

Robert Bialik
Mariusz Majdański
Mateusz Moskalik *Editors*

Achievements, History and Challenges in Geophysics

60th Anniversary of the
Institute of Geophysics,
Polish Academy of Sciences

GeoPlanet: Earth and Planetary Sciences

Editor-in-Chief

Paweł Rowiński

Series editors

Marek Banaszkiewicz

Janusz Pempkowiak

Marek Lewandowski

Marek Sarna

For further volumes:

<http://www.springer.com/series/8821>

Robert Bialik · Mariusz Majdański
Mateusz Moskalik
Editors

Achievements, History and Challenges in Geophysics

60th Anniversary of the Institute of
Geophysics, Polish Academy of Sciences



Springer

Editors

Robert Bialik
Department of Hydrology and
Hydrodynamics, Institute of Geophysics
Polish Academy of Sciences
Warsaw
Mazowieckie
Poland

Mateusz Moskalik
Department of Polar Research, Institute
of Geophysics
Polish Academy of Sciences
Warsaw
Mazowieckie
Poland

Mariusz Majdański
Department of the Lithospheric Research,
Institute of Geophysics
Polish Academy of Sciences
Warsaw
Mazowieckie
Poland

The GeoPlanet: Earth and Planetary Sciences Book Series is in part a continuation of Monographic Volumes of Publications of the Institute of Geophysics, Polish Academy of Sciences, the journal published since 1962 (<http://pub.igf.edu.pl/index.php>).

ISSN 2190-5193

ISSN 2190-5207 (electronic)

ISBN 978-3-319-07598-3

ISBN 978-3-319-07599-0 (eBook)

DOI 10.1007/978-3-319-07599-0

Springer Cham Heidelberg New York Dordrecht London

Library of Congress Control Number: 2014944554

© Springer International Publishing Switzerland 2014

This work is subject to copyright. All rights are reserved by the Publisher, whether the whole or part of the material is concerned, specifically the rights of translation, reprinting, reuse of illustrations, recitation, broadcasting, reproduction on microfilms or in any other physical way, and transmission or information storage and retrieval, electronic adaptation, computer software, or by similar or dissimilar methodology now known or hereafter developed. Exempted from this legal reservation are brief excerpts in connection with reviews or scholarly analysis or material supplied specifically for the purpose of being entered and executed on a computer system, for exclusive use by the purchaser of the work. Duplication of this publication or parts thereof is permitted only under the provisions of the Copyright Law of the Publisher's location, in its current version, and permission for use must always be obtained from Springer. Permissions for use may be obtained through RightsLink at the Copyright Clearance Center. Violations are liable to prosecution under the respective Copyright Law. The use of general descriptive names, registered names, trademarks, service marks, etc. in this publication does not imply, even in the absence of a specific statement, that such names are exempt from the relevant protective laws and regulations and therefore free for general use.

While the advice and information in this book are believed to be true and accurate at the date of publication, neither the authors nor the editors nor the publisher can accept any legal responsibility for any errors or omissions that may be made. The publisher makes no warranty, express or implied, with respect to the material contained herein.

Printed on acid-free paper

Springer is part of Springer Science+Business Media (www.springer.com)

Series Editors

Geophysics:

Paweł Rowiński
Editor-in-Chief
Institute of Geophysics
Polish Academy of Sciences
ul. Ks. Janusza 64
01-452 Warszawa, Poland
p.rowinski@igf.edu.pl

Space Sciences:

Marek Banaszkiewicz
Space Research Centre
Polish Academy of Sciences
ul. Bartycka 18A
00-716 Warszawa, Poland

Oceanology:

Janusz Pempkowiak
Institute of Oceanology
Polish Academy of Sciences
Powstańców Warszawy 55
81-712 Sopot, Poland

Geology:

Marek Lewandowski
Institute of Geological Sciences
Polish Academy of Sciences
ul. Twarda 51/55
00-818 Warszawa, Poland

Astronomy:

Marek Sarna
Nicolaus Copernicus Astronomical Centre
Polish Academy of Sciences
ul. Bartycka 18
00-716 Warszawa, Poland
sarna@camk.edu.pl

Managing Editor

Anna Dziembowska

Institute of Geophysics, Polish Academy of Sciences

Advisory Board

Robert Anczkiewicz

Research Centre in Kraków
Institute of Geological Sciences
Kraków, Poland

Aleksander Brzeziński

Space Research Centre
Polish Academy of Sciences
Warszawa, Poland

Javier Cuadros

Department of Mineralogy
Natural History Museum
London, UK

Jerzy Dera

Institute of Oceanology
Polish Academy of Sciences
Sopot, Poland

Evgeni Fedorovich

School of Meteorology
University of Oklahoma
Norman, USA

Wolfgang Franke

Geologisch-Paläontologisches Institut
Johann Wolfgang Goethe-Universität
Frankfurt/Main, Germany

Bertrand Fritz

Ecole et Observatoire des
Sciences de la Terre,
Laboratoire d'Hydrologie
et de Géochimie de Strasbourg
Université de Strasbourg et CNRS
Strasbourg, France

Truls Johannessen

Geophysical Institute
University of Bergen
Bergen, Norway

Michael A. Kaminski

Department of Earth Sciences
University College London
London, UK

Andrzej Kijko

Aon Benfield
Natural Hazards Research Centre
University of Pretoria
Pretoria, South Africa

Francois Leblanc

Laboratoire Atmosphères, Milieux
Observations Spatiales, CNRS/IPSL
Paris, France

Kon-Kee Liu

Institute of Hydrological
and Oceanic Sciences
National Central University Jhongli
Jhongli, Taiwan

Teresa Madeyska

Research Centre in Warsaw
Institute of Geological Sciences
Warszawa, Poland

Stanisław Massel

Institute of Oceanology
Polish Academy of Sciences
Sopot, Polska

Antonio Meloni

Istituto Nazionale di Geofisica
Rome, Italy

Evangelos Papathanassiou

Hellenic Centre for Marine Research
Anavissos, Greece

Kaja Pietsch

AGH University of Science and
Technology
Kraków, Poland

Dušan Plašienka

Prírodovedecká fakulta, UK
Univerzita Komenského
Bratislava, Slovakia

Barbara Popielawska

Space Research Centre
Polish Academy of Sciences
Warszawa, Poland

Tilman Spohn

Deutsches Zentrum für Luft und
Raumfahrt in der Helmholtz
Gemeinschaft
Institut für Planetenforschung
Berlin, Germany

Krzysztof Stasiewicz

Swedish Institute of Space Physics
Uppsala, Sweden

Ewa Szuszkiewicz

Department of Astronomy and
Astrophysics
University of Szczecin
Szczecin, Poland

Roman Teisseyre

Earth's Interior Dynamics Lab
Institute of Geophysics
Polish Academy of Sciences
Warszawa, Poland

Jacek Troncynski

Laboratory of Biogeochemistry
of Organic Contaminants
IFREMER DCN_BE
Nantes, France

Steve Wallis

School of the Built Environment
Heriot-Watt University
Riccarton, Edinburgh
Scotland, UK

Wacław M. Zuberek

Department of Applied Geology
University of Silesia
Sosnowiec, Poland

Piotr Życki

Nicolaus Copernicus Astronomical
Centre
Polish Academy of Sciences
Warsaw, Poland

Preface

During the last half century Geophysics has experienced a rapid development. Seismic methods, magnetic studies, hydrology, and atmospheric sciences expanded thanks to a boom in the computer sciences and progress in measurement techniques. During those times we also moved the frontiers of geophysics, reaching with our research to polar areas, both Arctic and Antarctic. All these events have been clearly reflected in the 60-year long history of the Institute of Geophysics, Polish Academy of Sciences (PAS). The current volume, being a result of the Jubilee Conference on the occasion of the 60th Anniversary of the Institute that took place on June 14, 2013, in Hotel Windsor in Jachranka near Warsaw, presents the most prominent achievements, the history of research, and also the future potential of the Institute. It also describes measurements in various projects, methods of interpretation of scientific data, and, last but not least, the people who drove the above-mentioned research in many scientific involvements. It is obvious that the rich history of the Institute may be only partially outlined in one volume but it definitely provides a valuable material for well-established researchers and especially for students who are the future of geophysics as a discipline and our Institute as well. For the preparation of the various chapters of the book, representatives of all Institutes' Departments were invited, the Ph.D. students in line with senior scientists.

The Jubilee Conference gave also an opportunity to honor four outstanding scientists with commemorative medals (see Fig. 1) for their great contributions to the development of the Institute of Geophysics. Professor Roman Teisseyre was awarded for his outstanding and creative work in the field of seismology, Prof. Jerzy Jankowski for his outstanding scientific achievements in the field of geomagnetism, Prof. Aleksander Guterch for his outstanding scientific and organizational achievements in the modeling of the structure of the Earth's crust and upper mantle, and Doctor Maciej Zalewski was awarded for his commitment to the development of the Polish Polar Station Hornsund in Spitsbergen.

There are several people that have to be acknowledged herein, as without their contributions, this book would have never been prepared. First of all, special thanks are dedicated to all the members of the organizing committee of the 60th Anniversary Conference in Jachranka, namely Robert Bialik, Janusz Borkowski, Zbigniew Czechowski, Anna Łukanowska, Mariusz Majdański, Mateusz Moskalik, Beata Orlecka-Sikora, Krzysztof Otto, Paweł Urban, Tomasz Werner, and Anna

Fig. 1 Jubilee medal

Zdunek. The members decided to entrust us with the task of editing this book and we hope that we have been able to meet their expectations. All chapters have been reviewed by at least two reviewers, including national and international specialists, and we are grateful to all of them, including Mariusz Białycki, Janusz Borkowski, Leszek Czechowski, Wojciech Czuba, Benoit Demars, Tomasz Ernst, Edward Gaczyński, Wolfram Geissler, Alireza Goudarzi, Marek Górski, Dariusz Jakubas, Grzegorz Karasiński, Mikołaj Karpiński, Jacek Kopeć, Marek Kubicki, Leszek Książek, Marek Lewandowski, Bartłomiej Luks, Sławomir Maj, Russel Manson, Iwona Markiewicz, Krzysztof Migala, Krzysztof Mizerski, Krzysztof Nowożyński, Krzysztof Opaliński, Marzena Osuch, Tomasz Petelski, Erin Pettit, Piotr Senatorski, Joanna Szczucka, Piotr Środa, Krzysztof Teisseyre, Luciano Telesca, Timo Tiira, Tomasz Werner, Joanna Wibig, Monika Wilde-Piórko, Marcin Witek, and Paweł Rowiński who assured high professional standard of all contributions. It should be mentioned that few of these people did their job several times, which is strongly appreciated. In addition, Anna Dziembowska did titanic job assuring the good quality of English of all chapters and helped us with handing this book, as well. She prepared the appendix to this preface honoring the previous Institute's workers who passed away during the last decade, which we think is strongly required to be included in this book. Finally, we would like to thank all the authors of the chapters for their involvement and the passion which resulted in provision of unique information about the history of the Institute of Geophysics PAS. The book is divided into two parts. In the first, the history and achievements of the Institute of Geophysics PAS are comprehensively described, whereas in the second part the exemplary current research results and the method used in geophysics are presented.

Robert Bialik
Mariusz Majdański
Mateusz Moskalik

In Memoriam (2004–2013)

It is our duty to commemorate our mentors, colleagues, and friends who passed away in the last decade.¹

Hanna Bojanowska (1933–2006), Employed at the Institute over the years 1955–1989. Worked in the Accounting Division. Deputy Chief Accountant in 1959–1989.

Dr. Bogusław Domański (1956–2011), physicist, geophysicist. Employed at the Institute in 1985–2009. Worked in the Department of Seismology.

Jakub Dopierała, M.Sc. (1976–2008), employed at the Institute in 2007–2008. Worked in the Department of Atmospheric Physics.

Associate Professor Aniela Dziewulska-Łosiowa (1916–2004), astronomer and geophysicist, graduated from the Stefan Batory University in Wilno, political exile to Siberia in 1945–1955. Employed at the Institute in 1959–1990, head of the Department of Atmospheric Physics over the years 1974–1981; pioneer of atmospheric ozone measurements in Poland. Obituaries: *Przegląd Geofiz.* 2005 No. 1–2; *Urania-PA*, 2004, No. 3; *Biul. Inf. ZZ AK*, 2004, No. 1.

Associate Professor Bożenna Gadomska (nee Wojtczak) (1931–2011), geophysicist, seismologist. Employed at the Institute in 1954–2001, associated with the Department of Seismology and Physics of the Earth's Interior. Since 1972 she was heading the Scientific Secretariate, and then, in the years 1976–1988, she was the Scientific Secretary of the Institute. Obituary: *Przegląd Geofiz.*, 2014, 59, No. 3.

Professor Sławomir Jerzy Gibowicz (1933–2011), geophysicist, renowned seismologist, with invaluable contribution to mining seismology. Associated with the Institute since 1956. Head of the Department of Seismology in the years 1979–2003. Obituary: *Acta Geophys.*, 2012, No. 1.

¹ Those who passed away prior to 2004 have been commemorated in the *Publs. Inst. Geophys. Pol. Acad. Sc.*, 2004, M-26(348), issued on the occasion of the 50th Anniversary of the Institute.

Halina Gizejewska (nee Kowalewska) (1952–2009), engineer, employed at the Institute since 1981, as a specialist at the Department of Polar and Marine Research.

Adam Gnoiński (1930–2006), magnetologist. Worked at the Geophysical Observatory at Świder in 1953–1975, then at the Central Geophysical Observatory at Belsk until 1989.

Professor Zdzisław Kaczmarek (1928–2008), employed at the Institute since 1981. Full member of the Polish Academy of Sciences, eminent hydrologist, contributing to the IPPC report which awarded the 2007 Nobel Peace Prize. Head of the Water Resources Department in 1982–2004 Obituaries: *Przegląd Geofiz.* 2008, No. 2; *WMO Newsletter MeteoWorld*, December 2009; *Gospodarka Wodna* 2008, Vol. 8.

Jacek Tadeusz Kowalski, M.Sc. (1926–2006), physicist, geophysicist, employed at the Institute in 1966–1981, first at the Observatory in Cracow, and then at the Central Geophysical Observatory at Belsk, to join the Seismology Department in 1976.

Wiesław Kozłowski (1942–2012), worked at the Geophysical Observatory at Świder in 1962–2008, in the atmospheric electricity laboratory.

Dr. Janusz Marianiuk (1936–2012), physicist, magnetologist. Employed at the Institute in 1957–2008, first at the Geophysical Observatory at Świder, and since 1965 at the Central Geophysical Observatory at Belsk, as head of the Geomagnetic Laboratory and then head of the whole Observatory over the years 2000–2006. Obituaries: *Przegląd Geofiz.*, 2012, 57(3–4); *Publs. Inst. Geophys* 2013, C-16(416, internet edition).

Rufin Materzok, M.Sc. (1935–2004), seismologist, employed at the Institute in 1970–2001, worked at the Department of Seismology, engaged in deep seismic sounding projects

Professor Janusz Niewiadomski (1940–2005), seismologist, employed at the Institute in 1974–2005. Associated with the Department of Seismology, being its head since 1993. Deputy Director for Science in 1990–1993.

Janina Przygodzińska (1920–2005), employed by the Institute in 1974–1991. Head of the Institute's library.

Professor Kacper Mieczysław Rafał Rybicki (1940–2008), geophysicist, planetologist, astrophysicist. Associated with the Institute since 1966: first as a Ph.D. student, and then, since 1972, employed at the Department of Earth Interior Dynamics until his death. He was the Deputy Director for Science since 1991, and

the Director of the Institute since 2004. Founded a scholarship for outstanding young geophysicists. Obituaries: *Acta Geophys.* 2008, No. 4, *Przegląd. Geofiz.* 2008, No. 3–4.

Associate Professor Jan Stomka (1925–2005), Climatologist. Employed at the Institute in 1956–1992. Strongly engaged in building the Central Geophysical Observatory at Belsk, organized the atmospheric physics and solar radiation laboratories there. Became the Director of the Observatory in 1962.

Urszula Staszkiewicz-Szwarc (1938–2008), Chief Accountant at the Institute over the years 1988–1996.

Professor Romuald Wielądek (1923–2004), Mathematician, magnetologist. Employed at the Institute in 1954–2000, specialist in time series analysis algorithms for magnetic data processing.

Anna Wiśniewska (nee Pac), M.Sc. (1976–2008), employed at the Institute' Accounting Division in 2001–2008.

Anna Dziembowska

Contents

Part I History and Achievements

| | |
|---|------------|
| Best Practices in Earth Sciences: The National and International Experience of the Institute of Geophysics, Polish Academy of Sciences | 3 |
| Paweł M. Rowiński and Anna Zdunek | |
| On the Roots of the Institute of Geophysics, Polish Academy of Sciences | 27 |
| Sławomir Maj and Krzysztof P. Teisseyre | |
| Fifty Years of Palaeomagnetic Studies in the Institute of Geophysics, Polish Academy of Sciences | 39 |
| Magdalena Kądziałko-Hofmokl, Tomasz Werner and Jadwiga Kruczyk | |
| Natural Variations of the Geomagnetic Field: Observations and Application to Study of the Earth's Interior and Ionosphere | 65 |
| Waldemar Jóźwiak, Jerzy Jankowski and Tomasz Ernst | |
| Half Century of the Ozone Observations at the Central Geophysical Observatory, IGF PAS, Belsk, Poland | 85 |
| Janusz W. Krzyścin, Janusz Borkowski, Anna Główacka, Janusz Jarosławski, Jerzy Podgócki, Aleksander Pietruszuk, Bonawentura Rajewska-Więch, Anna Sawicka, Piotr Sobolewski, Jakub Wink and Wiesława Zawisza | |
| Forty Years of Water Research at the Institute of Geophysics, Polish Academy of Sciences | 109 |
| Robert J. Bialik, Jarosław J. Napiórkowski, Paweł M. Rowiński and Witold G. Strupczewski | |

| | |
|---|------------|
| Changes in Catchment Hydrology Caused by Changes in the Environment: A Contribution of the Water Resources Department, Institute of Geophysics PAS | 127 |
| Emilia Karamuz and Renata J. Romanowicz | |
| Five Polish Seismic Expeditions to the West Antarctica (1979–2007) | 137 |
| Tomasz Janik, Marek Grad and Aleksander Guterch | |
| Department of Polar and Marine Research: The Hornsund Station and Other Activities in the Arctic and Antarctic Regions | 159 |
| Marek Górski | |
| Seismology and Earth Dynamics: A Variety of Scientific Approaches | 173 |
| Krzysztof P. Teisseyre, Paweł Wiejacz and Jacek Trojanowski | |
| Sixty Years of Publishing with the Institute of Geophysics | 197 |
| Anna Dziembowska and Maria Wernik | |

Part II Exemplary Current Research and Geophysical Methods

| | |
|--|------------|
| Discharge Measurements in Lowland Rivers: Field Comparison Between an Electromagnetic Open Channel Flow Meter (EOCFM) and an Acoustic Doppler Current Profiler (ADCP) | 213 |
| Robert J. Bialik, Mikołaj Karpiński and Agnieszka Rajwa | |
| Random Domino Automaton: Modeling Macroscopic Properties by Means of Microscopic Rules | 223 |
| Mariusz Bialecki and Zbigniew Czechowski | |
| Continental Passive Margin West of Svalbard and Barents Sea in Polish Arctic Seismic Studies | 243 |
| Wojciech Czuba | |
| Selected Theoretical Methods in Solid Earth Physics: Contribution from the Institute of Geophysics PAS | 253 |
| Wojciech Dębski, Roman Teisseyre and Włodzimierz Bielski | |
| Application of Passive Hydroacoustics in the Studies of Sea-Ice, Icebergs and Glaciers: Issues, Approaches and Future Needs | 271 |
| Oskar Glowacki and Mateusz Moskalik | |

| | |
|--|------|
| Contents | xvii |
| Pigeon Navigation Model Based on a Vector Magnetometer | 297 |
| Jerzy Jankowski | |
| Analysis of Surface Ozone Variations Based on the Long-Term Measurement Series in Kraków (1854–1878), (2005–2013) and Belsk (1995–2012) | 313 |
| Izabela Pawlak and Janusz Jarosławski | |
| Dissolved Oxygen in Rivers: Concepts and Measuring Techniques | 337 |
| Agnieszka Rajwa, Robert J. Bialik, Mikołaj Karpiński and Bartłomiej Luks | |
| Gradient-Based Similarity in the Stable Atmospheric Boundary Layer | 351 |
| Zbigniew Sorbjan | |
| Asymmetric Continuum Theory: Fracture Processes in Seismology and Extreme Fluid Dynamics | 377 |
| Roman Teisseyre | |
| Time Scales: Towards Extending the Finite Difference Technique for Non-homogeneous Grids | 397 |
| Kamil Waśkiewicz and Wojciech Dębski | |

Part I

History and Achievements

Best Practices in Earth Sciences: The National and International Experience of the Institute of Geophysics, Polish Academy of Sciences

Paweł M. Rowiński and Anna Zdunek

There is no national science just as there is no national multiplication table; what is national is no longer science.

Anton Chekhov

Abstract The Institute of Geophysics of the Polish Academy of Sciences is the natural successor to the glorious tradition of geophysical research in Poland. It plays the leading role in exploration of the Earth, beginning from the atmosphere across hydrosphere to the lithosphere at the end. This chapter is prepared on the occasion of the 60th anniversary of establishment of this Institution and it shows its activities in the past and nowadays.

Keywords Geophysics · Earth sciences · Polar research · Atmosphere · Hydrosphere · Lithosphere · Geomagnetism · History of the institute of geophysics PAS

1 The Institute of Geophysics PAS in the Service Towards Better Understanding of the Earth

Geophysics is an integral part of Earth Sciences. It is a field that has generated its own methodology and draws on the achievements of other sciences—especially physics, mathematics, chemistry, computer science and what we can broadly

This chapter is an updated and substantially extended version of the earlier published article in Polish (Rowiński and Zdunek 2011).

P. M. Rowiński (✉) · A. Zdunek
Institute of Geophysics, Polish Academy of Sciences, ul. księcia Janusza 64,
01-452 Warsaw, Poland
e-mail: p.rowinski@igf.edu.pl

conceive as the engineering sciences. Humankind has almost always been interested in the phenomena observed on the planet, and the beginnings of the history of geophysics as a separate science can probably be seen in the times of Thales of Miletus. The Greeks associated with him the creation of a new concept of the accumulation of knowledge—a scientific concept that we also use to a certain extent. It was Thales who created what was perhaps the first cosmological doctrine, according to which everything that exists floats on giant masses of water, and the Earth as a floating island is only a temporary product of the water. The first specifically geophysical achievement was the calculation of the radius of the Earth by Eratosthenes of Cyrene, based on an examination of differences in the angle of incidence of sunlight.

The current understanding of geophysics as a science is obviously different now, although the object of study remains the same. The website of the largest geophysical organisation, the American Geophysical Union (AGU), states that the Earth is a complex system consisting of four components—rocks, water, air and life, all of which are immersed in outer space. The work of scientists can therefore be classified according to which part of the system they explore. Such a comprehensive approach, taking into account all of the elements of the system, underlies the organisation of the research undertaken at the Institute of Geophysics of the Polish Academy of Sciences (IGF PAS). In other words IGF PAS works to understand how planet Earth works in all of its physical manifestations.

Deep theoretical studies play a role of great importance in the development of geophysics, but we can only obtain meaningful results if we combine this with well-conducted experiments and observations of nature. The subject of research in geophysics is the physical processes taking place now and in the past in the geospheres: the lithosphere, atmosphere, and hydrosphere, and the purpose of the research is to explain the phenomena that are observed.

The Institute of Geophysics PAS conducts basic research in virtually all areas related to the physics of the Earth—its interior, hydrosphere and atmosphere. At the same time, the Institute conducts continuous monitoring of global geophysical fields, seismic events and selected parameters of the atmosphere. In recent years, the main organisational and logistical objectives pursued by the Institute have focused on strengthening the research and application potential of its work by consolidating coordinated activities with other national and international institutions.

The contemporary challenges that are posed to science, and particularly to Earth Sciences, require an integrated, multidisciplinary approach to research. Only by developing research in this direction it is possible to orientate it towards current socio-economic needs while ensuring the ability to address and solve increasingly complex scientific issues. In response to this challenge, on 30 March 2009 at the premises of the Institute of Geophysics PAS, an agreement was signed on the establishment of a consortium under the title of the GeoPlanet: Earth and Planetary Research Centre, which united four research institutes at the Polish Academy of Sciences: the Institute of Geophysics, the Institute of Oceanology, the Space Research Centre and the Institute of Geological Sciences. On 3 October 2012,

Fig. 1 The GeoPlanet logo

GeoPlanet was joined by the Nicolaus Copernicus Astronomical Center, which extended its scopes towards astronomical investigations.

The base of the GeoPlanet Centre was created at the Institute of Geophysics (see the GeoPlanet logo in Fig. 1). An important factor cementing the joint scientific activity of these units is their similar—and often common—research methodology, which uses the conceptual apparatus of physical and chemical sciences, mathematics and geology. On the other hand, the complementarity of the disciplines represented by those institutions allows the Centre to cover the essential spectrum of cognitive studies of the Earth and other planets. With its research and infrastructure potential, common databases and research groups, the Centre constitutes an important added value, which is of importance both nationally and in the international scientific community.

GeoPlanet is a centre that integrates Polish research on the physical and chemical processes occurring on the Earth, its environment and the solar system. It is actively involved in national and international programmes, and is creating its own research tools. It has an important role to fulfil as regards conducting observations of the Earth (lands and oceans) using its own network of observatories and vessels, and in the creation of models interpreting the data so acquired. In parallel with its research activities, GeoPlanet is to become a centre of education for professionals at Ph.D. level and of the dissemination of knowledge about the Earth and the solar system in society. Internationally, GeoPlanet will hopefully participate in relevant European programmes, as well as in bilateral and multi-lateral research projects, enabling its use of international databases in the field of planetary science, geophysics, oceanography and geology. The role of the Center and its high international activity has been notably appreciated by invitation to join the newly established Consortium of leading European institutions dealing with Earth science, namely Earth Science National Labs that also includes: German Research Centre for Geosciences (GFZ, Potsdam, Germany), Natural Environment Research Council, British Geological Survey (NERC-BGS, UK), Instituto Nazionale di Geofisica e Vulcanologia (INGV, Italy), Die Eidgenössische Technische Hochschule (ETH, Zürich, Switzerland), L'institut de physique du Globe (IPGP, Paris, France), Institute of Earth Sciences “Jaume Almera” (ICTJA-CSIC,

Barcelona, Spain), Utrecht University (The Netherlands). The relevant agreement was solemnly signed in Paris on October 17, 2012. That important event had been preceded by signing the Letter of Intent on Bilateral Collaboration with the Helmholtz Centre Potsdam, GFZ German Research Centre for Geosciences.

At the same time, the Institute of Geophysics PAS acknowledges the increasing utilitarian importance of the research that it conducts. The results of its huge long-term projects concerning the exploration of the Earth's crust are an extremely valuable material for companies involved, for example, in prospecting for natural gas deposits. The development of this trend in the Institute's activities resulted in creation in 2009 of a scientific and industrial consortium led by the Institute of Geophysics PAS, and formed by Polskie Górnictwo Naftowe i Gazownictwo S.A. (Polish Oil and Gas Company) and Geofizyka Toruń S.A. The establishment of this consortium is the result of many years of joint work. The consortium has already proceeded to the implementation of a task that is extremely important for the economy: a programme of deep seismic reflection studies of the Earth's crust in the Lublin region and the Eastern Carpathians. The Institute has also actively participated in the very dynamic discussion on the existence of unconventional gas deposits in claystones (so-called shale gas), and the possibility of their extraction. In 2010 IGF PAS together with the Institute of Geological Sciences PAS and American corporation ION initiated the so-called PolandSPAN project which is a large regional 2D seismic research project covering all of Poland with the goal of improving the overall scientific knowledge of the geology of Poland. Within this unique huge project, a 2D seismic survey uses state-of-the-art geophysical technology to produce detailed images of the deep geological strata under the earth's surface along linear profiles. From these data, detailed maps are constructed and used to understand the geologic history. This one-of-a-kind program will provide the foundation of integrated geologic knowledge and a consistent seismic framework from which to build future studies. An interesting initiative is also a common project with the UK's Hutton Energy and again with the Institute of Geological Sciences PAS, the so-called Jurashale project, which focuses on tapping Jurassic shale plays. The project studies how to best achieve shale extraction from the Jurassic shale in Poland.

In sense of the applicability of the research done at the Institute, extremely important is its involvement in the so-called EPOS project (European Plate Observing System) which aims to promote and make possible innovative approaches for a better understanding of the physical processes controlling earthquakes, volcanic eruptions, tsunamis and other geohazards as well as those driving internal and surface geodynamics. All is about integration of the existing national and trans-national research infrastructures. IGF PAS is the Polish leading institution in the project and the leader of one of crucial work packages with the goal to integrate the research and research infrastructures in the area of seismicity induced by human activity and one its main priorities is to strengthen the cooperation between industry and science. Note that the socio-economic impact of induced seismicity is of crucial importance; this phenomenon is in fact an unwanted rockmass response to human technological processes which links

seriously the research and industry. The induced earthquakes accompany underground and open-pit mining, conventional and unconventional hydrocarbon production, reservoir impoundment, geothermal energy production, underground fluid and gas storage including carbon sequestration and many other technological processes that perturb the boundary conditions in the affected rockmass. In this respect, the institute successfully applied for an accompanying project IS-EPOS (funded by European Regional Development Fund) allowing for the significant improvement of Polish infrastructure. This project is realized, among other institutions, with the industrial partner, Kompania Węglowa, the largest coal mining company in Poland and Europe. The induced seismicity lies also at the front of the long-lasting collaboration with KGHM Polska Miedź S.A, a global producer of copper and silver. The collaboration concerns mainly the safety of exploitation of “Żelazny Most”—the largest tailings storage facility in Europe, and one of the largest worldwide.

From completely different angle, the Institute has collaborated with the designing companies of, e.g., gas steam power plants (DHV Hydroprojekt Sp.zo.o., Lemitor Ochrona Środowiska Sp.zo.o.), for which the Institute prepared parts of Environmental Impact Assessment Studies, namely the studies related to heat pollution transport in rivers.

Additionally, the scope of cooperation of IGF PAS has been extended to research centres not directly related to Earth Sciences (for example, the Medical University of Łódz), for which both the long experience of the Institute and its research infrastructure are key elements for further application and development work. As an example, let us mention the studies on the ultraviolet (UV) therapy of psoriasis, the disease that can have a substantial impact on quality of life, and its treatment yields substantial economic costs to patients and to the health care system. Another surprising example is the project realized in cooperation with the Miele Company, truly global premium brand of domestic appliances and commercial machines in the field of laundry care, dishwashing and disinfection. The project consists in the investigations of magnetic properties of the dust at various locations in Warsaw (see <http://odkurzonawarszawa.pl/>).

The multi-year project, Monitoring of Seismic Hazards in Poland, carried out at the request of the Minister of the Environment, is of a utilitarian nature and is financed by the National Fund for Environmental Protection and Water Management. This extremely important project (taking into account every kind of seismic event with an epicentre in Poland) is essential for planning large engineering investments, such as nuclear power plants and dams. The result of these observations are the so-called seismic hazard maps showing the spatial distribution of the probability of seismic activity in a given area at a given time. Information about meaningful earthquakes is transmitted to the Government Centre for Security. The Institute also conducts the measurement of gaseous pollutants, total ozone content and the intensity of UV-B radiation at the request of the Chief Inspectorate of Environmental Protection. The works conducted by the Institute in the field of water management, especially in relation to protected areas of

north-eastern Poland (such as Narew National Park), are also of utilitarian nature and are vital for the economy in general.

A very important aspect of the Institute's activities is its participation in the creation of global databases based on the monitoring of geophysical fields in Poland (10 stations and observatories) and at the Polish Polar Station on Spitsbergen. The Institute runs observatories across a wide spectrum of research: the Central Geophysical Observatory in Belsk, observatories in Świdra, Ojców, Racibórz, Książ and on Hel, as well as permanent seismic stations located in Suwałki, Niedzica, Góra Klasztorna Kalwaria Pacławska. The above mentioned activity is associated with cooperation and transfer of the results of geophysical observations to the World Data Centres, fulfilling the obligations incumbent upon Poland in this regard. Participation in this geophysical monitoring requires work on the development and modernisation of geophysical instruments and on the application of modern information and communication technologies to the collection and exchange of measurement data. The Institute also conducts innovative research and construction work in this field.

In 2002, the Ministry of Science granted the Institute the status of a Centre of Excellence on Geophysical Methods and Observations for Sustainable Development (GEODEV). That initiative was kind of a response to the paradigm of changing global environment and a need for closer cooperation of natural and social sciences in coping with possible consequences of these changes. On the other side, the risk of natural (atmospheric, hydrological, seismic) hazards, as a threat to sustainable development of national economy, is not adequately taken into consideration. The aims of GEODEV were therefore to enhance the role of Polish geophysicists in securing the sustainable growth of national economy, and to intensify cooperation with European centres involved in similar research.

The Institute can boast of active participation in the international studies of the polar regions, particularly the Arctic. The research on the physical characteristics of the natural environment that is being carried out at the Polish Polar Station at Hornsund Fjord on Spitsbergen constitutes an important contribution to the determination of global processes included in many international programmes considered as priorities by both the European Science Foundation in Strasbourg and the European Commission in Brussels. Hornsund Fjord, with the Polar Station, has been recognised as a flagship site in Europe in the field of research on terrestrial and marine ecosystems (European Marine Biodiversity Flagship Site). The level of the research being conducted at the station resulted in the Institute of Geophysics PAS being invited to join the SIOS (Svalbard Integrated Arctic Earth Observing System) consortium as coordinator of logistics enterprises across the entire Svalbard area. This project was one of the initiatives selected for the Polish Roadmap for Research Infrastructures. It is also worth mentioning that IGF PAS was the initiator of creating the Polish Multidisciplinary Laboratory for Polar Research with the research infrastructure based upon Polish Polar Station in Spitsbergen, Research Vessel Oceania, Horyzont II research-training vessel, highly specialized laboratories operated by Scientific Polar Network, and other infrastructure operated by nearly sixteen Polish institutions. The Laboratory is

going to strengthen the Polish contribution to creating worldwide network for research and monitoring of land and marine environments in polar zones which are crucial for understanding the dynamics of environmental changes all over the globe (global warming and raising sea levels especially). This lab has also been successful to be included on the Polish Roadmap for Research Infrastructures. On top of that, based on the national contest, the Institute has recently been awarded the prestigious title of Leading National Research Center, the highest rank for institutions that might be received in Poland. More precisely, that award went to the newly established Center for Polar Studies in collaboration with the University of Silesia and the Institute of Oceanology of the Polish Academy of Sciences.

The research, that is, the mainstream activity of the Institute, is focused on fundamental issues in the physics of the processes taking place on our globe, and covers the following areas: seismology, the dynamics of the Earth's interior, geomagnetism, physics of the atmosphere, hydrology, environmental hydrodynamics and polar research.

Research in the field of seismology covers a wide range of issues based on the analysis of earthquakes, especially in relation to the seismicity of Polish territory. The results of many years of research on tremors caused by mining activity make Poland stand out in this field. Recently, a great emphasis has been placed on the development of methods in the field of seismic hazards. The Institute has also achieved an outstanding success in performing the leading role in the conduction of large-scale international deep seismic soundings. These activities are aimed at understanding the structure and geodynamics of the Earth's crust and upper mantle in Europe and in the polar regions. For example, the CELEBRATION 2000 seismic experiment, carried out in Central and Eastern Europe over an area of approximately 500,000 km² by 1,250 cutting-edge seismic stations, provided mainly by US research centres in Washington and New Mexico, has been recognised in the report of the European Science Foundation (ESF) as the greatest research project of its kind in the history of world geophysics. In the opinion of the international scientific community, the area of Central Europe under investigation is the region with the currently best-explored deep structure of the Earth's crust and lithosphere to a depth of 100 km.

Geomagnetic research focuses on developing magnetotelluric methods and the numerical modelling of processes of electromagnetic induction within the Earth. The Institute also carries out regional studies on the structure of the Earth's crust, which complement the results obtained from deep seismic soundings. Paleomagnetic studies and studies of the magnetic properties of intrusive and sedimentary rocks represent an important part of the activities of the Department of Terrestrial Magnetism; these are carried out using a modern, well-equipped laboratory.

The Institute's mainstream research also includes the study of the dynamics of the Earth's interior, in particular the physics of seismically active regions. The Institute has developed theoretical models of the generation and propagation of seismic waves. The Institute has been actively involved in the development of the rotational seismology, an emerging field of study concerned with all aspects of rotational motions induced by earthquakes, explosions, and ambient vibrations.

In this respect, a concise Asymmetric Continuum Theory, including the relations between stresses, strains, interaction fields and defects has been recently proposed to the research community. The Institute also carried out several analyses of the Earth's future from the perspective of the evolution of the Sun and the solar system, using the research methodology of planetary science and astrophysics.

The studies on the atmosphere conducted by the Institute have a long history and extensive scope. In recent years, particular emphasis has been placed on an analysis of the variability of the ozone layer and solar radiation over different timescales. In 2013, the Institute celebrated the 50th anniversary of the initiation of ozone observations by the Dobson spectrophotometer at the Belsk Observatory, one of the longest observational series worldwide. The Institute has also achieved significant results in LIDAR measurements of atmospheric aerosol and the research of the atmospheric electricity.

The Institute's research also focuses on the hydrosphere, in particular on the physical processes occurring in surface waters. The Institute carries out theoretical and experimental work on the transport and mixing of pollutants in rivers, flood wave transformation and the determination of flood risk. The impact of projected global changes on water resources is also subject to analysis.

Polar and marine research includes in particular the analysis of geophysical data and information concerning the natural environment, which is obtained by the Polish Polar Station on Spitsbergen. The Institute of Geophysics PAS coordinated a large part of the Polish scientific activity during the globally reaching Fourth International Polar Year 2007–2009, which engaged numerous research teams from more than 60 countries worldwide.

The activity of Polish scientific institutions during the Fourth International Polar Year has been of great importance, not only scientifically, but also geopolitically and economically. Currently, intensive international negotiations are ongoing concerning the legal status of the Arctic and Antarctic. The Institute is in close contact with the Polish Ministry of Foreign Affairs, whose representative is systematically involved in the political negotiations. On an on-going basis, the Institute has been preparing materials and data which form the basis for legal and political negotiations, especially on the future of the Arctic. After the formal end of Fourth International Polar Year, the Decade of the Polar Year was announced.

Recent years have also seen the dynamic development of the Institute's flagship publishing house. The first issue of *Acta Polonica Geophysica* was published in 1953 and was edited by Edward Stenz. After nearly 53 years, in 2006, *Acta Geophysica Polonica* was transformed into *Acta Geophysica*. (for details see Dziembowska and Wernik (2014) in this Issue). The Editorial Board includes the most prominent world scientists, including the Crafoord Prize laureate Prof. Adam Dziewoński and professors Barbara Romanowicz, Randy Keller, James Dooge and Vijay Singh. The journal was published in collaboration with the publishers Versita and Springer. These activities resulted in the introduction of *Acta Geophysica* to the so-called Philadelphia List—Science Citation Index Expanded (currently Thomson Reuters Journal Citation Report) as early as 2007. Extremely quickly, by 2009, *Acta Geophysica* had been assigned its impact factor (IF). Currently, we can see a

rapid increase in both the IF and the number of authors involved from the world's leading geophysical centres. The journal has become a major player in the international scientific publishing market. The impact factor of *Acta Geophysica* for the year 2013, as expected to be specified in Journal Citation Reports (ca in June 2014) exceeds 1.2. The Institute also publishes a monographic series entitled Publications of the Institute of Geophysics, Polish Academy of Sciences. A total of over 400 volumes have been published as part of this series. Recently, in collaboration with the Springer-Verlag publishing house, the Institute has initiated (in partial continuation of the Publications of the Institute of Geophysics) a new series of publications to which we plan to assign world-class importance. The series is entitled *GeoPlanet: Earth and Planetary Sciences*. It grew from the great publishing traditions of the Institute, the excellent ratings of the monographs it has issued, and the established cooperation with other institutions. The first volume of this series was released in the summer of 2010 and at the moment 12 monographs are released and Four more are expected to be released still in 2014. A few of them may be found on the prestigious Web of Science of Thomson Reuters (for details about IGF PAS publication history, see Dziembowska and Wernik (2014) in this Issue).

With our emphasis on research, there can be no doubting the importance that the Institute places on our vibrant and growing Ph.D. programme. Students can participate in a wide range of dedicated courses and gain access to the in-depth research resources in various departments and observatories. We provide strong support to all of our Ph.D. students. They obtain decent scholarships and can apply for internal research projects on a competitive basis. We should also mention a generous inheritance of Prof. Kacper Rybicki who donated to the Institute for the purpose of funding scholarships for outstanding young geophysicists. A special fund name after Prof. Rybicki has been established and young researchers as well as Ph.D. students rival annually for this prestigious award.

An important element of the Institute's activities in recent years has been the expansion of its educational activity and its broadly conceived public awareness of science activities related to the research it conducts. In addition to active participation in the education of Ph.D. students and young university scientists, the Institute is actively developing the Geophysics at School programme. This is a project aimed at junior and upper high school students, promoting not only the role of Earth Sciences in sustainable social development, but also the history of research on the planet Earth, issues of natural hazards and environmental responsibility in this environment.

Since March 2011, the Institute has been also the leader of the project "Improving students' competences in science and mathematics by employing innovative methods and technology—Eduscience". The logo of this project is presented in the Fig. 2.

The project is carried out within the Human Capital Operational Programme and is co-financed by European Union within the range of European Social Fund. It is the largest Polish innovative project in the field of education. The main aim of the project is to rise the interest in mathematical-natural sciences among schoolchildren, which would lead to an increase in the number of young people deciding



Fig. 2 The Eduscience logo

to study subjects related to those sciences. That is also very important from the point of view of Poland's economy, which needs more young specialists educated in those fields. The aim is being achieved by designing, development, pilot implementation and promotion of innovative school syllabuses with the use of an interactive e-learning platform, by running numerous festivals of science and science picnics, school trips and by active collaboration with scientists at various observatories, including the Polish Polar Station (Goździk 2013).

The outreach activities include the presentation of the Institute at science picnics and festivals, as well as active participation in work coordinated by the Council for the Promotion of the Public Understanding of Science PAS. The Institute sets much store by cooperation with the media, which is particularly important after natural disasters. The Institute's employees are invited to contribute to programmes, and they inform the public about the mechanisms that cause these hazards (earthquakes, floods, and recently the spread of volcanic ash) on radio and television.

The pride of the Institute resides primarily in its staff. The Institute employed or currently employs many world-renowned scholars. In this context, it is worth mentioning Prof. Adam Dziewoński, winner of the Crafoord Prize in 1998 for his study of the structure and processes taking place within the Earth. This is an award of Nobel Prize rank, which has been awarded since 1982 for research in fields such as mathematics, astronomy and life sciences. After graduation, Prof. Adam Dziewoński undertook his first job at the Institute of Geophysics PAS. Professors Zbigniew Kundzewicz and Zdzisław Kaczmarek, for many years affiliated with the Institute, took an active part in the work of the Intergovernmental Panel on Climate Change, which awarded the Nobel Peace Prize in 2007. In 1990, Prof. Zdzisław Kaczmarek, a long-term head of the Department of Water Resources at the Institute (currently the Department of Hydrology and Hydrodynamics) received the prestigious International Hydrological Prize awarded by the International Association of Hydrological Sciences (IAHS) to the most outstanding hydrologist in the world. The Institute has also employed other scholars who have had a great influence on the development of Polish science, many of whom have been honoured with membership of the Polish Academy of Sciences. Currently, the Institute employs three such scientists: Prof. Aleksander Guterch, Prof. Roman Teissrey and Prof. Paweł Rowiński but in the past it used to be a bigger number.

The consecutive directors of the Institute (formerly the Department of Geophysics) were: Prof. Edward Stenz (1953–1954), a prominent meteorologist, climatologist but also a specialist in geomagnetism; famous, e.g., for pioneering works on geography of Afghanistan (see Olczak 1957; Fedirko 2011); Prof. Tadeusz Olczak (1954–1960), a seismologist and geomagnetist (Maj and Guterch 1990); Prof. Stefan Manczarski (1960–1970), outstanding engineer-constructor, radioelectrician, geophysicist but also a biophysicist, known, e.g., for his works on geomagnetic wave propagation (Fiett i Mangel 2009); Prof. Roman Teisseyre (1970–1972), still working, internationally well-known specialist in the physics of the Earth interior, one of the creators of rotational seismology, head of the Polish geophysical expedition to Vietnam in 1957; Prof. Jerzy Jankowski (1972–2004), leader of Polish investigations on magnetotelluric and geomagnetic deep soundings, Prof. Kacper Rybicki (2004–2008), a geophysicist, planetologist, astrophysicist, best known for his works on the mechanics of earthquake faulting and later on the evolution of the Earth and solar system in the far future (Rowiński 2008) and Prof. Paweł Rowiński (from 2008), a specialist in environmental hydrodynamics, known for his studies on heat and mass transport in rivers. One should also note the consecutive Presidents of the Scientific Council of the Institute Professors Julian Lambor, Stefan Piotrowski, Tadeusz Olczak, Teodor Kopcewicz, Roman Ney, Stanisław Małoszewski, Roman Teisseyre, Jerzy Jankowski and currently is Stanisław Lasocki. The deputy directors for science were the following professors: Edward Stenz, Romuald Wielądek, Roman Teisseyre, Aniela Dziewulska-Łosiowa, Sławomir Gibowicz, Jerzy Jankowski, Roman Teisseyre, Kacper Rybicki, Janusz Niewiadomski, Marek Lewandowski, Paweł Rowiński, Wojciech Dębski and at present this duty fulfils Beata Orlecka-Sikora. There are plenty of other people that influenced not only the development of the Institute but also the entire field of Earth Sciences and it is beyond the scope of this chapter to even mention their role. Some interesting information about the people who were crucial for the Institute throughout its history may be found in (Jankowski and Teisseyre 1991). In this chapter let us only remind those employees who at some point, not necessarily working at IGF were conferred the title of full professor either by President of Poland or formerly by the so-called Chairman of the State. Only those who have not been mentioned above are listed herein: Stanisław Szymborski, Józef Hordejuk, Sławomir Gibowicz, Andrzej Wernik, Stanisław Małoszewski, Jacek Leliwa-Kopystyński, Andrzej Hanyga, Krzysztof Haman, Andrzej Kijko, Magdalena Kądziałko-Hofmokl, Maria Teisseyre-Jeleńska, Janusz Pempkowiak, Jerzy Dera, Witold Strupczewski, Zygmunt Klusek, Jarosław Napiórkowski, Renata Romanowicz, Janusz Borkowski, Janusz Krzyścin, Henryk Mitosek and Stanisław Rudowski.

Recently, the Institute has undergone profound organisational changes. Its structure was designed to enable it to function effectively in the dynamically changing conditions of the current Polish scientific environment and to be ready to meet difficult challenges, including the coordination of large international projects. The Institute has withdrawn from the creation of permanent laboratories in favour of appointing project teams. Currently, the Institute consists of the following

thematic departments: the Department of Seismology and Physics of the Earth's Interior, the Department of Lithospheric Research, the Department of Magnetism, the Department of Polar Research, the Department of Hydrology and Hydrodynamics, and the Department of Physics of the Atmosphere. The Department of Theoretical Geophysics is under construction and will formally start its activities in a few months. The Institute also has a standalone division dealing with geo-physical monitoring, which serves the needs of different State institutions.

2 The Genesis of the Institute of Geophysics PAS

The Institute of Geophysics of the Polish Academy of Sciences (originally bearing the name the Department of Geophysics) was established by a resolution of the Presiding Board of the Polish Academy of Sciences on 18 December 1952 (Jankowski and Teisseyre 2004). It was based on three geophysical observatories: the Magnetic Observatory in Świdra, the Seismic Station in Warszawa and the Silesian Geophysical Station in Racibórz. It was one of the first institutions established by the Polish Academy of Sciences. The Institute became the natural successor to the glorious tradition of geophysical research in Poland. It is worth mentioning in this context that the pioneer in the field of geophysics in Poland was Prof. Maurycy Pius Rudzki, who in 1898 created the world's first Department of Geophysics at the Jagiellonian University in Kraków (Kowalcuk 2001). Despite such a significant and spectacular event, there were few geophysicists in Poland in the first half of the twentieth century. Most of them dealt with applied research, mainly in the fields of meteorology and hydrology, as well as the search for resources using geophysical methods. Therefore, the task of creating the foundations of Polish geophysics was carried out in the context of huge staff shortages. The research conducted in the Department was limited to seismology, geomagnetism and a strongly reduced level of atmospheric physics.

The statutory tasks of the Department of Geophysics of the Polish Academy of Sciences included, apart from purely research activities, the modernisation and extension of the continuous geophysical observations in Poland, as well as the inclusion of its observatories in the world measurement network that was being created at that time. It was at that point that the seismic station in Kraków was launched, the destroyed observatory in Hel was rebuilt, and the Marine Station of the Polish Academy of Sciences in Sopot was incorporated into the Department.

The governmental decision issued in 1955 to join on the organisation of the International Geophysical Year in 1957–1958 was not without significance for the development of Polish geophysics. The occasion brought additional grants and funds for research, the purchase of modern equipment and trips abroad, which contributed to the further extremely rapid development of this branch of science in our country. The two geophysical expeditions—to Vietnam and to Spitsbergen—proved particularly successful. The research undertaken during these expeditions contributed to the strengthening and consolidation of the geophysical staff and

expanded the Department's circle of research. The Department also launched the Central Geophysical Observatory in Belsk near Grójec, rebuilt the observatory on the Hel peninsula which had been destroyed during the war, and created the Department of Satellite Geodesy, which undertook activities in the field of satellite research, the rotation and shape of the Earth.

Another pioneering change in the activities of the Department was directly related to the person of Prof. Stefan Manczarski, who became the Director of the Department after Prof. Tadeusz Olczak. This very interesting man, a prominent specialist in the field of radio wave propagation and ionospheric studies, demonstrated huge initiative and, based on his technical education, organised the Department of Geophysical Equipment Construction within the Department of Geophysics. This was important because, with the large number of observatories, funds did not allow for the purchase of sufficient equipment. Since then, the Department of Geophysics has used mainly instruments of its own design.

During this period, the research area of the Department was specified in detail. It included particular research on mining seismology, deep geomagnetic soundings and the application of the methods of explosion seismology to deep lithospheric research. At this time, several theoretical works appeared on the application of the methods of continuum mechanics to seismology. The Department started to organise its paleomagnetic laboratory and initiated research on ionospheric inhomogeneities. The Marine Station in Sopot was transformed into the Department of Oceanography, which focused on the dynamics, chemistry and physics of the sea. This rapid development was not limited to the realm of research. In 1967, the Department of Geophysics acquired the right to confer the degree of doctor of physical sciences as the main basis for the entire environment associated with basic research in geophysics. In 1972, this success resulted in the establishment of four-year doctoral studies courses, which, with occasional short breaks, have been training young scientists up until now.

The growing importance of the achievements and activities of the Department of Geophysics led to its transformation in 1970 into the Institute of Geophysics of the Polish Academy of Sciences. At that time, Prof. Stefan Manczarski left the Institute and the position of Director was assumed by Prof. Roman Teisseyre, who after two years passed it to Prof. Jerzy Jankowski, remaining himself as the deputy director for research. Prof. Roman Teisseyre still works at the Institute, Prof. Jerzy Jankowski just recently (in 2011) retired and they both are the pride of the Institute in the country and far beyond its borders. This was also the management team that has led the Institute for the longest time in its history. New departments were created, including the Department of Oceanology and Satellite Geodesy and the Experimental Department GEOPAN, which was involved in the creation of geophysical equipment for external orders. The Institute also established the Hydrological Systems Laboratory, and in 1979, the Department of Polar Research, which included the geophysical station in Hornsund which conducts year-round geophysical observations. Another seismological observatory was opened in Ojców, which replaced the prototype in Kraków

and the auxiliary station in Niedzica. The research of the Department of Oceanography gained such momentum that it was transformed into an independent Institute of the Polish Academy of Sciences, and the Department of Satellite Geodesy was incorporated into the newly created Space Research Centre PAS.

The 1980s represented a revolution in geophysical research methods, driven by the introduction of computers, and thus the digitisation of registration, methods of analysis of time series in observatories and field studies. The numerical methods of one- and two-dimensional modelling and inversion algorithms were applied to interpret data.

Another advancement was the acquisition of the right to confer the degree of doctor habilitated, which benefited employees of the Institute and geophysicists from various research centres and universities in the country.

It is worth noting that, since its creation, the Department of Geophysics has not had one permanent home. Over the years, it has used various locations provided by the Academy. At one point, the Institute's laboratories were located in seven different locations in Warszawa, which made its management and research activities extremely difficult. It was only in the 1980s that the Institute gained its own building on Księcia Janusza Street in Warszawa, where it has been located until the present day.

With the political changes in the early 1990s, new opportunities opened up for the Institute, particularly regarding the access to the latest equipment and scientific contacts with the leading geophysical centres of the world. In addition, the rules for financing institutes of the Polish Academy of Sciences were changed. The State Committee for Scientific Research was established, which was the nucleus of the current Ministry of Science and Higher Education. The Research Committee completely took over the supervision of activities and control of grants to the institutes from the state budget.

The Institute of Geophysics continued to grow vigorously. It created two new seismic stations, in Suwałki and Kalwaria Paławska. All the observatories were modernised. Digital recording was introduced, along with the online transmission of data to global networks. It is worth mentioning that, almost from its inception, the Institute has carried out publishing activities. Since 1953, it has published the *Acta Geophysica* quarterly journal (until 2006 published under the name of *Acta Geophysica Polonica*), which has achieved a very high international standing.

3 Commitment to Build for Scientific Leadership

IGF PAS fosters excellence in research within the lithosphere, atmosphere, hydrology and polar sciences. Further we mention just a few, selected achievements that favour the Institute among other institutions dealing with Earth sciences. For more details we refer the reader to other comprehensive chapters of this volume focusing on particular branches of investigations.

3.1 Geophysical Investigations of the Lithosphere

The dynamics of the processes taking place within the Earth and issues related to seismology—both global and caused by mining activities—have been the core of the Institute's research almost since the inception of the Institute of Geophysics PAS (formerly the Department of Geophysics). Currently, research in this area is carried out by the Department of Seismology and Physics of the Earth's Interior. A number of theoretical results have been achieved in this field concerning the physics of earthquakes and the processes taking place in the crust before earthquakes, where the evolution of a stress field leads to the release of internal energy accumulated primarily as a result of the movement of lithospheric plates. As achievements in this field, we can mention the development of the dislocation theory of earthquakes, the theory of stress evolution and the process of dynamic decompression in mediums with a dense distribution of defects, the theory of earthquake precursors, as well as earthquake thermodynamics and laminar shear rupture. The Department has carried out the physical interpretation of seismic source parameters, such as seismic energy and seismic moment, and the statistical relationship between the two (thermodynamics of the seismic source), based on both observations and theoretical models, for different types of earthquake, including tectonic phenomena and mine-induced seismicity.

The Department has developed a kinetic model of evolution (i.e., nucleation, propagation and coalescence) of cracks during the rupture process in the earthquake source and the reasons for the emergence of reverse-power distributions in many geophysical phenomena through the ‘privilege’ mechanism, which includes and unifies the various reasons for these distributions previously reported in the literature.

Also of particular note are the Institute's studies of mining tremors. It was on the initiative of the Institute that the world's first underground network of seismic stations was created in 1964 in the Miechowice mine. Mines experience two types of seismic events: those directly related to mining work and those induced by movements over geological discontinuities in the rock mass: it was only at the Institute that these were shown to have different natures.

Since its inception, the Institute has also carried out research in the field of geomagnetism. One of the greatest achievements of the team of magneticians has been the discovery and interpretation of two large anomalies in conductivity distribution in Poland. The first is related to the Polish basin, and the other to the Carpathian Mountains. Both of those anomalies are among the largest in Europe and are well known in the global literature. During their mapping and interpretation, the Institute cooperated with scientists from the Czech Republic, Slovakia, Ukraine, Russia, Germany and Sweden. The quantitative interpretation of the geophysical data indicates that the bottom of the basins consists of highly conductive rocks, probably porous rocks filled with mineralised water.

Another important result is the development of a number of methods for the design and interpretation of data for magnetotelluric and geomagnetic soundings.

These include the method for calculating the transfer function in the time domain, inversion algorithms for flat and spherical earth models, inversion algorithms for two-dimensional structures and a magnetic tensor reconstruction method based on the so-called tippers. The sets of programmes that have been thus developed have been used not only for the Institute's own work, but also by foreign teams.

Using the methodology developed by the magneticians, a global (average) model of electrical conductivity in the Earth's mantle has been constructed, demonstrating the existence of a well-conductive layer in the middle mantle (650–800 km). The Institute has also developed a number of regional models documenting horizontal heterogeneities in the construction of the mantle and pointing to a fairly good correlation of the deep mantle structure with the identified tectonic units. This highly original issue has been explored by relatively few research centres around the world.

The three geomagnetic observatories—in Belsk, Hel, and Hornsund—belong to the best reference centres in the world. A number of devices for measuring the Earth's magnetic field have been constructed. Two of these, the PSM station (vector magnetometer) and the proton magnetometer, have very good technical parameters and have gained recognition in other countries, including Finland, Spain, Slovakia and Ukraine. In recent years, a marine magnetometer has also been built, which is used for measuring the magnetic field at the bottom of the sea. Also noteworthy are the global achievements of the Paleomagnetism Team, operating within the Department of Magnetism. This has specified the path of the apparent polar wandering (APWP) in the Sudetes for the Upper Palaeozoic. The results of this research on paleomagnetism and magnetic properties have been used to answer tectonic issues.

The position of Baltica at the turn of Precambrian/Cambrian has been established, as well as the Jurassic position of the pole from the Kraków-Częstochowa Jurassic Highland, which has been placed in the reference databases. Field inversion has been observed in the Jurassic highland in Poland and Bulgaria. Paleomagnetic results regarding the Carpathians have been used to explain the oroclinal bend of the Carpathian chain and to determine the position of the Pieniny sedimentary basins in the Jurassic period.

Periodic changes have been identified in the paleomagnetic record of varved clays (studies of Quaternary sediments loess, varved clay and Holocene sediments of the lakes of northern Poland). The positions of the structural units of Spitsbergen have been determined in relation to other continents in the Palaeozoic.

The Paleomagnetic Laboratory has achieved a strong international position, as evidenced by the numerous visits of foreign scientists and the best laboratory equipment in Europe.

The pride of the Institute is its research on the deep structure of the lithosphere of the Earth, using the methods of explosion seismology. In the current organisational structure, research in this field is conducted by the Department of Lithospheric Research (previously a part of the Department of Seismology, and later the Independent Deep Structures Laboratory). This subject has formed an important part of the Institute's research since the 1960s. It was the first research of

this type performed in Poland and one of the first in Europe. The systematic work has allowed for the identification of the main tectonophysical properties of the lithosphere on Polish territory. Already in the 1960s, it had been established beyond reasonable doubt that the so-called Teisseyre-Tornquist line, determined in the early twentieth century by geologists, is not a line, but a 60–80 km wide zone with a highly anomalous structure and physical properties of the Earth's lower crust, reaching a depth of 50 km. This zone, extending from north-western Poland towards the south east, is of continental range and rank.

In 1997–2003, in cooperation with 35 research and industrial institutions from 15 European countries and the United States and Canada, the Institute participated in a large research programme on the deep structures of the Earth's lithosphere in Central Europe, using seismic methods, which are the basis of modern geophysics. These were the seismic experiments commonly known as international projects: POLONAISE'97, CELEBRATION 2000, ALP 2002, SUDETES 2003 and GRUNDY 2003, initiated and coordinated by the Department of Lithospheric Research of the Institute of Geophysics PAS. All of the major geological structures of Central Europe between the Baltic and Adriatic Seas, with particular emphasis on the Polish territory, which is of crucial importance as regards the geodynamics of the European continent, were covered by a system of cutting-edge seismic profiles with a total length of around 20,000 km. In its publication entitled *MAGIC UNIVERSE, Oxford Guide to Modern Science* (2003), Oxford University Press included the CELEBRATION 2000 seismic experiment carried out in Central and Eastern Europe across an area of approximately 500,000 km² with and the use of 1,350 cutting-edge seismic stations, in the class of experiments that have brought science into the twenty-first century. In the opinion of the international scientific community, the area of Central Europe under investigation is the region with the currently best-explored deep structure of the Earth's crust and lower lithosphere to a depth of 100 km. The results achieved, sharing the rank of a discovery, formed the basis for a new geophysical and geological interpretation of the deep structures of the lithosphere, which is of fundamental importance for basic and applied research related to prospecting for hydrocarbons.

Since 1976, the Department has carried out systematic research on the deep structure of the lithosphere using experimental seismology methods in the area of the Svalbard Archipelago in the Arctic and in West Antarctica. This research has been carried out within the framework of broad international cooperation on programmes of international importance. In 1976–2008, the Institute of Geophysics of the Polish Academy of Sciences organised a total of six geodynamic expeditions to the Arctic in collaboration with academic institutions from Norway, Germany, Japan and the US. In 1979–2008, it organised five expeditions to West Antarctica. The result of these expeditions was the exact determination of the tectonophysical properties of the lithosphere up to a depth of 50 km in areas of key importance for the geodynamics of the Earth.

3.2 Geophysical Investigations of the Atmosphere

The activities of the Department of Physics of the Atmosphere have always been aimed at solving fundamental research issues in the field of physics of the atmosphere associated with the assessment of the impact of natural factors and human activities on atmospheric processes and the evaluation of risk to the environment. In the last few decades, changes in the amount and spatial distribution of ozone in the atmosphere have become a serious problem on a global scale. They have raised considerable concern among scientists and the public. Measurements of total ozone in the atmosphere and its vertical distribution by the Umkehr method have been conducted at the Central Geophysical Observatory of the Institute of Geophysics PAS in Belsk continuously since 1963. Currently, only five stations in the world have carried out systematic measurements of the ozone profile for decades (up to about 50 km from the Earth's surface). The Institute's work on the methodology of measurement and careful revaluation of the measurement results have meant that the long-term series of measurements have been recognised as one of the most reliable data sets by the international community of scholars studying the ozone layer. The measurement data from Belsk have been used, among others, for the revalorisation of satellite measurements, as well as in many designs and statistical models. In particular, the theoretical work of the Department has established current opinion about the 'recovery' of the ozone layer since the mid-1990s in some areas of the globe.

Interest in UV radiation reaching the Earth's surface arose in the 1980s and 1990s, along with the discovery of significant losses in the ozone layer enveloping the Earth and protecting it from harmful UV-B radiation. Measurements of UV radiation have been conducted at the Central Geophysical Observatory of the Institute of Geophysics in Belsk since 1975, with the use of different gauges. In recent years, the UV measurement series from Belsk has been standardised, and at the moment it is the longest UV measurement series in the world. Statistical analysis has revealed that the current level of UV radiation is about 15 % higher than that in the 1970s, which may have serious health implications. The UV series from Belsk has confirmed the quality of data on the global distribution of UV radiation since 1979, having been obtained from the models defining daily doses of UV radiation from satellite measurements of ozone and cloud cover, which has enabled the evaluation of trends and the severity of excessive UV radiation risk in areas where no terrestrial measurements are carried out.

The study of the factors responsible for changes in UV radiation reaching the Earth's surface with the use of comprehensive measurements of atmosphere parameters in Belsk (ozone, aerosol and cloud parameters) has pointed to a significant and previously unknown specific effect of aerosols on the intensity of UV radiation. Daily monitoring of aerosol properties has become a necessity. Measurement in the field of atmospheric optics with standard instruments used in weather stations has evolved into a study of the optical properties of atmospheric aerosol with the use of remote sensing techniques (LIDAR, sun photometers) and in situ techniques (aerosol

spectrometers). The comprehensive aerosol observation system has worked well in the monitoring of extreme phenomena, such as the movement of an aerosol cloud over the Polish area associated with the burning of biomass, desert sand and volcanic eruptions (Pinatubo in 1991 and Eyjafjoell in 2010).

Continuous measurement of parameters of atmospheric electricity such as electric field strength, positive and negative electrical conductivity of the air and ionosphere-Earth current density have been conducted at the observatory in Świder since 1958. Along with complex meteorological measurements, measurements of gaseous, aerosol and radioactive air pollutants constitute a unique database used mainly in studies on the global electrical circuit, air pollution and changes in climate.

The Polish Polar Station in Hornsund has been carrying out measurements of electric field strength since 1986, and currently it periodically conducts measurements of Maxwell current density and light ion concentration. On the basis of these measurements and additional magneto-helio-geophysical data, the couplings between the solar wind, magnetosphere, ionosphere and the lower atmosphere are analysed.

Simultaneous analysis of electrical parameters in mid-latitudes (Świder) and in the polar regions (Hornsund) allows us to analyse the propagation of magnetospheric effects. Research on storm electricity in Warszawa has been conducted by the Department of Atmospheric Physics since the 1970s.

Recently, the Department has attained a number of spectacular successes in the field of the boundary-layer meteorology (in the air layer directly above earth's surface), pertaining especially to large-eddy simulations and similarity theory analyses.

3.3 Geophysical Investigations of the Hydrosphere

The research on the aquatic environment at the Institute of Geophysics of the Polish Academy of Sciences is currently carried out by the Department of Hydrology and Hydrodynamics (formerly the Department of Water Resources). The history of hydrological studies at the Institute began in 1974, when a new unit, the Hydrological Systems Laboratory, was established. The laboratory undertook work on improving the methods of modern dynamic hydrology, including elements of hydrology, hydrodynamics and systems theory. The laboratory collaborated with renowned international research centres, in particular with University College Dublin and the University of Karlsruhe.

In particular, in the late 1970s and 1980s, the laboratory carried out works on linearised hydrodynamic models of river flow and their adjustment in practice. It analysed the inter-relationships between conceptual linear and non-linear models and simplified hydrodynamic models, and within this part of hydrology was at the forefront of the investigations at the international scale.

In the early 1980s, the laboratory underwent many changes, both personal and structural. Research subject areas were expanded into issues related to the stochastic structure of hydrological processes. In 1982, the Institute of Geophysics established the Department of Water Resources. From then on, the activity of the Department of Water Resources focused on the aspects of quality and quantity of water resources, the evolution of their structure due to economic activity and the control of water resources. The Department implemented a comprehensive programme of research assessing the impact of climate change on water resources in Poland. For this purpose, potential climate change scenarios in particular areas were developed and assessment of the state of water resources carried out. The CLIRUN programme for the assessment of water balance developed by the Department was recommended by the US Team Country Study for use in more than fifty countries of the world. The Department also proposed methods for the adaptation of water management to observed changes in climate.

In 2003–2005, the Department coordinated a spectacular project funded by the US Agency of International Development, the US-Poland Technology Transfer Project, in the field of numerical methods for the sustainable development of Polish water resources. The project was implemented in cooperation with the US National Centre for Computational Hydroscience and Engineering, Oxford (Mississippi).

An important part of the work carried out in the Department is dedicated to issues related to the hydrodynamics of river flows. Understanding the turbulence structure in flowing surface waters has been the subject of a number of national and international projects, both experimental and theoretical. The Department has focused its attention on situations that ‘escape’ traditional approaches due to the unsteadiness of the flow (caused, for example, by movement of a flood wave) or the geometrical complexity of the channel under consideration and presence of vegetation in the flow. In this regard, the Institute has achieved pioneering results, published in the world’s leading specialist journals.

The study of transport processes in rivers has undoubtedly made an important contribution to the international scientific knowledge. The Institute has developed a number of mathematical models describing the processes of mixing and transport of pollutants and sediment in rivers. In 2006, the Department carried out the world’s largest (in terms of time scale, space and number of test sections) tracer study in collaboration with the University of Warwick (United Kingdom). Before that, the Department carried out the first tracer study in a multi-channel river reach.

In addition, the Department has been developing the components of a decision support system for the control of flood waves within systems of storage reservoirs on various rivers. The Department has also created a number of models defining numerical precipitation forecasts, transforming the rainfall into runoff, the models describing the functioning of systems of storage reservoirs, or the models of transformation of flood waves in the river channels. It has also developed the optimisation techniques for the performance of the entire system of reservoirs, ensuring minimisation of the maximum flow in the selected sites.

The Department's research on statistical hydrology also enjoys great international esteem. The Department has virtually created the foundations of this field of science. At present, emphasis is placed on the development of statistical techniques applied to the modelling of extreme events (floods, droughts). Recently, the Department has been exploring the so-called bi-seasonal approach to the assessment of the probable maximum annual flow and evaluating the usefulness of this approach for different hydrological regimes of Polish rivers. It has formulated the foundations for an objective comparison of the accuracy of this approach with the traditional approach based on annual maxima.

The research carried out in the Department, in addition to its large cognitive significance, is of considerable utilitarian importance. The Department carries out environmental impact assessments of planned hydro-technical facilities, prepares expert opinions for local authorities, and develops cooperation with national and international NGOs.

3.4 Polar Research

The Polish Polar Station on Spitsbergen is a particularly interesting place in which to conduct research. Since its establishment in 1957, it has belonged to the Institute of Geophysics of the Polish Academy of Sciences. Due to its location, it is a modern platform for scientific research both in the country and abroad. The Department of Polar Research was established in 1977 as a result of the development of the polar and marine research programme in the Arctic and Antarctic.

The main task of the Department was originally to organise expeditions to the Polish Polar Station, Hornsund, and control its operation. The Department was also responsible for the logistical preparation and protection of marine geophysical expeditions to the Arctic and Antarctic organised in 1978–1988. During this period, the Department developed, in particular, the acoustic and sedimentological studies conducted in the basins revealed by retreating glaciers, their forefields and fjords. Also extensive seismological research of glaciers was carried out.

As the Department was involved in programmes monitoring geophysical fields in the Hornsund Station on Spitsbergen and Henryk Arctowski Station in the Antarctic, it also processed the findings of those observations, which were published in special magnetic and seismic annual reports.

In 1997, the Department began to change its academic profile towards the study of dynamic changes in the abiotic characteristics of the natural environment in polar zones and in reference regions, also towards the use and development of new geophysical methods in polar research and comparative studies in the areas of Pleistocene glaciation in Poland.

After 2000, there was a significant expansion of cooperation and academic exchange with foreign countries. Among other projects, an agreement was concluded between the Polish and the Russian Academy of Sciences for the studies of the dynamics of glaciers and snow cover in the Arctic and in the mountainous

regions of Russia. The Department also cooperated with the Finnish Academy of Sciences. It soon began to exchange data obtained from the monitoring carried out at the Hornsund Station on Spitsbergen with 15 other scientific institutions in Europe.

In 2001, the Department prepared the concept and technical assumptions of the modernisation of the Hornsund Station and the full implementation of the investment process took place in 2002–2008. As a result of these actions, the Hornsund Station has been recognised as a leading modern European platform for research in Svalbard. A breakthrough for the Department and the Station was the launch of a communications satellite with online data transmission to the international databases and data centres, WMO, IMAGE, INTERMAGNET, AE-RONET, and NORSAR. It is worth emphasising the fact that the Department has participated as a partner in the following Framework Programmes of the European Union: GISICE—(FP5), EUROPOLAR—(FP6), ICE2SEA and SIOS—(FP7), and SVAL-GLAC (European Science Foundation).

As part of preparations for the Fourth International Polar Year (IPY 2007–2008), the Department coordinated the activities of the commissioned project aimed at investigating the structure, evolution and dynamics of the lithosphere, cryosphere and biosphere in the European sector of the Arctic and Antarctic, which brought together the whole Polish polar research community. This resulted in active participation in the Fourth IPY 2007–2009, which was a great success. The Department has been a major partner in three international projects (GLACIODYN, TOPOCLIM, and POLARCAT) carried out in the Arctic (Svalbard) and in the Antarctic (South Shetland Islands). The Department also coordinated the KINNVIKA project implemented on the North East Land.

Major research achievements of the Department in recent years include the discovery and documentation of the existence of a subglacial lake under the 650 m Amundsenisen Icefield on Spitsbergen. The result of several years of research by an international team of glaciologists and geophysicists may in the coming years be crowned with core drilling and the sampling of ice and water, which will be of great importance for climate scientists and biologists.

Another important scientific achievement is the result of the use of the latest measurement and geophysical methods in the study of the dynamics of glaciers. Unique comprehensive studies related to the mechanisms governing the dynamics of glaciers have given rise to the creation of the so-called “Polish glaciological school”. This results in young scientists staying at the Hornsund Polish Polar Station and the cooperation of national and international partners in the implementation and testing of modern equipment for the study of the polar regions, and the correlation of their results with satellite data. The Hansbreen Glacier, monitored by the staff of the Department, is one of the best-known glaciers in the international World Glacier Monitoring Service network.

In 2008, the Department was entrusted by the Ministry of Science and Higher Education with the coordination of the Research Network “Multidisciplinary research on the geobiosystem of the polar regions”, which associates 7 institutes of the Polish Academy of Sciences and 11 faculties of Polish universities. In 2010,

the Polish Polar Research Multidisciplinary Laboratory (PolarPOL) was included in the Polish Roadmap of Research Infrastructure. Both of those events demonstrate the leading position of the Department, not only within the Institute of Geophysics, but also among Polish scientific institutions.

Acknowledgments Our special thanks go to all colleagues who have prepared various materials throughout last few years, namely to Zbigniew Czechowski, Piotr Głowacki, Aleksander Guterch, Waldemar Jóźwiak, Janusz Krzyścin, Stanisław Lasocki, Jarosław Napiórkowski, Roman Teisseyre, and to the late Bożenna Gadomska.

References

- Dziembowska A, Wernik M (2014) Sixty years of publishing with the institute of geophysics, In: GeoPlanet: earth and planetary sciences: achievements, history and challenges in geophysics: 60th anniversary of the institute of geophysics, Polish Academy of Sciences, Warsaw
- Fedirko J (2011) Edward Stenz—geograf, wybitny badacz Afganistanu (Edward Stenz—geographer, outstanding explorer of Afghanistan), Prace Geograficzne. Instytut Geografii i Gospodarki Przestrzennej UJ Kraków 127:31–48
- Fiett J, Mangel K (2009) Konferencja naukowo-techniczna “Prof. Stefan Manczarski—świat elektromagnetyzmu” (Scientific-technical conference “Prof. Stefan Manczarski—the world of geomagnetism). Spektrum 11–12:13–15
- Goździk A (2013) Eduscience project – effective way of teaching natural sciences at Polish schools, In: Science education and guidance in schools: the way forward, Firenze, Oct 21–22
- Jankowski J, Teisseyre R (eds) (2004) 50 lat Instytutu Geofizyki PAN 1952–2003; Bibliografia 1994–2003 (50 years of the Institute of Geophysics PAS, 1952–2003; Bibliography 1994–2003, Publs Inst Geophys, Pol Acad Sc, M-26(348). Warsaw, p 210
- Jankowski J, Teisseyre R (1991) Niektóre fakty z historii instytutu, wspomnienia o ludziach z nim związanych (Some facts from the Institute's history), Publications of the Institute of Geophysics, Polish Academy of Sciences, M-14 (232), Warsaw, pp 203–212
- Kowalcuk J (2001) 100-lecie Geofizyki Polskiej 1895–1995, Kalendarium (100 Years of Polish Geophysics, 1895–1995, Calendarium) 2nd edn, extended. ARBOR, Kraków
- Maj S, Guterch A (1990) Professor Tadeusz Olczak—a Polish geophysicist. Acta Geoph Pol 38(2):207–212
- Olczak T (1957) Edward Stenz. Rocznik Towarzystwa Geologicznego 26(4):349–352 (in Polish)
- Rowiński PM (2008) Kacper Mieczysław Rafał Rybicki a geophysicist, planetologist, astrophysicist. Acta Geophys 56(4):935–938
- Rowiński PM, Zdunek A (2011) Instytut Geofizyki Polskiej Akademii Nauk, Lider badania Ziemi wczoraj i dziś (Institute of Geophysics, Polish Academy of Sciences, leader of the Earth studies yesterday and today), Nauka Polska, jej potrzeby, organizacja i rozwój, XIX(XLIV), Rocznik Kasji im. Józefa Mianowskiego, Fundacja Popierania Nauki, 195–216

On the Roots of the Institute of Geophysics, Polish Academy of Sciences

Sławomir Maj and Krzysztof P. Teisseyre

Abstract The Institute of Geophysics, Polish Academy of Sciences, established in 1952, continues the long tradition of geophysical research done by the Poles in the past. The ample history of geophysical sciences, predominantly associated with academic centers in Kraków (Cracow), Lwów (Lviv), Warszawa (Warsaw), and also Wilno (Vilnius) and Poznań, is briefly outlined. The world's first Chair of Geophysics was established at the Jagiellonian University in Kraków in 1895 by Prof. Maurycy P. Rudzki. Various geophysical observatories and stations are mentioned, some of them having roots in the 19th century.

Keywords Geophysics · Geophysical observatories · Seismological observations · Geomagnetic measurements

1 Geophysics Amidst the Earth Sciences

The most general definition of geophysics is that it is a major branch of the Earth Sciences that applies the principles and methods of physics to the study of the Earth. Geophysics is a highly interdisciplinary subject and geophysicists contribute to every area of the Earth Sciences.

The very term *geophysics* was initially referred predominantly to the solid Earth study, quite often interchanged with geology. Presently, modern geophysical organizations use a broader definition that includes the atmospheric physics, hydrology, fluid dynamics, solar-terrestrial relations, and analogous problems associated with the Moon and other planets. Strongly interrelated with geophysics are many other disciplines, to mention only: space physics, geodesy, physical

S. Maj · K. P. Teisseyre (✉)

Institute of Geophysics, Polish Academy of Sciences, Księcia Janusza 64,
01-452 Warszawa, Poland
e-mail: kt@igf.edu.pl

geography, geomorphology, climatology, oceanology, polar research, ecology, glaciology, as well as astronomy and physics.

As concerns the Institute of Geophysics PAS, its main research topics have been evolving over the years. Here we will focus on some historical facts relevant to the research done there in the 1950s. We made use of the comprehensive treatise by Olpińska-Warzechowa (1995) and the book by Jerzy Kowalcuk (2001), as well as other publications: Olczak (1958), (1991), Mikulski (1991), Kowalcuk (2009), Dormus (2011), Hanik (1986), Maj (2003a, b), Michalski and Małkowska (1947).

2 Early Years of Polish Geophysics

Roots of geophysics in Poland, as systematically practiced science, may be sought in the 19th century, in the time when our state was absent from maps. It sprouted, under various names, in Cracow (Kraków in Polish) and its surroundings where meteorological, magnetic and other physical observations were conducted, partly in the framework of the Astronomical Observatory. This Observatory, together with its meteorological station, started to work at the dusk of former free Poland, in 1792. Both astronomical and meteorological observations were initially led by Prof. Jan Śniadecki (1756–1830). In 19th century, connection of Polish research with world's science was facilitated by the fact that south-eastern part of Poland was then ruled by the Austrian Empire.

In the years 1839–1885, a small magnetic observatory created by Austrian scientist Maximilian Weisse (1798–1863) was in operation in Cracow; it was the first on Polish lands. Like the Astronomical Observatory, also this small facility belonged to the Jagiellonian University. Scientists tended to be comprehensive in those times. Ludwik Antoni Birkenmajer (1855–1929), one of many Cracovian erudits, was not only a physicist, astronomer and historian of science, but also a geophysicist, deeply involved in gravimetric research. His habilitation treatise in 1881 was devoted to the Earth's shape and structure.

Taking things formally, geophysics as a separate science emerged in Poland on October 1, 1895, when at the Jagiellonian University in Cracow, at the Faculty of Philosophy, the Chair of Mathematical Geophysics and Meteorology started functioning; it was headed by Prof. Maurycy Pius Rudzki (1862–1916), eminent Polish geophysicist, mathematician, geographer, astronomer, author of textbooks. **This was the first Chair of Geophysics in the world** (3 years later, in 1898, great German physicist Emil J. Wiechert (1861–1928) was nominated Professor of Geophysics at the University of Göttingen, bringing to life the first Institute of Geophysics—see Schweitzer 2003).

After some years, the newly established Chair was combined with the Chair of Astronomy and named the Chair of Astronomy and Geophysics. The main scientific and organizational achievements of Prof. Rudzki included the establishing

of a modern (as for those times) Seismological Observatory, and reactivation of measurements of the Earth magnetic field components; he was also supervising meteorological stations in Zakopane.

At the same time (1895) in Lwów (Lviv, now: Lviv in the Ukraine), the Chair of Higher Geodesy and Spherical Astronomy at the Polytechnical School (from 1920—the Lvov Polytechnic) was offered to Prof. Václav Láska (1862–1943), prominent Czech geodesist, astronomer, geophysicist and mathematician, with versatile scientific interests. He worked there until 1911 dealing, beside geodesy and astronomy, also with mathematical geography, hydrology, meteorology and the space physics. In the framework of geophysics, he was mainly interested in seismology (earthquakes). In 1899, Prof. Láska organized at the Polytechnical School the first seismological station on Polish lands, equipped with two horizontal Bosch-Omori seismographs (see, e.g., Berezowski 1972).

The Lvov Polytechnic was also the institution with which Prof. Wawrzyniec (Laurentius) Teisseyre (1860–1939), eminent Polish scientist of French ancestry, has been associated over most of his scientific life (see, e.g., Teisseyre 1998). His name is widely present on geological maps of Europe for his discovery of the central part of an important tectonic line cutting Europe from NW in Denmark to SE, towards the Black Sea. He introduced the term “cryptotectonique,” meaning “buried tectonics.” In recent times, his achievements have been recollected, e.g., in EOS Transactions (Teisseyre and Teisseyre 2002; the first author is his grandson). Wawrzyniec Teisseyre first described his discovery in 1893, and in 1903 he published a relevant map. His results have been corroborated in 1908 by Swedish magnetologist A. J. H. Törnquist (1868–1944), who studied the areas NW of the Teisseyre line. The whole system, originally named the Teisseyre-Tornquist (or Tornquist-Teisseyre) line/zone and presently known as the Trans European Suture Zone (TESZ) is still extensively studied with many geophysical techniques, mainly the deep seismic sounding methods, in which the Institute of Geophysics PAS has been deeply involved for years (see other chapters of this issue; also Korja 2007).

In Cracow, at the Jagiellonian University, the second Polish seismological observatory was established in 1901, in the cellar of Astronomical Observatory (in the same cellar, gravimetric measurements were sporadically made, interfering with seismic observations). In 1903, Prof. Rudzki managed to equip this station with two horizontal seismographs of Bosch-Omori type. The recording was made on smoked paper (e.g. Mazur 1993).

From the early 20th century, in the Polish lands annexed to Russia—called the Congress Kingdom—physicist and geophysicist Stanisław Kalinowski (1873–1946), under the auspices of the Museum of Industry and Agriculture, started preparations for implementing systematic measurements of the Earth magnetic field components and establishing a magnetic observatory at Świder near Warsaw. In this way, Prof. Kalinowski has incorporated Poland into international campaign on producing magnetic maps of our planet, initiated by the Carnegie Institution in Washington. The design of the Świder Observatory was similar to that of the Magnetic Observatory in Potsdam. The construction works started in

1910 and were completed in rather unusual, war-time circumstances in 1915. The Observatory began regular observations in 1921. The basic magnetic map of Polish Republic has been compiled through the years 1923–1930. In 1928 the Magnetic Observatory was renamed as the Geophysical Observatory, since its scope has widened by including the atmospheric electricity observations (see, e.g., Ołpińska-Warzechowa 1985). Nowadays, atmospheric electricity has become the main domain of research done there, since magnetic measurements had to be terminated because of interfering noise produced by electric railroad (more details in Jóźwiak et al. 2014; this issue). Now the Observatory (housing also a museum of old magnetic instruments, see Fig. 1) bears the name of Prof. Stanisław Kalinowski.

The outbreak of the First World War on 28 July 1914 disorganized the scientific life in the area. In Cracow, this was soon followed by the death of Prof. Rudzki. His Chair was taken over by the well-known physicist Marian Smoluchowski (1872–1917), for a short time unfortunately. Later it was headed by Władysław Dziewulski (1878–1962), notable astronomer. Subsequently, in 1919, the Chair of Astronomy and Geophysics became just the Chair of Astronomy, led by Prof. Tadeusz Banachiewicz (1882–1954), eminent astronomer, geodesist and mathematician. Certain research in the domain of geophysics, e.g. in gravimetry, was conducted there, but the Cracow seismological station declined because of technical problems. It restored full functioning in 1927 (after 6 year break). When Prof. Rudzki passed away, seismological reports from Cracow ceased to be published till 1955.

After the First World War, in reborn Poland, two academic centres for geophysics have been established. These were: (i) the Institute of Geophysics and Meteorology at the Jan Kazimierz University in Lwów, headed by Prof. Henryk Arctowski (1871–1958), prominent Polish geophysicist, geochemist and polar explorer, and (ii) the Free Polish University (Wolna Wszechnica Polska) acting in 1918–1952 in Warsaw, where, in the framework of the Faculty of Mathematics and Natural Sciences, geophysics was extensively taught and studied under the guidance of Prof. Stanisław Kalinowski, initiator and director of the previously mentioned Magnetic Observatory at Świdra (see, e.g., Maj 2013).

At the Jan Kazimierz University in Lwów, the scope of research included, among other things, the measurements of the geothermal gradient and the Earth magnetic field. In 1928, first geomagnetic measurements (of inclination) were performed near Lwów. The next comprehensive surveys were done in this region in the years 1929–1930. This was possible due to cooperation with the firm “Pionier” SA from Lwów, and governmental financial help. These measurements served both prospecting and purely scientific purposes. In June 1929, magnetic station in Daszawa near Stryj was erected, equipped with high-class instruments, including the Askania-Werke magnetograph. Daszawa station worked till 16 May 1931, when heavy storm and rain destroyed it. Next station, in Janów near Lwów, was operative in the years 1933–1939 (see, e.g., Ołpińska-Warzechowa 1988).

In Mikołów in Upper Silesia, the Society of The Experimental Mine “Barbara” built a magnetic station, which worked in the years 1925–1939. Magnetic declination was measured for the mine surveying purposes.



Fig. 1 Some of the modern instruments installed in the 1920s at the newly-built Świdra Observatory. *Top* The Kew magnetometer of the Cambridge Scient. Instr. Co. *Bottom* The Sartorius magnetometer for magnetic declination measurements. *Photos taken in the observatory museum by K. P. Teisseyre in 2006*

Some branches of geophysics, like meteorology and climatology, were also among the disciplines taught and studied at the Stefan Batory University in Wilno (presently the Vilnius University), Poznań University (founded in 1919; presently the Adam Mickiewicz University in Poznań), or in the Main Agricultural School (presently the Warsaw University of Life Sciences SGGW). The role of the Mining Academy in Cracow, instituted in 1919 (now the AGH University of Mining and Technology), was also significant.

Not surprisingly, elements of geophysics were included in the mainstream research of the State Meteorological Institute (PIM) and the State Geological Institute (PIG), both established in 1919. Besides, gravity force surveys in Poland were conducted by the Central Office of Measures (Główny Urząd Miar) in Warsaw (see, e.g., Olczak 1932, or Kwiatkowski 1937), and the geomagnetic measurements belonged to the sphere of interest of the Military Institute of Geography (known for issuing excellent maps). Since 1921, in the Free Town of Gdańsk operated the Marine Department of PIM, transferred in 1927 to the newly built city of Gdynia. In addition to typical oceanographic/meteorological studies, it provided meteorological and hydrographic service for marine administration of the Polish Republic.

On the initiative of the Marine Department of PIM, a Magnetic Station was erected on the Hel Peninsula. It was built in 1931 and opened on 1 August 1932. Many magnetic field measurements were done in the Polish coastal region from Gdynia to Karwia and from Gdynia to Hel—see, e.g., Czyszek and Czyszek (1984), Jóźwiak et al. (this issue). The Hel station had to terminate its activity in its original shape after the outbreak of the Second World War on 1 September 1939. The Germans seized the last Polish outpost, which happened to be the little town of Hel with surroundings, on 2 October. In recent times, an interesting story of three quartz horizontal magnetometers (QHM) from Hel has been presented, with optimistic end, by Voppel and Schulz (2002).

In 1930, Polish geophysicists established their first organization, the Society of Geophysicists in Warsaw (Towarzystwo Geofizyków w Warszawie), with Prof. Antoni B. Dobrowolski (1872–1954) as chairman. Plans for its activities, wide and deliberate, included the development of the geophysical research in Poland and international cooperation. This society strongly enhanced the position of geophysics among the earth sciences in our country (see, e.g., Mikulski 1984; Maj 2011). One of the effects was the creation of Seismological Observatory at the Józef Piłsudski University in Warsaw. Organization of this observatory started in 1935. The Observatory, headed by Dr. Irena Bóbr-Modrakowa (1889–1959), was located in a basement in one of main buildings of the University campus. It was equipped in seismometers of Golicyn-Wilip type, with galvanometric (photographic) registration. The Seismological Observatory in Warsaw started to record distant earthquakes in 1937, but official opening took place on 1 January 1939 (see also Jankowska 1986).

The Society of Geophysicists supported also the organization of Polish Polar Expedition during the Second International Polar Year 1932/1933. In this case, a



Fig. 2 The former Józef Piłsudski Astronomical-Meteorological Observatory on the Pop Ivan Mount in Czarnohora Mts. *Photo* by K. P. Teisseyre taken in 2010

leading role was played by the State Meteorological Institute (PIM) in Warsaw, directed then by Jean Lugeon (1898–1976), Swiss engineer and meteorologist. During this expedition, observations in the fields of meteorology, physics of atmosphere and geomagnetism were done; there was also a temporary magnetic station (see e.g., Lugeon 1933). The successful First Polish Polar Expedition (with wintering!) gave an impulse for organizing consecutive expeditions (which came to effect after the Second World War) (Gizejewski 2011).

Professor Jean Lugeon was promoting the construction of the High Mountain Meteorological Observatory on the summit of Kasprowy Wierch in Polish Tatra Mountains. This modern research center, constructed incredibly fast (in about 12 months), started functioning on 1 January 1938; its first director was Dr Edward Stenz (1897–1956), physicist and geophysicist.

The other noteworthy facility was the high-class Józef Piłsudski Astronomical-Meteorological Observatory on the top of Pop Ivan mount in the Czarnohora range in eastern Carpathians (now the Ukraine). It was built in the years 1936–1938 due to donations from the Polish paramilitary organization named Air and Anti-gas Defense League. It was intended to be part of Astronomical Observatory at Józef Piłsudski University in Warsaw; its director was Włodzimierz Midowicz (1907–1993), meteorologist and geographer. The seizure of this observatory (together with the whole eastern part of Poland) by the Soviet Union in 1939 marked the beginning of its devastation, which lasted through the war and much later (see Fig. 2) (Kreiner and Rymarowicz 1992). Since 2011, the building has

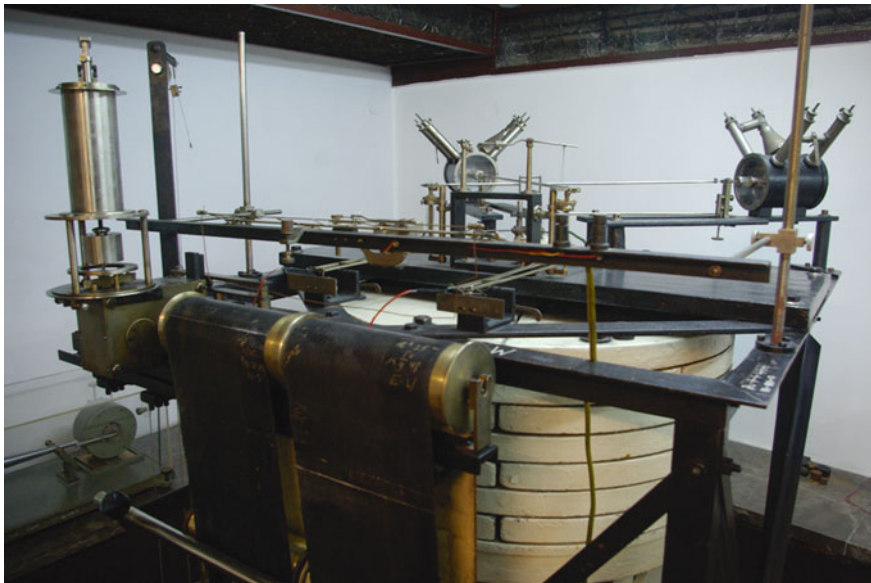


Fig. 3 The Wiechert horizontal seismograph, originally installed in Wrocław, then transported to the Racibórz Observatory. *Photo taken in the museum part of the seismological station at the Silesian Planetarium in Chorzów by K. P. Teisseyre in 2013*

been overhauled, with participation of Polish Republic. There are some plans to commercialize this building, strongly opposed by the defenders of wildlife nature in this small mountain range.

Seismic observations were also conducted in those parts of today's Poland, which before or during the Second World War belonged to Germany; they were under supervision of the observatory in Królewiec (German name Königsberg, now Kaliningrad, Russia), or in Wrocław (then Breslau); see Tams (1950) and Schweitzer (2003). The latter was founded by Prof. Gustav H. G. von dem Borne (1867–1918) in 1908, in then suburban district Krietern (now Krzyki) in Wrocław, and was named "Erdbebenwarte Breslau-Krietern". It started functioning in 1909 and worked till 1916. In 1910, Königliche Technische Hochschule Breslau was instituted and took over the management of the observatory (since 1945 the Hochschule's buildings have been occupied by the Wrocław University of Technology). In the years 1928–1929 the operation of the observatory was temporarily stopped, but registration re-started in 1929. During military operations in 1945, the building of observatory was completely ruined, but the Wiechert's seismographs survived in the basement. These were excavated in 1945 by Professors Edward Stenz and Tadeusz Olczak (1907–1983), and in 1954 transported to the Racibórz Observatory (Olczak 1991). These valuable historical instruments are now displayed in the seismological station at the Chorzów Planetarium (Fig. 3).

3 From the Outbreak of the Second World War to 1952

The Second World War, started on 1 September 1939 with German aggression on Poland and Soviet invasion from the East on 17 September, caused a several-year break in the promising development of Earth Sciences in this part of the world. It is to be noted, though, that two observatories, in Świder and at the Warsaw University, were functioning under German occupation, as entities subject to the Geological Institute of Warsaw District of General Gubernatory, the so-called “Amt für Bodenforschung”.

The Geological Institute was allowed, at least in first years of German occupation, to conduct certain geophysical field surveys, for example measurements of magnetic declination (*nota bene*, useful for production of maps for military forces of the Polish Underground State—ZWZ and later AK, i.e., the Home Army). Germans soon activated the High Mountain Meteorological Observatory at Kasprowy Wierch and used it for their purposes, the same concerns Marine Department of PIM in Gdynia. Generally, both invaders, Germans and Soviets, tried to wipe out Polish identity of the science and education in enslaved lands; they sometimes destroyed even the publications.

The scientific centers in Lwów and Wilno were, after Soviet aggression on 17 September 1939, lost for Poland. Scientists have dispersed, many of them met repressions, were killed in mass murders or sent to German concentration camps or Soviet lagers (forced labor camps). Many people did not survive harsh conditions. Quite a lot reached Western Europe or USA, via different ways, joined the Polish Forces in the West and after the war did not return to homeland for political reasons. Human and material loss of Polish science and higher education, in the effect of the Second World War, are enormous and even hard to estimate. Those scientists from Lwów or Wilno who survived all these hard times and returned to Poland, settled in Wrocław, Toruń or elsewhere, joining or organizing the scientific centers there.

After the war, the works on reconstruction of education and structures of science started immediately. The plans for reconstruction and reforms were already prepared before, by educational agendas of the Polish Underground State (as, e.g., the Secret Organization of Teachers “TON”). In 1945, reactivated were (among other) the State Geological Institute (PIG) and the PIM, under the name of State Institute of Hydrology and Meteorology (PIHM). The first of these took over the management of the Magnetic Observatory at Świder and Seismological Observatory at the University of Warsaw. The State Geological Institute soon started gravimetric, magnetic and seismic surveys, mainly in the Kujawy district (search for the salt deposits). The High Mountain Meteorological Observatory at Kasprowy Wierch was activated after a few-month break.

Because of territorial changes after the war, borders of Polish state embraced the meteorological observatory on the top of Śnieżka mount (Schneekoppe in German), built in 1900, and the Silesian Geophysical Observatory in Racibórz

which was ruined in major part. The latter started working in 1929, in then German Ratibor, arranged and directed by Silesian-German seismologist Prof. Karl (Carl) Mainka (1873–1943), inventor of the long-period seismographs, known as the Mainka seismographs (also the magnetic measurements were made in this observatory in the years 1932–1933). After the war, this observatory started to work in 1947 (see Olczak 1948); in 1953 it was taken over by the Institute of Geophysics PAS. Due to overwhelming disturbances caused by heavy traffic, this observatory was removed from the network of seismic stations in 2010. Now the Geophysical Observatory in Racibórz is only a museum and educational facility, where the huge, old Mainka seismographs may still be admired.

In Polish capital, the Warsaw Seismological Observatory re-started normal functioning in 1946, run by still the same person, Dr. Irena Bóbr-Modrakowa (then replaced by Wiesława Jankowska). In September 1947, the Society of Geophysicists in Warsaw was reactivated under a new name: Polish Society of Geophysicists (Maj 2011). Its main goals included proposals for geophysical studies programs and edition of monographs on the Earth sciences. In the same time, another society relating to geophysics, the Polish Meteorological-Hydrological Society, came into being.

At the Mining Academy, Prof. Edward Walery Janczewski (1887–1959) organized, already in 1945, the Chair of Geophysics, the first after the war. It was mostly focused on prospecting geophysics (see, e.g., Kowalcuk 2011). In the Faculty of Mathematics, Physics and Chemistry at Warsaw University, the Department of Geophysics was organized in 1948, under the guidance of Prof. Teodor Kopcewicz (1910–1976). It was concerned with physics of the atmosphere, seismology, gravimetry and general geophysics. In the next year, it was split in two: the Chair of Geophysics I (since 1952: Physics of the Lithosphere), headed by Prof. Edward Stenz (1897–1956), who had just returned from the Kingdom of Afghanistan, and the Chair of Geophysics II (since 1952: Physics of the Atmosphere) headed by Prof. Teodor Kopcewicz (Kozłowski 1990).

On the turn of June and July 1951, Polish state authorities organized in Warsaw the First Congress of Polish Science, when the plans to bring into being the Polish Academy of Sciences (PAS) were announced, basing on scheme of the Academy of Science of the USSR. This decision was authorized by governmental edict of 30 October 1951. At the same time, the Polish Academy of Arts and Sciences (in Cracow), Polish Academy of Technical Sciences and the Warsaw Scientific Society were closed. Within the Polish Academy of Sciences, numerous departments/institutes dealing with various branches of science were instituted by the end of 1952. These included the Department of Geophysics, later transformed into the Institute of Geophysics PAS. The following observatories constituted its main experimental background: the Magnetic Observatory at Świdra, Seismological Observatory at the University of Warsaw, Silesian Geophysical Observatory in Racibórz, and the Marine Station Sopot-Molo.

Acknowledgments The authors want to express their sincere gratitude to Mrs Anna Dziewińska for her help in preparing this chapter for publication.

References

- Berezowski E (1972) Vaclav Laska (1862–1943). *Kwart Hist Nauki Tech* 17(1):71–77
- Czyszek Z, Czyszek W (1984) *Obserwatorium Geofizyczne w Helu 1932–1982 (Geophysical Observatory at Hel, 1932–1982)*. Przegląd Geof 29(2):199–212
- Dormus K (2011) Fizyka Ziemi i jej światowe początki w Uniwersytecie Jagiellońskim (Physics of the Earth and its global beginnings at the Jagiellonian University). *Prace Geograf* 127:7–30
- Giżejewski J (2011) Działalność polarna Towarzystwa Geofizyków w Warszawie (The polar activities of the Society of Geophysicists in Warsaw). *Przegląd Geof* 56(3–4):291–296
- Hanik J (1986) Katedra Geofizyki Uniwersytetu Jagiellońskiego (1895–1919) (Chair of Geophysics at the Jagiellonian University, 1895–1919). *Przegląd Geof* 31(3):339–345
- Jankowska WA (1986) Obserwatorium Sejsmologiczne imienia Ireny Bóbr-Modrakowej w Warszawie (seismological observatory in warsaw). *Przegląd Geof* 31(2):193–200
- Jóźwiak W, Jankowski J, Ernst T (this issue) Natural variations of the geomagnetic field—observations and application to study of the Earth's interior and ionosphere
- Korja T (2007) How is the European lithosphere imaged by magnetotellurics? *Surv Geophys* 28:239–272. doi:[10.1007/s10712-007-9024-9](https://doi.org/10.1007/s10712-007-9024-9)
- Kowalcuk J (2009) Organizacja życia naukowego w dwudziestoleciu międzywojennym we Lwowie (Scientific life in 20-year inter-war period in Lwów). *Przegląd Geof* 54(1–2):33–51
- Kowalcuk J (2001) 100-lecie Geofizyki Polskiej 1895–1995, Kalendarium (Hundred Years of Polish Geophysics 1895–1995. Calendarium). 2edn, Wydawnictwo Arbor, Kraków, pp 234
- Kowalcuk J (2011) Edward Walery Janczewski (1887–1959): życie i działalność naukowa (Edward Walery Janczewski 1887–1959 Biography and scientific activity). *Przegląd Geof* 56(3–4):297–304
- Kozłowski MF (1990) Początki geofizyki na Wydziale Fizyki Uniwersytetu Warszawskiego (Beginnings of geophysics at the Faculty of Physics, Warsaw University). *Przegląd Geof* 35(1–2):97–106
- Kreiner JM, Rymarowicz L (1992) Obserwatorium Meteorologiczno-Astronomiczne im. Marszałka Józefa Piłsudskiego na Popie Iwanie (Meteorological-astronomical observatory at pop Ivan). *Przegląd Geof* 37(1–2):77–85
- Kwiatkowski A (1937) Pomiary polowe 1935 r. (Field measurements in 1935), *Prace Grawimetryczne* in 1935 (seria V), Główny Urząd Miar, Warszawa, pp 43
- Lugeon J (1933) Polski Rok Polarny na Wyspie Niedźwiedziej (Polish Polar Year on the bears' Island). *Przegląd Geograf* 13(1):1–49
- Maj S (2003a) Rudzki Maurycy Pius (1862–1916). In: Lee WHK, Kanamori H, Jennings BC, Kisslinger C (eds) *International handbook of earthquake and engineering seismology*. Academic Press, Part B, p 1774
- Maj S (2003b) Pięćdziesięciolecie Komitetu Geofizyki PAN, 1952–2002 (Fifty years of the committee of geophysics PAS, 1952–2002). *Przegląd Geof* 48(1–2):91–103
- Maj S (2011) Działalność Towarzystwa Geofizyków w Warszawie (1930–1947) (On the society of geophysicists in Warsaw, 1930–1947). *Przegląd Geof* 56(3–4):265–277
- Maj S (2013) Studia geofizyczne w Wolnej Wszechnicy Polskiej w Warszawie (1918–1939) (Geophysical study at the Polish free university in Warsaw, 1918–1939). *Przegląd Geof* 58(3–4):211–228
- Mazur M (1993) Stacja sejsmologiczna Uniwersytetu Jagiellońskiego (1903–1956) (Seismological station of the Jagiellonian University, 1903–1956). *Kwart Hist Nauki Tech* 38:5–35
- Michalski S, Małkowska J (Eds) (1947) *Nauka polska: jej potrzeby, organizacja i rozwój* (Science and letters in Poland: its needs, organization and progress), vol XXV, Wyd. Kasy im. Mianowskiego Inst. Popierania Nauki, Warszawa–Uniwersytet, pp 590
- Mikulski Z (1984) Towarzystwo Geofizyków w Warszawie (1929–1939) (Society of Geophysicists in Warsaw, 1929–1939). *Przegląd Geof* 29(2):181–190

- Mikulski Z (1991) Wybrane zagadnienia nauk o Ziemi w Cesarskim Uniwersytecie Warszawskim (1869–1917) (Selected problems of Earth sciences at the Imperial University of Warsaw, 1869–917). *Przegląd Geof* 36(4):329–338
- Olczak T (1932) Stan prac nad pomiarami siły ciężkości w Polsce (Gravity force measurements in Poland). *Wiad Geograf* 10:13–18
- Olczak T (1948) Śląska Stacja Geofizyczna Państwowego Instytutu Geologicznego w Raciborzu (Silesian Geophysical Station of the State Geological Institute in Racibórz), Biul. Śląskiej Stacji Geofiz. Nr 1, Wyd. Geologiczne
- Olczak T (1958), Badania nad magnetyzmem ziemskim w Polsce (Research on the earth magnetism in Poland), In: Janowski BM, Magnetyzm Ziemska PWN (eds) Warszawa
- Olczak T (1991) Studia z historii geofizyki na ziemiach polskich (Studies on the history of geophysics in Poland). *Przegląd Geof* 36(1):37–54
- Ołpińska-Warzechowa K (1985) Obserwatorium Geofizyczne imienia Stanisława Kalinowskiego w Świdrze (The Stanisław Kalinowski Geophysical Observatory at Świdra) *Przegląd Geof*. 30:2, 213–229
- Ołpińska-Warzechowa K (1995) Geofizyka (Geophysics), In: Historia nauki Polskiej, Wiek XX, Nauki o Ziemi, Wyd. Instytut Historii Nauki PAN, pp 37–82
- Ołpińska-Warzechowa K (1988) Instytut Geofizyki i Meteorologii Uniwersytetu Jana Kazimierza we Lwowie (1920–1939), (Institute of Geophysics and Meteorology at the Jan Kazimierz University in Lwów, 1920–1939). *Przegląd Geof* 33(1):65–81
- Schweitzer J (2003) Early german contributions to modern seismology, In: Lee WHK, Kanamori H, Jennings P, Kisslinger C (eds) International handbook of earthquake and engineering seismology, Part B, Academic Press, pp 1347–1352
- Tams E (1950) Materialien zur Geschichte der deutschen Erdbebenforschung bis zur Wende des 19. zum 20. Jahrhundert Teil II und Teil III. Mitteilungen des Deutschen Erdbebendienstes, Sonderheft 2, Akademie Verlag, Berlin, pp 169
- Teisseyre B (1998) Uwagi o życiu Wawrzyńca Teisseyre'a z okazji jubileuszu 150-lecia Politechniki Lwowskiej (Notes on the life of Wawrzyniec Teisseyre, on the occasion of 150-year jubilee of Lvov Polytechnic), *Acta Univeristatis Vratislaviensis*, No 2004, Prace Geologiczno-Mineralogiczne LXIV, pp 11–40
- Teisseyre R, Teisseyre B (2002) Wawrzyniec Karol de Teisseyre, A Pioneer in the Study of Cryptotectonics, *Eos, Transactions American Geophysical Union*, 83(47):541, 556
- Voppel D, Schulz G (2002) An episode in the history of geophysics against the background of world events. In: Proceedings of the Tenth IAGA workshop on geomagnetic instruments, data acquisition and processing. Hermanus Magnetic Observatory, pp 281–286

Fifty Years of Palaeomagnetic Studies in the Institute of Geophysics, Polish Academy of Sciences

Magdalena Kądziałko-Hofmokl, Tomasz Werner
and Jadwiga Kruczyk

Abstract Palaeo- and archaeomagnetic investigations in the Institute of Geophysics were initiated at the beginning of 1960s. The archaeomagnetic study was performed in the Geomagnetic Observatory in Hel till the mid-1980s and was resumed lately in the Warsaw laboratory. Palaeomagnetic study begun in 1963 but the palaeomagnetic group obtained necessary place for the laboratory in the Central Geophysical Observatory in the newly finished building in Belsk later in 1966. Formally, the Paleomagnetic Laboratory was established in 1972. From the very beginning, palaeomagnetic studies were accompanied by studies of magnetic properties of rocks and minerals-carriers of natural remanence and by measurements of magnetic susceptibility and its anisotropy. Therefore, the laboratory became successively equipped with the apparatus for strictly palaeomagnetic study (astatic and spinner magnetometers and demagnetizing devices) as well as with devices for rock-magnetic investigations (apparatus for thermoanalysis, system for measuring of hysteresis parameters and for study of magnetic remanence at low temperatures, torsion balance, device for study of magnetic properties under mechanical stress and temperature, device for study of alterations of magnetic minerals based on thermally stimulated emission of exo-electrons (TSEE). The last three devices have not been in use for several years. At the end of 1980s, the Institute moved to a new building and the whole laboratory was moved to Warsaw. Moving palaeomagnetic measurements to town was possible due to the replacement of spinner magnetometer by the cryogenic magnetometer SQUID, which is much more sensitive and less affected by the urban disturbances. Computer software packages that are written in the Institute or obtained from their inventors became a great help in the interpretation of experimental results. Palaeomagnetic investigations have been performed in our laboratory on rocks of various origins and age, coming from various regions of Poland and other countries often in cooperation with scientists from foreign laboratories. Numerous palaeomagnetic results that are obtained in our laboratory are in

M. Kądziałko-Hofmokl · T. Werner (✉) · J. Kruczyk
Institute of Geophysics, Polish Academy of Sciences, ul. Księcia Janusza 64,
01-452 Warsaw, Poland
e-mail: twerner@igf.edu.pl

the world data palaeomagnetic basis and on Apparent Polar Wander Paths constructed for various regions. Study of anisotropy of magnetic susceptibility brought interesting results concerning problems of tectonics; study of rock-magnetic properties helped to identify carriers of primary and secondary components of natural magnetic remanence in many cases. In the last 10 years, a group in our laboratory has been studying very important problems connected with environmental magnetism by applying of magnetometric methods for investigations of soil and air pollution.

Keywords Geophysics • Earth sciences • Palaeomagnetism • History of the Institute of Geophysics PAS

1 Introduction

In this short resume we would like to present the history of palaeomagnetic investigations in our Institute, the history that begun 50 years ago. We will show how the laboratory, that started from nothing half a century ago and grew to very well equipped establishment where numerous palaeomagnetic and rockmagnetic problems have been and are resolved. In the passing of time, the staff of our laboratory grew and all of us tried to equip the laboratory with modern devices, to investigate interesting problems, often in cooperation with foreign laboratories, to invent new methods of investigations and analyse the experimental results. In our narrative you will see that we worked often in groups of two-three persons and that members of the groups moved from one group to the other, depending on the investigated problems, and individually as well. In many cases, our working groups included scientists from various Polish geological institutions and scientists from foreign laboratories. Thanks to this way of organization we were able to investigate a great number of problems connected with various regions, time spans, types of rocks, magnetic mineralogy, and, lately, soils and dust pollution. In this place we have to mention that in our laboratory, apart of scientists, worked also technicians who helped in field work, prepared rock specimens of standard size and shape and performed numerous measurements.

Now in our laboratory work eight palaeomagneticians and a technician Anna Norberciak, a great help in our experimental work since 1984.

2 The Beginnings of the Palaeomagnetic Laboratory

Palaeo- and archaeomagnetic investigations in the Institute of Geophysics started at the beginning of 1960s.

The archaeomagnetic study was initiated and performed in the Geomagnetic Observatory in Hel by Zofia Czyszek and Waclaw Czyszek. The necessary equipment was constructed according to Czyszeks' requirements in the Institute,

with help of engineer Włodzimierz Romaniuk. The Czyszek' couple investigated well dated archaeological objects (bricks, fragments of potteries, whorls etc.) encompassing last 3,000 years and coming from places situated along the meridian passing through Gdańsk, Sieradz and Cieszyn, in order to obtain secular variations of inclination of the geomagnetic field. Both scientists obtained Ph.D. degrees on the basis of the results of this project (Czyszek and Czyszek 1976, 1987). The archaeomagnetic studies in Hel took place till the middle of 1980s and were not continued afterwards. Some archaeomagnetic studies were also performed in the 1960s by Warsaw group together with a team of scientists from the Institute of Physics of the Earth of Soviet Academy of Sciences from Moscow on the objects from the Kielce and Kraków regions (Burlackaja et al. 1969). Lately the archaeomagnetic studies have been resumed in the cooperation with scientists from Ukraine.

Palaeomagnetic studies were started in our Institute in 1963, when two Ph.D. students, Jadwiga Kruczyk and Magdalena Kądziałko-Hofmokl started to work under the supervision of Dr. Zdzisław Małkowski. Thanks to him, in the years 1964–1965 both Ph.D. students obtained fellowships in palaeomagnetic laboratories of good standards: Jadwiga Kruczyk in the Institute of the Physics of the Earth of Academy of Sciences of Soviet Union in Moscow and Magdalena Kądziałko-Hofmokl in the Institute of the Physics of the Earth of the Academy of Sciences of German Democratic Republic in Potsdam. During their stays they learned the importance of performing, together with palaeomagnetic investigations, also investigations of magnetic properties of magnetic minerals that are carriers of natural remanence.

Such experience led to the efforts to equip our laboratory from the very beginning not only in instruments for strictly palaeomagnetic study (magnetometers, susceptibility bridge and demagnetizing devices) but also in devices for rock-magnetic investigations. The rock-magnetic studies were complemented nearly from the beginning with optical microscopic study of ore minerals performed in Polish Geological Institute by Dr. Jacek Siemiatowski. This cooperation has lasted for a long time and was extended in the recent 20 years by electronic microscopy (SEM) and microprobe measurements (in the Polish Geological Institute and the Faculty of Geology of the University of Warsaw).

The first palaeomagnetic investigations in the Institute, performed partly in Moscow and partly in Poland by Jadwiga Kruczyk, concerned the Tertiary andesites from Wżar Mt. in Pieniny. The results obtained were compatible with the results for Tertiary rocks from Stable Europe and shown that Wżar andesites formed during several lava outflows (Kruczyk 1970).

The first set of instruments in our laboratory consisted of astatic magnetometer LAM1 and later LAM3 as well as two spinner magnetometers ION1(all purchased in the Soviet Union) and the equipment constructed in our Institute (devices for measurements of hysteresis parameters and for study of remanent magnetization in low-liquid nitrogen—temperatures, Fig. 1b). The two latter devices worked, at the beginning, in the Students First Physics Laboratory of the Faculty of Physics of the University of Warsaw thanks to Prof. Jerzy Pniewski, director of the

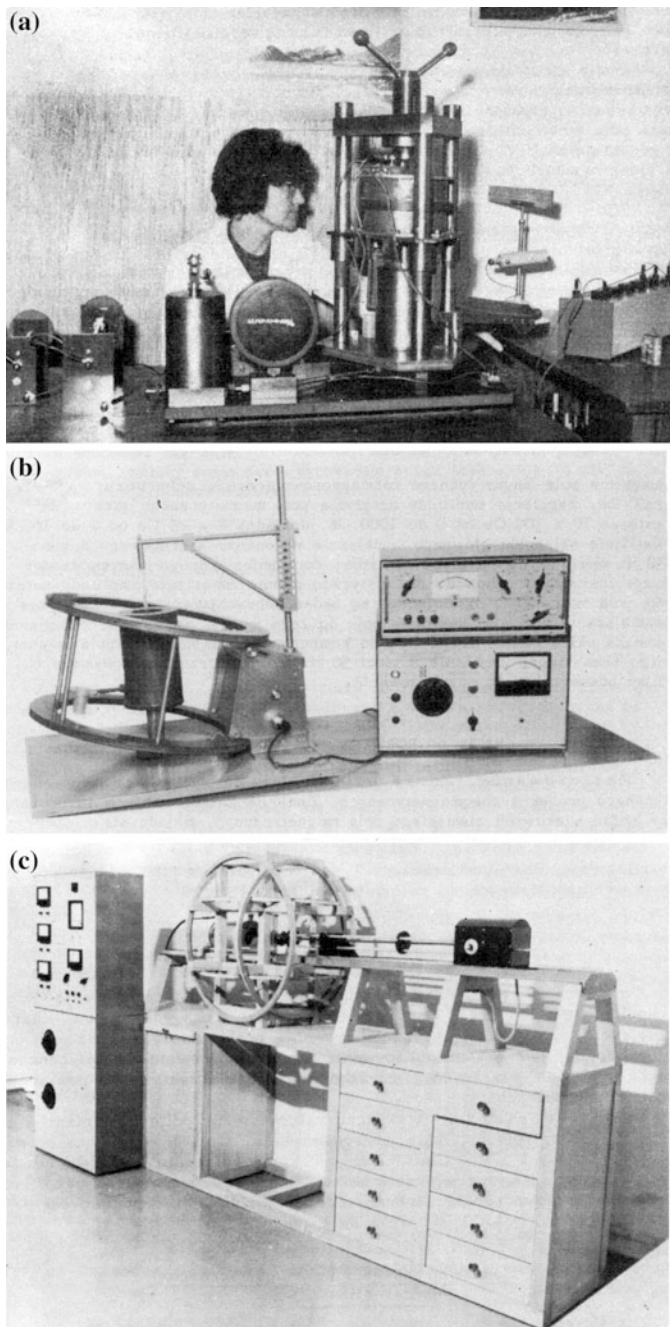


Fig. 1 Equipment made in the Institute of Geophysics in 1968–1980: **a** amagnetic press for measurements of induced magnetization and magnetic remanence under uniaxial pressure at 20–300 °C temperatures (concept of Jeleńska and Jeleński); **b** cryomagnetic unit (ZUK-257-69) for measurements of rock magnetic properties of rocks in -190 to 0 °C temperature range (concept of M. Kądziałko-Hofmokl and M. Jeleńska); **c** apparatus for AF demagnetizing of rock samples (UR-1-S-68, concept of M.Kądziałko-Hofmokl, M.Jeleńska and J.Kruczyk)

Institute of Experimental Physics of the University at that time. The Faculty provided also the galvanometric system of measurements for hysteresis study. The first results obtained in low temperatures in the Institute were published by Kądziałko-Hofmokl and Kruczyk (1968).

In 1967 the palaeomagnetic group was joined by the third PhD student (Maria Jeleńska). Thanks to invention of all three PhD students, engineer Włodzimierz Romanik built a device for demagnetization of natural remanence with alternating field (AF) UR1-S-68 (Fig. 1c). With the use of AF demagnetizer and magnetometers we could start standard palaeomagnetic investigations. The first device for thermal demagnetization (operating, unfortunately, only in limited temperature range up to 300 °C due to limitations of permalloy box) was bought a few years later. Due to limited maximum demagnetization temperature, only NRM components of low thermal stability were demagnetized. Nevertheless, the results of even such imperfect cleaning helped in the interpretation of obtained data.

At the end of 1960s, the palaeomagnetic group obtained some rooms for the experimental laboratory in the newly built buildings of the Central Geophysical Observatory in Belsk Duży (close to Grójec, some 50 km from Warsaw). In a new locality all palaeomagnetic and rock-magnetic devices were installed. In Belsk we had also mechanical workshop where a technician cut our oriented hand-samples taken during field trips into standard specimens for palaeomagnetic and rock magnetic measurements and a storage place for the remaining parts of hand samples. A new instrument—the susceptibility bridge, KLY2 (by Geofyzika Brno), supplementing the above palaeomagnetic equipment, was installed during this time in Warsaw.

In the second half of 1970s, the old spinner magnetometers were replaced by a new spinner magnetometer JR-3 of Geofyzika Brno (Czechoslovakia), and further by its new version (JR-4, 1982) that improved speed, accuracy and ease of palaeomagnetic measurements.

The Palaeomagnetic Laboratory in Belsk was fitted in following palaeo- and rock-magnetic equipment working till 1989:

A. Palaeomagnetic equipment:

1. Astatic magnetometer LAM-1 (SU) replaced in 1973 by LAM-3 installed in the magnetic absolute pavilion
2. Spinner magnetometer ION-1 (SU) replaced by spinner JR-3 (Geofyzika Brno, Czechoslovakia) and later JR-4
3. Alternating field demagnetizer with maximal AC field of 100 mT
4. Furnace for demagnetizing specimens in non-magnetic permalloy box in temperatures up to 300 °C.

B. Rock-magnetic equipment:

1. Apparatus for low-temperature study.
2. Apparatus for thermoanalysis built on the basis of one of ION1 spinners by J. Kruczyk, M. Jeleńska, M. Kądziałko-Hofmokl, and C. Sanojca, (certificate nr 112480) enabling identification of magnetic minerals-carriers of magnetic

properties by their blocking temperatures Tb. The great advantage of this apparatus has been (and still is) heating samples to 700 °C within the non-magnetic space.

3. Pulse magnetizer for magnetizing rock samples to 1 T constructed in the State Institute for Geophysical Prospecting by engineer Jadwiga Mednis.
4. Device for study of magnetic properties under mechanical stress and various temperatures invented by Maria Jeleńska and Janusz Jeleński and constructed according to Maria Jeleńska's idea in the Institute, which served as a basis for her Ph.D. dissertation (Jeleńska 1975, Fig. 1a).
5. Torsion balance constructed according to idea of Magdalena Kądziałko-Hofmokl in the Institute of Nuclear Research in Świeck for the study of rotational hysteresis and various types of torsion curves characteristic for various magnetic minerals. The results were a basis for her habilitation (Kądziałko-Hofmokl 1981).
6. At the end of 1980s engineers Wojciech Turewicz and Jerzy Suchcicki (TUS) built on the basis of the first apparatus for thermoanalysis its successive modernized version STEPS1, with data collected by computer. Now in the Laboratory in Warsaw its fourth generation STEPS4 is used.

3 The New Research Directions Since 1970s

At the end of 1960s and beginning of 1970s Jadwiga Kruczyk, Magdalena Kądziałko-Hofmokl and Maria Jeleńska obtained their PhD degrees. Formally, the Palaeomagnetic Laboratory was established in 1972 with Dr. Zdzisław Małkowski as the head of laboratory.

When our laboratory was acceptably equipped, the group of Jadwiga Kruczyk, Maria Jeleńska, Magdalena Kądziałko-Hofmokl with Prof. Krzysztof Birkenmajer, geologist from the Institute of Geological Sciences PAS, started detailed palaeomagnetic study of Tertiary basaltic rocks from Lower Silesia, situated between the Sudetic Boundary Fault and the Odra Fault. The geochronological study of these rocks was performed by M. Arakelyants in the Moscow laboratory; the results of K–Ar method dated them at 28 ± 3 – 15 ± 2.5 Ma. The investigations took several years; the most important results consisted of construction of magnetostratigraphic scale, recognition of several phases of volcanic activity, recognition of six polarity events within the studied basaltic succession (Kruczyk et al. 1977) and observation of self-reversal of magnetic remanence occurring in some samples due to presence of partly oxidized titanomagnetites (Kądziałko-Hofmokl and Kruczyk 1976).

In the mid-1970s Jadwiga Kruczyk applied the method of thermo-stimulated emission of exo-electrons (TSEE) to study oxidation and phase transitions of iron oxides and sulfides (Kruczyk 1978) that was the basis of her habilitation (Kruczyk 1983). All measurements were performed on the equipment installed in the Military Institute of Chemistry and Radiometry in Warsaw.

At the same time, the palaeomagnetic team worked together with Czechoslovak palaeomagneticians on magnetic properties of basaltic rocks from the Bohemian Massif, belonging to the same basaltic province as the Lower Silesian ones (Jeleńska et al. 1978a). In the 1970s the Institute became a partner in so-called KAPG project (Planetary Geophysical Study of the Academies of Socialistic Countries). Our cooperation with the Institute of Geophysics of the Czechoslovak Academy of Sciences took place in the frame of this project.

To the variety of palaeomagnetic investigations, Maria Jeleńska added in the 1970s the study of Mesozoic and Palaeozoic rocks from Spitsbergen, as a Polish leader of palaeomagnetic project “Geodynamic study of Spitsbergen” financed by the American Marie Skłodowska-Curie funds. The working group included also Jadwiga Kruczyk and Magdalena Kądziałko-Hofmokl. From the American side, the study was headed by Prof. Stanisław A. Vincenz from St Louis University. Thanks to her determination, Maria Jeleńska organized two expeditions to Spitsbergen to sample selected rocks units for investigations presented in several papers and during international conferences and leading to her habilitation. A very detailed analysis of magnetic mineralogy performed with rock-magnetic and microscopic methods enabled identifying carriers of natural remanence and obtaining reliable palaeomagnetic pole positions. The most important results concerned the construction of Devonian-Triassic segment of Apparent Polar Wander Path for Spitsbergen indicating its shift against the corresponding segment of the Path for the Stable Europe (Jeleńska et al. 1978b; Vincenz et al. 1984; Vincenz and Jeleńska 1985). In the frame of this program, Maria Jeleńska spent three times several months in St. Louis working with S.A. Vincenz on Spitsbergen rocks.

In the 1970s three new Ph.D. students: Bibianna Szumańska-Pajchel, Elżbieta Niedziółka-Król and Piotr Tuchołka joined the Laboratory. Bibianna Szumańska-Pajchel in her Ph.D. project studied alterations of titanomagnetite from basaltic rocks with rock-magnetic and Mössbauer methods. After dissertation, she returned to her previous institution. Elżbieta Niedziółka-Król and Piotr Tuchołka studied Quaternary sediments. Their most important project concerned longtime variations of geomagnetic field in Holocene lake sediments (gytia) from northern Poland performed in cooperation with scientists from the Geophysical Faculty of University of Edinburgh (Creer et al. 1979, 1983). The authors presented the correlation of observed secular changes with the reference data from the Lake Windermere in Great Britain. They also obtained new parameters helping to estimate velocity of sedimentation in the studied Polish lakes. In 1983 Piotr Tuchołka left for Great Britain and the Quaternary rocks were further investigated only by Elżbieta Król. She worked on rocks from Poland and other countries, in part in cooperation with the University of Edinburgh (sediments from maar lakes), where she twice obtained a fellowship, and in part in the frame of KAPG in cooperation with scientists from Bulgaria, Rumania, Soviet Union and Ukraine. Elżbieta Król was also interested in rock-magnetism—she investigated Tertiary sediments of Parathetys containing magnetic sulphide minerals and magnetic properties of meteorites (Polish meteorite Baszkówka and Japanese Mt. Tazerzeit chondrite, Król at al. 1996). In the last years she joined the group of Maria

Teisseyre-Jeleńska investigating air pollution on archival air filters and indoor dust from Warsaw. In last few years she worked in cooperation with the University of Kielce (project on the Quaternary sediments from Holy Cross Mts.), the Faculty of Geography of Warsaw University (project on magnetic susceptibility of continental and lake sediments from Holocene profiles) and University of Łódź (project of anisotropy of susceptibility from sediments of Vistulian age).

At the end of 1970s the palaeomagnetic group was joined by Marek Lewandowski. In order to be able to demagnetize thermally rock samples in the whole necessary range of temperatures (up to 700 °C), he constructed the non-magnetic thermal demagnetizer (certificate 112480) which was installed in Warsaw together the susceptibility bridge KLY-2 and later with spinner magnetometer JR-4 bought in 1988.

As a geologist, he started to apply the results of his palaeomagnetic investigations for geological, tectonic and palinspastic interpretations and reconstructions. He studied, at the beginning, Palaeozoic rocks from the Holy Cross Mts. His results, summarized in his dissertation (Lewandowski 1981) shown that Devonian fold structures of the Holy Cross Mts. formed during the Variscan tectogenesis.

Apart of construction of non-magnetic furnace at the beginning of his work in our laboratory, Marek Lewandowski, together with Krzysztof Nowożyński, prepared computer program package for analysis of results of palaeomagnetic experiments, based on the Kirschvink's method of fitted lines to demagnetization paths, modernized later with the help of Tomasz Werner (Lewandowski et al. 1997). It contributed in a very important way to analysis and interpretation of our palaeomagnetic results making our work much easier and quicker.

At the end of 1970s and beginning of 1980s Jadwiga Kruczyk, Magdalena Kądziałko-Hofmokl and Maria Jeleńska started to study Jurassic sediments from Poland, Bulgaria, and Slovakia (the latter two in cooperation with Bulgarian and Slovak scientists in the frame of KAPG) and France in the frame of international cooperation with the Strasbourg University. Out of numerous results the most important are: Upper Jurassic pole positions for the Cracow-Częstochowa Upland (Kruczyk et al. 1980; Kądziałko-Hofmokl and Kruczyk 1987), Jurassic pole position obtained for the Tatra Mts., for halokinetic structure in Kujawy, for Central and Southern Bulgaria (Kruczyk et al. 1990), Jurassic pole position obtained for Rheingraben in France, all compatible with data for the Stable Europe. The team found also fan-like distribution of Jurassic pole positions obtained for nappe slices in the Western Inner Carpathians, interpreted as being due to fan-like movements of nappes (Kruczyk et al. 1992), and the Callovian field reversal in the Cracow-Częstochowa Upland (Poland) and Central Balkan (Bulgaria) (Kruczyk and Kądziałko-Hofmokl 1988; Kruczyk et al. 1988, 1990). In 1989 the Polish-Bulgarian working group obtained the Prize of the Scientific Secretary of Bulgarian Academy of Sciences. In the meantime Maria Jeleńska and Magdalena Kądziałko-Hofmokl investigated the influence of temperature on anisotropy of magnetic susceptibility of rocks. They showed how heating may enhance this anisotropy (Jeleńska and Kądziałko-Hofmokl 1990).

In 1983 the head of our laboratory Dr Zdzisław Małkowski died, and Ass. Prof. Jadwiga Kruczyk became a new head of the Paleomagnetic Laboratory.

At the end of 1980s Maria Jeleńska returned to study of palaeomagnetism of polar regions together with scientists from Norway (R. Løvlie, University of Bergen), leading the project titled “Paleomagnetism of some regions of the Northern Europe” (Løvlie et al. 1984). In addition, a collaboration with Norwegian team resulted in a project dealing with palaeomagnetism of Sudetic granitoids (Halvorsen et al. 1989). She also continued studies of Spitsbergen rocks together with Marek Lewandowski. During the 1980s, scientists from the laboratory obtained four prizes of the Scientific Secretary of Polish Academy of Sciences.

4 The Next Stage of Palaeomagnetic Laboratory in a New Institute Location at Księcia Janusza

In 1988 the Institute moved to a new building where the Paleomagnetic Laboratory obtained enough space to move all necessary equipment from Belsk to Warsaw (Fig. 2). The frequent trips from Warsaw to Belsk and back in order to perform experiments were no longer necessary and our working conditions and possibilities improved enormously. In 1991 the Laboratory obtained the most modern device for measurements of natural remanence—the cryogenic magnetometer AC SQUID (model 755 made by 2G Enterprises, USA), connected with alternating field demagnetizer. It was the first cryogenic magnetometer for palaeomagnetic studies installed in Central Europe. It let us study even rocks of very weak remanence that were not measurable with the JR4 spinners. The SQUID magnetometer was upgraded to DC model of higher sensitivity in 2001. This magnetometer together with non-magnetic furnace of Magnetic Measurements, Gr. Britain, MMTD for 18 specimens was installed within the cage of magnetic field compensating coils of Magnetic Measurements.

In 1986 Maria Jeleńska and Magdalena Kądziałko-Hofmokl begun investigations of Palaeozoic rocks from European Variscans in the frame of prolonged cooperation with French scientists from the universities in Strasbourg (M. Westphal, J.B. Edel) and Rennes (T. Aifa) and, in the first years with scientists from Munich, Germany (H. Soffel and N. Petersen). These Variscan units were studied either in the frame of international cooperation or only by the Polish group and consisted of Ślęza Massif, Wałbrzych Basin, Świebodzice Basin, Izera and Karkonosze Mts., Rudawy Janowickie Mts., Kłodzko Metamorphic Massif, Jordanów-Gogółów Massif, Braszowice-Brzeźnica Massif, Niemcza Zone, Intrasudetic Basin, Śnieżnik Metamorphic Massif. In the frame of this cooperation Maria Jeleńska spent several months in laboratories of Strasbourg and Rennes, and went, together with Magdalena Kądziałko-Hofmokl, for numerous short visits for scientific discussions and sampling expeditions. Both of them worked also in Munich (Germany) in the frame of DAAD fellowships. Scientists from France took part in several sampling expeditions in Poland.



Fig. 2 The farewell group photo of the members of Department of Magnetism at the front of Zielna location of Institute at the last day before moving to Księcia Janusza locality (Autumn 1988). From the left: (*standing*) Krzysztof Nowożynski, Jan Pawliszyn, Jerzy Jankowski, Romuald Wieladek, Jadwiga Kruczyk, Waldemar Józwiak, Jadwiga Radzikowska, Magdalena Kądziałko-Hofmokl, Tomasz Ernst, Anna Norberciak, Jan Brojek, Maria Jeleńska and as two guest members of “moving team” Janusz Niewadomski and Andrzej Zawada; (*bottom row*) Elżbieta Król and Marek Lewandowski

In the studies of Carboniferous sediments from the Intrasudetic Basin took part Ibrahim A. El-Hemaly who was the Ph.D. student from the National Research Institute of Astronomy and Geophysics of Egyptian National Academy of Sciences in Helwan. He obtained the Ph.D. title under supervision of Magdalena Kądziałko-Hofmokl. His Ph.D. project initiated a long and fruitful cooperation of our laboratory with the Palaeomagnetic Laboratory in Helwan (e.g., Kądziałko-Hofmokl and El-Hemaly 1997).

The results of the study of Sudetic rocks became compiled in Jeleńska et al. (2003 and references within), as the Devonian–Permian segment of Apparent Polar Wander Path for the Sudetes. The authors stated the general similarity of this Path with the reference Path for the Stable Europe by Torsvik, but with one difference—the eastern shift of the Permian part of the Sudetic Path in relation to the Torsvik’s one (Fig. 3). The results obtained later for circum-Sowie Góry ophiolitic belt and Kłodzko and Śnieżnik Massifs are compatible with this path. (Kądziałko-Hofmokl et al. 2003, 2013). Generally speaking, the many-year study of the Sudetic rocks brought numerous interesting results concerning palaeomagnetic data, rock-magnetic and magnetic mineralogical data and data joining anisotropy of magnetic susceptibility with tectonics.

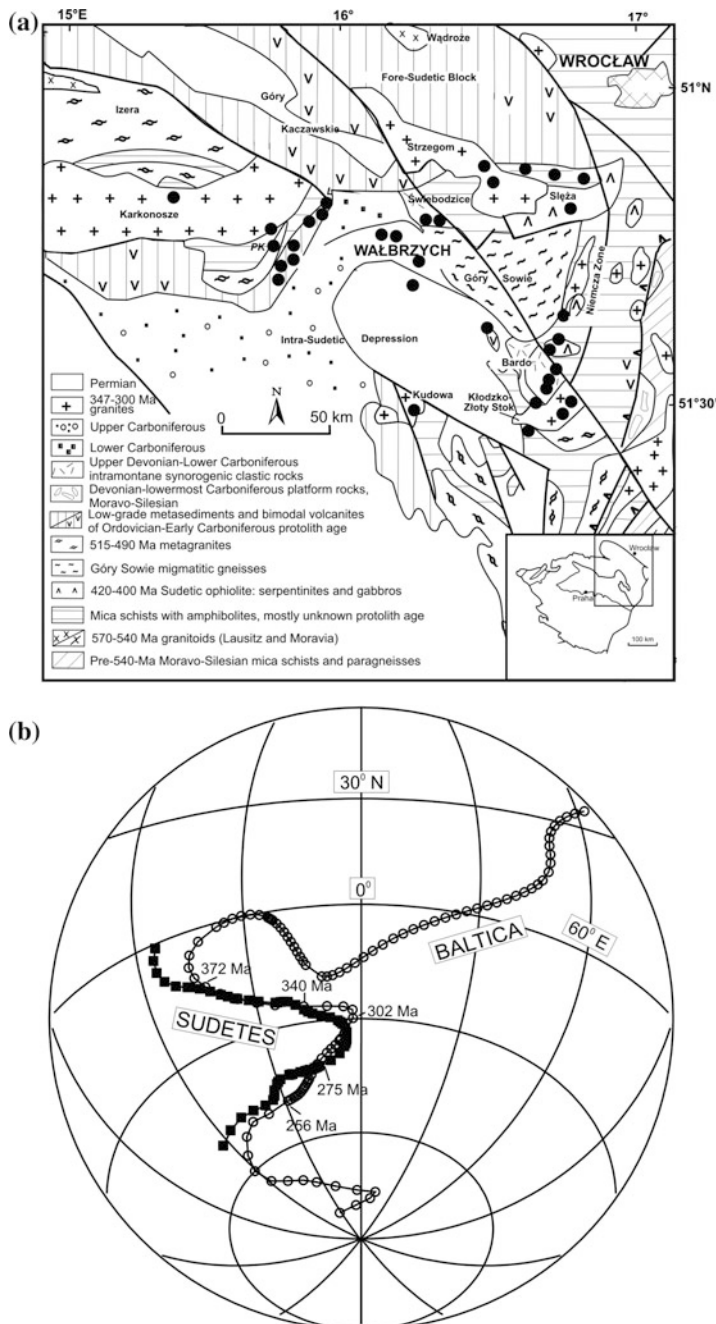


Fig. 3 **a** Geological sketch map of the West Sudetes showing sites of sampling for palaeomagnetic studies. Inset shows position of the study area in the Bohemian Massif. **b** The comparison of the APWP for Sudetes (squares) and for Baltica (open circles). Modified after Jeleńska et al. (2003)

In 1990s Maria Jeleńska returned to the previous study of influence of compression on remagnetization (Jeleńska and Kapicka 1999) and investigated anisotropy of magnetic susceptibility of rocks from the Sudetes (Werner et al. 2000) and also from Brittany (in the frame of cooperation with France, Lefort et al. 2001). Magdalena Kądziałko-Hofmokl with Maria Jeleńska and group of mineralogists performed numerous rock-magnetic experiments identifying magnetic chromitites (Kądziałko-Hofmokl et al. 2008), surface oxidized magnetites (Kądziałko-Hofmokl 2001), hemoilmenites rich in ilmenite part present in Sudetic ophiolitic rocks and in Kłodzko metamorphic rocks (Kądziałko-Hofmokl et al. 2003). In the same years Maria Jeleńska and Elżbieta Król investigated Miocene deposits from the Carpathian Foredeep obtaining local magnetostratigraphic scale (Król and Jeleńska 1999).

The cooperation with Slovakia, continued in these years, concerned palaeomagnetism of Triassic sediments and serpentinites from Silica and Meliata units, as well as Carboniferous sediments from Gosau Group. The authors showed that rocks were remagnetized during the latest Cretaceous when the study area was of African affinity (Tunyi et al. 2008). The other problems investigated in the frame of cooperation with Slovakia concerned palaeomagnetism and anisotropy of magnetic susceptibility of Palaeozoic rocks from Gemerides (Kruczyk et al. 2000) and Slovak part of Pieniny Klippen Belt (Jeleńska et al. 2011b).

Marek Lewandowski in the 1990s continued palaeomagnetic studies of Palaeozoic units of Holy Cross Mountains. His works concerning Małopolska and Łysogóry blocks brought evidence of shift of the Małopolska block against Łysogóry during the Variscan orogeny (Lewandowski 1993). Investigating calcite veins occurring in Holy Cross Mts he showed the possibility of dating diamagnetic rocks by palaeomagnetic methods (Lewandowski 1999). The results of his further study of the Holy Cross Mts. performed together with the French group from the University of Lille (France) were presented in several articles (Lamarche et al. 1999; Lamarche et al. 2003; Lamarche et al. 2002; Lacquement et al. 2005). In the same years together with scientist from Denmark he studied origin of natural magnetic remanence of Cambrian sandstones from Nexø (Lewandowski and Abrahamsen 2003). His scientific interests were focused on Pangaea applying palaeomagnetic and palaeoclimatic data for revealing its history (Lewandowski 2003, Fig. 4) and showing palaeomagnetic evidence of formation of proto-ocean Magura during the Middle-Upper Jurassic (Lewandowski et al. 2005). In 2005 Lewandowski together with a Croatian team began palaeomagnetic studies of Permian-Mesozoic rocks of Dinarides (Lewandowski et al. 2009) and performed rock-magnetic study of pre-Cenozoic rocks of Croatia (Lewandowski et al. 2012).

In 1990 the Palaeomagnetic Laboratory was joined by Tomasz Werner who, after obtaining M.Sc. degree under supervision of Maria Jeleńska (Werner and Jeleńska 1992), spent 2 years in Canada (1991–1993), at the Lakehead University, studying application of magnetic anisotropy for tectonic problems under direction of Dr G. Borradaile (Borradaile et al. 1993c, d; Werner 1993; Borradaile et al. 1994; Werner and Borradaile 1996). He also got familiar with magnetic hysteresis studies with a new high-sensitivity equipment (Borradaile et al. 1993a, b) taking part in some pioneering studies of hysteresis properties of single crystals (Borradaile and

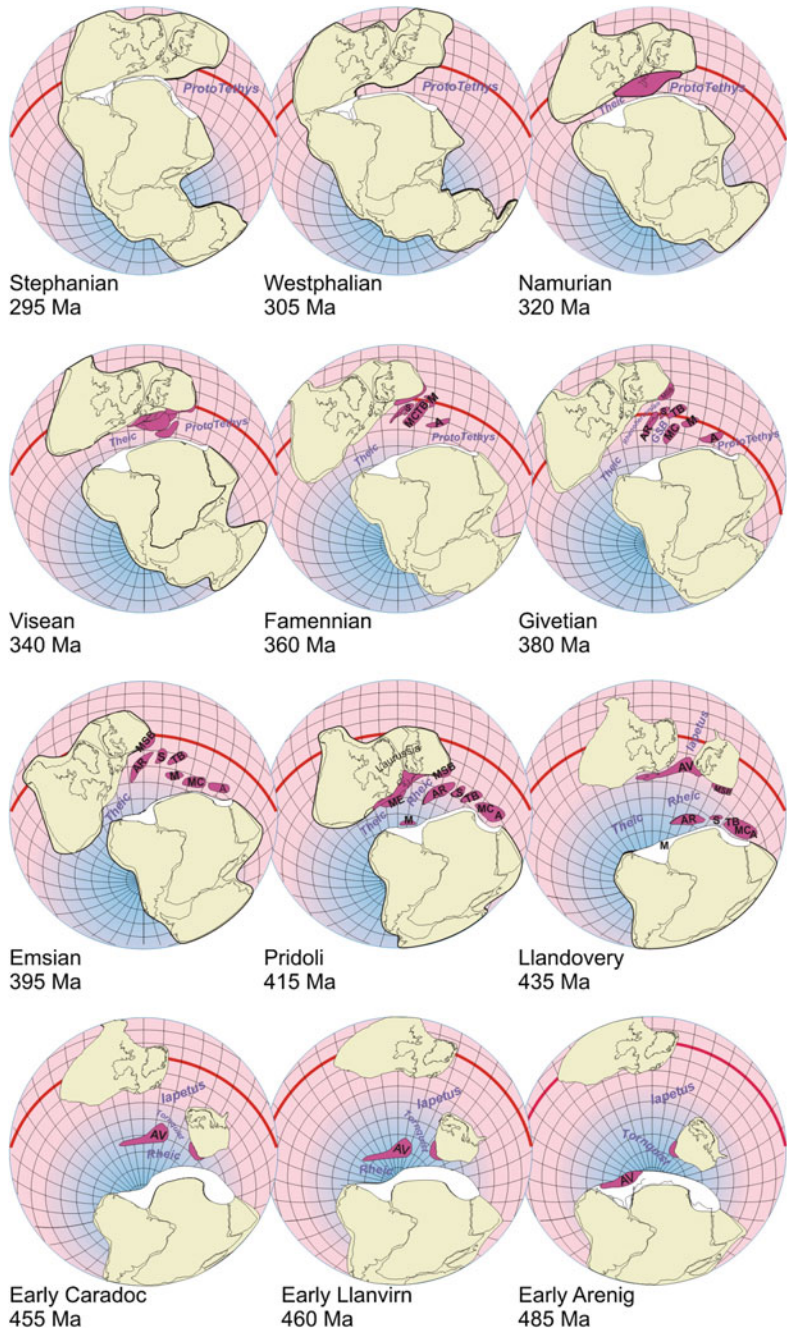
Werner 1994). The collaboration in both fields with Canadian team continued until the early 2000s, resulting in papers on tectonics (Borradaile et al. 1999; Borradaile et al. 1993a, b) and hysteresis studies of tektites (Werner and Borradaile 1998). After returning to Poland he focused on the applicability of methods of magnetic fabrics (AMS, AARM) for tectonic problems for the Sudetes (Jeleńska et al. 1996; Werner 1997; Werner et al. 2000; Jeleńska and Werner 1997; Jeleńska et al. 2000; Jeleńska et al. 2002a, b; Kądziałko-Hofmokl et al. 2004; Werner and Białek 2004). The problems of anisotropy served as a basis of his dissertation performed under supervision of M. Jeleńska (Werner 2002). He also took part in the studies coordinated by Maria Jeleńska of magnetic anisotropy of rocks from borehole cores from Borek Strzeliński (Jeleńska et al. 1996) and regional anisotropy studies of Rudawy Janowickie (Jeleńska et al. 2000). Studies of magnetic anisotropy were continued by Maria Jeleńska in cooperation with dr E. Márton from Etvos Geophysical Laboratory from Budapest dealing with anisotropy of remanence and its applications in palaeomagnetism (Márton et al. 2009).

In next years he used the potential of our rockmagnetic equipment in studies of hysteresis properties and magnetic fabrics of various rock collections mostly in collaboration with the palaeomagnetic team of the Polish Geological Institute (e.g., Nawrocki et al. 2005; Nawrocki et al. 2008a, b). Since 2007s he also took part in the palaeomagnetic studies of Śnieżnik-Orlica massif (Kądziałko-Hofmokl et al. 2013) and palaeomagnetism of Palaeozoic and Mesozoic rock units in Dinarides (in Marek Lewandowski group). Thanks to activity of T. Werner, the labs' software for palaeomagnetic and magnetic fabric analysis was continuously modified and upgraded.

In the 1990s Maria Jeleńska begun to continue the study of Palaeozoic rocks in the eastern part of Europe—in the Podole region (Ukraine) in cooperation with V. Bakhmutov from the Institute of Geophysics of the Ukrainian Academy of Sciences. The results obtained for Silurian (Jeleńska et al. 2005) and, later, Devonian (Bakhmutov et al. 2012) sediments reveal primary Silurian and Devonian poles and Permian remagnetization of rocks with Permian pole positions shifted against the reference Torsvik's APWP in the same way, as observed for the Sudetic results.

In 2000 Magdalena Kądziałko-Hofmokl, in 2001 Maria Jeleńska, and in 2006 Marek Lewandowski obtained the scientific titles of professor. In 2004 Marek Lewandowski became the deputy director of the Institute of Geological Sciences PAS and since 2008 he is a director of the Institute of Geological Sciences PAS but remained employed for part time in our laboratory.

In 1997 the palaeomagnetic team was joined by Rafał Szaniawski, who prepared his M.Sc. thesis under supervision of Prof. Marek Lewandowski and Prof. Michał Szulczewski from the Warsaw University and continued to study palaeomagnetism of Holy Cross Mts. In a short time he gained a competition for a co-tutelle Ph.D. fellowship for the years 1998–2003 and begun his investigations partly in our Laboratory and partly in the Lille 1 University (France). He expanded study of European Variscans further to the west with his thesis concerning palaeomagnetism and tectogenesis of European Variscans of Northern France and



◀Fig. 4 Continents disposition in the Pangea-A reconstruction. Main continents: Ba, Baltica; Ga, Gondwana; La, Laurentia. Crustal units related to the Avalonian–Cadomian orogenic belt (ACOB) in red. A, Alpine basement units; AR, Armorica; AV, Avalonia (Western and Eastern, not separated); FL, Florida composite unit (including Oxaquia/Yucatan—OX, and Carolina—CA; unseparated); M, Moravian; MC, Massif Central–Moldanubia; ME, Meguma; MSB, Małopolska–Silesian Massifs (unseparated); S, Saxothuringian; TB, Tepla–Barrandian; White area, presumable extend of the ACOB remnants in the North Africa (most speculative in the easternmost sector). Boundaries and configuration of the ACOB crustal units compiled from various sources (see text). Equator is drawn by a *red line*. Climatic zonations are crudely shown by shades transforming from *blue* (cold realm) to *pink* (warm realm) colors. Equal area projection, grid every 10°. Palaeogeographic time-slices for 485–295 Ma. Modified after Lewandowski (2003)

Southern Belgium (Lewandowski et al. 1999; Szaniawski et al. 2003; Averbuch et al. 2002, 2006; Lacquement et al. 2005). After finishing of his thesis he performed interdisciplinary study in the Holy Cross Mts (Szaniawski 2008; Szaniawski and Lewandowski 2009; Szaniawski et al. 2011) and Carpathians in cooperation with the Geological Faculty of Warsaw University, Polish Geological Institute, and universities in Padua and Naples (Italy) (Grabowski et al. 2009, Szaniawski et al. 2012; Mazzoli et al. 2010; Zattin et al. 2011; Szaniawski et al. 2013, Andreucci et al. 2013) as well as Apennines (Mazzoli et al. 2012). He was a leader of one and co-author of three scientific projects, concerning the study of the Inner Carpathians in SE Poland and Western Ukraine, palaeomagnetism of Devonian carbonates in the Holy Cross Mts., Early Palaeozoic tectonics of the southern part of Holy Cross Mts, and palaeogeography of Baltica in the Early Palaeozoic based on the study of Bornholm deposits.

The palaeomagnetic study in polar regions led earlier by Maria Jeleńska and Marek Lewandowski is continued by Dr Krzysztof Michalski, who joined the Laboratory in 2001. After finishing in 1999 his M.Sc. thesis prepared at the Faculty of Geology of the University of Warsaw under the supervision of Prof. Marek Lewandowski he took part in winter expedition to Polish Polar Station in Hornsund in the season 1999–2000, where he begun his first palaeomagnetic project dealing with Spitsbergen rocks (S Wedel Jarlsberg Land, SW Torell Land). In the years 2002, 2004, and 2006, he was the leader of three other palaeomagnetic expeditions to southwestern and western Spitsbergen where he collected material for his Ph.D. thesis concerning palaeotectonics and palaeogeography of southern Spitsbergen based on the palaeomagnetic study of Cambrian, Carboniferous and Devonian rocks (Michalski and Lewandowski 2004; Błażejowski et al. 2006; Szlachta et al. 2008). He was also the coordinator of two projects funded by the Polish State Committee for Scientific Research concerning palaeomagnetism of southern Spitsbergen). In 2006 he was also leader of international group preparing interdisciplinary geo-physical—geological—oceanological investigations of the Franz Joseph Land Archipelago, Russian Arctic. After finishing his Ph.D. thesis in 2007 he continued his investigations concerning palaeogeography and tectonics of the NW sector of the Barents Sea and extended his study to all “so called” Svalbard Caledonian terranes (including Nordaustlandet). In 2008 he started close cooperation in this

matter with the Department of Geology of University of Warsaw and University of Greenwich (UK) and in 2009 with Natural History Museum of London (UK). The compilation of palaeomagnetic results from southern Spitsbergen and $^{40}\text{Ar}/^{39}\text{Ar}$ isotopic datings of Billefjorden Fault Zone bounding Central and Western Caledonian Terranes (Dr Geoffrey Manby—Natural History of London) resulted in definition of the final age of the strike-slip movements along Svalbard Caledonian terranes (Michalski et al. 2012). From 2012 he is the leader of the project “Integration of palaeomagnetic, isotopic and structural data to understand Svalbard Caledonian Terranes assemblage (2012–2015)” funded by Polish National Science Centre. According to the project he led the following two expeditions to western Spitsbergen (2012) and northern Spitsbergen and western Nordaustlandet (2013). In 2013 he was one of the main coordinators of international geological workshop SvalGeoBase “Proterozoic and Lower Palaeozoic basement of Svalbard: state of knowledge and new perspectives of investigations” which took place in Svalbard, 1–8 September 2013 (the initiative and coordination of the Institute of Geophysics PAS, AGH University of Sciences and technology in Cracow and Norsk Polar Institute, Norway).

In 2001 Maria Jeleńska initiated study of environmental magnetism by obtaining a NATO grant for investigations of polluted and non-polluted soils in the Ukraine. The study was performed together with Ph.D. student Agata Hasso-Agopsowicz in cooperation with the University of Kiev (Jeleńska et al. 2004, 2008). In the next years M. Jeleńska organized a group consisting of Elżbieta Król, Beata Górkakoszubiec (who came to the Institute in 2008) and joined lately by the Ph.D. student Sylwia Dytłow. They perform thorough investigations in the Warsaw agglomeration concerning pollution of soil in numerous places of the town of various traffic, pollution retained by tree leaves, and pollution of domestic dust. In the project in cooperation with Miele company the map of pollution in Warsaw was constructed showing regions of higher and lower pollution (“Odkurzona Warszawa” 2012, Fig. 5). The project had a high public relations impact resulting in numerous interviews in TV, radio and press given by team members. The magnetometric method of investigation of dust pollution brings information about presence of heavy metals, that are often a cause of such illnesses as cancer, allergies, asthma. Results presented in Jeleńska et al. (2011a) and Król et. al. (2013) showed how important for health of the Warsaw population is the monitoring of pollution of outdoor and indoor dust.

At the end of 2000s Maria Jeleńska and Magdalena Kądziałko-Hofmokl joined the French group from the Centre de Géosciences, École des Mines de Paris, Fontainebleau, France (M.Thiry, Ch. Franke) in palaeomagnetic investigations of Carboniferous granitic rocks in Karkonosze Mts. The main purpose of this study concerns phenomenon of albitization of Carboniferous granitoids appearing in the European Variscan province during the Triassic. The data summarizing results from numerous regions of the European Variscans were presented up to now during several international conferences (Franke et al. 2010).

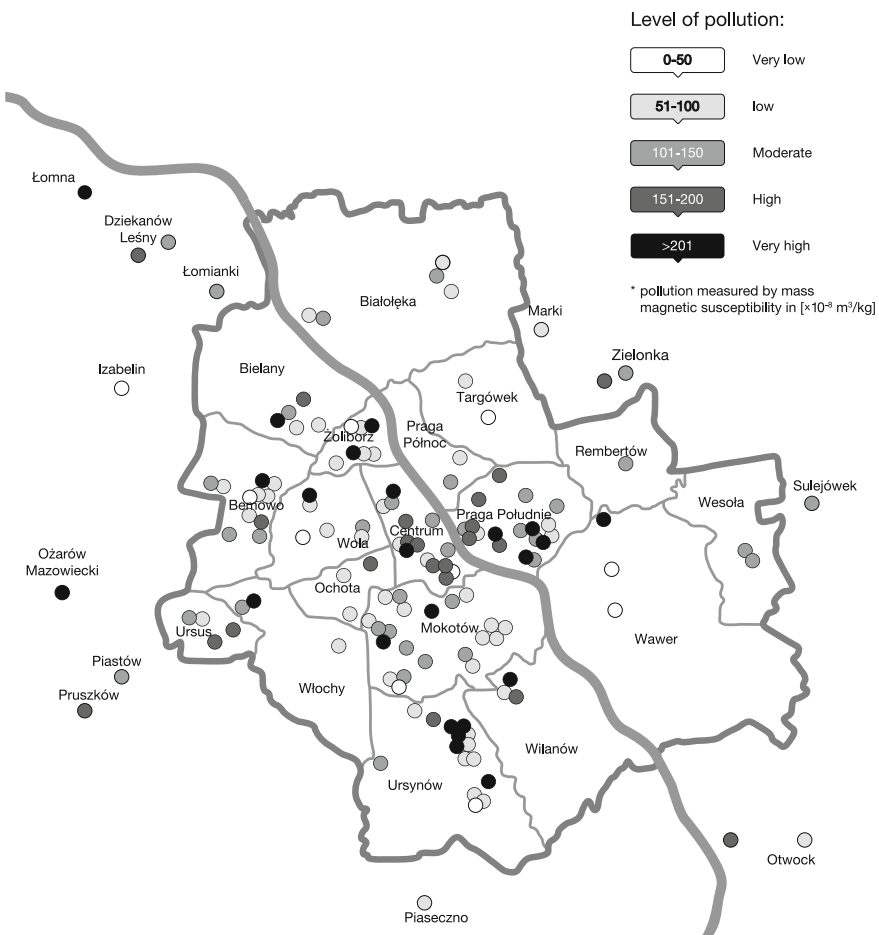


Fig. 5 Map of magnetic susceptibility of indoor dust in Warsaw (project Odkurzona Warszawa, cooperation with Miele in 2012)

5 The Development of the Laboratory Infrastructure Since 1990

At the beginning of 1990s, as it was mentioned before the laboratory gained the first high class equipment (cryogenic magnetometer SQUID, modern Magnetic Measurements furnace and low-field magnetic cage) that was the base for standard palaeomagnetic research for a growing team of palaeomagnetists and studies of new rock sample collections.

In 1990s the lab was gradually equipped with new devices for rock magnetic studies. We have obtained AF demagnetizer with a possibility of inducing anhysteretic remanence (LDA, 1998, Agico, Czech Republic) that let us to employ

methods of anhysteretic remanence and anisotropy of remanent magnetization. With a purchase of vibrating sample magnetometer (VSM, 1995, Molspin, Gr. Britain) we could start measurements of magnetic hysteresis of rock samples. More detailed experiments of magnetic hysteresis properties of small and low-susceptible samples (rock pieces, dusts and soils) were initiated after obtaining much more sensitive AGM 2900 MicroMag unit (2004, Princeton Measurements, USA).

Since the late 1990s we were able to measure the changes of magnetic susceptibility with temperature in the range of -196 to 700°C thanks to susceptibility bridge KLY3S/CS-3/CS-L (AGICO, Czech Republic). The use of this equipment let us determine Curie temperatures and temperatures of low-temperature transitions characteristic for magnetic minerals present in rocks. It also helped us to speed up the measurements of anisotropy of magnetic susceptibility comparing to older KLY-2 kappabridge. The laboratory obtained also two pulse magnetizers: one with 1.2T maximum field (SI6 by Sapphire Instruments, Canada) for IRM anisotropy studies and later MMPM10 (by Magnetic Measurements, UK) enabling magnetization of specimens of 10 cm^3 to 3 T and specimens of 1 cm^3 to 9 T.

The determinations of blocking temperatures of ferromagnetic phases was continued thanks to new generations of thermomagnetic system (STEPS3/ STEPS4) by TUS Poland. Problems with an old heavily used thermal demagnetizer MMTD18 performing day after day heating-cooling runs for 20 years were overcome when a new high capacity furnace (for 80 specimens) was obtained in 2009 (MMTD80, Magnetic Measurements, UK) that made palaeomagnetic measurements more effective.

The expansion of projects dealing with environmental magnetism required new multifrequency susceptibility bridge. We obtained in 2010 a MFK1 magnetic susceptibility meter (Agico, Czech Republic) that operated in fields of three various frequencies and varying field intensities that we found especially useful in study of environmental pollution. In the last years, the laboratory was also equipped in some devices for sample preparations and separations as well as with optical microscope. The environmental group was equipped with devices for measuring soil parameters such as pH, organic content and granulometry. A new device for low and high temperature studies of magnetic hysteresis properties (Advanced Variable Field Translation Balance, Magnetic Measurements, UK) was ordered in 2013.

In the last 25 years we have managed to keep most of the equipment in running conditions. The only pieces of equipment that have finished their 30 years' service are two JR4 spinner magnetometers and this gap has to be filled promptly.

Now the Laboratory is very well equipped and the working group deals with numerous various problems from palaeomagnetism of oldest rocks to every-day problems of pollution. We have decided to have the laboratory included in the EPOS laboratory framework and Dr Tomasz Werner was appointed the Polish representative in Working Group 6 of EPOS project. EPOS project correlates well with our policy to accept short-term visits of guest to use our facilities (mostly from Ukraine, Russia, Egypt).

In 1990, after the retirement of Jadwiga Kruczyk, the head of the Laboratory became Magdalena Kądziałko-Hofmokl. She held the positions till 2009 when she was replaced by Tomasz Werner.

During 50 years our laboratory served for 12 Ph.D. projects of our team members and students, and 4 habilitation projects. The laboratory infrastructure has been also extensively used for longer projects of students and guests from other institutions preparing their Ph.D. or M.Sc. thesis under the supervision of our lab' members.

Marek Lewandowski was the supervisor of M.Sc thesis of Jerzy Nawrocki and Jacek Grabowski. Magdalena Kądziałko-Hofmokl was a Ph.D. thesis supervisor for Jerzy Nawrocki (in 1994), present director of Polish Geological Institute, and Jacek Grabowski (in 1999), presently in the Polish Geological Institute. Marek Lewandowski supervised Ph.D. project of Piotr Ziółkowski (in 2007) from the Warsaw University. Rafał Szaniawski partly supervised M.Sc. project of Joanna Roszkowska (in 2008) from the Warsaw University and M.Sc. project of Benedetta Andreucci from University of Bologna (Italy). Our facilities were also used by students from other institutions for short term measurements of selected rockmagnetic parameters.

6 Conclusions

Numerous palaeomagnetic results obtained in our laboratory are in the world data palaeomagnetic bases and on Apparent Polar Wander Paths constructed for various regions. Studies of anisotropy of magnetic susceptibility brought interesting results concerning problems of tectonics, studies of rock-magnetic properties helped to identify carriers of primary and secondary components of natural magnetic remanence in many cases. Results obtained by the group studying very important problems connected with environmental magnetism by application of magneto-metric methods bring important knowledge concerning air and soil pollution. The results have been published in international journals of high impact factor, as well as in national journals. Our palaeomagnetists, from the beginning, presented their achievements during numerous international and national conferences.

References

- Andreucci B, Castelluccio A, Jankowski L, Mazzoli S, Szaniawski R, Zattin M (2013) Burial and exhumation history of the Polish Outer Carpathians: Discriminating the role of thrusting and post-thrusting extension. *Tectonophysics* (in press). doi: [10.1016/j.tecto.2013.07.030](https://doi.org/10.1016/j.tecto.2013.07.030)
- Averbuch O, Lacquement F, Mansy JL, Szaniawski R, Lewandowski M (2006) Deformation along the northern front of the Variscan belt: example of the French-Belgium Ardennes in the Givet area. *Géol Fr* 1–2:85–90

- Averbuch O, Lacquement F, Szaniawski R, Mansy JL, Lewandowski M (2002) Segmentation of the Variscan thrust front (N France, S Belgium): insights into the geometry of the Devonian Rheno-Hercynian Basin. *Aardk Mededel Geologica Belgica* 12:89–92
- Bakhmutov V, Teisseyre-Jeleńska M, Kądziałko-Hofmokl M, Konstantinienko L, Poliaczenko E (2012) Paleomagnitnyje issledovanija nizniedewonskikh serocvietnykh otlozeniy Podoli. *Geofizicheskii Zhurnal* 34(6):1–11
- Błażejowski B, Hołda-Michalska A, Michalski K (2006) Schellwienia arctica (Fusulinidae) from the Carboniferous–Permian strata of the Treskeladden Formation, south Spitsbergen. *Pol Polar Res* 27(1):91–103
- Borradaile GJ, Chow N, Werner T (1993a) Magnetic hysteresis of limestones: facies control? *Phys Earth Planet Inter* 76:241–252. doi:[10.1016/0031-9201\(93\)90016-3](https://doi.org/10.1016/0031-9201(93)90016-3)
- Borradaile GJ, Kehlenbeck MM, Werner T (1994) A magnetotectonic study correlating late Archean deformation in northwestern Ontario. *Can J Earth Sci* 31(9):1449–1460. doi:[10.1139/e94-128](https://doi.org/10.1139/e94-128)
- Borradaile GJ, Kissin SA, Stewart JD, Ross WA, Werner T (1993b) Magnetic and optical methods for detecting heat treatment of chert. *J Archeol Science* 20:57–66. doi:[10.1006/jasc.1993.1004](https://doi.org/10.1006/jasc.1993.1004)
- Borradaile GJ, Lemmetty TJ, Werner T (2003a) Apparent polar wander paths and the close of late Archean crustal transpression, northern Ontario. *J Geophys Res* 108(B8):2402. doi:[10.1029/2002JB002379](https://doi.org/10.1029/2002JB002379)
- Borradaile GJ, Stewart RA, Werner T (1993c) Archean uplift of a subprovince boundary in the Canadian Shield, revealed by magnetic fabrics. *Tectonophysics* 227:1–15. doi:[10.1016/0040-1951\(93\)90083-V](https://doi.org/10.1016/0040-1951(93)90083-V)
- Borradaile GJ, Werner T (1994) Magnetic anisotropy of some of phyllosilicates. *Tectonophysics* 235:223–248. doi:[10.1016/0040-1951\(94\)90196-1](https://doi.org/10.1016/0040-1951(94)90196-1)
- Borradaile GJ, Werner T, Dehls JF, Spark RN (1993d) Archean regional transpression and paleomagnetism in northwestern Ontario, Canada. *Tectonophysics* 220:117–125. doi:[10.1016/0040-1951\(93\)90226-A](https://doi.org/10.1016/0040-1951(93)90226-A)
- Borradaile GJ, Werner T, Lagroix F (1999) Magnetic Fabrics and Anisotropy-controlled thrusting in the Kapuskasing Structural Zone, Canada. *Tectonophysics* 302:241–256. doi:[10.1016/S0040-1951\(98\)00292-3](https://doi.org/10.1016/S0040-1951(98)00292-3)
- Borradaile GJ, Werner T, Lagroix F (2003b) Differences in paleomagnetic interpretations due to the choice of statistical, demagnetization and correction techniques: Kapuskasing Structural Zone, northern Ontario, Canada. *Tectonophysics* 363(1–2):103–125. doi:[10.1016/S0040-1951\(02\)00667-4](https://doi.org/10.1016/S0040-1951(02)00667-4)
- Burlakaja SP, Kruczyk J, Małkowski Z, Nechayeva TB, Petrova GN (1969) Magnetic field in the southern Polish territory over the last thousand years. *Acta Geophys Pol* 17:165–179
- Creer KM, Hogg TE, Małkowski Z, Mojski E, Niedziółka-Król E, Readman PW, Tuchołka P (1979) Paleomagnetism of Holocene lake sediments from north Poland. *Geophys J Roy As Soc* 59:287–314. doi:[10.1111/j.1365-246X.1979.tb06768.x](https://doi.org/10.1111/j.1365-246X.1979.tb06768.x)
- Creer KM, Tuchołka P, Barton CE (eds) (1983) *Geomagnetism of Baked Clays*. Elsevier, Amsterdam, p 324
- Czyszek Z, Czyszek W (1976) Application of archeomagnetic method for archeological investigations. *Archeol Pol* 22(1):7–33
- Czyszek Z, Czyszek W (1987) Secular variations of the magnetic field in Poland from archeomagnetic studies. *Acta Geophys Pol* 35(2):187–211
- Franke Ch, Thiry M, Gomez-Gras D, Jeleńska M, Kądziałko-Hofmokl M, Lagroix F, Parcerisa D, Spassov S, Szuszkievicz A, Turniak K (2010) Paleomagnetic age constrains and magneto-mineralogical implications for the Triassic paleosurface in Europe. *EGU General Assembly 2010*, 2010EGUGA, p 7858
- Grabowski J, Michalik J, Szaniawski R, Grotek I (2009) Synthrusting remagnetization of the Krízna nappe: high resolution palaeo—and rock magnetic study in the Strazovce section, Strazovske vrchy Mts, Central West Carpathians (Slovakia). *Acta Geol Pol* 59(2):137–155

- Halvorsen E, Lewandowski M, Jeleńska M (1989) Palaeomagnetism of the Upper Carboniferous Strzegom and Karkonosze Granites and the Kudowa Granitoid from the Sudet Mts. Poland *Phys Earth Planet Int* 55:54–69. doi:[10.1016/0031-9201\(89\)90233-1](https://doi.org/10.1016/0031-9201(89)90233-1)
- Jeleńska M (1975) Stress dependence of magnetization and magnetic properties of igneous rocks. *PAGEOPH* 113(4):635–649. doi:[10.1007/BF0159948](https://doi.org/10.1007/BF0159948)
- Jeleńska M, Bakhmutov V, Konstantinenko L (2005) Paleomagnetic and rock magnetic data from the Silurian succession of the Dniester basin. Ukraine *Phys Earth Planet Inter* 149:307–320. doi:[10.1016/j.pepi.2004.10.005](https://doi.org/10.1016/j.pepi.2004.10.005)
- Jeleńska M, Górką-Kostrubiec B, Król E (2011) Magnetic properties of dust as indicators of indoor air pollution. In: Dudzińska MR (ed) Management of Indoor Air Quality, CRC Press, Taylor & Francis Group, p 129–137
- Jeleńska M, Hasso-Agopsowicz A, Kędziałko-Hofmokl M, Sukhorada A, Bondar K, Matviishina Zh (2008) Magnetic iron oxides occurring in chernozem soil from Ukraine and Poland as indicators of pedogenic processes. *Studia Geophys Geod* 52:255–270. doi:[10.1007/s11200-008-0017-z](https://doi.org/10.1007/s11200-008-0017-z)
- Jeleńska M, Hasso-Agopsowicz A, Kopcewicz B, Sukhorada A, Tyamina K, Kadzialko-Hofmokl M, Matviishina Z (2004) Magnetic properties of the profiles of polluted and non-polluted soils. A case study from Ukraine. *Geophys J Int* 159(1):104–116. doi:[10.1111/j.1365-246X.2004.02370.x](https://doi.org/10.1111/j.1365-246X.2004.02370.x)
- Jeleńska M, Kędziałko-Hofmokl M (1990) Dependence of temperature on anisotropy of magnetic susceptibility of rocks. *Phys Earth. Planet Int* 62:19–31. doi:[10.1016/0031-9201\(90\)90189-5](https://doi.org/10.1016/0031-9201(90)90189-5)
- Jeleńska M, Kędziałko-Hofmokl M, Kropek V, Povondra P (1978a) Magnetic properties of basaltic rocks from Lower Silesia and their relationship to petrological characteristics. *Časopis pro Min a Geol, Praha* 23(2):159–169
- Jeleńska M, Kędziałko-Hofmokl M, Kruczyk J, Vincenz SA (1978b) Thermomagnetic properties of some Late Mesozoic diabase dikes of South Spitsbergen. *PAGEOPH* 117(4):784–794. doi:[10.1007/BF00879979](https://doi.org/10.1007/BF00879979)
- Jeleńska M, Kędziałko-Hofmokl M, Źelaźniewicz A (2003) The Devonian-Permian APWP for the West Sudetes, Poland. *Stud Geophys Geod* 47:419–434. doi:[10.1023/A:1023788127994](https://doi.org/10.1023/A:1023788127994)
- Jeleńska M, Kapička A (1999) Preliminary results of chemical remagnetization under uniaxial compression. *Phys Chem Earth, part A Solid Earth and Geodesy* 24(9):759–762. doi:[10.1016/S1464-1895\(99\)00111-8](https://doi.org/10.1016/S1464-1895(99)00111-8)
- Jeleńska M, Tunyi I, Aubrecht R (2011b) Low-latitude Oxfordian position of the Oravic crustal segment (Pieniny Klippen Belt, Western Carpathians). *Paleogeography, Palaeoclimatology, Palaeoecology* 302(3–4):338–348. doi:[10.1016/j.palaeo.2011.01.021](https://doi.org/10.1016/j.palaeo.2011.01.021)
- Jeleńska M, Werner T, Król E (1996) Paleomagnetic and rock magnetic study of ultramafic and gabbroic rocks from boreholes in the Sudetes, Poland. *Acta Geoph Pol* 46(4):361–382
- Jeleńska M, Werner T, Mazur St (2000) Paleomagnetic and rock magnetic study of the Early Paleozoic metamorphic complex of Rudawy Janowickie (West Sudetes; Poland). *Geologica Carpathica* 51(3):172–173
- Jeleńska M, Werner T, Mazur St (2002a) A paleomagnetic and rock magnetic properties of the Lower Paleozoic metamorphic complex of the Rudawy Janowickie (West Sudetes, Poland). *Geologica Carpathica* 54(5):283–294
- Jeleńska M, Werner T, Mazur St (2002b) The comparison of tectonic and magnetic fabric (AMS and AARM) in a thrust unit: an example from metamorphic series of Rudawy Janowickie (SW Poland). *Quaderni di Geofisica* 26:65–67
- Jeleńska M, Werner T (1997) Magnetic anisotropy parameters for the ultramafic and the gabbroic rocks from three boreholes from the Sudetes, Poland. *Phys Chem Earth* 22(1–2):161–165. doi:[10.1016/S0079-1946\(97\)00096-7](https://doi.org/10.1016/S0079-1946(97)00096-7)
- Kędziałko-Hofmokl M (1981) Magnetic anisotropy of magmatic rocks and its relationship to other magnetic characteristics (statistical analysis). *Acta Geophys Pol* 29(1):21–32
- Kędziałko-Hofmokl M (2001) Rock-magnetic study of the Gogołów-Jordanów serpentinite unit of the Paleozoic Sudetic ophiolite (South Poland). *Ophioliti* 26(2B):425–431. doi:[10.4454/ophioliti.v26i2b.164](https://doi.org/10.4454/ophioliti.v26i2b.164)

- Kądziałko-Hofmokl M, Delura K, Bylina P, Jeleńska M, Kruczyk J (2008) Mineralogy and magnetism of Fe–Cr spinel series minerals from podiform chromitites and dunites from Tąpadła (Sudetic ophiolite, SW Poland) and their relationship to palaeomagnetic results of the dunites. *Geophys J Int* 175:885–900. doi:[10.1111/j.1365-246X.2008.03933.x](https://doi.org/10.1111/j.1365-246X.2008.03933.x)
- Kądziałko-Hofmokl M, El-Hemaly IA (1997) Paleomagnetism of carboniferous sediments from the West Sudetes (SW Poland). *Geol Mijnbouw* 76(1–2):97–104. doi:[10.1023/A:1003189215073](https://doi.org/10.1023/A:1003189215073)
- Kądziałko-Hofmokl M, Kruczyk J (1968) Low temperature investigations of the composition of magnetic fraction of rocks. *Acta Geophys Pol* 16(3):249–255
- Kądziałko-Hofmokl M, Kruczyk J (1976) Complete and partial self-reversal of natural remanent magnetization in basaltic rocks from Lower Silesia. *PAGEOPH* 114:207–213. doi:[10.1007/BF00878946](https://doi.org/10.1007/BF00878946)
- Kądziałko-Hofmokl M, Kruczyk J, Mazur S, Siemiątkowski J (2003) Paleomagnetism of the Upper Proterozoic and Devonian rocks from the Kłodzko Metamorphic Complex in the West Sudetes (SW Poland): tectonic implications for the Variscan belt of Central Europe. *Tectonophysics* 377:83–99. doi:[10.1016/j.tecto.2003.08.021](https://doi.org/10.1016/j.tecto.2003.08.021)
- Kądziałko-Hofmokl M, Kruczyk J, Siemiątkowski J (2003) Identification of magnetic minerals in paleomagnetism. Papers of the Meeting of the Mineralogical Society of Poland and the Conference Perspectives of the Progress of Mineralogical Sciences in Poland. Cieszyn, 22, 19–20.09.2003
- Kądziałko-Hofmokl M, Mazur S, Werner T, Kruczyk J (2004) Relationship between magnetic and structural fabrics revealed by the Variscan basement rocks subjected to heterogenous deformation—a case study from the Kłodzko Metamorphic Complex (Central Sudetes, Poland). *Magn Fabr: Methods and Appl, Geol Soc London, Spec Pub* 238:475–491. doi:[10.1144/GSL.SP.2004.238.01.24](https://doi.org/10.1144/GSL.SP.2004.238.01.24)
- Kądziałko-Hofmokl M, Szczepański J, Werner T, Jeleńska M, Nejbert K (2013) Paleomagnetism and magnetic mineralogy of metabasites and granulites from Orlica-Śnieżnik Dome (Central Sudetes). *Acta Geophys* 61(3):535–568. doi:[10.2478/s11600-012-0092-y](https://doi.org/10.2478/s11600-012-0092-y)
- Kądziałko-Hofmokl M, Kruczyk J (1987) Paleomagnetism of Middle-Late Jurassic sediments from Poland and implications for polarity of the geomagnetic field. *Tectonophysics* 139:53–66. doi:[10.1016/0040-1951\(87\)90197-1](https://doi.org/10.1016/0040-1951(87)90197-1)
- Król E, Górka-Kostrubiec B, Jeleńska M (2013) The magnetometric study of indoor air pollution inside flats located in Warsaw and its suburbs. *Environ Eng IV* Ed by Lucjan Pawłowski CRC Press 2013:323–328. doi:[10.1201/b14894-50](https://doi.org/10.1201/b14894-50)
- Król E, Jeleńska M (1999) The local magnetostatigraphic scale for the supra-evaporitic Miocene deposits in the northern party of Carpathian Foredeep and its stratigraphic implications (drill-core Jamnica S-119). *Geol Q* 43(4):509–518
- Król E, Lang B, Siemiątkowski J (1996) The magnetic properties of the Baszkówka L5 chondrite. *Geol Carpath* 47(3):193–194
- Kruczyk J (1970) Paleomagnitnyje issledovanija andezitovykh intruzij iz gory Vzhar. *Publ Inst Geophys Pol Ac Sci* 35:35–83
- Kruczyk J (1978) Study of phase transition in iron sulphides using the TSEE method. *Acta Geophys Pol* 26:191–204
- Kruczyk J (1983) Phase transitions in iron oxides and sulphides and their relations to magnetic properties of rocks. *Publ Inst Geophys Pol Ac Sc* 164:C15
- Kruczyk J, Kądziałko-Hofmokl M (1988) Polarity of the geomagnetic field during the Callovian. In: 2nd International Symposium on Jurassic Stratigraphy 1139–1150
- Kruczyk J, Kądziałko-Hofmokl M, Jeleńska M (1980) Paleomagnetic and rock magnetic study of Jurassic sediments from Cracow Upland (Southern Poland). *Acta Geophys Pol* 29(4):309–323
- Kruczyk J, Kądziałko-Hofmokl M, Jeleńska M, Birkenmajker K, Arakelyants MM (1977) Tertiary polarity events in Lower Silesian basalts and their K-Ar age. *Acta Geophys Pol* 25(3):183–191

- Kruczyk J, Kądziałko-Hofmokl M, Jeleńska M, Tunyi I, Grecula P, Navesnak D (2000) Tectonic and structural implications of paleomagnetic and AMS study of highly metamorphosed Paleozoic rocks from Gmeric Superunit, Slovakia. *Geologica Carpathica* 51(3):133–144
- Kruczyk J, Kądziałko-Hofmokl M, Lefeld J, Pagač P, Tunyi I (1992) Paleomagnetism of oroclinal bending of the Western Inner Carpathians. *Tectonophysics* 196:315–324. doi:[10.1016/0040-1951\(92\)90383-H](https://doi.org/10.1016/0040-1951(92)90383-H)
- Kruczyk J, Kądziałko-Hofmokl M, Nozharov N, Nachev I (1988) Paleomagnetism of Jurassic sediments from Balkan, Bulgaria. *Acta Geophys Pol* 36(1):49–62
- Kruczyk J, Kądziałko-Hofmokl M, Nozharov P, Petkov N, Nachev I (1990) Paleomagnetic studies on sedimentary Jurassic rocks from Southern Bulgaria. *Phys Earth Planet Int* 62:82–96. doi:[10.1016/0031-9201\(90\)90194-3](https://doi.org/10.1016/0031-9201(90)90194-3)
- Lacquement F, Averbuch O, Mansy JL, Szaniawski R, Lewandowski M (2005) Transpressional deformations At Lateran boundaries of propagating thrust-sheets;the example of the Mouse Valley Recess within the Ardennes Variscan fold-and thrust belt (N France-S Belgium). *J Struct Geol* 27:1788–1802. doi:[10.1016/j.jsg.2005.05.017](https://doi.org/10.1016/j.jsg.2005.05.017)
- Lamarche J, Bergerat F, Lewandowski M, Mansy JL, Świdrowska J, Wieczorek J (2002) Variscan to Alpine heterogenous palaeo-stress field above a major paleozoic suture in the Carpathian foreland (southeastern Poland). *Tectonophysics* 357(1–4):55–80. doi:[10.1016/S0040-1951\(02\)00362-1](https://doi.org/10.1016/S0040-1951(02)00362-1)
- Lamarche J, Lewandowski M, Mansy JL, Szulczewski M (2003) Partitioning pre-syn- and post-Variscan deformation In the HolyCross Mts, eastern Variscan foreland. In: Mc Cann T, Saintot A (eds) Tracing Tectonic Deformation using the sedimentary record. *Geol Soc London Spec Publ* 208:159–184. doi:[10.1144/GSL.SP.2003.208.01.08](https://doi.org/10.1144/GSL.SP.2003.208.01.08)
- Lamarche J, Mansy JL, Bergerat F, Averbuch O, Hakenberg M, Lewandowski M, Stupnicka E, Świdrowska J, Wajsprych B, Wieczorek J (1999) Variscan tectonics in the Holy Cross Mts (Poland) and the role of structural inheritance during Alpine tectonics. *Tectonophysics* 313:171–186. doi:[10.1016/S0040-1951\(99\)00195-X](https://doi.org/10.1016/S0040-1951(99)00195-X)
- Lefort JP, Aifa T, Jeleńska M, Kądziałko-Hofmokl M, Max MD (2001) Paleomagnetic and AMS evidence for a Variscan ductile clockwise rotation of the ile de Groix blueschists (South Brittany, France): consequence on the Late Hercynian structural pattern of westernmost Europe. *Tectonophysics* 337(3–4):223–235. doi:[10.1016/S0040-1951\(01\)00118-4](https://doi.org/10.1016/S0040-1951(01)00118-4)
- Lewandowski M (1981) Post-folding characteristic of remanent magnetization of the Upper Devonian Kostomłoty Beds in the Holy Cross Mts. *Acta Geophys Pol* 31(3–4):265–272
- Lewandowski M (1993) Paleomagnetism of the Paleozoic rocks of the Holy Cross Mts (Central Poland) and the origin of the Variscan Orogeny. *Publ Inst Geophys Pol Ac Sci A* 23(265):1–85
- Lewandowski M (1999) A paleomagnetic study of fracture fills in the Holy Cross Mountains of Central Poland and its application in dating tectonic processes. *Geoph J Int* 317:783–792. doi:[10.1046/j.1365-246x.1999.00815.x](https://doi.org/10.1046/j.1365-246x.1999.00815.x)
- Lewandowski M (2003) Assembly of Pangea: combined paleomagnetic and paleoclimatic approach. *Adv Geophys* 46:199–236. doi:[10.1016/S0065-2687\(03\)46003-2](https://doi.org/10.1016/S0065-2687(03)46003-2)
- Lewandowski M, Abrahamsen N (2003) Paleomagnetic results from the Cambrian and Ordovician sediments of Bornholm (Denmark) and Southern Sweden and paleogeographical implications for Baltica. *J Geophys Res* 108(B11):2516. doi:[10.1029/2002JB002281](https://doi.org/10.1029/2002JB002281)
- Lewandowski M, Krobicki M, Matyja BA, Wierzbowski A (2005) Paleogeographic evolution of the Pieniny Klippen Basin using stratigraphic and palaeomagnetic data from the Veliky Kamenets section (Carpathians, Ukraine). *Palaeogeogr Palaeoclimatol Palaeoecol* 216(1–2):53–72. doi:[10.1016/j.palaeo.2004.10.002](https://doi.org/10.1016/j.palaeo.2004.10.002)
- Lewandowski M, Mansy JL, Averbuch O, Lamarche J, Szaniawski R (1999) Paleomagnetic dating of brittle tectonic structures: case studies on Ferques Fault (Boulonnais, France) and two faults from the Holy Cross MTS (Poland). *CR Geosci* 329:495–502
- Lewandowski M, Nowożyński K, Werner T (1997) PDA-package of FORTRAN programs for paleomagnetic analysis. Unpublished

- Lewandowski M, Velic I, Sidorczuk M, Vlahovic I, Velic J (2009) First rock-magnetic and paleomagnetic analyses of the Pre-Cenozoic rocks of the Velebit Mt (Croatia):prospects for applications in paleogeographic and geotectonic studies. *Geologia Croatica* 62(1):45–61
- Lewandowski M, Werner T, Vlahovic I, Środoń J, Anczkiewicz A, Velic I, Sidorczuk M (2012) Paleomagnetism and Thermal history of the Permian Succession of the Velebit Mt (Dinarides, Croatia). AGU Fall meeting GP21A-1136
- Løvlie R, Torsvik T, Jeleńska M, Lewandowski M (1984) Evidence for detrital remanent magnetizations carried by hematite In Devonian red beds from Spitsbergen: paleomagnetic implications. *Geophys J Roy Astron Soc* 79(2):573–588. doi:[10.1111/j.1365-246X.1984.tb02242.x](https://doi.org/10.1111/j.1365-246X.1984.tb02242.x)
- Márton E, Jeleńska M, Tokarski AK, Soták J, Kováč M, Spišiak J (2009) Current-independent paleomagnetic declinations in flysch basins: a case study from the Inner Carpathians. *Geodin Acta* 22:73–82. doi:[10.3166/ga.22.73-82](https://doi.org/10.3166/ga.22.73-82)
- Mazzoli S, Jankowski L, Szaniawski R, Zattin M (2010) Low-T thermochronometric evidence for post-thrusting (<11 Ma) exhumation in the Western Outer Carpathians, Poland. *Comptes Rendus Geosci* 342(2):162–169. doi:[10.1016/j.crte.2009.11.001](https://doi.org/10.1016/j.crte.2009.11.001)
- Mazzoli S, Szaniawski R, Mittiga F, Ascione A, Capalbo A (2012) Tectonic evolution of Pliocene-Pleistocene wedge-top basins of the southern Apennines: new constraints from magnetic fabric analysis. *Can J Earth Sci* 49(3):492–509. doi:[10.1139/e11-067](https://doi.org/10.1139/e11-067)
- Michalski K, Lewandowski M (2004) Palaeomagnetic results from the Middle Carboniferous rocks of the Hornsund region, southern Spitsbergen: preliminary report. *Pol Polar Res* 25(2):169–182
- Michalski K, Lewandowski M, Manby GM (2012) New palaeomagnetic, petrographic and 40Ar/39Ar data to test palaeogeographic reconstructions of Caledonide Svalbard. *Geol Mag* 149(4):696–721. doi:[10.1017/S0016756811000835](https://doi.org/10.1017/S0016756811000835)
- Nawrocki J, Fanning M, Lewandowska A, Polechońska O, Werner T (2008a) Palaeomagnetism and the age of the Cracow volcanic rocks (S Poland). *Geophys J Int* 174(2):475–488. doi:[10.1111/j.1365-246X.2008.03804.x](https://doi.org/10.1111/j.1365-246X.2008.03804.x)
- Nawrocki J, Polechońska O, Lewandowska A, Werner T (2005) On the palaeomagnetic age of the Zalas laccolith (southern Poland). *Acta Geol Pol* 55(3):229–236
- Nawrocki J, Polechońska O, Werner T (2008b) Magnetic susceptibility and selected geochemical-mineralogical data as proxies for the Early to Middle Frasnian (Late Devonian) palaeoenvironmental settings of limestone deposition in Holy Cross Mountains, southern Poland. *Palaeogeogr Palaeoclimatol Palaeoecol* 269(3–4):176–188. doi:[10.1016/j.palaeo.2008.04.032](https://doi.org/10.1016/j.palaeo.2008.04.032)
- Szaniawski R (2008) Late Paleozoic geodynamics of the Malopolska Massif in the light of new paleomagnetic data for the southern Holy Cross Mountains. *Acta Geol Pol* 58(1):1–12
- Szaniawski R, Konon A, Grabowski J, Schnabl P (2011) Palaeomagnetic age constraints on folding and faulting events in Devonian carbonates of the Kielce Fold Zone (southern Holy Cross Mountains, Central Poland). *Geol Q* 55(3):223–234
- Szaniawski R, Lewandowski M (2009) Palaeomagnetic age constraints indicate post-Variscan origin of massive breccia in Wietrzna Quarry (Holy Cross Mountains, Central Poland). *Geol Q* 53(3):357–362
- Szaniawski R, Ludwiniak M, Rubinkiewicz J (2012) Minor counterclockwise rotation of the Tatra Mountains (Central Western Carpathians) as derived from paleomagnetic results achieved in hematite-bearing Lower Triassic sandstones. *Tectonophysics* 560–561:51–61. doi:[10.1016/j.tecto.2012.06.027](https://doi.org/10.1016/j.tecto.2012.06.027)
- Szaniawski R, Mazzoli S, Jankowski L, Zattin M (2013) No large-magnitude tectonic rotations of the Subsilesian Unit of the Outer Western Carpathians: Evidence from primary magnetization recorder in hematite-bearing Węglówka Marls (Senonian to Eocene). *J Geodyn* 71:14–24. doi:[10.1016/j.jog.2013.07.001](https://doi.org/10.1016/j.jog.2013.07.001)
- Szaniawski R, Lewandowski M, Mansy JL, Averbuch O, Lacquement F (2003) Syn-folding magnetization in the French-Belgium Variscides as a marker of the fold belt tectonic evolution. *Bull Soc Geol Fr* 174(5):511–523. doi:[10.2113/174.5.511](https://doi.org/10.2113/174.5.511)

- Szlachta K, Michalski K, Brzózka K, Górką B, Gałazka-Friedman J (2008) Comparison of Magnetic and Mössbauer Results Obtained for Palaeozoic Rocks of Hornsund, Southern Spitsbergen, Arctic. Proceedings of the Polish Mössbauer Community Meeting 2008. *Acta Physica Polonica A* 114(6):1675–1682
- Tunyi I, Kruczky J, Kądzialko-Hofmokl M, Mello J (2008) Post-Cretaceous differential block rotation in the Slovensky raj Mts (Western Carpathians, Slovakia): inferences from paleomagnetic data. *Geol Carpath* 59(6):515–524
- Vincenz SA, Jeleńska M (1985) Paleomagnetic investigations of Mesozoic and Paleozoic rocks from Svalbard. *Tectonophysics* 114(1–4):163–180. doi:[10.1016/0040-1951\(85\)90011-3](https://doi.org/10.1016/0040-1951(85)90011-3)
- Vincenz SA, Jeleńska M, Aiinehsazian K, Birkenmajer K (1984) Paleomagnetism of some LateMesozoic dolerite sills of East Central Spitsbergen, Svalbard Archipelago. *Geophys J Royal Astron Soc* 78(3):751–773. doi:[10.1111/j.1365-246X.1984.tb05069.x](https://doi.org/10.1111/j.1365-246X.1984.tb05069.x)
- Werner T (1993) Paleomagnetism, structure and magnetic fabrics in a traverse of the Quetico Subprovince between Atikokan and Kashabowie, NW Ontario. M.Sc. thesis Lakehead University Thunder Bay Ontario Canada
- Werner T (1997) Experimental designs for determination of the anisotropy of remanence—test of the efficiency of least-square methods applied for highly metamorphic rocks from Southern Poland. *Phys Chem Earth* 22(1–2):131–136. doi:[10.1016/S0079-1946\(97\)00090-6](https://doi.org/10.1016/S0079-1946(97)00090-6)
- Werner T (2002) The correlation of magnetic anisotropies (AMS and AARM) with tectonic fabrics of the Niemcza shear zone (SW Poland). *Acta Geophysica Polonica* 50(1):79–107
- Werner T, Białek D (2004) The Jawornik granitoids: AMS fabric and its relationship with the Złoty Stok—Skrzynka shear zone (Sudetes, SW Poland). *Contrib Geophys Geodesy* 34:167
- Werner T, Borradaile GJ (1996) Paleoremanence dispersal across a transpressed Archean terrain: Deflection by anisotropy or by late compression? *J Geophys Res* 101(B3):5531–5546. doi:[10.1029/95JB03047](https://doi.org/10.1029/95JB03047)
- Werner T, Borradaile GJ (1998) Homogeneous magnetic susceptibility of Tektites: implications for extreme homogenization of source material. *Phys Earth Planet Int* 108(3):235–243. doi:[10.1016/S0031-9201\(98\)00098-3](https://doi.org/10.1016/S0031-9201(98)00098-3)
- Werner T, Jeleńska M (1992) The applicability of two computer techniques to separate the remanent magnetization (RM) components acquired in laboratory fields. *Phys Earth Planet Int* 70:194–200. doi:[10.1016/0031-9201\(92\)90182-U](https://doi.org/10.1016/0031-9201(92)90182-U)
- Werner T, Mazur S, Jeleńska M (2000) Changing direction of magnetic fabric in a thrust unit: an example from the Karkonosze-Izera massif, (SW Poland). *Phys. Chem. Earth Part A.* 25(5):511–517, doi:[10.1016/S1464-1895\(00\)00079-X](https://doi.org/10.1016/S1464-1895(00)00079-X)
- Zattin M, Andreucci B, Jankowski L, Mazzoli S, Szaniawski R (2011) Neogene exhumation in the Outer Western Carpathians. *Terra Nova* 23(5):283–291. doi:[10.1111/j.1365-3121.2011.01011.x](https://doi.org/10.1111/j.1365-3121.2011.01011.x)

Natural Variations of the Geomagnetic Field: Observations and Application to Study of the Earth's Interior and Ionosphere

Waldemar Józwiak, Jerzy Jankowski and Tomasz Ernst

Abstract The magnetic investigations carried out incessantly from the very moment the Institute of Geophysics was established in 1953 are outlined. Since that time, continuous observations of the natural magnetic field of the Earth, also called “magnetic service”, have been carried out. The research methods are discussed, which cover a wide scope of problems relating to the use of natural electromagnetic field variations, including the recognition of the Earth’s crust and upper mantle, search for electromagnetic earthquake precursors, and the ionosphere state monitoring via surface-based observations of the magnetic field. The reported investigations are of methodological nature, relating to recording and processing of data, as well as geophysical and geological modeling and interpretation. The major results obtained during 60-year activity, referring to the structure of the Earth’s crust and mantle in central Europe, are summarized.

Keywords Geophysics · Earth sciences · Geomagnetism · Ionosphere

1 Observatories

The Department of Geophysics (Zakład Geofizyki), of the Polish Academy of Sciences, later named the Institute of Geophysics, was established in 1953 on the basis of geophysical observatories in Warsaw, Świdra and Racibórz, with the aim of carrying out continuous studies and observations of geophysical elements, including the Earth’s magnetic field. Two magnetic observatories existed at that time in Poland: at Świdra and Hel. Their overhauling and assuring that the observations they provide are at a high level were among the most important goals

W. Józwiak (✉) · J. Jankowski · T. Ernst
Institute of Geophysics, Polish Academy of Sciences, Księcia Janusza 64,
01-452 Warsaw, Poland
e-mail: jozwiak@igf.edu.pl

of the newly created Department. Although the two observatories were established many years before, it is worthwhile to recollect their unusual history.

The first systematic observations of the Earth magnetic field date back to the beginning of the 20th century, when, on the initiative of L. A. Bauer, director of Earth's Magnetism Department of the Carnegie Institution in Washington, an international project of magnetic mapping at individual countries was initiated. There was a threat that the territory of Poland, because of the lack of proper facilities, would be surveyed by the Americans, as planned for other underdeveloped countries. Stanisław Kalinowski, head of the Physical Laboratory of the Industry and Agriculture Museum in Warsaw, decided to defend Poland's scientific esteem. On his own, he initiated in 1907 the Earth's magnetism surveys on the area of Congress Poland.¹ He executed test measurements in the Frascati Garden and Mokotowskie Field in Warsaw. In 1910, having acquired more accurate instruments, Kalinowski started systematic measurements at the 20×20 km grid, which was a deed envisioned for many years. To process the measurements made at various times and produce a magnetic map, they should have been reduced to one time moment. Hence, a continuous recording of the Earth's magnetic field must have been carried out, which is a task for magnetic observatories. He was initially using data from the observatory situated nearest to Warsaw, i.e., the one in Potsdam, located over 500 km away, but they turned out to be not representative for the Polish territory. In these circumstances, the idea was born to establish a Polish magnetic observatory. In 1911 Kalinowski addressed a letter "in urgent scientific matter", asking the Poles to donate financial means to build a Polish observatory and furnish it with instruments. The idea of creating the observatory was a scientific and patriotic deed. The request was met with wide response, and the collected funds enabled, already in 1914, to purchase a building lot for the observatory at Świder near Warsaw, and to begin the construction works there. The observatory buildings were designed taking as an example the Potsdam Observatory. The funds sufficed to buy the instrumentarium, i.e., three variometers produced by Cambridge Scient, and a set of variometers and recorders produced by Toepfler und Sohn. The construction works were finalized in 1915. In this manner, the first magnetic observatory on the Polish territory came into being, and continuous measurements of the Earth's magnetic field were initiated. In 1916 Kalinowski went with his family to the Ukraine, but in 1918 he returned and was able to resume the works on putting the Świder Observatory into service. Since 1921 the measurements have been made in a continuous manner, and even during the Second World War, owing to the energy and determination of Kalinowski and his co-workers, it was possible to protect the Observatory against destruction and robbery. After the war, in spite of advanced age, Kalinowski undertook the task of overhauling the buildings and expanding the scope of work of the survived geo-physical observatory. He was aided by his daughters: Zofia Kalinowska, who

¹ Congress Poland or the Kingdom of Poland (Kongresówka) was a limited-autonomy country on the territory of partitioned Poland, existing in 1815–1916.

succeeded her father as head of the Observatory after his death, and Ewa Kalinowska-Widomska, who, along with the Earth's magnetism, was engaged in atmospheric electricity and meteorological observations.

The other Polish magnetic observatory was established more than 10 years later. In the early 1930s, Prof. Stefan Hłasek-Hłasko, director of the State Meteorological Institute, put forward an initiative to create a Magnetic Station—Marine Observatory at Hel. The Station came into being in 1932; its goal was the study of the Earth's magnetism and verification of ship compasses. During the war, the objects of the station were destroyed. In 1951–1953 the State Institute of Hydrology and Meteorology began actions toward building a new station at Hel. In 1954, a new recording pavilion and dwelling house were handed over to the Institute of Geophysics. For many years, the Observatory has been led by Zofia and Wacław Czyszek (Wacław Czyszek was taking part in Warsaw Uprising when he lost a leg; after the war he was subject to political repressions). Upon the retirement of Dr. Zofia Czyszek, the Observatory was headed by her son Jarosław over the years 1990–2006, and since then by Stanisław Wójcik.

A strong increase of artificial disturbances, mainly magnetic, coming from the railroad (Otwock line) electrified in 1934, made it necessary to move the geomagnetic observations from Świder to another site, not far away from Warsaw, but such in which the level of artificial noise would be low. The selected area was located at the edge of natural reserve “Modrzewina”, some 2 km from the village Belsk Duży, 50 km south of Warsaw. It is an agricultural land, distant from urban and industrial regions and far away from railroad.

Both observatories were lacking instrumentation. In the 1950s, this was an extremely difficult problem, because of troubles with obtaining foreign currency for buying the suitable instruments, available only abroad. The situation improved only when, on account of the International Geophysical Year 1957/1958, the Institute obtained additional funds for purchasing up-to-date (as for those times) equipment for making geomagnetic observations at Belsk and Hel. The new instruments for magnetic field recording included two magnetometers of La Cour system, one Mating-Wiesenberg, and three portable Askania magnetometers for field surveys. The instruments for absolute magnetic field measurements consisted of two large theodolites, Mating-Wiesenberg and Ascania, two inductors for inclination measurement, and some QHM and BMZ magnetometers that were popular at that time.

The Belsk Observatory began its regular activity in the fall of 1965; the first magnetic yearbook listed the 1966 data. The Observatory implemented a recording system on a photopaper, based on Bobrov-system quartz sensors. Yet it turned out pretty soon that the photographic-analog recording system has become technically obsolete, which made it impossible to carry out the magnetic field recording on a level that would be sufficient for the World Data Center. As a remedy, we decided to initiate works on designing our own instruments. This brought about the first proton magnetometer (1963/1964), and then the vector magnetic stations with digital recording, based on Bobrov-type quartz sensors, constructed by Dr. Janusz Marianuk (1977). Both instruments, whose creation was forced by economic

reasons, turned out to be so successful that they have been the basic ones in our observatories up to now. Fluxgate-type magnetometers are used as stand-by sets. It is to be noted that many copies were sold abroad, and are still in use in some observatories. The recording on a photopaper has been carried out until 1986, but already since 1984 our observatories began a digital, initially employing the digital recorder that was storing data on a tape cartridge (constructed at Belsk), and then the digital recorders of our own make. A great contribution to the process of building, organizing and instituting the proper operation of the Observatory was brought by Prof. J. Jankowski and Dr. J. Marianuk.

Since 1978, the absolute measurements have been done by means of a proton vector magnetometer PMW-344-74. Since 1993, the absolute measurements consist of declination and inclination measurements based on a nonmagnetic theodolite equipped in transduced sensor produced by ELSEC and a Polish proton magnetometer PMP for total magnetic field measurement. In April 2013, the ELSEC magnetometer was replaced by the Ukrainian instrument GEOMAG-02.

It is to be noted that the instruments built in our Institute have also been the basic equipment of two Polish magnetic stations in Polar regions, in Antarctica and Spitsbergen. The Hornsund station in Spitsbergen has been operating up to now and the data recorded there are very useful due to its unique location.

In the 1980s we realized, together with the Institute of Meteorology in Helsinki, two research projects related to magnetic observatories. Polish-Finish induction studies begun around Nurmijarvi Observatory in Southern Finland in 1982 and were continued around Sodankyla Observatory in Northern Finland in 1988 (Jankowski et al. 1986; Kauristie et al. 1990). The purpose of the study was to obtain information about the spatial homogeneity of magnetic variations recorded in these observatories; in other words, we wanted to check the existence of any local induction effects that might occur there. Such effects, if they exist, should be taken into account by the scientists using observatory data in the reduction of secular variation measurements. In the frame of both projects, geomagnetic variations were recorded at four temporary stations around the Nurmijarvi and Sodankyla Observatories for 2–3 weeks. The distance from each station to the observatory was about 30 km. Finally, we concluded that the spatial distribution of the geomagnetic field variations is generally homogeneous in the periods range from 100 to 2,500 s.

Since the Belsk Observatory was established, Prof. Jerzy Jankowski took the responsibility for the organization of work and then the supervision over the current activity of all Polish observatories. His versatile knowledge of the subject and professional experience were internationally acknowledged. IAGA has asked him to write a handbook (manual) with guidelines and recommendations relating to the construction of observatories, their equipment and the organization of measurements. The book, co-authored by Dr. Christian Sucksdorff, was published in 1996 (Jankowski and Sucksdorff 1996). It has been, up to the present, the basic handbook for everybody engaged in magnetic observations over the world.

It is also to be noted that in our group we developed an algorithm and software for automatic determination of K indices (Nowożynski et al. 1991), which is presently used in most observatories over the world.

All our observatories are included in the world data collection system INTERMAGNET, and are among the world leaders in terms of data quality. This was acknowledged by the international community: Dr. Jan Reda, successor of Dr. Marianiuk as head of the magnetic laboratory at Belsk, is now responsible for the data quality in the whole INTERMAGNET network.

2 Beginning of Geomagnetic (Magnetovariational) Surveys

The instruments purchased in the previously mentioned Geophysical Year (1957/1958) included, along with instruments for observatories, also Askania-type portable magnetic stations. They turned out to be a very proper choice, enabling us to begin studies of local magnetic field variations generated by currents induced in the conducting Earth (magnetovariational sounding, previously called geomagnetic ones). This direction of research has later become one of the main tasks of the Alternating Magnetic Field Laboratory. Over consecutive decades, this research has brought about numerous important findings relating to the deep basement in Poland and Central Europe.

The research was began in 1958 by Jerzy Jankowski; the experimental surveys were based on deploying portable magnetic stations over the whole country. In the first stage, the data from 36 measurement points were collected; although the points were rather sparsely scattered over a large area, their analysis yielded very interesting results. The interpretation was made using the so-called geomagnetic vectors, according to Wiese's definition. They were calculated with a simplified method, without spectral analysis, as proposed by Wiese. The geomagnetic vector values depend upon the variation period. A simplified method employs only the bay-type variations, some 1,800 s in period, for which the phase shift between the magnetic field components is the smallest.

The first analysis of magnetovariation data was made in 1965 (Pozaryski et al. 1965), when the number of observational data was small. Nevertheless, the authors were already able to distinguish the three regions: Variscides, Caledonides, and Precambrian Platform. Already the first interpretations of the regularities observed in the vector distribution indicated that they are due to a complex of well-conducting rocks in the lower crust (Jankowski 1972). Such a result was not conformant to the views prevailing at that time. It was then generally believed that the sources of the observed anomalies are situated in the upper mantle (Schmucker 1970).

The interpretations made in the 1960s were not based on detailed numerical (inversion) models, since such algorithms did not exist at that time. Yet the qualitative interpretations, as to the location of the anomaly axis, were possible and yielded unequivocal conclusions. It was an original interpretation, and we were among the first countries which initiated research of this kind.

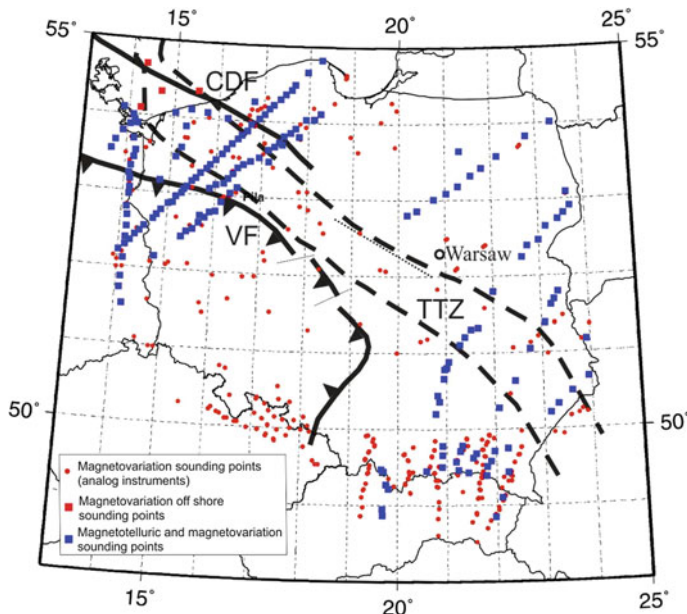


Fig. 1 Location of measurement points for magnetovariation and magnetotelluric soundings

In the next years, electromagnetic (magnetovariational and magnetotelluric) surveys have become our main area of research and brought about many achievements (Fig. 1). Along with field surveys, we have been developing, likewise other institutes in the world, methods and algorithms for data processing and numerical modelling of electric conductivity distribution in the basement. Measuring instruments have also been greatly updated; we are now using modern field stations based on fluxgate magnetometers. Due to methodological and instrumental progress, the huge regional, country-scale and international research projects realized by our team yielded very interesting, original data on the structure of the Earth's crust and upper mantle in Central Europe.

3 Theoretical (Methodological) Research

Electromagnetic (magnetovariation and magnetotelluric) methods use, as a source, the natural variations of the Earth's magnetic field are based on the electromagnetic induction. Electric currents are induced in the rocks constituting the Earth's interior; their directions and intensities depend on the electric conductivity distribution. An analysis of relations between the values of respective electromagnetic field components recorded at the surface enables us to draw conclusions on the values of electric conductivity of the basement. It is a very important physical

parameter, owing to which we can—with a relatively high accuracy—identify geological structures which differ in petrophysical properties.

The history of induction studies goes back to the 1950s, when Tikhonov (1950) and Cagniard (1953) developed theoretical background of the method. They showed that by analyzing a relation between the amplitudes of horizontal components of electric and magnetic fields observed at the Earth's surface one can obtain information on the conductivity distribution within the Earth. However, the MT method, initially introduced for recognition of layered structures, does not provide satisfying results in the regions of large horizontal inhomogeneities. In this situation, the other method, initially called the geomagnetic sounding and now named magnetovariation (MV) method, gains in importance. An inspiration for inventing the latter method came from a comparison of magnetic field variations observed at various points at the Earth's surface. It was noticed that the differences, visible mainly in the vertical component, are caused by horizontal inhomogeneities in the electric conductivity distribution in the Earth. The MV method, unappreciated for a long time in Western Europe, was widely used in countries of Central and Eastern Europe, providing very interesting results.

The first step in interpreting the results of electromagnetic soundings is to determine the so-called transfer function (i.e., induction vector in geomagnetic soundings and the impedance, and then the apparent resistivity and phase in magnetotelluric soundings). These are functions of location and the period of field changes; as the period grows, we obtain information from deeper and deeper layers of the Earth.

The transfer function calculation is a typical problem of studying a stationary linear system of two input and one output signals.

There are two approaches to the processing of magnetotelluric and geomagnetic sounding data. Most scientific centers have been using different variants of spectral analysis to estimate transfer functions in the frequency domain. However, our department from the very beginning (1973) has applied the method of least squares to estimate the coefficients determining impulse responses in the time domain. All the algorithms and programs invented and developed in our department (Wieladek, Ernst, Nowożyński) have been gradually refined and are successfully used until now.

The use of algorithms working in time domain gives, in our opinion, many advantages:

- estimation of the power spectra (frequency domain) requires the assumption that the signals are stationary, while the method of least squares (time domain) requires only the stationarity of noise (Ernst 1981; Ernst et al. 2001);
- using the methods of spectral analysis involves many steps of subjective character, such as the choice of shape and width of spectral windows;
- the impulse responses allow us to easily predict the output signal through the convolution of such responses with two input signals in time domain;
- finally, algorithms in the time domain enable us to make the correct selection of data much easier and better than in the frequency domain.

The algorithms and codes for calculations in the time domain were developed in our group by Wieladek and Ernst (1977) and then modified by Wieladek and Nowożyński (2001). A next modification (Nowożyński 2004) made it possible to use “long” impulse responses, thus enabling the determination of transfer functions for a very wide frequency range.

A next step in the interpretation is the numerical modeling of conductivity distribution on the basis of the determined transfer functions. To this end, the use is made of algorithms for forward and inverse modeling. In our group we created a few such algorithms, and they were developed in approximately the same time as in other leading research institutions over the world.

The first was a two-dimensional forward modeling algorithm based on the finite-difference method, developed by Tarłowski (1978). In this algorithm, Helmholtz’ equations are approximated by a five-point finite-difference scheme. It is also assumed that at the edges the structure is one-dimensional, i.e., the resistivity depends on depth only. The huge set of equations was solved with the help of an iterative Gauss-Seidl method. Model parameters were selected with a trial-and-error method, many times repeating the simple task problem. The method was then modified by Wieladek and Nowożyński (Wieladek and Nowożyński 1981; Wieladek et al. 1981), who were directly solving the equation system with the Cholesky-Banachiewicz method. At the same time, Antonina Bromeck independently developed an algorithm for forward modeling using a finite-element method. There were also elaborated an algorithm for “pseudo-three-dimensional” modeling with the so-called thin layer approximation (Jóźwiak and Baemish 1986), in which it is assumed there that 3D conducting structures are concentrated in a thin near-surface layer, while the deep basement is 1D in character.

In a subsequent step, a few inversion algorithms were produced. The first of these was the 1D stochastic inversion algorithm (Nowożyński 1981; Wieladek and Nowożyński 1989) for a plane medium. It was assumed that the differences between the model searched for and the half-space are stochastic and can be described by a combined process of moving average and autoregression. The maximum likelihood method and then Marquardt’s (1963) method were used. A similar algorithm has also been developed for spherical model of the Earth (Jozwiak 1993, 2001) to study the distribution in the Earth’s mantle conductivity. This algorithm has enabled global data inversion, for periods of up to 11-year changes, which makes it possible to estimate conductivity in the mantle down to a depth of 2,100 km. This approach is original; the model that is commonly used in such studies is a flat-parallel one, in spite of the fact that, from a depth of 400 km downward, the effect of Earth’s sphericity begins to be of significance.

In 2001, basing on the direct modeling algorithm using the finite difference method, there was created the first inversion algorithm for modeling a conductivity distribution of complex geometry (Nowożyński and Pushkarev 2001).

In the last years, an interesting method and an algorithm based on it was developed for reconstructing all magnetic field components and, further on, for determining the values of Horizontal Magnetic Field (HMT) on the basis of the knowledge of induction vectors over a certain area. The spatial distribution of some HMT

invariants, in particular the maximum eigenvalues, can very effectively locate the position of well-conducting structures, including three-dimensional ones. A new efficient iterative algorithm was proposed for the HMT determination. This technique takes advantage of the fact that the Earth's magnetic field is a potential field and its vertical component is associated with the horizontal component by Hilbert transform (Jozwiak et al. 2009; Jozwiak 2012; Nowozynski 2012). It uses approximation of tipper components on the area of a rectangle with the use of two-dimensional splines with separate variables and the algorithm for calculating the three-dimensional Hilbert transform for the vertical component of the magnetic field.

4 Regional Surveys

The main result of the geomagnetic sounding carried out in Poland since 1958 was the discovery of the two huge magnetic anomalies. The first of these, related to the Permian basin (Jankowski 1967; Pawliszyn and Jankowski 1973; Jankowski et al. 1995), turned out to be a continuation of the large North German-Danish anomaly discovered in the 1950s. It runs from North Germany towards Stargard Szczeciński, then turns ESE, and close to Inowrocław it turns further in the SE direction. Its course on the central Poland segment is recognised to the area of Holy Cross Mountains.

Studies of this anomaly were intensely continued in the last years in the frame of the large, international electromagnetic research project conducted in NW Poland and NE Germany. It was carried out by teams from Poland, Germany, Finland, the Czech Republic, Russia, Sweden, and Ukraine. The main objective was to study the deep geoelectrical structure of the Trans European Suture Zone (TESZ). Measurements were carried out in the years 2001–2005, primarily along the seismic profiles P2, LT-7, and LT-2. Later on, in 2005–2007, the area of research was extended toward the NW by additional profiles in NE Germany and with points lying in south Baltic region (Brasse et al. 2006; Ernst et al. 2008; Jóźwiak 2012). One of the aims of the surveys on the Baltic was also to implement a new research method based on using under-sea magnetic measurements performed with bottom magnetometer constructed at Belsk (Marianiuk et al. 2007). In the framework of EMTESZ, the magnetotelluric soundings were executed at over 300 points, so it was one of the world biggest projects of such type.

It was found that the obtained conductivity distribution models for both profiles show three different fragments of the crust (Fig. 2). The first of them, lying in the NE part of the profile, is highly resistant and is undoubtedly a part of the East European Platform. Its structure appears uniform, indicating that the changes that had taken place since its creation in the Precambrian were relatively small. In the second, middle fragment, the resistivity values are much lower. Due to the complicated structure of its upper floors, this area must have undergone numerous changes which led to the creation of a deep basin, which underwent inversion in the Triassic. The lower crust appears to be quite homogenous and lower resistivity values may indicate a higher temperature. The anomalous well-conducting region

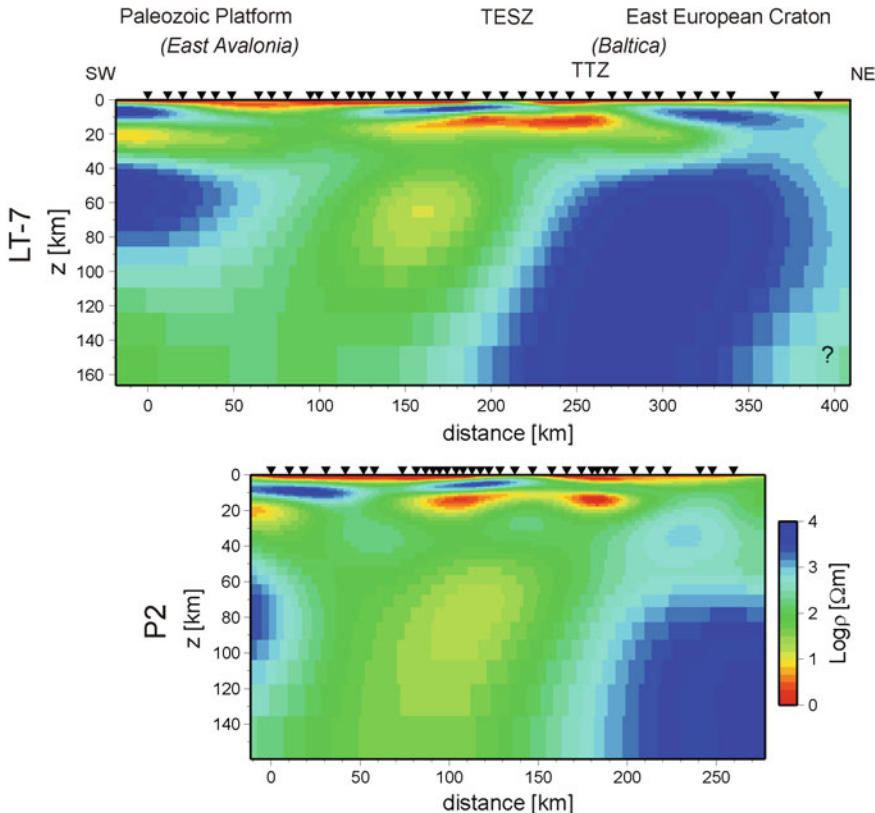


Fig. 2 Two-dimensional models of the deep conductivity distribution for the *LT-7* and *P2* profiles

visible in the upper mantle region, at depths of 60–120 km, correlates well with the thermal anomaly observed there (Majorowicz 2004). The third region adjacent to the former from SW is not as homogeneous as the East European Platform and it is undoubtedly the Palaeozoic Platform. Contacts between the platforms indicate very deep rooting of the sutures observed in the shallower layers. In the obtained conductivity distributions, we do not see a typical image of subduction in the lower crust, even though it is possible to find some elements of this model in the upper stages. The most striking feature is the presence of a very well conducting layer with minimal resistivity, of about 2 Ωm , and values of integral conductivity of the order of a few thousand S, which is located under the entire TESZ at a depth of 10–20 km. It is identified on the basis of seismic refraction data analysis as a pre-Variscan consolidated crust (Dadlez 2006) and is characterised by low P-wave velocity values. We cannot state clearly what the mechanism of electrical conductivity is. It can be mineralised waters (ionic conductivity), graphites or conductive shales (electronic conductivity).

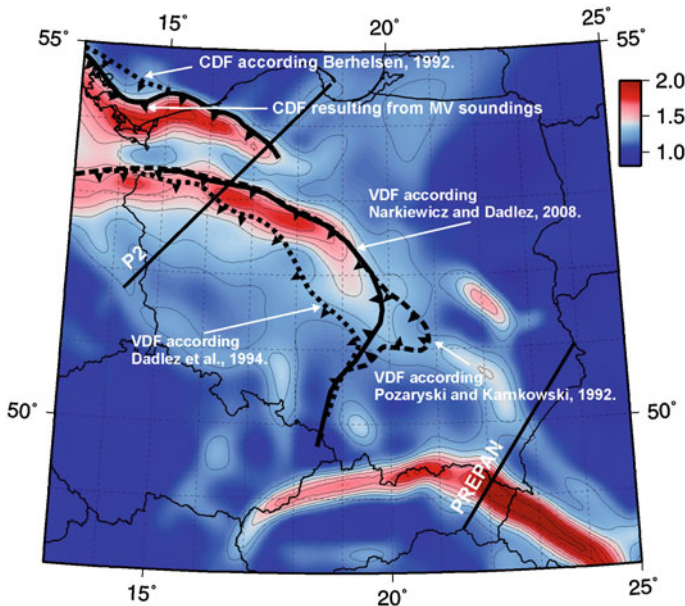


Fig. 3 Map of the spatial distribution of the most informative invariants of HMT (the largest singular value). The high values (red in color) show the locations of conducting structures. Hypothetical locations of the Caledonian Deformation Front (CDF) and the Variscan Deformation Front (VDF) are indicated by black lines with triangles (Jóźwiak 2012)

The new method of integrated interpretation of geomagnetic soundings enabled us to determine the course of these deep structures (Fig. 3). It turned out that they are amazingly well correlated with the position of Caledonian, Variscan and Alpine deformation fronts. Supposedly, the well-conducting rock complexes are most probably an effect of subsidence of sedimentary material in foredeeps in front of mountain chains.

Interestingly enough, the results indicate that the front of Caledonian foldings does not lie, as generally believed, somewhat NE of the Rügen-Koszalin line. Instead, north of Koszalin it turns westwards, goes further along the Baltic shore, to reach Uznam and turn towards Rügen, by-passing it from the NE. However, the location of the Variscan deformation front we obtained is very close to the one postulated by Narkiewicz and Dadlez (2008) (Fig. 3).

In the 1960s, there was also discovered the other one of the huge anomalies on the Polish territory, i.e., the Carpathian anomaly, extending under the whole Carpathian arc (Jankowski 1967). In the next years, it was thoroughly surveyed in cooperation with the Geophysical Institute of the Czech Academy of Sciences. The measurements in Poland were made by the Institute of Geophysics. The results were interpreted jointly (Jankowski et al. 1985, 1991; Jankowski and Ernst 1986; Lefeld and Jankowski 1985; Ernst et al. 1997). The behaviour of induction vectors in the Carpathians is typical for 2D conductivity distribution, since vectors rotate

by exactly 180° while passing through the so-called zero line of the anomaly, where the vector amplitudes are zero. This line runs nearby the Pieniny Klippen Belt. The course of the anomaly's zero line is well documented and it determines the anomaly axis. Already the first interpretations indicated that the anomaly is related to the existence of a large sedimentary basin filled with sedimentary rocks. More detailed studies have shown that the well-conducting rocks may reach depths of 10–18 km. These are complexes of very large integral conductivity values, up to 6,000 S. The mechanism of electric conductivity of these deep rock complexes is still a controversial problem; it has not been unequivocally solved up to now whether the good conductivity of rocks is an effect of saturation with mineralized waters (ionic conductivity) or the presence of graphites and shales (electronic conductivity). In our opinion, these are porous (cracked) rocks filled-in with mineralized waters, whose presence in deeper regions of the orogens is a result of diagenesis or metamorphism (Jankowski et al. 2008). It is also possible, however, that these are metamorphosed rocks, containing graphite layers formed secondarily at the discontinuity surfaces between crustal blocks, thrust zones, deep faults, or metal sulfides (black shales, alu shales). A comparison of conductivity distribution models with seismic results (Grad et al. 2006; Środa et al. 2006) indicates that the position of the area we documented is amazingly well correlated with the zone of low seismic velocities (Fig. 4). The geoelectric models, however, have been constructed years earlier than the seismic models.

In SE Poland, the depth of high-resistivity formation roof was determined along the Holy Cross Mountains (Semenov et al. 1998; Pushkariev et al. 2007) and PREPAN (PRECambrian Craton—PANonian Basin) profiles (Adam et al. 1997; Ernst et al. 2002). The two deep well-conducting faults (saturated with mineralized waters) were found. One of these is an eastward continuation of the Holy Cross dislocation. It separates two crustal blocks, the Małopolska Massif and the Radom-Łysa Góra block, contrasting in resistivity values. The other fault is associated with the SW margin of the East European Platform.

The deep magnetovariation and magnetotelluric soundings were also carried out in the Polish part of the East European Platform (Jankowski et al. 2004). The most surprising result was that the amplitudes of the real part of the induction arrows are very large, up to 0.8, which was not expected in the case of an old platform. All calculated vectors were superimposed on a tectonic map (Znosko 1998). It is easy to notice a striking correlation between the directions of the isolines of the crystalline basement depths and the directions of induction arrows—they are perpendicular to each other. Such a correlation suggests that the explanation of the observed behaviour of the induction arrows should be sought in the subsurface sedimentary layer. To clarify this, we developed a pseudo 3D model of a thin layer, assuming distribution of integral conductivity on the basis of geological data down to the crystalline basement depth.

The results of modelling confirmed the notion that the morphology of the sedimentary cover has a decisive impact on the nature of induction arrows. It was a new conclusion, not to be found elsewhere in the literature.

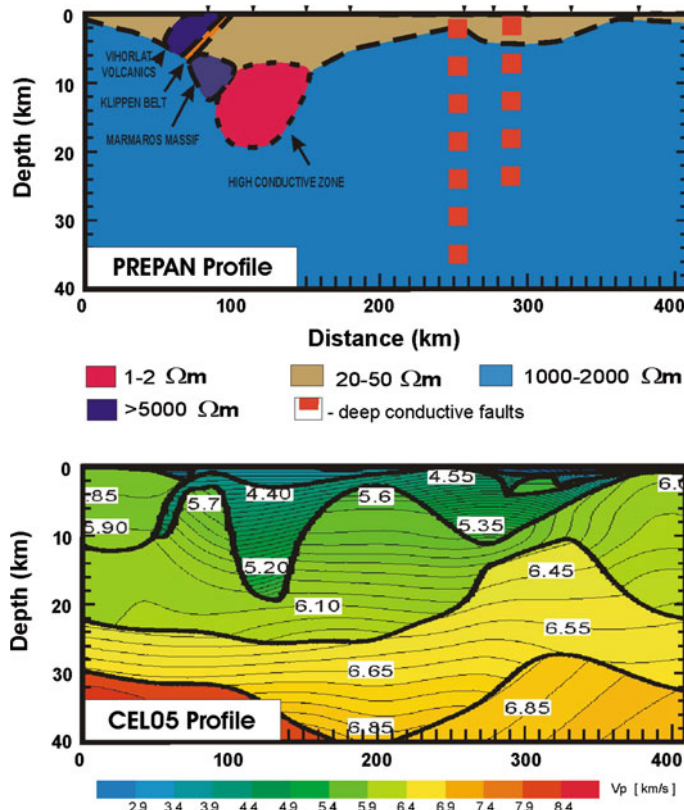


Fig. 4 Comparison of the geoelectric model PREPAN (Ernst et al. 2002) with the results of seismic modeling for CEL05 profile (Grad et al. 2006)

Interesting information on the geoelectric structure of the upper mantle is provided by the ultra-deep sounding carried out for more than 10 years. Already the first models pointed to the presence of a conducting anomaly in the earth's mantle, at depths of 150–250 km, clearly related to the TESZ zone (Semenov et al. 2002; Semenov and Józwiak 2005, 2006); its position amazingly well coincides with the position of heat flow anomaly (Majorowicz 2004). Additional information on the upper mantle structure comes from the results of CEMES project (Central Europe Mantle geoElectrical Structure), in the framework of which the deep electromagnetic sounding in more than ten magnetic observatories in Central Europe has been made (Semenov et al. 2003; Semenov et al. 2008). The results obtained confirm the presence of a well-conducting zone, corresponding to the asthenosphere, the correlation of its parameters with the tectonic division is very clear (Fig. 5). The lithosphere thickness estimated from these studies ranges from 100 km under the Paleozoic Platform of Western Europe to 250 km under the East European Craton.

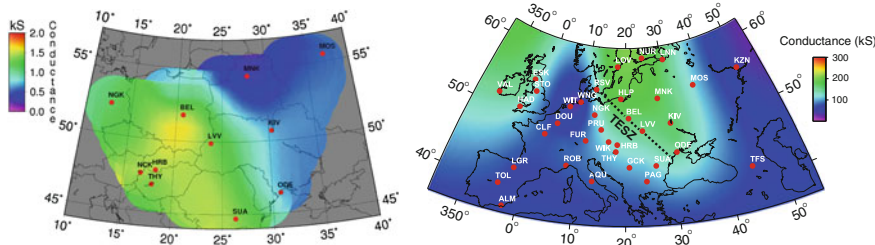


Fig. 5 Schematic maps of the mantle conductance from 50 to 200 km depth (*left*) and 50–770 km depth (*right*) beneath Central Europe

Noteworthy are also the short-period soundings made in many regions of the country, targetted at the recognition of near-surface structures. On their basis, the morphology of sedimentary layer has been determined, and an increase in conductivity values in lower parts of this layer has been found, which evidences the presence of mineral waters. In particular, owing to regional magnetotelluric surveys in the Carpathians, a map of sub-Tertiary basement has been compiled. Results of these studies were summarized in (Jankowski et al. 1991).

Worth mentioning is that most of the regional studies was made basing on funds from consecutive grants from Poland or abroad. The Department of Magnetism has realized a total of 35 projects financed by the State Committee for Scientific Research (KBN) and later the National Science Center (NCN); there were also two NATO projects.

5 Earthquake Precursors and State of the Ionosphere

Regional studies of the crust and upper mantle structure were the main topic of our research. Alongside, we were also dealing with a variety of problems, the most important being the studies of earthquake precursors and the state of the ionosphere.

As already mentioned, the transfer functions of magnetotelluric sounding are strictly related to local geological structure (conductivity distribution). If some pre-earthquake changes in the conductivity distribution in the lithosphere around the recording sites do occur, they will be revealed as changes of transfer function values (apparent resistivity, phase). Monitoring of these changes in time and analysis of their correlation with seismicity is a fairly popular procedure in a search for electromagnetic precursors of earthquakes. A shortcoming of such an approach is the necessity of using long time series for correct estimation of resistivity (phase), which disqualifies it.

That is why we proposed an original method based on an analysis of residual parts of electric components, which are defined as differences between the recorded electric components and their predictions (Ernst et al. 1991).

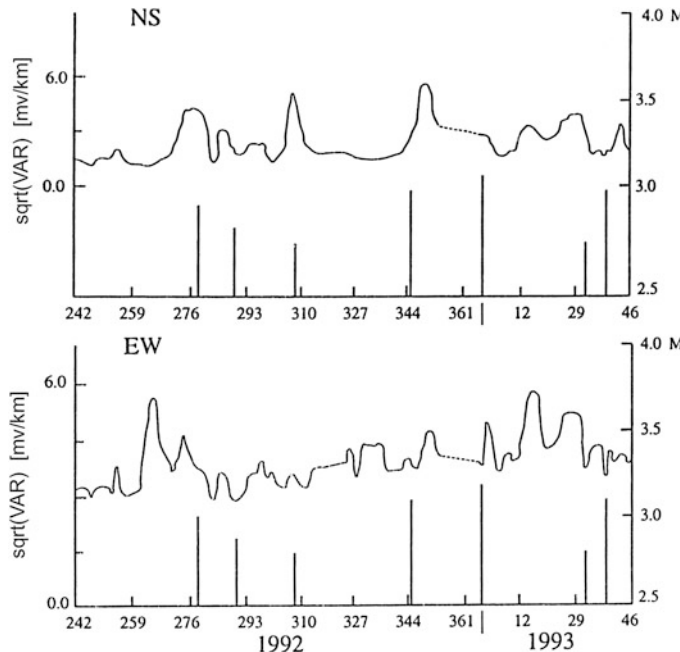


Fig. 6 Temporal changes of the estimated variances of residual electrical signals (left axis), together with magnitudes of selected earthquakes (right axis)

For statistical analysis of residual signals and search for their correlations with the occurrence of earthquakes, the use was made of variances of these signals, which can be determined in a practically continuous manner. The methodology was tested, with the use of Polish instruments, in many seismically active regions of Europe, in close cooperation with scientific institutions abroad. These were:

- Friuli region in North Italy, cooperation with the University in Trieste (1987–1988, measurement duration in excess of 1 year) (Zadro et al. 1990; Ernst et al. 1993),
- L’Abruzzo region in Central Italy, cooperation with Instituto Nazionale di Geofisica e Volcanologia in Rome (1992–1994; duration of 20 months) (Ernst et al. 1994),
- Sterea Ellas region in Greece, cooperation with the University of Athens, Greece. (1997; duration of 4 months) (Ernst 2005).

The numerical analysis of the rich data set was mainly made by our Institute, using our original software and methodology. In the study of precursors we obtained numerous important and interesting results. In the Friuli region we observed a considerable increase of residual signal variances in periods preceding the large earthquakes (Fig. 6). Also studies in Central Italy and Greece have shown that the research methodology we proposed (residual component analysis) is a

much better tool for the study of precursors than the analysis of a behavior of transfer function values (apparent resistivity or phase).

Also in recent years we actively joined the study of phenomena constituting the space weather, which can be observed at the earth's surface through geomagnetic field variations. We developed an innovative method for determining the state of the ionosphere, based on a new magnetic index η introduced by us, whose value is strictly related to the external part of vertical geomagnetic field (Ernst et al. 2010).

Of great importance in our method is to separate an external part from the vertical geomagnetic field (Ernst and Jankowski 2005). Our algorithm, operating in the time domain, enables us to achieve it without much trouble; the external part thus obtained is approximated by a residual part of the vertical geomagnetic component.

The index was subject to verification at the Space Research Center in Warsaw, and we showed in joint publications that the variations of η are very well correlated with the appearance of sporadic layer E in the ionosphere, as well as with large changes in other layers (Dziak-Jankowska et al. 2011). This index is likely to be successfully applied for efficient monitoring of the ionosphere.

6 Summary

The main achievements of the Geoelectromagnetic Laboratory can be summarized as follows:

1. The magnetic observatories at Belsk, Hel, and Hornsund have been established and kept at the world highest level; Schuman resonance observations have been implemented to the routine observatory practice at Belsk and Hornsund.
2. A new, original methodology of magnetotelluric and magnetovariational sounding has been developed (methods and algorithms for experimental data processing and construction of numerical models).
3. In close cooperation initiated and kept with numerous top-level European research groups, huge joint research projects have been realized. In some of these, we were playing the leading role.
4. It has been demonstrated that the large magnetic anomaly, called the German-Danish anomaly, has its continuation on the Polish territory, being related to Variscan orogenesis and localized the Caledonian and Variscan folding fronts.
5. The Carpathian Anomaly has been discovered and it was shown that it is rooted in the well-conducting rock complexes in the crust, most likely buried and metamorphosed sedimentary rocks saturated with mineralized waters.
6. The recognition of geoelectric structure of the Earth's crust and upper mantle in the transition zone between the East European Platform and Paleozoic Platform has been made. We have estimated the lithosphere–asthenosphere boundary (LAB) depth (220–240 km under the Precambrian Craton and 120–140 km under the Paleozoic Platform) and demonstrated that the differentiation of conductivity, which is visible in the crust, has its continuation into the upper mantle.

7. Numerous measuring instruments have been constructed (proton magnetometer, magnetic station, and field magnetotelluric station); our instruments were used in many countries for years.
8. A method for monitoring the state of the ionosphere from ground-based magnetic observations has been developed; we introduced a new parameter making it possible to “measure” the magnetic activity also in quiet days.
9. A new method for monitoring the pre-earthquake phenomena, based on an analysis of residual parts of electric components, has been proposed.

References

- Adam A, Ernst T, Jankowski J, Józwiak W, Hvozdara M, Szarka L, Wesztergom V, Logvinov I, Kulik S (1997) Electromagnetic induction profile (PREPAN 95) from the East European Platform (EEP) to the Pannonian Basin. *Acta Geodaet Geophys Hung* 32(1–2):203–223
- Brasse H, Cerv V, Ernst T, Hoffman N, Jankowski J, Jozwiak W, Korja T, Kreutzmann A, Neska A, Palshin NA, Pedersen LB, Schwartz G, Smirnov M, Sokolova EY, Varentsov IM (2006) Probing electrical conductivity of the Trans-European Suture Zone. *EOS Trans AGU* 87(29):281–287
- Cagniard L (1953) Basic theory of the magnetotelluric method of geophysical prospecting. *Geophysics* 18:605–635
- Dadlez R (2006) The Polish Basin-relationship between the crystalline, consolidated and sedimentary crust. *Geol Q* 50(1):43–58
- Dziak-Jankowska B, Stanisławska I, Ernst T, Tomaszik L (2011) Ionospheric reflection of the magnetic activity described by the index η . *Adv Space Res* 48:850–856
- Ernst T (1981) A comparison of two methods of the transfer function calculation using least squares criterion in time and frequency domain. *Publ Inst Geophys PAS G-2(143)*:13–24
- Ernst T, Marianuk J, Rozluski CP, Jankowski J, Palka A, Teisseyre R, Braitenberg C, Zadro M (1991) Analysis of the magnetotelluric recordings from the Friuli seismic zone, NE Italy. *Acta Geophys Pol* XXXIX(2):129–158
- Ernst T, Jankowski J, Rozluski CP, Teisseyre R (1993) Analysis of the electromagnetic Fidel recorded in the Friuli seismic zone, northeast Italy. *Tectonophysics* 224(1993):141–148
- Ernst T, Teisseyre R, Meloni A, Palangio P, Marchetti M (1994) Magneto-telluric studies in the Central Appenines, 1992–1993. *Acta Geophys Pol* 42(3):209–228
- Ernst T, Jankowski J (2005) On the plane wave approximation of the external geomagnetic field in the regional induction study. *Izv Phys Solid Earth* 41(5):363–370
- Ernst T, Jankowski J, Nowożyński K (2010) A new magnetic index based on the external part of vertical geomagnetic variations. *Acta Geophys* 58(6):963–972
- Ernst T (2005) Electrical conductivity inhomogeneities in Greece on the west margin of the Anatolian Fault. *Acta Geophys Pol* 53(1):103–114
- Ernst T, Jankowski J, Semenov V, Adam A, Hvozdara M, Józwiak W, Lefeld J, Pawliszyn J, Szarka L, Wesztergom V (1997) Electromagnetic sounding across the Tatra mountains. *Acta Geophys Pol* XLV(1):23–33
- Ernst T, Sokolova EY, Varentsov IM, Golubev NG (2001) Comparison of two techniques for magnetotelluric data processing using synthetic data sets. *Acta Geophys Pol* XLIX(2):2001
- Ernst T, Jankowski J, Józwiak W, Lefeld J, Logvinov I (2002) Geoelectrical model along a profile across the Tornquist-Teisseyre zone in southeastern Poland. *Acta Geophys Pol* 50(4):505–515
- Ernst T, Brasse H, Cerv V, Hoffmann N, Jankowski J, Jozwiak W, Kreutzmann A, Neska A, Palshin N, Pedersen L, Smirnov M, Sokolova E, Varentsov IM (2008) Electromagnetic

- images of the deep structure of the Trans European Suture Zone beneath Polish Pomerania. *Geophys Res Lett* 35. doi:[10.1029/2007GL034610](https://doi.org/10.1029/2007GL034610)
- Grad M, Guterch A, Keller GR, Janik T, Hegedűs E, Vozár J, Ślączka A, Tiira T, Yliniemi J (2006) Lithospheric structure beneath trans-Carpathian transect from Precambrian platform to Pannonian basin: CELEBRATION 2000 seismic profile CEL05. *J Geophys Res* 111:B03301
- Jankowski J (1967) The marginal structure of the East European Platform in Poland on the basis of data on geomagnetic field variations. *Publ Inst Geophys Pol Acad Sci* 14:93–102
- Jankowski J (1972) Techniques and results of magnetotelluric and geomagnetic deep soundings. *Publ Inst Geophys Pol Acad Sci* 54:135
- Jankowski J, Tarłowski Z, Praus O, Pecova J, Petr V (1985) The results of deep geomagnetic sounding in the West Carpathians. *Geophys J R Astr Soc* 80:561–574
- Jankowski J, Pirjola R, Ernst T (1986) Homogeneity of magnetic variations around the Nurmijarvi observatory. *Geophysica* 22(1–2):3–13
- Jankowski J, Pawliszyn J, Jóźwiak W, Ernst T (1991) Synthesis of electric conductivity surveys performed on the Polish part of the Carpathians with geomagnetic and magnetotelluric sounding methods. *Publ Inst Geophys Pol Acad Sci A-19* (236)
- Jankowski J, Ernst T, Jozwiak W, Pawliszyn J (1995) Results of induction study within the Precambrian segment of the Tornquist-Tesseyre tectonic zone. *Acta Geophys Pol* 43:2
- Jankowski J, Sucsdorff Ch (1996) Guide for magnetic measurements and observatory practice, Edited by International Association of Geomagnetism and Aeronomy
- Jankowski J, Ernst T, Jozwiak W (2004) Effect of thin near-surface layer on the geomagnetic induction arrows: an example from the East European platform. *Acta Geophys Pol* 52(3):349–361
- Jankowski J, Jóźwiak W, Vozar J (2008) Arguments for ionic nature of the Carpathian electric conductivity anomaly. *Acta Geophys* 56(2):455–465
- Jóźwiak W, Beamish D (1986) A thin-sheet model of electromagnetic induction in northern England and southern Scotland. *Geophys J R Astr Soc* 85(3):629–643
- Jóźwiak, W. (2001), Stochastic inversion method for modeling the electrical conductivity distribution within the Earth's mantle. *Publ Inst Geophys Pol Acad Sci C-78(327):75*
- Jóźwiak W (1993) Application of stochastic method to the global inverse problem. *Acta Geophys Pol* 41:2
- Jozwiak W, Kovacikova S, Nowozynski K, Varentsov IM (2009) Comparison of techniques to extract geomagnetic field components from array of induction arrows using spline hilbert transform, IAGA 11th Scientific Assembly, Sopron, 2009; *abstract book*, ed. Szarka László
- Jozwiak W (2012) Large-scale crustal conductivity pattern in central Europe and its correlation to deep tectonic structures. *Pure Appl Geophys* 169:1737–1747. doi:[10.1007/s00024-011-0435-7](https://doi.org/10.1007/s00024-011-0435-7)
- Kauristie K, Ernst T, Jankowski J, Viljanen A, Kultima J, Pirjola R (1990) Homogeneity of geomagnetic variations at the Sodankyla Observatory. Finnish Academy of Science and Letters publications, p 76
- Lefeld J, Jankowski J (1985) Model of deep structure of the Polish Inner Carpathians. *Publ Inst Geophys Pol Acad Sci A-16:175*
- Majorowicz JA (2004) Thermal lithosphere across the Trans-European Suture Zone in Poland. *Geol Q* 48:1–14
- Marianiuk J (1977) Photoelectric converter for recording the geomagnetic field elements: construction and principle of operation. *Publ Inst Geophys Pol Acad Sci C-4(114):57–82*
- Marianiuk J, Jozwiak W, Neska A, M. Neska (2007) Underwater magnetometer MG-01/2003 for geomagnetic offshore soundings. In: XII IAGA Workshop on geomagnetic observatory instruments, data acquisition and processing, vol C-99, Issue 398. Publications of the Institute of Geophysics Polish Academy of Sciences, pp 87–92
- Marquardt D (1963) An algorithm for least-squares estimation of nonlinear parameters. *SIAM J Appl Math* 11(2):431–441

- Narkiewicz M, Dadlez R (2008) Geological regional subdivision of Poland: general guidelines and proposed schemes of sub-Cenozoic and sub-Permian units. *Prz Geol* 56:391–397 (in Polish with English abstract)
- Nowożyński K (1981) Methods of solving one-dimensional magnetotelluric inverse problem. *Publ Inst Geophys Pol Acad Sci G-3*
- Nowożyński K, Ernst T, Jankowski J (1991) Adaptive smoothing method for computer derivation of K-indices. *Geophys J Int* 104:85–93
- Nowożyński K, Pushkarev PYu (2001) The efficiency analysis of programs for two-dimensional inversion of Magnetotelluric Data. *Fiz Zemli* 6
- Nowożyński K (2004) Estimation of magnetotelluric transfer functions in the time domain over a wide frequency band. *Geophys J Int* 158:32–41
- Nowożyński K (2012) Splines in the approximation of geomagnetic fields and their transforms at the Earth's surface. *Geophys J Int* 189:1369–1382. doi:[10.1111/j.365-246X.2012.05458.x](https://doi.org/10.1111/j.365-246X.2012.05458.x)
- Pawliszyn J, Jankowski J (1973) The results of preliminary treatment of magnetotelluric investigations on the VII international profile. *Publ Inst Geophys Pol Acad Sci* (60)
- Pożaryski Wł, Małkowski Z, Jankowski J (1965) Distribution of shortperiod geomagnetic variations related to tectonics in Central Europe. *Rocznik Pol Tow Geol* 97–102
- Pushkarev PYu, Ernst T, Jankowski J, Józwiak W, Lewandowski M, Nowożyński K, Semenov VYu (2007) Deep resistivity structure of the Trans-European Suture Zone in Central Poland. *Geophys J Int* 169(3):926–940
- Schmucker U (1970) Anomalies of geomagnetic variations in the southwestern United States. University of California Press, Berkley
- Semenov VYu, Jankowski J, Ernst T, Józwiak W, Pawliszyn J, Lewandowski M (1998) Electromagnetic sounding across the Holly Cross Mountains, Poland. *Acta Geophys Pol* XLVI(2):171–185
- Semenov VYu, Jankowski J, Józwiak W (2002) New evidence of the anomalously conductive mantle beneath the Tornquist-Tesseyre zone in Poland. *Acta Geophys Pol* 50(4):517–526
- Semenov VYu, Józwiak W, Pek J (2003) Deep electromagnetic soundings conducted in Trans-European Suture Zone. *EOS Trans AGU* 84(52):581, 584
- Semenov V, Józwiak W (2005) Estimation of the upper mantle conductance at the Polish margin of the East European platform. *Izv Phys Solid Earth* 41(4):326–332
- Semenov VYu, Józwiak W (2006) Lateral variations of the mid-mantle conductance beneath Europe. *Tectonophysics* 416:279–288
- Semenov VYu, Pek J, Ádám A, Józwiak W, Ladanyvskyy B, Logvinov IM, Pushkarev P, Vozar J (2008) Electrical structure of the upper mantle beneath Central Europe: results of the CEMES project. *Acta Geophys* 56(4):957–981
- Środa P, Czuba W, Grad M, Guternik A, Tokarski AK, Janik T, Rauch M, Keller GR, Hegedus E, Vozar J, CELEBRATION 2000 Working Group (2006) Crustal and upper mantle structure of the Western Carpathians from CELEBRATION 2000 profiles CEL01 and CEL04: seismic models and geological implications. *Geophys J Int* 167:737
- Tarłowski Z (1978) Application of the finite difference method to explain the electromagnetic induction in two-dimensional structures. Ph.D. thesis, Institute of Geophysics of Polish Academy of Sciences
- Tikhonov AN (1950) On investigation of electrical characteristic of deep strata of Earth's crust. *Dokl Akad Nauk SSSR* 73:295–297
- Wieladek R, Ernst T (1977) Application of the method of least squares to determining impulse responses and transfer functions. *Publ Inst Geophys Pol Acad Sci G-1(110)*:3–12
- Wieladek R, Nowożyński K (1981) Modified method of minimal residuals for large systems of linear equations. *Publ Inst Geophys PAN G-2:143*
- Wieladek R, Nowożyński K, Tarłowski Z (1981) Application of the Cholesky-Banachiewich method to solving some linear systems of equations approximating Helmholtz's equation. *Publ Inst Geophys Pol Acad Sci G-2(12)*: 3–12
- Wieladek R, Nowożyński K (1989) The accuracy of solution of one-dimensional magnetotelluric inverse problem. *Acta Geophys Pol* 37(1):37–70

- Wielądek R, Nowożyński K (2001) Determination of transfer function through solution in time domain. *Acta Geophys Pol* XLIX(1):131–142
- Zadro M, Ernst T, Teisseyre R, Jankowski J (1990) The magnetotelluric recordings from seismic zone Friuli, N-E Italy. *Tectonophysics* 180:303–308
- Znosko J (1998) Tectonic Atlas of Poland, Państwowy Instytut Geologiczny i Wydawnictwa

Half Century of the Ozone Observations at the Central Geophysical Observatory, IGF PAS, Belsk, Poland

Janusz W. Krzyścin, Janusz Borkowski, Anna Głowiak, Janusz Jarosławski, Jerzy Podgócki, Aleksander Pietruczuk, Bonawentura Rajewska-Więch, Anna Sawicka, Piotr Sobolewski, Jakub Wink and Wiesława Zawisza

Abstract The history of ozone observations at Belsk (51.84°N , 20.79°E) is shortly described and the results of a novel statistical model are presented to show various aspects of the long-term variability of Belsk's ozone in the period 1963–2012. The model stems from previous experiences of the Department of the Atmospheric Physics, Institute of Geophysics, Polish Academy of Sciences (IGF PAS), in the statistical modeling of the ozone layer. The analysis corroborates our earlier finding of the first stage of the ozone recovery over Belsk, i.e., a weakening of the negative ozone trend there. The second stage of the ozone recovery, i.e., an appearance of the statistically significant positive trend in series having had removed the “natural variability”, could not be yet announced. Generally, the long-term variability of the Belsk's total ozone follows the anthropogenic trend, which is forced by changes of the man-made ozone depleting substances concentration in the mid-stratosphere. It provides a strong support for the effectiveness of the Montreal Protocol 1987 (and its subsequent amendments) regulations for protection of the ozone layer. The slowing down of the ozone recovery and the first sign of returning back to the negative tendency, which previously existed in the period 1980–1996, are found in the Belsk's ozone time series since 2005, especially in the summer data. Such changes in the ozone layer are of special interest as they will induce an increase of the ground level solar UV-B intensity in the season of the naturally high UV radiation and frequent outdoor activity. Thus, in spite of evidence of the ongoing ozone recovery over the globe, the ozone issue, especially its local aspect, still needs attention of both scientists and public.

Keywords Geophysics · Ozone observations · Atmosphere · History of the Institute of Geophysics PAS

J. W. Krzyścin (✉) · J. Borkowski · A. Głowiak · J. Jarosławski · J. Podgócki · A. Pietruczuk · B. Rajewska-Więch · A. Sawicka · P. Sobolewski · J. Wink · W. Zawisza
Polish Academy of Sciences, Institute of Geophysics, Warsaw, Poland
e-mail: jkrzys@igf.edu.pl

1 Introduction

The atmospheric ozone variability has been an important research topic since the mid-1970s, after Crutzen (1973), Molina and Rowland (1974), the 1996 Nobel prize winners in chemistry, have found a possibility of thinning of the ozone layer due to increasing concentration of man-made ozone depleting substances (ODS) in the mid-altitude stratosphere. The thinning of the ozone layer became one of the most important ecological issues in 20th century as the ozone layer is a shield protecting the Earth from harmful extraterrestrial solar ultra violet (UV) radiation. Ozone is the only chemical compound in the atmosphere, which is capable of absorbing solar UV in the biologically active part of the UV spectrum, 290–315 nm, i.e., in the so-called UV-B range.

The discovery of the ozone hole over the Antarctica in 1984 (Chubachi 1984; Farman et al. 1985), and the anthropogenic origin of the hole (Solomon et al. 1986) alarmed both scientists and the public of a growing danger to the Earth ecosystems due to the anticipated increase of the surface UV radiation. Awareness of this threat to life on Earth led to cooperation between politicians, scientists, and industrialists that resulted in signing (16 September 1987) the international treaty between United Nations countries, the Montreal Protocol, to monitor and reduce the ODS production. The first papers showing the ozone depletion over the densely populated regions (NH midlatitudes) appeared at the Quadrennial Ozone Symposium in 1988 at Göttingen (Rowland et al. 1989; Degórska et al. 1989). In subsequent years, there were several MP amendments (London 1990, Copenhagen 1992, Montreal 1997, and Beijing 1999) setting even more rigorous restrictions to the ODS production and consumption. All these efforts brought an apparent lowering of the ODS level in the mid-altitude stratosphere since the mid-1990s (over the extratropics) and since the end of 1990s (over the high latitude regions—Antarctica) and the corresponding total ozone trend overturning (WMO 2011). Many statistical analyses focused on detection of the anthropogenic trend component in the ozone data and search for ways leading to the recovery of the ozone layer. The apparent negative TO_3 trends, which were found in the mid- and high latitude before the maximum of ODS level (~ 1995) in the stratosphere, were replaced afterwards by slight positive ones. For some sites and regions these trends were highly statistically significant (e.g., Vyushin et al. 2007; Harris et al. 2008; Salby et al. 2011; WMO 2011; Krzyścin 2012; Nair et al. 2013).

Multi-decadal, quality-controlled, ground-based observations of the total amount of ozone contained in a vertical column of the atmosphere, i.e., the so-called total ozone (TO_3), are a basic source to delineate ozone variability with different time scales, ranging from intra-day oscillations up to decadal trend variability. There are only few stations in Europe with the continuous ozone observations for about 50 year period or longer: Arosa (Switzerland: since 1926), Hradec Kralove (the Czech Republic, since 1961), and Belsk (Poland, since 1963). The very recent papers concerning the analyses of the Belsk's ozone have shown the lowering of the total ozone trends since the mid 1990s and the trend

overturning in the upper stratosphere (~ 40 km) throughout the whole year and in the lower stratosphere (14–23 km) only in spring (Krzyścin and Rajewska-Wiech 2009a, b).

Here we present the history of the ozone observations at Belsk and results of a novel trend model applied to updated Belsk's total ozone data for the period 1963–2012 to find: (i) the ozone trend variability in this period, (ii) effectiveness of MP regulations in changing the Belsk's ozone, (iii) the long-term variability of the ozone pattern due to combined chemical and dynamical forcing on the ozone layer.

2 History of the Ozone Observations at Belsk

An idea to start ozone measurements at Belsk appeared around 1960. Professor Teodor Kopcewicz (\dagger 1976), from the Warsaw University, proposed to install the Dobson spectrophotometer at Belsk Observatory, at that time being under construction. There was a hope that the measurements of the column amount of ozone in the atmosphere from the surface level up to the end of stratosphere and the ozone vertical profiles (by the Umkehr method) would have been able to improve the weather forecasting models because of the existing strong correlation between the ozone changes and the weather pattern variability. Fortunately, some money directed by the government to the Polish participation in the First International Geophysical Year 1957/1958 was not totally spent and the rest could have been used for purchasing the spectrophotometer. Dr. Aniela Dziewulska-Łosiowa (\dagger 2004), from the Institute of Geophysics PAS, went through numerous bureaucracy steps of the purchasing procedure, finally resulting in the spectrophotometer being set up at the Belsk Observatory in the early 1963. She was also a pioneer of the ozone measurements in Poland, which she carried out during the first few years of the instrument operation at Belsk. The ozone data appeared regularly (on the yearly basis) in the Publications of the Institute of Geophysics, Polish Academy of Sciences, since 1965. Figure 1 shows Dr. Aniela Dziewulska-Łosiowa (pioneer of the ozone measurements in Poland and the author of comprehensive monograph on ozone in the atmosphere: Dziewulska-Łosiowa 1991) and Prof. Teodor Kopcewicz (the initiator of the ozone measurements in Poland) during a non-formal meeting in Warsaw (Institute of Geology, Warsaw University) around 1958.

The Belsk's ozone record by the Dobson instrument No. 84 started on 23 March 1963, i.e., long-before the ozone issue became the key ecological problem. First observations were carried out on the ground-level terrace and the instrument was stored in a wooden pavilion (Fig. 2). Since 1965, i.e., after completion of the new building for the atmospheric observations (Fig. 3), the Dobson spectrophotometer measurements have been performed continuously up to now at the same place—terrace on the second floor of the atmospheric physics laboratory (Fig. 3). There were only a few short breaks of the ozone observations at Belsk (lasting maximally few weeks) due to the international calibration campaigns with other Dobson spectrophotometers.



Fig. 1 Scientists who contributed to setting up the ozone measurements at Belsk. Dr. Aniela Dziewulsko-Łosiowa (IGF PAS) and Prof. Teodor Kopcewicz (Warsaw University). (*Source* Archives of the Department of the Atmospheric Physics, IGF PAS)

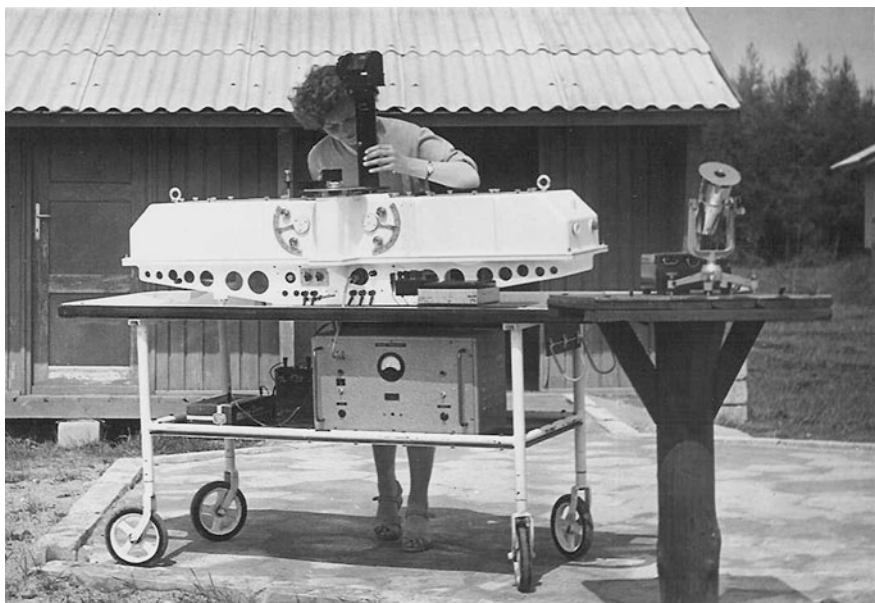


Fig. 2 The ozone observation at Belsk in summer 1963. (*Source* Archives of the Department of the Atmospheric Physics, IGF PAS)

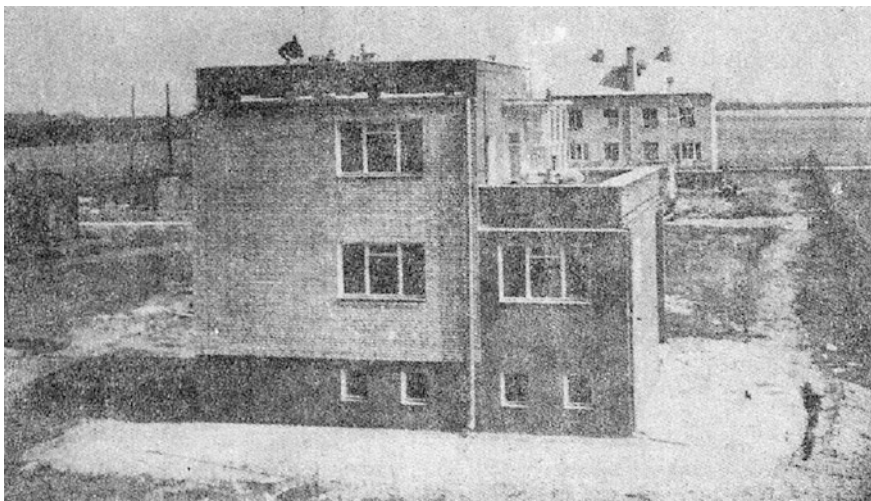


Fig. 3 The view (around 1964) of the Atmospheric Physics Laboratory at Belsk where ozone measurements by the Dobson spectrophotometer have been carried up to now. (*Source* Archives of the Department of the Atmospheric Physics, IGF PAS)

Having the high quality ozone data, appropriate for long-term statistical analyses, has always been the major concern of the IGF PAS ozone team. The data quality procedures of Dobson measurements were strengthened since the mid-1970s. Frequent international intercomparisons of the Belsk's Dobson with the world standard instrument were an essential point of the quality control procedure of the instrument. It is worth mentioning that the first Dobson instrument intercomparison took place at Belsk in June/July 1974 (Fig. 4) due to the initiative of Dr. Aniela Dziewulska-Łosiowa (with the support from World Meteorological Organization—WMO) to homogenize the ozone data collected by various spectrophotometers. Since then the Dobson calibration campaigns were organized on regular basis. There were the calibration campaigns at Belsk (1974), Potsdam (1979), Arosa (1986, 1990, and 1995) with the world standard Dobson instrument No. 83 (e.g., WMO 1995). Subsequent campaigns (2001, 2005, 2009) were organized at the European regional Dobson calibration center, the Meteorological Observatory Hohenpeissenberg, Germany. Local European sub-standard, the Dobson spectrophotometer No. 64, was used as the reference instrument during the inter-comparisons at the center.

The complementary measurements of the total ozone and vertical profiles by the fully automated instrument, the Brewer spectrophotometer (BS), has begun at Belsk by single monochromator BS No. 64 in 1991 and by double monochromator BS No. 207 in 2010. Thus, the Dobson quality control procedure between the intercomparisons could be accomplished by the cross-comparisons with the collocated BS measurements and with the satellite data taken during the Belsk's station overpasses (Rajewska-Więch et al. 2006).



Fig. 4 The view (from the Atmospheric Physics Laboratory terrace) of the first international intercomparison campaign carried out at the Belsk's premises in June/July 1974. (*Source* Archives of the Department of the Atmospheric Physics, IGF PAS)

Some part of the Dobson data has been re-evaluated on the reading-by-reading basis using the Bass-Pour ozone absorption coefficients (for all the data collected before 1992) and adding to the standard calculation retrieval the results of the intercomparisons, i.e., changes in R-N tables if they happened (Dziewulska-Łosiowa et al. 1983; Degórska and Rajewska-Więch 1991; Degórska et al. 1995). As a result of these quality control and quality insurance efforts, the homogenized time series of the Belsk's ozone have been appropriate for the long-term analyses. The Belsk's total ozone and the Umkehr ozone profiles were used in numerous trend analyses, starting from the paper of Degórska et al. (1989) showing negative trend in the Belsk's TO_3 in winter.

The ozone observations at Belsk contribute to the international efforts of monitoring the ozone layer and analyzing sources of the ozone variability in the Earth's atmosphere. The MP 1987 and its subsequent amendments also called for strengthening scientific activity and international cooperation in the area of the ozone monitoring. The key point was a delineation of the ozone response to changes in ODS level in the atmosphere, which were forced by MP 1987 regulations to limit production and usage of ODS. The importance of the ozone issue has been recognized by the Polish Government. The IGF PAS has been receiving regular financial support for the ozone monitoring at Belsk for more than 20 years.



Fig. 5 The scientific staff and the technicians presently involved (September 2013) in the ozone observations and data analyses: (*upper row, left*) Prof. Janusz W. Krzyścin, M.Sc. Jerzy Podgócki, Dr. Piotr S. Sobolewski, M.Sc. Jakub Wink, Dr. Aleksander Pietruszuk. (*bottom row, left*) M.Sc. Bonawentura Rajewska-Więch, Wiesława Zawisza, Dorota Sawicka, M.Sc. Izabela Pawlak, Dr. Janusz Jarosławski. *Photo* was made on the Dobson spectrophotometer observing terrace at Belsk (Source Archives of the Department of the Atmospheric Physics, IGF PAS)

The staff from the Department of the Atmospheric Physics and the Belsk's Observatory, Institute of Geophysics, PAS presently involved in the ozone monitoring is presented in Fig. 5.

3 The Ozone Explanatory Variables

Ozone depleting substances (ODS) belong to a category of chlorofluorocarbons (CFCs) and hydrochlorofluorocarbons (HCFCs), i.e., chemicals containing bromine, chlorine, fluorine, carbon, and hydrogen (only HCFCs) in varying proportions. The ODS released at the ground-level migrate to the stratosphere where strong solar UV radiation breaks down CFCs and HCFCs, freeing the chlorine and bromine that have a large ozone destructive potential through numerous catalytic reactions, which are summarized by the reaction: $O_3 + O + M \rightarrow 2O_2 + M$.

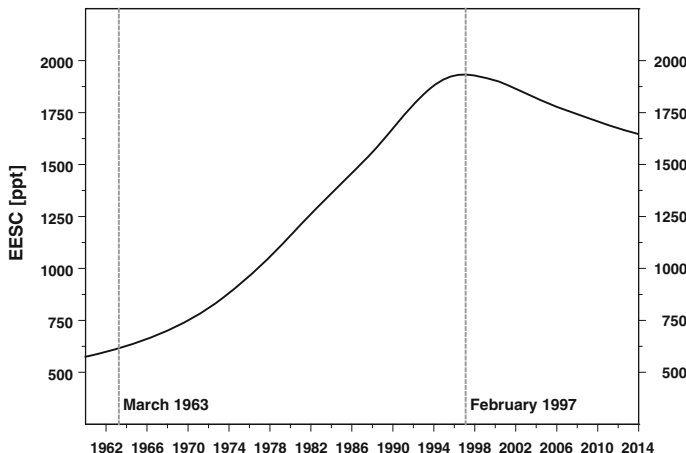


Fig. 6 The time series of the Equivalent Effective Stratospheric Chlorine (EESC) in the NH extratropics in the middle-altitude stratosphere calculated assuming mean air age of 3 year and age-of-air spectrum width of 1.5 year. The vertical lines show the start time of the ozone observations at Belsk and the time of EESC maximum

The total destructive potential of these chemicals is expressed using the equivalent effective stratospheric chlorine (EESC) (e.g., Newman et al. 2007). The EESC changes with time are used to monitor anthropogenic forcing on the ozone layer and to find out the effectiveness of the MP regulations on ODS production limits. In statistical modeling, the EESC time series is used for attribution of ODS effects to the ozone layer changes. Here we calculate the EESC time series using the software (http://acdb-ext.gsfc.nasa.gov/Data_services/automailer/) assuming mean air age of 3 year and age-of-air spectrum width of 1.5 year that represent typical values for the mid-altitude extratropical stratosphere (WMO 2011). The selected EESC time series is shown in Fig. 6.

Various proxies related to dynamical processes known to affect the ozone variability in the NH midlatitudes are selected to explain the long-term TO_3 changes at Belsk. These are: (i) the zonal component of wind at 30 and 50 hPa averaged over the tropics for the Quasi Biennial Oscillation (QBO) attribution, (ii) the Arctic Oscillation (AO) Index, (iii) Penticton/Ottawa 2800 MHz solar flux to search for the 11 year solar cycle effects, (iv) the El Niño/Southern Oscillation (ENSO) index, sea surface temperature (SST) anomaly in the Niño-3.4 region, used to search for effects of quasi-periodical SST temperature fluctuations in the equatorial Pacific, (v) cumulative Eliassen-Palm (EP) flux at 100 hPa averaged over 45–75°N region for description of the ozone changes induced by the variability of the Brewer-Dobson circulation, (vi) stratospheric aerosol optical depth at 550 nm for attribution of the ozone variability to the volcanic eruptions, (vii) local (over Belsk) meteorological variables (from Reanalysis 2 data base); temperature at 50 and 10 hPa, and the tropopause pressure used as proxies for local dynamical

effects on ozone. These proxies were commonly used in the previous ozone trend studies (e.g., Krzyścin 2006; Vyushin et al. 2007; Mader et al. 2007; Harris et al. 2008; Nair et al. 2013).

4 Statistical Model

Original statistical software was developed in IGF PAS to determine factors responsible for the ozone variability in different time scales, using wavelets (e.g., Borkowski 2004; Krzyścin and Borkowski 2008); Multiple Adaptive Regression Splines (MARS) (e.g., Krzyścin, 2008); as well as the neural Network (NN) (e.g., Jarosławski 2013). We focused in particular on a quantification of the man-made effects on ozone, which are related to the ODS level change in the mid-altitude stratosphere, from the noisy time series of ozone that contains various oscillations of different origin and over wide range of time scales. Here we present a novel statistical trend model being a synthesis of our previous trend studies to disclose the long-term variability of the Belsk's total ozone for the period 1963–2012.

The TO_3 monthly means, $O_3(t_{i,j})$, for year i ($i = 1$ in 1963) and calendar month j are calculated from all daily means, averaging the results of intra-day ozone measurements (i.e., direct Sun, zenith blue and cloudy TO_3 measurements). Next, the fractional TO_3 deviations (deseasonalized monthly means), $\Delta O_3(t_{i,j})$, are derived and further used as the dependent (output) variable in a statistical model:

$$\Delta O_3(t_{i,j}) = (O_3(t_{i,j}) - O_3(j)) / O_3(j) \times 100\%, \quad (1)$$

where $O_3(j)$ is the long-term (1963–2012) TO_3 monthly mean for calendar month j obtained as the mean from all monthly means in the period 1963–2012.

The trend pattern will be revealed from the proposed three-step statistical model:

- **First step**—finding chemical and dynamical part of the ozone variability

Variability of $\Delta O_3(t_{i,j})$ is assumed to be a superposition of slow component having the chemical origin (related to ODS changes) and various components due to dynamical processes affecting the ozone transport.

$$\Delta O_3(t_{i,j}) = \text{Trend}_{\text{ODS}}(t_{i,j}) + \text{Dynamics}(t_{i,j}) + \text{Noise}(t_{i,j}), \quad (2)$$

$\text{Trend}_{\text{ODS}}(t_{i,j})$, represents the anthropogenic trend component of the ozone time series that is assumed to be proportional to the EESC time series change from the beginning of the Belsk time series (March 1963, i.e., $i = 1$ and $j = 3$),

$$\text{Trend}_{\text{ODS}}(t_{i,j}) = \alpha_{\text{EESC}}(\text{EESC}(t_{i,j}) - \text{EESC}(t_{1,3})) \quad (3)$$

where α_{EESC} is the regression constant to be determined by the standard multiple regression fit $Dynamics(t_{i,j})$ is a linear combination of the potential proxies (regressors) of the ozone variability, $X_M(t_{i,j})$, which are commonly used indices of dynamical process affecting on the ozone variability (see Sect. 3 for the proxies selection);

$$Dynamics(t_{i,j}) = \alpha_o + \sum_M \alpha_M X_M(t_{i,j-\Delta M}) \quad (4)$$

where constants α_o and α_M are calculated by standard multi-linear statistical analysis, ΔM represents the time lag (in months) necessary for M -th proxy to start its influence on ozone at Belsk. Various combinations of ΔM values (between 0 and 6 month) for all the proxies are examined to select optimal set of ΔM values giving the best fit to the observed data, $Noise(t_{i,j})$ represents the noise term that can be partially linked to the presently unknown short-term forcing.

Model (2) is run to find $Dynamics(t_{i,j})$ part of model (2) for the four seasonal subsets of the yearly data: winter, $j = \{12, 1, 2\}$; spring, $j = \{3, 4, 5\}$; summer, $j = \{6, 7, 8\}$; autumn, $j = \{9, 10, 11\}$; and for the year-round data $j = \{1, \dots, 12\}$. Such trend model has been extensively used in various estimates of the long-term ozone changes (e.g., Reinsel et al. 2005; Mäder et al. 2007; Harris et al. 2008) to find the ozone response to the chemical (due to ODS) and dynamical forcing on the ozone layer.

- **Second step**—extraction of the overall trend and local trend time series

A smooth function, $Trend_{ALL}(t_{i,j})$, which represents the trend component comprising both the chemical effects and the long-term dynamical effects with yet unknown origin is filtered out from the residual time series of model (2), $Resid(t_{i,j})$, having removed dynamical signal due to the selected (Sect. 3) ozone dynamical proxies,

$$Resid(t_{i,j}) = \Delta O_3(t_{i,j}) - \sum_i \alpha_i X_i(t_{i,j}) = Trend_{ALL}(t_{i,j}) + Noise^*(t_{i,j}) \quad (5)$$

where $Trend_{ALL}(t_{i,j})$ is the smooth function obtained by LOWES smoother (Cleveland 1979) applied to $Resid(t_{i,j})$ time series. The level of smoothing is chosen to have $Trend_{ALL}(t_{i,j})$ series free from short-term oscillations with periodicities up to about one decade, thus $Noise^*(t_{i,j})$ comprises only the short-term oscillations. It is worth mentioning that the trend curve by model (5) does not possess a pre-defined analytical form. The shape of trend curve is revealed by the smoothing of the fractional ozone time series having “natural” variability removed. It could be a non-linear with a number of local extremes. The first time derivative of the $Trend_{ALL}(t_{i,j})$ time series provides an estimate of the local trend values,

$$Local_Trend(t_{i,j}) = 0.5(Trend_{ALL}(t_{i,j+1}) - Trend_{ALL}(t_{i,j-1})) \% / \text{per month} \quad (6)$$

Examination of the local trend time series allows to find periods with extreme rate of changes and the year of the trend overturning.

- **Third step**—comparison between the overall and the anthropogenic trend pattern

The anthropogenic trend pattern is calculated in the first step of the statistical model by Eq. 3. It provides the ozone long-term changes induced by the EESC variations throughout the whole of the analyzed period. The overall trend term, found in the second step, could not be linked with a specific process. It represents the long-term pattern that exists in the ozone time series having removed combined signal due to known dynamical forcing. Thus, the overall trend is a superposition of signals due to various mostly unknown chemicals and/or dynamical processes.

A difference between the overall and anthropogenic trend pattern allows us to assess to what extent the ozone long-term variability is determined by the EESC changes reflecting the ODS production and consumption limits, which were forced by the MP 1987 and its subsequent amendments. Thus, the effectiveness of the MP 1987 regulations and their subsequent amendments to protect of the ozone layer could be confirmed by analysis of the differences between the overall and the anthropogenic trend pattern.

Calculation of the uncertainty range of the differences requires special re-sampling procedure. We consider a re-sampling family of the hypothetical $Trend_{ALL}^*(t_{i,j})$, $n = \{1, \dots, N\}$ trend time series to estimate the statistical properties of the differences between the overall and the anthropogenic trend time series. The block bootstrap technique is used to generate hypothetical $Trend_{ALL}^*(t_{i,j})$ time series by the LOWES smoothing applied to the bootstrapped $Resid(t_{i,j})$ time series, $Resid^*(t_{i,j})$,

$$Resid_n^*(t_{i,j}) = Trend_{ALL}(t_{i,j}) + Noise_n^*(t_{i,j}), \quad n = \{1, \dots, N = 1000\} \quad (7)$$

where $Noise_n^*(t_{i,j})$ is the n -th hypothetical representative of $Noise^*(t_{i,j})$ term that is built from consecutive 3 month seasonal blocks randomly drawn from the seasonal subset (DJF, MAM, JJA, SON) of the $Noise^*(t_{i,j})$ time series (see Eq. 5). Finally, $Trend_{ALL}^*(t_{i,j})$ time series are retrieved by the LOWES smoothing applied to $Resid_n^*(t_{i,j})$ term.

Figure 7 shows an example set of 5 bootstrapped representatives of the trend time series in the year-round data i.e., $Trend_{ALL}^*(t_{i,j})$, $i = \{1, \dots, 50\}$, $j = \{1, \dots, 12\}$, $n = \{1, \dots, 5\}$. For each data point, $t_{i,j}$, the statistical parameters (median, 97.5 percentile, and 2.5 percentile) of the difference between the overall and the anthropogenic (\sim EESC) trend, $\delta Trend(t_{i,j})$, is calculated from the set of the bootstrapped $\delta Trend_n^*(t_{i,j})$ time series,

$$\delta Trend_n^*(t_{i,j}) = Trend_{ALL}^*(t_{i,j}) - Trend_{ODS}(t_{i,j}); \quad n = \{1, \dots, 1000\} \quad (8)$$

Our interest is not only in the trend pattern estimate, i.e., in a smooth time series that is extracted from the fractional ozone variations after removal of the dynamical part of ozone variability as defined by Eq. 4. Such a trend pattern could be called an anthropogenic one if $\delta Trend_n(t_{i,j})$ values are close to zero.

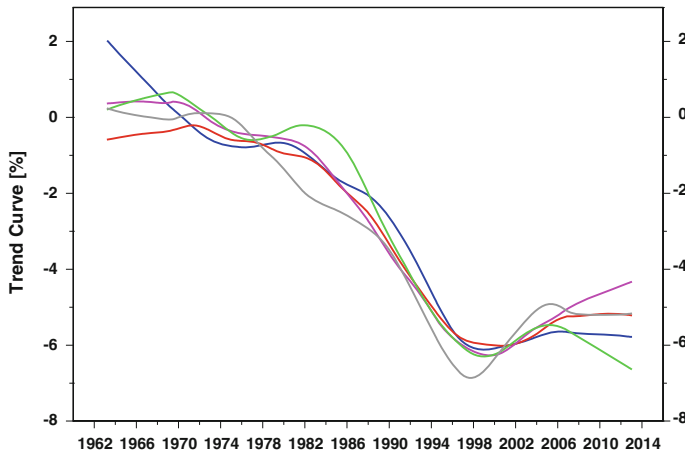


Fig. 7 Examples of the bootstrap representative of the overall trend component in the year-round monthly fractional deviations for the period 1963–2012

To search for the long-term UV response to changing ozone, it is necessary to deal with the ozone tendency that is defined as the long-term component extracted from the whole time series of the fractional deviations. The anthropogenic trend is a part of the overall trend and consequently the overall trend is a part of the ozone tendency. The long-term changes in the ground-level UV are anti-correlated with the ozone tendency variability.

The uncertainty range of the ozone tendency is obtained by examining the bootstrap representatives of the ozone tendencies that are filtered out from the bootstrap sample of ozone fractional deviations $\Delta O_3^*(t_{ij})$,

$$\begin{aligned} \Delta O_{3n}^*(t_{ij}) = & \text{Trend}_{\text{ALL}}(t_{ij}) + \alpha_o \\ & + \sum_M \alpha_M X_M(t_{ij-M}) + \text{Noise}_n^*(t_{ij}), \quad n = \{1, \dots, N = 1000\} \end{aligned} \quad (9)$$

The methodology of calculating uncertainties of the trend and tendency time series based on the bootstrap sample was described in more details in our previous paper (Krzyścin 2006).

5 Results

Figure 8 shows the TO_3 monthly means subset for all seasons of the year and the year-round monthly mean series. The tendency curves, by the LOWES smoother applied to the whole time series, are superposed on the monthly means to illustrate the long-term ozone variability comprising all (chemical + dynamical) effects.

The following phases of the long-term variability of the Belsk's TO_3 could be identified in the year-round data: (i) a stable ozone up to the end of 1970s, (ii) strong decline in the period 1980–1996, (iii) a long term oscillation in the period 1997–2012 with the local maximum around 2005 and the local minimum at the end of the time series with the ozone decline comparable to that in 1996. The ozone behaviour in the third phase is quite surprising as a positive trend is rather expected from the recent ODS decrease than the oscillation around the mid 1990s level. It is worth mentioning that the negative or positive tendencies could be revealed in the early ozone observations up to 1980 in the winter and summer subset of the yearly data, respectively. Moreover, the summer and autumn data exhibit a steady ozone decline starting around 1975–1980 and lasting up to the end of the data.

Figure 9 presents a relationship between modeled Eqs. (2)–(3) and the observed TO_3 monthly means. The scatter plots are for all the seasons and for the yearly data. Both modeled and observed TO_3 values are in a close agreement as the model/observation points in Fig. 9 are grouped along the diagonal of the model/observation square. The percentage of the variance explained by the regression model (defined in the first step of the proposed model) is equal to 81, 73, 73, 75, and 72 % in winter, spring, summer, autumn, and in the year-round data, respectively. The last value matches that obtained in other trend studies; for example, Nair et al. (2013) found $R^2 = 65\%$ for the regression model applied to the year-round monthly TO_3 data taken by the Dobson spectrophotometer at Haute-Provence Observatory for the period 1984–2010.

The linear combination of the proxies with the optimal ΔM lags was used to find the composite dynamical signal in the Belsk's ozone (see Eq. 4). The regression constants, which determine the ozone response to the explanatory variables, are from the standard multi-linear least-squares fit. It seems possible that more sophisticated statistical model would result in much better estimation of the dynamical part of the Belsk's ozone variability. Thus we also examine the performance of the multilayer perceptron (MLP) neural network (NN), similar to that used in the modeling of the ozone vertical profile at Belsk (Jaroslawski 2013), to estimate the TO_3 response to the dynamical forcing.

Network complexity (number of neurons in the hidden layer) is chosen experimentally to give the best agreement between NN output and the reference dynamical TO_3 variability, $\Delta O_3(t_{i,j})\text{-Trend}_{\text{ODS}}(t_{i,j})$. The MLP structure is taken as 9–x–1 where 9 is the total number of dynamical proxies, x = 8 is the number of neurons in the hidden layer and 1 represents a single value for the output neuron providing the TO_3 value due to combined effects of all dynamical proxies.

The year-round signal due to the selected dynamical proxies is simulated by NN algorithm. It appears that the NN does not provide a better estimation of the dynamical part of ozone variability as $R^2 = 70\%$, i.e., a few percent lower than that by the multi-linear model. Further in the paper we will present results of both approaches (linear and NN) for estimation of the dynamical component of the series in the year-round data.

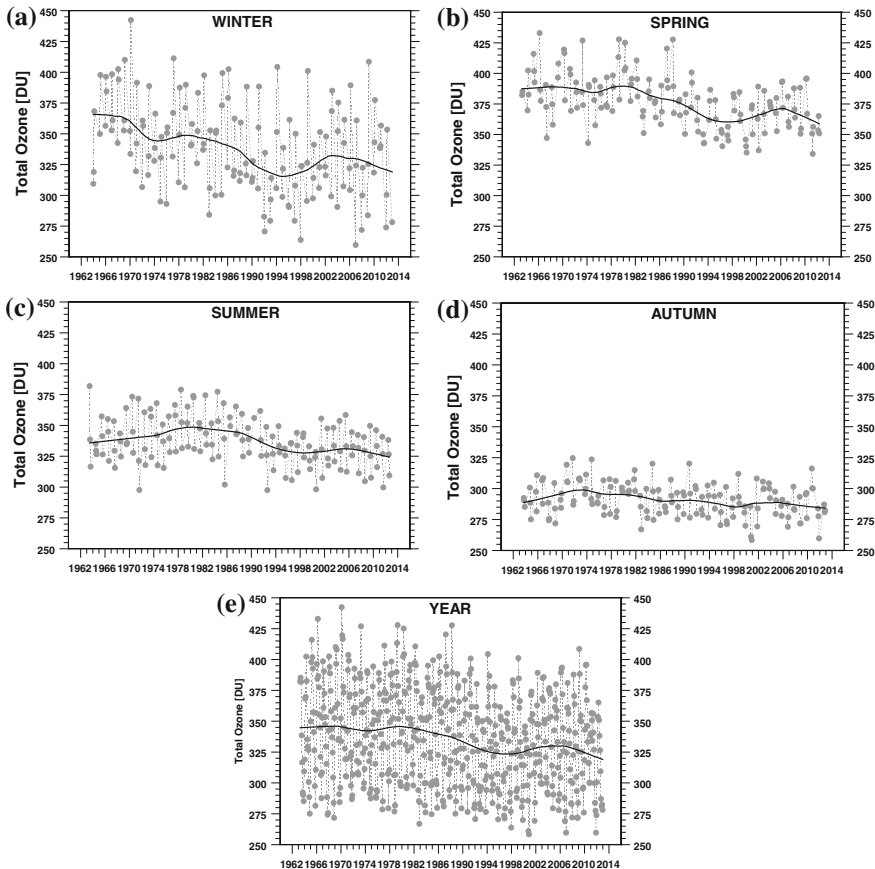


Fig. 8 The seasonal and the year-round total ozone monthly means (points) calculated from the Belsk's daily values. Curves represent the smoothed patterns by LOWES. **a–e** show the seasonal and year-round results by the multiple regression model, respectively

The seasonal and the year-round trend curves, $Trend_{ALL}(t_{i,j})$, are presented in Fig. 10. The ozone decline for the whole analyzed period (1963–2010) can be estimated as 10, 5, 4, 3 % for winter, spring, summer, and autumn, respectively, and 5 % decline is found in the year-round data. Two year-round trend curves (Fig. 10e, f), based on the model using multi-linear and NN approach in description of the dynamical component, are practically the same. The 95 % uncertainty range of the trend pattern changes from 1 % (in summer) to 2 % (in winter). It increases approximately twice at the start and end of the times series.

The rate of ozone decline was the largest in the end of 1980s and in the early 1990s, i.e., 4–5 % per decade in winter spring, and the year-round data (Fig. 11) but ~2 % per decade in autumn. The local trend curve (Fig. 11) shows that the trend overturning, i.e. the time when the local trend curve crosses the zero line, is found in the early 1970s (summer and autumn), in the late 1990s (all seasons, and

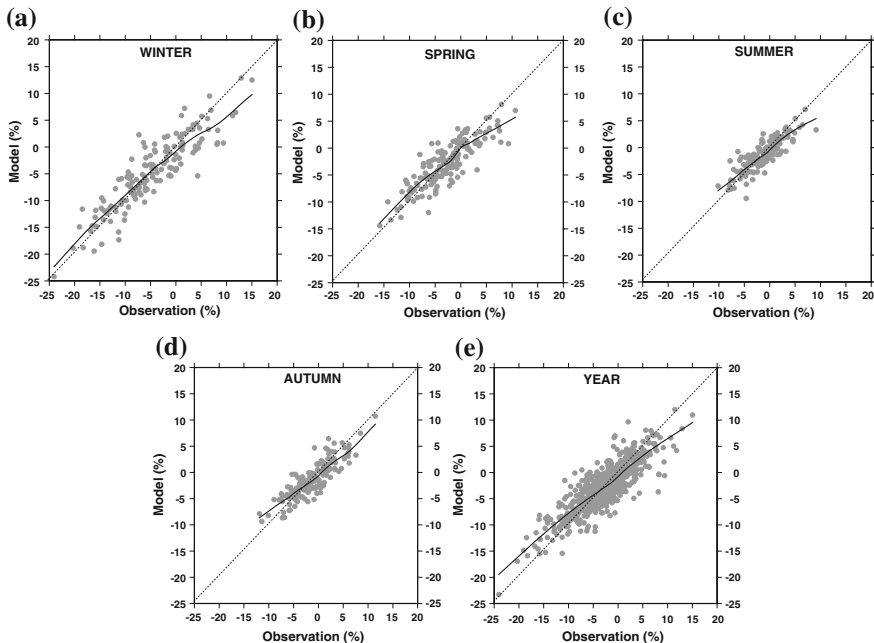


Fig. 9 The modeled versus the observed monthly fractional deviations of total ozone for the period 1963–2012 in the four seasons of the year and in the whole year. The dotted line shows the diagonal of the square and the solid curve represents the smoothed pattern by LOWES. **a–e** show the seasonal and year-round results by the multiple regression model, respectively

year-round data), and around 2005 (winter, spring, and year round-data). However, the positive trends are not statistically significant after the trend overturning in the late of 1990s. Thus, the second step of the ozone recovery could not be announced at Belsk. It is worth mentioning that the trends appeared in the early ozone data (before 1980), i.e., before onset of the strong anthropogenic forcing on ozone layer. The winter negative trend of about 4 % continued up to the early 1990s, the positive one (2 % per decade) in autumn data appeared at the end of the 1960s.

Seasonal and year-round tendency curve, i.e., the long-term variability in the fractional ozone deviations, are presented in Fig. 12. Almost similar patterns are revealed in comparisons between the trend curves (Fig. 10) and the corresponding tendency curves. Tendency curves exhibit only stronger oscillations in the first and last 15 year of the data. It is seen that the long-term pattern was only slightly affected by the combined dynamical forcing, so it means that the dynamical oscillations due to the selected proxies were practically smoothed out over longer periods.

The trends in ozone are usually expressed in % per decade. This value is frequently calculated as a slope of the straight line fit to the data. The long-term changes of Belsk's ozone are far from being linear, so the linear trend equivalent is estimated to represent the rate of ozone change over longer periods (for the local trend values see Fig. 11). The linear trend equivalent in the selected period is

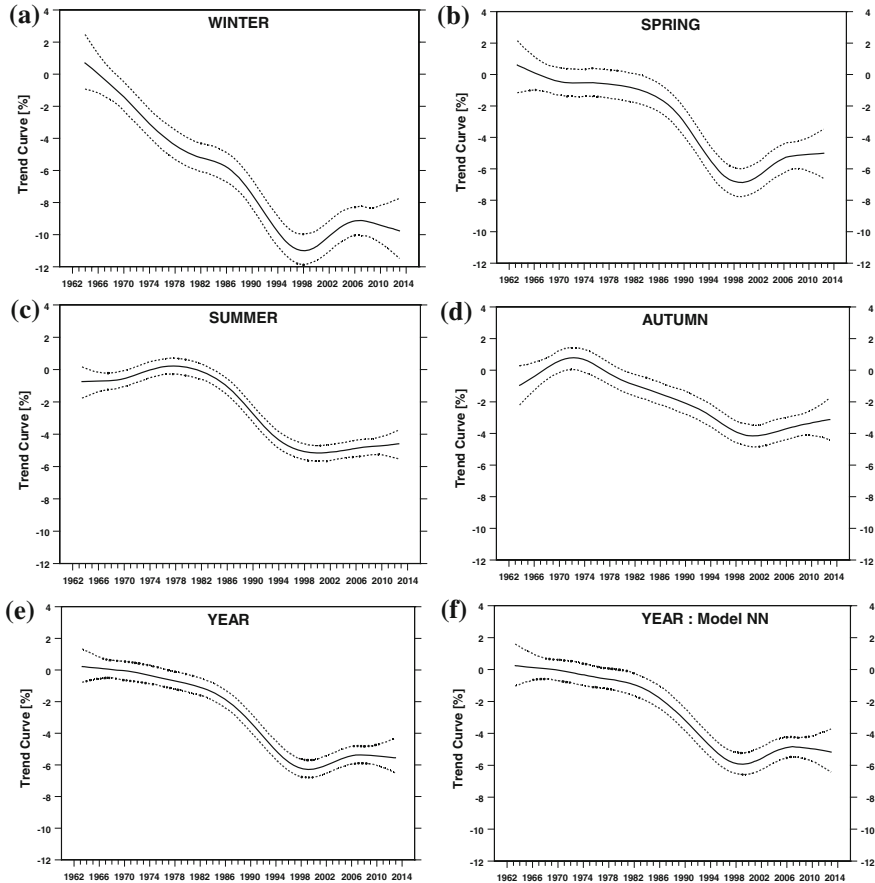


Fig. 10 The overall trend pattern and the 95 % uncertainty range from the total ozone monthly fractional deviations in the data subsets for the four seasons of the year and in the year-round data. The trends are derived by the model assuming that the dynamical signal hidden in the data is: (i) a linear combination of the ozone dynamical proxy individual effects (Fig. 10a–e) and (ii) inferred by the neural network (NN) simulations (Fig. 10f)

calculated as the ozone change, derived from the trend (or tendency) curve differences between the end and onset of the period, divided by the duration of the period. The linear equivalent of trends and tendencies in the seasonal and the yearly-data are shown in Tables 1 and 2, respectively, for the 17 year periods 1964–1980, 1980–1996, 1996–2012, and for the period 2005–2012.

The statistically significant negative trends ($\sim 2\text{--}4\%$ per decade) and tendencies ($\sim 2\text{--}5\%$ per decade), which were found in the period 1980–1996, i.e., in the ODS increasing phase, do not continue afterwards in the decreasing ODS phase. The trends and tendencies are not statistically significant in the period 1996–2012 (between -1 and 2% per decade for the trends, and between -2 and

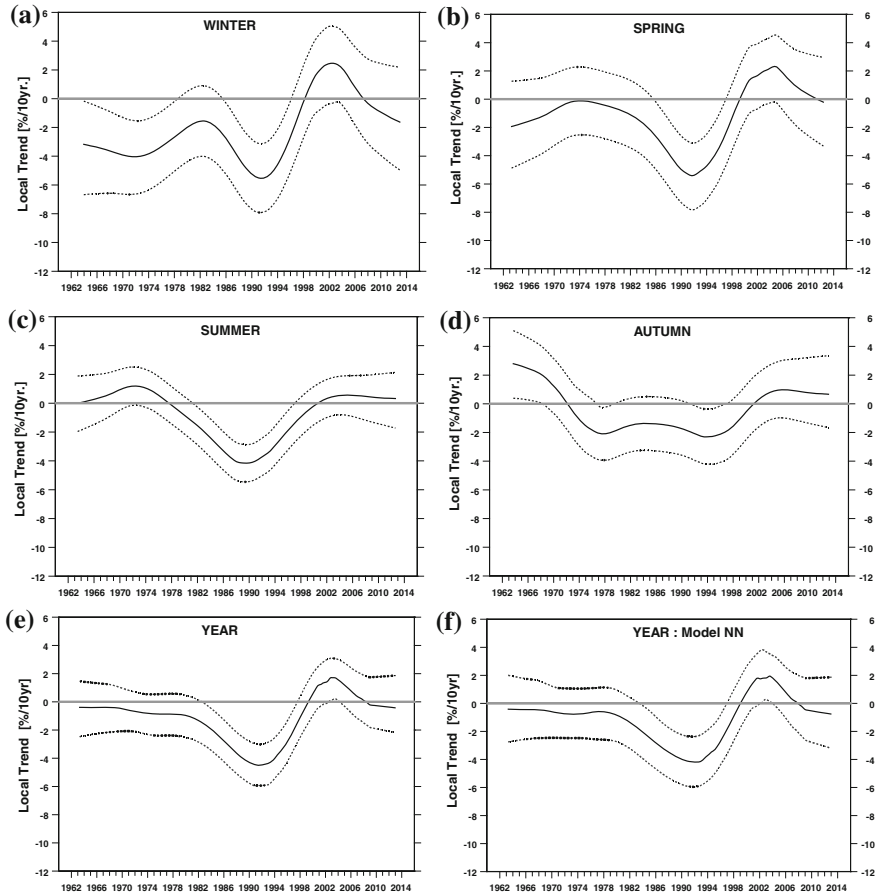


Fig. 11 The same as Fig. 10 but the time series represent the local trend values, i.e., the time derivative of the overall trend time series shown in Fig. 10. **a–e** show the seasonal and year-round results by the multiple regression model, respectively. **f** shows the year-round results by the neural network (NN) model

2 % for the tendencies). A lessening of the ozone trend and tendencies could be, at least, announced since the overturning of ODS tendency that might be linked to the success of MP 1987 and its subsequent amendments regulations to save the ozone layer. Figures 10 and 12 suggest that the local the maximum of trend and tendency curve, respectively, appeared around 2005. The maximum is more evident in case of the tendency time series. However, both trend and tendency do not exhibit the statistically significant negative trends in the period 2005–2012. It is worth mentioning that all estimates of the tendencies for the period 2005–2012 are negative (between -2.6% per decade in winter up to -1.2% per decade in autumn). The trend values for this period are a mixture of positive and negative values (-0.6% per decade in winter and 0.8% per decade in autumn). Thus it

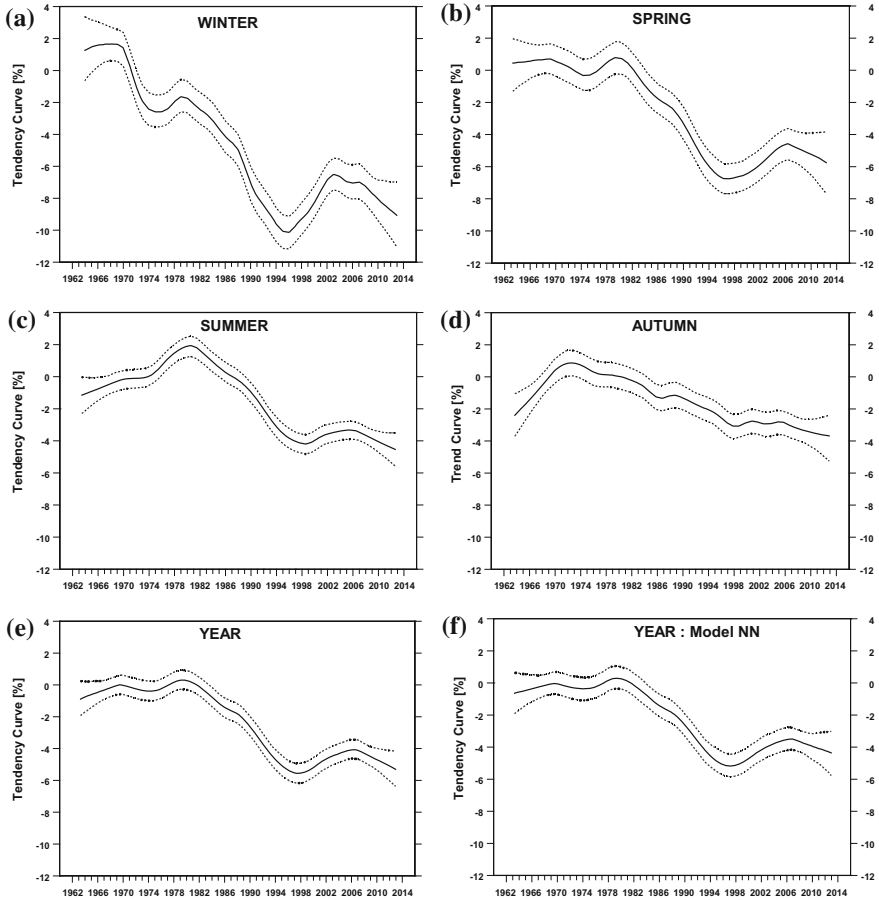


Fig. 12 The same as Fig. 10 but the time series represent the tendency, i.e., the smooth component extracted from the monthly fractional deviations. **a–e** show the seasonal and year-round results by the multiple regression model, respectively. **f** shows the year-round results by the neural network (NN) model

seems possible that a superposition of the recent dynamical changes in total ozone drives declining tendency for the period 2005–2012. This period is too short and the uncertainties ranges are larger at the end of the time series, so at the moment a more precise estimation is not possible.

Surprisingly statistically significant negative trend and tendency are found in the Belsk's early data (1964–1980) for winter. This result should be treated with care as at the time (up to 1974) specific wavelength pair CC' (Dobson 1957) was used in the TO_3 calculation especially in winter that could yield the TO_3 overestimate of few percent before 1974. A group of months with large fractional deviations appeared in summer and autumn for the late 1970 and late 1960s,

Table 1 Linear equivalent of the overall ozone trend in the selected periods

| Season | Trend (%/decade) | | | |
|-------------------|-----------------------------|-----------------------------|--------------------|---------------------|
| | 1964–1980 | 1980–1996 | 1996–2012 | 2005–2012 |
| Winter | -3.46 (-4.97, -2.16) | -3.63 (-4.55, -2.65) | 0.65 (-0.64, 2.06) | -0.59 (-3.49, 2.63) |
| Spring | -0.75 (-1.92, 0.65) | -3.54 (-4.59, -2.59) | 0.87 (-0.49, 2.18) | 0.56 (-2.54, 3.66) |
| Summer | 0.49 (-0.19, 1.20) | -3.10 (-3.58, -2.58) | 0.19 (-0.63, 0.93) | 0.43 (-1.47, 2.01) |
| Autumn | 0.06 (-0.93, 0.89) | -1.81 (-2.49, -1.06) | 0.32 (-0.68, 1.42) | 0.79 (-1.54, 3.41) |
| Year | -0.67 (-1.46, 0.09) | -3.14 (-3.70, -2.56) | 0.26 (-0.59, 1.20) | -0.64 (-1.88, 2.19) |
| Year ^a | -0.60 (-1.52, 0.37) | -3.02 (-3.79, -2.32) | 0.31 (-0.63, 1.35) | -0.27 (-2.76, 2.27) |

^a Results based on NN model. 95 % confidence intervals are in the parentheses, statistically significant results are in bold font

Table 2 Linear equivalent of the ozone tendency in the selected periods

| Season | Trend (%/decade) | | | |
|-------------------|-----------------------------|-----------------------------|---------------------|---------------------|
| | 1964–1980 | 1980–1996 | 1996–2012 | 2005–2012 |
| Winter | -1.90 (-3.62, -0.31) | -5.26 (-6.33, -4.21) | 0.87 (-0.59, 2.35) | -2.61 (-5.89, 0.67) |
| Spring | 0.14 (-1.02, 1.47) | -4.66 (-5.64, -3.68) | 0.63 (-1.04, 2.27) | -1.35 (-5.02, 1.87) |
| Summer | 1.82 (1.00, 2.70) | -3.68 (-4.32, -3.02) | -0.34 (-1.21, 0.53) | -1.69 (-3.71, 0.30) |
| Autumn | 1.18 (0.21, 2.21) | -1.76 (-2.55, -0.95) | -0.56 (-1.75, 0.61) | -1.19 (-3.96, 1.35) |
| Year | 0.57 (-0.24, 1.40) | -3.55 (-4.17, -2.91) | 0.18 (-0.78, 1.05) | -1.52 (-3.51, 0.41) |
| Year ^a | 0.45 (-0.47, 1.39) | -3.33 (-4.05, -2.61) | 0.52 (-0.57, 1.54) | -1.05 (-3.58, 1.29) |

^a Results based on NN model, 95 % confidence intervals are in the parentheses, statistically significant results are in bold font

respectively. As a result, the statistically significant positive tendencies are found for the whole period 1964–1980. However, the corresponding insignificant trends are found in this period, thus it seems that the positive tendencies have a dynamical origin.

The key point of the study is to find how the ozone trend and tendencies differ from the reference anthropogenic trend reflecting ODS level changes in the stratosphere. Figure 13 presents the differences in regard of the overall ozone trends (the seasonal and year-round data). The overall trend curve almost follows the reference curve, i.e., the difference is within the range (-1.5, 1 %). The statistically significant differences are found around 1990 in all seasonal and yearly data. The chemical ozone destruction, at that time, was stronger than the modeled trend, which comprises all the forcing factors. Maybe, unknown yet dynamical processes affected the ozone layer at that time.

The statistically significant negative differences appeared since about 2005 in summer and in the yearly data. At the present time the summer and yearly trend become significantly lower than the reference anthropogenic trend. Table 3 shows the differences at the end of time series (2012) between the overall trend curve (or the tendency curve) and the reference anthropogenic trend values. All the differences are negative but statistically significant (of about 2 %) only in the summer

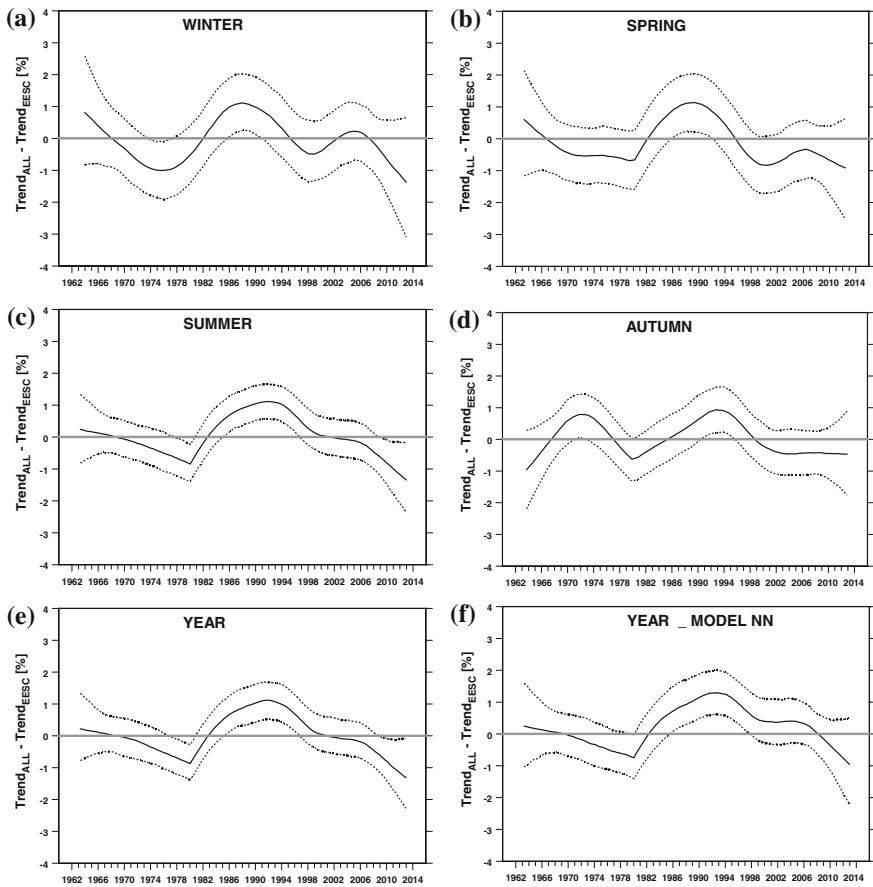


Fig. 13 The same as Fig. 10 but the time series represent the difference between the overall trend and the reference anthropogenic trend related exclusively to the EESC changes (Fig. 6). **a–e** show the seasonal and year-round results by the multiple regression model, respectively. **f** shows the year-round results by the neural network (NN) model

Table 3 Difference between the overall trend curve and the anthropogenic trend curve (due to ODS variability) at the end of the 1963–2012 time series of total ozone observations at Belsk

| Season | Difference (%) | |
|-------------------|-----------------------------|-----------------------------|
| | Trend | Tendency |
| Winter | -0.99 (-3.07, 1.25) | -0.65 (-2.99, 1.72) |
| Spring | -0.71 (-2.88, 1.40) | -1.08 (-3.76, 1.53) |
| Summer | -1.54 (-2.86, -0.37) | -2.41 (-3.80, -1.01) |
| Autumn | -0.92 (-2.51, 0.85) | -2.32 (-4.23, -0.45) |
| Year | -1.82 (-3.19, -0.32) | -1.96 (-3.49, -0.55) |
| Year ^a | -1.73 (-3.23, -0.05) | -3.33 (-3.15, 0.23) |

^a Results based on NN model, 95 % confidence intervals are in the parentheses, statistically significant results are in bold font

and year-round data (for the differences between the overall trend curve and the anthropogenic trend) and in summer and autumn (for the differences between the tendency curve and the anthropogenic trend). Thus, it seems possible than the unknown yet process has started to influence the Belsk's ozone since about 2005.

6 Summary and Conclusions

The ozone observations at Belsk have been carried out at the same site since 23 March 1963 up to now with only a few short breaks undertaken for the instrument maintenance. The time series of the daily ozone observations is one of the longest ozone observation series in the world. Moreover, this series is even more valuable for a trend estimate because of careful the data homogenization done in the 1980 and 1990s, and permanent quality control/quality assurance procedures applied to every result of the ozone measurements. The analysis of the Belsk's data by our original statistical software is an important part of the global scientific activity in area of quantification of the man-made changes in the ozone shield that protects the Earth from the solar UV-B radiation.

In the paper we propose a novel statistical 3-step model, which summarize our previous experiences in the statistical modeling of the ozone layer. The model estimates the ozone variability in various time scales (ranging from few years up to many decades) and focuses on the quantification of the man-made effects in the ozone layer. Moreover, besides the calculation of the overall trends, the model estimates the ozone tendency, i.e., the long-term smoothed ozone pattern comprising all dynamical and chemical forcing on ozone, that enables us to calculate the ground level UV irradiation response to the long-term ozone changes.

The analyses of the total ozone trends in the four seasons of the year and in the year-round data show that the first stage of the ozone recovery, defined by the World Meteorological Organization, i.e., a weakening of the ozone negative trend, has appeared over Belsk since the mid of 1990s. However, the second stage of the ozone recovery, i.e., an appearance of the statistically significant positive trend in series having removed "natural variability", could not yet be announced. The ozone trend and ozone long-term pattern follow the anthropogenic trend (due to ODS changes) for all seasons of the year and in the whole of the analyzed period. The uncertainty of the overall trend estimate is still too high to find statistically significant trends after the mid 1990s because the statistical model accounted for only a limited number of the ozone dynamical proxies. However, using more sophisticated statistical technique (NN) to reveal the dynamical effects on ozone does not improve the model's performance. Thus, maybe searching for new explanatory variables will provide a solution?

The slowing down of the ozone recovery found at Belsk's since 2005 and return back to negative tendency, that previously existed in the period 1980–1996, especially in summer, warn that the ozone issue still needs attention of scientists. The MP 1987 regulation and its subsequent amendments to protect the ozone layer

helped to stop the midlatitudinal ozone decline but still the ozone monitoring is necessary as evidently not all problems are solved. The first sign of the ozone decline in the summer since about 2005, i.e., in the season with naturally high UV radiation and a frequent outdoor activity in Poland, need further studies to find a driver of such variability.

Acknowledgments The ozone observations at Belsk have been partially founded by the Chief Inspectorate of Environmental Protection in Poland since 1989.

References

- Borkowski JL (2004) Wavelets—a tool in ozone and UV time series analysis. *Publ Inst Geophys Pol Acad Sc* vol D-64(371):135–138
- Chubachi S (1984) Preliminary result of ozone observations at Syowa station from February 1982 to January 1983. *Mem Natl Inst Polar Res Spec Issue Jpn* 34:13–20
- Cleveland WS (1979) Robust locally weighted regression and smoothing scatterplots. *J Amer Statist Assoc* 74(368):829–846
- Crutzen P (1973) A discussion of the chemistry of some minor constituents in the stratosphere and troposphere. *PAGEOPH* 106–108(1):1385–1399
- Degórska M, Krzyścin JW, Rajewska-Więch R (1989) Ozone trends from Dobson station at Belsk, Poland, ozone in the atmosphere. In: Bojkov RD, Fabian P (eds) *Proceedings of the quadrennial ozone symposium 1988 and tropospheric ozone workshop*, 4–13 August, 1988 in Göttingen, FRG. Edited by . Hampton, VA: A. Deepak Publishing, 1989, p 120–123
- Degórska M, Rajewska-Więch B (1991) Retrospective reevaluation of total ozone and Umkehr profile data from Belsk, Poland. *Publ. Inst. Geophys. Pol. Acad. Sc. D-36(246)*:71–76
- Degórska M, Rajewska-Więch B, Krzyścin J (1995) Reduction of variance of total ozone and Umkehr profiles after re-evaluation of the Belsk records. *Publ. Inst. Geophys. Pol. Acad. Sci. D-42(269)*:91–101
- Dobson GMB (1957) Observers' handbook for the ozone spectrophotometer. *Ann Int Geophys Year* V(1):46–89
- Dziewulska-Łosiowa A (1991) Ozon w atmosferze (Ozone in the Atmosphere). PWN, Warszawa p 395
- Dziewulska-Łosiowa A, Degórska M, Rajewska-Więch B (1983) The normalized total ozone data record, Belsk, 1963–1983. *Publ Inst Geophys Pol Acad Sc D-18(169)*:23–73
- Farman JC, Gardiner BG, Shanklin JD (1985) Large losses of total ozone in Antarctica reveal seasonal ClO_X/NO_X interaction. *Nature* 315:207–210
- Harris NRP, Kyrö E, Staehelin J, Brunner D, Andersen S-B, Godin-Beekmann S, Dhomse S, Hadjinicolaou P, Hansen G, Isaksen I, Jrrar A, Karpetchko A, Kivi R, Knudsen B, Krizan P, Lastovicka J, Maeder J, Orsolini Y, Pyle JA, Rex M, Vanicek K, Weber M, Wohltmann I, Zanis P, Zerefos C (2008) Ozone trends at northern mid- and high latitudes—a European perspective. *Ann Geophys* 26:1207–1220. doi:[10.5194/angeo-26-1207-2008](https://doi.org/10.5194/angeo-26-1207-2008)
- Jaroslawski J (2013) Improvement of the Umkehr ozone profile by the neural network method: analysis of the Belsk (51.80 N, 20.80E) Umkehr data. *IJRS* 34(15):5541–5550. doi:<http://dx.doi.org/10.1080/01431161.2013.79346>
- Krzyścin JW (2006) Change in ozone depletion rates beginning in the mid 1990s: trend analyses of the TOMS/ SBUV merged total ozone data, 1978–2003. *Ann Geophys* 24(2):493–502. doi:[10.5194/angeo-24-493-2006](https://doi.org/10.5194/angeo-24-493-2006)

- Krzyścin J, Borkowski JL (2008) Variability of the total ozone trend over Europe for the period 1950–2004 derived from reconstruction data. *Atmos Chem Phys* 8:2847–2857. doi:[10.5194/acp-8-2847-2008](https://doi.org/10.5194/acp-8-2847-2008)
- Krzyścin JW (2008) Statistical reconstruction of daily total ozone over Europe 1950 to 2004. *J Geophys Res* 113:D07112. doi:[10.1029/2007JD008881](https://doi.org/10.1029/2007JD008881)
- Krzyścin J, Rajewska-Więch B (2009a) Trends in the ozone vertical distribution from the Umkehr observations at Belsk 1963–2007, *IJRS* 30(15):3917–3926. doi: <http://dx.doi.org/10.1080/01431160902821866>
- Krzyścin J, Rajewska-Więch B (2009b) Ozone recovery as seen in perspective of the Dobson spectrophotometer measurements at Belsk (52 N, 21E) in the period 1963–2008. *Atmos Environ* 43(40):6369–6375. doi:[10.1016/j.atmosenv.2009.09.018](https://doi.org/10.1016/j.atmosenv.2009.09.018)
- Krzyścin JW (2012) Onset of the total ozone increase based on statistical analyses of global ground-based data for the period 1964–2008. *JOC* 32(2):240–246. doi:[10.1002/joc.2264](https://doi.org/10.1002/joc.2264)
- Mäder JA, Staehelin J, Brunner JD, Stahel WA, Wohltmann I, Peter T (2007) Statistical modeling of total ozone: selection of appropriate explanatory variables. *J Geophys Res* 112:D11108. doi:[10.1029/2006JD007694](https://doi.org/10.1029/2006JD007694)
- Molina MJ, Rowland FS (1974) Stratospheric sink for chlorofluoromethanes: chlorine atom-catalysed destruction of ozone. *Nature* 246:810–812
- Nair PJ, Godin-Beekmann S, Kuttippurath J, Ancellet G, Goutail F, Pazmiño A, Froidevaux L, Zawodny JM, Evans RD, Pastel M (2013) Ozone trends derived from the total column and vertical profiles at a northern mid-latitude station. *Atmos Chem Phys Discuss* 13:7081–7112. doi:[10.5194/acpd-13-7081-2013](https://doi.org/10.5194/acpd-13-7081-2013)
- Newman PA, Daniel JS, Waugh DW, Nash ER (2007) A new formulation of equivalent effective stratospheric chlorine (EESC). *Atmos Chem Phys* 7:4537–4552. doi:[10.5194/acp-7-4537-2007](https://doi.org/10.5194/acp-7-4537-2007)
- Reinsel GC, Miller AJ, Weatherhead EC, Flynn LE, Nagatani RM, Tiao GC, Wuebbles DJ (2005) Trend analysis of total ozone data for turnaround and dynamical contributions. *J Geophys Res* 110:D16306. doi:[10.1029/2004JD004662](https://doi.org/10.1029/2004JD004662)
- Rowland FS, Harris NRP, Bojkov RD, Bloomfield P (1989) Statistical error analyses of ozone trends—winter depletion in the northern hemisphere. *Ozone in the atmosphere*. In: Bojkov RD, Fabian P (eds) *Proceedings of the quadrennial ozone symposium 1988 and tropospheric ozone Workshop*, 4–13 August, 1988 in Göttingen, FRG. Hampton, VA: A. Deepak Publishing, p 71–75
- Rajewska-Więch B, Białek M, Krzyścin JW (2006) Quality control of Belsk's Dobson spectrophotometer: comparison with the European sub-standard Dobson spectrophotometer and satellite (OMI) overpasses. *Publ Inst Geophys Pol. Acad. Sci.* D-67(382):115–121
- Salby M, Titova E, Deschamps L (2011) Rebound of Antarctic ozone. *Geophys Res Lett* 38:L09702. doi:[10.1029/2011GL047266](https://doi.org/10.1029/2011GL047266)
- Solomon S, Garcia RR, Rowland FS, Wuebbles DJ (1986) On the depletion of stratospheric ozone. *Nature* 321:755–758. doi:[10.1038/321755a0](https://doi.org/10.1038/321755a0)
- Vyushin D, Fioletov VE, Shepherd TG (2007) Impact of long-range correlations on trend detection in total ozone. *J Geophys Res* 112(D14307):1–18. doi:[10.1029/2006JD008168](https://doi.org/10.1029/2006JD008168)
- World Meteorological Organization (WMO) (1995) *Scientific Assessment of Ozone Depletion: 1994*. Global Ozone Research and Monitoring Project—Report No. 37, Geneva, Switzerland, p 457
- World Meteorological Organization (WMO) (2011) *Scientific Assessment of Ozone Depletion: 2010*. Global Ozone Research and Monitoring Project—Report No. 52, Geneva, Switzerland, p 516

Forty Years of Water Research at the Institute of Geophysics, Polish Academy of Sciences

**Robert J. Bialik, Jarosław J. Napiórkowski, Paweł M. Rowiński
and Witold G. Strupczewski**

Abstract The history of research on hydrological and hydrodynamic processes carried out at the Department of Hydrology and Hydrodynamics, Institute of Geophysics, Polish Academy of Sciences is discussed. The genesis and development of the Department are briefly presented. The chapter focuses on the structure of the Department as well as the people associated with it at different stages of its history. The main research and organisational achievements of the Department team are summarised and supported by selected references.

Keywords Floods · Optimization algorithms · Pollutant transport · Rivers · Statistical hydrology · Turbulent open-channel flow · Water research

1 History and Recent Achievements

On 1 August 1974, a small group of young idealists (Roman Budzianowski, Zbigniew Kundzewicz, Jarosław Napiórkowski and Renata Romanowicz), recent graduates of the Department of Electronics, Warsaw University of Technology, initiated intensive research in the field of dynamic hydrology at the Institute of Geophysics of the Polish Academy of Sciences (IGF PAS). This group was led by Dr. Witold Strupczewski who moved in February 1972 from the Chair in Hydrology and Water Management at Warsaw Technical University to the IGF PAS. Initially, continuing Dr. Strupczewski's previous research interests, the team focused on the development and application of Markov dynamic programming models for optimal control of water storage reservoirs (e.g., Strupczewski et al. 1977).

R. J. Bialik (✉) · J. J. Napiórkowski · P. M. Rowiński · W. G. Strupczewski
Institute of Geophysics, Polish Academy of Sciences, Warsaw, Poland
e-mail: rbialik@igf.edu.pl



Fig. 1 Professor Zdzisław Kaczmarek (*left*) and Professor Julian Lambor (*right*)

The Hydrologic System Laboratory was formally established on 1 October 1974 as one of the initiatives of the Water Resources Committee of the Polish Academy of Sciences and its main aim was to stimulate research in hydrology and water management in Poland. It should be stressed that two famous members of this committee (Professor Julian Lambor and Professor Zdzisław Kaczmarek, see Fig. 1) were at that time members of the Scientific Board of the IGF PAS. Figure 2 shows the original document listing members of the first Scientific Board of the IGF PAS. It should be noted that Professor Lambor was the honorary chairman of the board. *Inter alia* he was the supervisor of the doctoral dissertation of Witold Strupczewski, one of the leading scientists who influenced the development of the Department.

Until 1977, the Hydrologic System Laboratory was part of the Department of Physics of the Atmosphere and Outer Space and from 1977 until 1982 was part of the Department of Atmospheric Physics and Hydrology, headed by Associate Professor Aniela Dziewulska-Łosiowa. It should be noted, however, that the laboratory operated quite independently at that time, and the research directions were decided by Associate Professor Strupczewski. The group's unique focus was on the application of optimisation methods and system theory to hydrological problems. Their results were presented at international conferences and published as a series of articles in leading international journals (e.g., Strupczewski et al. 1977; Napiórkowski and Strupczewski 1979, 1981; Strupczewski and Kundzewicz 1980, 1981; Kundzewicz 1980; Kundzewicz and Strupczewski 1982; Strupczewski and Budzianowski 1983) to mention just a few of them. In addition, one of the group's great achievements was the establishment of extensive cooperation with

| Szwad Radzy Naukowej IGF PAN | | |
|------------------------------------|--|---------------------------|
| | | IV 1972 |
| 1. prof.dr Julian Lembar | | honorowy przewodniczący |
| 2. prof.dr Teodor Kopcewicz | | przewodniczący |
| 3. prof.dr Henryk Orkisz | | zastępca przewodniczącego |
| 4. dr Bosuald Wielądek | | sekretarz naukowy |
| 5. dr Tadeusz Chojnicki | | członek |
| 6. dr hab. Jerzy Dera | | " |
| 7. dr hab. Weneda Dobaczewska | | " |
| 8. doc.dr hab. Krzysztof Haman | | " |
| 9. dr hab. Jerzy Jankowski | | " |
| 10. prof.dr Zdzisław Kaczmerek | | " |
| 11. prof.dr Czesław Kamela | | " |
| 12. dr hab. Zygmunt Kowalik | | " |
| 13. dr Jadwiga Kruczyk | | " |
| 14. doc. Stanisław Kryński | | " |
| 15. dr Zdzisław Małkowski | | " |
| 16. prof.dr Stanisław Małoszewski | | " |
| 17. prof.dr Stefan ManczarSKI | | " |
| 18. prof.dr Roman Ney | | " |
| 19. prof.dr Włodzimierz Parczewski | | " |
| 20. prof.dr Janusz Paszyński | | " |
| 21. prof.dr Stefan Pietrowski | | " |
| 22. dr hab. Jan Szomka | | " |
| 23. prof.dr Kazimierz Smulikowski | | " |
| 24. prof. Stanisław Szymborski | | " |
| 25. prof.dr Roman Teisseyre | | " |
| 26. prof.dr Włodzimierz Zonn | | " |
| 27. prof.dr Roman Żelazny | | " |

Fig. 2 List of members of the first Scientific Board of the IGF PAS in 1972

leading centres abroad, in particular with University College Dublin, represented by James Clement Dooge (see Fig. 3), who was not only a famous scientist (hydrologist and climatologist) but also a notable politician (Irish Minister for



Fig. 3 Professor Dooge (*second from left, front row*), Professor Kuchment (*first from right, front row*), Associate Professor Jarosław Napiórkowski (*first from left, middle row*), Professor Zdzisław Kaczmarek (*fourth from left, back row*) and Associate Professor Zbigniew Kundzewicz (*seventh from left, back row*) (Balice 1982)

Foreign Affairs and Chairman of the Irish Senate, President of the International Association of Hydrological Sciences (IAHS) from 1975 to 1979, Secretary General of the International Council for Science (ICSU) (1980–1982), President of the Royal Irish Academy (1986–1990) and President of ICSU (1993–1996).

This collaboration resulted in short-term (Z. Kundzewicz and W. Strupczewski) and long-term stays of young researchers at University College Dublin (J. Napiórkowski 1981–1983 and R. Romanowicz 1983–1984), and in a substantial number of joint international publications (e.g., Dooge et al. 1982, 1983, 1988; Kundzewicz and Dooge 1985; Romanowicz et al. 1988; Dooge and Napiórkowski 1987, 1993; Napiórkowski and Dooge 1988; Strupczewski and Dooge 1995, 1996) with the main focus on the linearisation of mathematical representations of hydrological processes.

It should be noted that as a result of co-operation with Professor Dooge, the 1989 Tison Award, awarded for an outstanding chapter by a young scientist in IAHS publications, went to Dr. Jarosław Napiórkowski for ‘Analytical solution of channel flow model with downstream control’. This chapter was published in the *Hydrological Sciences Journal* in 1988.

All the young scientists in the lab defended their doctoral dissertations under the supervision of Associate Professor Witold Strupczewski (see Fig. 4) in the late seventies or early eighties: Jarosław Napiórkowski (1979), Zbigniew Kundzewicz (1979), Renata Romanowicz (1981) and Roman Budzianowski (1982).

Fig. 4 Professor Witold Strupczewski (*front*) and Professor Jarosław Napiórkowski (*back*)



On 1 April 1982 the five-person team of Water Management Modellers was transferred by Professor Zdzisław Kaczmarek from the State Institute of Meteorology and Water Management to the Institute of Geophysics and a new Water Resources Department was established there. This Department was headed by Professor Kaczmarek, who officially joined the Institute and worked there for the next 25 years. From the very beginning, the challenges at the Department were considerable and both the research field and human resources were substantially extended. In 1986 the Water Resources Department consisted of three laboratories: (1) Hydrologic System Laboratory; (2) Water Management System Laboratory; and (3) Laboratory of Hydrodynamics.

The Hydrologic System Laboratory continued its research on the mathematical modelling of flood wave transformation with St Venant equations, their linearised forms and conceptual models, the application of Volterra series in dynamic hydrology, flood routing and the operational control of reservoir systems with stochastic inflows. Until 2004 it was headed by Witold Strupczewski. In the meantime, in 1983, the head of the laboratory obtained the title of Full Professor. In 1980 Dr. Henryk Mitosek joined the lab from Warsaw Technical University; he also served temporarily as the chief of the laboratory. His scientific interests extended the laboratory field to include stochastic problems in hydrological processes. In the mid-eighties, Dr. Tomasz Terlikowski and Dr. Andrzej Łodziński also joined this research group, working together with Associate Professor Jarosław Napiórkowski on control of storage reservoirs' systems. Some of their colleagues left the laboratory in the late eighties and early nineties: for example, Dr. Zbigniew Kundzewicz moved to the Institute for Agricultural and Forest Environment (IAFE) of the Polish Academy of Sciences in Poznań and Dr. Renata Romanowicz remained abroad, working at University College Dublin and Lancaster University. Besides the series of articles co-authored with James Dooge, a number of chapters prepared by the lab team appeared in international journals at

Fig. 5 Marzena Osuch (*left*) and Małgorzata Liszewska (*right*)



that time (i.e., Strupczewski and Napiórkowski 1990; Mitosek 1995; Strupczewski and Kaczmarek 2001; Strupczewski et al. 2001a, b). The lab was arguably one of the leading hydrological units in Europe.

On the other hand, the Water Management Systems Laboratory orientated the research interests of the Department towards control of water resources, evolution of their structure caused by economic activities and the quality and quantity aspects of hydrological processes, including climate changes. It was headed by Dr. Kazimierz Salewicz, who was the link between the Water Resources Department and the International Institute for Applied Systems Analysis (IIASA) in Vienna where many young researchers from the Department were subsequently sent for short-term internships. After the resignation of Dr. Salewicz at the beginning of the nineties, Jarosław Napiórkowski moved to the laboratory and became its chief. Professor Kaczmarek worked at this laboratory as well and in the mid-nineties Marzena Osuch and Małgorzata Liszewska (see Fig. 5) also joined this group, focusing on the interaction between anticipated climate changes and water resources. Several significant chapters were published on this subject (e.g., Kaczmarek and Napiórkowski 1996; Kundzewicz and Kaczmarek 2000).

From 1994 to 1995 Professor Kaczmarek was the leader of the project ‘SE12—Strategy of Polish water resources management in face of climatic change’, realised in the frame of the agreement between the US government and the Polish Ministry of Environmental Protection, Natural Resources, and Forestry—‘Strategies of GHG’s emission reduction and adaptation of Polish economy to the changed climate’. The first goal of the project was to analyse possible changes in the quantity and quality of Polish water resources on the basis of historical data, assumed climate scenarios, and models developed in the Department of Water

Resources. On the basis of those analyses, the most vulnerable regions were selected for further phases of the study. Model calculations were based on: climatic observations (1951–1990) at 41 stations, hydrologic data (1951–1990) for 31 river basins, two climate scenarios (GFDL-R15 and GISS) and a set of water balance and energy balance models developed at the Institute of Geophysics and the Institute of Meteorology and Water Management. The conclusion was that there was a possibility of serious disturbances in water resources processes in Poland, particularly in the central regions of the country. Consequently, two regions were selected for further analyses: the Warta-Pilica catchments ($57,000 \text{ km}^2$) supplying about seven million people (18 % of the Polish population) and the Wieprz-Krzna catchments ($13,300 \text{ km}^2$) supplying about 1.4 million people.

Four tasks were performed:

- Re-evaluation of water demand for selected water resource systems and for alternative climate scenarios.
- Development (adaptation) of methodological tools for regional water resources analysis under climatic change.
- Analysis of water resources situation in selected regions aimed at elaboration of the adaptation policy.
- Economic and institutional constraints.

The material gained by the research team at the Institute of Geophysics created a basis for the final report of project SE12 prepared by Professor Z. Kaczmarek and Dr. J. J. Napiórkowski. The key conclusion was, that in spite of expected water shortages in Poland's Central Lowlands (particularly for the GFDL scenario), effective adaptation measures (mostly non-structural) could be applied to supply enough water for the out-stream users. Some difficulties might arise in the case of in-stream water use, mostly because of changes in water temperature and consequently in biological processes.

It should be mentioned that at the request of the US Country Study Team (Professor K. Strzepek) the Polish water balance model CLIRUN3 developed in the Water Resources Department (Kaczmarek 1993; Kaczmarek and Napiórkowski 1996; Kaczmarek et al. 1996, 1998) had been adapted to the needs of other countries participating in the so-called US Country Study Program. A computer program had been made available for general use, and a user's manual prepared for those interested in applying this program. The CLIRUN3 model was demonstrated and discussed at the Training Workshop in Washington in February 1994. The extended version of CLIRUN3 is still used for evaluation of the effects of climate change on hydrological indicators across 8,413 basins in World Bank client countries (Strzepek et al. 2011).

Last but not least, the Laboratory of Hydrodynamics was created in 1986 when Associate Professor Włodzimierz Czernuszenko, the former Ph.D. student of Professor Kaczmarek, moved to the Institute of Geophysics from the Institute of Meteorology and Water Management to become its head. He expanded the research interest of the Department to cover theoretical and experimental



Fig. 6 (From *left*) Vladimir Nikora, Paweł Rowiński, Georgy Shalar, Alexander Sukhodolov during the measurement campaign on the Wilga River, Poland in 1993

investigations on flow modelling, the turbulent structure of flow in surface waters and heat and mass transport in rivers. Paweł Rowiński joined the Department in 1988, almost from the beginning, as the research assistant of Professor Czernuszenko. Those scientists were at the forefront of investigations of physical processes in rivers. At that time they were the only scientists in Poland working on river turbulence both experimentally and numerically. An important part of their investigations related to the spread of pollutants over long distances that, among others, resulted in chapters on the inclusion of the effect of dead-zone trapping of pollutants in models of pollution transfer in rivers (Czernuszenko and Rowiński 1997; Czernuszenko et al. 1998). These chapters are still cited today. Their crucial studies also aimed at determining the paths of single grains in turbulent open channel flows, drawing on the theory of two-phase flows (Czernuszenko 1997). The lab has established strong collaboration with a number of well recognised research centres, such as Institut für Gewässerökologie und Binnenfischerei im Forschungsverbund in Berlin, the National Center for Hydroscience and Engineering, University of Mississippi, USA, the State University of New York at Stony Brook, USA, where both Czernuszenko and Rowiński spent a substantial amount of time working with top experts in the field such as Professor Sam S.Y. Wang and Professor Richard S.L. Lee, to mention just two. Probably the most rewarding and long-lasting collaboration was that with the Institute of Geophysics and Geology of the Academy of Sciences of Moldova (Professor Vladimir Nikora and Dr. Alexander Sukhodolov; see Fig. 6) and later with all the institutions to which researchers from Moldova moved. They published a number of joint articles

in prestigious international journals focusing mostly on experimental hydraulics (Nikora et al. 1994, 1997; Sukhodolov et al. 1997; Czernuszenko et al. 1998). It should be noted that Dr. Alexander Sukhodolov was the first of several scientists to enjoy long-term stays at the Department, followed by Dr. Abdulgader Ali Almabruk from Libya, Dr. Alexey Rylov from Russia and Dr. Jean Marc Pretre from Switzerland. These stays at IGF resulted in numerous joint publications (Czernuszenko and Rylov 2000, 2002; Rowiński et al. 2000). The work of the Laboratory of Hydrodynamics was well recognized internationally, as shown by the invitation to Professor Czernuszenko and Professor Rowiński to prepare special chapters on the theme ‘Fresh Surface Waters’ for the monumental *Encyclopaedia of Life Support Systems*, presenting the state of the art within their fields of expertise (Czernuszenko 2002; Rowiński 2002).

Also fundamental to the development of the Laboratory was collaboration with a number of Polish research institutions. In this respect, one should mention the Institute of Meteorology and Water Management and the Faculty of Land Reclamation and Environmental Engineering of Warsaw Agricultural University. The first collaboration resulted, among others, in the world’s first tracer test in a multithread river reach (Rowiński et al. 2003) and one of the first attempts on an international scale to evaluate the bed shear stresses in rivers under unsteady flow conditions (Rowiński et al. 2000). The second collaboration mainly focused on flume experiments on the turbulence structure in compound channels and on unique experiments on the flow through vegetated channels (Rowiński and Kubrak 2002).

In summary, as regards the period from 1982 to 2004 it is important to note that the Department coordinated many national and international projects through the unique US-Poland Technology Transfer Program financed by the US Agency for International Development, in which the Water Resources Department cooperated with the National Center for Computational Hydroscience and Engineering (NCCHE) of the University of Mississippi. The project was led by Professors Czernuszenko and Rowiński and aimed at equipping Polish researchers and engineers with state-of-the-art research and engineering tools to carry out more effective investigations and engineering projects intended to improve water resources management. Another important landmark was the establishment of the Centre of Excellence on Geophysical Methods and Observations for Sustainable Development (GEODEV) which was coordinated by Professor Zdzisław Kaczmarek between 2002 and 2005. The Centre involved all the Institute’s departments and focused mainly on the role played by human activity in climate variation, ozone layer depletion, implementation of national policies in the field of environmental protection, and rational use of natural resources. At this point the role of Professor Kaczmarek, the Head of the Department, should be emphasised. Professor Kaczmarek’s outstanding contribution to international hydrology was recognized in 1990 by the International Association of Hydrological Sciences when he was awarded the International Hydrology Prize. This award reflected the high regard that Professor Kaczmarek enjoyed among the international community



Fig. 7 (From left) Antoni Kozłowski, Associate Professor Jarosław Napiórkowski, Professor Zdzisław Kaczmarek, Dr. Alexey Rylov, Professor Włodzimierz Czernuszenko, Dr. Paweł Rowiński and Dr. Tomasz Terlikowski in the office at the Institute of Geophysics in 1998

of both hydrologists and water resources engineers and he was the only Polish scientist to receive the prestigious prize. Figure 7 shows members of the Department in 1998.

2 Current Situation and Future Challenges

The year 2004 began with a series of huge changes in the Department. First of all, after many years of leading the Department, Professor Zdzisław Kaczmarek resigned and was replaced by Professor Jarosław Napiórkowski. That time the following scientists formed the Department: Professor Witold Strupczewski, Professor Włodzimierz Czernuszenko, and Associate Professor Paweł Rowiński who was elected in 2004 as the Director of Research of the Institute of Geophysics PAS, Dr. Tomasz Terlikowski, Dr. Krzysztof Kochanek, Dr. Małgorzata Liszewska, Marzena Osuch, Tomasz Dysarz and Antoni Kozłowski. Moreover, Associate Professor Henryk Mitosek left the Institute and moved to the Kielce University of Technology. It should be stressed that Professor Napiórkowski also served as the coordinator of the Ph.D. programme at the Institute of Geophysics (from 2000 to 2009). His involvement attracted a new group of young people who undertook Ph.D. Studies at the Department, i.e., Agata Mazurczyk (under the supervision of P. Rowiński), Adam Piotrowski (J. Napiórkowski), Monika Kalinowska (P. Rowiński), Iwona Markiewicz (W. Strupczewski), Robert Bialik (W. Czernuszenko) and Adam Kiczko (J. Napiórkowski). Moreover, Marzena

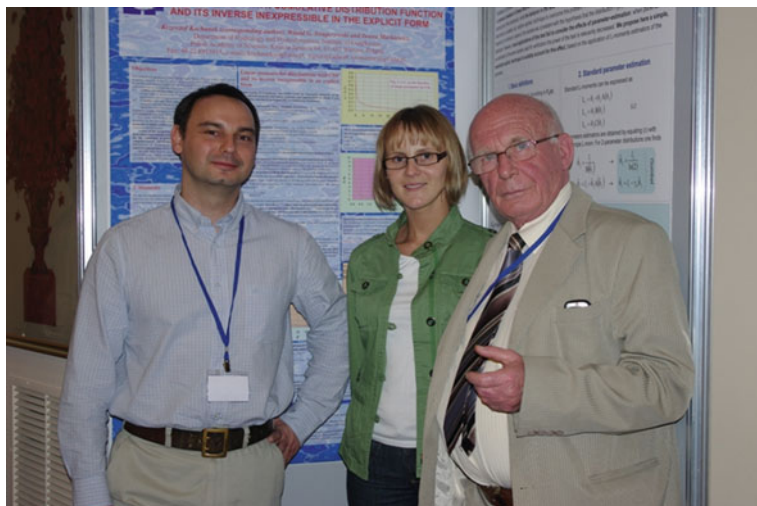


Fig. 8 The Environmental Hydrology Laboratory members. (From *left*) Dr. Krzysztof Kochanek, Dr. Iwona Markiewicz, Professor Witold G. Strupczewski

Osuch defended her Ph.D. under the co-supervision of Professors Napiórkowski and Romanowicz.

The second major change was the restructuring of the Department. In place of three previous laboratories two new ones were set up: (1) Environmental Hydrology Laboratory; and (2) Laboratory of Hydrophysics.

The Environmental Hydrology Laboratory was headed by Professor Strupczewski and continued the tradition of the Hydrologic System Laboratory with the main focus on the analysis of extreme hydrological phenomena, statistical and stochastic flood modelling, risk assessment and risk management, anthropogenic change impact on flood regime and hydrologic forecasting. The team actively participated in the International Hydrological Programme of UNESCO, where Professor Witold Strupczewski was for several years a national representative, serving two terms as Vice-Chairman of the Programme. He has also served as the Polish Representative of IAHS in the International Union of Geodesy and Geophysics (IUGG).

Since 2001, Professor Vijay P. Singh (originally from Louisiana State University and now at Texas A and M University) has participated in the work of the team as the co-author of 38 publications in reputable journals and conference proceedings. In cooperation with the Institute of Meteorology and Water Management the group worked closely with Dr. Ewa Bogdanowicz and published a number of chapters in high-rank international journals (e.g., Kochanek et al. 2008, 2012; Markiewicz et al. 2006, 2010; Markiewicz and Strupczewski 2009; Strupczewski et al. 2007, 2011, 2012, 2013). Since 2009, the team has participated in the COST Action ES0901 ‘European Procedures for Flood Frequency Estimation’. Figure 8 shows major members of the Environmental Hydrology Lab.



Fig. 9 Group photo of participants of the 32nd School of Hydraulics held in Łochów, Poland in 2012

The Laboratory of Hydrophysics continued the research done by the Laboratory of Hydrodynamics and was headed by Professor Włodzimierz Czernuszenko. Two major initiatives of the laboratory deserve special attention. The first was a unique, large-scale tracer test performed along a 90 km reach of the Narew River (Rowiński et al. 2008), which involved a number of people from the Department. It was actually the world's largest experiment of that kind; it was designed by Professor Rowiński and was run in collaboration with a team from the University of Warwick, UK (headed by Professor Ian Guymer). The second initiative that promoted the Institute well beyond the borders of Poland was the organisation of the International Schools of Hydraulics at which a bench of the best experts in the world have presented their work. The School is organised every second year in various parts of Poland and is already a well recognised international event organized, among others, under the umbrella of the International Association for Hydro-Environment Engineering and Research (IAHR); its chair is Professor Paweł Rowiński (see Fig. 9 for the last School in 2012). The proceedings from all the Schools are published. It is worth mentioning that Professor Rowiński was twice elected as a member of IAHR Europe Regional Division Leadership Team.

The year 2008 was a very sad one for the Institute as a whole and in particular for the Water Resources Department. In February of that year Professor Zdzisław Kaczmarek died and in April the Director of the Institute Professor Kacper Rafał

Rybicki passed away, both after long illnesses. Just 1 year earlier Professor Kaczmarek received the greatest recognition that a scientist can enjoy: he was listed as one of the Nobel Peace Prize recipients as a co-author of the report of the Intergovernmental Panel on Climate Change (IPCC). The death of both scientists led to meaningful changes. Professor Paweł Rowiński was elected as a new Director (CEO) of the Institute and one of his first decisions was to change the name of the Water Resources Department to the Department of Hydrology and Hydrodynamics to describe more precisely the research carried out at the Department. Moreover, in 2010, as the result of structural changes within the Institute, two existing laboratories were also liquidated with the option of eventually creating special task or project teams. This decision resulted in the emergence of four informal, thematic groups operating within the Department. Below only a brief description of these groups is presented.

First, the so-called Optimisation Methods in Hydrology Group which was created in 2004 and has been headed since then by the Head of the Department, Professor Jarosław Napiórkowski. It focuses on the development of evolution algorithms and application of neural networks to hydrological problems (Piotrowski et al. 2006, 2012; Piotrowski and Napiórkowski 2011, 2012) to mention a few. The second was the former Environmental Hydrology Laboratory, still headed by Professor Witold Strupczewski, which has continued its research on extreme hydrological phenomena with the use of statistics and stochastic analysis (Kochanek et al. 2012; Strupczewski et al. 2012, 2013). The third is the Hydrodynamics Group, which since the retirement in 2010 of Professor Czernuszenko has been informally headed by Professor Paweł Rowiński. The group mainly focuses on the modelling of heat and mass transfer in rivers (Kalinowska and Rowiński 2012; Kalinowska et al. 2012), the modelling of bed load transport (Bialik 2011; Bialik et al. 2012; Bialik and Czernuszenko 2013), the problem of resistance to flow in open channels and flows through vegetated channels. The only formal team dealing with experimentation relating to river hydraulics has been recently established within this group. The team is led by Dr. Robert Bialik and is relatively well equipped with field experimental instruments, working on river velocity fields, pollution transport and bed form development (see Bialik et al. 2014 and Rajwa et al. 2014 in this issue). The last group is the one dealing with stochastic analysis of hydrological problems and climate change, headed by Professor Renata Romanowicz who returned to the Institute in 2006. The group mostly focuses on the uncertainty and sensitivity analysis of hydrological processes, including pollutant transport and the application of statistical tools, including nonstationary frequency analysis of extreme events (low and high flows), to assess the relationships between external forcing and simulated catchment responses at varying temporal scales (Romanowicz et al. 2010, 2013; Romanowicz and Osuch 2011; Kiczko et al. 2011). Recently, the group has successfully applied for the project ‘Climate Change Impact on Hydrological Extremes’ funded by a Polish-Norwegian research fund. The main goal of the project is to analyse the adaptation of flood and drought under future climate changes with the use of a nonstationary framework. These groups obviously collaborate with one another and extremely interesting works

arise from common undertakings. Examples of such works are those in which optimisation methods are successfully used for typical hydrodynamics problems (Rowiński et al. 2005; Piotrowski et al. 2006, 2012, 2014; Piotrowski and Napiórkowski 2013).

At present 19 scientists and Ph.D. students work for the Department, including four full professors and one corresponding member of the Polish Academy of Sciences. The mix creates a team with substantial potential to undertake the most important tasks in water management in Poland and to solve crucial research problems. This group is probably the most well-known hydro-research Polish team on a European scale.

Acknowledgments This work was supported within statutory activities No 3841/E-41/S/2014 of the Ministry of Science and Higher Education of Poland. We would like to thank all colleagues from the Department of Hydrology and Hydrodynamics for providing photos and for helpful comments and discussions which recalled past incidents.

References

- Bialik RJ (2011) Particle-particle collision in lagrangian modeling of saltating grains. *J Hydraul Res* 49(1):23–31
- Bialik RJ, Nikora VI, Rowiński PM (2012) 3D Lagrangian modeling of saltating particles diffusion in turbulent water flow. *Acta Geophys* 60(6):1639–1660
- Bialik RJ, Czernuszenko W (2013) On the numerical analysis of bed-load transport of saltating grains. *Int J Sediment Res* 28(3):413, 420
- Bialik RJ, Karpiński M, Rajwa A (2014) Discharge measurements in lowland rivers: field comparison between an electromagnetic open channel flow meter (EOCFM) and an acoustic doppler current profiler (ADCP). *GeoPlanet: Earth and Planetary Sciences: Achievements, History and Challenges in Geophysics: 60th Anniversary of the Institute of Geophysics, Polish Academy of Sciences*. Bialik et al. (eds.) 213–222 (in this issue)
- Czernuszenko W (1997) Drift velocity concept for sediment-laden flows. *J Hydraul Eng* 124(10):1026–1033
- Czernuszenko W, Rowiński PM (1997) Properties of the dead-zone model of longitudinal dispersion in rivers. *J Hydraul Res* 35(4):491–504
- Czernuszenko W, Rowiński PM, Sukhodolov A (1998) Experimental and numerical validation of the dead-zone model. *J Hydraul Res* 36(2):269–280
- Czernuszenko W, Rylov A (2000) A generalization of prandtl's model for 3D open channel flows. *J Hydraul Res* 38(2):133–139
- Czernuszenko W (2002) Transport processes in river systems, in fresh surface waters. In: Dooge JCI (ed) *In encyclopaedia of life support systems (EOLSS)*, developed under the auspices of the UNESCO, Eolss Publishers Co., Oxford. (<http://www.eolss.net>)
- Czernuszenko W, Rylov A (2002) Modeling of three-dimensional velocity field in open channel flows. *J Hydraul Res* 40(2):135–143
- Dooge JCI, Strupczewski WG, Napiórkowski JJ (1982) Hydrodynamic derivation of storage parameters of the muskingum model. *J Hydrol* 54:371–387
- Dooge JCI, Kundzewicz ZW, Napiórkowski JJ (1983) On backwater effects in linear diffusion flood routing. *Hydrol Sci J* 28(3):391–402
- Dooge JCI, Napiórkowski JJ (1987) The effect of the downstream boundary conditions in the linearized St. Venant equations. *Q J Mech Appl Math* 40:245–256

- Dooge JCI, Napiórkowski JJ, Strupczewski WG (1988) The linear downstream response of a generalized uniform channel. *Acta Geophys Pol* 35(3):277–291
- Dooge JCI, Napiórkowski JJ (1993) Study of open-channel dynamics as controlled process. *J Hydraul Eng ASCE* 119(4):542–543
- Kaczmarek Z (1993) Water balance model for climate impact analysis. *Acta Geophys Pol* 41(4):423–437
- Kaczmarek Z, Napiórkowski JJ (1996) Water resources adaptation strategy in an uncertain environment. *Adapting in climate change*: 211–224, Springer, Berlin
- Kaczmarek Z, Napiórkowski JJ, Strzepek KM (1996) Climate change impact on the water supply system in the warta river catchment, Poland. *Water Resour Develop* 12(2):165–180
- Kaczmarek Z, Napiórkowski JJ, Rowiński, PM (1998) Conceptual catchment water balance model. In: Babovic V, Larsen LC (eds.) *Hydroinformatics*, A.A. Balkema/Rotterdam/Brookfield, p 143–148
- Kalinowska MB, Rowiński PM (2012) Uncertainty in computations of the spread of warm water in a river—lessons from environmental impact assessment. *Hydrol Earth Syst Sci* 16:4177–4190
- Kalinowska MB, Rowiński PM, Kubrak J, Mirosław-Świątek D (2012) Scenarios of the spread of a waste heat discharge in a river vistula river case study. *Acta Geophys* 60(1):214–231
- Kiczko A, Romanowicz RJ, Osuch M (2011) Impact of water management policy on flow conditions in wetland areas. *Phys Chem Earth* 36(13):638–645
- Kochanek K, Strupczewski WG, Singh VP, Weglarczyk S (2008) The PWM large quantile estimates of heavy tailed distributions from samples deprived of their largest element. *Hydrol Sci J* 53(2):367–386
- Kochanek K, Strupczewski WG, Bogdanowicz E (2012) On seasonal approach to flood frequency modeling Part II flood frequency analysis of polish rivers. *Hydrol Process* 26(5):717–730
- Kundzewicz ZW (1980) Approximate flood routing modeling methods: a review-discussion. *J Hydraul Div ASCE* 106:2072–2075
- Kundzewicz ZW, Strupczewski WG (1982) Approximate translation in the muskingum model. *Hydrol Sci J* 27:19–27
- Kundzewicz ZW, Dooge JCI (1985) Unified structural approach to linear flood routing. *Adv Water Resour* 8(1):37–43
- Kundzewicz ZW, Kaczmarek Z (2000) Coping with hydrological extremes. *Water Int* 25(1):66–75
- Markiewicz I, Strupczewski WG, Kochanek K, Singh VP (2006) Relationships between three dispersion measures used in flood frequency analysis. *Stoch Env Res Risk A* 20(6):391–405
- Markiewicz I, Strupczewski WG (2009) Dispersion measures for flood frequency analysis. *Phys Chem Earth* 34:670–678
- Markiewicz I, Strupczewski WG, Kochanek K (2010) On accuracy of upper quantiles estimation. *Hydrol Earth Syst Sc* 14(11):2167–2175
- Mitosek HT (1995) Climate variability and change within the discharge time series: a statistical approach. *Clim Chang* 29(1):101–116
- Napiórkowski JJ, Strupczewski WG (1979) The analytical determination of the kernels of the volterra series describing the cascade of nonlinear reservoirs. *J Hydrol Sci* 6:121–142
- Napiórkowski JJ, Strupczewski WG (1981) The properties of the kernels of the volterra series describing flow deviation from a steady state in an open channel. *J Hydrol* 52:185–198
- Napiórkowski JJ, Dooge JCI (1988) Analytical solution of channel flow model with downstream control. *Hydrol Sci J* 33(3):269–287
- Nikora VI, Rowiński PM, Sukhodolov A, Krasuski D (1994) Structure of river turbulence behind warm water discharge. *J Hydraul Eng-ASCE* 120(2):191–208
- Nikora VI, Sukhodolov A, Rowiński PM (1997) Statistical sand waves dynamics in one-directional water flows. *J Fluid Mech* 351:17–39
- Piotrowski A, Napiórkowski JJ, Rowiński PM (2006) Flash-flood forecasting by means of neural networks and nearest neighbour approach—a comparative study. *Nonlinear Proc Geoph* 13:443–448

- Piotrowski AP, Napiórkowski JJ (2011) Optimizing neural networks for river flow forecasting—evolutionary computation methods versus levenberg—marquardt approach. *J Hydrol* 407:12–27
- Piotrowski AP, Napiórkowski JJ (2012) Product-units neural networks for catchment runoff forecasting. *Adv Water Resour* 47:97–113
- Piotrowski A, Rowiński PM, Napiórkowski JJ (2012) Comparison of evolutionary computation techniques for noise injected neural network training to estimate longitudinal dispersion coefficients in rivers. *Expert Syst Appl* 39(1):1354–1361
- Piotrowski AP, Napiórkowski JJ (2013) A comparison of methods to avoid overfitting in neural networks training in the case of catchment runoff modeling. *J Hydrol* 476:97–111
- Piotrowski AP, Osuch M, Napiórkowski MJ, Rowiński PM, Napiórkowski JJ (2014) Comparing large number of metaheuristics for artificial neural networks training to predict water temperature in a natural river. *Comput Geosci* 64:136–151
- Rajwa A, Bialik RJ, Karpiński M, Luks B (2014) Dissolved oxygen in rivers: concepts and measuring techniques. *GeoPlanet: Earth and Planetary Sciences: Achievements, History and Challenges in Geophysics: 60th Anniversary of the Institute of Geophysics, Polish Academy of Sciences*. Bialik et al. (eds.) 337–350 (in this issue)
- Romanowicz RJ, Dooge JCI, Kundzewicz ZW (1988) Moments and cumulants of linearized St. Venant equation. *Adv Water Resour* 11(2):92–100
- Romanowicz RJ, Kiczko A, Napiórkowski JJ (2010) Stochastic transfer function model applied to combined reservoir management and flow routing. *Hydrol Sci J* 55(1):27–40
- Romanowicz RJ, Osuch M (2011) Assessment of land use and water management induced changes in flow regime of the upper narew. *Phys Chem Earth* 36(13):662–672
- Romanowicz RJ, Osuch M, Wallis S (2013) Modeling of solute transport in rivers under different flow rates: a case study without transient storage. *Acta Geophys* 61(1):98–125
- Rowiński PM, Czernuszenko W, Pretre JM (2000) Time-dependent shear velocities in channel routing. *Hydrol Sci J* 45(6):881–895
- Rowiński PM (2002) Constituent transport in fresh surface waters. In: Dooge JCI (ed) *In encyclopaedia of life support systems (EOLSS)*, developed under the auspices of the UNESCO. Eolss Publishers Co., Oxford. (<http://www.eolss.net>)
- Rowiński PM, Kubrak J (2002) A mixing-length model for predicting vertical velocity distribution in flows through emergent vegetation. *Hydrol Sci J* 46(6):893–904
- Rowiński PM, Napiórkowski JJ, Szkutnicki J (2003) Transport of passive admixture in a multi-channel river system—the Upper Narew case study. Part 1. *Hydrol Surv Ecohydrol Hydrobiol* 3(4):371–379
- Rowiński PM, Piotrowski A, Napiórkowski JJ (2005) Are artificial neural networks techniques relevant for the estimates of longitudinal dispersion coefficient in rivers? *Hydrol Sci J* 50(1):175–187
- Rowiński PM, Guymer I, Kwiatkowski K (2008) Response to the slug injection of a tracer—large scale experiment in a natural river. *Hydrol Sci J* 53(6):1300–1309
- Sukhodolov AN, Nikora VI, Rowiński PM, Czernuszenko W (1997) A case study of longitudinal dispersion in small lowland rivers. *Water Environ Res* 69(7):1246–1253
- Strupczewski WG, Romanowicz RJ, Budzianowski R (1977) Markovian programming for flow regulation. *J Hydrol Sci* 4:1–16
- Strupczewski WG, Kundzewicz ZW (1980) Translatory characteristics of the muskingum method of flood routing—a comment. *J Hydrol* 48:363–372
- Strupczewski WG, Kundzewicz ZW (1981) Linear reservoirs and numerical diffusion—discussion. *J Hydraul Div ASCE* 107:251–253
- Strupczewski WG, Budzianowski RJ (1983) Identification of the input-output stochastic model with correlated errors. *J Hydrol* 67:13–23
- Strupczewski WG, Napiórkowski JJ (1990) Linear flood routing model for rapid flow. *Hydrol Sci J* 35:49–64
- Strupczewski WG, Dooge JCI (1995) Relationships between higher cumulants of channel response I Properties of the linear channel response. *Hydrol Sci J* 40(6):675–687

- Strupczewski WG, Dooge JCI (1996) Relationships between higher cumulants of channel response II Accuracy of linear interpolation. *Hydrol Sci J* 41(1):61–73
- Strupczewski WG, Kaczmarek Z (2001) Non-stationary approach to at-site flood-frequency modeling Part II Weighted least squares estimation. *J Hydrol* 248:143–151
- Strupczewski WG, Singh VP, Feluch W (2001a) Non-stationary approach to at-site flood-frequency modeling Part I Maximum likelihood estimation. *J Hydrol* 248:123–142
- Strupczewski WG, Singh VP, Mitosek HT (2001b) Non-stationary approach to at-site flood-frequency modeling Part III Flood analysis of polish rivers. *J Hydrol* 248:152–167
- Strupczewski WG, Kochanek K, Weglarczyk S, Singh VP (2007) On robustness of large quantile estimates to largest elements of the observation series. *Hydrol Process* 21(10):1328–1344
- Strupczewski WG, Kochanek K, Markiewicz I, Bogdanowicz E, Singh VP (2011) On the tails of distributions of annual peak flow. *Hydrol Res.* 42(2–3):171–192
- Strupczewski WG, Kochanek K, Bogdanowicz E, Markiewicz I (2012) On seasonal approach to flood frequency modeling Part I Two-component distribution revisited. *Hydrol Process* 26(5):705–716
- Strupczewski WG, Kochanek K, Bogdanowicz E, Markiewicz I (2013) Inundation risk of embanked rivers. *Hydrol Earth Syst Sci* 10:2987–3025
- Strzepek K, McCluskey A, Boehlert B, Jacobsen M, Fant IV C (2011) Climate variability and change: a basin scale indicator approach to understanding the risk to water resources development and management: in water papers. World Bank, Washington

Changes in Catchment Hydrology Caused by Changes in the Environment: A Contribution of the Water Resources Department, Institute of Geophysics PAS

Emilia Karamuz and Renata J. Romanowicz

Abstract A number of hydrological studies focus on identifying and examining the main processes in the catchment area that shape water conditions in the basin. Every change in the environment affects the processes controlling the outflow from the basin. It is thus very difficult to distinguish the driving forces responsible for changing the processes. Previous studies have shown the problem to be complex and not fully explained. Many environmental factors (natural and anthropogenic) are responsible for changes in catchment hydrology. To detect changes in catchment response and to identify the source of changes, it is necessary to apply a number of methods which explain different aspects of the changes. This chapter outlines the contributions of the Water Resources Department (at present, the Department of Hydrology and Hydrodynamics), Institute of Geophysics, Polish Academy of Sciences, to research in the field of widely appreciated environmental changes (i.e., climate, land use and water management changes) with respect to catchment hydrology.

Keywords Hydrology · Environmental study · Climate change · Earth sciences

1 Introduction

Problems of environmental change and their impact on water conditions in the basin are of on-going interest to researchers. The catchment hydrology may have changed due to a range of forcing factors, both natural as well as anthropogenic. Under the term “environmental change” we understand here changes in climatic conditions, land use and water management.

E. Karamuz (✉) · R. J. Romanowicz
Institute of Geophysics, Polish Academy of Sciences, Ks. Janusza 64,
01-452 Warsaw, Poland
e-mail: emikar@igf.edu.pl; emilia_karamuz@igf.edu.pl

We have now strong evidence that the climate is changing (IPCC 2001, 2007). Various natural processes show large variations in recent decades. It is very easy to detect them on a global scale. Observable change in the composition of the atmosphere is reflected in the changes in the flow of energy due to the absorption of infra-red radiation. A current picture of the Earth's climate system is quite different from that of the preindustrial era. The global surface temperature rise of 0.6 ± 0.2 °C over the 20th century was greater than in any other century in the last 1,000 years. A global map of temperature changes over the last quarter of the 20th century indicates warming in the vast majority of grid cells.

Changed climatic conditions have inevitably become the focus of hydrological study. Climate is a major driving force of hydrological processes. Any change in the climate system modifies also the hydrological conditions. In the 1980s and 1990s the challenge for researchers was to provide proof of the on-going changes, develop the tools for modelling climate change and to indicate the direction of change. Existing General Circulation Models (GCMs) are sophisticated tools for a quantitative representation of the expected changes in climate on a global scale. But we have still a problem with the quantitative assessment of the impact of global warming on a smaller scale. There are many difficulties in applying GCM data as inputs in hydrological assessment studies, arising from the inadequate resolution of the available data.

A problematic issue seems to be how to separate factors on a regional scale which are responsible for changes in catchment hydrology. Human activities in the catchment area disrupt the natural balance of ecosystems. Dams and artificial reservoirs significantly change natural flow regimes. Land use changes lead to changes in land cover, translating into changes in rainfall-runoff relationships. Deforestation and intensive urbanization and a decreasing proportion of wetlands decrease the water storage capacity and increase the runoff coefficient. Regulation of rivers (channel straightening and shortening, construction of embankments) shortens the time of water conveyance.

We have observed that extreme hydrological events have become more destructive in many parts of the globe. A warmer Earth becomes wetter. In accordance with the Clausius-Clapeyron physical law, there is more space in the warmer atmosphere for water vapour, which increases the probability of intense precipitation. Observations have shown a growth of land-surface precipitation, especially in mid- and high-latitudes of the North Hemisphere (changes in the mean stream flow usually correspond well to changes in total precipitation, IPCC 2001). Climate changes induce an acceleration of the hydrological cycle which may be reflected in an increase in the frequency and severity of extreme hydrological events.

The best way to detect disturbances in catchment response due to environmental changes is finding changes in flow data series. But here the question arises, what kind of driving force is responsible for the shifts? This requires more detailed studies on a regional scale. The complexity of interactions between forcing factors and catchment response creates difficulties in separating different causes of the change of hydrological regime.

As mentioned above, catchment responses to environmental change are best captured by flow data series. This all results in a great interest in detecting change in flow time series. The key issue seems to be how to provide appropriate methods and tools for detecting the changes and identifying their sources.

2 Contribution to Research

Scientific staff of the Department of Hydrology and Hydrodynamics, Institute of Geophysics PAS, have participated extensively in research in the field of environmental changes and their impact on hydrological processes. Research related to the above-mentioned issues coincides with the global trends and has provided important insights into the effects of climate change on hydrology. Engagement in research on an international level has resulted in exchange of knowledge and experience. Membership of professional societies (such as IAHS—International Association of Hydrological Sciences, AGU—American Geophysical Union and many others) and participation in international initiatives and projects, have contributed to intensification and major expansion of research in the field of climate change and its impact on the environment, especially on hydrological systems. Particularly involved in these topics was Professor Zdzisław Kaczmarek, long-standing head of the Water Resources Department and the leader of a group of IGF PAS scientists working on climate change-related issues, including Małgorzata Liszewska, Dariusz Krasuski and Marzena Osuch. He was the co-ordinating lead author of the water chapter in the IPCC Second Assessment Report and a lead author of the European regional chapter in the IPCC Third Assessment Report. Professor Kaczmarek was a founding member of the Baltic Sea Experiment (BALTEX) Science Steering Group (BSSG), and acted as vice-chairman of the BSSG from 1994 to 2001. He was among the few key hydrologists who shaped the profile of BALTEX during this period. Professor Kaczmarek held the opinion that science is responsible for developing methodologies for climate impact assessment and for providing a rational basis for undertaking the necessary adaptive measures. Scientists should also inform decision-makers and the general public of the possible global threats and their accompanying uncertainties (Kaczmarek 1993a). Research in the Department of Hydrology and Hydrodynamics has been carried out following these aims.

We can distinguish at least six main areas of research related to the climate-water resource interface, which have been conducted in the Water Resources Department. They include:

- (1) Sensitivity analysis of water balance components to changes in climate characteristics (Kaczmarek 1990; Kaczmarek and Krasuski 1991);
- (2) Studies aimed at detecting changes in hydro-meteorological observations by means of hydrological indicators (Mitosek 1992, 1995, 1998; Mitosek and Strupczewski 1996; Strupczewski and Feluch 1998a; Strupczewski and

- Kaczmarek 1998; Strupczewski and Mitosek 1998; Liszewska and Osuch 1997, 2002; Strupczewski 2000; Osuch et al. 2012);
- (3) Assessing the possible implication of climate fluctuations on water supply and demand and consequently on water management (Kaczmarek and Kindler 1989; Kaczmarek et al. 1995);
 - (4) Studies on adaptation activities to the environmental change (Kaczmarek and Napiórkowski 1996; Kaczmarek and Kindler 1996; Kaczmarek et al. 1996; Osuch et al. 2012);
 - (5) Hydrological models to assess the impact of climate change on water resources on a regional scale (Kaczmarek and Krasuski 1991; Kaczmarek 1993b; Kaczmarek et al. 1998);
 - (6) Analysis of nonstationarity of flood frequency curves (Strupczewski and Feluch 1998a; Strupczewski et al. 2001a, b; Strupczewski and Kaczmarek 2001);

In the early years of research on global climate change, when the concept was gaining popularity, the greatest emphasis was put on the detection of changes in a series of available data. This approach started to undermine the widely accepted concept of the stationarity of climatic and hydrological processes. At that time in the Water Resources Department a number of methodological techniques were developed to detect non-stationarity in long-time series of temperature, precipitation and discharge data. The work was carried out mainly by a group including Profs. Kaczmarek, Strupczewski, Mitosek and Feluch. In many of his studies Prof. Kaczmarek (2002, 2003, 2005) cited an uncommon (but quite simple) procedure, based on a hyper-geometric distribution, that can be useful for testing changes in the frequency of hydrological and meteorological phenomena and for inferences about their stationarity.

A major contribution to the study of non-stationarity in flood frequency analysis was provided by Professor Strupczewski. He was especially interested in the development of methods of flood frequency analysis under non-stationarity conditions (Strupczewski and Mitosek 1991, 1995; Strupczewski and Feluch 1998b). In a series of studies a non-stationary approach to at-site flood-frequency modeling was outlined (Strupczewski et al. 2001a, b; Strupczewski and Kaczmarek 2001).

At the same time, in the Water Resources Department, work on the assessment of the impact of environmental change on hydrological regimes has been continued. Professor Kaczmarek was especially interested in climate impact analysis with respect to water resource and water management. He studied the sensitivity of river runoff (which represents the available regional water supply) to changes in precipitation, air temperature and net radiation in order to acquire the quantitative assessment of runoff changes due to variations in climate forcing that is prerequisite for rational decision-making in water management (Kaczmarek 1990). His methodological work contributed to a better understanding of the complex interdependence of climatic and hydrological phenomena. Continuing the work on the climate impact analysis, he focused on providing methodological tools for the sensitivity analysis of water balance components to changing climatic forcing.

A new meso-scale hydrological model (CLIRUN—CLImate/RUNoff model), based on stochastic storage theory, was a result. The model, originated by Kaczmarek, was developed by Napiórkowski and Rowiński (Kaczmarek et al. 1998). It was used in sensitivity analysis and in water balance impact studies (Kaczmarek and Krasuski 1991). The model allows for the calculation of runoff characteristics, evaporation and catchment storage on the basis of standard climatological data, and more importantly, on the basis of alternative climate scenarios from the Global Climate Models (GCMs). CLIRUN became a standard tool for climate change impact analysis within the program of US Country Study Computer Implementation Management Team. Subsequent versions of the model were created: CLIRUN_3 (Kaczmarek 1993a, b) and CLIRUN_4 (Kaczmarek et al. 1998). The model has gained recognition in other scientific institutions, where it has been modified and expanded (Yates 1996; Strzepek and Fant 2010; Strzepek et al. 2008). Three existing versions of CLIRUN created at the Institute of Geophysics PAS differ in their overall structure, in their parameterization and methods of calibration. The last version of the model (CLIRUN_4) has a better performance than former versions. The concept of this (latest) model is based on two connected reservoirs. The computer system based on the model consists of two main independent parts: CLIRUN_4 s and CLIRUN_4 g. The first simulates water balance components on the basis of measured values of catchment precipitation and potential evapotranspiration. In the second, the input climatic data are obtained by means of stochastic generation procedures.

Conceptual catchment water balance models developed at the Institute of Geophysics PAS have been used in many case studies to assess the vulnerability of water resources in Poland to climate change (Kaczmarek and Kindler 1996; Kaczmarek et al. 1996; Liszewska and Osuch 1997; Osuch and Liszewska 1997). CLIRUN has been also successfully used to model climate impact in other regions (Salewicz 1996; Kaczmarek 1998; Strzepek et al. 2008).

In recent years, work in the field of environmental change in the Department of Hydrology and Hydrodynamics has focused on assessing shifts in flow regime induced by land use modification and water management practices (Romanowicz and Osuch 2011; Kiczko et al. 2011). At this point, the international research project LUWR (Impacts of Land Use and Water Resources management on hydrological processes under varying climatic conditions) should be mentioned (<http://luwr.igf.edu.pl>). It was developed by Professor Renata Romanowicz and her colleagues, Dr. Marzena Osuch from IG PAS and Dr. Martijn Booij, from the University of Twente, Netherlands. LUWR is an open international research project aimed at analysing the impacts of historical, current and future changes in climate variability, land use and water management on hydrological processes, of mitigation of present and future risks to the public and ecosystems from extreme events (droughts and floods). The project focuses on detecting changes in a data-based hydrological process description and relating them to changes in meteorological processes and other external forcing factors, such as changes in water management practices and land use. Changes in catchment retention and flow dynamics will affect flow in different ways, depending on the hydrological conditions

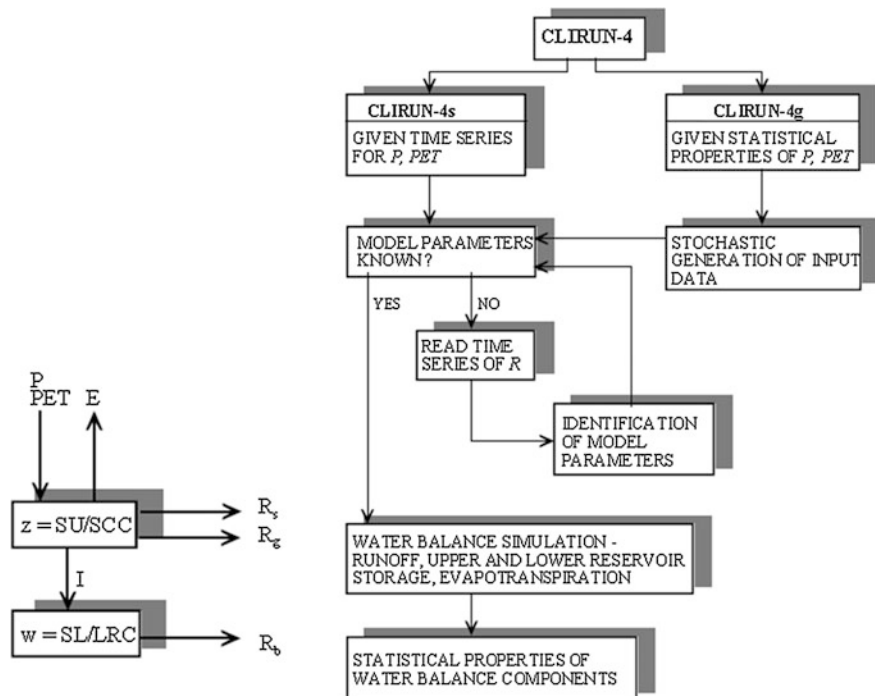


Fig. 1 CLIRUN_4 water balance model structure and flow diagram; *source* Kaczmarek et al. (1998)

in the catchment. Therefore, the classification of the events according to different soil moisture and flow regimes should help in separating the changes related to land use and water management from the natural changes related to climatic variability. Activities in the framework of the project contributed to the development of international cooperation. LUWR resulted also in a session (HS4.10) at the General Assembly of European Geosciences Union (EGU) in 2010 and in Special Issue of Physics and Chemistry of the Earth (Volume 36, issue 13, 2011).

3 Ongoing Work and Challenges for the Future

Assessment of hydrological processes under changing environmental conditions remains one of the main tasks of the Department of Hydrology and Hydrodynamics. Special emphasis is placed on designing and developing appropriate methods for detecting change in hydrological processes and identification of their source (Fig. 1).

A research team, including Professor Strupczewski, Professor Napiórkowski, Professor Romanowicz and Dr Osuch, is starting a new project, Climate Change

Impact on Hydrological Extremes(CHIHE, web page: <http://chihe.igf.edu.pl>), which aims to estimate the influence of climate change on extreme (low and high) river flows and to evaluate their impact on the frequency of hydrological extremes occurrence. The project is being done in cooperation with the Norwegian Water Resources and Energy Directorate (NVE). The main tasks of the project are:

- a statistical analysis of observed hydrological time series, especially extreme events,
- the development and application of methods for flood and drought frequency analysis in a non-stationary framework,
- the development of hydrological projections for likely changes in extremes and assessment of the uncertainty of the projections,
- recommendations for an adaptation strategy for managing the impact of climate change on hydrological extremes in the context of the European Flood Directive.

The challenges and scientific novelty of the project are the development of new non-stationary approaches to the analysis of changes in quantiles of hydrological extremes on a catchment scale for past events and future climate scenarios and an adaptation to possible future hydrological extremes. The research will follow the path set by Professor Kaczmarek and his co-worker, Professor Strupczewski, a globally recognized specialist on flood frequency analysis.

4 Conclusion

Over the years, the Department of Hydrology and Hydrodynamics has examined hydrological processes under varying environmental conditions. In particular, Professor Kaczmarek was a precursor of the present-day scientific interest in the impact of climate change on water resources in Poland. His work was complemented by the work of Professor Strupczewski on non-stationary flood frequency analysis; this work is being continued in the Department. The strength of the research carried out in the Department lies in the quality of the scientists employed and their insights. Changing water conditions in the catchments have significant economic, social and environmental consequences. Therefore, an understanding of their origin and the consequences is of the utmost importance.

References

- IPCC (2001) Climate change 2001: synthesis report. A contribution of working groups I, II, and III to the third assessment report of the intergovernmental panel on climate change. Cambridge University Press, Cambridge, United Kingdom
- IPCC (2007) Climate change 2007: synthesis report. A contribution of working groups I, II, and III to the fourth assessment report of the intergovernmental panel on climate change. Cambridge University Press, Cambridge, United Kingdom

- Kaczmarek Z, Kindler J (1989) The impacts of climate variability and change on urban and industrial water demand and waste water disposal. In: Proceedings of the conference on climate and water, vol 2. Valtion Painatuskeskus, Helsinki, pp 161–176
- Kaczmarek Z (1990) On the sensitivity of runoff to climate change. WP-90-58, international institute for applied systems analysis, Laxenburg, Austria
- Kaczmarek Z, Krasuski D (1991) Sensitivity of water balance to climate change and variability. WP-91-047, international institute for applied systems analysis, Laxenburg, Austria
- Kaczmarek Z (1993a) Sensitivity of water resources systems to climate change. In: Proceedings of Vth symposium on the protection of forest ecosystems
- Kaczmarek Z (1993b) Water balance model for climate impact analysis. *Acta Geophys Pol* 41(4):423–437
- Kaczmarek Z, Niestepski M, Osuch M (1995) Climate change impact on water availability and use. WP-95-48, international institute for applied systems analysis, Laxenburg, Austria
- Kaczmarek Z, Kindler J (1996) National assessment-Poland. In: Kaczmarek Z et al (eds) Water resources management in the face of climatic and hydrologic uncertainties. Kluwer Academic Publishers, Dordrecht
- Kaczmarek Z, Napiórkowski JJ (1996) Water resources adaptation strategy in uncertain environment. In: Smith JB et al (ed) Adapting to climate change—assessments and issues. Springer, Berlin
- Kaczmarek Z, Napiórkowski JJ, Strzepek KM (1996) Climate change impact on the water supply system in the Warta river catchment, Poland. *Water Resour Dev* 12(2):165–180
- Kaczmarek Z (1998) Human impact on yellow river water management. IR-98-016, international institute for applied systems analysis, Laxenburg, Austria
- Kaczmarek Z, Napiórkowski JJ, Rowiński PM (1998) Conceptual catchment water balance model. In: Babovic V, Larsen LC (ed) Hydroinformatics. A.A. Balkema, Rotterdam, Brookfield
- Kaczmarek Z (2002) Hydrological processes in a catchment scale under global climate change. *Ecohydrol Hydrobiol* 2(1–4):29–38
- Kaczmarek Z (2003) The impact of climate variability on flood risk in Poland. *Risk Anal* 23(3):559–566
- Kaczmarek Z (2005) Risk and uncertainty in water management. *Acta Geophys Pol* 53(4):343–355
- Kiczko A, Romanowicz RJ, Osuch M (2011) Impact of water management policy on flow conditions in wetland areas. *J Phys Chem Earth* 36(13):638–645
- Liszewska M, Osuch M (2002) Climate changes in Central Europe projected by general circulation models. *GeoJournal* 57(3):139–147
- Liszewska M, Osuch M (1997) Assessment of the impact of global climate change simulated by the ECHAM1/LSG general circulation model onto hydrological regime of three polish catchments. *Acta Geophys Pol* 45(4):363–386
- Mitosek HT (1992) Occurrence of climate variability and change within the hydrological time series. A statistical approach. CP-92-05. International institute for applied systems analysis, Laxenburg, Austria
- Mitosek HT (1995) Climate variability and change within the discharge time series: a statistical approach. *Clim Change* 29:101–116
- Mitosek HT, Strupczewski WG (1996) Can series of maximal annual flow discharges be treated as realizations of stationary process? *Acta Geophys Pol* 44(1):61–77
- Mitosek HT (1998) Some remarks on detecting non-stationarity in natural processes. *Geogr Pol* 71:35–38
- Osuch M, Liszewska M (1997) Climate change impact on water resources in three Polish catchments: Narew, Warta and Upper Vistula. Book of abstracts, European water resources and climate change processes, University College Cork, Irlandia
- Osuch M, Kindler J, Romanowicz RJ, Berbeka K, Baranowska A (2012) Strategy of adaptation in Poland to climate change in sector “water resources and water management”. Institute of environment technical report (in Polish)
- Romanowicz RJ, Osuch M (2011) Assessment of land use and water management induced changes in flow regime of the Upper Narew. *Phys Chem Earth* 36(13):662–672

- Salewicz KA (1996) Impact of climate change on the Lake Kariba hydropower scheme. In: Kaczmarek Z et al (eds) Water resources management in the face of climatic and hydrologic uncertainties. Kluwer Academic Publishers, Dordrecht
- Strupczewski WG, Mitosek HT (1991) How to deal with nonstationary time series in the hydrologic projects. *Mitteilungsblatt des Hydrographischen Dienstes in Österreich* 65/66:36–40
- Strupczewski WG, Mitosek HT (1995) Some aspects of hydrological design under non-stationarity. In: Kundzewicz Z (ed) New uncertainty concepts in hydrology and water resources. Cambridge University Press, Cambridge
- Strupczewski WG, Feluch W (1998a) Flood frequency analysis under non-stationarity. *Geogr Pol* 71:19–34
- Strupczewski WG, Feluch W (1998b) Investigation of trend in annual peak flow series. Part I Maximum likelihood estimation. In: Proceedings of the second international conference on climate and water, vol 1, pp 241–250
- Strupczewski WG, Kaczmarek Z (1998) Investigation of trend in annual peak flow series. Part II Weighted least squares estimation. In: Proceedings of the second international conference on climate and water, vol 1, pp 251–263
- Strupczewski WG, Mitosek HT (1998) Investigation of trend in annual peak flow series. Part III Flood analysis of Polish rivers. In: Proceedings of the second international conference on climate and water, vol 1, pp 264–272
- Strupczewski WG (2000) Simultaneous estimation of trends in mean and variance. In: Kundzewicz Z, Robson A (ed) Detecting trend and other changes in hydrological data. World Climate Programme and Monitoring, WMO
- Strupczewski WG, Singh VP, Feluch W (2001a) Non-stationary approach to at-site flood-frequency modelling. Part I Maximum likelihood estimation. *J Hydrol* 248:123–142
- Strupczewski WG, Singh VP, Mitosek HT (2001b) Non-stationary approach to at-site flood-frequency modelling. Part III Flood analysis of Polish rivers. *J Hydrol* 248:152–167
- Strupczewski WG, Kaczmarek Z (2001) Non-stationary approach to at-site flood-frequency modelling. Part II Weighted least squares estimation. *J Hydrol* 248:143–151
- Strzepka K, Balaji R, Rajaram H, and Strzepek J (2008) A water balance model for climate impact analysis of runoff with emphasis on extreme events. Report prepared for the World Bank. Washington, DC: World Bank
- Strzepek KM, Fant CW (2010) Water and climate change: modeling the impact of climate change on hydrology and water availability. University of Colorado and Massachusetts Institute of Technology
- Yates DN (1996) WatBal: An Integrated water balance model for climate impact assessment of river basin runoff. *Inter J Water Res Develop* 12(2):121–139

Five Polish Seismic Expeditions to the West Antarctica (1979–2007)

Tomasz Janik, Marek Grad and Aleksander Guterch

Abstract The chapter presents results of five Polish expeditions which realised an extensive programme of wide-angle refraction experiments in the northern Antarctic Peninsula region in the period of 1979–2007. The main achievement was the interpretation of materials collected along 20 deep seismic sounding profiles located along western part of the Antarctic Peninsula. Additionally, few shallow profiles in the area of Deception Island and the net of 10 reflection profiles from the Bransfield Strait and Drake Passage, and 3D experiment in the Admiralty Bay (King George Island) were carried out. Crustal velocity models extending across the Antarctic continental shelf between Adelaide Island and Bransfield Strait show typical continental crustal structure, with crustal thicknesses of 36–42 km near the coast, decreasing to 25–28 km beneath the outer continental shelf. Farther north, in the Bransfield Strait region, the models describe a crustal structure with the Moho dipping southeastward from a depth of 10 km beneath the South Shetland Trench to 40 km under the northern tip of the Antarctic Peninsula. Beneath the trough of the Bransfield Strait, the presence of a high-velocity body, with compressional-wave velocities exceeding 7.0 km/s, was detected at a depth range of 6–32 km.

Keywords Antarctic Peninsula · Bransfield Strait · West Antarctica · Crustal structure · Moho depth · Subduction zone

T. Janik (✉) · A. Guterch
Polish Academy of Sciences, Institute of Geophysics, Księcia Janusza 64,
01-452 Warsaw, Poland
e-mail: janik@igf.edu.pl

M. Grad
Faculty of Physics, Institute of Geophysics, University of Warsaw,
Pasteura 7, 02-093 Warsaw, Poland

1 Introduction

Between 1979 and 2007, the Institute of Geophysics, Polish Academy of Sciences, conducted five Antarctic expeditions, in 1979/1980, 1984/1985, 1987/1988, 1990/1991 and 2007. Wide-angle refraction projects were carried out on ships: ORP “Kopernik” (hydrographic research ship), M/S “Jantar”, M/S “Jantar”, D/E “Neptunia” (oceanic tugs), and M/V “Polar Pioneer”, respectively. The first four geodynamical expeditions performed deep seismic sounding (DSS) measurements in the transition zone between the Drake and South Shetland microplates and the Antarctic plate, West Antarctica. The network of 20 DSS profiles, ranging in length from 150 to 320 km, crossed the Antarctic Peninsula (AP) continental shelf off Graham Land, Bransfield Strait, and the continental margin northwest of the South Shetland Islands, from Adelaide Island in the south to Elephant Island on the north. The total length of the profiles was about 4500 km (Fig. 1). Seismic energy from ca. 525 explosive sources with charge from 25 to 150 kg of TNT were recorded by land stations and ocean-bottom seismic stations (OBS) in 25 positions. The seismic results obtained during four expeditions were published in a number of chapters (Guterch et al. 1985, 1990, 1991, 1998; Grad et al. 1992, 1993a, b, 1997a, b, 2002; Janik 1997a, b; Janik et al. 2006; Środa et al. 1997; Środa 2001, 2002).

During fifth expedition in 2007, 3D seismic local survey experiment was performed in the Admiralty Bay (King George Island, South Shetland Islands). It targeted the shallow crustal structure of the volcanic arc. The air-gun shots were recorded using 47 seismic land stations deployed at the coast of the bay. As a source, two air-guns with the total capacity of 40 l were used, and generated 449 shots along 21 profiles. Good quality data allowed for 3D tomographic modelling of the study area (Majdański et al. 2008).

2 Tectonic Setting

The AP is a composite magmatic arc terrane formed at the Pacific margin of Gondwana. Ocean crust formed at the Antarctic-Phenix Ridge (Fig. 1) must have been subducted beneath the peninsula, until segments of the ridge itself arrived at the margin and the subduction stopped. Through the late Mesozoic and Cenozoic, subduction has been stopping progressively from southwest to northeast as a result of a series of ridge trench collisions; the spreading ridge topography disappeared and the zone where the ridge segment had arrived became a passive margin. These processes repeated in successive segments of the subducting plate, separated by numerous fracture zones. According to Larter and Barker (1991), this process occurred until about 5.5–3.1 million years ago when the last segment of the ridge reached the section of the margin south of the Hero Fracture Zone (HFZ). The landward projection of HFZ separates the South Shetland Islands and the Bransfield

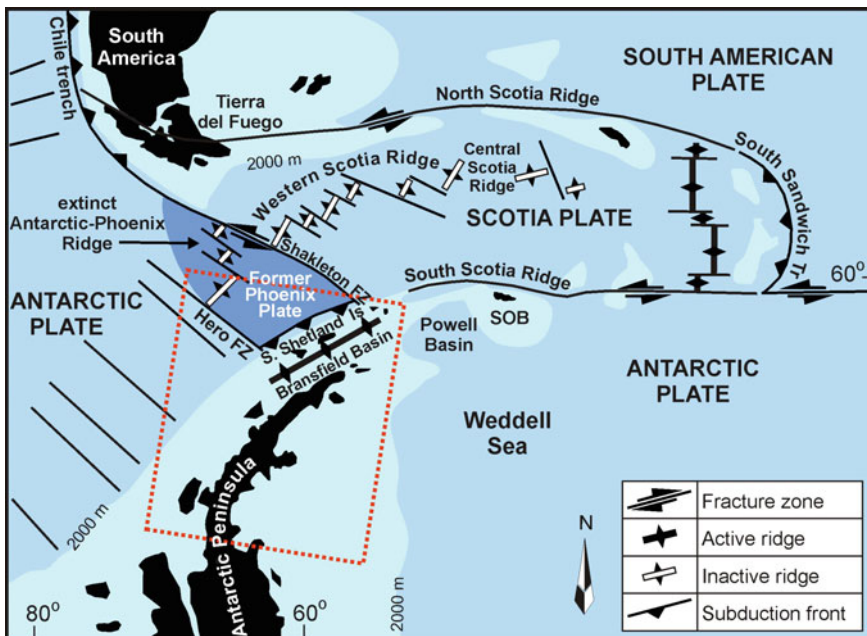


Fig. 1 Main tectonic units of Antarctic Peninsula and Scotia Sea (Larter and Barker 1991). Dashed red line rectangle indicates the study area. Light blue shows bathymetry shallower than 2000 m. SOB—South Orkney Block (*upper*)

basin from a continental, passive zone further to the south (Herron and Tucholke 1976). Subduction may be active today in the northern part of the AP adjacent to the South Shetland Islands. Several tectonic lineaments, discontinuities and geological structures between Deception and Low Islands were presented in many chapters and interpreted as landward projections of HFZ.

3 Reflection Investigations

The seismic reflection measurements programme carried out during the first expedition (1979/1980) was mainly concentrated on the shelf of the AP, in axial part of the Bransfield Strait and of the South Shetland Islands on the side of the Drake Passage (Fig. 2). Altogether, seismic reflection measurements were made along profiles about 1100 km long. The seismic source at sea was an array of air-guns with the total capacity of ca. 30 l aboard the ORP “Copernik”. Recordings were made by the DFS-IV equipment with a 1150 m long streamer system consisting of 24 active channels. The depth of shooting was ca. 11 m but the depth of streamer was ca. 25 m. Geometry of the measurement system was provided by of the Magnavox system. The reflection sections from the axial part of the Bransfield

Strait, which is most probably formed by a young rift system, are of special interest. The reflection section crossing the Bransfield Strait is presented in Fig. 3.

The reflection data collected in this region by expeditions from different countries are available in the base of reflection Antarctic data “The Antarctic Seismic Data Library System”, ANTOSTRAT (<http://www.scar.org/publications/reports/9/>).

4 Results of Deep Seismic Soundings Investigations

4.1 Bransfield Strait

The first results of DSS investigations of Polish Antarctic Expeditions were presented by Guterch et al. (1985), while the first results of 2-D seismic modelling along profile DSS-1 were published by Guterch et al. (1991). This profile detected the top of the high velocity body (HVB) in the central part of the Bransfield Strait, which confirmed previous results obtained by Ashcroft (1972).

Pioneer seismic investigations inside and outside of the caldera of Deception Island were published by Grad et al. (1992) (Fig. 4). In the caldera and immediate vicinity of Deception Island, a layer of unconsolidated and poorly consolidated young sediments of 1.9–2.2 km s/s P-wave velocity was found. Velocities of 4.1–4.3 km/s were found in the depth interval from 0.6–1.3 to about 3 km. Lateral differences in the upper crustal structure between the south-eastern and western sectors were identified. In the region between Deception and Livingston islands, an inclined boundary with a velocity of about 6.1 km/s occurs. A deep fault zone dividing crustal blocks beneath Deception Island is associated with a prominent volcanic line within Bransfield Strait, extending between Deception and Bridgeman islands.

The second and fourth expeditions extended research area to the south of Bransfield Strait, crossed landward projection of HFZ which is a zone dividing the passive and active margins of the northwestern coast of AP shelf. M/S “Jantar” landed the seismic groups on many islands of Gerlache Strait (Fig. 5). The collection of crustal and upper mantle velocity models along selected transects and profiles is present in Fig. 6a, b, c.

One of most prominent profiles carried out during the third expedition was 310 km long profile DSS-17 (Fig. 6c), with 30 shots fired in the transition zone between the Drake plate and the Antarctic plate. The seismic model was prepared with the use of seismic records of four land stations in the South Shetland Islands and AP (Grad et al. 1993a, b). The Moho boundary depth ranges from 10 km in the South Shetland Trench area to 40 km under the AP. In the subduction zone, from the Drake Passage to the South Shetland Islands, a seismic boundary in the lower lithosphere occurs at a depth ranging from 35 to 80 km. The Moho and this

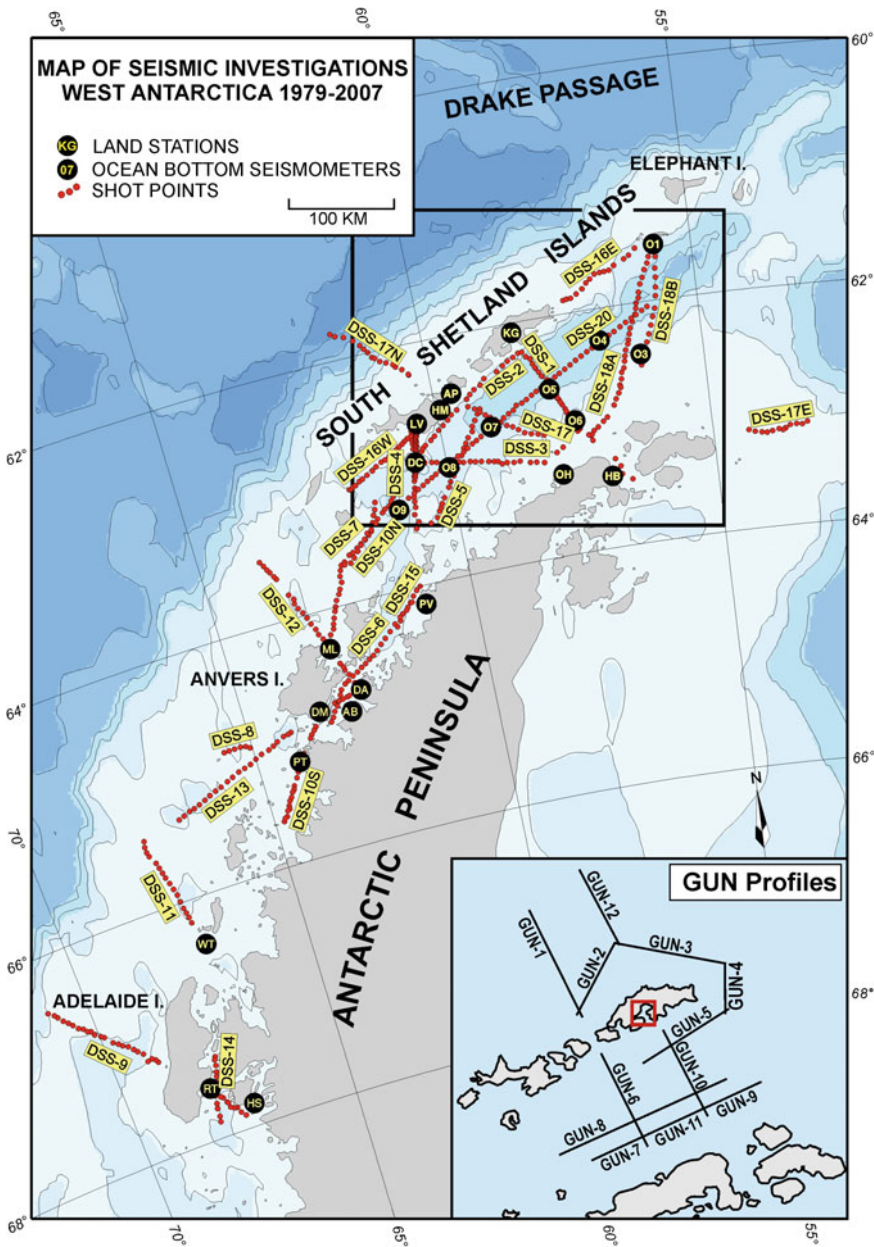


Fig. 2 Location of deep seismic sounding (DSS) profiles and transects in West Antarctica. Seismic stations: AB Almirante Brown, AP Arturo Prat, DA Danco, DC at Deception Island, DM Damoy, HB Hope Bay, HM at Half Moon Island, HS Horse Shoe, KG at King George Island, LV at Livingston Island, ML Melchior, OH O'Higgins, PT Petermann, PV Primavera; RT Rothera, WT Watkins, 01–09: ocean bottom seismographs. Bathymetry contours are plotted at 500 m intervals (ETOPO5 data file, NOAA's NGDC), using GMT software by Wessel and Smith (1995). Location of seismic reflection (*air-gun*) profiles (the first expedition—1979/1980) (bottom rectangle). Red inset the target of 2007 air-gun measurements—Admiralty Bay (King George Island)

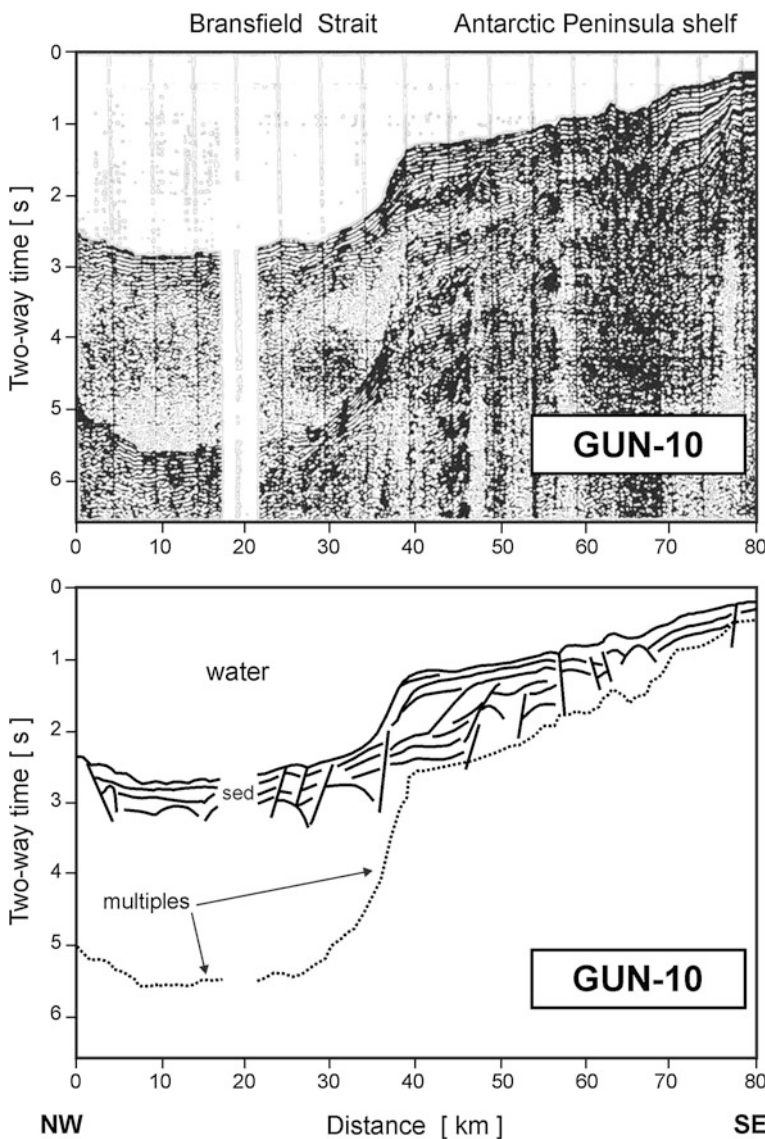
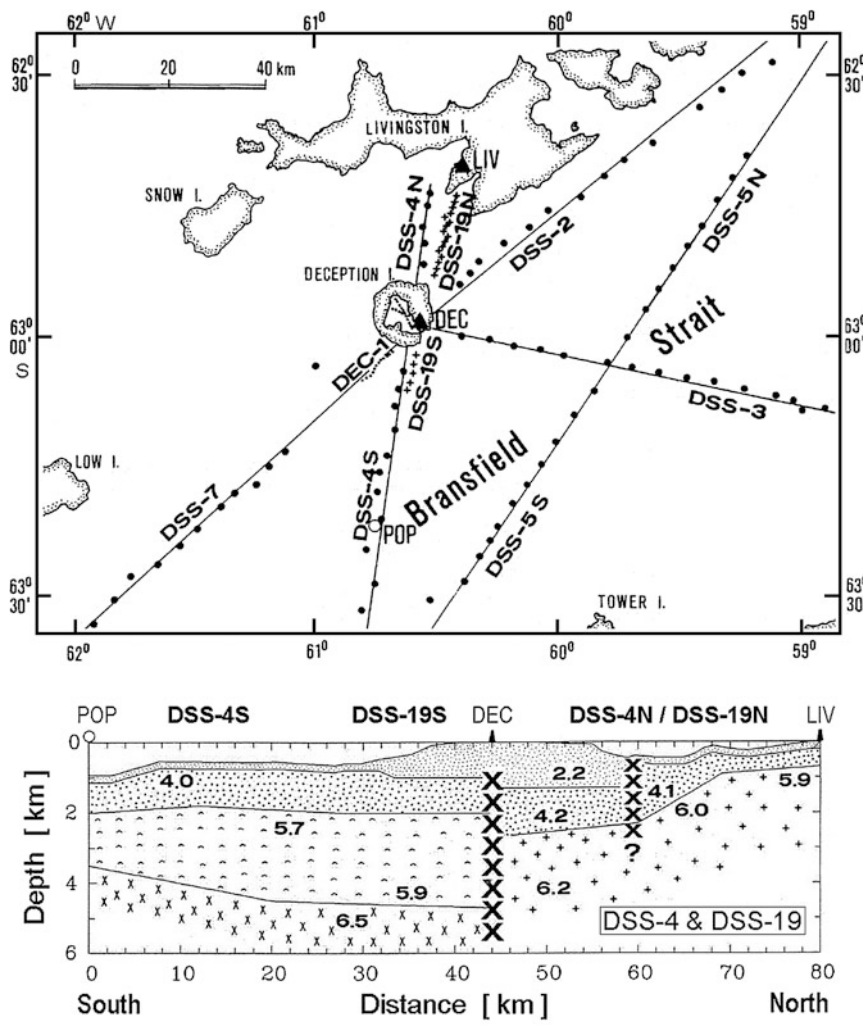


Fig. 3 Seismic reflection profile (see Fig. 2): GUN-10—across the Bransfield Strait

boundary indicate the direction of subduction of the lithosphere of the Drake plate under the Antarctic plate. Obtained results were compared with earlier results of seismic, gravity and magnetic surveys in West Antarctica. A scheme of geotectonic division and a geodynamical model of the zone of subduction of the Drake plate under the Antarctic plate is compared with subduction zones in other areas of the circum-Pacific belt. The crustal structure beneath the trough of Bransfield



Profile Bransfield Strait - Deception I. - Livingston I.

Fig. 4 Location of seismic profiles in the vicinity of Deception Island made during Polish Antarctic Geodynamical Expeditions 1979–1980 and 1987–1988 (*upper diagram*). ● ● = large-size shot points (50–120 kg TNT) along deep seismic sounding (DSS) profiles; + + + = shot points (2 kg TNT) along profile DSS-19; • • • = airgun shots along profile DEC-1 and profiles inside the caldera of Deception Island; ▲ = location of seismic stations on Deception Island (DEC) and Livingston Island (LIV); POP is the beginning of the two-dimensional profile. Seismic model of the upper crust structure along profile Bransfield Strait–Deception Island–Livingston Island (DSS-19). Crosses show locations of inferred faults; velocity in km/s (*lower diagram*). Modified from Grad et al. (1992)

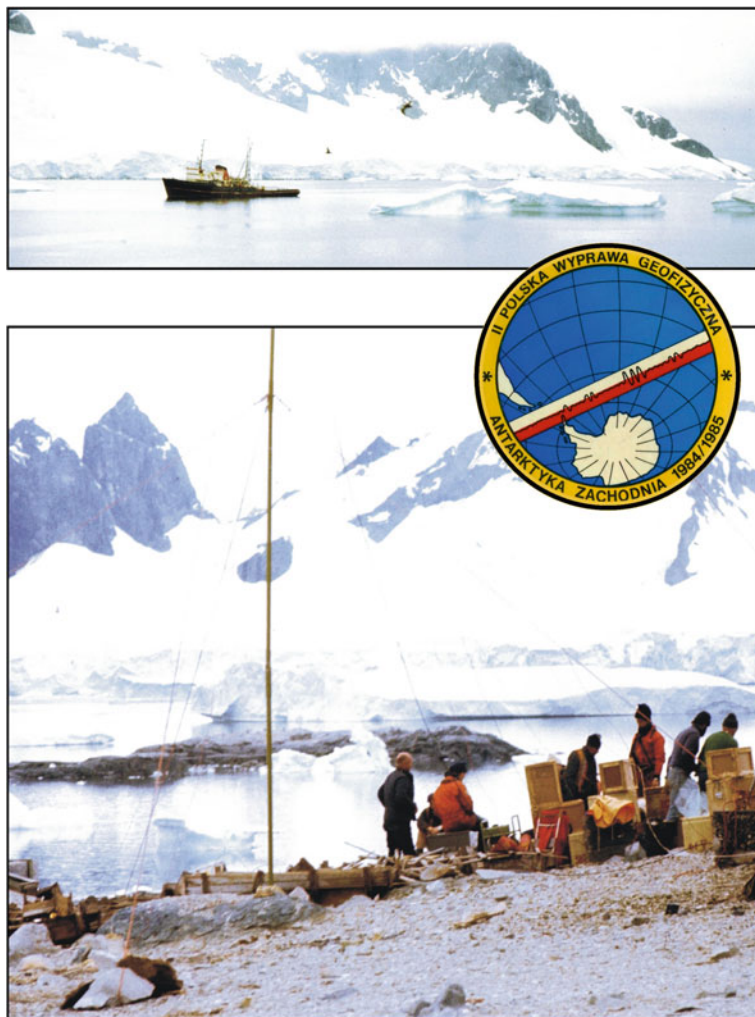


Fig. 5 The landing of the seismic group on Danco Island (Gerlache Strait) from M/S "Jantar". In the middle, the emblem of the Second Polish Geophysical Expedition to the West Antarctica. Photos taken by M. Grad, January 1985

Strait is highly anomalous. The presence of a HVB, with longitudinal seismic wave velocities >7.0 km/s, was detected in the 6–30 km depth range.

The first detailed deep seismic refraction study in the Bransfield Strait, using (nine) sensitive OBSs (ocean-bottom seismic stations) was carried out successfully during the Antarctic summer of 1990/1991 (the forth expedition). The experiment focused on the deep crustal structure beneath the axis of the Bransfield Rift. Seismic profile DSS-20 was located exactly in the Bransfield Trough, which is

suspected to be a young rift system. Five OBSs deployed at spacings of 50–70 km recorded seismic energy from 51 shots fired along 310 km long profile. A detailed model of the crustal structure was obtained by modelling using a 2D ray-tracing technique (Grad et al. 1997a, b). The presence of a high-velocity body with velocities $V_p = 7.3\text{--}7.7 \text{ km/s}$ (similar as on DSS-17 profile), was detected in the 14–32 km depth range in the central part of the profile. Velocities of 8.1 km/s, characteristic of the Moho, are observed along the profile at a depth of 30–32 km (Fig. 4).

Results of 2D modelling obtained for the net of five crossing each other profiles in the Bransfield Strait (Fig. 6b, c), and summary seismic geodynamical model were present by Janik (1997a, b). Further modification of the model along DSS-17 was presented in the chapter by Yegorova et al. (2011). Structure of the Earth's crust in the Bransfield Strait is strongly anomalous. Beneath a water body there are recent poorly consolidated sediments with seismic wave velocities equal to 1.9–2.9 km/s. The uppermost (sedimentary?) cover, with velocities of 2.0–5.5 km/s, reaches a depth of up to 8 km. The next two beds with velocities of 3.5 km/s and 4.0 km/s comprise presumably older and more consolidated sediments and pillow lavas. Beneath a sedimentary cover there is a bed with velocities of 5.2–5.8 km/s, typical for metamorphic and acid crystalline rocks. It is underlain by crystalline bedrock itself, with velocities of 6.4–6.9 km/s. Below this, a complex with velocities of 6.4–6.8 km/s is observed. In any case, close to the station HB, beneath a body with velocity of 6.4 km/s, at depths of 2–4 km, there is a bed with lower velocities, being presumably a continuation of the previously mentioned bed (with $V_p > 5.2 \text{ km/s}$).

The main element of the Bransfield Strait seismic models is the HVB (Fig. 6), detected also in previous investigations, with $V_p = 7.1\text{--}7.4 \text{ km/s}$ in the upper part of the body and high vertical velocity gradient, discovered at depths from about 10–15 km to about 25 km on all examined profiles, with the only exception of profile DSS-4. Range of the HVB (mushroom-shaped) deduced from two-dimensional modelling of the net of intersecting deep seismic profiles is present on the top-left box of Fig. 6b. Thickness of the HVB increases from several kilometres in southeastern parts of profiles DSS-3 and DSS-17, reaching 30 km depths on profile DSS-20 in central part of the Bransfield Strait. Beneath the HVB, to depths of 30–35 km in southeastern parts of profiles DSS-17 and DSS-3, crustal velocities from 6.8 to 7.2 km/s were detected. From our data it is not possible to make a detailed determination of seismic wave velocities distribution beneath the HVB in its northwestern part. It is known that the velocity must be over 7.0 km/s or presumably the same as in the HVB. Location of the lower boundary of 'the body' cannot be easily determined, as the observations of the lower crust are distinctly masked. Structure of the Earth's crust under the Deception Island below a depth of 6 km still remains unknown, as long as our data are concerned. On the other hand, the HVB does not occur in a southern part of profile DSS-4, close to the station PV. On profile DSS-4 in a southeastern part of the Bransfield Strait, a zone with lower velocities (assumed $V_p = 6.1 \text{ km/s}$) was found beneath a bed with velocity $V_p > 6.4 \text{ km/s}$ at depths of 7–17 km. The Moho discontinuity with

Fig. 6 **a** Location of seismic refraction transect along the continental shelf of the Antarctic Peninsula and Bransfield Strait in West Antarctica: ca 1,000 km long transect between Marguerite Bay (MAB) and Elephant Island (*yellow stripe*), Grad et al. (2002). Thin red lines locate deep seismic profiles. Lower diagram shows two-dimensional seismic velocity model of P-wave. Vertical exaggeration is 5:1. Crosses show crustal discontinuities, corresponding in some cases to fracture zones. HVB—high-velocity body. Numbers indicate P-wave velocity in km/s. Other abbreviations as in Fig. 2. **b** Velocity models along lines crossing the Bransfield Strait: DSS-1, DSS-3, DSS-4, Janik (1997a, b), and velocity model along the DSS-20 line, Janik (1997a, b) modified from Grad et al. (1997a, b). Numbers indicate P-wave velocity in km/s. Vertical exaggeration is 2.5:1. Other abbreviations are as in Fig. 6a. *The top-left diagram*: P-wave velocity anomalies detected in the crust in the Bransfield Strait marginal basin against of the South Shetland Islands. Range of the previously identified high velocity (mushroom-shaped) body (HVB) with $V_p > 7.2$ km/s in the Bransfield Strait, detected at a depth of 10–18 km, deduced from two-dimensional modelling of the net of intersecting deep seismic profiles. *Violet colour* shows the places where the depth of HVB reaches 30 km. At other places (*yellow colour*), the thickness of the body is relatively small (southern part) or unknown (northwest part). Modified from Janik et al. (2006). **c** Velocity models along lines: DSS-17 crossing the Bransfield Strait, Yegorova et al. (2011) modified from Grad et al. (1993a, b) and Janik (1997a, b); profile DSS-12 between Bellingshausen sea and Antarctic Peninsula, Środa et al. (1997); transect along profiles DSS-6, DSS-15 and DSS-5 which cross the land projection of the hero fracture zone, Janik et al. (2006). Vertical exaggeration is 2.5:1. Other abbreviations are as in Fig. 6a

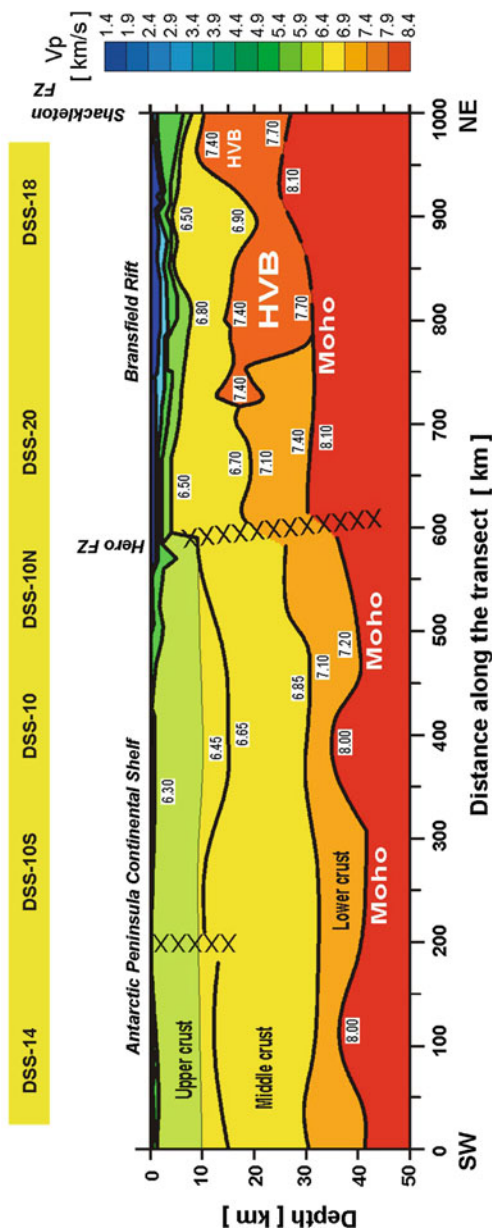
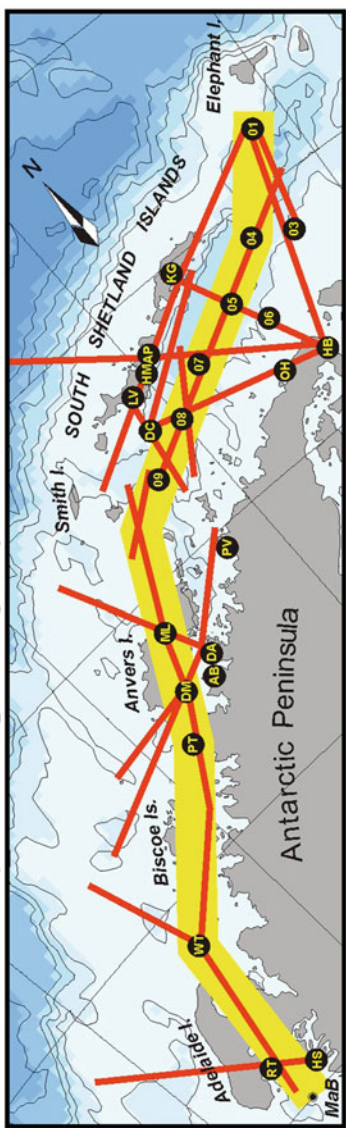
velocity $V_p > 8.1$ km/s was detected below, at depths of 30–32 km on profile DDS-20. Fragments of the Moho discontinuity were also discovered on profiles DSS-17 and DSS-3, and presumably also DSS-4 at depths of 30–37 km.

4.2 Main Transects

Figure 6a shows the crustal structure beneath the AP shelf and Bransfield Strait along a 1000 km SW–NE transect corridor between Marguerite Bay and Elephant Island (*yellow strip*). This crustal velocity model is derived from profiles DSS-14, DSS-10 (southern, central, and northern parts), DSS-20, and DSS-18 (Grad et al. 1997a, b; Środa et al. 1997). The second transect between Petermann station and King George Island (Fig. 6c) shows crustal velocity models crossing the HFZ (profiles DSS-6, DSS-15 and DSS-5) and the tectonically active Bransfield Strait region (Janik 1997a, b; Środa et al. 1997; Środa 2001, 2002; Janik et al. 2006).

The seismic models of the crust and uppermost mantle along both transects cross the transition zone between the passive and active margins of the north-western coast of the AP and the main structures of the Bransfield Strait. Changes in the crustal structure along the Marguerite Bay–Elephant Island transect suggest the presence of structural discontinuity in the crust at 600 km, corresponding perhaps to the landward projections of the HFZs. On the second transect, the HVB body was modelled (on landward projection of HFZ) at km 170 at a depth of 15 km; it was ca. 80 km long and 5 km thick. The body is separated by a low velocity zone with $V_p < 6.4$ km/s from the HVB in the central part of Bransfield Strait. In the central part of the transect, velocities $V_p \sim 6.7$ km/s, typical for middle crust,

(a) West Antarctica, transect Marguerite Bay - Elephant Island



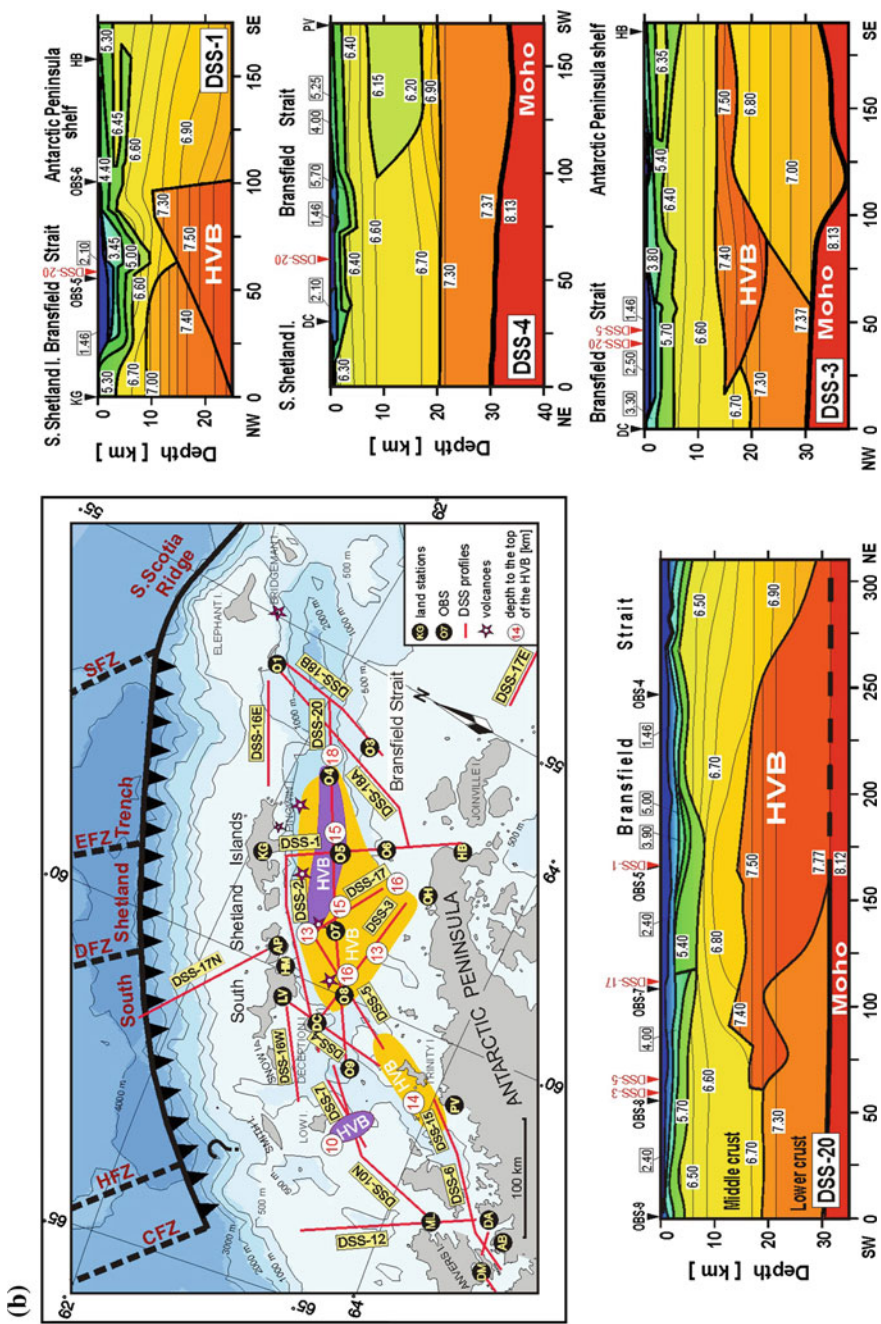


Fig. 6 continued

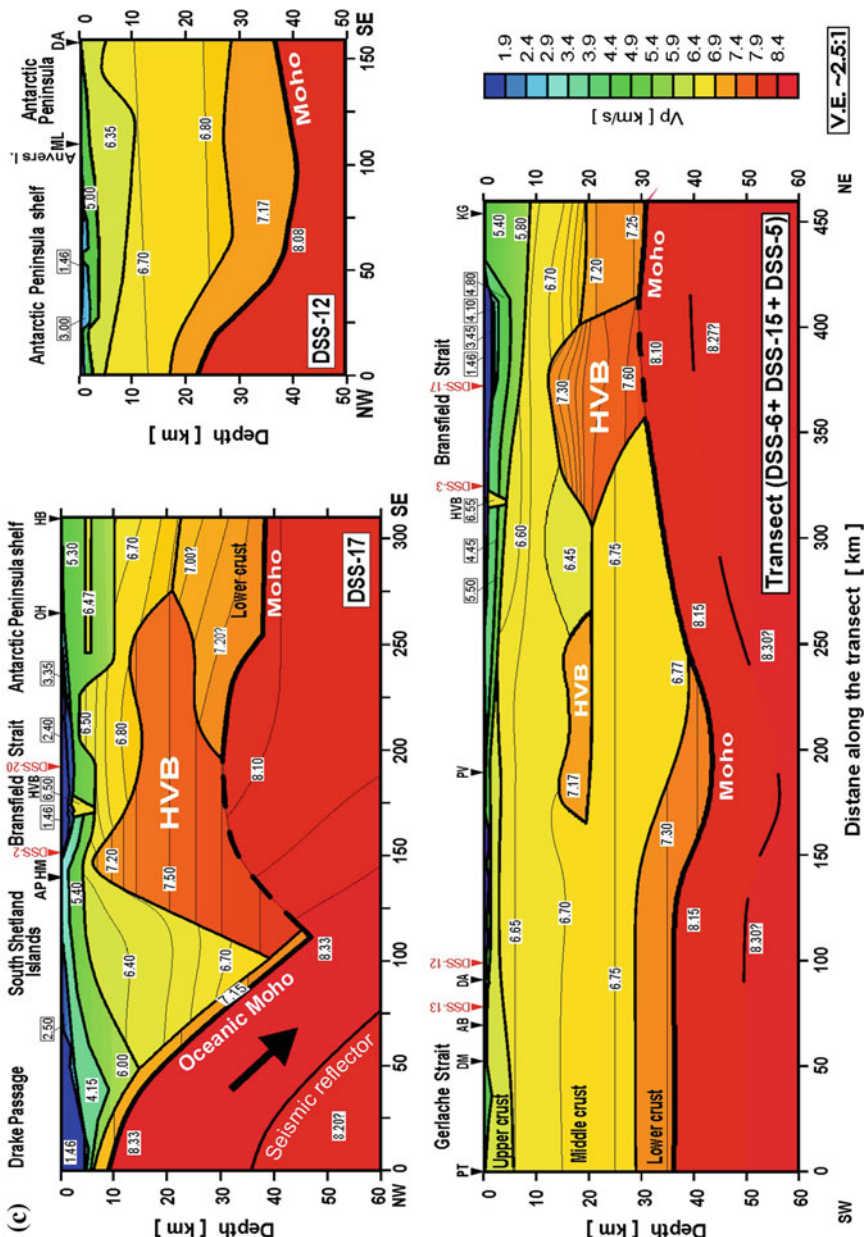


Fig. 6 continued

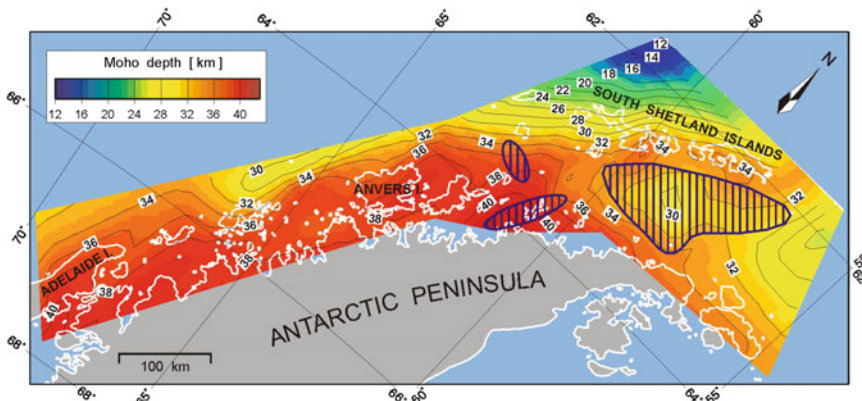


Fig. 7 Map of the depth to the Moho boundary along the Antarctic Peninsula, based on data from ray-tracing models of the crustal structure. Areas filled with *blue lines* in the central part of the Bransfield Strait mark the extent of the high velocity anomaly, where at a depth of 13–18 km P-wave velocities reach 7.2 km/s, as well as the extent of two other areas of anomalously high velocity. In the NE part of this area, due to possible existence of a thick crust-mantle transition, the isolines do not reflect the actual Moho depth. Modified from Janik et al. (2006)

were modelled down to the Moho boundary which reaches a depth of 42 km in this area. The lower crustal velocities are 7.3 km/s in the 7 km thick southwestern part and 7.2 km/s in the 12 km thick northeastern part of the model. Sub-Moho velocities of 8.10–8.15 km/s and a deep reflector (55–40 km) at distances 100–400 km were modelled for the upper mantle. Existence of a HVB was not confirmed further to the NE.

4.3 Moho Depth and Crustal Features

Based on the collected DSSs models of crustal structure (Fig. 6a, b, c), a map of isolines of depth to the Moho discontinuity along the AP was prepared (Fig. 7, Janik et al. 2006). The depths to the Moho were taken where available along all profiles. Between the data points, the Moho depth values were interpolated to create a 2D surface. The map shows that the maximum crustal thickness, 38–42 km, occurs along the AP shelf between Adelaide Island and Palmer archipelago. Towards the Pacific, the Moho depth decreases and reaches 30–32 km at the edge of study area. In central part of the Bransfield Strait, seismic velocities reach anomalously high value of 7.2 km/s at a body that is asymmetric “mushroom”-shaped in a three-dimensional form, shaded with blue lines, at depths of 12–18 km. Below NE part of this body, Moho depth is not well resolved. Along the coast of the AP, the Moho depth is about 34 km, and along South Shetland Islands the crustal thickness reaches 35 km. The latter area separates Bransfield Strait from the South Shetland Trench, where the minimum Moho depth in the area occurs (12 km).

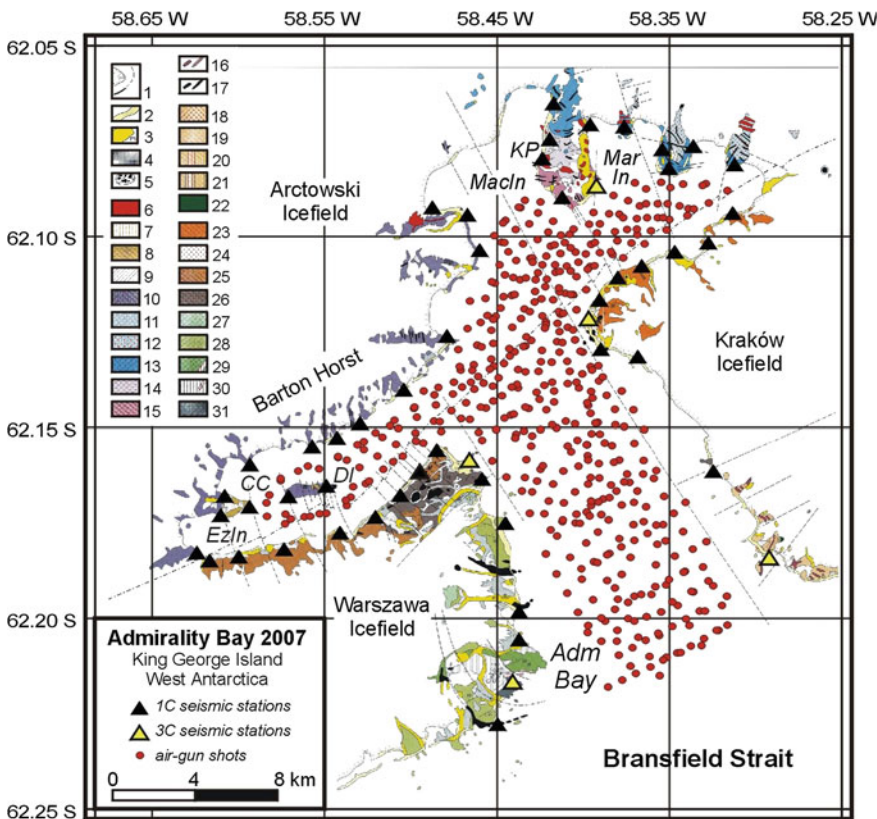


Fig. 8 The Map of the Admiralty Bay (after Birkenmajer 2003) with location of experiment's air gun shots (red dots), and receivers (triangles) deployed at the coast of the Bay. Inlet shows localization of the experiment area at the South Shetland Islands archipelago. Modified from Majdański et al. (2008)

5 Shallow Refraction: 3D Experiment

Schematic location of air gun shots and land receivers from the 2007 experiment in the Admiralty Bay, is presented in Fig. 8. The idea of the experiment was to recognize the main fault system in the area composed of the Ezcurra and Mackellar faults, and to localize the edge of the Barton Horst. It was also necessary to compare the shallow structures with known surface geology. The structure of the upper most crust was modelled using two software packages IBP by Hole (1992), and JIVE3D by Hobbs (1999). The total of 11341 verified travel times were inverted for velocity distribution. A strong effect of the water layer was recognized and had to be included in the inversion. The bathymetry map of the bay was prepared based on echosounder measurements taken at each shot point. The obtained bathymetry was

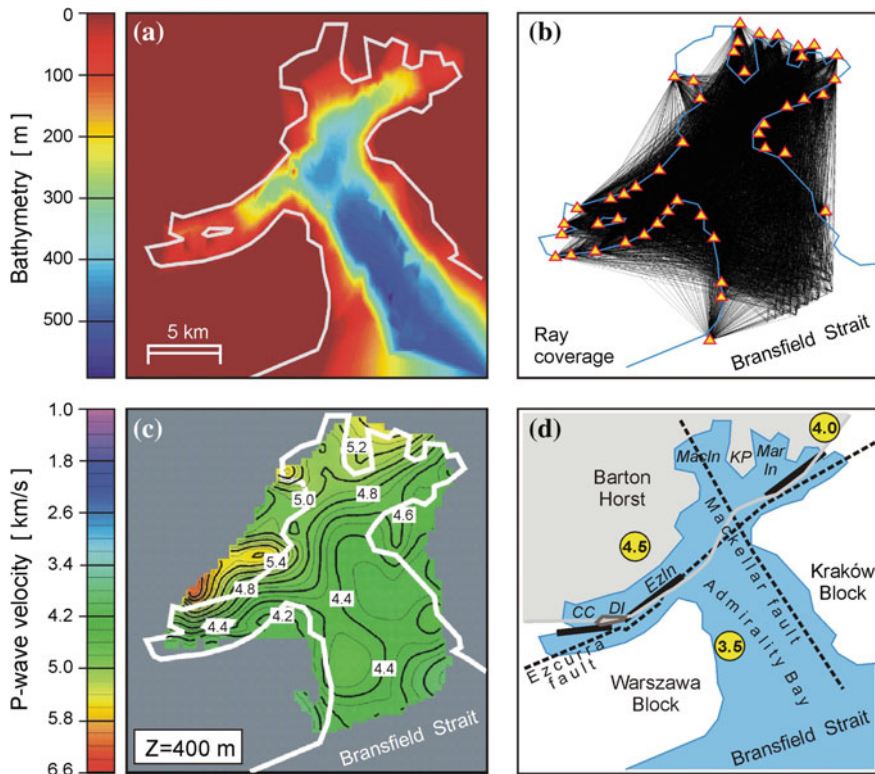


Fig. 9 The collection of the diagrams from the Admiralty Bay: **a** estimated shape of the sea floor with coast line marked with white line; **b** the distribution Pg waves rays. The triangles mark the position of the stations; **c** horizontal slice through the tomographic inversion model at 400 m. High gradients zones indicate the faults; **d** schematic interpretation with marked localization of confirmed faults (*thick black lines*) Dashed lines marks faults recognized in the surface geology. The difference in the velocities suggest the uplift of the Barton Horst, and the Horst edge is marked with 4.0 km/s velocity isoline

included in IBP as time corrections for travel times, and as an additional water layer modeled in JIVE3D. This procedure significantly improved the resolution of the final model.

During the interpretation it was possible to recognize the main features of the shallow crustal structure in the Admiralty Bay. The 3D tomographic image was obtained thanks to good quality of the data, especially Pg arrivals. The location of the Ezcurra Fault was verified from the Ezcurra Inlet to the Martel Inlet (Fig. 9). The ray coverage in the Kraków Block was not good enough to verify the location of the Mackellar Fault. The edge of the Barton Horst was defined as a 4 km/s isoline between the area of higher velocities of the Horst (about 4.5 km/s) in the shallow structures and smaller velocities of Warszawa and Kraków Blocks.

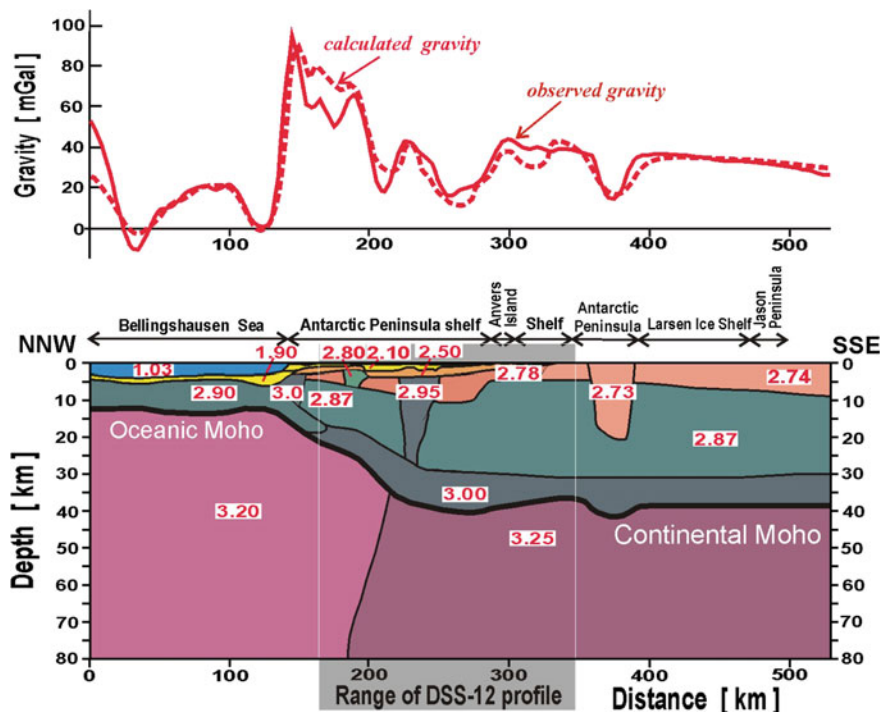


Fig. 10 Density model of the crust and upper mantle from the Bellingshausen Sea to the Antarctic Peninsula as an extension of the seismic velocity model along DSS-12 profile (ca. 120 km long, see Figs. 2 and 6c) is taken from Yegorova et al. (2011), modified from Środa et al. (1997). Observed and calculated anomalies are shown in the upper diagram. Numbers on the cross-section indicate density values in g/cm^3

6 Gravity and Magnetic Models

The magmatic arc of the AP continental margin is marked by high-amplitude gravity and magnetic anomaly belts reaching highest amplitudes in the region of the South Shetland Islands and trench. The sources for these anomalies are highly magnetic and dense batholiths of mafic bulk composition, which were intruded in the Cretaceous, due to partial melting of upper-mantle and lower-crustal rocks.

Incorporating data on our seismic refraction profiles (DSS-17, DSS12 and DSS-13) and physical properties, Yegorova et al. (2011) and Yegorova and Bakhmutov (2013) prepared 2D (600–900 km long) gravity and magnetic models which provide new insights into crustal and upper-mantle structure of the active and passive margin segments of the northern AP.

This enables a better constraining of both Moho geometry and petrological interpretations in the crust and upper mantle. Model along the DSS-12 profile (Fig. 10) crosses the AP margin near the Anvers Island and shows typical features

of a passive continental margin (Yegorova et al. 2011). The second model along the DSS-17 profile extends from the Drake Passage through the South Shetland Trench/ Islands system and Bransfield Strait to the AP and indicates an active continental margin linked to slow subduction and on-going continental rifting in the back arc region. Continental rifting beneath the Bransfield Strait is associated with an upward of hot upper mantle rocks and with extensive magmatic underplating.

7 Discussion

Seismic refraction profiles were obtained across the AP continental shelf between the projected southeastward positions of the Tula and HFZs. Near the coast of the AP, crustal velocity models reveal sediments with a thickness of 0.2–1.5 km. Farther northwest, sediments with a thickness of up to 5 km are observed beneath the mid–outer continental shelf. The crustal velocity models also describe high velocities of 6.3–6.4 km/s at depths <1 km in a wide belt beneath the AP continental shelf, increasing to 6.6 km/s at depths of 5–15 km. Near the Graham Land coast, the AP has a typical continental structure, and has been modelled with three layers with velocities of 6.3–6.4, 6.6–6.8, and 7.1–7.2 km/s. The total thickness of the crust varies from 36 to 42 km, and maximum crustal thicknesses are observed beneath Adelaide Island, the Biscoe Islands, and Anvers Island. The models also show that the AP crust thins oceanward to a thickness of 25–30 km beneath the mid–outer shelf.

The crustal structure of Bransfield Strait between the Shackleton and HFZs differs from that of the AP shelf to the southwest. Our data describe a major crustal boundary, which corresponds to the southeastward projection of the HFZ. This zone separates the three-layer continental crust of the AP to the southwest from the two-layer crust and the presence of the high-velocity body beneath Bransfield Strait to the northeast.

On the SW edge of landward projection of HFZ we detected two HVBs with $V_p > 7.2$ km/s. The geometry of our network of measurements, for obvious reasons, was not optimal for detecting details of the structure of the whole landward projection of HFZ. From our data we can not prove or disprove connection between the HVBs in the south; but we are sure of their separation from the HVB of Bransfield Strait by a zone of lower velocities. The boundary of the HVB in Bransfield Strait is controlled by rifting processes at its NE limit. Can we connect the existence expressed on both transects of HVB's with the landward extension of HFZ? One explanation could be movements on the boundary between the passive and an active margin (?rotation of South Shetland microplate), which could have created conditions for injection of upper mantle material into the crust, or uplift of the lower crust.

In the NE part of Bransfield Strait where the larger HVB “mushroom” body has its root, velocity increases continuously to 7.8 km/s at 30 km depth. This suggests the existence of a thick crust-mantle transition zone, often encountered in active

rift zones, rather than a step-like Moho boundary. Therefore, the area, marked by violet colour in Fig. 5, indicates that the velocity isolines do not reflect the Moho discontinuity depth. There are no data that could confirm the depth of the HVB in the northwestern part of the Bransfield Strait (particularly the area close to the King George Island) and whether the Moho discontinuity with $V_p = 8.1$ km/s is to be found there, but alimentary zones with the upper mantle material seem to occur there too. The HVB spreads far southeastwards from the main axis of the rift (profiles DDS-3 and DSS-17). It becomes thinner at larger and larger distances, and continues a horizontal intrusion into the continental crust of the AP. The maximum distance from the rift axis is about 80 km. Dimensions, thickness and extents exclude the existence of a single huge magmatic chamber.

The chapters by Barker et al. (2003) and Christeson et al. (2003) present the results of a wide-angle seismic experiment with a net of eight profiles, conducted in Bransfield Strait in 2000. Christeson et al. (2003) detected, as in our investigations, velocities >7.25 km/s at a depths 10–15 km at the central part of Bransfield Strait, which they interpreted as the Moho boundary. In our interpretation, it is a top of HVB. The well-documented upper mantle velocity of $V_p > 8.0$ km/s on the record sections along 300 km of DSS-20 profile (Grad et al. 1997a, b), strong reflections from the Moho boundary observed on DSS-17 profile (Grad et al. 1993a, b; Yegorova et al. 2011) and lower velocities (~ 6.9 km/s) detected below HVB along DSS-3 profile (Janik, 1997a, b) confirm our interpretation of the Moho boundary at a depth of ~ 30 km below the Bransfield Strait.

8 Summary

- The maximum crustal thickness occurs along the AP shelf, between Adelaide Island and Palmer Archipelago; it amounts to 38–42 km.
- Towards the Pacific, the Moho depth decreases and reaches 30–32 km at the edge of study area.
- The minimum Moho depth in the study area is beneath the South Shetland Trench (12 km).
- In the central part of the Bransfield Strait, seismic velocities reach an anomalously high value of 7.2 km/s at 13–18 km depth in the “mushroom”-shaped body.
- In the NE part of the Bransfield Strait, near the axis of the active rift, velocities increasing from 7.2 to 7.7 km/s were found.
- The area of shallow Moho depths (ca. 30 km) in central part of the Bransfield Strait extends between the coast of the AP, with a Moho depth about 34 km, and South Shetland Islands, with a Moho depth of 35 km.
- On the landward projection of the HFZ, two high velocity bodies with $V_p > 7.2$ km/s were detected, both separated from the HVB of the Bransfield Strait by zone of lower velocities with $V_p < 6.6$ km/s.

Acknowledgments The Polish Antarctic Expeditions were helped by numerous Antarctic stations: Argentinian (Almirante Brown, Esperanca and Primavera); Brasilian (Comendante Ferraz); British (Rothera,R); Chilean (O'Higgins and Arturo Prat); and Spanish (Livingston Island). The land teams also used inactive stations: Half Moon, Melchior (Argentinian); Hope Bay, Damoy (A), Danco (O), Deception (B), Faraday (F), Horse Shoe (Y), Admiralty Bay (G) (British). The Expeditions collaborated closely with the Polish Arctowski Antarctic Station on King George Island. The members of the Expeditions are grateful to all persons and organisations responsible for the Antarctic stations they used. The cooperation and assistance of Polish scientists, technicians and captains and the crews of the hydrographic research ship ORP "Kopernik", oceanic tugs M/S "Jantar" and D/E "Neptunia", and M/V "Polar Pioneer", during the experiments are gratefully acknowledged. The first four expeditions were led by Aleksander Guterch. Members of five Polish Antarctic Expeditions, included many people working at the Institute of Geophysics PAS: Zbigniew Czerwiński, Wojciech Czuba, Edward Gaczyński, Zbigniew Gajewski, Marek Górski, Aleksander Guterch, Tomasz Janik, Włodzimierz Kowalewski, Jerzy Krajczyński, Marek Kubicki, Mariusz Majdański, Michał Malinowski, Jan Pajchel, Robert Pietrasiać, Edward Perchuć, Stanisław Rudowski, Kazimierz Skowroński, and Maciej Zalewski.

We are indebted to Geofizyka Toruń S.A. for providing instrumentation and staff support during our expedition operation.

During the Antarctic summer of 1990/91, a detailed deep seismic refraction survey was undertaken in the Bransfield Strait using sensitive ocean bottom-seismic stations in co-operation with the Hokkaido University in Sapporo.

For map preparation and coordinate calculations we used GMT software (Wessel and Smith 1998).

We greatly appreciate the constructive and helpful review by Wolfram Geissler.

References

- Ashcroft WA (1972) Crustal structure of the South Shetland Islands and Bransfield Strait. British Antarctic Survey Scientific Report 66. p 43
- Barker DHN, Christeson GL, Austin JA, Dalziel IWD (2003) Backarc basin evolution and cordilleran orogenesis: Insights from new ocean-bottom seismograph refraction profiling in Bransfield Strait. *Antarct Geol* 31(2):107–110
- Birkenmajer K (2003) Admiralty Bay, King George Island (South Shetland Islands, West Antarctica): a geological monograph. In: K Birkenmajer (ed) Geological results of the Polish Antarctic expeditions. *Studia Geologica Polonica* 120:5–73
- Christeson GL, Barker DHN, Austin JA, Dalziel IWD (2003) Deep crustal structure of Bransfield Strait: initiation of a backarc basin by rift reactivation and propagation. *J Geophys Res* 108(B10):2492. doi:[10.1029/2003JB002468](https://doi.org/10.1029/2003JB002468)
- Grad M, Guterch A, Środa P (1992) Upper crustal structure of deception Island area, Bransfield Strait, West Antarctica. *Antarct Sci* 4:469–476
- Grad M, Guterch A, Janik T (1993a) Seismic structure of the lithosphere across the zone of subducted Drake plate under the Antarctic plate, West Antarctica. *Geophys J Int* 115:586–600
- Grad M, Guterch A, Janik T, Środa P (1993b) 2-D seismic models of the lithosphere in the area of the Bransfield Strait, West Antarctica. *Pol Polar Res* 14:123–151
- Grad M, Shiobara H, Janik T, Guterch A, Shimamura H (1997a) Crustal model of the Bransfield Rift, West Antarctica, from detailed OBS refraction experiments. *Geophys J Int* 130:506–518
- Grad M, Shiobara H, Janik T, Guterch A, Shimamura H (1997b) Crustal model of the Bransfield Rift, West Antarctica, from detailed OBS refraction experiments. In: Ricci CA (ed) The Antarctic region: geological evolution and processes. Terra Antartica Publication, Siena, pp 675–678

- Grad M, Guterch A, Janik T, Środa P (2002) Seismic characteristic of the crust in the transition zone from the Pacific Ocean to the northern Antarctic Peninsula, West Antarctica. In: Gamble JA Skinner DNB, Henrys S (eds) Antarctica at the close of a millennium. Royal Society of New Zealand Bulletin 35:493–498
- Guterch A, Grad M, Janik T, Perchuć E, Pajchel J (1985) Seismic studies of the crustal structure in West Antarctica 1979–1980—preliminary results. In: Husebye ES, Johnson GL, Kristoffersen Y (eds) Geophysics of the polar regions. Tectonophysics 114:411–429
- Guterch A, Grad M, Janik T, Perchuć E (1990) Deep crustal structure in the region of the Antarctic Peninsula from seismic refraction modelling (next step of data discussion). Pol Polar Res 11:215–239
- Guterch A, Grad M, Janik T, Perchuć E (1991) Tectonophysical models of the crust between the Antarctic Peninsula and the South Shetland trench. In: Thomson MRA, Crame JA, Thomson JW (eds) Geological evolution of Antarctica. Cambridge University Press, Cambridge, pp 499–504
- Guterch A, Grad M, Janik T, Środa P (1998) Polish Geodynamical Expeditions—seismic structure of West Antarctica. Pol Polar Res 19:113–123
- Herron EM, Tucholke BE (1976) Sea-floor magnetic patterns and basement structure in the southeastern Pacific. In: Hollister CD, Craddock C et al (eds) Initial reports of the deep sea drilling project. Government Printing Office, Washington, pp 263–278
- Hobro JWD (1999) Three-dimensional tomographic inversion of combined reflection and refraction seismic travel-time data. Ph.D. thesis, Department of Earth Sciences, University Cambridge p 240
- Hole JR (1992) Non-linear high resolution three-dimensional seismic travel time tomography. J Geophys Res 97:6553–6562
- Janik T (1997a) Seismic crustal structure in the transition zone between Antarctic Peninsula and South Shetland Islands. In: Ricci CA (ed) The Antarctic region: geological evolution and processes. Terra Antarctica Publication, Siena, pp 679–684
- Janik T (1997b) Seismic crustal structure of the Bransfield Strait, West Antarctica. Pol Polar Res 18:171–225
- Janik T, Środa P, Grad M, Guterch A (2006) Moho depth along the Antarctic Peninsula and crustal structure across the landward projection of the hero fracture zone. In: Fütterer DK, Damaske D, Kleinschmidt G, Miller H, Tessensohn F (eds) Antarctica: contributions to global earth sciences. Springer, Berlin, pp 229–236
- Larter RD, Barker PF (1991) Effects of ridge crest-trench interaction on Antarctic-Phoenix spreading: forces on a young subducting plate. J Geophys Res 96(12):19583–19604
- Majdański M, Środa P, Malinowski M, Czuba W, Grad M, Guterch A, Hegedűs E (2008) 3D seismic model of the uppermost crust of the Admiralty Bay area King George Island, West Antarctica. Pol Polar Res 29(4):303–318
- Środa P, Grad M, Guterch A (1997) Seismic models of the Earth's crustal structure between the South Pacific and the Antarctic Peninsula. In: Ricci CA (ed) The Antarctic region: geological evolution and processes. Terra Antarctica Publication, Siena, pp 685–689
- Środa P (2001) Three-dimensional modelling of the crustal structure in the contact zone between Antarctic Peninsula and South Pacific from seismic data. Pol Polar Res 22:129–146
- Środa P (2002) Three-dimensional seismic modelling of the crustal structure between the South Pacific and the Antarctic Peninsula. In: Gamble JA, Skinner DNB, Henrys S (eds) Antarctica at the close of a millennium, vol 35. Royal society of New Zealand Bulletin, pp 555–561
- Wessel P, Smith WHF (1995) New version of generic mapping tools released. EOS 76:329
- Yegorova T, Bakhmutov V, Janik T, Grad M (2011) Joint geophysical and petrological models for the lithosphere structure of Antarctic Peninsula continental margin. Geophys J Int 184:90–110. doi:10.1111/j.1365-246X.2010.04867.x
- Yegorova T, Bakhmutov V (2013) Crustal structure of the Antarctic Peninsula sector of the Gondwana margin around Anvers Island from geophysical data. Tectonophysics 585:77–89

Department of Polar and Marine Research: The Hornsund Station and Other Activities in the Arctic and Antarctic Regions

Marek Górska

Abstract The activity of the Department of Polar and Marine Research at the Institute of Geophysics PAS has been briefly outlined by a participant and witness of the reported events, working there over the years 1977–2002.

Keywords Polish polar research · Polish Polar Station Hornsund

1 Historical Background

The Polar and Marine Research Laboratory was established at the Institute of Geophysics PAS in 1977; it was headed by Maciej Zalewski. In 1979 it became the Department of Polar and Marine Research, and since 2010 it bears the name of Department of Polar Research (in the whole text we will refer to it as the Department). Its first mission was to organize systematic studies in Arctic regions on the basis of a permanent polar station.

The creation of the Department was possible owing to the former achievements and many-year experience of Polish scientists in exploration and survey of polar regions. At the end of the 19th century, Poles were among the explorers of Antarctica. Henryk Arctowski and Antoni Bolesław Dobrowolski took part in the Antarctic expedition onboard the ship “Belgica”, led by Captain Adrien de Gerlache (the expedition started in 1897, and wintered in 1898–1899). Our exploration of the Arctic begun a century earlier: Polish explorers (political exiles, but not only) were engaged in exploration of the Russian Arctic. Vast expansion of Polish research in

M. Górska (✉)
Polish Academy of Sciences, Institute of Geophysics,
Księcia Janusza 64, 01-452 Warsaw, Poland
e-mail: mgorski@igf.edu.pl

the Arctic took place in the 1930s. The meaningful events were, in particular, the wintering on the Bear Island in the framework of the Second International Polar Year 1932/1933, and seasonal research campaigns in the region of Spitsbergen and Greenland. The very favorable circumstance was the fact that polaristics was a very popular issue at that time, as evidenced by ample and informative literature in Polish language.

After the Second World War, of great importance for the development of Polish polaristics was our participation in the International Geophysical Year 1957/1958. During the wintering in Spitsbergen, a polar station was established at the Isbjørnhamna in Hornsund Fjord. In the summer seasons of 1957, 1958, 1959, and 1962, researchers from Polish scientific institutions have worked in different areas of South Spitsbergen, realizing projects of very wide thematic scope. In later years, various academic institutions were engaged in seasonal surveys over Spitsbergen, making use of trapper huts existing there, or building their own stations.

Our activity around Hornsund has intensified again in the years 1970–1975. On the initiative of Krzysztof Birkenmajer, under the auspices of the Geophysical Expeditions Commission of the Polish Academy of Sciences, six expeditions to the Hornsund region were organized. They were executed by the Institute of Geography, University of Wrocław, in cooperation with the Institute of Geophysics, Polish Academy of Sciences, and other scientific institutions engaged in polar research. The expeditions were realizable owing to the agreement between the Polish Academy of Sciences and the State Maritime School in Gdynia to enable transport of scientists to Spitsbergen. The cruises to Spitsbergen were also used for systematic maritime studies. Most of the expeditions were headed by Stanisław Baranowski¹ from the University of Wrocław. The Institute of Geophysics was represented by Maciej Zalewski (Fig. 1), who actively participated in putting the station into service and marine research in the framework of project realized by the Marine Station in Sopot.

In the Antarctic region, the Department got at its disposal the station established in 1957 by the Soviet Union under the name Oasis, located in Bunger Oasis. It was handed over to Poland on January 21, 1959, and renamed as A. B. Dobrowolski Polar Station, to commemorate the Polish geophysicist and explorer. Because of difficult access (the station is located hinterland), it was used by short time only, being the site of research by the First Polish Antarctic Expedition 1958–1959. The last Polish expedition, making geodetic, geomorphological and meteorological observations, went there in 1978–1979.

The A. B. Dobrowolski Station is now inactive. The actively operating Polish station in the Antarctic region is the Henryk Arctowski Antarctic Station opened on February 26, 1977, presently managed by the Department of Antarctic Biology, Institute of Biochemistry and Biophysics, Polish Academy of Sciences.

¹ Stanisław Baranowski died in Poland in 1978, after a tragic accident during the Polish Antarctic Expedition to King George Island.



Fig. 1 *Left* Maciej Zalewski, long-standing head of the Department of Polar and Marine Research, performing oceanological experiments during the cruise to Spitsbergen (the 1970s). *Right* Engineer Janusz Jeleński inside the Polish Polar Station Hornsund in Isbjørnhamna during reconstruction works (summer 1978)

2 Polish Polar Station Hornsund Begins Working Permanently

Maciej Zalewski, a person with large experience in geophysical expeditions, has been nominated to the position of head of the Department of Polar and Marine Research. He had been taking part in the wintering in Spitsbergen in the framework of the International Geophysical Year 1957/1958, and was a leader of Polish geophysical expedition to Vietnam in 1964. Zalewski spent the winter 1966 in the Russian station Molodezhnaya in Antarctica. During this wintering he also visited the A. B. Dobrowolski Polar Station in Bunger Oasis (The wintering team included Ryszard Czajkowski, later on employed by the Institute of Geophysics).

In the late 1970s, political forces of the so-called “Eastern Block” tended to expose and publicize their presence in polar regions. Scientific communities took an advantage of this fact to expand the scientific exploration. The main objective of the Department of Polar and Marine Research was to put back into service the year-round operating Polish Polar Station in Hornsund Fiord. The station building erected during the International Geophysical Year 1957/1958 was meant for just one wintering, though it was often used by summer scientific teams doing research in Spitsbergen. In spite of systematic repairing, the building was not apt to further exploitation. To make the Station ready for permanent work, the building needed thorough overhauling or replacement by a new one. Due to the favorable fact of keeping the original engineering construction plans, it was possible to arrange the



Fig. 2 The opening ceremony at the Polish Polar Station Hornsund, September 1978

needed works as a major repairing. This turned out to be crucial for the existence of the Station in the Isbjørnhamna, since Norwegian regulations would not allow to erect any new construction within the South Spitsbergen National Park that was enacted in this area in 1973.

Preparations for making the Station suitable for permanent work started, under the supervision of Jerzy Jankowski, Director of the Institute of Geophysics, in the first days of January 1978, after the appropriate team has been gathered. The first group of scientific and technical workers consisted of:

- Wojciech Krzemiński, deputy director of the Department
- Janusz Jeleński, engineer, responsible for the entire overhauling and making the Station operative (Fig. 2)
- Jan Szumański, architect
- Marek Górska, geophysicist,
- Krystyna Źakowicz, geophysicist

Later on, the group incorporated more persons, including:

- Antoni Szymański, geophysicist
- Ryszard Czajkowski, geophysicist
- Jacek Kowalski, geophysicist
- Stanisław Rudowski, geologist

In the fall of 1977 Maciej Zalewski went to the Henryk Arctowski Antarctic Station, to be a leader of wintering. The team remaining in Warsaw kept in radio contact with him. At the Arctowski station, established by the Institute of Ecology



Fig. 3 *Left* view on the Polish Polar Station Hornsund in Isbjørnhamna Bay in the 1980s. *Right* construction works on the so-called summer base in the summer of 1979

PAS, the main research was concerned with ecology, but a geophysical program was incorporated. The recordings from seismological and magnetic stations established there were processed at the Department of Polar and Marine Research.

The entire organization of construction works at the Hornsund Station and preparations for the 10-person wintering in the remodeled Station were led by Janusz Jeleński, aided by Wojciech Krzemieński, who was at the same time responsible for organizing the second expedition of the Polish Academy of Sciences to the A. B. Dobrowolski Station in the Bunger Oasis (East Antarctica) in 1978/1979, and then led this expedition. Its aim was to perform geophysical, geological, geodetic, topographic, glaciological and geomorphological surveys.

Most of the instruments for various projects carried out by the Department of Polar and Marine Research have been designed and built by other departments of the Institute of Geophysics PAS. In July 1978 the Hornsund Station was visited by a group of researchers doing deep seismic sounding surveys in Svalbard region, led by Aleksander Guterch.

A very important task was to prepare a team of ten researchers to spend the winter in the planned Station. Finally, the group heading for Spitsbergen at the end of June consisted of a total of 70 scientists and technicians. The means of transportation were provided owing to the cooperation with the State Maritime School. The works in the Isbjørnhamna, carried out until the mid-September, were fully successful. At the ambient temperature of -17°C , the Station was officially opened. A photo of the opening ceremony, in the presence of the Institute's Director Jerzy Jankowski, is shown in Fig. 2.

After successful wintering, the Station was subject to further improvements; in the summer of 1979 a new pavilion was added for summer research groups working in the region of Hornsund (Fig. 3).

In next years, the Station has been systematically amended, according to the needs of current research projects. The data coming from the Hornsund Station were processed and prepared for publication in yearbooks (in the series *Publications of the Institute of Geophysics*) and original research papers. Magnetic and



Fig. 4 Left one of the sites of the Seismological Station array. Right magnetic pavilions

seismological data have been regularly submitted to World Data Centers (Two photos to illustrate the measurement sites are in Fig. 4). In summer seasons, few-person groups have been visiting the Station for realizing short-term projects, making instrument calibration, and technical servicing to enable the Station to function. The main research projects carried out at the Station in a continuous manner were related to the following fields:

- seismology,
- earth's magnetism,
- meteorology,
- physics of the ionosphere

The processing of seismological, magnetic and ionospheric data was made at the Institute of Geophysics PAS. Ionospheric research in Hornsund Station was designed and led by Andrzej Wernik from the Space Research Centre PAS. Hornsund meteorological data were transmitted to the Maritime Branch of the Institute of Meteorology and Water Management in Gdynia. Magnetic data were processed and prepared for publication by Adam Gnoiński and Włodzimierz Glegolski. Geophysical data from the Arctowski Station in the Antarctic were processed by Jacek Kowalski and Antoni Szymański. In 1986 the scope of continuous measurements at the Hornsund station was enlarged by including those of the electric field; the instruments were installed by Marek Kubicki, who supervised the project.

The activation of the Hornsund station in 1978 coincided with the breakthrough in measurement technologies and the data processing relating to dynamic development of computerization. The necessary updating of the measuring instruments was made gradually. A problem was with the access to the station, possible only in the summer. The analog instruments were ultimately replaced by digital ones. The data processing software has been developed at the Institute of Geophysics PAS. The updating was possible owing to close cooperation between the Departments of Seismology, Magnetism and the Scientific Instruments Laboratory. The seismological instruments were designed and prepared by Jerzy



Fig. 5 *Left* before departure to Hornsund from Longyearbyen (Piotr Głowacki on the *left*, Marek Górska in the *middle* and Maciej Zalewski on the *right*). *Right* Marek Górska measuring seismic events in the ablation zone of the Hans Glacier

Suchcicki and Bogusław Domański, who was the author of ingenious software enabling the data recording and analysing; the data processing software was later on updated by Jan Wiszniewski. Modern magnetic field recorders were constructed at the Central Geophysical Observatory at Belsk under the guidance of Janusz Marianuk. In the region of Hornsund, the sites of seismometers in the array were optimized to enable the location of both the earthquakes and the glacial seismic events generated in the region of Hans Glacier.

The station has been subsequently enlarged by adding pavilions for the needs of environmental studies, which began to be systematically performed there. For such studies, suitable laboratories and complicated analytical equipment were indispensable. The analytical laboratories were also used for seasonal biological studies carried out at the Station by scientific institutions collaborating with the Department.

The Seismological Station HSP has been recording not only earthquakes but also glacial seismic events generated in the nearby Hans Glacier. The observation of these phenomena enabled monitoring the dynamical activity of the glacier. There were also made seasonal recordings of icequakes using seismometers placed directly on the glacier's surface. These recordings refer to the studies begun in the summer of 1962 by Roman Teisseyre (Lewandowska and Teisseyre 1964) and continued by the Institute of Geophysics in the Hornsund expeditions in the first half of 1970s. The monitoring of seismic glacial events enabled a detailed determination of their character and relation to dynamic processes within the glacier. The research was led by Marek Górska (Fig. 5).

Photographs illustrating the history of Hornsund Station, together with recollections of Maciej Zalewski, Marek Górski, Marcin Węsławski and Piotr Głowiak, and excerpts from unpublished texts by Lucjan Nowosielski, have been gathered in an album commemorating the Fiftieth Anniversary of the Station, edited by Magdalena Puczko ([2007](#)).

3 Logistics and Transportation

A major issue to be solved every year was to assemble a wintering group. The head and participants of the group were selected in consultation with the authorities of the Institute and the departments. The initial health check-up of candidates and medical care over the wintering group was made by the Military Institute of Aviation Medicine, which also realized its own research project. The maintenance of station and care over current technical problems of the wintering group were carried out by the logistics team of the Department of Polar and Marine Research. The number of persons involved varied depending on the needs. In the 1980s and 1990s the organizational works were headed by the late Halina Giżejewska and Grażyna Dziurla (performing this duty up to now). It was a difficult task, especially in the 1980s, because of harsh economic conditions and political situation in Poland. The food supply was mostly provided by the Foreign Trade Company Baltona. The marine transportation was initially performed by the State Maritime School, then the use was made of the vessels belonging to the Polish Ship Salvage and other maritime enterprises. In recent years, the permanent collaboration with the State Maritime School was resumed, including joint scientific workshops.

Several technical problems relating to the maintenance of the station have been solved gradually, e.g., a sewage-treatment plant was implemented (exporting the waste material), and fuel storage tanks were modernized to enable a continuous operation of electric current generators. However, after 20 years of exploitation, in spite of systematically performed maintenance and updating works, the station must have been thoroughly renovated. This was done in the early 2000s (see later in the text), under the guidance of Jan Szumański—the architect who was responsible for the construction works in 1978.

4 Further Research Programs, Cooperating Institutions

In summer seasons, the Station was used for making measurements by various field groups and for projects realized by various scientific institutions in Poland. These included the following: University of Silesia, Nicolaus Copernicus University in Toruń, University of Wrocław, Adam Mickiewicz University in Poznań, Maria Curie-Skłodowska University in Lublin, University of Gdańsk, AGH University of Science and Technology in Cracow, Institute of Meteorology and Water

Management, Institute of Geological Sciences PAS, and the Institute of Oceanology in Sopot (its representative Marcin Węsławski was involved since 1970s; he also wintered in 1981/1982). There was also a broad international cooperation.

Along with the works associated with the construction of the Station and wintering, the Department was engaged in research programs. In 1976, the Institute of Geophysics initiated a huge, many-year international deep seismic sounding project in polar regions. This project, led by Aleksander Guterch, was finalized by the Antarctic expedition in 1991, but the deep seismic sounding studies in polar regions have been continued up to the present. The deep seismic sounding campaign was accompanied by projects realized by the Department of Polar and Marin Research: the study of local seismicity in selected areas of Svalbard and the Antarctica, led by Marek Górska, and the study of bottom sediments, led by Maciej Zalewski. The bottom sediment research, however, was initiated in 1982 in the Hans Glacier forefield, Hornsund Fjord, by Stanisław Rudowski, head of the 1982/1983 wintering.

In the years 1981–1988, another very active person, Krystyna Żakowicz, joined the works on organization of polar research. Previously, in the summer of 1979, she was engaged in the project of applying geophysical methods to study medium-scale ice structures in the Hans Glacier, led by Marian Pulina, head of the wintering in 1979/1990. Alongside, the radar sounding of the glacier was performed by Ryszard Czajkowski.

In Polish science, the 1980s were the era when central research projects were strongly promoted. Various long-term projects were initiated by Scientific Committees of the Polish Academy of Sciences, and the respective institutes of the Academy. The Institute of Geophysics was one of these, leading the Central Polar Research Project in the Earth' Sciences, co-ordinated by the Committee on Polar Research. For many years, the Chairman of the latter was Aleksander Guterch, and the Secretariate, led by Stanisław Rudowski, was housed by the Polar and Marine Department of the Institute of Geophysics. The research topics included: the study of seismic architecture and seismostratigraphy of sedimentary cover of fiord and shelf bottoms in the region of Spitsbergen and South Shetlands, using seismoaoustic profiling and taking core samples of sediments. The results, serving also for recognition of the course of deglaciation of the study regions and determining the glacial-marine sedimentation conditions, were presented in publications and at numerous conferences in Poland and abroad, in cooperation with the International Arctic Science Committee (IASC). The Department has been closely collaborating with the National Earthquake Information Center (NEIC), Cooperative Arctic Seismological Project (COASP) and NORSAR. In the framework of this collaboration, the author attended yearly seminars.

The collaboration with other scientific Polish and foreign institutions covered not only the joint elaboration of routine data from the Hornsund Station. The Station was also a base for various specific research projects, realized mainly in spring and summer seasons, related to glaciological, geomorphological, environmental, biological, oceanological topics, as well as deep seismic sounding. Quite



Fig. 6 *Left* in front of the Station—discussion before the measurements at the Hans Glacier (Marek Górski on the *left*, Jacek Jania in the *middle*, and Jon Ove Hagen on the *right*). *Right* the group from Finland (Anja Palli on the *left* and John C. Moore in the *middle*) during measurements

often, the wintering crew included a scientist from the respective institution, supervising a given project. Of particular importance was the cooperation with the University of Silesia, initiated by Marian Pulina and then continued by Jacek Jania. This cooperation gave grounds for joint projects with Andreas Vieli and other scientists from the ETH Zurich, Switzerland, as well as John C. Moore and Anja Palli from the Arctic Centre, University of Lapland, Finland (see, e.g., Vieli et al. 2004; Palli et al. 2003, 2004). The scientists involved included also Jon Ove Hagen from the Department of Physical Geography, University of Oslo, and Andrei F. Glazovsky from the Institute of Geography, Russian Academy of Sciences (Fig. 6).

The fast development of the studies on many glaciers in the region of Hornsund Fjord was possible owing to the use of modern measuring instruments and snow scooters for field surveys and transportation of scientific teams from the Longyearbyen airport to Hornsund in winter seasons.

Piotr Głowacki, the present head of the Department, appeared in Hornsund in 1980. He has been strongly involved in polar research, participating in many projects carried out by the University of Silesia, his employer until 1997. Then he became hired by the Institute of Geophysics PAS. His skills helped to solve many scientific problems, as well as organizational and technical ones. One of more important organizational accomplishments of Piotr was to equip the station in modern snow scooters for permanent use. His glaciological studies were summarized in the book: Głowacki (2007). In 2003 Piotr Głowacki was decorated by the King Harald V of Norway with the Commander Cross of Royal Norwegian Order of Merit for his activity in Polish-Norwegian scientific cooperation in the region of Spitsbergen.

In spring 1992, at the initiative of the University of Silesia, an international glaciological symposium was organized at the Hornsund Station. The chairman



Fig. 7 Spring seismometric measurements. *Left* Maciej Zalewski on the way to the Hans glacier. *Right* Jerzy Suchcicki reading data from the computer at the central site of the seismometer array in the ablation zone of the Hans Glacier

was Jacek Jania. The symposium was attended by several persons from various institutions; the Department was represented by Maciej Zalewski and Jerzy Gizejewski, leader of the 1991/1992 wintering.

In summer seasons of 1993–2000 systematic studies of seismic glacial events occurring in the Hans Glacier region were made. The recordings were carried out by an array of seismometers placed directly on ice. The works were led by Marek Górska; the team included Maciej Zalewski, Jerzy Suchcicki (Fig. 7) and a current seismological observer at the Station. The results obtained over the 50-year period of glacial events study (initiated by Roman Teisseyre in 1962) were later on summarized in the monograph issued by Springer (Górska 2014).

Other important investigations were headed by Jacek Bednarek (leader of 1990/1991, 1993/1994, 1995/1996 wintering) and Jerzy Gizejewski (leader of 1991/1992, 1996/1997 wintering). Jacek Bednarek was executing the project: “Genesis of Spitsbergen fjords based on a study of tectonic structures in the Hornsund Fjord region, including the study of tectonic structures in the glacier’s basement with the use of geomagnetic surveys”. This many-year project involved a variety of field measurements. Jerzy Gizejewski was heading the project: “Seismoacoustic methods as a tool for studying the variability and diversity of geological environment of sedimentary basins”. The measurements were performed in Isbjørnhamna, Spitsbergen, and comparatively at the contemporary pro-glacial lake Jokulsarlon in Iceland and post-glacial lake Drawsko in Poland.

The beginning of the year 2000 was a very difficult period. The Hornsund station was deteriorating and urgently needed to be overhauled. It was necessary to

find financial means for this undertaking. This coincided with a serious illness of Maciej Zalewski. His duties as head of the Department were taken over by his deputy, Marek Górski. Maciej Zalewski, upon awarding the Officer's Cross of Polonia Restitura, retired in March 2001. In 2002 Piotr Głowacki was nominated the head of the Department and is holding this position until now.

Of great importance for the exchange of information on the current polar research results have been the Polar Symposia, convened every year. The symposia, associated with meetings of the Polar Club established in the 1970s, were housed by various scientific centers over the country. The proceedings have been published in the series *Polish Polar Studies*; see, e.g. the issues devoted to sixty years of Polish research of Spitsbergen (edited by Zalewski 1994) and the one devoted to the forties anniversary of the Polish Polar Station Hornsund (edited by Głowacki 1997).

All the publications relating to the results obtained in the Hornsund region have been listed in two comprehensive volumes: *Bibliography of Polish Research in Spitsbergen Archipelago, Part I, years 1932–1996* (Zalewski 2000) and *Bibliography of Polish Research in Spitsbergen Archipelago, Part II, years 1997–2006* (Gizejewski 2010).

The yearbooks of all routine Polar measurements have been published in the series *Publications of the Institute of Geophysics, Polish Academy of Sciences*. Hornsund magnetic yearbooks are still published, together with other yearbooks from Polish Magnetic Stations, in internet edition of Series C (the most recent one: Reda et al. 2013). Seismological yearbooks in printed form were terminated at the data from the year 1995 (Górski 2000). Recent seismological data are available from the Department of Seismology at the Institute of Geophysics PAS. Meteorological yearbooks were published in Series D of *Publications of the Institute of Geophysics, Polish Academy of Sciences* over the years 2000–2005 (the last issue: Kwaczyński 2008). Recent meteorological bulletins are available at the address: glaco-topoclim.org .

5 Rejuvenation of the Hornsund Station and Current Research at the Department

In 2002 the Hornsund Station, along with the whole Hornsund region, was selected as one of the European biodiversity flagship sites. The previously mentioned thorough renovation of the station was made under very strict nature protection regulations. In addition to overhauling, some new pavilions and an urgently needed large storehouse were implemented. New facilities included a power plant system, fuel installation, and biological sewage treatment plant. Great emphasis has been put on waste segregation. The ecological waste management system includes two hydraulic compactors and a waste incinerator.

More information about the past and current research and seasonal measurements in the Hornsund station region, including the full list of wintering teams, can be found at the Station's homepage <http://hornsund.igf.edu.pl/>.

The research at the Department is currently done within the general topic: "Study of abiotic environmental features and the use and development of new geophysical methods in polar zones and comparative regions". Specifically, there are three main projects:

- Meteorology and optical methods of the atmosphere research
- Geophysical methods of marine polar environment
- Balance of glaciated and non-glaciated polar catchments

The research team, led by Piotr Główacki, includes Grzegorz Karasiński, Bartłomiej Luks, Mateusz Moskalik, Adam Nawrot, and Ph.D students: Magda Bloch, Tomasz Wawrzyniak, and Oskar Główacki.

Acknowledgments I am grateful to all my colleagues from the Polar Community for their help in collecting the materials for writing this historical outline, in particular to Maciej Zalewski, the many-year head of the Department of Polar and Marine Research. Thanks are also due to my friends from the Editorial Office of the Institute of Geophysics, Anna Dziembowska and Zofia Okrasińska, for editing the text.

References

- Giżejewski J (ed) (2010) Bibliography of Polish Research in Spitsbergen Archipelago, part II, 1997–2006. Publs Inst Geoph Pol Acad. Sc M-31(407):149
- Główacki P (ed) (1997) 40th Anniversary of the Polish Polar Station Hornsund—Spitsbergen, 24th Polar Symposium, Polish Polar Studies, IGF PAN, Warszawa, p 388
- Główacki P (2007) Rola procesów fizyczno-chemicznych w kształtowaniu struktury wewnętrznej i obiegu masy lodowców Spitsbergenu (Role of physical and chemical processes in the internal structure formation and mass circulation of Spitsbergen glaciers). Publs Inst Geophys Pol Acad Sc. M-30(400):147
- Górski M (2000) Seismological Bulletin, Arctowski Antarctic Station, Hornsund Polish Station 1992–1995. Publs Inst Geophys Pol Acad Sc B-18(284):70
- Górski M (2014) Seismic events in glaciers, Series: Geoplanet: Earth and Planetary Sciences. Springer, p 99
- Kwaczyński J (2008) Meteorological Conditions, Hornsund, Spitsbergen, 2004/2005. Publs Inst Geophys Pol Acad Sc D-69(384):84
- Lewandowska H, Teisseyre R (1964) Investigations of the ice microtremors on Spitsbergen in 1962. Biul Inf Komisji Wypraw Geof PAN 37:1–5
- Palli A, Moore JC, Jania J, Kolondra L, Główacki P (2003) The drainage pattern of Hansbreen and Werenskioldbreen, two polythermal glaciers in Svalbard. Polar Res 22(2):355–371
- Palli A, Moore JC, Jania J, Kolondra L, Główacki P (2004) Glacier changes in Southern Spitsbergen, Svalbard, 1901–2000. Ann Glaciol 37:219–255
- Puczko M (ed) (2007) 50 lat Polskiej Stacji Polarnej im. Stanisława Siedleckiego (Spitsbergen, Hornsund) (50 Years of the Hornsund Polar Station), Naviga Krzysztof Makowski, Warsaw, p 120
- Reda J, Neska M, Wójcik S (2013) Results of geomagnetic observations—Belsk, Hel, Hornsund 2012. Publs Inst Geophys Pol Acad Sc C-106(414):68

- Vieli A, Jania J, Blatter H, Funk M (2004) Short-term velocity variations on Hansbreen, a tidewater glacier in Spitsbergen. *J Glaciol* 50(170):389–398
- Zalewski SM (ed) (2000) Bibliography of Polish research in Spitsbergen Archipelago, Part I, 1930–1996. Publs Inst Geophys Pol Acad Sc M-23(314):p 194
- Zalewski SM (ed) (1994) 60 Years of Polish research of Spitsbergen. In: 21st Polar symposium. Polish Polar Studies, IGF PAN, Warszawa, p 371

Seismology and Earth Dynamics: A Variety of Scientific Approaches

Krzysztof P. Teisseyre, Paweł Wiejacz and Jacek Trojanowski

Abstract Seismology and related fields were among the basic disciplines constituting the Institute of Geophysics, Polish Academy of Sciences, from its inception. During 60 years, various experimental and theoretical researches have been conducted, and a network of seismic observatories has been managed and gradually updated, as part of international network. Novel theories of the propagation of seismic waves and the processes in the lithosphere and the Earth's interior, especially in the seismic event preparation areas, have been developed and gradually modified. The statistical studies and profound research on innovative mathematical techniques brought about a real progress in the assessment of seismic hazard and the probability of other extreme events.

Keywords Seismology · Elastic waves · Continuum theory · Dislocations · Anisotropy · Earth structure · Geoelectricity · Heat transfer

1 The Beginnings

The Institute of Geophysics PAS started functioning in 1953, initially (until 1971) bearing the name of the Department of Geophysics PAS. The Department of Seismology and Physics of the Earth's Interior was established as one of the Institute's units in 1971. In 1979, it split in two parts: Department of Seismology and Department of the Earth's Interior Dynamics, to unite again into the Department of Seismology and Physics of the Earth's Interior in 2008.

In the Department of the Earth's Interior Dynamics, a very diversified research was conducted, from theory to field surveys and laboratory experiments. In the

K. P. Teisseyre (✉) · P. Wiejacz · J. Trojanowski
Institute of Geophysics, Polish Academy of Sciences, Księcia Janusza 64,
01-452 Warszawa, Poland
e-mail: kt@igf.edu.pl

Department of Seismology, mainly the observational projects were executed. These included building, updating and managing of the network of observatories, exchanging and processing of data, publishing reports, and participating in international projects.

Back in 1953, the first head of seismological division and its organizer was Roman Teisseyre. The topics of work included practice and theory of seismic measurements and observations, theory and studies on the earthquakes, mining rockbursts, the processes in the Earth's interior, and the deep seismic sounding. Later on, the last branch was transformed into an independent Department of the Lithospheric Research.

From the beginning, adaptation of scientific equipment and manufacturing of new models took place, basing on the instrumentation that already existed at the Silesian Geophysical Observatory in Racibórz. Consecutive technical directors of the Institute have been putting much effort on producing seismic sensors and the recording systems. A small handbook by Droste and Hordejuk (1964) gathers basic information on the seismic equipment that was in use in Polish seismic stations, as well as the principles of seismometry and characteristics of seismographs and seismograph-galvanometer pairs, in the form of tables. Nine seismographs (seismometers) are presented, three of which were constructed in the Institute by the engineers Tadeusz Siemek and Jan Uchman: SD-57, SK-58, and SU-59.

The Department of Geophysics PAS, soon participated in the huge international project—the International Geophysical Year 1957–1958. Concurrently, two geophysical expeditions were organized—to Spitsbergen and Vietnam, the latter directed by Roman Teisseyre. In Spitsbergen, the expedition led by Dr. Stanisław Siedlecki has established the first Polish Polar Station. In Vietnam, already in 1957, two geophysical observatories were built and equipped: in Phu-Lien by Hanoi and at Cha-Pa. These were serviced and modified during consecutive expeditions. The last small expedition, which serviced the Phu-Lien observatory, took place in 1964.

The distribution of earthquakes belongs to basic problems of geophysics. It was investigated in our Department in relation to the studies on the Earth's structure. Bożenna Gadomska (nee Wojtczak) studied the Earth structure (Wojtczak-Gadomska et al. 1964) and patterns of regional seismicity (e.g., Gadomska and Korhonen 1989). In cooperation with the Institute of Seismology, University of Helsinki, she participated in studies on global seismicity and tectonic features, and symmetry/asymmetry in the Earth structure (see, e.g., Gadomska and Teisseyre (1984)).

2 Polish Seismological Network

The Polish Seismological Network (PLSN) is managed by the Institute of Geophysics PAS. The network consists of seven broadband stations in Poland: Góra Klasztorna (code: GKP), Suwałki (SUW), Belsk (BEL), Książ (KSP), Ojców (OJC),

Niedzica (NIE), Kalwaria Pacławska (KWP) and the eighth broadband site at Hornsund (HSPB, Spitsbergen, Svalbard). Data is transferred in real time. Data and results of analyses are shared with international seismological centers and organizations (EMSC, ORFEUS EIDA, ORFEUS VEBSN, ISC, FDSN, NEIC) and seismological networks of neighbouring countries. The team supplies seismological data to the web pages of the Institute.

This network has been deployed gradually. Older instruments have been replaced by new-generation devices; methods of recording and data analysis evolved too. Transition from analog to digital recording and transfer of data has taken place over the years 1989–2004. Updating and maintenance of the PLSN, as well as data processing were the main duties of Paweł Wiejacz in the years 1996–2012.

On technical side, seismologists collaborated with the Department of Scientific Instruments, especially with Jerzy Suchcicki, in locating and servicing the seismological stations and Jan Wiszniewski in computer analysis of signals and calibration of equipment.

In 2013, registration from three new local networks has started. These are: LUMINEOS in the copper mining area and in the vicinity of Żelazny Most repository basin, SENTINELS near Niedzica in southern Poland, and VERIS in Vietnam, around a river dam.

3 Mining Seismicity: A Challenge for Polish Seismology

Seismicity of Poland is dominated by mining-induced events; therefore, mining and engineering geophysics is a very important field of research at the Institute of Geophysics PAS. Over the years, the Institute has become the leading research institution on mining seismicity.

Research on mining seismicity on the territory of present-day Poland dates back to 1929, when Prof. Karl Mainka created the geophysical observatory at Racibórz (then in Germany), aimed at the study of induced seismic events in Upper Silesia. Recording at Racibórz was continued after World War 2. Having taken care of this observatory, the Institute has created a local network of seismic stations in Upper Silesia (Bytom, Dąbrowa Górnica, Rybnik, Zabrze, Chorzów), transferred in the 1970s to the Central Mining Institute (in Katowice) to initiate their local seismic network.

Józef Hordejuk studied spectral and dynamic character of seismic sources, including dimensions of foci in time domain (see, e.g., Hordejuk et al. 1984). The research was based on analog data. Strong mining tremors in the copper mining region were studied by Hordejuk et al. (1979). He was also involved in designing new seismic equipment.

Studies on statistical structure of induced seismicity applied to the mining problems have been also made by Jankowska (1971) and Kijko et al. (1982). The

energy statistics for mining events and correlation of the extracted deposit volume with the energy released by mining were dealt with by Główacka et al. (1990).

Cooperation of Zofia Droste with Roman Teisseyre has led to a preliminary classification of mining tremors based on signs of the first motions (Droste and Teisseyre 1972). Droste was one of the promoters of setting up the first underground three-dimensional seismic network in Poland—at Miechowice coal mine (in 1964). Her research, jointly with other scientists in Poland and abroad, concerned many problems, such as the seismicity in the Upper Silesian Coal Basin and the Legnica-Głogów Copper Mining District, and seismic hazard related to dams and other industrial objects.

The Institute was the first in the world to develop methods of determination of magnitude and energy of mining events and the first to study their return period patterns (Gibowicz 1962). It was also the first in the world to implement algorithms to locate sources of induced seismic events. Gibowicz estimated the seismic source parameters from wave spectra (see Gibowicz 1975). This approach has been applied to studies on the mechanisms of mining tremors (Gibowicz et al. 1989).

Seismic events in mines were found to be of two types—one directly associated with mining, the other associated with dislocations along faults in the rockmass, the motion being triggered by the change of stress field as result of mining. The source studies carried out since the 1970s have shown that the dislocation-type events have shear-type mechanisms, just as earthquakes. The events directly associated with mining show some discrepancy from the shear model, and the Institute has developed the first source model accounting for the non-shear components.

Spectral source models have been applied to events from America, South Africa and Poland, and enabled the determination of physical parameters of those events. Worth noting are the location algorithms by Andrzej Kijko and his results in terms of optimal planning of seismic networks in mines (see, e.g., Kijko and Wcisło 1980).

Janusz Niewiadomski (1989) applied the Singular Value Decomposition Method to the location of mining seismic events and optimization of seismic networks, both with linear and nonlinear techniques. He also applied the neural networks approach to seismogram analysis (Niewiadomski 2004). Considerations on the theory of source time function of an earthquake, describing the process of energy release, can be found, e.g., in the paper by Mendecki and Niewiadomski (1997).

The Institute was the first in the world to apply the source time function approach to the analysis of mining events (Domański et al. 2002). Search for slow initial phase in the seismic events generated at a copper mine was undertaken by Kwiatek (2003).

Modern numerical, probabilistic methods enable better evaluation of natural hazards and the event location (see, e.g., Dębski 2004, 2008). Also the probabilistic inverse theory has been studied and seismic parameter estimators have been analyzed. Rudziński and Dębski (2013) presented an adaptation of the double-difference



Fig. 1 During the expedition to Vietnam, from *left* Józef Hordejuk, Vietnamese seismologist, and Sławomir Gibowicz. From the archives of the Institute of Geophysics PAS

seismic event location technique to the studies on the mining seismic events, and a further development of this technique, to enable a more precise determination of the origin time and epicenter location.

The Institute's leading role in mining geophysics may be best documented by the first in the world textbook on mining seismology—Introduction to Mining Seismology by Gibowicz and Kijko (1994); the recent developments in this field were in-depth summarized by Gibowicz (2009, and references therein).

In 1997, the Institute of Geophysics PAS and the University of Mining and Metallurgy in Kraków organized the Fifth International Symposium on Rockbursts and Seismicity in Mines; the main organizer was Stanisław Lasocki, at the Academy of Mining and Metallurgy in that time. Since 1971, the Institute has been co-organizing the yearly Polish-Czech-Slovakian Conferences on Mining Geophysics.

Some photos relating to early seismological investigations are reproduced in Figs. 1, 2, 3, 4, 5, 6 and 7.

4 Induced Seismicity: Recent Developments

Nowadays, the main topics of research on mining-induced seismic processes, based mainly on the data recorded by the local seismic networks, include: investigation on the seismic source properties and their relation with geomechanics, tectonics, geology, and the seismic hazard; the ground motion prediction with the use of neural network simulation; assessment of time-varying seismic



Fig. 2 At the Niedzica castle, from *left* Z. Gajewski, J. Hordejuk, W. Romaniuk, and M. Pętkowski. From the archives of the Institute of Geophysics PAS

Fig. 3 In Budapest in the 1980s, from *left* Roman Teisseyre, Edward Perchuć, Sławomir Jerzy Gibowicz, Aleksander Guterch. From the archives of the Institute of Geophysics PAS



hazard in various areas and at specific mining situations; application of the seismic tomography for controlling the rockmass parameters in mines.

Methods of estimating the largest possible earthquake are discussed by Lasocki and Urban (2011). Studies of the Coulomb stress transfer (e.g., Orlecka-Sikora et al. 2012) show that the coseismic stress transfer plays significant role in seismogenic process. This influence manifests itself with strong dependency between the location of new events and the stress distribution after a strong event.

A next important topic was the introduction, by Stanisław Lasocki, of the equivalent dimension (ED) space and the transformation methods for seismic data (such as magnitude, location and time intervals between consecutive events) into this multidimensional space (Lasocki 2014). Lizurek and Lasocki (2012) unveiled



Fig. 4 In the courtyard of Wawel royal castle, 1989, from *left* Barbara Dudek, Maria Hojny-Kołoś, Andrzej Zawada, Ewa Zarzycka. Except of A. Zawada, this was crew of the Kraków Seismological Observatory (code: KRA). From the archives of the Institute of Geophysics PAS



Fig. 5 In the Racibórz Observatory (code: RAC), 1986. From *left* Andrzej Zawada, Krystyna Wiktorowicz, Bolesław Bylica, Maria Bylica, Łucja Zimny, Józef Hordejuk, and Wojciech Wojtak. Except of A. Zawada and J. Hordejuk, this was the crew of the Observatory, W. Wojtak being its head



Fig. 6 At the entrance to Książ Observatory (code: KSP), in the castle, 1989, from *left* Zbigniew Skoczeń and Dorota Stempowska in the *upper row*, and Paweł Wiejacz, John Poetschke (Teledyne Geotec), Józef Weiss and John Brooks (Teledyne Geotec) in the *lower row*. Photo by Jerzy Speil, from the archives of the Institute of Geophysics PAS



Fig. 7 Crew of the Książ Observatory, 1991: Leopold Stempowski, his mother Dorota Stempowska, Jerzy Speil and Józef Weiss. From the archives of the Institute of Geophysics PAS

the potential of the equivalent dimension method in studies of interaction between events in the mining seismicity.

Stanisław Lasocki and Beata Orlecka-Sikora initiated the Teamwork for Hazard Assessment for Induced Seismicity initiative (THAIS). The overall intention of THAIS initiative is to integrate research groups and improve the efficiency of knowledge transfer by creating the international platform of cooperation between scientists and industry representatives in the field of man-induced seismicity. An infrastructural component of the initiative will be ensured by EPOS Working Group 10 “Infrastructures for Georesources” conducted by Orlecka-Sikora.

This Working Group is part of the EPOS (European Plate Observing System) project, that was prepared for integration of European research infrastructure in Earth Sciences and producing the common scientific services based on cloud computing (which will stand as standards for Solid Earth computational infrastructure). WG10 has been created to integrate research infrastructures in the area of anthropogenic seismicity and to strengthen dialogue and cooperation between the scientific community and industry.

5 The Seismic Hazard Monitoring of Poland

Poland is a region of very low seismicity; nevertheless, earthquakes occur here from time to time. The historical catalogue consists of less than 100 earthquakes in the time span of almost 1,000 years. The existing permanent seismic network in Poland is sparse and meant rather for being part of a global network than for measuring local seismicity. The Polish Seismic Network is not sufficient to detect all local earthquakes with magnitudes less than 3.

For more precise hazard assessment, more dense and more sensitive seismic networks had to be deployed. On the order of the Ministry of Environment, the project of Seismic Hazard Monitoring of Poland (SHMP) was executed over the years 2007–2012. On the Institute’s side, the key role in settling the agreement was played by Prof. Aleksander Guterch and the Deputy Director Marian Hościliowicz. Two new employees, Beata Plesiewicz and Jacek Trojanowski, were appointed.

The SHMP project was focused on events at magnitudes lower than 2. Because the whole area of Poland is too large area to be monitored with 24 stations assigned for the project, it was decided to monitor only selected areas with relatively high probability of seismic events occurrence.

The project was divided into two 2.5-year stages. In the SHMP the stress was put on mobility and immediate data transfer. It was assumed that in case of a sudden earthquake anywhere in Poland, some of the stations would be moved in 2 days from current positions to new ones around the epicenter. At the end of the project, the seismic hazard assessment for monitored regions had to be updated.

The first stage of the project covered the southern Polish border with a strong belief to record some activity. Indeed, it has been confirmed that Podhale is seismically active (over 100 events). There were also two microearthquakes

recorded near Krynica in Beskid Sądecki which goes with previous activity of the region. In other places monitored during the first stage of SHMP, no event was recorded. Places of well confirmed earthquakes in the Teisseyre-Tornquist Zone became the object of seismic monitoring in the second stage of the project.

Five regions were selected: West Pomerania near Koszalin, Pomerania near Żarnowiec, central Poland near Płock and near Łuków, and Holly Cross Mountains. Additionally, three stations remained in the Podhale—the area where seismic activity was ascertained in the first stage of survey.

In some regions, recording conditions were very bad, as near Łuków, where the high noise level in the whole region was a reason for moving the stations elsewhere. Generally, most of the stations were put in regions with thick sediment and soil layers, which makes the noise level high. From this point of view, stations in the Holly Cross Mountains had good recording conditions but a great problem was with high activity of numerous quarries in the region. Several quarry blasts each day were difficult to be precisely analyzed and hardly distinguishable from natural events. Finally, no natural seismic event was found in the whole Teisseyre-Tornquist Zone during SHMP.

Surprisingly, a relatively strong earthquake appeared on 6 January 2012 near Jarocin. It had magnitude $ML = 3.8$ and was felt in a radius of 60 km. Immediately after the earthquake, five stations were moved there from other regions. By the end of the project, no more events have been recorded there, but a discovery was made of two previous events: one in seismic records of 2007 and the other in local museum archive as a short note in a diary of 1824.

Organization of this new kind of experiment brought new challenges at each stage of the execution. The new data logger (NDL) developed at the Institute, which meets high quality requirements and low price, was adopted for the purpose of the project. Then, an acquisition and archiving system was innovatively developed for storing the data and making them available in near-real-time mode. Additional tools for data analysis (SWIP) and the detection algorithm were significantly improved.

SHMP was the first project of this scale in Poland that focused on local seismicity. The project confirmed that some regions of Poland are seismically active and that it is advisable to run local monitoring in such places, as it is one of very few methods to measure current dynamical processes of the Earth's crust.

6 Studies on the Earth's Upper Mantle

Seismic sounding of the Earth's crust and the upper mantle are conducted mainly in the Department of the Lithospheric Research. Here, we present only some results of the investigations by Edward Perchuć and his co-workers.

The 8° discontinuity was detected (Perchuć and Thybo 1996; Thybo and Perchuć 1997), which corresponds to the top of a low-velocity zone below

approximately 100 km depth, first found beneath the Baltic shield and then in Europe, Asia and North America. This zone is identified with the asthenosphere—a layer of our planet which lies below the lithosphere and consists of partly melted material. In these studies, two kinds of mantle and crust regions in the continents are found. One is tectonically stable and thus aseismic, the other being unstable and seismically active. Lateral transition from passive to active regions in North America demarks a narrow, deep zone of high accumulation of stress. This explains the occurrence of intraplate earthquakes in this zone (Thybo et al. 2000).

Strong seismic scattering from around the top of the mantle's Transition Zone in the high resolution explosion seismic profiles from Siberia and North America was investigated by Thybo et al. (2003). This seismic reflectivity refers to the “410 km” discontinuity, explained by mantle heterogeneity, which is attributed to widening of the zone of α - β - γ spinel transformations. If this explanation has to be probable, high iron content is required at these depths.

Reinterpretation of seismic data along two crossing profiles in Yakutian kimberlite province in Russia, after digitization of seismograms, has led to finding the extremely large sub-Moho P-wave velocities, up to >8.7 km/s in some areas (Suvorov et al. 2006). Crustal structure was revealed and relation of the velocity to the kimberlite field was discussed.

Another seismic discontinuity, located at a depth around 300 km, with the P-wave the basis of records at single station, SUW velocity increasing to 9 km/s, has been observed for all the sub-Alpine raypaths (see Nita et al. 2012). This discontinuity is considered to have originated as a result of Alpine orogen subduction. Studies support the contention that the 300-km discontinuity is a regional feature—the subduction regime beneath the younger orogen.

Monika Dec studied structures at the western rim of the East European craton on the basis of records at single station, SUW. Travel time and other features of the waveforms were analyzed in order to reveal the influence of deep structures.

7 Theoretical Description of Seismic Sources

Earthquake source models can be divided into three groups. The first group deals with body force distribution in a focus region, the second one presents dislocation processes as responsible for internal energy releases in earthquakes, and in the third group the crack mechanics is considered in order to describe fracturing. The first and second groups are mutually connected by the theorem of stress equivalency caused by dislocation and by point force distribution. The second and third group are related to the theory of continuous distribution of dislocations.

Roman Teisseyre initiated theoretical program related to the defects in a continuum and to the formation of dislocations and cracks. The main task faced by these theoretical works was to formulate a fracture theory based on the dislocation arrays; these theoretical attempts considered not a single array, but two arrays of opposite sign dislocations under the same strain conditions. Due to the mutual

annihilation, these processes lead to formation of fracture and release of energy (see Droste and Teisseyre 1959).

Dislocational approach introduced some concepts of medium inhomogeneities, while cracks describe a further stage—rupturing (lost of cohesion in part of the medium). Crack formation energetics in processes of an earthquake preparation was studied by Dmowska et al. (1972). The premonitory processes were considered by Teisseyre (1980). Crack formation was studied with the use of physical model by Niewiadomski et al. (1980).

Main geophysical interests of Kacper Rafał Rybicki were the theory of dislocations, fractures, cracks-and-stress field evolution (Niewiadomski and Rybicki 1984), especially in the presence of layers (Rybicki and Kasahara 1977) or discontinuities in media of various rigidity (Rybicki 1992). Mechanical interaction between neighbouring faults was investigated by Rybicki et al. (1985).

Contact problems on tectonic faults were modelled and analyzed by Włodzimierz Bielski with co-workers (see Bielski and Telega 2001). The problems are formulated as variational inequalities, in terms of the tangent component stresses only, on contact or fault surfaces. Such a task is difficult since the stress-strain relations are not uniquely reversible; hence, the theory of convex analysis was used to solve the problem.

The studies on seismic release-rebound theory pertain both to seismic wave propagation and the theory of the seismic focus (see Teisseyre 1985). Droste (1991) has analyzed energy of simulated earthquake and the earthquake sequences, for various seismic rebound models, various friction and stress field levels. Five models of rebound process were taken into account, basing on theoretical background provided by seismic rebound theory applied to stress drop conditions (Droste and Teisseyre 1988).

Teisseyre and Wiejacz (1993) have modelled the stress history in earthquake sequences, studying four earthquake series. Earthquake source—the fracture—was approximated as a disc. Several assumptions relating to the thickness of this disc have been compared. Application of release-rebound theory to the study of a parallel crack system has been presented by Niewiadomski et al. (1991).

The release-rebound mechanism applied to the energy release problem resulted later in devising the Asymmetric Continuum Theory (see Teisseyre 2014, this issue, and Dębski et al. 2014, this issue). Also the fracture-band model of seismic focus plays a role in the formation of this theory.

The Micromorphic Theory of Continuum developed by Eringen and co-workers (for references see Teisseyre 2014, this issue) introduces microstructure and its deformations into the earthquake processes occurring in the focal zone, and into the seismic field as well. In the framework of such an approach, let us quote papers by Teisseyre (1974) and Teisseyre and Bielski (1995). Applicability of micromorphic theory to the problem of the medium influence on P-waves was proven with physical modeling (see Teisseyre et al. 1985).

According to the shear-band model, and its modification—the fracture-band model, in the earthquake process the seismic moment density and the released total energy density can be expressed by the number of coalescences of line

defects—dislocations (see Teisseyre 1996). For these studies, an approach was taken inspired by thermodynamics of point defects with relations to bulk properties.

Applications to the depth variation of earthquake entropy and to the dislocation network, or superlattice parameter, have been shown by Gadomska et al. (1995). This superlattice contains both the dislocations and “points” with no dislocation—vacancies. The presence of these vacancies is necessary if the system has to be able to obtain thermodynamical equilibrium. See also the paper by Kuklińska (1996), where the method is shown how to numerically develop a superlattice from elements distributed at random. Energetics of earthquake process in accord with fracture-band model is presented by Teisseyre and Majewski (2002).

In several papers, seismic events’ sequences were analyzed and simulated. As the input data, tectonic events, mining events from South Africa, and icequakes were taken (see Teisseyre et al. 2001b). The volcanic earthquakes were also subject to theoretical analysis, by Teisseyre and Nishimura (2001). Here the zone of stress-related fracturing is large, these fractures are a result of magma-imposed pressure. But the rupture and volcanic eruption are prepared and occur in a narrow channel, somewhere in middle of pressure-affected zone.

Some scientific activities of Andrzej Hanyga comprised studies in which an earthquake is explained by physico-chemical process—that is, by detonation-like phase transformations in the Earth (see Hanyga 1974). His studies include shock waves which are the aspects of rapidly propagating phase transformations. A theory of transverse waves: sonic shock waves, reaction waves and others, was presented by Hanyga (1975). His monograph of non-linear elasticity (Hanyga 1985) comprises, e.g., elastostatics with monotone operator theory and convex functions; elastodynamics with simple and shock waves; and geometry of elasticity, dislocations including.

8 Modelling of Earthquakes and Earthquake Cycles

Earthquakes, from the angle of models and methods of physics, using both theoretical research and computer modelling of earthquake-related processes, were investigated by Piotr Senatorski. Specificity of this approach is that it takes into account spatial heterogeneity of considered systems and slip-dependent friction law.

The investigations started from the continuous dislocation theory. The theory relates stresses in the earth’s crust to distribution of slips on tectonic faults, which enables us to formulate realistic models of interacting faults as seismic sources. Original derivations of the slip versus stress relations for faults in 2D and 3D elastic medium have been presented. In the next stage, by combination of the theory of dislocations and dynamical systems methods, an original model of fault dynamics with slip-dependent friction was constructed (Senatorski 1997). The model, as one of the first in seismology, allowed to simulate fault dynamics in the scales of both, single earthquakes and many seismic cycles. Computer simulations

enable to recognize relations between fault interactions and irregularity of seismic cycles. An important result was the formula for radiated seismic energy in accord with earthquake kinematic models.

During the third stage, the model was adapted to a more realistic case of faults embedded in 3D medium, which allowed to compare directly the simulated fault behaviour and statistics of earthquake parameters with real-world seismicity (Seniorski 2005).

In the next stage, the earthquake rupture process was analyzed from the angle of statistical physics, i.e., as represented by two linked description levels: the detailed one formulated in terms of the stress and slip fields, and the averaged one, expressed in terms of earthquake parameters and statistical relations among them. In analogy to thermodynamics, the seismic state equation is proposed to explain diversity of the so-called scaling relations in seismology, such as the radiated energy versus seismic moment scaling. At first, such relations were recognized in the computer simulation results. Then, they were found for real sets of earthquakes.

Next, the relations have been explained in terms of the proposed seismic state equation. Furthermore, some other scaling of earthquake parameters has been predicted and confirmed within the same scheme, revealing a consistent image of seismicity. These considerations resulted in several publications (e.g., Seniorski 2012).

Seniorski's recent studies are motivated by recent great mega-thrust earthquakes (Sumatra, 2004; Chile, 2010; Japan, 2011). They provided a large amount of new data revealing details of earthquake rupture complexity and recurrence patterns of large earthquakes.

9 Stochastic Description of Geophysical Processes

Earthquakes are a result of fracture of the crust due to tectonic stresses. The fracture of solids is preceded by nucleation of microcracks population which can propagate and coalesce. In order to describe this complex process, the kinetic model of crack evolution was derived by Czechowski (1993). The kinetic description lies at a level intermediate between the purely stochastic models and the fully microscopic treatment. The state of the crack system is described by the size distribution function which satisfies an integro-differential equation (similar to the coagulation equation). Such an approach explains the exponential form of crack size distribution, typical for metals and the inverse-power form for brittle materials like rocks, dependently on fusion cross-section. The model was generalized in order to describe the process of macrocrack growth by swallowing microcracks which nucleate in the vicinity of its tip. The kinetic model enabled us to calculate the evolution of field of internal stresses relating with cracks and can be treated as a description of fracturing processes parallel to the dislocation theory by Roman Teisseyre.

The inverse-power distributions appear in many phenomena: physical, geophysical, biological and economical. Phase transitions, deterministic chaos in nonlinear systems, large interacting systems with Self-Organized Criticality and

fractals are classical examples of mathematical models leading to this type of distributions. However, in spite of some different ways of explanation, common reasons of the power statistics are unknown.

The privilege mechanism was proposed as a unified cause of long tail distributions. It was shown (Czechowski 2001, 2005) that in many cases (i.e., percolation processes, cellular automata, Cantor set, resource redistribution model, return-to-the-origin problem in random walk, multiplicative processes, multiplication of probabilities), the hidden privilege can be extracted. A relevance was found between the privilege concept and the nonlinear approach, as well as connection between these processes and Ito equations or master equations.

Ito equations for observable quantities can constitute nonlinear macroscopic models of complex phenomena. Modelling of time series requires methods of model reconstruction from data. Some procedures for construction of Ito-like equations with persistence or periodical correlation function were derived and tested by Czechowski and Telesca (2013). They were based on the histogram method which was applied in our papers to geophysical time series (see Telesca and Czechowski 2012).

A recent field of activity are the studies on properties of simple cellular automata models. The approach aimed at obtaining elements of analytical description of the model, to draw precise conclusions on general properties of the system. Such methods are inspired by some works in the field of the so-called integrable systems, which is effective in obtaining exact formulas for cellular automata. This subject, although considered as being not strictly geophysical, was advanced by some studies performed in our department.

A systematic method of construction of cellular automata over finite fields was initiated by Doliwa et al. (2003) and developed by Białycki and Doliwa (2005) and Białycki (2005).

In order to study fundamental aspects of seismicity, a simple cellular automaton model was introduced by Białycki and Czechowski (2013), which reflects only two properties of earthquakes: the process of slow accumulation of energy and the abrupt release of energy. The model was used to an analysis of selected aspects of seismicity. In particular, it was shown that the universal curve for earthquakes recurrence time is of a combinatorial nature and it results from these two main characteristics of earthquakes.

Because of one-to-one correspondence between the rebound parameters and the avalanche distribution in the model, the non-trivial task of how to infer the properties of the microscopic physical interactions from a given distribution of avalanches, could be solved (Białycki and Czechowski 2013).

Another use of such simple cellular automata models is to show that the Ito equation may be a macroscopic model of the phenomenon. It resulted in a three-level description of a complex system, modelled by the domino cellular automaton (which is related to the Motzkin numbers, well known object in combinatorics)—see Czechowski and Białycki (2012).

10 Studies on the Heat Transfer, Liquid Flow and Electric Properties of Rocks

Heat transfer and geothermal gradient in the Earth mantle are important issues, as they have influence on many geophysical processes (see, e.g., Maj 1991). The problem of phonon conductivity was investigated, and estimation for molar heat at a constant volume for silicate minerals was done (see Maj 2005).

Diffusion problems in composite media, particularly the heat transfer and flow of electric charge, were also investigated. The homogenization theory was used and numerical calculations were applied to verify compatibility between experimental data and theory. The problems of controllability with boundary conditions in continuum mechanics, particularly in elastic and thermoelastic bodies, and in heat transfer problems, were discussed by Galka et al. (1994). Exploration of underground resources requires the knowledge of liquid flows through porous rocks. Transport problems in rocks are of significance also in waste storage, CO₂ sequestration, geothermal exploitation. Therefore, nonstationary flow of viscous incompressible fluid through deformable skeleton has been investigated. Derivation of macroscopic models, constitutive relations and generalized filtration laws was a subject of interest in many papers (e.g., Telega and Bielski 2003 and Bielski 2005).

Laboratory investigations of electric properties of rocks with water in pores, conducted by Lech Rusiniak, led to important results concerning the water itself, especially when it is contained in small compartments, as reported by Rusiniak (2002). A new conductivity model for dipole liquid with domain structure was proposed. Results of experiments suggest that the obtained dielectric permittivity curves are superpositions of two Debye's curves with different relaxation times and two different values of static dielectric constant. Debye's resonance for lower frequency is associated with oxygen's domain structure and for higher frequency with hydrogen's domain structure. For thin samples, damping of the Debye's resonance and interaction of the domains' structures is observed. On the basis of the experiments, Rusiniak inferred that water (including ice) behaves as a dielectric and ferroelectric material (Rusiniak 2004).

The paper by Teisseyre et al. (2001a) presents an interpretation of experiments on electric polarization of the rock samples subject to load, conducted in at the Solid Earth Institute, University of Athens. From shapes of the obtained curves compared to the numerical simulation results, a kind of piezoelectric stimulation is assumed. Supposedly, at least two relaxation processes, with different relaxation times, occur simultaneously. If the stimulation (episode of increased load) is abrupt and ends also abruptly, a bay of reversed polarization follows the initial one and is followed by visible relaxation. Also this effect was included in the numerical modelling.

Electric processes in the earthquake preparation stage were discussed by Teisseyre (1995). Various charge separation phenomena in rocks subject to varying loads were reviewed also by Teisseyre (2008).

11 Coupled Fields and Electric Resistivity Studies

Experimental relations between seismic, mechanic and electrical phenomena have led to concepts of coupled fields. The influence of non-mechanical, i.e., magnetic and/or electric fields on wave propagation in elastic solids is of interest in geo-physical problems. The wave propagation was studied within the coupled-field theory in linear elastic isotropic space and half-space using Green's functions. The loss of isotropy was found. Moreover, surface wave propagation in periodically layered media was investigated using a homogenization approach (see Bielski and Matysiak 1992).

Relation between rock and aquatic solution resistivity, charge separation and other electric and magnetic effects, and on the other hand—state and evolution of dislocation and crack fields were the theme of theoretical investigations conducted by Renata Dmowska and others (see, e.g., Dmowska et al. 1986). The dynamics of cracks system in the context of earthquake preparation was also extensively studied and reconstructed by means of numerical simulation by Czechowski (1993).

Measurements of soil or rock resistivity, especially with the use of four-electrode method, may reveal presence of hidden cavities and other structures. The electric resistivity research conducted by Wojciech Stopiński with partners from other institutions, was applied to engineering and archaeological problems.

Experimental investigations of electric resistivity variations were carried in mines (see Stopiński 1985). Measurements in the copper mines show that the local electric resistivity variations can be treated as precursors to upcoming seismic events. The resistivity variations in rocks subjected to stress are explained first by dilatation-diffusion theory, then by its modification, the dilatation–percolation theory (see Stopiński and Teisseyre 1982; Stopiński 1985). Observed curves of resistivity versus time may be explained by creation of open cracks, leading to their coalescence and formation of planes of the forthcoming rupture, with simultaneous water infiltration. This concerns both the tectonic earthquakes and mining tremors. Experiments in laboratories, as in Stopiński et al. (1991), confirmed dependence of resistivity on the cracks/fractures system, evolving in the rocks under variable, anisotropic load.

Krzysztof P. Teisseyre, inspired by these investigations, tried to construct a numerical model of electric resistivity of the complex medium, which would take into account: resistivity of matrix between inclusions (cracks and pores), resistivity of material or materials inside these inclusions, inclusions volume, geometry and orientation. A few versions of the model were developed in sequence (these are quoted in Teisseyre and Teisseyre 1999).

The idea of such a geometrical model contrasts with the typical approach—the percolation theory, in which connections between cracks or pores are decisive for compound medium resistivity. Here, connections are not taken into account. Nevertheless, the model has been partly confirmed in laboratory and by results found in the literature. Explanation to resistivity variations has been proposed, first

of all—to the opposite bays in the resistivity recorded with two perpendicularly oriented electrode arrays, known from the literature.

Long period resistivity variation of the dam bedrock related to varying water levels has been shown, e.g., by Stopiński (2003), and a model of the bedrock saturation with water has been given. Basing on Stopiński's data, Teisseyre and Teisseyre (1999) performed numerical simulations of electric resistivity changes caused by water infiltration.

12 Experimental Research on Seismic Rotation

The theory of rotation strains—Asymmetric Continuum Theory—is described by Teisseyre (2014, this issue) and Dębski et al. (2014, this issue). In this section, certain experimental results on seismic rotation are recalled.

The seismograms described by Droste and Teisseyre (1976) are probably the first rotational seismograms ever obtained. They were obtained from microarray of six horizontal seismometers distributed at different azimuths at the Miechowice coal mine (located in Upper Silesia, region of frequent seismic events of mining provenience). In macro scale, symmetric medium does not allow for rotations in the ground, except of those which are caused by local inhomogeneities. The above-mentioned rotations, however, were found very near to the event epicenter (1–3 km), and were explained by inertia of microblocks.

Distinction should be made between rotational components of seismic field and the rotational effects of earthquakes; some of the latter may be attributed to the interplay between straight (not rotational) elastic waves and the medium inhomogeneity or anisotropy. In our department we deal with the rotational components and their generation in a seismic source. Pure rotation and twist may be drawn out from the seismic field generated by the source. These motions/deformations are treated as components of deviatoric shear and, at the same time, as components of the seismic waves.

In order to measure rotational components of the seismic field, special rotational seismometers were manufactured in our Institute. The microarray comprises two such rotational seismometers. Each of them is constructed from a pair of two short-period SM-3 seismometers; which are antiparallel-oriented and mounted in common chassis in the position appropriate for detection of the horizontal motions.

One such microarray operates in the Książ observatory, the other in Ojców. The first is most suitable for analysis of the seismic mining events in the Legnica-Głogów Copper Mining District, the second—for research on Upper Silesian mining events.

Measurements with these seismometers were conducted also in Greece and central Italy (in cooperation with Istituto Nazionale di Geofisica e Vulcanologia in Rome and its field branch—the Seismological Observatory in l'Aquila). The obtained series of data enabled finding certain group-specific features of small earthquakes in three areas around l'Aquila (see Teisseyre 2007). Preliminary

results show that rotational components are present also in the mechanical waves generated by seismic events in glaciers (see Górski and Teisseyre 2006).

The Institute of Geophysics PAS cooperates with the Military University of Technology in Warszawa. There, the team of Leszek Jaroszewicz devised optical, inertia-free gyroscope AFORS, one of very few such instruments designed for work as a seismometer. It is based on the Sagnac interferometer principle. AFORS is already used at Książ observatory; it records rotations coming with seismic waves generated by mining events in the Legnica-Głogów Copper Mining District.

13 Some Other Projects

Out of other investigations done in our department, which cannot be easily classified to the afore-presented sections, we will emphasize the following two topics: the seismo-glaciological studies and research into the future of the Earth.

Seismic measurements on a glacier were first performed in 1962 in Spitsbergen. Measurements were done on the Hans Glacier by R. Teisseyre with help of Stanisław Siedlecki, the leader of a small expedition. Next seismic measurements on Spitsbergen glaciers started in 1970 and were directed by Marek Górski.

Seismic investigations on the Hans Glacier in 1980 (Cichowicz 1983) were the first attempt to determine physical parameters of icequakes. The presence of open cracks in glaciers was discussed and theory of glacier extensional cracking is referred to opening of dislocation cracks.

Moreover, in the years 2000–2006, short expeditions went to Pasterze Glacier in the Alps (photo in Fig. 8), where the glacier seismicity was investigated, including recording of tilt, related to the rotations and probably caused by them, but obtained from an array of vertical seismometers (see Górski and Teisseyre 2006). Because of creeping/tilting of the ice surface, the recording had to be limited to vertical motions.

The recent publications of Górski show his main results of the glacier seismicity research (see Górski 2014). The detection of a second type of seismic event occurring in the glacier is one of them. The first type is an icequake, the second type being icevibration—a long-duration tremor, from few to tens of seconds, bearing lower frequency waves (of predominant frequencies at 2–3 Hz). These events are related to glaciodynamical processes occurring in the main stream of the glacier, especially to episodes of relatively quick crawling of the glacier. Of importance are also resonant vibrations of large elements in the glacier.

Quite different problems were dealt with by Rafał Rybicki; in addition to his study of crack and fault dynamics, he was deeply engaged in research into the evolution of the Earth. He proposed a vision on the fate of the Solar System and especially that of our planet in next few milliard (10^6) years (Rybicki and Denis 2001), studied the effects of the Earth's evolution on the length of the day, and some aspects of the evolution of the Earth's core (Denis et al. 2011). His last results, of purely astrophysical nature (Rybicki 2006), show quantitatively how the



Fig. 8 Marek Górski at the Pasterze Glacier, Austria, 2006. Installation of micro-array of seismographs for tilt oscillation measurement. *Photo by K. P. Teisseyre*

XUV energy fluxes vary during star evolution, and how such fluxes emitted by the evolving Sun affect the Earth and other planets. These results were highly recognized by broad scientific audience, being quoted in the columns of *Nature* and other highest-rank science promoting journals, including *Sky and Telescope*; they were also reported in the *New York Times* (Rowiński 2008).

Acknowledgments We express our sincere thanks to all the colleagues who helped in preparation of this chapter, especially to Zbigniew Czechowski.

References

- Białycki M (2005) Integrable KP and KdV cellular automata out of a hyperelliptic curve. *Glasgow Math J* 47a: 33–44
- Białycki M, Czechowski Z (2013) On one-to-one dependence of rebound parameters on statistics of clusters: exponential and inverse-power distributions out of random domino automaton. *J Phys Soc Jpn* 82:014003. doi:[10.7566/JPSJ.82.014003](https://doi.org/10.7566/JPSJ.82.014003)
- Białycki M, Doliwa A (2005) Algebro-geometric solution of the discrete KP equation over a finite field out of a hyperelliptic curve. *Comm Math Phys* 253:157–170
- Bielski WR (2005) Nonstationary flows of viscous fluids through porous elastic media. Homogenization method. *Publ Inst Geophys Pol Acad Sci A-29(388)*:1–147
- Bielski WR, Matysiak SJ (1992) Surface waves in a periodic two-layered elastic half-space. *Acta Mech* 91(1–2):47–55
- Bielski WR, Telega JJ (2001) Modelling contact problems with friction in fault mechanics. *J Theor Appl Mech* 39(3):475–505

- Cichowicz A (1983) Icequakes and glacier motion: the Hans Glacier, Spitsbergen. *Pure Appl Geophys* 121:27–36
- Czechowski Z (1993) A kinetic model of nucleation, propagation and fusion of cracks. *J Phys Earth* 41:127–137
- Czechowski Z (2001) Transformation of random distributions into power-like distributions due to non-linearities: application to geophysical phenomena. *Geophys J Int* 144:197–205
- Czechowski Z (2005) The importance of the privilege in resource redistribution models for appearance of inverse-power solutions. *J Phys A: Math Stat Mech Appl* 345:92–106
- Czechowski Z, Białecki M (2012) Three-level description of the domino cellular automaton. *J Phys A: Math Theor* 45:155101. doi:[10.1088/1751-8113/45/15/155101](https://doi.org/10.1088/1751-8113/45/15/155101)
- Czechowski Z, Telesca L (2013) Construction of a Langevin model from time series with a periodical correlation function: application to wind speed data. *Phys A: Stat Mech Appl* 392:5592–5603
- Denis C, Rybicki KR, Schreider AA, Tomecka-Suchoń S, Varga P (2011) Length of the day and evolution of the Earth's core in the geological past. *Astronom Nachr* 332(1):24–35
- Dębski W (2004) Application of Monte Carlo techniques for solving selected seismological inverse problems. *Publs Inst Geophys Pol Acad Sci B-34*(367):1–207
- Dębski W (2008) Estimating the earthquake source time function by Markov Chain Monte Carlo sampling. *Pure Appl Geophys* 165:1263–1287
- Dębski W et al (2014) Selected theoretical methods in solid Earth physics—contribution from the Institute of Geophysics PAS this issue
- Dmowska R, Bielski W, Teisseyre R (1986) Electromechanical and magnetochemical coupling. In: Teisseyre R (ed) *Continuum theories in solid earth physics* Political Science Publications PWN–Elsevier, pp 399–475
- Dmowska R, Rybicki K, Teisseyre R (1972) Focal mechanism in connection with energy storage before crack formation. *Tectonophys* 14(3–4):309–318
- Doliwa A, Białecki M, Klimczewski P (2003) The Hirota equation over finite-fields: algebro-geometric approach and-multisoliton solutions. *J Phys A: Math Theor* 36:4827–4839
- Domański B, Gibowicz SJ, Wiejacz P (2002) Source time function of seismic events at Rudna copper mine, Poland. *Pure Appl Geophys* 159(1–3):131–144
- Droste Z (1991) Energy release in the earthquake rebound modeling. *Acta Geophys Pol* 39(2):159–178
- Droste Z, Hordejuk J (1964) Determination of frequency response for the seismographs of the Polish seismic network (in Polish). *Mater Pr Zakł Geof* (Publs. Inst. Geophys. Pol. Acad.) 2:175
- Droste Z, Teisseyre R (1959) The mechanism of earthquakes according to dislocation theory. *Rep Tohoku Univ Ser 5, Geophys* 11(1): 55–71
- Droste Z, Teisseyre R (1972) Shock classification according to P-wave signs for a system of seismographs in the region of Miechowice mine. *Acta Mont* 22:7–27
- Droste Z, Teisseyre R (1976) Rotational and displacemental components of ground motion as deduced from data of the azimuth system of seismographs (in Polish). *Publ Inst Geophys Pol Acad Sci M-1*(97):157–167
- Droste Z, Teisseyre R (1988) Earthquake rebound theory: properties of earthquake sequences. *Acta Geophys Pol* 36(4):293–299
- Gadomska B, Korhonen H (1989) Isoseismal distribution and focal mechanisms in the Balkan Region. *Acta Geophys Pol* 37(2):133–145
- Gadomska B, Teisseyre R (1984) Density anomalies, geoid shape and stresses. *Acta Geophys Pol* 32(1):1–24
- Gadomska B, Maj S, Teisseyre R (1995) Variation of seismic source parameters and earthquake entropy with depth. *Acta Geophys Pol* 43(4):285–302
- Gałka A, Telega JJ, Bielski WR (1994) Contribution to dual variational principles for nonlinear elastic beams. *Control Cybern* 23(4):641–670
- Gibowicz SJ (1962) The magnitude, energy and frequency of subterranean shocks in Upper Silesia. *Bull Acad Pol Sci Sér Géol Géogr* 10(2):113–119

- Gibowicz SJ (1975) Variation of source properties: the Inangahua, New Zealand, aftershocks of 1968. *Bull Seismol Soc Am* 65(1):261–276
- Gibowicz SJ (2009) Seismicity induced by mining: recent research. *Adv Geophys* 51:1–53
- Gibowicz SJ, Kijko A (1994) An introduction to mining seismology. Academic Press, San Diego, p 399
- Gibowicz SJ, Niewiadomski J, Wiejacz P, Domański B (1989) Source study of the Lubin, Poland, mine tremor of 20 June 1987. *Acta Geophys Pol* 27(2):111–132
- Główacka E, Stankiewicz T, Holub K (1990) Seismic hazard estimate based on the extracted deposit volume and bimodal character of seismic activity. *Gerland's Beitr Geophys* 99(1):35–43
- Górski M (2014) Seismic events in glaciers, geoplanet: earth and planetary sciences. Springer, Berlin, p 99
- Górski M, Teisseyre KP (2006) Glacier motion: seismic events and rotation/tilt phenomena. In: Teisseyre R, Takeo M, Majewski E (eds) *Earthquake source asymmetry, structural media and rotation effects*. Springer, Heidelberg, pp 199–215
- Hanyga A (1974) Evolutionary condition in the theory of detonation and deflagration waves. *Bull Ac Polon Sci Sér Techn* 22:1–11
- Hanyga A (1975) Shear waves. *Publ Inst Geophys Pol Acad Sci* 87:3–61
- Hanyga A (1985) Mathematical theory of non-linear elasticity (1985). Ellis Horwood, New York, p 432
- Hordejuk J, Aleksandrowicz D, Droste Z (1984) Analogue determination of seismic source parameters and seismic wave dynamics. *Acta Geophys Pol* 32:239–251
- Hordejuk J, Gibowicz SJ, Bober A, Cichowicz A, Droste Z, Dychtowicz Z, Kazimierczyk M, Kijko A (1979) Source study of the Lubin, Poland, tremor of 24 March 1977. *Acta Geophys Pol* 27:3–38
- Jankowska W (1971) Próba określenia powtarzalności wstrząsów w rejonie kopalni Lubin (The recurrence of tremors in the Lubin mine). *Mater Pr Inst Geof* 47:179–183
- Kijko A, Dessokey MM, Główacka E, Kazimierczyk M (1982) Periodicity of strong mining tremors in the Lubin copper mine. *Acta Geophys Pol* 30(3):221–230
- Kijko A, Wcisło A (1980) An analysis of the optimum extension of the regional seismic network in Upper Silesia. *Publ Inst Geophys Pol Acad Sci M-3(134)*:21–28
- Kuklińska M (1996) Thermodynamics of line defects: construction of a dislocation superlattice. *Acta Geophys Pol* 44(3):237–249
- Kwiatek G (2003) A search for the slow initial phase generated by seismic events at a copper mine in Poland. *Acta Geophys Pol* 51(4):369–385
- Lasocki S (2014) Transformation to equivalent dimensions—a new methodology to study earthquake clustering. *J Int Geophys*. doi:[10.1093/gji/gju062](https://doi.org/10.1093/gji/gju062)
- Lasocki S, Urban P (2011) Bias, variance and computational properties of Kijko's estimators of the upper limit of magnitude distribution, M_{max} . *Acta Geophys* 59(4):659–673
- Lizurek G, Lasocki S (2012) Studies of induced seismic events clustering in equivalent dimension spaces in chosen Rudna Mine panels. *AGH J Min Geoeng* 36:203–216
- Maj S (1991) On the Energy Gap for Fe-Poor Oxide and Silicate Minerals. *Phys Chem Miner* 17:711–715
- Maj S (2005) Geothermal features of the Earth's lower mantle: phonon thermal conductivity. *Acta Geophys* 53(2):183–196
- Mendecki AJ, Niewiadomski J (1997) Spectral analysis and seismic source parameters. In: Mendecki AJ (ed) *Seismic monitoring in mines*. Chapman & Hall, London, pp 144–158
- Niewiadomski J (1989) Application of singular value decomposition method. *Pure Appl Geophys* 129(3–4):553–570
- Niewiadomski J (2004) Extraction of information from seismograms by neural networks. *Acta Geophys Pol* 52(4):143–153
- Niewiadomski J, Górska M, Kozák J (1980) Tensional crack development in physical models with inhomogeneities under load. *Studia Geoph et Geod* 4:373–381

- Niewiadomski J, Rybicki K (1984) The stress field induced by antiplane shear cracks—application to earthquake study. *Bull Seism Soc Am* 59:67–81
- Niewiadomski J, Senatorski P, Teisseyre R (1991) Rebound geometry of dislocation distribution in the parallel crack system. *Acta Geophys Pol* 39(4):349–359
- Nita B, Dobrzhinetskaya L, Maguire P, Perchuc E (2012) Age-differentiated subduction regime: an explanation of regional scale upper mantle differences beneath the Alps and the Variscides of Central Europe. *Phys Earth Planet Inter* 206–207:1–15
- Orlecka-Sikora B, Lasocki S, Lizurek G, Rudziński Ł (2012) Response of seismic activity in mines to the stress changes due to mining induced strong seismic events. *Intern J Rock Mech Min Sci* 53:151–158
- Perchuc E, Thybo H (1996) A new model of upper mantle P-wave velocity below the Baltic Shield: indication of partial melt in the 95–160 km depth range. *Tectonophysics* 253:227–245
- Rowiński PM (2008) Kacper Mieczysław Rafał Rybicki, a geophysicist, planetologist, seismophysicist—obituary. *Acta Geophys* 56(4):935–938
- Rudziński Ł, Dębski W (2013) Extending the double difference location technique—improving hypocenter depth determination. *J Seismol* 17:83–94
- Rusiniak L (2002) Spontaneous polarization of water in porous structure of a solid body. *Geophys J Int* 148(2):313–319
- Rusiniak L (2004) Electric properties of water. New experimental data in 5–13 MHz frequency range. *Acta Geophys Pol* 52(1):63–76
- Rybicki K (1992) Strike-slip faulting in the presence of a low rigidity inhomogeneities. *Bull Seism Soc Am* 82(5):2170–2190
- Rybicki KR (2006) On the energy flux reaching planets during the parent star's evolutionary track: the Earth-Sun system. *Publ Astron Soc Pacific* 118(846):1124–1135
- Rybicki KR, Denis C (2001) On the final destiny of the Earth and the solar system. *Icarus* 151(1):130–137
- Rybicki K, Kasahara K (1977) Strike-slip fault in a laterally inhomogenous medium. *Tectonophysics* 42(2–4):127–138
- Rybicki K, Kato T, Kasahara K (1985) Mechanical interaction between neighboring active faults—static and dynamic stress induced by faulting. *Bull Earth Res Inst* 60:1–21
- Senatorski P (1997) Interactive dynamics of faults. *Tectonophys* 277(1–3):199–207
- Senatorski P (2005) A macroscopic approach towards earthquake physics: the meaning of the apparent stress. *Phys A* 358:551–574
- Senatorski P (2012) Effect of seismic moment-area scaling on apparent stress–seismic moment relationship. *Phys Earth planet Int* 196–197:14–22
- Stopiński W (1985) Model dylatacyjno-progowy zmian oporności skał nienasyconych (Dilatational-threshold model of resistivity changes in partly saturated rocks) *Publ Inst Geophys Pol Acad Sci M-6*(176):199–232
- Stopiński W (2003) Bedrock monitoring by means of the electric resistivity method during the construction and operation of the Czorsztyn-Niedzica dam. *Acta Geophys Pol* 2:215–226
- Stopiński W, Ponomaryov AV, Los V (1991) Fast-changing processes in a medium subject to loading as detected by resistivity measurements. *Pure Appl Geophys* 136(1):49–58
- Stopiński W, Teisseyre R (1982) Precursory rock resistivity variations related to mining tremors. *Acta Geophys Pol* 30(4):293–320
- Suvorov VD, Melnik EA, Thybo H, Perchuc E, Parasotka BS (2006) Seismic velocity model of the crust and uppermost mantle around the Mirnyi kimberlite field in Siberia. *Tectonophysics* 420:49–73
- Teisseyre KP (2007) Analysis of a group of seismic events using rotational components. *Acta Geophys* 55(4):535–553
- Teisseyre KP (2008) Charged dislocations and various sources of electric field excitation. In: Teisseyre R, Nagahama H, Majewski E (eds) *Physics of asymmetric continuum:extreme and fracture processes*. Springer, Berlin, pp 137–161
- Teisseyre KP, Hadjicontis V, Mavromatou C (2001a) Anomalous piezoelectric effect: analysis of experimental data and numerical simulation. *Acta Geophys Pol* 49(4):449–462

- Teisseyre KP, Teisseyre R (1999) Numerical simulation of resistivity changes caused by water infiltration. *Acta Geophys Pol* 47(1):41–57
- Teisseyre R (1974) Symmetric micromorphic continuum: wave propagation, point source solutions and some applications to earthquake processes. In: P Thoft-Christensen (ed) Continuum mechanics aspects of geodynamics and rock fracture mechanics, pp 201–244
- Teisseyre R (1980) Earthquake premonitory sequence—dislocation processes and fracturing. *Boll Geofis Teor Appl* 22:245–254
- Teisseyre R (1985) Creep-flow and earthquake rebound: system of the internal stress evolution. *Acta Geophys Pol* 33(1):11–23
- Teisseyre R (1995) Electric field generation in earthquake premonitory process. In: Teisseyre R (ed) Theory of earthquake premonitory and fracture processes. Political Science Publications PWN, Warszawa, pp 282–303
- Teisseyre R (1996) Shear band thermodynamical earthquake model. *Acta Geophys Pol* 44(3):219–236
- Teisseyre R (2014) Asymmetric continuum theory: Fracture processes in seismology and extreme fluid dynamics, this issue
- Teisseyre R, Bielski W (1995) Micromorphic model of a seismic source zone. In: R Teisseyre (ed) Theory of earthquake premonitory and fracture processes. Political Science Publications PWN, pp 613–640
- Teisseyre R, Dresen L, Kozák JT, Waniek L (1985) Physical properties of micromorphic medium: theory and experiment. *Acta Geophys Pol* 33(4):341–356
- Teisseyre R, Majewski E (2002) Physics of earthquake. In: Lee WHK, Kanamori H, Jennings PC, Kisslinger C (eds) International handbook of earthquake and engineering seismology, part A, pp 229–235
- Teisseyre R, Nishimura Y (2001) Application of the fracture-band model to volcanic-quake series of 1977 at Usu, Hokkaido, Japan. *Acta Geophys Pol* 49:481–496
- Teisseyre R, Teisseyre KP, Górska M (2001b) Earthquake fracture-band theory. *Acta Geophys Pol* 49(4):463–479
- Teisseyre R, Wiejacz P (1993) Earthquake sequences: stress diagrams. *Acta Geophys Pol* 41:85–99
- Telega JJ, Bielski WR (2003) Flows in random porous media: effective models. *Comput Geotech* 30(4):271–288
- Telesca L, Czechowski Z (2012) Discriminating geoelectrical signals measured in seismic and aseismic areas by using Ito models. *Phys A: Stat Mech Appl* 391:809–818
- Thybo H, Nielsen L, Perchuc E (2003) Seismic scattering at the top of the mantle Transition zone. *Earth Planet Sci Lett* 216:259–269
- Thybo H, Perchuc E (1997) The seismic 8° discontinuity and partial melting in continental mantle. *Science* 275:1626–1629
- Thybo H, Perchuc E, Zhou S (2000) Intraplate earthquakes and a seismically defined lateral transition in the upper mantle. *Geophys Res Lett* 27(23):3953–3956
- Wojtczak-Gadomska B, Guterch A, Uchman J (1964) Preliminary results of deep seismic sounding in Poland. *Bull Acad Pol Sci Ser Geol et Geogr* 12(4):205–211

Sixty Years of Publishing with the Institute of Geophysics

Anna Dziembowska and Maria Wernik

Abstract The main publications written by people associated with the Institute of Geophysics PAS are outlined. Presently, the major titles are *Acta Geophysica* and the *GeoPlanet Book Series*. The journal *Acta Geophysica*, formerly *Acta Geophysica Polonica*, is of the same age as the Institute. The *GeoPlanet Book Series* evolved from Monographic Volumes of the *Publications of the Institute of Geophysics*. Also many significant, pioneering monographs are recalled, along with some remarks on the Institute's history.

Keywords *Acta Geophysica* · *Geoplanet Book Series*

1 Introduction

The 60-year editorial output of the Institute¹ of Geophysics, Polish Academy of Sciences, is very rich, both in terms of thematic variety and the number of publications. The topics varied over the years, but have always been related to geophysical problems dealt with by the Institute's staff.

The leading topics were: seismology and physics of the Earth's interior, study of deep structures of the Earth, magnetism and paleomagnetism, atmospheric optics, study of ozone and atmospheric electricity, physics and ionosphere structure, cosmic rays and planetary geodesy, polar research, oceanology and hydrology.

¹ Strictly speaking, until 1970 it was the Department of Geophysics (Zakład Geofizyki), but we will use the name Institute throughout the whole article.

A. Dziembowska (✉) · M. Wernik
Institute of Geophysics, Polish Academy of Sciences, Warsaw, Poland
e-mail: anna@igf.edu.pl

The history of publishing mirrors the 60-year history of the Institute. The Institute of Geophysics was founded as one of units of the Polish Academy of Sciences, established in 1952. The newly created Institute followed the long tradition of world-renown achievements of Polish geophysicists. The first Chair of Geophysics was established by **Prof. Maurycey P. Rudzki** at the Jagiellonian University in Cracow in 1895. The Teisseyre-Tornquist transcontinental tectonic zone, presently called the Trans-European Suture Zone, was recognized by Polish geologist **Prof. Wawrzyniec Teisseyre** in the late 1890s. More about the history of geophysics in Poland can be found, e.g., in: Ołpińska-Warzechowa (1995), Kowalczuk (2001) and Gadowska (2004).

The Institute incorporated geophysical observatories with long history, in particular those in Warsaw, Świdra, Racibórz, and Hel, and developed new ones, the main being the Central Geophysical Observatory at Belsk, and the Polish Polar Station Hornsund, Spitsbergen. Our publications document the vast amount of data collected. In some fields, the long series of best-quality observation results are unique in the world scale (e.g., ozone data) and provide excellent source for studying the long-term tendencies.

Great influence on the early period of Institute's activity was exerted by the International Geophysical Year 1957/1958, which brought about a lot of research results and publications. They included vast documentation of expeditions to the Arctic, where the Polish Polar Station was established, to the Antarctic region, and to North Vietnam, where permanent geophysical stations were organized and long-lasting cooperation was initiated. In the next years, the resulting documents were edited and published jointly with the Vietnamese Committee for International Cooperation.

2 Own Publications

The early publications were mainly concerned with experimental results from the observatories, and were issued as separate bulletins/yearbooks of a given observatory. Since 1964 they have been gradually incorporated into the newly created series *Materiały i Prace*.

2.1 Seismological Bulletins

Seismological bulletins issued as separate publications were the following: *Bulletyn Obserwatorium Sejsmologicznego w Warszawie* (*Bulletin of the Seismological Observatory in Warsaw*), *Bulletyn Śląskiej Stacji Geofizycznej w Raciborzu* (*Bulletin of the Silesian Geophysical Station in Racibórz*), and *Bulletyn Obserwatorium Sejsmologicznego w Krakowie* (*Bulletin of the Seismological Observatory in Cracow*).

The first two titles were previously issued by the State Geological Institute. The publication of all three titles was terminated on the data from the year 1958. Data since 1959 have been included to the series *Materiały i Prace* discussed later on. The editor was **Prof. Tadeusz Olczak**.

2.2 Prace Obserwatorium Geofizycznego im St. Kalinowskiego w Świdrze (1959–1976)

It contained the magnetic recording through the years 1953–1967 and atmospheric electricity recordings through the years 1957–1965, as well as related papers. A total of 21 magnetic yearbooks and 9 atmospheric electricity yearbooks, and a Yubilee Book to commemorate the 50-th anniversary of the Observatory (cover is reproduced in Sect. 4) were published. The editors were: **Prof. Tadeusz Olczak** and then **Dr. Zdzisław Małkowski**.

2.3 Materiały i Prace Zakładu Geofizyki PAN (1963–1976)

The separate titles enumerated above were included into the newly created broad series *Materiały i Prace Zakładu Geofizyki PAN*, covering, along with observatory results, also original scientific papers, selected habilitation treatises, selected doctoral theses, conference materials, and the like. The first issue was published in 1963.

2.4 Publications of the Institute of Geophysics, Polish Academy of Sciences (Until 2010 in Printed Form, Then, on a Smaller Scale, as an Internet Edition)

It was a continuation of *Materiały i Prace Zakładu Geofizyki PAN*, but under English-language title; the continuity of numbering was kept. The last printed issue, published in mid-2013, was bearing the number 415.

Publications of the Institute of Geophysics (abbreviated *Publs. Inst. Geophys. Pol. Acad. Sc.*) has become the basic editorial series, serving as a main platform for publishing the observatory results, conference proceedings, some doctoral theses and habilitation treatises. The proceedings were related to important international conferences, like General Assembly of the European Seismological Commission in 1976, Europrobe Symposium in 1991, IAGA Workshop in 2006, consecutive Polish-Czech-Slovakian Mining Geophysics Conferences, some meetings of the International School of Hydraulics, and many other.

Upon acquiring the English-language title, the publication was divided into thematic series as follows:

- A Physics of the Earth's Interior
- B Seismology
- C Geomagnetism
- D Physics of the Atmosphere
- E Ionosphere (1976–1980); Hydrology (since 1997)
- F Planetary Geodesy (1976–2008)

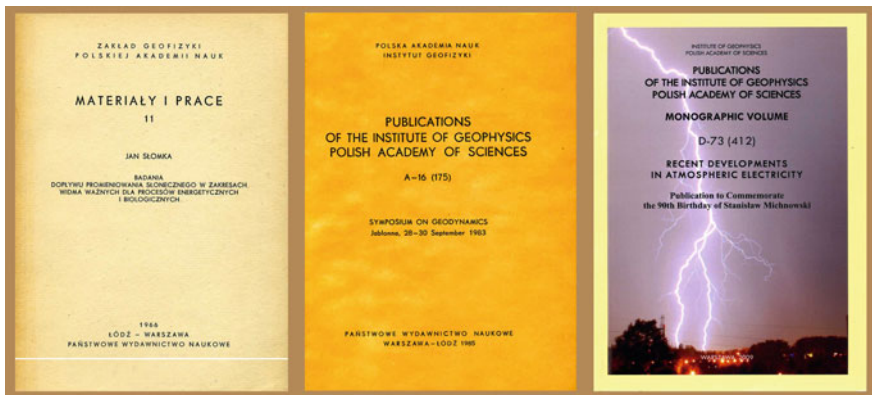


Fig. 1 Three covers of illustrating the evolution of the series *Publications of the Institute of Geophysics*

G Numerical Methods in Geophysics

M Miscellanea.

The full texts of some issues are available through Publication's Website. **Professor Roman Teisseyre** has been the Editor-in-Chief since the very beginning up to now.

Since 2001 the most important issues were labeled with a subtitle Monographic Volume, and were in fact monographs. Some covers to illustrate the evolution of the journal are shown in Fig. 1. In 2010, the Institute of Geophysics signed an agreement with Springer-Verlag to transform them into a new editorial series named *GeoPlanet*, which will be discussed in Sect. 5. *Publications of the Institute of Geophysics* is now issued in much reduced form in the internet.

3 Acta Geophysica Polonica/Acta Geophysica

3.1 History

The first issue of *Acta Geophysica Polonica* (*AGP*) bears the date of March 25, 1953. The Editorial included the following declaration: "... we expect Polish geophysicists to acknowledge with pleasure the appearance of *Acta Geophysica Polonica*—a forum for presenting the results of their research. We hope, it will contribute to the development of geophysics in Poland and promote the exchange of achievements of our scientists with those in other countries." And this line has been kept until the present times. Under a slightly modified title of *Acta Geophysica* (*AG*), it is the leading geophysical journal in Poland and highly recognized abroad (some covers are reproduced in Fig. 2). For early scientometric evaluations - see Maj (1966) and Racki (2004).

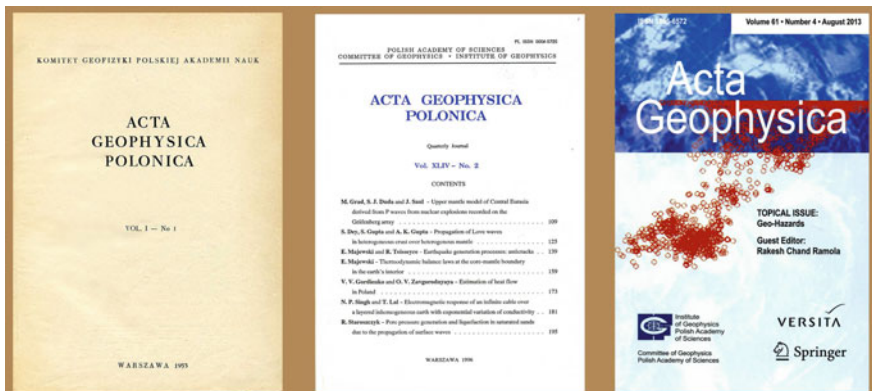


Fig. 2 Three covers illustrating the evolution of *Acta Geophysica Polonica/Acta Geophysica*

Looking over the back issues we may observe some impact of politics. The most vivid example is already in the first issue, whose publication coincided with the death of Joseph Stalin, hence it began with his photo and a servile note, as in most Polish journals. The evolution of language of articles is another example. The Russian-language abstracts were gradually disappearing, while English was becoming dominant, and since 1982 the only language for publication. Polish abstracts to English-language papers were kept until 1991. The number of authors from abroad has been growing.

These changes were in line with political transformations in our country and elsewhere. The international recognition of scientific publications was becoming more and more important. Since 2007 *Acta Geophysica* has been covered by the Science Citation Index Expanded (Thomson Scientific, Philadelphia) and Current Contents/Physical, Chemical and Earth Sciences. The most popular measure of journal's ranking, the Impact Factor trend, is demonstrated in Fig. 3.

Acta Geophysica is mainly focused on original scientific contributions. Alongside, there have also been many articles commemorating the achievements of Polish scientists associated with the journal or other prominent geophysicists (often as a post-mortem tribute). Already in vol. 2 there is an article devoted to 50-year anniversary of scientific work of **A.B. Dobrowolski**, world-famous Antarctic explorer. In the next volume there is an obituary of **Prof. Tadeusz Banachiewicz**—famous mathematician, emphasizing his contribution to astronomy, geodesy and geophysics. Of course, the death (in 1954) of **Prof. Edward Stenz**, the Editor-in-Chief, was followed by an article devoted to his life and scientific output, including a broad bibliography. Also the 100-th anniversary of his birth has been commemorated (Maj 1997). The tribute was also paid to **Prof. M. P. Rudzki** on the occasion of the 100-th anniversary of his birth.

Other prominent persons associated with the journal included two physicists, Professors **Stefan Pieńkowski** and **Czesław Białobrzeski**, Professors **Edward W. Janczewski** from the Academy of Mines in Cracow, **Teodor Kopcewicz** from the

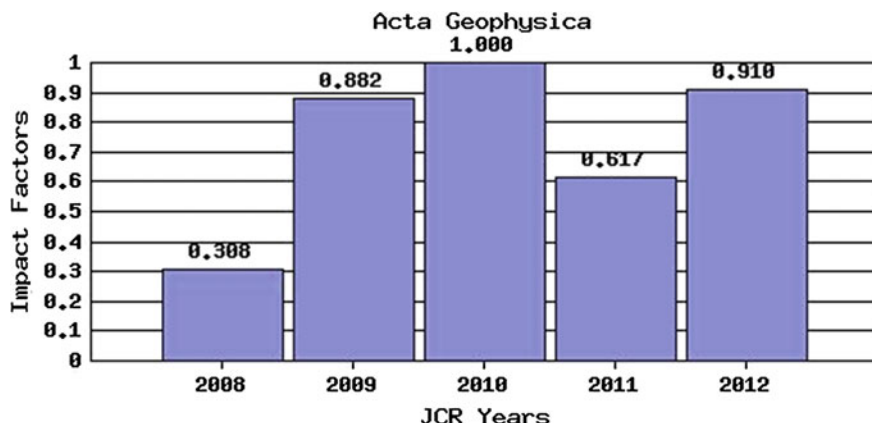


Fig. 3 Impact Factor trend of *Acta Geophysica* (Web of Knowledge). Impact Factor for 2013 is estimated to be above 1.2

University of Warsaw, **Stefan Manczarski**, former Director of our Institute, and **Stanisław Małoszewski**. After the death of **Prof. Henryk B. Arctowski**, the most eminent Polish explorer of Polar regions and well-known meteorologist and climatologist, a special issue to honor him was published.

In more recent times, the journal lost two persons of great merits: the former Editor-in-Chief **Sławomir Jerzy Gibowicz** (1933–2011), well-known seismologist, who established fundamentals of mining geophysics, and **Prof. Kacper Mieczysław Rafał Rybicki** (1940–2008), Director of the Institute of Geophysics PAS, highly esteemed geophysicist, planetologist, astrophysicist.

Last but not least, it is to be emphasized with satisfaction that **Adam M. Dziewnowski**, the 1998 Crafoord Prize winner, Professor of Harvard University, Cambridge, MA, USA, began his scientific career in Poland, publishing his first three papers in *Acta Geophysica Polonica*. He is now member of the AG Advisory Board. The Crafoord Prize winners are treated as Noblists.

3.2 Publishers and Editors

Since the very beginning, *AGP* was co-published by the Institute of Geophysics PAS and the Committee of Geophysics PAS. Until 1991, the editing and printing was carried out by the Polish Scientific Publishers PWN. Afterwards, in relation to the change in financing conditions, the camera-ready copies were prepared at the Editorial Office of the Institute of Geophysics and printed by the Editorial Team of the Space Research Center, and then the private enterprise Remigraf.

In 2005 the journal acquired a new co-publisher, Central European Science Journals (presently Versita), and since 2006 it has become one of Springer-Verlag journals accessible through Springerlink at <http://www.springer.com/journal/11600>.

The Institute of Geophysics is the owner of the journal, responsible for all editorial work. These changes strongly enhanced the availability of *AG* around the world.

Also the editorial and scientific standard of publications has been growing. The review, performed by at least two referees, is now quite rigorous and many papers are rejected.

The first Editor-in-Chief of *AGP*, as we already mentioned, was **Prof. Edward Stenz**, holding this position from 1953 to his death in 1956. He was superseded by **Prof. Tadeusz Olczak** (1956–1982) and then **Prof. Stanisław J. Gibowicz** (1982–1994). The next Editor-in-Chief was **Prof. Roman Teisseyre** (1995–2005), strongly associated with the journal from the very beginning, probably the most frequent author up to the present. He was followed by **Prof. Stanisław Lasocki** (2006–2010), who expanded the Editorial and Advisory Board, incorporated Associate Editors responsible for papers in particular areas of geophysics, and included a Special Section on Triggered and Induced Seismicity. Since 2010 up to now, the Editor-in-Chief has been **Prof. Jarosław Napiórkowski**. Under his guidance, the hitherto quarterly journal has expanded into a bi-monthly one.

The Advisory Board includes prominent scientists from the leading universities, mostly in the United States and Europe. The current list of Advisory Board members and Associate Editors is available at <http://agp.igf.edu.pl/>.

Over the years, eight persons performed the duty of Managing Editor, including **Maria Wernik** (co-author of this paper) in the years 1976–2009, **Iwona Escreat (née Brzuska)** in 2010–2012, and **Dr. Zbigniew Wiśniewski** since then. A photo of the *Acta Geophysica* team in 2007 is in Fig. 4.

3.3 Special/Topical Issues

Special or Topical Issues have been published throughout the whole 60-year history of the journal, starting with the issue devoted to the International Geophysical Year 1957/58. The present policy is to increase the number of issues to be focused on specific, hot topics of utmost interest. The Special/Topical Issues published since 2006 are listed below.

Vol. 55 (1): Environmental Hydraulics. Editor: Paweł M. Rowiński Vol. 56 (1): Recent Topics in Boundary-Layer Meteorology. Editor: Zbigniew W. Sorbjan
Vol. 56 (1): Recent Topics in Boundary-Layer Meteorology. Editor: Zbigniew W. Sorbjan

Vol. 56 (3): Rough-bed Flows in Geophysical, Environmental, and Engineering Systems: Double Averaging Approach and its Applications. Editors: Vladimir I. Nikora and Paweł M. Rowiński

Vol. 57 (1): Developing the Scientific Basis for Monitoring, Modelling and Predicting Space Weather. Editors: Jean Liliensten, Mauro Messerotti, Rami Vainio, and Jurgen Watermann

Vol. 57 (4): Boundary Layer Flows Along Sloping Surfaces. Editors: Alan Shapiro and Evgeni Fedorovich



Fig. 4 *Acta Geophysica Editorial Team on 23 January 2007. Standing (from the left): Roman Teisseyre, Sławomir Gibowicz, Kacper Rybicki, Zbigniew Sorbjan, Stanisław Lasocki, Szymon Malinowski, Zbigniew Czechowski, Janusz Borkowski, Andrzej Wernik, Andrzej Leśniak, Jarosław Napiórkowski, Wojciech Dębski, Marek Grad, Paweł Rowiński. Sitting (from the left): Iwona Brzuska, Małgorzata Czarnecka, Jadwiga Jarzyna, Anna Dziembowska, Maria Wernik, Iwona Stanisławska (Photo by Marek Górska)*

- Vol. 58 (1): Geophysics in Near Surface Investigations. Editor: Jadwiga Jarzyna
- Vol. 58 (3): EURIPOS: Observing and Modeling the Earth's Ionosphere and Plasmasphere. Editors: Anna Belehaki, Lili R. Cander, and Bruno Zolesi
- Vol. 58 (5): Multi-Disciplinary Research on Geo- and Man-Made Hazards. Editors: Eleftheria E. Papadimitriou and Sedat Inan
- Vol. 59 (4): Statistical Tools for Earthquake and Mining Seismology. Editors: George M. Tsaklidis, Eleftheria E. Papadimitriou, and Nikolaos Limnios
- Vol. 59 (6): Modeling Atmospheric Circulations with Sound-Proof Equations. Editors: Szymon P. Malinowski, Andrzej A. Wyszogrodzki, and Michał Z. Ziemiński
- Vol. 60 (3): Statistical Mechanics in Earth Physics and Natural Hazards. Editors: Filippou Vallianatos and Luciano Telesca
- Vol. 60 (5): Remote Sensing and Sounding of the Atmospheric Boundary Layer. Editors: Zbigniew Sorbjan and Tadeusz Stacewicz
- Vol. 60 (6): Sediment Transport Mechanics. Editors: Francesco Ballio and Simon Tait
- Vol. 61 (4): Geo-Hazards. Editor: Rakesh Chand Ramola
- Vol. 61 (6): Advances in Geophysical Processes—Models and Methods. Editors: Zbigniew Czechowski and Mariusz Bialecki.

4 Books by External Publishers

Members of the Institute's staff have produced numerous valuable, often pioneering monographs in various branches of geophysics, as well as academic handbooks and popular science books, which were published by renowned publishers



Fig. 5 Six volumes of the monograph *Physics and Evolution of the Earth's Interior* edited by R. Teisseyre

in Poland and elsewhere. Initially, it was predominantly the major publishing house in our country, the Polish Scientific Publishers PWN, then Elsevier, Springer and other. The books published in the framework of *Publications of the Institute of Geophysics* and *GeoPlanet Series* are discussed separately in Sects. 2 and 5.

Looking over the Institute's output in terms of monographs, the role of **Prof. Roman Teisseyre** is crucial. It was due to his initiative, patience and diligence that the widely recognized 6-volume series under the common title *Physics and Evolution of the Earth's Interior* was completed (Fig. 5). It was preceded by a two-volume monograph in Polish, and followed by next monographs, including two newest ones in the *GeoPlanet Series* discussed separately. At the wide theoretical and experimental background, the books present various stages of developments in earthquake physics.

We are listing here, in roughly chronological order, the titles of books, including some special issues of journals, that are, in our opinion, most important and representative for the Institute's 60 years. The books were initially mostly written for Polish readers, being gradually addressed to international audience, so the English language began to prevail. Some covers are reproduced in Figs. 6, 7 and 8.

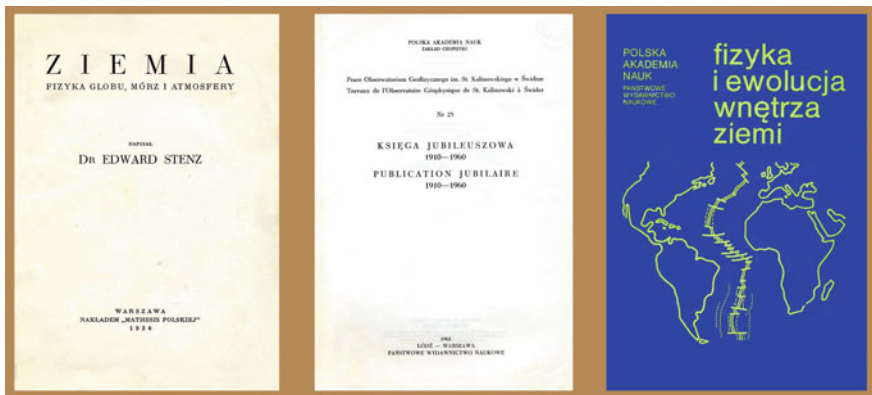


Fig. 6 Three covers of early books listed in this review. Included is also a cover of Jubilee Book commemorating the 50-th anniversary of the Świdra Observatory established in 1920 (as discussed in Sect. 2.2)

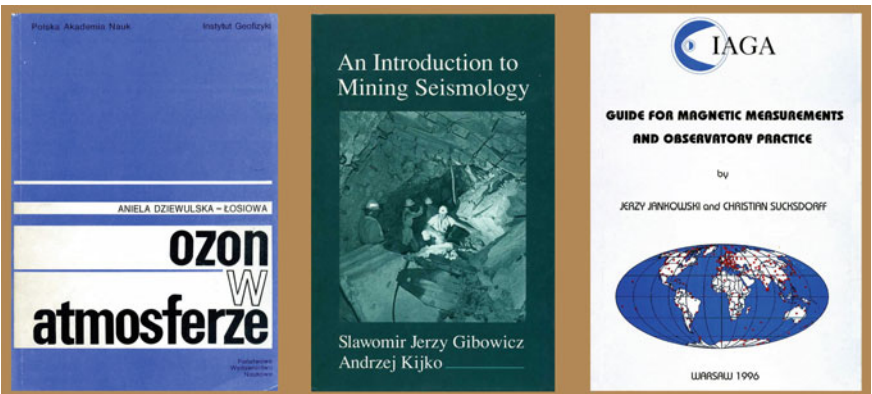


Fig. 7 More covers of books listed here, including the widely recognized, pioneering textbook on mining seismology and a basic comprehensive guide for geomagnetic observatories

1954 *Wstęp do geofizyki* (*Introduction to Geophysics*), E. Stenz, PWN, Warszawa, 179 pp.

1956 *Ziemia, fizyka wnętrza Ziemi, mórz i atmosfery* (*Earth, Physics of the Earth's Interior, Seas and Atmosphere*), E. Stenz, PWN, Warszawa, 389 pp. II edition (updated version of two former editions, in 1936 and 1953; see Fig. 6).

1960 *Introduction into Problems of Atmospheric Electricity*, S. Michnowski, Hanoi, Vietnam, 135 pp (in Vietnamese).

1964 *Geofizyka ogólna* (*General Geophysics*), E. Stenz and M. Mackiewicz, PWN, Warszawa, 647 pp.

1965 *Astronomia sferyczna* (*Spherical Astronomy*), L. Cichowicz, Wyd. Politechniki Warszawskiej, Warszawa, 179 pp.

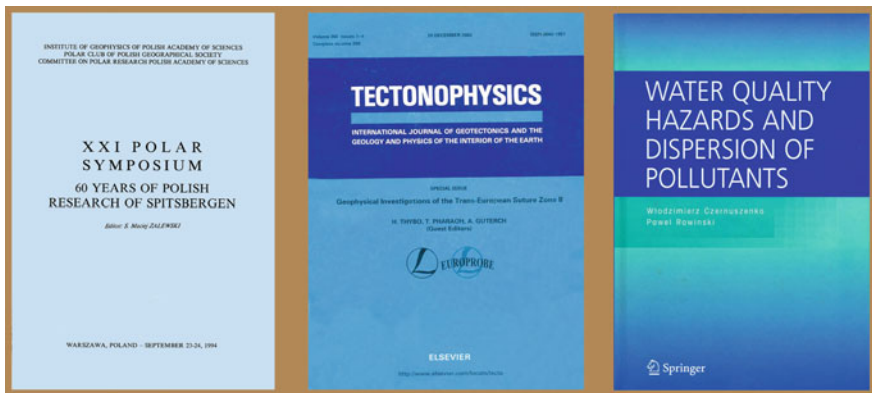


Fig. 8 More covers: one of the Polish Polar Studies issues, one of several Special Issues of Tectonophysics devoted to deep seismic sounding projects, and the first of hydrological monographs published with Springer (next ones are in the GeoPlanet Series)

- 1970** *Dynamika morza (Dynamics of the Sea)*, Z. Kowalik and C. Druet, Wyd. Morskie, Gdańsk, 428 pp.
- 1983** *Geomagnetism of Baked Clays and Recent Sediments*, K.M. Creer, P. Tuchołka, and C.E. Barton (eds.), Elsevier, Amsterdam, 324 pp.
- 1983 *Fizyka i ewolucja wnętrza Ziemi (Physics and Evolution of the Earth's Interior)*, two volumes, R. Teisseyre (ed.), PWN, Warszawa, vol. 1: 584 pp, vol. 2: 679 pp (see Fig. 6)
- 1984–1993** *Physics and Evolution of the Earth's Interior* (6 volumes), PWN, Warszawa—Elsevier, Amsterdam (see Fig. 5)
- 1985** *Mathematical Theory of non-Linear Elasticity*, A. Hanyga, PWN, Warszawa—Ellis Horwood Ltd, Chichester, 432 pp.
- 1989** *Seismicity in Mines*, S.J. Gibowicz (ed.), Pure Appl. Geophys. Special Issue. V.129, No. 3–4, 283–680.
- 1991** *Ozon w atmosferze (Ozone in the Atmosphere)* A. Dziewulska-Łosiowa, PWN, Warszawa, 395 pp (see Fig. 7).
- 1991** *Współczesna termodynamika ośrodków ciągłych (Contemporary Thermodynamics of Continuous Media)*, A. Hanyga, PWN, Warszawa, 316 pp.
- 1994** *Współczesne modele matematyczne procesów transportu i mieszania zanieczyszczeń w rzekach (Contemporary Mathematical Models of Contaminant Transport and Mixing in Rivers)*, W. Czernuszenko and P. Rowiński, Monogr. Kom. Gosp. Wodnej PAN, No. 6, Oficyna Wyd. Politechniki Warszawskiej, Warszawa, 61 pp.
- 1994** *An Introduction to Mining Seismology*, S.J. Gibowicz and A. Kijko, Academic Press, San Diego, 399 pp (see Fig. 7).
- 1994** *60 Years of Polish Research of Spitsbergen, XXI Polar Symposium. Polish Polar Studies*, M.S. Zalewski (ed.), IGF PAN, Warszawa, 371 pp (see Fig. 8).
- 1995** *Guide for Magnetic Measurements and Observatory Practice*, J. Jankowski and Ch. Sucksdorff, IAGA, Boulder-Warszawa, 236 pp.

- 1995** *Theory of Earthquake Premonitory and Fracture Processes*, R. Teisseyre (ed.), PWN, Warszawa, 648 pp.
- 1996** *Water Resources Management in the Face of Climatic/Hydrologic Uncertainties*, Z. Kaczmarek et al. (eds.), Kluwer Academic Publishers, Dordrecht, 395 pp.
- 1996** *Wpływ niestacjonarności globalnych procesów geofizycznych na zasoby wodne Polski (Effect of Nonstationarity of Global Geophysical Processes on Water Resources in Poland)*, Z. Kaczmarek (ed.), Monogr. Kom. Gosp. Wodnej PAN, No.12, Oficyna Wyd. Politechniki Warszawskiej, Warszawa, 96 pp.
- 1997** *Rockbursts and Seismicity in Mines*. S.J. Gibowicz and S. Lasocki (eds.), Kraków, Poland, A.A. Balkema, Rotterdam, 437 pp.
- 1997** *40th Anniversary of the Polish Polar Station Hornsund—Spitsbergen, 24th Polar Symposium, Polish Polar Studies*, P. Głowiak (ed.), IGF PAN, Warszawa, 388 pp.
- 1999** *Geophysical Investigations of the Trans-European Suture Zone*, H. Thybo, T. Pharaoh, and A. Guterch (eds.), Tectonophysics, Special Issue, vol. 314, nos.1–3, 352 pp.
- 2001** *Earthquake Thermodynamics and Phase Transformations in the Earth's Interior*, R. Teisseyre and E. Majewski (eds.), Academic Press, San Diego, 674 pp.
- 2001** *EUROBRIDGE: Palaeoproterozoic Accretion of Fennoscandia and Sarmatia*, S.V. Bogdanova, R. Gorbatschev, R.A. Stephenson, and A. Guterch (eds.), Tectonophysics, Special Issue, vol.339, nos. 1–2, 238 pp.
- 2002** *Geophysical Investigations of the Trans-European Suture Zone*, H. Thybo, T. Pharaoh, and A. Guterch (eds.), Tectonophysics, Special Issue, vol.360, nos. 1–4, 314 pp.
- 2005** *Water Quality Hazards and Dispersion of Pollutants*, W. Czernuszenko and P. Rowiński (eds.), Springer, New York, 250 pp (see Fig. 8).
- 2006** *Earthquake Source Asymmetry, Structural Media and Rotation Effects*, R. Teisseyre, M. Takeo, and E. Majewski (eds.), Springer, Berlin, 582 pp.
- 2008**. *Physics of Asymmetric Continuum: Extreme and Fracture Processes—Earthquake Rotation and Soliton Waves*, R. Teisseyre, H. Nagahama, and E. Majewski (eds.), Springer, Berlin, 293 pp.
- 2008** *Models and Methods of Magnetotellurics*, M. N. Berdichevsky and V. I. Dmitriev, Springer, 564 pp.

5 GeoPlanet: Earth and Planetary Sciences Series

The idea to create a new editorial series was born once a new interdisciplinary center, gathering four institutes of the Polish Academy of Sciences, came into being. The GeoPlanet Center was established in March 2009. At present, it is composed of the following five institutes affiliated with the Polish Academy of Sciences: Institute of Geophysics, Space Research Centre, Institute of Oceanology, Institute of Geological Sciences, and Nicolaus Copernicus Astronomical Center (Fig. 9).

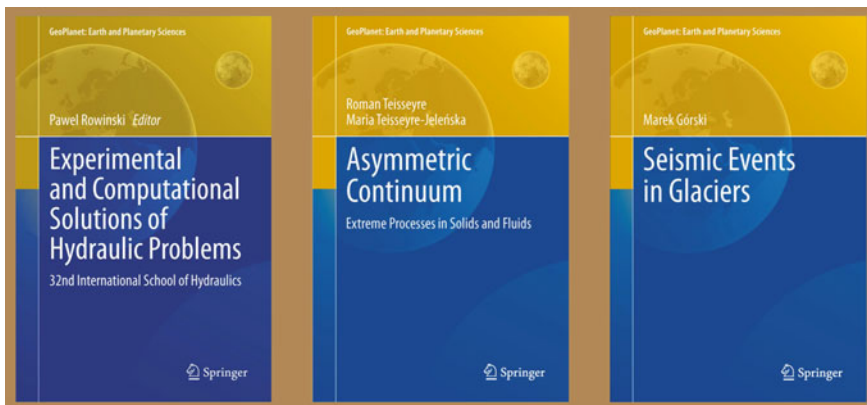


Fig. 9 Covers of three recent issues of *GeoPlanet Series* books

The publications encompass topical monographs and selected conference proceedings, authored or edited by leading experts of international repute as well as by promising young scientists.

The Editor-in-Chief is **Prof. Paweł Rowiński**. Associate Editors: Profs. **Marek Banaszkiewicz** (Space Sciences), **Janusz Pempkowiak** (Oceanology), **Marek Lewandowski** (Geology), and **Marek Sarna** (Astronomy). The Advisory Board is composed of renown scientists from many countries. Managing Editor is **Anna Dziembowska**, co-author of the present article.

The publications are produced in close cooperation between the GeoPlanet Series Editors and Springer-Verlag. The issues are available through the Springerlink and distributed by Springer-Verlag. From the Springer's side, the publication is managed by Agata Oelschlaeger. More information is available at the addresses: http://www.igf.edu.pl/pl/publikacje/geoplanet_series and <http://www.springer.com/series/8821>.

The interest in publishing books within the *GeoPlanet Series* is large. The editing of five new books is well advanced. The already published titles are listed below. Covers of three recent issues are reproduced in Fig. 6.

- 2010** *Synchronization and Triggering: from Fracture to Earthquake Processes*, V. de Rubeis, Z. Czechowski, and R. Teisseyre (eds.)
- 2011** *Experimental Methods in Hydraulic Research*, P. Rowiński (ed.)
- 2011** *Modelling of Hydrological Processes in the Narew Catchment*, D. Świątek and T. Okruszko (eds.)
- 2011** *Geophysics in Mining and Environmental Protection*, A. F. Idziak and R. Dubiel (eds.)
- 2012** *Carbon Cycling in the Baltic Sea*, K. Kuliński and J. Pempkowiak
- 2013** *Modelling Water Flow in Unsaturated Porous Media*, A. Szymkiewicz
- 2013** *Experimental and Computational Solutions of Hydraulic Problems*, P. Rowiński (ed.)

- 2013** *Aerospace Robotics*, J. Sąsiadek (ed.)
- 2013** *Seismic Events in Glaciers*, M. Górska
- 2013** *Asymmetric Continuum: Extreme Processes in Solids and Fluids*, R. Teisseyre and M. Teisseyre-Jeleńska
- 2014** *Atlantic Water in the Nordic Seas*, W. Walczowski (ed.)
- 2014** *Determination of Atmospheric Parameters of B, A, F and G Type Stars* E. Niemczura, B. Smalley, and W. Pych (eds.)
- 2014** *Insights on Environmental Changes: Where the World is Heading* T. Zielinski, K. Pazdro, A. Dragan-Górska, and A. Weydmann (eds.)

6 Bibliographic Databases

Bibliographic databases relating to the Institute of Geophysics have been regularly published in printed form until 1993 in *Publications of the Institute of Geophysics* (Vols. 73, 138, 232, 266), and since 1994 to 2008 in the internet at http://www.igf.edu.pl/en/publikacje/bibliographical_database.

The professional bibliographies were prepared by the experienced documentalist Dr. **Kazimiera Warzechowa**, and then, after her death, by **Zofia Okrasinska**. Worth mentioning is also a two-volume of bibliography of Polish research in Spitsbergen (Zalewski 2000; Giżejewski 2010).

Acknowledgments We made use of historical articles and obituaries written by our late colleagues, Dr. Kazimiera Warzechowa and Dr. Bożenna Gadomska. We also acknowledge the great help from numerous articles relating to the history of the Institute of Geophysics, its publications and the people involved, written by Prof. Sławomir Maj. It is due to their work that many achievements and facts of importance are commemorated.

References

- Gadomska B (2004) Kronika Instytutu Geofizyki PAN, 1952–2002. Chronicle of the Institute of Geophysics PAS. Publs Inst Geophys Pol Acad Sci M-26(348):48–50
- Giżejewski J (ed) 2010 Bibliography of Polish Research in Spitsbergen Archipelago, Part II, 1997–2006. Publs Inst Geophys Pol Acad Sci M-31(407):149
- Kowalcuk J (2001) 100-lecie Geofizyki Polskiej 1895–1995, Kalendarium (100 years of Polish geophysics, 1895–1995, Calendarium), 2nd edn. ARBOR, Kraków, p 234
- Maj S (1996) Kwartalnik “Acta Geophysica Polonica” (Quarterly Journal “Acta Geophysica Polonica”) Prz. Geofiz 41(1–2):93–100
- Maj S (1997) Edward Stenz (1897–1956). First Editor of “Acta Geophysica Polonica”. Acta Geophys Pol 45(4): 411–413
- Ołpińska-Warzechowa K (1995) Geofizyka (Geophysics). In: Mikulski Z (ed) Historia Nauki Polskiej, wiek XX, Nauki o Ziemi. IHN PAN, Warszawa, pp 37–82
- Racki G (2004) Role of Acta Geophysica Polonica in International Scientific Communication 1996–2003. Publs Inst Geophys Pol Acad Sci M-26(348):72–92 (in Polish with English abstract)
- Zalewski SM (ed) (2000) Bibliography of Polish Research in Spitsbergen Archipelago, Part I, 1930–1996. Publs Inst Geophys Pol Acad Sci M-23(314):194

Part II

**Exemplary Current Research
and Geophysical Methods**

Discharge Measurements in Lowland Rivers: Field Comparison Between an Electromagnetic Open Channel Flow Meter (EOCFM) and an Acoustic Doppler Current Profiler (ADCP)

Robert J. Bialik, Mikołaj Karpiński and Agnieszka Rajwa

Abstract Field tests were carried out on two lowland rivers in Poland, namely Narew and Wilga, both being right tributaries of the Vistula River, in order to compare the results of flow velocity and discharge measurements. Both measurements were completed with the use of an acoustic Doppler current profiler (ADCP RiverSurveyor S5) manufactured by SonTek and an electromagnetic open channel flow meter (model 801) manufactured by Valeport. Narew is one of Europe's few anastomosing and vegetated rivers. The field measurements were done in the central part of the Narew National Park. By contrast, Wilga is mostly a sandy and meandering river, and the measurements were carried out on the regulated channel that is part of the river. In both cases, field tests in each cross-section were made using both methods. The chapter mostly focuses on the potential errors and differences in the measurements of flow velocity and discharge resulting from: (1) the existence of vegetation on the river bottom; (2) the influence of obstacles such as islands or large fluvial dunes above the measuring cross-section; and (3) the quantity of measuring profiles and measuring execution time for the method using the electromagnetic flow meter. For the latter method a simple but accurate procedure, which is also briefly presented in the chapter, was applied to obtain the flow discharge. It is shown that the differences in the measured values of the flow discharge are from 12 to 35 %, depending on the method of measurement, the nature of the river and flow conditions. The findings of this study may be a suitable tutorial material for education in hydrology, civil engineering and environmental hydraulics.

Keywords Acoustic doppler current profiler · Field measurements · Discharge measurements · Electromagnetic open channel flow meter · Hydrology

R. J. Bialik (✉) · M. Karpiński · A. Rajwa
Department of Hydrology and Hydrodynamics, Institute of Geophysics PAS,
ul. Ks. Janusza 64, 01-452 Warsaw, Poland
e-mail: rbialik@igf.edu.pl

1 Introduction

Water discharge is one of the main characteristics describing a river and is associated with other issues such as water levels, erosion or decomposition and sediment and other transport processes. Therefore, scientists have devoted attention to discharge measurement and tried to develop new measurement techniques and improve their accuracy.

At the Department of Hydrology and Hydrodynamics of the Institute of Geophysics, Polish Academy of Sciences (IGF PAS), the first field campaigns of discharge and velocity measurements were organized at the end of the 1980s by Professor Włodzimierz Czernuszenko. These analyzed the impact of power stations on aquatic environments in Połaniec on the Vistula River (Lebiecki and Czernuszenko 1987; Czernuszenko and Lebiecki 1989) and in Ostrołęka on the Narew River (Czernuszenko and Rowiński 1989; Nikora et al. 1994). In the later studies at the IGF PAS, the water discharge was measured from an estimation of shear velocity during the flooding in the natural conditions by Rowiński and Czernuszenko (1998) and Rowiński et al. (2000). In all of the above works, the water discharge was estimated based on measurements of instantaneous flow velocity made with the use of mechanical current meters in which the flow velocity is proportional to the number of rotations of a propeller. Depending on the depth and width of the river, measurements are usually made from a few to several hydrometric cross-section and at different depths. The same methodology is usually applied to measure the flow discharge with the use of electromagnetic current meters and this will be discussed in the next section of this work. It is worth noting here that the typical current meter is still used in field work, in particular in locations where magnetic or acoustic methods do not work. However, further progress in the techniques for measuring flow velocity means that more accurate devices have usually been employed in the field. For example, Rowiński et al. (2008) used an electromagnetic open channel flow meter (EOCFM) during a large tracer test on the Narew River. This device is based on the Faraday principle of electromagnetic induction. Generally, the water flow through the magnetic field which is generated by this device will produce an electrical potential difference that is proportional to the velocity of the water. Recently, in order to measure the water discharge, the IGF PAS has started to use the acoustic Doppler current profiler (ADCP) which is based on the Doppler effect of acoustic waves. The velocity is calculated from the phase lag between two received acoustic signals that are transmitted with different energies and time intervals. Preliminary results of such measurements from the Narew and Wilga Rivers are presented in this chapter.

The purpose of this work is to compare the results of flow velocity and discharge measurements obtained using both the ADCP and EOCFM devices. MacVicar et al. (2007) have already argued that it is necessary to answer the following questions: (1) can the data on measured discharge and flow velocities collected using both methods be at all comparable; (2) can any of these devices be

used interchangeably; and (3) are the conclusions drawn from the use of the EOCFM still valid. Despite the involvement of numerous scientists, these questions are still open, and the use of these devices for each river needs further investigation. As one of the first, Guza et al. (1988) checked the available electromagnetic current meters and concluded that, in the field, many factors can affect the accuracy of flow measurements using that equipment. On the other hand, acoustic methods based on the Doppler effect have been investigated more closely in recent years (i.e., Muste et al. 2004; Mueller et al. 2007; Stone and Hotchkiss 2007). This work supplements the earlier studies and mainly focuses on the specific problems associated with flow velocity and discharge measurements using both methods, such as the duration of the velocity measurements, the number of verticals and the existence of obstacles or vegetation in rivers.

2 Study Sites

Measurements were carried out in two lowland rivers in Poland, namely Narew and Wilga, both being right tributaries of the Vistula River (see Fig. 1). The Wilga River is located 55 km south of Warsaw, Poland, and the cross-section was selected on the straight channel of the trapezoidal shape, which is located close to the village of Wilga (Fig. 2b). The Wilga basin area covers 231.6 km² (Szkutnicki 1996) and the channel bed consists of fine sand with regular sand-waves 10–40 cm in length and 1–5 cm in height. The discharge measurement on this river was performed on 4 October 2012. On the other hand, the Narew River is one of Europe's few anastomosing and moreover vegetated rivers. The Narew basin has a total area of 75,200 km² and is located in north-east Poland. The field measurements were done on 25 September 2012 in the central part of the Narew National Park and the cross-section has a trapezoidal shape and is located close to the village of Topilec Kolonia (Fig. 2a).

3 Results

The instruments used for comparison of measurements of water discharge in rivers were an acoustic Doppler current profiler (ADCP RiverSurveyor S5) manufactured by SonTek and an electromagnetic open channel flow meter (model 801) manufactured by Valeport. Using the ADCP device, the flow discharge is obtained directly, while using the EOCFM the point flow velocities are measured and the water discharge value is estimated by integrating the velocities distribution over the entire area of the measuring subsections based on the number of point velocities. Depending on the width of the river and its depth, the procedure commonly used in Poland to determine the average flow velocity is as follows (Bajkiewicz-Grabowska et al. 1993):

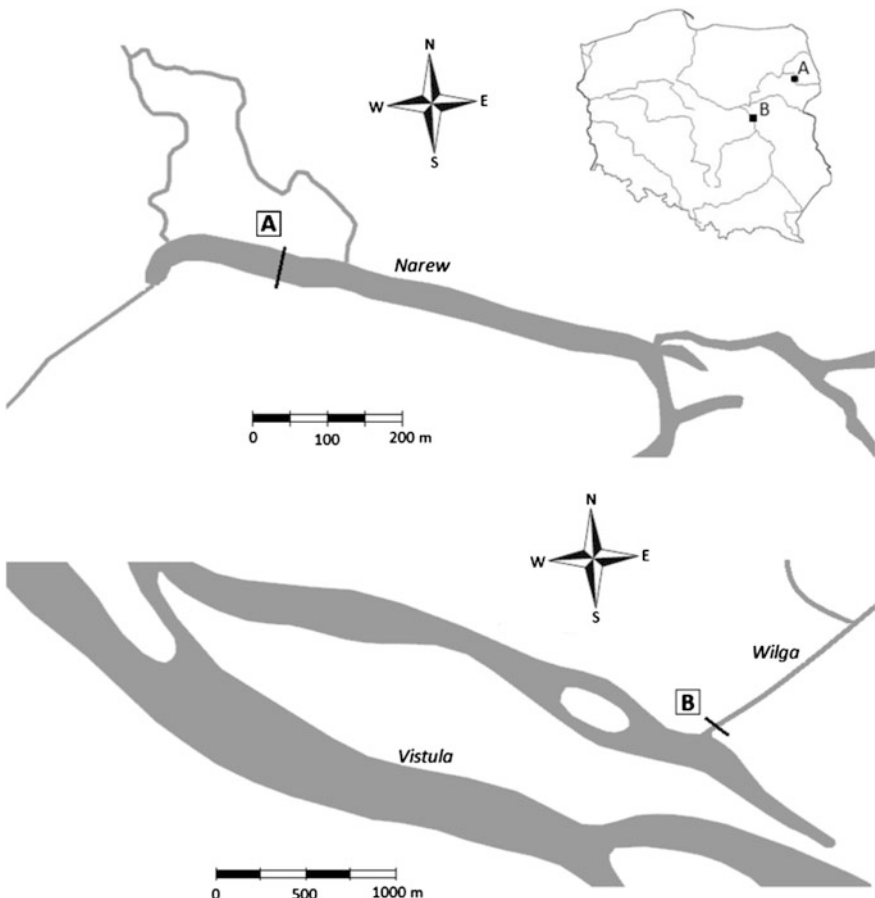


Fig. 1 Location of study sites

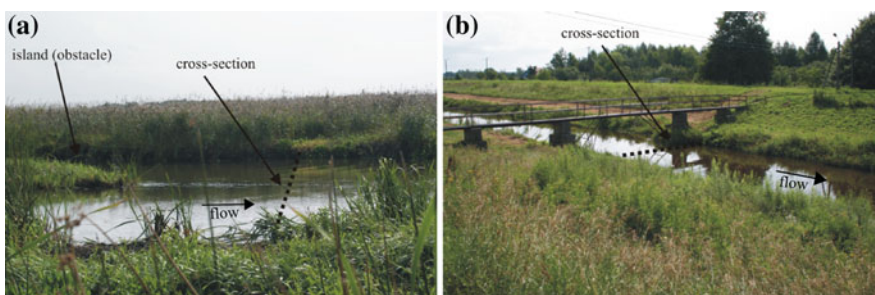


Fig. 2 Location of cross-sections, **a** the Narew River and **b** the Wilga River

- if the river depth $h < 0.2$ m, then the velocity \bar{v} is measured once for each subsection at 0.4 h measured from the river bed and the average velocity is equal to:

$$\bar{v} = v_{0.4h}$$

- if the river depth h is in the range $0.2 < h < 0.6$ m, then the velocity \bar{v} is measured three times for each subsection at 0.2, 0.4, 0.8 h, and the following expression is used to determine the average velocity:

$$\bar{v} = 0.25(v_{0.2h} + 2v_{0.4h} + v_{0.8h})$$

- if the river depth $h > 0.6$ m, then the velocity \bar{v} is measured five times for each subsection: close to the river bed v_b , at 0.2, 0.4, 0.8 h, and close to the free surface v_f . The average velocity is then calculated from the following formula:

$$\bar{v} = 0.1(v_b + 2v_{0.2h} + 3v_{0.4h} + 3v_{0.8h} + v_f)$$

If the water velocities and river bathymetry at given cross-sections have already been measured for each subsection, then the water discharge, in general, may be calculated from the following formula:

$$Q = \sum A\bar{v}$$

where Q is the total discharge, A is the subsection cross-sectional area, and \bar{v} is the mean velocity in a given subsection. Moreover, general recommendations state that the speed at each point of the subsection should be measured for at least 40 s and that the number of subsections depends on the river width as well as its morphology, and for regular cross-section shape (Byczkowski 1999).

- if the river width $d < 10$ m, then the minimum number of subsections should be 4–6;
- if the river width d is in the range $10 < d < 30$ m, then the minimum number of subsections should be up to 8.

In this section, the number of measuring subsections and the measuring execution time for the method using the electromagnetic flow meter will also be discussed among other goals of this chapter.

Figure 3 shows flow velocities across the river section measured using both the ADCP and EOCFM devices on the Narew River. It is important to note here that the velocity fields calculated from point measurements with the EOCFM were obtained using a simple linear interpolation method. In general, for both cases, the ranges of average speed are very similar. However, note that when applying the ADCP device, a clearly visible mosaic occurs close to the left bank. This results

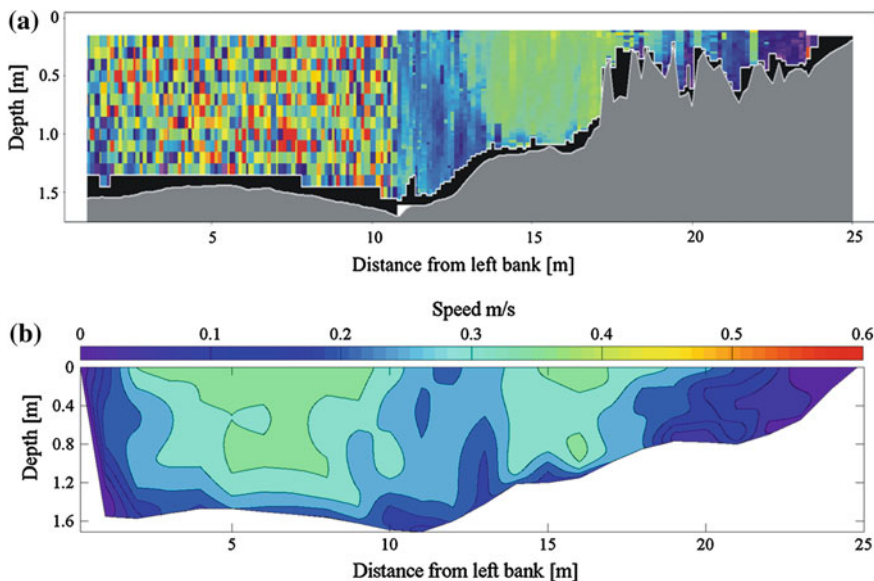


Fig. 3 Velocity spatial distribution on the Narew River measured using an **a** acoustic Doppler current profiler, and **b** electromagnetic open channel flow meter; the same legend is applied to both figures

from the presence of a large island upstream the measured section (see Fig. 2a). This was chosen deliberately to examine its effect on the recorded measurements. Its presence at the above measurement cross-section causes vortices, which occur as the water flows around an obstacle. However, this mosaic appears as a result of the device itself. The ADCP RiverSurveyor S5 transmits and receives the signal from four beams oriented outward 25° from the vertical, and the measurements are done in the measuring cells (easily recognized in Fig. 3). Since during the measurement it is able to capture the occurrence of the vortex, i.e., the positive and negative velocities are recorded. It is revealed as a mosaic pattern. On the other hand, on the right bank the difference in bathymetry, which was obtained with both methods, is shown. It stems from the presence of vegetation at this location. The growth of vegetation is one of the main problems in flow measurements as it increases the channel roughness. This problem occurs in both acoustic and magnetic methods. Regarding the acoustic method, vegetation disrupts the signal transmitted and the device is not able to measure, whereas in the magnetic method, the vegetation can disturb the magnetic field. It is recommended that, if possible, the measurement profile should be cleaned of vegetation before the measurements are started.

Tables 1 and 2 summarize the water discharge calculated on the Narew River using both devices. The ADCP measurements were performed four times, and in the table the maximum, minimum and the mean values are presented. On the other hand, in the case of the EOCFM, the procedure provides that, if the river width is

Table 1 Discharges on the Narew River measured using acoustic doppler current profiler (ADCP)

| ADCP [m ³ /s] |
|---------------------------|
| $Q_{\text{mean}} = 7.176$ |
| $Q_{\text{max}} = 7.339$ |
| $Q_{\text{min}} = 6.998$ |

Table 2 Discharges on the Narew River measured using electromagnetic open channel flow meter (EOCFM)

| Distances between verticals [m] | EOCFM [m ³ /s] |
|---------------------------------|---------------------------|
| 1 | $Q = 7.841$ |
| 2 | $Q = 7.758$ |
| 3 | $Q = 7.401$ |

in the range of 10–30 m, the measurement of the velocity should be done at least 8 times across the river. Due to the very complex cross-section, measurements were collected at every meter. The table shows the estimated value of the water discharge in cases of measurements performed at distances of 1, 2 and 3 m. Significant differences, of up to 12 %, are shown between the ADCP and EOCFM. It seems that the most accurate measurement was made using the EOCFM, in the case when the measurement was made in 25 measurement profiles (i.e., at every meter). On the one hand, this difference may be explained by the existence of vegetation on the right bank which interfered with the measurement of velocities by the ADCP. However, on the other hand, taking measurements with the EOCFM was very time-consuming, and the collection for the whole profile took about 3 h; during this period the flow was repeatedly affected, for example, by sudden gusts, which could increase the local value of the discharge.

A comparison of these two devices was made also on the second river, namely Wilga, to verify the above statements and to check how the averaging time using the EOCFM affects the results of discharge. As stated before, the measurement at each point of the subsection should be done for at least 40 s. In our case, measurements were made for 30–60 s. Figure 4 shows flow velocities across the river section measured using both the ADCP and EOCFM devices on the Wilga River and the ranges of the average speeds are found to be very similar for both cases.

Tables 3 and 4 summarize the water discharge calculated using both devices on the Wilga River. The same procedures were used as at the Narew River for the ADCP and EOCFM. It should be noted that measurements made with both methods gave the same water discharge values in the case when the EOCFM measurements were done every meter, which is a simplicity to the recommended procedure, according to which the minimum number of measuring subsections should be about 6. When distances are 2 m, the flow discharge is about 35 % higher than that obtained when both methods are used, i.e., by the ADCP as well as the EOCFM, wherein the distances between the subsections were one meter. However, there is no clear difference in the measured discharge when the duration of the averaging was equal to 30 or 60 s.

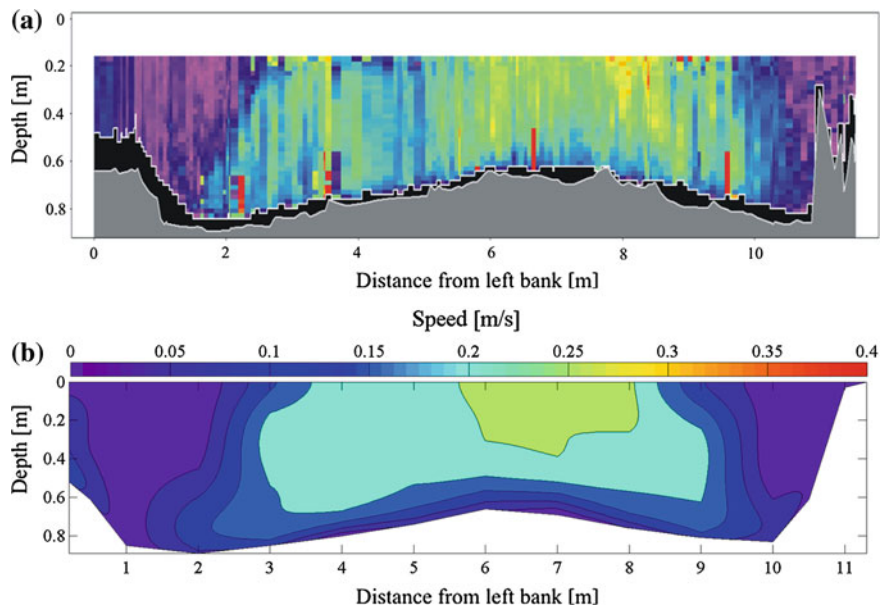


Fig. 4 Velocity spatial distribution on the Wilga River measured using **a** acoustic doppler current profiler, and **b** electromagnetic open channel flow meter; the same legend is applied to both figures

Table 3 Discharge on the Wilga River measured by the acoustic doppler current profiler (ADCP)

| ADCP [m^3/s] |
|--------------------------------|
| $Q_{\text{mean}} = 1.113$ |
| $Q_{\text{max}} = 1.139$ |
| $Q_{\text{min}} = 1.078$ |

Table 4 Discharge on the Wilga River measured by the electromagnetic open channel flow meter (EOCFM)

| Distances between verticals [m] | EOCFM [m^3/s] | Measuring time [s] |
|---------------------------------|---------------------------------|--------------------|
| 1 | $Q = 1.131$ | 30 |
| 1 | $Q = 1.150$ | 60 |
| 2 | $Q = 1.516$ | 60 |

4 Conclusions

In this chapter, the flow velocity and discharge measurements made using an acoustic Doppler current profiler (ADCP RiverSurveyor S5) manufactured by SonTek and an electromagnetic open channel flow meter (model 801)

manufactured by Valeport were presented in order to compare the results obtained by each method. Measurements were done on the rivers Narew and Wilga, and in general the mean flow velocities were the same across the whole measuring sections. However, the maximum differences in the measured values of the flow discharge ranged from 12 to 35 % depending on the method of measurement, the nature of the river and flow conditions. It has been shown that a major problem in measuring the velocity of the water is densely growing vegetation and, if possible, it should be removed before the measurements. Moreover, it is also important to make a proper selection of the location, and close attention should be paid to the probable obstacles above the cross-section to avoid interference, particularly when the ADCP is used. Attention has been also drawn to the time of the averaging as well as the number of measuring subsections when using the electromagnetic open channel flow meter. While in the first case there was no significant difference when the averaging was done by 30 or 60 s, in the second case it was clear that the number of vertical measurements should be as great as possible. On the one hand, this may extend the time of measurement, but on the other hand the quality of the results should not be a compromise. In this case, the great advantage of the ADCP to note here is that it can take measurements of the flow discharge very fast, yielding high quality measurement results.

Acknowledgement The study is supported by the Ministry of Science and Higher Education "IUVENTUS PLUS II" project No. 0028/IP2/2011/71.

References

- Bajkiewicz-Grabowska E, Magnuszewski A, Mikulski Z (1993) Hydrometria (Hydrometry). PWN, Warsaw
- Byczkowski A (1999) Hydrologia (Hydrology), vol 1. SGGW, Warsaw
- Czernuszenko W, Lebiecki P (1989) Turbulence in the river flow (in Polish). Archiwum Hydrotechniki 36(1-2):17-34
- Czernuszenko W, Rowiński PM (1989) Measurements of turbulence in heated water jet. In: Proceedings of 23rd IAHR Congress, Ottawa, pp A71-A76
- Guza RT, Clifton MC, Rezvani F (1988) Field intercomparisons of electromagnetic current meters. J Geophys Res 93(C8):9302-9314
- Lebiecki P, Czernuszenko W (1987) Measurements of basic characteristics of river turbulence (in Polish). Gospodarka Wodna 3:52-56
- MacVicar BJ, Beaulieu E, Champagne V, Roy AG (2007) Measuring water velocity in highly turbulent flows: field tests of an electromagnetic current meter (ECM) and an acoustic doppler velocimetry (ADV). Earth Surf Proc Land 32:1412-1432
- Mueller DS, Abad JD, Garcia CM, Gartner JW, Garcia MH, Oberg KA (2007) Errors in acoustic doppler velocity measurements caused by flow disturbance. J Hydraul Eng ASCE 133(12):1411-1420
- Muste M, Yu K, Spasojevic M (2004) Practical aspects of ADCP data use for quantification of mean river flow characteristics; Part I: moving-vessel measurements. Flow Meas Instrum 15:1-16
- Nikora VI, Rowiński P, Sukhodolov A, Krasuski D (1994) Structure of river turbulence behind warm-water discharge. J Hydraul Eng 120(2):191-208

- Rowiński PM, Czernuszenko W (1998) Experimental study of river turbulence under unsteady conditions. *Acta Geophys Pol* XLVI(4):461–480
- Rowiński PM, Czernuszenko W, Prete JM (2000) Time-dependent shear velocities in channel routing. *Hydrolog Sci J* 45(6):881–895
- Rowiński PM, Guymer I, Kwiatkowski K (2008) Response to the slug injection of a tracer—a large-scale experiment in a natural river. *Hydrolog Sci J* 53(6):1300–1309
- Stone MC, Hotchkiss RH (2007) Evaluating velocity measurement techniques in shallow streams. *J Hydraul Res* 45(6):752–762
- Szkutnicki J (1996) Ocena szorstkości koryt rzecznych na podstawie badań eksperymentalnych. (An experimental estimation of the roughness of river's beds). *Mat Bad Ser Hydrol Meteor* 19, IMiGW Warsaw

Random Domino Automaton: Modeling Macroscopic Properties by Means of Microscopic Rules

Mariusz Bialecki and Zbigniew Czechowski

Abstract A stochastic cellular automaton called Random Domino Automaton (RDA) was set up to model basic properties of earthquakes. This review presents definition of the automaton as well as investigates its properties in detail. It emphasizes transparent structures of the automaton and their relations to seismology, statistical physics and combinatorics. In particular, a role of RDA for modeling time series with Ito equation is emphasized.

Keywords Stochastic cellular automaton · Toy models of earthquakes · Earthquakes' recurrence time · Ito equation · Avalanches · Motzkin numbers · Forest-fire models

1 Introduction

In geophysics, as well as in other natural sciences, observations are of crucial importance. However, direct observations of relevant processes for many geophysical phenomena are beyond our reach. This is the case of seismology—earthquakes' hypocenters are located too deep to make the appropriate measurements. While the phenomena associated with the propagation of seismic waves are relatively well understood—thus we can interpret the seismogram records to reconstruct histories of faults—our knowledge of the physical processes leading to successive shifts on a fault during an earthquake initiation is still quite limited.

M. Bialecki (✉) · Z. Czechowski
Institute of Geophysics, Polish Academy of Sciences, Ks. Janusza 64,
01-452 Warszawa, Poland
e-mail: bialecki@igf.edu.pl

Z. Czechowski
e-mail: zczech@igf.edu.pl

Although the mechanics of destruction is quite a well-developed field of science, in the event of seismic processes we are dealing with an extremely complex task. Areas of tectonic faults are substantially diversified, full of cracks and dislocations, for which distributions of size and location are unknown. Thus, stress distributions inside media and the form of a friction law on the fault are unknown too. Also, a role of other processes, such as plasticity, migration of fluids, chemical reactions, etc. is not known. In particular, interactions between them also remain unclear (Corral 2007; Holliday et al. 2009; Rundle et al. 2003). Information about all of these processes is crucial for the correct description of the process of destruction of the complex geological medium with mathematical and physical models. At the same time, it should be stressed, boundary and initial conditions are unknown either. It is also important that, in contrast to many other natural sciences, the ability to conduct experiments for earthquakes is very limited.

Earthquakes themselves are very complex phenomena, and it is very difficult to fully reflect their complexity in theoretical models. As well as for other geo-physical phenomena, their models introduce considerable simplifications in order to control their physical/mathematical structure. However, even substantial simplifications do not guarantee obtaining of transparent formulas, nor exact solutions.

Earthquakes' models largely belong to the domain of complex systems (Newman 2011). Due to the above-mentioned difficulties, stochastic models are widely considered (Rundle et al. 2003). Introduction of stochastic aspects helps to avoid problems of complex interactions, if they compose in a proper manner (see e.g. (Czechowski 1991, 1993)). However, it is impossible to eliminate another crucial feature of complex systems—nonlinearity, which makes their description complicated. In this context, even relatively simple-looking equations of a model can lead to significant difficulties in solving them or even in performing any exact analysis. For this reason, any links of earthquakes' models with other mathematical or physical disciplines are helpful, because they enable to use various methods developed there.

For those complex phenomena whose physical nature is difficult to understand and explain on the basis of the equations of physics, it appears that cellular automata turn out to be good models (Bhattacharyya and Chakrabarti 2007; Jimenez 2013). Cellular automata—completely discrete dynamical systems—are defined by specifying the geometry of the system and giving the rule of evolution. Basically, these two components encode essential properties of the modelled phenomena. The rule that defines the automaton can be very simple, but it can lead to very complex evolution of the system and produce a rich structure (patterns), often resulting from nonlinear interactions present in the system.

In the context of applications of cellular automata to modeling complex phenomena, they can be divided into two separate fundamental classes. The aim of the first is to capture the essential features of the phenomenon, while neglecting the majority of “irrelevant” properties. The most important task in this class is an “understanding” of the phenomenon. Models in the second class are designed to

reconstruct the actual data. Properly tested models of the second type are used for planning and forecasting. Often they are created by the significant completion of models of the first type (Newman 2011; Vere-Jones 2009).

Cellular automata, and more specifically the rules that define their evolution, are sometimes treated as a kind of replacement of equations, or even as something opposite to equations—if evolution is given by a simple rule, then equations of evolution may seem unnecessary. There is also another approach, shared by the authors of the presented work, namely taking advantage of both analytical properties of equations and simulations of automata governed by the respective rules. This approach is natural, when the automata are constructed as a counterpart of a particular equation (i.e., Boltzmann equation (Chopard and Droz 2005)).

It should be noted here that the problem of transformation of continuous models (equations) to the discrete domain is not simple to perform. Substituting the discrete counterparts of derivatives into equations usually results in cancelling out important properties. In particular, this is the case of non-trivial complex systems, which exhibit self-similarity property. An example of a paper explaining the subtleties of this topic is the work (Nishiyama and Tokihiro 2011). Difficulties associated with finding discrete counterparts of continuous equations, while maintaining their properties, are thoroughly examined in the theory of integrable systems (see Białecki 2005a, b, 2009; Białecki and Doliwa et al. 2003, 2005; Białecki and Nimmo 2007; Doliwa et al. 2003; Kanki et al. 2012; Takahashi and Satsuma 1990; Tokihiro 2004; Tokihiro et al. 1996).

Models presented in the papers described below can be interpreted as a substantial extension of the well-known model of forest fires (Drossel and Schwabl 1992). Similar methods of analysis of equations were used in paper (Paczuski and Bak 1993), although, as is discussed in more detail in (Czechowski and Biały 2012) and (Biały and Czechowski 2013), both the context and the purpose of the analysis were completely different.

In the literature there are many studies devoted to applications of cellular automata to seismicity. Except of a vast diversity of works related to the self-organizing criticality (Bak et al. 1988), for example (Lee et al. 2012), also publications (Gonzalez et al. 2006; Tejedor et al. 2008, 2009, 2010; Vazquez-Prada et al. 2002) certainly deserve to be mentioned. Those works consider cellular automata, and apply them to the analysis of the selected aspects of seismicity.

2 Definition of Random Domino Automaton

In order to study basic aspects of seismicity there was introduced a simple model that reflects only two properties of earthquakes (Biały and Czechowski 2010, 2013). The first one is the process of accumulation of energy, under assumption that it is supplied to the system at a constant (average) rate. This property, in a simplified way, reflects slow growth of stress caused by the relative movement of

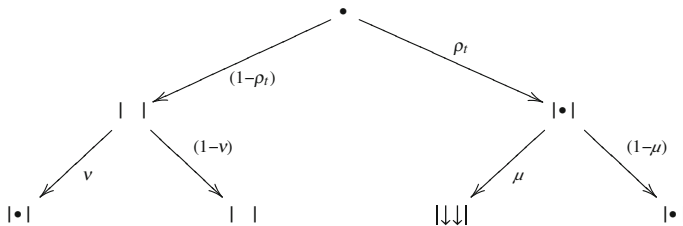


Fig. 1 All possibilities for a single time step of evolution of RDA. An incoming ball can hit an empty cell (on the *left*) or an occupied cell (on the *right*) with respective probabilities depending on actual density of the system. In both cases it may be rebounded (with respective probabilities $(1 - v)$ and $(1 - \mu)$) or it may change the state of the cell (with probabilities v for occupation of the cell and μ for triggering an avalanche)

tectonic plates. The second feature is the occurrence of an abrupt release of energy—the occurrence of avalanches in the context of the automaton—as it happens when the stress exceeds in a certain place a given threshold and an earthquake is triggered. The model is an example of slowly driven system.

In order to construct the model and incorporate into it those two basic characteristics, the papers (Białecki and Czechowski 2010, 2013) establish geometry and rules of evolution for the automaton with stochastic mechanism for ‘pumping’ energy. The model has to meet two criteria: be simple enough to allow a description by the equation, yet be complex enough to give a wide range of behaviors.

In the Random Domino Automaton (RDA) model, the space is \mathbb{Z}_N , i.e., one-dimensional finite lattice of length N with periodic boundary conditions. Each cell may be empty or occupied—which means that it contains a single ball. The density ρ_t defined for the state of the automaton in time t is equal to the number of occupied cells, in a given time t , divided by the size of the system N . The update procedure performed in each discrete time step is defined as follows. A ball is added to the system to the randomly chosen cell (with uniform distribution). If the chosen cell is empty (which corresponds to probability $1 - \rho_t$), there are two possibilities: it becomes occupied with probability v or the ball is rebounded with probability $(1 - v)$, leaving the state of the automaton unchanged. If the chosen place is already occupied (which corresponds to probability ρ_t), there are also two possibilities: the ball is rebounded with probability $(1 - \mu)$ or the incoming ball triggers a relaxation with probability μ . The relaxation means that the ball from the chosen cell and balls from all its adjacent occupied cells (i.e., the whole cluster) are removed simultaneously. In such a way there is triggered an avalanche of size equal to the number of cells that becomes empty. Then the update procedure is repeated in the next time step. All possibilities for the single time step are shown schematically in Fig. 1. An avalanche is represented by the symbol $\downarrow\downarrow$. An example of relaxation of the size *three* is presented in Fig. 2.

Note that RDA is a dissipative system, because of two reasons: avalanches and rebounded balls. The definition of the size of an avalanche presented above results

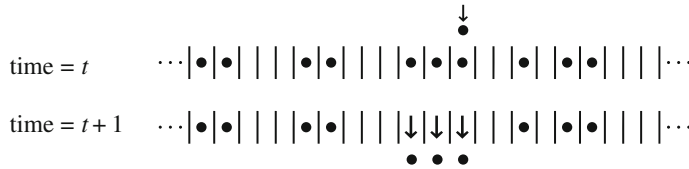


Fig. 2 A relaxation of the size three for an exemplary state of the automaton

in that a system of size N produces avalanches of size ranging from 1 up to N (see (Bialecki and Czechowski 2013) for more details).

The name ‘domino’ for the automaton is related with the interpretation of occupied cells as standing domino blocks (with some distance between consecutive stones) and empty cells are interpreted as an empty space. The new ball incoming to an empty space means that a domino block is added there with probability v . If the incoming ball strikes a domino block, with probability μ it falls down the chosen block and all its adjacent neighbours on both sides.

3 Equations of Random Domino Automaton

In applications, we are usually interested in lasting rather than transient phenomena and so the automaton is described in stationary state and the variables used in the equations, like density and others, are average values and do not depend on time. The stationarity condition: “flow in” is equal to “flow out” can be formulated more precisely when RDA is described as a Markov chain (Bialecki 2012b). Then a statistically stationary state is given by

$$v \cdot P = v, \quad (1)$$

where v is a state vector and P is a transition matrix. In consequence, variables describing statistically stationary state are interpreted as probability rates (or just probabilities after normalization). In particular, variables counting the number of various objects (as clusters, see below) do not have to be integers.

Note, the space of states of the RDA is irreducible, aperiodic and recurrent. An arbitrary state i leads to an arbitrary state j in some finite number of time steps. Thus, properties of a stationary state of the automaton do not depend on initial conditions.

A state of the automaton is given by a sequence of occupied and empty cells. A sequence of i consecutive occupied cells is called the cluster of length i (shortly i -cluster); a sequence of i consecutive empty cells is called empty cluster of length i , where $i = 1, 2, \dots, N$. The size of the lattice N is assumed to be big enough to make limit for the size of clusters negligible. In other words, the system is considered in a thermodynamic limit. The size limits and its consequences are studied

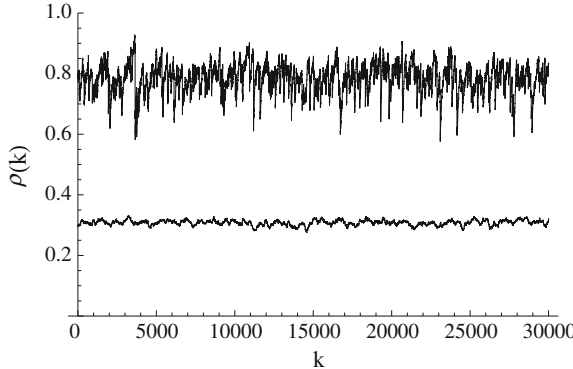


Fig. 3 Examples of simulation results for time series of density $\rho(k)$ of the 1D domino automaton in two cases: constant rebound parameters $\mu/v = 1$ (lower curve) and rebound parameters depending on a cluster size $\mu/v = \frac{0.25}{i}$ (upper curve). The lattice size was set as $N = 4000$. The parameter k numbers subsequent avalanches, the total number of avalanches is $k_T = 30000$

in detail in a separate paper (Białycki 2012b), where properties of finite RDA are investigated.

The number of i -clusters is denoted by n_i and the number of empty i -clusters by n_i^0 . Then the total number of clusters n

$$n = \sum_{i \geq 1} n_i \quad (2)$$

and the total number of empty clusters n^0

$$n^0 = \sum_{i \geq 1} n_i^0 \quad (3)$$

are equal with good approximation (see Białycki 2012b) due to periodic boundary conditions. The density ρ is given by

$$\rho = \frac{1}{N} \sum_{i \geq 1} n_i i. \quad (4)$$

The variations of the density (see Fig. 3) are subjected to ‘v-shape’ potential (Białycki and Czechowski 2013).

In the model we make the following assumptions for a form of rebound parameters. The coefficient $\mu = \mu_i$ does not depend on the position of the chosen cell, but may depend on the size i of the chosen cluster. The parameter v is set to be constant.

Analytical description of the statistically stationary state of automaton (hereinafter referred to as just stationary) was developed in (Białycki and Czechowski 2013). Balance equations were derived for density and for the total number of clusters are as follows

$$v(1 - \rho)N = \sum_{i \geq 1} \mu_i n_i i^2, \quad (5)$$

$$v[(1 - \rho)N - 2n] = \sum_{i \geq 1} \mu_i n_i i, \quad (6)$$

The equations for number of clusters n_i and empty clusters n_i^0 with a given size i are of the form

$$n_1 = \frac{1}{\frac{\mu_1}{v} + 2} [(1 - \rho)N - 2n + n_1^0], \quad (7)$$

$$n_2 = \frac{2}{2\frac{\mu_2}{v} + 2} \left(1 - \frac{n_1^0}{n} \right) n_1, \quad (8)$$

$$n_i = \frac{1}{\frac{\mu_i}{v} i + 2} \left[2n_{i-1} \left(1 - \frac{n_1^0}{n} \right) + \frac{n_1^0}{n^2} \sum_{k=1}^{i-2} n_k n_{i-1-k} \right], \quad \text{for } i \geq 3, \quad (9)$$

$$n_k^0 = \frac{2(n - \sum_{i=1}^{k-1} n_i^0)}{(k+2) + \frac{2}{n} \sum_{i \geq 1} \frac{\mu_i}{v} i n_i}, \quad \text{for } k = 1, 2, \quad (10)$$

$$n_k^0 = \frac{2(n - \sum_{i=1}^{k-1} n_i^0) + \sum_{j=1}^{k-2} \sum_{l=1}^{k-1-j} \frac{\mu_j j n_l}{v N} \frac{n_l^0}{n^0} \frac{n_{k-j-l}^0}{n^0}}{(k+2) + \frac{2}{n} \sum_{i \geq 1} \frac{\mu_i}{v} i n_i}, \quad \text{for } k \geq 3. \quad (11)$$

Variable n_1^0 can be cancelled from the set of Eqs. (7)–(9) for clusters by substitution of n_i^0 obtained from the Eq. (10), namely

$$n_1^0 = \frac{2n}{(3 + \frac{2}{vn} \sum_{i \geq 1} \mu_i n_i i)}. \quad (12)$$

Thus, Eqs. (7)–(9) form a closed set for variables $\{n_1, n_2, \dots\}$. Equations (10) and (11) allow us to find n_k^0 for all $k = 1, 2, \dots$ because on right hand sides there are terms n_j^0 with $j < k$ only.

The above Eqs. (5)–(7) are exact. The remaining ones are derived under the assumption that *clusters are distributed independently*, which means that the length of the “next” cluster is not correlated with the length of the “previous” one. This assumption appears to be justified for small and moderate densities. For big

Table 1 The average density $\langle \rho \rangle$, the average size of a cluster $\langle i \rangle$, and the average size of an avalanche $\langle w \rangle$ from simulation results ($N = 4000$, $k_T = 30000$), equations of the model and percolation approximation for case $\mu/v = 1$

| | Simulation | Equations | Percolation |
|------------------------|------------|-----------|-------------|
| $\langle \rho \rangle$ | 0.3076 | 0.308 | 1/3 |
| $\langle i \rangle$ | 1.5974 | 1.597 | 3/2 |
| $\langle w \rangle$ | 2.2513 | 2.252 | 2 |

Data taken from (Białecki and Czechowski 2013)

densities, when the lattice is almost fully occupied, correlations are not negligible and the assumption cannot be valid (Białecki 2012b). The presented approach may be regarded as a generalization of percolation (Stauffer and Aharony 1992), where subsequent *cells* are treated as independent. The adequacy of this approach was tested both by comparing to the percolation approximation and by comparing to the results of numerical experiments. Agreement of the analytical results with the simulation results is very good, much better than for those obtained within the percolation approximation—see Table 1 and (Białecki and Czechowski 2013) for more details.

The form of the above equations enables us to show the direct existence of a one-to-one correspondence between the efficiency parameters and the function of distribution of clusters and, consequently, distribution of avalanches generated by the automaton. This relationship shows how to infer about properties of the microscopic interactions (i.e., about functional form of the efficiency parameters) from a given distribution of clusters.

For given rebound parameters μ_i/v , details of intrinsic dynamics are fixed, and the system evolves producing specific distributions of clusters n_i . The opposite direction—obtaining parameters of internal dynamics from a given distribution—is usually ambiguous and more complicated to achieve. For RDA the procedure is straightforward: having all n_i (and hence n , ρ and n_1^0) it is possible to designate consecutively all μ_i/v from Eqs. (7)–(9). For $i \geq 3$ the formula is as follows

$$\frac{\mu_i}{v} = \frac{1}{i} \left\{ 2 \left[\frac{n_{i-1}}{n_i} \left(1 - \frac{n_1^0}{n} \right) - 1 \right] + \frac{n_1^0}{n_i n^2} \sum_{k=1}^{i-2} n_k n_{i-1-k} \right\}. \quad (13)$$

We note that formula (13) was typed incorrectly in (Białecki and Czechowski 2013). In particular, to obtain inverse-power distribution of the form $n_i = \alpha/i^\beta$ for some constant α and β , the respective rebound parameters read

$$\frac{\mu_i}{v} = \frac{1}{i} \left\{ 2 \left[\left(\frac{i}{i-1} \right)^\beta \left(1 - \frac{n_1^0}{n} \right) - 1 \right] + \alpha i^\beta \frac{n_1^0}{n^2} \sum_{k=1}^{i-2} \frac{1}{k^\beta (i-1-k)^\beta} \right\}. \quad (14)$$

Again, formula (14) was typed incorrectly in (Białecki and Czechowski 2013).

The procedure is a priori valid for an arbitrary distribution of clusters n_i . The one-to-one relation $\mu_i = f(n_i)$ allows to establish a one-to-one correspondence between rebound parameters μ_i and avalanches distribution w_i . Some details related with this task are considered in (Bialecki 2013).

4 Moments of Cluster Distributions and Selection of Special Cases

The balance equations are valid for general efficiency parameters in the form described above. Thus the equations allow to derive a hierarchy of equations for moments (of any level). Analysis of this hierarchy enables us to select some special cases, including the exponential and inverse-power ones. For n_i , $i = 1, 2, \dots$, we define a moment of order γ by

$$m_\gamma = \frac{1}{N} \sum_{i \geq 1} n_i i^\gamma. \quad (15)$$

Then, the density ρ is equal to the first moment m_1 , and the normalized number of clusters $\frac{n}{N}$ is equal to the zero moment m_0 . We define also *weighted* moments \hat{m}_γ as follows

$$\hat{m}_\gamma = \frac{1}{N} \sum_{i \geq 1} \frac{\mu_i}{v} n_i i^\gamma. \quad (16)$$

Definition of moments, Eq. (15), leads to particularly neat form of expressions for the average size of a cluster

$$\langle i \rangle = \frac{\sum_{i \geq 1} n_i i}{\sum_{i \geq 1} n_i} = \frac{m_1}{m_0}, \quad (17)$$

and the average size of an avalanche

$$\langle w \rangle = \frac{\sum_{i \geq 1} \mu_i n_i i^2}{\sum_{i \geq 1} \mu_i n_i i} = \frac{\hat{m}_2}{\hat{m}_1} = \frac{1 - m_1}{1 - m_1 - 2m_0}. \quad (18)$$

From the set of Eqs. (7)–(9), and (12), one obtains (see Bialecki and Czechowski 2013)

$$\begin{aligned}\widehat{m}_{z+1} &= 1 - m_1 - 2m_0 + 2 \sum_{k=0}^{z-1} \binom{z}{k} m_k \\ &+ \frac{2}{3m_0 + 2\widehat{m}_1} \sum_{l,p=1}^{l+p \leq z} \binom{z}{l+p} \binom{l+p}{l} m_l m_p.\end{aligned}\quad (19)$$

The above equation for $z = 0$ and $z = 1$ takes the following forms:

$$\widehat{m}_1 = 1 - m_1 - 2m_0, \quad (20)$$

$$\widehat{m}_2 = 1 - m_1. \quad (21)$$

The first one is the equation for balance of n —Eq. (6)—and the second one is the equation for balance of ρ —Eq. (5).

Equations of moments for subsequent values of z allow to choose particular forms of rebound parameters (like Eq. (22)), for which weighted moments become just moments and isolate interesting cases as presented below. For rebound parameters in the form

$$\mu_i = \frac{\delta}{i^\sigma}, \quad v = \text{const.}, \quad (22)$$

where δ , σ and $\theta = \frac{\delta}{v}$ are constants, Eqs. (20) and (21) take the form

$$m_1 + \theta m_{2-\sigma} = 1, \quad (23)$$

$$2m_0 + m_1 + \theta m_{1-\sigma} = 1. \quad (24)$$

Choosing $\sigma = 1$ the above set gives values of m_0 and m_1 (hence n and ρ); choosing $\sigma = 0$ it gives a linear dependence between them.

Case $\sigma = 0$ or equivalently $\mu = \beta = \text{const}$ means equal probability of triggering relaxation for each occupied cell. Approximate solution for n_i in this case can be obtained by substituting in Eq. (9) the following formula

$$n_i = k e^{-\gamma i} \quad \text{for } i = 3, 4, \dots \quad (25)$$

where k and γ are some constants. For $i \gg 1$ this gives

$$e^{-\gamma} = \frac{v}{\beta} \frac{k n_1^0}{n^2}, \quad \text{or} \quad n_i = k \left(\frac{v}{\beta} \frac{k n_1^0}{n^2} \right)^i. \quad (26)$$

The value of the constant k can be found from Eq. (4). The above result indicates a close relation to the percolation dependence for n_i (where $n_i = c(1 - \rho)^2 \rho^i$).

Case $\sigma = 1$ or equivalently $\mu = \mu_i = \delta/i$ means equal probability of triggering relaxation for each cluster. For $\mu_i = \frac{\delta}{i}$, where $\delta = \text{const}$, the density ρ and the total number of clusters n can be obtained directly:

$$\rho = \frac{1}{(\theta + 1)} \quad \text{and} \quad n = N \frac{\theta}{(\theta + 1)(\theta + 2)}, \quad (27)$$

where $\theta = \frac{\delta}{v}$, which relates the density with the ratio of coefficients δ and v only.

The average size of a cluster is the same as the average size of an avalanche, because any cluster, regardless of its size, has the same chance to become an avalanche. Hence, both balance equations lead to the same result

$$\langle i \rangle = \langle w \rangle = 1 + \frac{2}{\theta}. \quad (28)$$

In this case, a simple form of $n_1^0 = 2n/(3 + 2\theta)$ together with balance Eqs. (27) allows to reduce the set of Eqs. (7)–(9) to the solvable recurrence. The formulas for n_i are rational functions of θ and N only. The explicit form of solutions is related to the Motzkin numbers (Bialecki 2012c).

5 Relation to Combinatorial Numbers

The Motzkin sequence is an important example of Catalan sequences and thus related to orthogonal polynomials, continued fractions, Hankel matrices and operator calculus (Aigner 2007; Flajolet and Sadgewick 2008; Sloane and Plouffe 1995). A *Motzkin path* P of the length n is a lattice path from $(0, 0)$ to $(n, 0)$ with all steps horizontally or diagonally up or down to the right (i.e., $U = (1, 1)$, $F = (1, 0)$ and $D = (1, -1)$) that never falls below the axis $y = 0$. The *Motzkin number* M_n is the number of Motzkin paths of length n . The first Motzkin numbers are

$$1, 1, 2, 4, 9, 21, 51, 127, 323, 835, 2188, \dots,$$

and they satisfy the following recurrence

$$M_{m+2} = M_{m+1} + \sum_{k=0}^m M_k M_{m-k}. \quad (29)$$

Introducing new variables c_i for $i = 0, 1, \dots$, by

$$c_i = \frac{\beta}{\alpha^{i+1}} n_{i+1}, \quad (30)$$

where

$$\alpha = \frac{2}{(\theta + 2)} \left(\frac{2\theta + 1}{2\theta + 3} \right), \quad \beta = \frac{(\theta + 1)(\theta + 2)}{N\theta(2\theta + 1)}. \quad (31)$$

Equation (9) can be rewritten in the form of Motzkin numbers recurrence (29)

$$c_{m+2} = c_{m+1} + \sum_{k=0}^m c_k c_{m-k}, \quad (32)$$

valid for $m \geq 0$ ($m = i - 2$). Initial data c_0 and c_1 , obtained from Eqs. (7)–(8), are

$$c_0 = c_1 = \frac{1 + \frac{3}{2}\theta + \theta^2}{1 + 4\theta + 4\theta^2}. \quad (33)$$

For the limit case, $\theta \rightarrow 0$, we start with $c_0 = c_1 = 1$. Thus, it is explicitly shown, how to obtain Motzkin from the RDA.

The explicit solution of the set (7)–(9) in the case $\mu = \mu_i = \delta/i$ can be derived using generating function method (see Białycki 2012c):

$$c_m = \frac{1}{2} \sum_{j=0}^{\left[\frac{m+2}{2}\right]} \frac{(2c_0 - \frac{1}{2})^j}{(m-j+2)2^{m-j}} \binom{2(m-j)+1}{m-j+1} \binom{m-j+2}{j}. \quad (34)$$

Thus, formula (30) gives explicit solution of Eqs. (7)–(9) for the distribution n_i for any value of θ .

Asymptotic distribution of the n_i in the limit case $\theta \rightarrow 0$ with the total number of clusters n kept constant ($N\theta = \text{const.}$) is given by an inverse-power distribution

$$n_{i+1} \sim \frac{1}{i^2}. \quad (35)$$

6 The Ito Equation and Time Series Modeling

Moment Eqs. (19) are related to the statistically stationary state only; therefore, an evolution equation for the chosen macroscopic variable would complete the description of RDA.

The automaton rules provide that time fluctuations of density $\rho(t)$ around the stationary state ρ can be treated as a Markov process of order 1. Evolution of the

stochastic diffusion Markov process $\rho(t)$ can be described by the adequate Ito equation:

$$d\rho = a(\rho)dt + \sqrt{b(\rho)}dW(t), \quad (36)$$

in which functions $a(\rho)$ and $b(\rho)$ have to be determined, $W(t)$ is the Wiener process.

Thus, in our papers (Czechowski and Białycki 2012a, b), we constructed the Ito equations in two independent ways. The first one, the time series modeling, is based on data for $\rho(t)$ generated by numerical simulations of RDA and uses histograms of the joint distribution function.

In the second method, the Ito equation is derived analytically under the assumption that geometric-like form for cluster distribution $n_k(\rho(t))$ is maintained (see Czechowski and Białycki 2012b; Czechowski and Białycki 2012a). This let us to find the following formulas (see Czechowski and Białycki 2012a) for functions $a(\rho)$ and $b(\rho)$ in the Ito equation:

$$a(\rho) \propto \frac{v_e(1-\rho)}{1-v_e(1-\rho)} - \frac{1}{\rho} \sum_{k \geq 1} k^2 n_k, \quad (37)$$

$$b(\rho) \propto \frac{v_e(1-\rho)(1+v_e(1-\rho))}{(1-v_e(1-\rho))^2} - \frac{2v_e(1-\rho)}{\rho(1-v_e(1-\rho))} \sum_{k \geq 1} k^2 n_k + \frac{1}{\rho} \sum_{k \geq 1} k^3 n_k. \quad (38)$$

which are given in terms of the first, second and third moment of $n_k(\rho(t))$. Here, the rebound parameter v was replaced by the effective parameter v_e :

$$v_e = \frac{v}{\mu\rho + v(1-\rho)} = \frac{1}{\eta\rho + 1 - \rho}. \quad (39)$$

because we consider only active (not rebounded) balls in the stochastic process of fluctuations of density $\rho(t)$.

In papers (Czechowski and Białycki 2012b; Czechowski and Białycki 2012a) results of the both methods were compared. A good fit for reconstructed functions $a(\rho)$ and $b(\rho)$, given by the analytical formulas (37) and (38) and those obtained by the time series modeling, was shown. This result is important for the utility of the histogram procedure of reconstruction of Ito equations from time series generated by natural complex systems (here RDA is an example of the system). The procedure fills a gap between linear stochastic models (ARMA) and nonlinear deterministic models (Takens 1981) because it is both stochastic and nonlinear.

It should be stressed that in many cases geophysical registered variables are macroscopic, hence the Ito equations can be considered as macroscopic models of these phenomena, in which microscopic details were averaged in some way during complex process of intrinsic interactions.

According to this idea, adequate Ito models were constructed for the following geophysical time series: geoelectrical signals measured in seismic and aseismic areas (Czechowski and Telesca 2011; Telesca and Czechowski 2012), daily mean discharges measured on the river Sauzay catchment (Czechowski 2013) and wind speed data (Czechowski and Telesca 2013). In the two last cases, modified histogram methods were derived in order to take into account the persistent time series and the time series with periodic correlations.

7 Finite RDA and Universal Curve of Recurrence Time for Earthquakes

The above results have been used for further development of both the description of stochastic cellular automata and the analysis of selected aspects of seismicity. In particular, the extension of the results of the work (Białycki and Czechowski 2013) is included in preprint (Białycki 2012b). A paper (Białycki 2013) presents a detailed reconstruction procedure of the rules governing the microscopic dynamics of the automaton (i.e., the efficiency parameters) on the basis of (any) specified distribution of avalanches for finite cellular automaton. Another work (Białycki 2012a) presents an explanation of the universal of curve for earthquakes recurrence time. It is a direct indication that the domino cellular automaton can be useful for clarifying important issues of seismology.

Finite domino automaton (Białycki 2012b) was created to study limits of the assumptions of the analytical description of the domino automaton; in particular, in order to examine the size of the correlations and to perform comparison of the accurate values obtained within the framework of Markov chains with those obtained from the balance equations. For this purpose, it was necessary to develop an analytical description of the finite version of stochastic domino automaton, which incorporates the effect of finite size.

There were derived respective equations describing the steady-state cellular automaton, namely: the equation of balance of density, the total amount of clusters and the number of clusters of a certain size. It was shown that some of the equations are exact, i.e., they take into account all occurring correlations. There was also shown that certain factors (of combinatorial origin) can not be exactly expressed by the variables used in the equations for the size of the automaton greater than four, and the corresponding approximate formulas were proposed. Moreover, there was considered the thermodynamic limit of the obtained equations—obtained equations are identical to the equations previously derived in (Białycki and Czechowski 2013).

The paper (Białycki 2012b) presents also a description of the automaton as a Markov chain: adequate space of states has been described (irreducible, aperiodic and recurrent). The steady state was precisely defined in terms of the transition matrix. It should be noted that the terminology of Markov chains enables us to

directly conclude the existence of a steady state—which is not trivial to establish, without these concepts.

There were derived various relations specific to a number of selected cases. Appropriate parameters in the finite cases can be chosen from significantly greater range comparing to the infinite version, because all sequences are finite, and there is no need to impose proper conditions for their convergence. This enables the consideration of new classes of efficiency parameters, leading to a quasi-periodic evolution of the system. In this way, within the uniform description of domino cellular automaton, one more important new class of automata was constructed.

There were considered expected values of return times between states with empty lattice and also between states with fully occupied lattice. There were derived the formula for the average time between any avalanches

$$t_{av} = \frac{\langle w \rangle + 1}{1 - P_r}, \quad (40)$$

which connect the macroscopic quantities (average size of avalanches $\langle w \rangle$) and the microscopic quantities (the probability of rebound of incoming particles P_r). There are also presented two other formulas for the average time between any avalanches, as well as the method of determining the average time between avalanches of a given size.

Distributions of clusters were tested for various densities of the system, also for those close to zero and close to unity. The approximate coefficients of equations were compared with the exact values (derived from Markov chains) and their accuracy was evaluated. The analysis leads to the following conclusion: investigated various cases show similar qualitative behavior for sizes 5, 7 and 10. It supports the natural assumption that the results for small sizes can be transferred (mutatis mutandis) to larger systems. Therefore, studies of relatively small systems help to understand the behavior of such automata in general.

Based on the above results, paper (Białecki 2013) presents an analytical procedure for the determination of the efficiency parameters characterizing the internal dynamics from a given distribution of avalanches. There is presented a system of equations (with no a priori unknown efficiency parameters), which allows to determine the distribution of clusters on the basis of the distribution of avalanches. Knowing the distribution of those two kinds of parameters, efficiency parameters can be easily determined.

Another important conclusion from the results presented above is the observation that the domino automaton allows to explain the shape of the universal curve of recurrence time of earthquakes (Białecki 2012a).

This curve, introduced in (Corral 2004), is a universal characteristic of seismic activity on the Earth (see also Corral 2007). Following an approach presented in paper (Bak et al. 2002), earthquakes are described by the point process (in time). Then, the difference of occurrence time between two consecutive earthquakes (sometimes called a return time) is investigated. After appropriate rescaling by the average seismicity of the region, a universal curve for earthquake recurrence time

distribution, independent of the choice of the region was obtained. This curve is approximated by a generalized gamma distribution, but for small values of recurrence time, deviations from the gamma fit have been observed (Corral 2004; Marekova 2012).

Based on the combinatorial properties of a finite domino automaton, paper (Białecki 2012a) shows both the mechanism leading to the correct shape of the curve and to the formation of deviations for small return times. Notice, many accepted models of earthquakes can not reproduce return time distribution properly (Weatherley 2006).

Thus, studies of a simple cellular automaton model of earthquakes suggest the conclusion that the shape of the universal curve of earthquake recurrence time distribution is of a combinatorial nature, and it results from the two main characteristics of earthquakes: the slow accumulation of energy and its rapid release (according to the rules implemented in the domino automaton).

8 Conclusions

RDA can be treated as an extension of 1-D forest-fire model proposed by Drossel and Schwabl (1992) or Paczuski and Bak (1993). The assumption we made that rebound parameters are dependent on a cluster size changes the automaton behavior essentially. In particular, in papers (Drossel and Schwabl 1992; Paczuski and Bak 1993) Self-Organized Criticality was investigated and the required critical state could be realized only in the limit $\rho \rightarrow 1$. However, in natural phenomena this condition seems artificial. Note also two important mistakes in equations derived in (Paczuski and Bak 1993), for details see (Czechowski and Biały 2012b).

RDA evolves to statistically stationary states which are characterized by a wide class of cluster size distributions (e.g., exponential or inverse-power) depending on an appropriate form of rebound parameters. Therefore, the model can describe self-organized critical states (for ρ not close to one) but also other self-organized states. Transition from one to another behaviour is smooth, given by a tuning of rebound parameters.

RDA is a rather simple model, but the obtained exact and approximated results provide a new insight into non-equilibrium statistical mechanical models of earthquakes and forest fires. Several formulas—Eqs. (5)–(7), (17), (18), and its consequences—are exact. Other equations are derived under the assumption of independence of clusters.

For inversely proportional dependence between the rebound parameter and a cluster size, the link to combinatorial objects allows the use of well-developed combinatorial methods for the analysis of RDA. In particular, the method of generating functions allows to determine an explicit form of the general solution of the recurrence and thus to find explicit formulas for the distribution of clusters for the automaton in this case.

The remarkable feature of the RDA is the one-to-one relation between details of dynamical rules of the automaton (represented by rebound parameters) and the produced stationary size distribution of clusters, and in consequence distribution of avalanches. These enables to find such microscopic characteristics of the automaton which lead to assumed macroscopic behavior given by the avalanche size distribution function.

Properties of RDA reflects basic characteristics of earthquakes. In particular, it can help to explain the shape of the universal curve of earthquake recurrence time distribution.

The rules and geometry of RDA, equations for cluster size distribution and expressions for moments present respectively: microscopic, mesoscopic and macroscopic description of our automaton in the statistically stationary state. The Ito equation for density fluctuations introduces additionally the time evolution of the chosen macroscopic quantity. This approach, motivated by the kinetic theory of gases, enables an explanation of the macroscopic aspects and behavior of the automaton by microscopic mechanisms.

Acknowledgment This work is supported by the National Science Centre project DEC-2012/05/B/ST10/00598.

References

- Aigner M (2007) A course in enumeration. Graduate text in mathematics, vol 238. Springer, Berlin
- Bak P, Christensen K, Danon L, Scanlon T (2002) Unified scaling law for earthquakes. *Phys Rev Lett* 88:178501
- Bak P, Tang C, Wiesenfeld K (1988) Self-organized criticality. *Phys Rev A* 38:364–374
- Bhattacharyya P, Chakrabarti BK (eds) (2007). Modelling critical and Catastrophic phenomena in geoscience. Lecture notes in physics, vol 705. Springer, Berlin
- Białecki M (2005a) Integrable 1D Toda cellular automata. *J Nonlinear Math Phys* 12 Suppl 2:28–35. doi: [10.2991/jnmp.2005.12.s2.3](https://doi.org/10.2991/jnmp.2005.12.s2.3)
- Białecki M (2005b) Integrable KP and KdV cellular automata out of a hyperelliptic curve. *Glasgow Math J* 47A:33–44. doi:[10.1017/S0017089505002260](https://doi.org/10.1017/S0017089505002260)
- Białecki M (2009) On discrete Sato-like theory with some specializations for finite fields (recent trends in integrable systems). *RIMS Kokyuroku* 1650:154–161
- Białecki M (2012a) An explanation of the shape of the universal curve of the Scaling Law for the earthquake recurrence time distributions. arXiv:1210.7142 [physics.geo-ph]
- Białecki M (2012b) Finite random domino automaton. arXiv:1208.5886 [nlin.CG]
- Białecki M (2012c) Motzkin numbers out of random domino automaton. *Phys. Lett A* 376:3098–3100. doi: [10.1016/j.physleta.2012.09.022](https://doi.org/10.1016/j.physleta.2012.09.022)
- Białecki M (2013) From statistics of avalanches to microscopic dynamics parameters in a Toy model of earthquakes. *Acta Geophys* 61(6):1677–1689
- Białecki M, Czechowski Z (2010) On a simple stochastic cellular automaton with avalanches: simulation and analytical results. In: De Rubeis V, Czechowski Z, Teisseire R (eds) *Synchronization and triggering: from fracture to earthquake processes, geoplanet-earth and planetary sciences*, Springer, Berlin, pp 63–75. doi: [10.1007/978-3-642-12300-9_5](https://doi.org/10.1007/978-3-642-12300-9_5)

- Białycki M, Czechowski Z (2013) On one-to-one dependence of rebound parameters on statistics of clusters: exponential and inverse-power distributions out of random domino automaton. *J Phys Soc Jpn* 82:014003. doi: [10.7566/JPSJ.82.014003](https://doi.org/10.7566/JPSJ.82.014003)
- Białycki M, Doliwa A (2003) The discrete KP and KdV equations over finite fields. *Theor Math Phys* 137:1412–1418. doi: [10.1023/A:1026000605865](https://doi.org/10.1023/A:1026000605865)
- Białycki M, Doliwa A (2005) Algebro-geometric solution of the dKP equation over a finite fieldout of a hyperelliptic curve. *Commun Math Phys* 253:157–170. doi: [10.1007/s00220-004-1207-3](https://doi.org/10.1007/s00220-004-1207-3)
- Białycki M, Nimmo JJC (2007) On pattern structures of the N-soliton solution of the discrete KP equation over a finite field. *J Phys A Math Theor* 40:949–959. doi: [10.1088/1751-8113/40/5/006](https://doi.org/10.1088/1751-8113/40/5/006)
- Chopard B, Droz M (2005) Cellular automata modeling of physical systems. Cambridge University Press, Cambridge
- Corral A (2004) Unified scaling law for earthquakes. *Phys Rev Lett* 92:108501
- Corral A (2007) Statistical features of earthquake temporal occurrence. In: Bhattacharyya P, Chkrobarti BK (eds) Modelling critical and catastrophic phenomena in geoscience. Lecture notes in physics, vol 705. Springer, Berlin, pp 191–221
- Czechowski Z (1991) A kinetic model of crack fusion. *Geophys J Int* 104:419–422
- Czechowski Z (1993) A kinetic model of nucleation, propagation and fusion of cracks. *J Phys Earth* 41:127–137
- Czechowski Z (2013) On reconstruction of the Ito-like equation from persistent time series. *Acta Geophys* 61(6):1504–1521
- Czechowski Z, Białycki M (2012a) Ito equations out of domino cellular automaton with efficiency parameters. *Acta Geophys* 60:846–857. doi: [10.2478/s11600-012-0021-0](https://doi.org/10.2478/s11600-012-0021-0)
- Czechowski Z, Białycki M (2012b) Three-level description of the domino cellular automaton. *J Phys A Math Theor* 45:155101. doi: [10.1088/1751-8113/45/15/155101](https://doi.org/10.1088/1751-8113/45/15/155101)
- Czechowski Z, Telesca L (2011) Construction of Ito model for geoelectrical signals. *Phys A* 390:2511–2519
- Czechowski Z, Telesca L (2013) Construction of a Langevin model from time series with a periodical correlation function: Application to wind speed data. *Physica A* 392:55925603
- Doliwa A, Białycki M, Klimczewski P (2003) The Hirota equation over finite fields: algebro-geometric approach and multisoliton solutions. *J Phys A Math Gen* 36:4827–4839. doi: [10.1088/0305-4470/36/17/309](https://doi.org/10.1088/0305-4470/36/17/309)
- Drossel B, Schwabl F (1992) Self-organized critical forest-fire model. *Phys Rev Lett* 69:1629–1632
- Flajolet P, Sedgewick R (2008) Analytic combinatorics. Cambridge University Press, Cambridge
- Gonzalez A, Vazquez-Prada M, Gomez JB, Pacheco AF (2006) A way to synchronize models with seismic faults for earthquake forecasting: Insights from a simple stochastic model. *Tectonophysics* 424:319–334
- Holliday JR, Rundle JB, Turcotte DL (2009) Earthquake forecasting and verification. In: Meyers RA (ed) Encyclopedia of complexity and systems science. Springer, New York, pp 2438–2449
- Jimenez A (2013) Cellular automata to describe seismicity: a review. *Acta Geophys* 61(6):1325–1350
- Kanki M, Mada J, Tokihiro T (2012) Discrete integrable equations over finite fields. *Symmetry Integr Geom* 8:054
- Lee Y-T, Telesca L, Chen C-C (2012) Negative correlation between frequency-magnitude power-law exponent and Hurst coefficient in the long-range Connective Sandpile model for earthquakes and for real seismicity. *EPL* 99:29001
- Marekova E (2012) Testing a scaling law for the earthquake recurrence time distributions. *Acta Geophys* 60:858–873
- Newman MEJ (2011) Complex systems: a survey. *Am J Phys* 79:800–810
- Nishiyama A, Tokihiro T (2011) Construction of an isotropic cellular automaton for a reaction-diffusion equation by means of a random walk. *J Phys Soc Jpn* 80:054003

- Paczuski M, Bak P (1993) Theory of the one-dimensional forest-fire model. *Phys Rev E* 48:R3214–R3216
- Rundle JB, Turcotte DL, Shcherbakov R, Klein W, Sammis C (2003) Statistical physics approach to understanding the multiscale dynamics of earthquake fault systems. *Rev Geophys* 41(4):1019
- Sloane NJA, Plouffe S (1995) *The Encyclopedia of integer sequences*. Academic Press, San Diego
- Stauffer D, Aharony A (1992) *Introduction to percolation theory*. Taylor & Francis, London
- Takahashi D, Satsuma J (1990) A soliton cellular automaton. *J Phys Soc Jpn* 59(10):3514–3519
- Takens F (1981) Dynamical systems and turbulence. In: Rand DA, Young LS (eds) *Detecting strange attractors in turbulence*. Lecture notes in mathematics, vol 898. Springer, Berlin, pp 366–381
- Tejedor A, Ambroj S, Gomez JB, Pacheco AF (2008) Predictability of the large relaxations in a cellular automaton model. *J Phys A Math Theor* 41:375102
- Tejedor A, Gomez JB, Pacheco AF (2009) Earthquake size-frequency statistics in a forest-fire model of individual faults. *Phys Rev E* 79:046102
- Tejedor A, Gomez JB, Pacheco AF (2010) Hierarchical model for disturbed seismicity. *Phys Rev E* 82:016118
- Telesca L, Czechowski Z (2012) Discriminating geoelectrical signals measured in seismic and aseismic areas by using Ito models. *Phys A* 391:809–818
- Tokihiro T (2004) Ultradiscrete systems (cellular automata). In: Grammaticos B, Kosmann-Schwarzbach T, Tamizhmani T (eds) *Discrete integrable systems*. Lecture notes in physics, vol 644. Springer, Berlin, pp 383–424
- Tokihiro T, Takahashi D, Matsukidaira J, Satsuma J (1996) From solitonequations to integrable cellular automata through a limiting procedure. *Phys Rev Lett* 76:3247–3250
- Vazquez-Prada M, Gonzalez A, Gomez JB, Pacheco AF (2002) A minimalist model of characteristic earthquakes. *Nonlinear Processes Geophys* 9:513–519
- Vere-Jones D (2009) Earthquake occurrence and mechanisms, stochastic models for. In: Meyers RA (ed) *Encyclopedia of complexity and systems science*. Springer, New York, pp 2555–2580
- Weatherley D (2006) Recurrence interval statistics of cellular automaton seismicity models. *Pure Appl Geophys* 163:1933–1947

Continental Passive Margin West of Svalbard and Barents Sea in Polish Arctic Seismic Studies

Wojciech Czuba

Abstract Deep seismic sounding measurements were performed in the continent-ocean transition zone of the western Svalbard and Barents Sea margin, during the Polish–international expeditions in 1976–2008. Seismic energy (airgun and TNT shots) was recorded along several profiles by onshore seismic stations, ocean bottom seismometers (OBS) and hydrophone systems (OBH). Good quality reflected and refracted P waves provided an excellent data base for a seismic modelling along the profiles. TNT sources were recorded up to 300 km distances. A minimal depth of about 6 km of the Moho interface was found east of the Molloy Deep. The Moho discontinuity dips down to 28 km beneath the continental part of the northernmost profile and down to maximum 32 km beneath other profiles. The evolution of the region is considered to be within a shear-rift tectonic setting.

Keywords Seismological observations • Geophysics • Svalbard • Arctic studies

1 Introduction

Svalbard Archipelago is located at the north-western corner of the Barents Sea continental platform bordered to the west by passive continental margin (Fig. 1, insert map). Spitsbergen is the main island of the archipelago. This region is an interesting and important area for understanding the evolution of the North Atlantic and Arctic Oceans. This is the youngest region of the Atlantic and Arctic Oceans giving a good opportunity to study processes leading to their opening. Rifting and subsequent sea-floor spreading processes in the North Atlantic Ocean and the development of the passive sheared continental margin of the Barents Sea

W. Czuba (✉)

Institute of Geophysics, Polish Academy of Sciences, ks. Janusza 64,
01-452 Warsaw, Poland
e-mail: wojt@igf.edu.pl

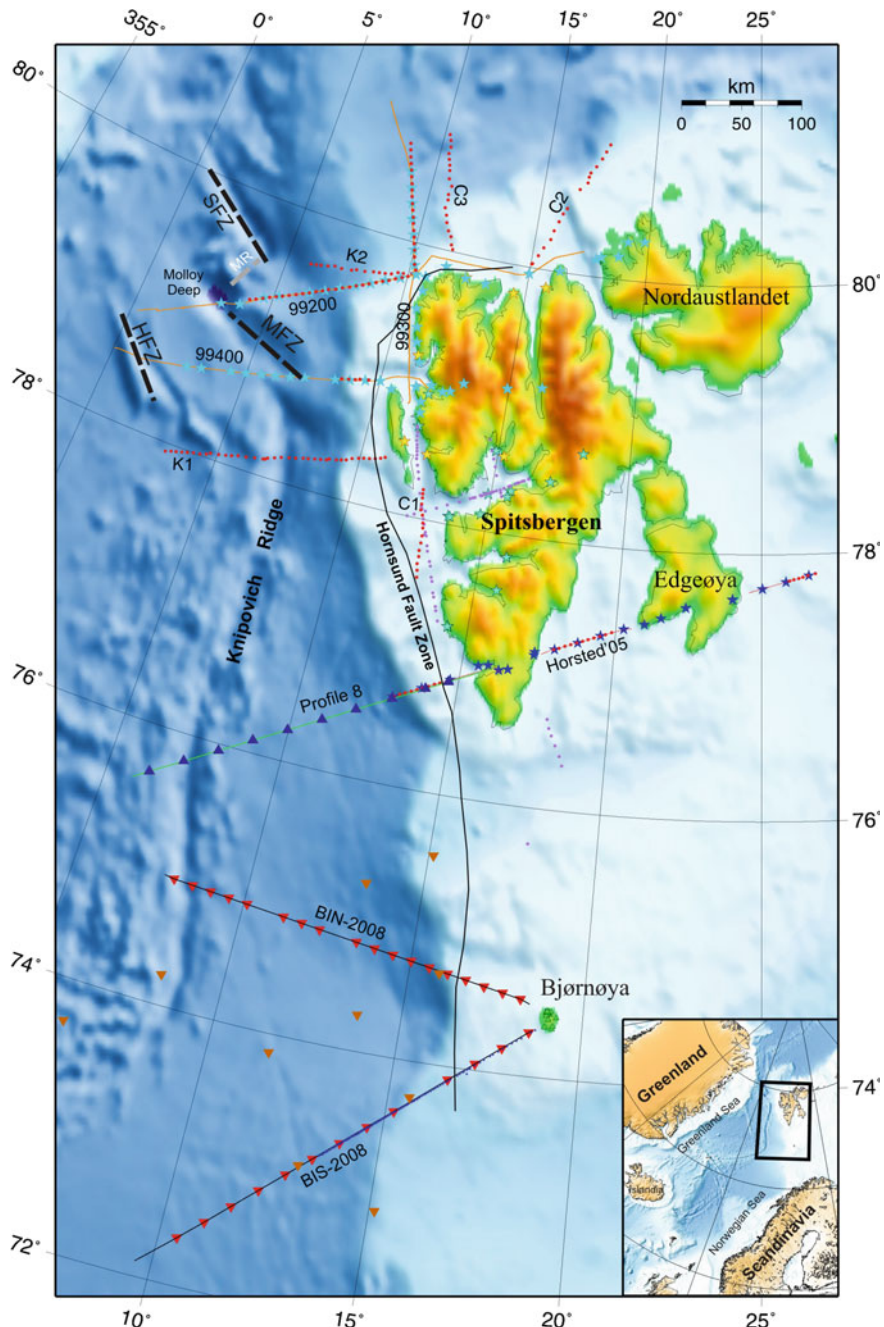


Fig. 1 Location map of the seismic profiles in the ocean-continent transition zone in the western Svalbard and Barents Sea margin on the background of topography/bathymetry map (Jakobsson et al. 2000) and simplified tectonic elements (Gabrielsen et al. 1990; Faleide et al. 2008). Stars and triangles are receivers, thin lines and dots are airgun and chemical (TNT) shots, respectively. HFZ—Hovgård Fracture Zone, MFZ—Molloy Fault Zone, MR—Molloy Ridge, SFZ—Spitsbergen Fault Zone

continental platform are the processes which form the today's face of the Earth. The development of this margin is strongly connected with the history of opening of the North Atlantic Ocean (Jackson et al. 1990; Lyberis and Manby 1993a, b; Ohta 1994).

The Svalbard passive continental margin has been investigated by geophysical research over the last 40 years, mainly based on multichannel seismic reflection, sonobuoy refraction, gravity and magnetic measurements. The continent-ocean boundary (COB) in the region between Svalbard in the north and Scandinavia in the south has been relatively well studied by use of multichannel reflection seismics—for review see, e.g., Gabrielsen et al. (1990) and Faleide et al. (2008). These investigations provided only limited information about the crystalline basement and deep crustal structure of this area.

Deep seismic sounding with the use of refraction technique generally provides information about the crystalline basement and crust-mantle transition (e.g., Mjelde et al. 2002; Davydova et al. 1985; Faleide et al. 1991; Ljones et al. 2004). This leads to important knowledge on the lithospheric structure, tectonic and sedimentary dynamics as well as the hydrocarbon potential.

The Department of Lithospheric Research (former Deep Seismic Lab) of the Institute of Geophysics, Polish Academy of Sciences, focuses on deep seismic sounding for years. One of the areas of interest is Svalbard and Barents Sea. Several DSS profiles were realized in international cooperation during polar expeditions starting from the seismic reconnaissance in 1976 (refraction profiles PAN 1, PAN 2, PAN 3 and reflection profiles PAN 4, PAN 5) (Guterch et al. 1978). These investigations were continued in 1978 (profiles named Coastal, Isfjorden, and Central) (Sellevoll 1982; Guterch and Perchuc 1990; Sellevoll et al. 1991). After the success of the first experiment, next investigations were performed in 1985 (profiles K1, K2, C1, C2, C3) (Czuba et al. 1999) and 1999 (profiles 99200, 99300, 99400) (Jokat et al. 2000). During the expedition in 2005 (transect Horsted'05), a deep seismic sounding of the Earth's crust was performed in the southern Svalbard area. It was an introduction to the large international project “IPY Plate Tectonics and Polar Gateways” closely related to the 4th International Polar Year (Czuba et al. 2008). The last study was made in 2008 (profiles BIN-2008 and BIS-2008) within the 4th International Polar Year (IPY) in the frame of the international project “The Dynamic Continental Margin Between the Mid-Atlantic-Ridge (Mohns Ridge, Knipovich Ridge) and the Bear Island Region” (Czuba et al. 2011; Libak et al. 2012). Apart of seismic refraction investigations, the project comprised seismic reflection profiling, installation of 3 broadband seismic stations on Bear Island, Hopen and southern Spitsbergen at the Polish Polar Station in Hornsund, as well as 1 year deployment of 12 broadband OBSs (Schweitzer et al. 2008; Wilde-Piorko et al. 2009; Pirli et al. 2010).

During refraction experiments, seismic energy (TNT explosions and airgun) was recorded along several transects by onshore (land) seismic stations, ocean bottom seismographs (OBS) and hydrophone systems (OBH). Good seismic records from airgun shots were obtained up to 200 km distances at onshore stations and 50 km at OBSs. TNT shooting was recorded up to 300 km distances.

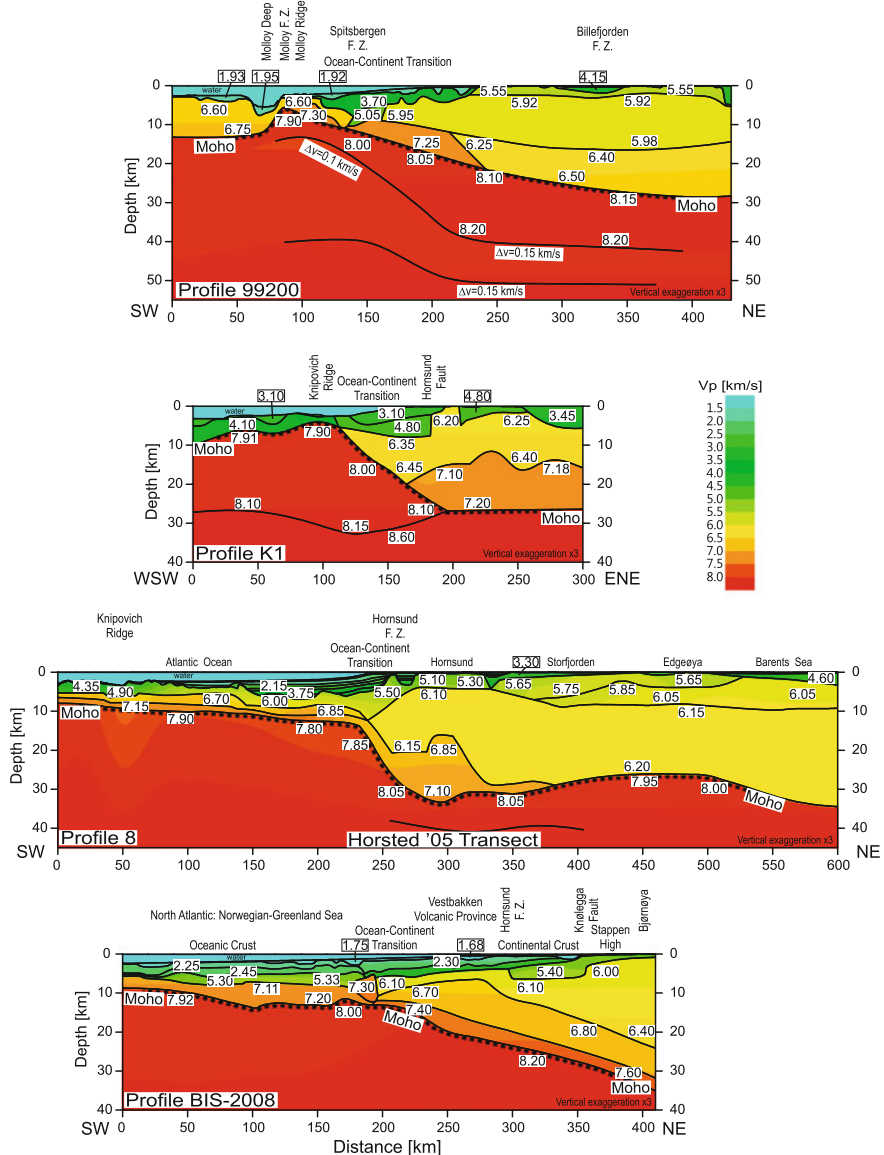


Fig. 2 Examples of 2-D seismic P-wave velocity models developed by ray-tracing technique along selected profiles from Fig. 1, from north (top) to south (bottom), respectively. Black lines represent seismic discontinuities (boundaries); colours represent the distribution of the P-wave velocity and numbers in the model are P-wave velocities in km/s. All the models are in the same geometric and colour scale

2 Tectonic Setting of the Study Area

The geological history of Svalbard Archipelago is ranging in age from Precambrian to Cenozoic (e.g., Birkenmajer 1993; Ohta 1994; Harland 1997; Dallmann 1999). Its structure reflects the relative activity of the Eurasian and the North American plates (Eldholm et al. 1987) and shows a multiorogenic development with several prominent tectonic stages (e.g., Dallmann 1999; Harland 1997). The tectonic history of the region can be simplified into terms of three main geological stages (Sellevoll et al. 1991).

The first important tectonic event is related to the Caledonian Orogeny. Its effects are particularly well visible in the eastern Svalbard (Sellevoll et al. 1991). The next main tectonic stage is called the Late Devonian Svalbardian event. During this event, the eastern Spitsbergen and Nordaustlandet have moved northward from eastern Greenland to a position north of Greenland (Sellevoll et al. 1991). This is a disputable hypothesis (Harland 1997). Thus, the eastern part of Svalbard has attached to the western Spitsbergen.

Cenozoic tectonic processes in the Svalbard area were related to the structural history of the western Barents Sea margin. The relative motion between Svalbard and Greenland took place along the Hornsund Fault Zone, traced from just south of Bjørnøya at ca. 75°N to about 79°N (Sundvor and Eldholm 1979, 1980). This regional fault zone has acted as an incipient plate boundary between the opening Arctic Ocean and the Barents Sea shelf.

The evolution of the North Atlantic Ocean can be divided into two main phases. During the first phase, the continental break-up occurred and sea floor spreading started along the Reykjanes, Aegir and Mohns Ridges (Talwani and Eldholm 1977) in the Early Eocene. The shearing along faults between northeast Greenland and Svalbard has created the Spitsbergen fold and thrust belt to the north. Dense mantle material was intruded most abundantly at the Vestbakken Volcanic Province after thinning and weakening of the crust caused by trans-tension (Eiken and Austegard 1987; Eldholm et al. 1987; Sundvor and Eldholm 1979).

The second phase of North Atlantic evolution was marked by a change in the spreading direction from NNW–SSE to NW–SE. This has begun in Early Oligocene when spreading in the Labrador sea stopped (Mosar et al. 2002; Talwani and Eldholm 1977). The beginning of the phase has unlocked the northward development of the Mid Atlantic Ridge. The spreading axis has developed into the Spitsbergen Shear Zone creating the asymmetric, ultraslow and obliquely-spreading Knipovich Ridge. Around 23 Ma ago the spreading started further, along the Molloy Ridge, and around 10 Ma ago a continental break-up occurred along the Fram Strait. This has established connection between the Arctic and the Northern Atlantic ridges (Lundin and Doré 2002; Crane et al. 1991).

3 Experimental Setup

Good quality records of refracted and reflected P waves were obtained along the entire profiles lengths (Fig. 1). They were an excellent data base for subsequent seismic modelling along the profiles. The details about the experiments, data processing and quality, as well as modelling procedures and interpretations are described in Czuba et al. (1999, 2005, 2008, 2011), Krysiński et al. (2013), Libak et al. (2012), Ljones et al. (2004), Ritzmann et al. (2004), Ritzmann and Jokat (2003) and Sellevoll et al. (1991). Although all the profiles are DSS profiles, their setup was different because of polar region logistics, instruments availability and land geometry. Seismic sources were used in the sea for all the profiles. The profiles in 1976, 1978 and 1985 were performed using TNT sources and seismic land stations (vertical component) only. Later, in 1999, 2005 and 2008, the profiles were performed using seismic land stations, OBSs and OBHs (99200 and 99400 only) as receivers, and dense system of airgun shots as well as TNT shots to extend distance of recording. The profile 99200 geometry setup was partly off-line, but seismic modelling was performed like for full in-line setup using real distances between sources and receivers. Later, the 2.5-D (Czuba et al. 2007) tomographic inversion methods were used with additional data from crossing profiles. The Profile 8 was full marine profile with airgun shots and OBSs only. This profile was then connected with the Horsted'05 profile and other available data from the region to perform a gravimetry modelling along the whole transect (Krysiński et al. 2013). The profile BIN-2008 was performed using seismic land stations, OBSs and airgun shots.

All the data from 1985 were processed in the same way and transformed to SEG-Y format with 100 Hz sampling. Different filters (range of 1–20 Hz) were used dynamically during picking of arrivals of seismic energy. Seismic models were calculated using P waves by ray-tracing trial-and-error method using wide available software.

4 Seismic Results

The results are shown in Fig. 2. A minimal depth of about 6 km of the Moho discontinuity was determined east of the Molloy Deep. Here, the upper mantle exhibits P-wave velocity of about 7.9 km/s, and the crustal thickness does not exceed 4 km, which is an extremely low value. The crustal thickness in the area is differentiated, from about 13 km (Knipovich Ridge and Yermak Plateau) to 25 km (K2 profile) beneath the sea. The Moho discontinuity dips down to 28 km beneath the continental part of the 99200 (northernmost profile) and K1 profiles and down to maximum 32 km beneath the other profiles. The P-wave velocity below the Moho interface increases generally up to 8.2 km/s, reaching a maximum of 8.6 km/s beneath the continental part of the profile located in the central part of the west coast of Spitsbergen (K1).

The continental crust consists of two or three crystalline layers. The lowermost crustal continental layer with the P-wave velocity in the order of 7 km/s does not exist in the continental crust along three of the profiles described in this chapter. It is completely missing (BIN-2008) or it exists in the transition zone only (99200, Horsted'05). A layer characterised by P-wave velocities significantly above 7 km/s is found along the continental part of the BIS-2008 profile but it is very thin and it can hardly be considered as a part of normal continental lower crust. Profiles 99400 and K1 show clearly continental lower crustal layer characterised by P-wave velocities 6.7–7.0 and 7.1–7.2 km/s, respectively.

The oceanic crust is generally similar in terms of thickness along all the profiles studied here, but it is more differentiated in three southern profiles, where opening of Northern Atlantic happened earlier. Differences in crustal thickness are the result of different spreading rate in the tectonic history. The thickness is minimal in the vicinity of the mid-oceanic ridge. There, the P-wave upper mantle velocities are lowest along these profiles, being even lower than 7.9 km/s (Profile 8, BIN-2008). The sedimentary part of the continent–ocean transition zone is characterised by a complex basin structure, known in the Spitsbergen region as west Spitsbergen foreland basin (Eiken and Austegard 1987). The P-wave velocity at the topmost layers is very low, being even 1.8–1.9 km/s (BIS-2008, 99200), which indicates high water saturation of the rock body.

The margin intersected by several profiles studied here have the character of sheared margin with rather short continent–ocean transition and abrupt change of the crustal thickness (99400, K1, Horsted'05). The shearing took place mostly along the Hornsund Fault Zone (Faleide et al. 1991, 2008). The margin intersected by the other profiles (99200, BIN-2008, BIS-2008) have more complex history and their transition zone structure indicates the transform character in the past, but in the present they can be classified rather as rifted margins with ultra-slow spreading.

5 Conclusions

Thanks to the dense system of airgun shots it was possible to model very accurately the seismic crustal structure along profiles located in the Svalbard and Barents Sea continental passive margin. TNT shots allowed to reach deeper parts of the Earth's crust and uppermost mantle. During numerous seismic projects in the Svalbard region, mainly in the continent–ocean transition zone, we have determined the seismic structure of the lithosphere down to the Moho discontinuity or deeper. The continent–ocean transition zone is characterised by a complex seismic structure covered by deep sedimentary basins. The evolution of the region appears to be within a shear-rift tectonic setting. The last stage of the development of the margin at the northernmost profile (99200) can be classified as rifting. The margin of the central and southern Spitsbergen are rather of sheared character, while the western Barents Sea margin are of slow to ultraslow spreading type.

The use of in-line and off-line data recorded from two seismic experiments (realized in 1985 and 1999) allowed 3-D seismic modelling to be performed, which is the first attempt of such crustal modelling in this region.

Results of deep seismic studies are very important base for geological interpretation and for modelling of deeper layers or more distant structures.

Acknowledgments The public domain GMT software (Wessel and Smith 1991, 1998) has been used.

References

- Birkenmajer K (1993) Tertiary and cretaceous faulting in a proterozoic metamorphic Terrain, SE Wedel Jarlsberg Land, Spitsbergen. *Bull Pol Acad Sci Earth Sci* 41(3):181–189
- Crane K, Sundvor E, Buck R, Martinez F (1991) Rifting in the northern Norwegian-Greenland Sea: thermal tests of asymmetric spreading. *J Geophys Res* 96:14529–14550
- Czuba W, Grad M, Guterch A (1999) Crustal structure of north-western Spitsbergen from DSS measurements. *Pol Polar Res* 20(2):131–148
- Czuba W, Ritzmann O, Nishimura Y, Grad M, Mjelde R, Guterch A, Jokat W (2005) Crustal structure of northern Spitsbergen along the deep seismic transect between the Molloy Deep and Nordaustlandet. *Geophys J Int* 161:347–364
- Czuba W (2007) 2.5-D seismic tomographic modelling of the crustal structure of north-western Spitsbergen based on deep seismic soundings. *Mar Geophys Res*. doi:[10.1007/s11001-007-9028-3](https://doi.org/10.1007/s11001-007-9028-3)
- Czuba W, Grad M, Guterch A, Majdański M, Malinowski M, Mjelde R, Moskalik M, Środa P, Wilde-Piórko M, Nishimura Y (2008) Seismic crustal structure along the deep transect Horsted'05, Svalbard. *Pol Polar Res* 29(3):279–290
- Czuba W, Grad M, Mjelde R, Guterch A, Libak A, Krüger F, Murai Y, Schweitzer J, the IPY Project Group (2011) Continent-ocean-transition across a trans-tensional margin segment: off Bear Island, Barents Sea. *Geophys J Int* 184:541–554 doi:[10.1111/j.1365-246X.2010.04873.x](https://doi.org/10.1111/j.1365-246X.2010.04873.x)
- Dallmann WK (1999) Lithostratigraphic Lexicon of Svalbard. Review and recommendations for nomenclature use. Upper Palaeozoic to Quarternary Bedrock. Committee on the Stratigraphy of Svalbard, Norsk Polarinstitutt, Tromsø, pp 318
- Davydova NI, Pavlenkova NI, Tulina YUV, Zverev SM (1985) Crustal structure of the Barents Sea from seismic data. *Tectonophysics* 114:213–231
- Eiken O, Austegard A (1987) The tertiary orogenic belt of West Spitsbergen: seismic expressions of the offshore sedimentary basins. *Nor Geol Tidsskr* 67:383–394
- Eldholm O, Faleide JI, Myhre AM (1987) Continental-ocean transition at the western Barents Sea/Svalbard continental margin. *Geology* 15:1118–1122
- Faleide JI, Gudlaugsson ST, Eldholm O, Myhre AM, Jackson HR (1991) Deep seismic transects across the western Barents Sea continental margin. *Tectonophysics* 189:73–89
- Faleide JI, Tsikalas F, Breivik AJ, Mjelde R, Ritzmann O, Engen Ø, Wilson J, Eldholm O (2008) Structure and evolution of the continental margin off Norway and the Barents Sea. *Episodes* 31(1):82–91
- Gabrielsen RH, Færseth RB, Jensen LN, Kalheim JE, Riis F (1990) Structural elements of the Norwegian continental shelf, Part I: The Barents Sea Region. *NPD-Bull* 6:1–33, Oljedirektoratet
- Guterch A, Pajchel J, Perchuć E, Kowalski J, Duda S, Komber J, Bojdys G, Sellevoll MA (1978) Seismic reconnaissance measurement on the crustal structure in the Spitsbergen region 1976. *Geophysical Research on Svalbard, Bergen*, pp. 61

- Guterch A, Perchuć E (1990) Seismic crustal structure of the sedimentary basin of central Spitsbergen (discussion of results). *Pol Polar Res* 11(3–4):267–276
- Harland WB (1997) The geology of Svalbard. Geological Society Memoir No. 17, The Geological Society, London, pp 521
- Jackson HR, Faleide JI, Eldholm O (1990) Crustal Structure of the Sheared Southwestern Barents Sea Continental Margin. *Mar Geol* 93:119–146
- Jakobsson M, Cherkis NZ, Woodward J, Macnab R, Coakley B (2000) New grid of Arctic bathymetry aids scientists and mapmakers. *EOS Trans AGU* 81(9):89, 93, 96
- Jokat W, Czuba W, Dzewas J, Ehrhardt A, Gierlichs A, Kühn D, Martens H, Lensch N, Nicolaus M, Nishimura Y, Ritzmann O, Schmidt-Aursch M, Środa P, Wildeboer-Schut E (2000) Marine Geophysics, In: Jokat W (ed) The Expedition ARKTIS-XV/2 of Polarstern in 1999, Berichte zur Polarforschung 368:8–26, Alfred Wegener Institute for Polar and Marine Research, Bremerhaven
- Krysiński L, Grad M, Mjelde R, Czuba W, Guterch A (2013) Seismic and density structure of the lithosphere–asthenosphere system along transect Knipovich Ridge–Spitsbergen–Barents Sea—geological and petrophysical implications. *Pol Polar Res* 34(2):111–138. doi:[10.2478/popore-2013-0011](https://doi.org/10.2478/popore-2013-0011)
- Libak A, Eide CH, Mjelde R, Keers H, Flüh ER (2012) From pull-apart basins to ultraslow spreading: results from the western Barents Sea Margin. *Tectonophysics* 514:44–61
- Ljones F, Kuwano A, Mjelde R, Breivik A, Shimamura H, Murai Y, Nishimura Y (2004) Crustal transect from the North Atlantic Knipovich Ridge to the Svalbard Margin west of Hornsund. *Tectonophysics* 378:17–41
- Lundin E, Doré AG (2002) Mid-Cenozoic post break-up deformation in the “passive” margins bordering the Norwegian-Greenland Sea. *Mar Pet Geol* 19:79–93
- Lyberis N, Manby G (1993a) The origin of the west Spitsbergen Fold belt from geological constraints and plate kinematics: implications for the Arctic. *Tectonophysics* 224:371–391
- Lyberis N, Manby G (1993b) The west Spitsbergen Fold Belt: the result of Late Cretaceous-Palaeocene Greenland-Svalbard Convergence? *Geol J* 28:125–136
- Mjelde R, Breivik AJ, Elstad H, Ryseth AE, Skilbrei JR, Opsal RR, Shimamura H, Murai Y, Nishimura Y (2002) Geological development of the Sørvestsnaget Basin, SW Barents Sea, from ocean bottom seismic, surface seismic and potential field data. *Norw J Geol* 82:183–202
- Mosar J, Eide EA, Osmundsen PT, Sommarunga A, Torsvik TH (2002) Greenland-Norway separation: a geodynamic model for the North Atlantic. *Norw J Geol* 82(4):282–299
- Ohta Y (1994) Caledonian and Precambrian history in Svalbard: a review, and an implication of escape tectonics. *Tectonophysics* 231:183–194
- Pirli M, Schweitzer J, Ottemöller L, Raeesi M, Mjelde R, Atakan K, Guterch A, Gibbons SJ, Paulsen B, Dębski W, Wiejacz P, Kværna T (2010) Preliminary analysis of the 21 February 2008, Svalbard (Norway), Seismic Sequence. *Seism Res Lett* 81:63–72
- Ritzmann O, Jokat W (2003) Crustal structure of northwestern Svalbard and the adjacent Yermak Plateau: evidence for Oligocene detachment tectonics and non-volcanic breakup. *Geophys J Int* 152:139–159
- Ritzmann O, Jokat W, Czuba W, Guterch A, Mjelde R, Nishimura Y (2004) A deep seismic transect from Hovgård Ridge to northwestern Svalbard across the continental-ocean transition. A sheared margin study. *Geophys J Int* 157:683–702
- Schweitzer J, Guterch A, Krüger F, Schmidt-Aursch M, Mjelde R, Grad M, Faleide JI (2008) The IPY Project 77—The dynamic continental margin between the Mid-Atlantic-Ridge system (Mohns Ridge, Knipovich Ridge) and the Bear Island Region. In: 33 International Geological Congress, Oslo, 6–14 August 2008, CD-ROM Proceedings
- Sellevoll MA (coordinator) (1982) Seismic crustal studies on Spitsbergen 1978. Geophysical Research on Spitsbergen, Bergen, pp 62
- Sellevoll MA, Duda SJ, Guterch A, Pajchel J, Perchuć E, Thyssen F (1991) Crustal structure in the Svalbard region from seismic measurements. *Tectonophysics* 189:55–71
- Sundvor E, Eldholm O (1979) The western and northern margin off Svalbard. *Tectonophysics* 59:239–250

- Sundvor E, Eldholm O (1980) The continental margin of the Norwegian-Greenland Sea: recent and outstanding problems. *Trans Royal Soc Lond Ser A* 294:77–82
- Talwani M, Eldholm O (1977) The evolution of the Norwegian-Greenland Sea: recent results and outstanding problems. *Geol Soc Am Bull* 88:969–999
- Wessel P, Smith WHF (1991) Free software helps map and display data. *EOS Trans AGU* 72:441
- Wessel P, Smith WHF (1998) New, improved version of the Generic Mapping Tools released. *EOS Trans AGU* 79:579
- Wilde-Piórko M, Grad M, Wiejacz P, Schweitzer J (2009) HSPB seismic broadband station in Southern Spitsbergen: first results on crustal and mantle structure from receiver functions and SKS splitting. *Pol Polar Res* 30(4):301–316

Selected Theoretical Methods in Solid Earth Physics: Contribution from the Institute of Geophysics PAS

Wojciech Dębski, Roman Teisseyre and Włodzimierz Bielski

Abstract Solid Earth Physics, including Seismology, Physics of the Earth, Earth Magnetism to name a few more topical disciplines, strongly relies on mathematical and numerical possibilities of modeling very complex physical processes ongoing in the Earth interior. Tremendous progress in geophysical instrumentation and still increasing quality and quantity of observational data also prompts for advanced processing methods in order to get more reliable interpretations. The goal of this chapter is to review some contributions from the Institute of Geophysics, Polish Academy of Sciences (IGF PAS) to physical and mathematical concepts used in Solid Earth Physics. We have selected some topics which are general enough to be interesting for a wide range of readers, leaving many topical issues uncovered in this review.

Keywords Computational geophysics · Inverse theory · Asymmetric continuum · Flow in porous media

1 Introduction

The distinguished position of geophysics among other earth sciences comes from the fact that geophysics attempts to describe the earth system using generally physical methodologies. It comprises observational techniques of physical parameters of the earth systems, often based on the very advanced technologies like satellite telemetry, very sensitive seismometric observations, or technologically very advanced deep and fast deep crust drilling to name a few techniques concerning solid earth observations. Moreover, most of observational sites have

W. Dębski (✉) · R. Teisseyre · W. Bielski
Institute of Geophysics, Polish Academy of Sciences, ul. Ks. Janusza 64,
01-452 Warsaw, Poland
e-mail: debski@igf.edu.pl

recently been networked together and infrastructures like international data centers have been created. Thus, nowadays we can talk about the Earth's *global observational system* providing enormous quantity of information on the Earth system and comparable only to the most advanced physical experimental facilities. Another particular feature of geophysics is using the physical approach to understand the natural and anthropogenic-caused processes occurring in the Earth system starting from the very basic physical principles like energy or momentum conservation, second thermodynamic law, etc. However, geophysics not only uses the concepts and methodologies developed by other physical disciplines. It also significantly contributes to development of various physical observational technologies, theories and computational techniques. This development was quite often inspired by pragmatic industrial and/or social requests and needs. For example, development of the very advanced numerical data processing techniques was inspired and founded by the prospecting industry, very much interested in more detailed and efficient mapping of underground structures. On the other hand, an advanced analysis of earthquake hazard, physics of earthquake sources or volcanic processes is of the greatest importance for contemporary societies. This particular demand of a "practice" of geophysical research has formed the third distinguished feature of geophysics—its pragmatism in formulating and solving the real scientific tasks.

At the early stage of the development of geophysical research, the most important research tasks were accumulating an evidence of some natural processes and linking them as much as possible to known physical principles, models and ideas. This stage of geophysical qualitative-type research was very soon finished by formulated demands of a quantitative analysis of gathered evidence and searching for possible physical description of observed phenomena. This refocusing of geophysical thinking from qualitative evidence accumulation to quantitative description has opened a way for introducing mathematical methods to generally understood Earth sciences. Many of the analyzed problems have been found out to be extremely complex so specific scientific methods needed to be developed. Let us concentrate on some of them.

Geophysical data used to infer the properties of the Earth's interior and/or provide information on processes undergoing in its depth are gathered practically on surface of the Earth or from the space. In such a case, an inference about the thought properties of the Earth or process in hand become a nontrivial inverse task. In consequence special data interpretation methods called inverse theory have been developed by geophysicists. The need for a quantitative estimation of accuracy of observational data analysis has lead to probabilistic formulation of the inverse theory.

Another astonishing example of development of general physical theory inspired by solid Earth problem analysis is the formulation of Asymmetric Continuum Media theory. This theory appears from very simple observations that damages of some constructions during earthquakes pointed out on relative rotational movements of different parts of constructions. However, the classical

continuum elastic mechanics, which is the corner stone of contemporary seismology, predicts no rotational effects. Analysis of this apparent contradiction has lead to an idea of extending the classical theory of continuum elastic media.

In this chapter we concentrate on the mathematical and data analysis aspects of the geophysical research connected to the above tasks. This particular choice is by no means arbitrary. It simply follows from the fact of a significant contribution of IGF PAS to development of these particular types of geophysical research and personal authors' attachments.

2 Probabilistic Inverse Theory

2.1 General Concept

In geophysical investigations, when interpreting observational data we deal with the forward problem (also called forward modeling), and inverse problems. The forward problem aims at mathematical, or more often numerical simulations of given physical processes like energy release from seismic source, propagation of elastic waves, generation of electromagnetic signals at earthquake preparation stage, to name a few. On the contrary, the inverse tasks aim at quantitative description of process in hand. In this section we present the probabilistic approach to inverse problems, actively developed and promoted by IGF PAS.

While the forward problems intend to explain the nature of phenomena at hand, the inverse questions concern its precise and quantitative description. The simplest answer to such tasks would be a direct measurement of a quantity we are interested in. However, the capacity to carry out direct measurements is very limited in geophysics (Tarantola 2005). In cases where we cannot directly observe given parameters \mathbf{m} we are interested in, we need to carry out an “indirect” measurement. We measure another parameter \mathbf{d} and using the forward modeling relation (Eq. 1) try to infer information about the sought \mathbf{m} .

Contrary to the forward problem, inverse tasks are quite often non-unique, which happens frequently in the case of nonlinear multi-parameter inverse problems. Non-uniqueness means that there may be many different sets of parameters \mathbf{m} which will predict the same observational effect (Tarantola 2005). It can happen, for example, when the observational data contain no information about the sought parameters or forward modeling results do not depend on the particular parameters. In any case, some sought parameters remain unresolved by experimental data. In such a situation, to obtain any solution we need to use an additional piece of information, called a priori information. It allows to choose the desired solution from the set of equivalent (from the observational point of view) models.

Let us consider the most often met inverse problem: a task of estimating unknown parameters. To achieve our goal we need:

- observational data
- a model (theory) which provides a theoretical prediction for any set of model parameters
- a priori information (expectations) about the sought parameters

All three elements: the data, model and a priori expectations provide us with some knowledge (information) about the problem. Experimental data tell us what the “reality” is. The model (theory) is a kind of theoretical knowledge (information) which allows us to predict the possible outcome of a given experiment. Finally, the a priori expectations come from subjective experience, previous experiments, knowledge accumulated during similar research and so forth. Thus, solving the parameter estimation task we actually use the above-mentioned three kinds of information and combine them into final a posteriori knowledge. Thus, inversion can be regarded not just as a mathematical method of fitting parameters to data but rather as a process of handling, accumulation and inference of pieces of information. This generalization which is the corner-stone of the probabilistic inverse theory (Tarantola 2005) allows to treat a variety of inverse problems like parameter estimation, error analysis, discrimination among different theories (models), planning new experiments and so forth in a homogeneous way.

Currently, the inverse theory faces now a new challenge in its development. In many applications, the classical solution leading to an optimum “best data fitting” model according to a selected optimization criterion is no longer sufficient. We need to know how plausible the obtained model is or, in other words, how large the uncertainties are in the final solutions (Malinverno 2002; Dębski 2010). Actually, the necessity of estimating the inversion uncertainties within the parameter estimation class of inverse problems is one of the most important requirements imposed on any modern inverse theory. It can only partially be fulfilled within the classical approaches. For example, assuming Gaussian-type inversion errors, inversion uncertainty analysis can, in principle, be performed for linear inverse problems (see, e.g., Zhdanov 2002), although in the case of large inverse tasks like seismic tomography this can be quite difficult (Nolet et al. 1999; Yao et al. 1999). On the other hand, in the case of non-linear tasks a comprehensive evaluation of the inversion errors is usually impossible. In such a case, only a linearization of the inverse problem around the optimum model allows the inversion errors to be estimated, provided that the original nonlinearity does not lead to multiple solutions, null space, etc. (see, e.g., Dębski 2004). The probabilistic technique based on the information inferring principle offers a very general, flexible and unified approach outperforms any classical inversion technique in such applications.

2.2 Inverse Problem: A Probabilistic Point of View

As already mentioned, solving the inverse problem can be regarded as an inference process in which available information is combined into the final, a posteriori knowledge of the system. The strict mathematical formulation of this inference

process has been proposed by Tarantola (2005) in terms of the probabilistic language. The main points are the following.

Following the Bayesian interpretation of mathematical notion of probability, all available information, including theoretical predictions, priori knowledge, and posteriori one, can be represented by probability distributions (Tarantola 2005). According to this reasoning, the solution of the inverse problem is not a single, optimum model, but rather the a posteriori probability distribution. This makes the most important difference with respect to the classical approach which casts the inverse tasks into the optimization, parameter-fitting type problem. The crucial point of this approach is the proper construction of the a posteriori probability providing we have all necessary a priori observational and theoretical information.

Let us denote the data and model spaces by (\mathcal{D}) and (\mathcal{M}), respectively. These are space of all possible values of the measurements (data space) and possible values of the model parameters (model space) (Tarantola 2005). Let the forward (modelling) task be described by the G operator acting between these two spaces (Eq. 1), allowing calculation of observational effects (d) for a given model m .

$$d = G(m) \quad (1)$$

Based on the Bayesian paradigm, each of the pieces of information we have in hand about d , m , and G can be described by an appropriate probability density functions (Tarantola 2005). We can join them using, for example, the Bayesian theorem to get the a posteriori probability $p(m|d)$ expressing our belief that the true value of the thought parameters is m provided that we have measured the data d and the relation between m and d given in Eq. 1 is subjected to some modeling errors described by a conditional probability $p(d|m)$. It reads (Tarantola 2005)

$$p(m|d) = k p_{apr}(m) p(d|m) \quad (2)$$

where k is the constant (normalization factor independent of m) and $p_{apr}(m)$ is the probability distribution describing the a priori information. The so-called likelihood function $p(d|m)$ being the conditional probability of predicting the data d provided the model parameters are m is often taken in the form (Tarantola 2005; Debski 2010)

$$p(d|m) = \exp(-||d^{obs} - G(m)||) \quad (3)$$

where d^{obs} are data measured in the experiment.

Having defined the a posteriori distribution, the question is how to inspect it to extract the required information. The point is that in most of practical cases the a posteriori *PDF* is a complicated, multi-parameter function. Basically, there are two different strategies to explore the a posteriori probability density function, either by the evaluation of some point estimators or by the calculation of the marginal a posteriori *PDF* distributions.

The first approach relies on calculation of some integrals, among which the most popular are the lowest-order moments of the a posteriori PDF (Tarantola 2005; Debski 2010):

1. The maximum likelihood model

$$\mathbf{m}^{ml} = \max_{\mathbf{m} \in \mathcal{M}} p(\mathbf{d}|\mathbf{m}), \quad (4)$$

2. The average model

$$\mathbf{m}^{avr} = \int_{\mathcal{M}} \mathbf{m} p(\mathbf{d}|\mathbf{m}) d\mathbf{m}, \quad (5)$$

3. The covariance matrix

$$C_{ij}^{PO} = \int_{\mathcal{M}} (\mathbf{m}_i - \mathbf{m}_i^{avr})(\mathbf{m}_j - \mathbf{m}_j^{avr}) p(\mathbf{d}|\mathbf{m}) d\mathbf{m}. \quad (6)$$

If a more comprehensive description of $p(\mathbf{d}|\mathbf{m})$ is required, higher-order moments can also be calculated (Jeffreys 1983).

The exhaustive description of the probabilistic inverse theory can be found, for example, in an excellent book by Tarantola (2005).

2.3 Practical Applications: Examples

For a long time the probabilistic inverse theory was treated as an interesting proposition of managing inverse problems but limited computational resources prevented using it in real geophysical applications. Situation started to change with a wide availability of high speed computers, and development of the very efficient numerical techniques of sampling in multidimensional spaces (see, e.g., Debski 2010; Sambridge 1999). Here we describe a few examples of such applications.

One of the first real seismological task which has been addressed by probabilistic inverse theory is location of seismic sources (Lomax et al. 2000; Gibowicz and Kijko 1994). In this problem we try to estimate the coordinates of hypocenter and rupture time of a seismic source on the basis of the recorded seismic waves. What probabilistic approach is bringing to the problem is an exhaustive and a reliable evaluation of location uncertainties (see, e.g., Lomax et al. 2000; Rudzinski and Debski 2012). It allows also a comprehensive analysis of efficiency

and accuracy of different location techniques (Rudzinski and Debski 2012) and seismic network sensitivity (Gibowicz and Kijko 1994). While in first applications of the Bayesian technique the source location problem was solved by using observed time onsets of given seismic waves, now it is possible to use the full seismograms to enhance the location reliability or to locate events like volcanic tremors, ice-quake tremors etc. (see, e.g., Larmat et al. 2008). The idea behind this approach relies in two elements: using the time-reversal symmetry of the wave equation to perform the back-propagation of the recorded signal (the so-called time-reversal mirroring; (Fink 1997) and performing implicit sampling simultaneously with back-propagation of the recorded seismograms.

Another seismological analysis where probabilistic approach has been proved to be very important is an analysis of kinematics of seismic sources including such detailed tasks like energy release, rupture duration, static and dynamic stress drop to name a few (Debski 2008; Kwiatek 2008). This, very fundamental seismological task requires a very careful analysis of inversion uncertainties, because the obtained results are being currently the only available observational information on rupture physics. Thus, their interpretation in terms of physical models of material failure is critically dependent on the inversion errors. Again, the probabilistic approach provides tools for the reliable estimation of the final uncertainties in the solutions found. Debski (2008) has managed to obtain the relative source time function for mining induced events with magnitude between 2.4 and 3.0. He has demonstrated that while the obtained source time functions suggested some complexity of the rupture process and two modal energy releases, the analysis of the a posteriori errors showed that such an interpretation has no justification. Kwiatek (2008) performed a similar analysis to check whether the complexity of calculated source time functions was only a numerical artefact or a reliable signature of the complexity of the rupture processes.

The maturity of the probabilistic inversion technique allows to apply the method to large scale inversion problems like tomographic imaging of the velocity heterogeneities at least in the regional or local scales (Debski 2013). Some first attempts of the full seismic waveform inversion have also been recently undertaken (Bodin and Sambridge 2009). In tomographic applications the possibility of evaluation of the reliability of obtained results is again the biggest advantage of the method. The fully nonlinear estimation of the a posteriori errors and their spatial distribution possible in the framework of the approach significantly outperforms other semi-quantitative methods based on various types of resolution tests (Debski 2013). Moreover, using the advanced techniques of exploring the a posteriori distribution based on trans-dimensional sampling techniques (Green 1995; Bodin and Sambridge 2009) allows to optimally adjust achieved spatial resolution to data at hand.

The applications of the probabilistic inversion, as discussed above, were essentially the classical parameter estimation tasks. What really brings the probabilistic technique to this problems is the possibility of an exhaustive error analysis. However, the power of the method is most apparently visible when non-parametric inversion tasks are concerned. One of such problems is discussed by (Debski and

Tarantola 1995) in the context of the AVO (Amplitude Vs. Offset) prospecting techniques. The question which authors posed and answered was whether the AVO data can distinguish between different sets of physical parameters used equivalently to describe the elastic medium. If so, which parameters are the best resolved by seismic data? This is an example of the non-parametric inverse problem, where we are interested not in an (accurate) estimation of numerical values of some physical parameters, but we are comparing different relations between physical parameters. The answer was, that in a wide angle refraction experiment the P-wave impedance contrast and the Poisson's ratio are best resolved by the data, while the density remains unresolved. A similar problem has recently been addressed in the context of verification of assumptions about characteristics of the a posteriori probability functions constructed for time-reversal based location algorithm when statistic of observational or/and modeling errors are unknown. None of these tasks can be easily treated with the classical approach.

3 Rotational Waves and Asymmetric Theory of Elasticity

Classical theory of elasticity (Aki and Richards 1985) which describes the behavior of the elastic material under a small external perturbation is the symmetric theory in the sense that the strain and stress tensors remain symmetric. Let us denote by u a displacement field in the body and let x_i be a set of Cartesian coordinates $x_i = (x, yz)$. Then, the strain tensor for infinitesimally small deformation u can be written down in the differential form (Aki and Richards 1985)

$$E_{ij}^c = \frac{1}{2} \left(\frac{\partial u_i}{\partial x_j} + \frac{\partial u_j}{\partial x_i} \right). \quad (7)$$

According to the constitutive relation, the deformation of the body described by the strain tensor E_{ij}^c is related to stresses acting on/within the body: any deformation rises internal stresses and vice versa any external load causes deformation of the body. In the case of perfectly elastic, isotropic and homogeneous medium, this constitutive relation takes the form of Hook's law

$$\sigma_{ij} = \lambda \delta_{ij} E_{kk}^c + 2\mu E_{jk}^c \quad (8)$$

where σ_{ij} is the stress tensor, δ_{ij} stands for the Kronecker's symbol, summation over repeated indexes is assumed and λ and μ are two Lame's parameters. This relation is symmetric with respect to interchange of i and j indexes.

The wave equation describing the propagation of small disturbances can now be obtained by equating the total internal forces $\partial \sigma_{ij} / \partial x_i$ to the derivative of momentum for infinitesimally small volume of body and reads (Aki and Richards 1985)

$$\rho \frac{\partial^2 u_i}{\partial t^2} = \sum_j \frac{\partial \sigma_{ij}}{\partial x_j} + F_i(x, t) \quad (9)$$

where a source term $F_i(x, t)$ describing external forces acting on the medium has been introduced. The solution of this equation consists of two types of waves called P and S waves propagating with constant velocities (Aki and Richards 1985; Gibowicz and Kijko 1994)

$$\begin{aligned} v_p &= \sqrt{(\lambda + 2\mu)/\rho} \\ v_s &= \sqrt{\mu/\rho}. \end{aligned} \quad (10)$$

These two types of waves differ essentially in the sense of movements of medium's particle through which waves are passing. In case of P waves, the particles are moving parallel to wave propagation direction. In case of the S-waves, the particle's displacement is perpendicular to the wave propagation direction and the waves can obviously have two perpendicular polarizations. From mathematical point of view, the P-wave corresponds to the solution with null rotation, while the S-wave is the solution with the null divergence. In this classical elastodynamics any mechanical wave in an infinite elastic body can be described as a superposition of these two waves.

However, as it has already been mentioned, the observations of damages caused by earthquakes provide evidence on rotational movements connected with seismic waves (Trifunac 2009; Zembaty 2009). Being inspired by this observation, Tessseyre and Gorski (2009) proposed another way of extending the classical elastodynamics towards the theory including rotational effects. The basic idea is to split the total (observable) rotations and displacements into elastic and "internal" or self-field components connected with existing internal micro-structure of the medium. This basic idea is implemented in terms of the shearing and rotational stress tensors rather than the displacements like in the classical approach (Tessseyre and Gorski 2007) The idea of using stresses as the "elementary fields" instead of displacements (deformations) comes from observations that in the solid continuum point transports and point rotations are actually non-important (rotations can even be hardly defined at the continuum level) but an important role is played by the deformations between neighborhood points, that is, the rotational and shear stresses. We shall come back to this point latter on.

The main points of the theory are following.

Let us consider waves propagation in solids. The wave motion equations follow directly from the derivatives of the classic Newton formula. Balancing all acting forces within the body we obtain the equation of motion similar to those in the classical elasticity theory. However, the deformation tensor E is now assumed to have both symmetric and antisymmetric parts and in general can be decomposed as follows

$$E_{ij} = \frac{\partial u_i}{\partial x_j}; \quad E_{ij} = E_{(ij)} + E_{[ij]} = \delta_{ij}\bar{E} + \hat{E}_{(ij)} + \check{E}_{[ij]} \quad (11)$$

where u is the displacement field, symbols (ij) and $[ij]$ stands for symmetric and antisymmetric parts of the appropriate tensors, $\bar{E} = \frac{1}{3} \sum_i E_{ii}$ describes the elastic

deformation part while $\hat{E} = E_{ij} - \delta_{ij}\bar{E}$ and \check{E} are symmetric and antisymmetric self-field deformations due to an internal micro-structure of the body. Similar decomposition expressions for stress tensor can be easily obtained assuming linear Hook's law (Teisseyre and Gorski 2007). The resulting set of equation describing propagation of seismic waves in the body reads

$$\begin{aligned} (\lambda + 2\mu) \sum_s \frac{\partial^2 E}{\partial x_s \partial x_s} - \rho \frac{\partial^2 E}{\partial t^2} &= 0 \\ \mu \sum_s \frac{\partial^2 \hat{E}_{(ij)}}{\partial x_s \partial x_s} - \rho \frac{\partial^2 \hat{E}_{(ij)}}{\partial t^2} + (\lambda + \mu) \left(3 \frac{\partial^2 \bar{E}}{\partial x_i \partial x_j} - \delta_{ij} \sum_s \frac{\partial^2 \bar{E}}{\partial x_s \partial x_s} \right) &= 0 \\ \mu \sum_s \frac{\partial^2 \check{E}_{[ij]}}{\partial x_s \partial x_s} - \rho \frac{\partial^2 \check{E}_{[ij]}}{\partial t^2} &= 0 \end{aligned} \quad (12)$$

where the external force term was omitted. When considering only shear and rotation strains (at constant pressure) we will obtain:

$$\begin{aligned} \mu \sum_s \frac{\partial^2 \hat{E}_{(ij)}}{\partial x_s \partial x_s} - \rho \frac{\partial^2 \hat{E}_{(ij)}}{\partial t^2} &= 0 \\ \mu \sum_s \frac{\partial^2 \check{E}_{[ij]}}{\partial x_s \partial x_s} - \rho \frac{\partial^2 \check{E}_{[ij]}}{\partial t^2} &= 0 \end{aligned} \quad (13)$$

The interpretation of the above relation is that during an earthquake, or other fracture process, a few mechanisms are activated. First seismic waves are generated following the release-rebound mechanism (see, e.g., Teisseyre 2011): molecular bonds are breaking in the source area which leads to a release of rotation and shear fields. They are subsequently converting each other: rotation generates a shear field and vice versa, release of shears are generating rotation strains. Without such a mutually combined system it is difficult to understand the related propagation motions at least at meter scales (seismological) much larger than typical scales for molecular dynamics.

A difference between the Classic and Asymmetric theories shortly sketched above follows from the assumption that we have a simultaneous appearance of a number of fields independently released; we admit an independent release of some physical fields, e.g., shear strains or rotation strains, in an earthquake source. Formally, these released fields might be expressed again by some displacements, but such displacements do not exist in a continuum—we prefer to treat them as the potential fields only. In fact the recording of the seismic waves, even very long, means that we record only the deformation which becomes integrated during an adequate time by a seismometer to reveal the displacement motion.

The assumption about symmetricity of the observed tensors leads to the constraints on the symmetric and antisymmetric parts of the total stress and strain tensors. Simplifying the problem one can say that the symmetric parts of tensors can now be connected mainly to the translational deformations while the anti-symmetric ones to the rotations of nuclei in the body. From seismological point of view, the most important conclusion of the theory is that an existence of grains (or other nuclei) within the crust (more generally some micro-structure) allows propagation of rotational waves—an additional type of elastic waves not predicted by the classical theory of elasticity.

The proposed antisymmetric elastodynamics is mathematically a very elegant theory and it is already supported by seismological observations. However, its importance goes much beyond seismology and is actually related to a very basic principles underlying the continuum mechanics. Let us shortly discuss this point. Any macroscopic, rigid body (when plastic effects, creeping, and similar non-elastic effects are excluded) has six degrees of freedom: three translations and three rotation. They are canonically connected to three components of the momentum vector and moment of momentum, respectively. The continuum mechanics is built under the assumption that a given medium can be described as a set of infinitesimally small elements for which all forces can be balanced and this way the equation of dynamic evolution is constructed. The limit of the infinitesimally small elements is necessary to describe the medium dynamics in terms of differential equation. However, a way of approaching this limit is by no means obvious. The classical approach leads to disregarding the rotation and moment of momentum of such infinitesimally small elements. In consequence, the strain and stress tensors becomes symmetric. The other approach leads to micromorphic continuum mechanics (Eringen 1999). The asymmetric theory discussed here is another attempt of dealing with this “limit problem” which could be applied at the seismological scales (1 m–1 km) without going to microscopic scale of, for example, the micromorphic model of Eringen (1999).

4 Flow of Incompressible Viscous Fluids in Porous Media

The modeling of porous media and fluid flows through the media has a significant role in the Earth sciences, i.e., geophysics, seismology, exploration of underground resources or CO₂ sequestration to name a few. The properties of permeability of porous media and physics of volatile transport through the medium play a crucial role in building of appropriate mathematical models to be used in practical applications. For example, in seismology the pore fluids are known to be factor very important in earthquake triggering. Secondly, exploration of natural resources, i.e., oil, gases, or geothermal heated water is related to flow through a porous strata. Contamination transport is another example of an application of poromechanics. Last but not least, the underground acoustics describes wave propagating in the uppermost part of the strongly water-saturated, porous, ocean-bottom sediment layers.

In continuum mechanics, there are at least two approaches of the description and modeling of porous media. One approach is the phenomenological one (Coussy 2004) whereas the other is based on a contemporary continuum micro-mechanics and mathematical methods, based especially on the theory of asymptotic homogenization (see, e.g., Mikelic 2000). We use the second approach which exploits micro-structure of the medium.

The main task of the description of the porous media is to determine the filtration law, the classic example of which is the so-called Darcy's law which states that

$$\mathbf{v} = -K(\nabla p - \mathbf{f}), \quad (14)$$

where \mathbf{v} is the vector of fluid velocity. K is positive permeability coefficient (matrix for anisotropic flows), p is a pressure and \mathbf{f} are forces (gravitational, for example).

The homogenization method is particularly convenient to address this issue, because it does not require any a priori knowledge of an infiltration mechanisms. It follows from the suitable assumptions on the micro-structure of a porous skeleton. Let us shortly discuss this task important for geophysical problems.

In seismology, it is important to study properties of one-phase fluid flow through a porous medium, linearly deformable, i.e., liable to a small elastic deformation. The presence of fluid is of importance here because it influences such characteristics of the medium like seismic wave speed, intrinsic attenuation or seismic wave anisotropy (see, e.g., Carcione 2001).

The fluid flow is governed by the non-stationary Stokes equation. In typical geophysical applications the fluid can be assumed incompressible, the Reynolds number is low and for simplicity the periodic micro-structure of the porous skeleton can be assumed. In this case, the homogenization can be carried out in the following way.

Let us denote by $\mathbf{u} = \mathbf{u}(x, t)$ and $\mathbf{v} = \mathbf{v}(x, t)$ the displacement vector of solid phase and the velocity field of fluid phase, respectively; the tensor of elastic properties of the solid part is referred to as \mathbf{C} , and \mathbf{F}^L and \mathbf{F}^S are forces of liquid and solid part, respectively. Tensor $\mathbf{e}(\mathbf{u})$ is the symmetric gradient of the vector field \mathbf{u} and reads

$$\mathbf{e}(\mathbf{u}) = \frac{1}{2}(\nabla \mathbf{u} + \nabla \mathbf{u}^T) \quad (15)$$

or in the index notation

$$e_{ij}(\mathbf{u}) = \frac{1}{2}\left(\frac{\partial u_i}{\partial x_j} + \frac{\partial u_j}{\partial x_i}\right). \quad (16)$$

The system of equations for fluid flow through an elastic skeleton now reads:

$$\varrho^S \ddot{\mathbf{u}}^e = \nabla \cdot \mathbf{C} \mathbf{e}(\mathbf{u}^e) + \mathbf{F}^S, \quad x \in \Omega_e^S \quad (17)$$

$$\varrho^L \dot{\mathbf{v}}^e = \varepsilon^2 \eta \nabla \cdot \mathbf{e}(\mathbf{v}^e) - \nabla p^e + \mathbf{F}^L, \quad x \in \Omega_e^L \quad (18)$$

$$\nabla \cdot \mathbf{v}^\varepsilon = 0, \quad x \in \Omega_\varepsilon^L. \quad (19)$$

where η is the constant viscosity of the fluid. Here ϱ^S and ϱ^L are mass densities of solid and fluid part, respectively. The small parameter $\varepsilon \ll 1$ is used to characterize the micro-structure of the reservoir Ω . In the process of homogenization, the small parameters tend to zero and the asymptotic solution is obtained.

The reservoir occupied by porous medium Ω is divided onto two parts, Ω_S^ε and Ω_L^ε . The subscripts S and L denote solid and liquid part of the reservoir Ω , respectively. Interface between Ω_S^ε and Ω_L^ε is denoted by Γ^ε . For the solid part, the equation of linear theory of elasticity is satisfied and in the liquid part the Stokes equation of incompressible fluid is valid. The appropriate boundary and initial conditions must be added according to a physical problem considered; for example, we can assume that $\mathbf{u}^\varepsilon = \mathbf{v}^\varepsilon$ on the interface Γ^ε . It means that in this case the so-called non-slip condition is posed.

Homogenization means passing with parameter ε to zero. The small parameter characterizes the ratio of diameter (d) of periodic cell Y and diameter of reservoir (D). Usually we set $\varepsilon = \frac{d}{D} << 1$. This method requires at least two scales, say macroscopic denoted traditionally by $x \in \Omega$ and the microscopic denoted by $y = \frac{x}{\varepsilon} \in Y$, where Y is the so-called periodicity cell.

Through homogenization of the Stokes equations we can obtain the effective infiltration law and the dynamic equations for the poroelastic medium. The obtained equations describing the non-local in time filtration law are much more general than the Biot model providing important extensions and can be expressed in the form

$$\mathbf{v}_{rel}(x, t) = \frac{1}{\rho^L} \int_0^t \mathbf{A}(t - \tau) (\mathbf{F}^L(\tau, x) - \varrho^L \ddot{\mathbf{u}}(\tau, x) - \nabla p(\tau, x)) d\tau, \quad (20)$$

where \mathbf{A} is the permeability tensor obtained from the solution of an auxiliary *local problem* on the periodicity cell Y described by a set of equations:

$$\varrho^L \dot{\mathbf{w}}^{(i)}(y, t) = \eta \Delta \mathbf{w}^{(i)}(y, t) - \nabla_y q^{(i)}(y, t) + \mathbf{e}^i \quad \text{in } Y \quad (21)$$

$$\nabla \cdot \mathbf{w}^{(i)}(y, t) = 0 \quad \text{in } Y \quad (22)$$

$$\mathbf{w}(y, t) = 0 \quad \text{on } \partial Y. \quad (23)$$

Then, the permeability matrix $\mathbf{A}(t)$ given by

$$A_{ij}(t) = \frac{1}{|Y|} \int_{Y_L} \frac{\partial \mathbf{w}^{(i)}(t, y)}{\partial t} \cdot \mathbf{e}_j dy \quad (24)$$

is symmetric and positive definite.

The results of the study on porous media using homogenization theory, are included in the papers, for example, by Bielski et al. (2001); Bielski (2005); Bielski and Wojnar (2008); Telega and Bielski (2003).

Another important case is the two-phase fluid flow, i.e., dynamics of two immiscible fluids in a porous medium. In this case, the flow is significantly influenced by the presence of capillary forces at the interfaces between two fluids.

Modeling of hierarchical porous media appears to be of significance since over 20 % of the world oil reservoirs are found in rocks with double porosity properties. Some of the first models were introduced by Warren and Root (1963). The issue of description of the double-porosity properties can also be conveniently undertaken using the homogenization method. In this case we assume two scales of rock porosity. The results of this approach and modeling of double-porosity media may be found in the paper by Bielski and Wojnar (2008).

Porous media frequently exhibit a random micro-structure. Thus, it is crucial to derive a stochastic model of the media. The book by Torquato (2002) summarizes the results of finding effective quantities for the media with random micro-structures. In the paper Telega and Bielski (2003) various approaches to micro-macro passage for random porous media were reviewed. The results obtained by stochastic homogenization are very similar to those obtained for periodic micro-structures and the macroscopic filtration law (generalized Darcy's law) is expressed as

$$E(\chi_F(v - \dot{u})) = \frac{1}{\varrho^L} \int_0^t A(t-s, \omega) [F^L(s, x) - \varrho^L \ddot{u}(s, x, \omega) - \nabla_x p(s, x, \omega)] ds, \quad (25)$$

where $E()$ means the expected value over the probabilistic space and ω is an element of this space. The permeability matrix is defined by

$$A_{ij}(t, \omega) = E(\chi_F(\omega) \dot{w}^{(i)}(t, \omega) \cdot e_j), \quad i, j = 1, \dots, n, \quad (26)$$

where e_j denotes the j th standard basis vector in \mathbb{R}^n . The matrix A_{ij} is symmetric and positive definite. The functions $w^{(i)}, q^{(i)}$ are solutions to the following flow cell problem:

$$\varrho^L \frac{\partial w^{(i)}}{\partial t} + \nabla_\omega q^{(i)} - \eta \nabla_\omega w^{(i)} = e_i \quad \text{on } (0, \tau) \times F, \quad (27)$$

$$\nabla_\omega \cdot w^{(i)}(t, \omega) = 0 \quad \text{on } (0, \tau) \times F \quad (28)$$

$$w^{(i)}(t, \omega) = 0 \quad \text{on } (0, \tau) \times \Gamma(\omega). \quad (29)$$

The details on this stochastic calculus and results obtained are discussed by Telega and Wojnar (2007). Finally, let us note that the study of porous media has become an interdisciplinary area and the range of scientific and engineering applications of the poro-mechanics is still increasing.

5 Conclusion

In this chapter we have presented some selected elements of theoretical, data processing, and mathematical tasks which appear in various aspects of the solid Earth physical analysis emphasizing contributions of authors to their formulation, development and applications. The selection is by no means complete and many important elements have been obviously omitted. We made it keeping in mind first of all our personal competence in their description and secondly trying to make the review logically consistent and concise. Some of the presented techniques are further discussed in more depth in other chapters of this book.

The selected topics illustrate the broad range of a scientific activity undertaken and continuing at the IGF PAS with respect to the solid Earth problems. They cover advanced mathematical methods, an attempt of building more realistic physical models of wave propagations, and finally the advanced technique of observational data analysis. These three elements form a kind of a “full chain” of methods used for solving problems at hand. Such an approach, always visible in IGF PAS activity, is motivated by two complementary factors. Firstly, by the fact that all research activity we undertook in the past and are also addressing today always refers to real problems met by seismology and physics of the Earth and all the elements mentioned above are usually necessary. The second factor is connected to different personal attitudes of researchers towards mathematics, theoretical physics, observational data analysis, and so on. The topics covered in this chapter are just illustration of these facts.

Acknowledgments The development of the Asymmetric Theory of Elasticity presented in this chapter was partially supported by the grant No. 2011/01/B/ST10/07305 from the National Science Centre, Poland. Anonymous reviewers and editors are acknowledged for their help in improving the manuscript.

References

- Aki K, Richards PG (1985) Quantitative Seismology. Freeman and Co, San Francisco
- Bielski W (2005) Nonstationary flows of viscous fluids through porous elastic media. Homogenization method. Publs Inst Geophys Pol Acad Sc A-29(388)
- Bielski W, Telega J, Wojnar R (2001) Nonstationary two-phase flow through elastic porous medium. Arch Mech 33:333–366
- Bielski W, Wojnar R (2008) Homogenisation of flow through double scale porous medium, Analytic methods of analysis and differential equations. AMADE 2006, 6(12):27–44
- Bodin T, Cambridge M (2009) Seismic tomography with the reversible jump algorithm. Geophys J Int 178(3):1411–1436. doi:[10.1111/j.1365-246X.2009.04226.x](https://doi.org/10.1111/j.1365-246X.2009.04226.x)
- Carcione J (2001) Handbook of geophysical exploration: seismic Exploration. Elsevier Science, Oxford
- Coussy O (2004) Poromechanics. Wiley, New York
- Debski W (2004) Application of Monte Carlo techniques for solving selected seismological inverse problems. Publs Inst Geophys Pol Acad Sc 34(367):1–207

- Debski W (2008) Estimating the source time function by Markov Chain Monte Carlo sampling. *Pure appl Geophys* 165:1263–1287. doi:[10.1007/s0024-008-0357-1](https://doi.org/10.1007/s0024-008-0357-1)
- Debski W (2010) Probabilistic Inverse Theory. *Adv Geophys* 52:1–102. doi:[10.1016/S0065-2687\(10\)52001-6](https://doi.org/10.1016/S0065-2687(10)52001-6)
- Debski W (2013) Bayesian approach to tomographic imaging of rock-mass velocity heterogeneities. *Acta Geophys* 61(6):1395–1436. doi:[10.2478/s11600-013-0148-7](https://doi.org/10.2478/s11600-013-0148-7)
- Debski W, Tarantola A (1995) Information on elastic parameters obtained from the amplitudes of reflected waves. *Geophysics* 60(5):1426–1437. doi:[10.1190/1.1443877](https://doi.org/10.1190/1.1443877)
- Eringen A (1999) Microcontinuum field theories. Springer, Berlin
- Fink M (1997) Time reversed acoustic. *Phys Today* 50:34–40
- Gibowicz SJ, Kijko A (1994) An Introduction to Mining Seismology. Academic Press, San Diego
- Green P (1995) Reversible jump Markov chain Monte Carlo computation and Bayesian. *Biometrika* 82:711–732
- Jeffreys H (1983) Theory of Probability. Clarendon Press, Oxford
- Kwiatek G (2008) Relative source time functions of seismic events at the Rudna copper. *J Seismol* 12(4):499–517. doi:[10.1007/s10950-008-9100-8](https://doi.org/10.1007/s10950-008-9100-8)
- Larmat C, Tromp J, Liu Q, Montagner J-P (2008) Time reversal location of glacial earthquakes. *J Geophys Res* 113(B09314):1–9. doi:[10.1029/2008JB005607](https://doi.org/10.1029/2008JB005607)
- Lomax A, Virieux J, Volant P, Berge C (2000) Probabilistic earthquake location in 3D and layered models: introduction of a Metropolis-Gibbs method and comparison with linear locations. Kluwer, Amsterdam. doi:[10.1007/978-94-015-9536-0_5](https://doi.org/10.1007/978-94-015-9536-0_5)
- Malinverno A (2002) Parsimonious Bayesian Markov chain Monte Carlo inversion. *Geophys J Int* 151(3):675–688. doi:[10.1046/j.1365-246X.2002.01847.x](https://doi.org/10.1046/j.1365-246X.2002.01847.x)
- Mikelic A (2000) Homogenization theory and applications to filtration through porous media, volume 1734 of Lecture Notes in Mathematics. Springer, Berlin. doi: [10.1007/BFb0103977](https://doi.org/10.1007/BFb0103977)
- Nolet G, Montelli R, Virieux J (1999) Explicit approximate expressions for the resolution and a posteriori covariance of massive tomographic systems. *Geophys J Int* 138(1):36–44. doi:[10.1046/j.1365-246X.1999.00858.x](https://doi.org/10.1046/j.1365-246X.1999.00858.x)
- Rudzinski L, Debski W (2012) Extending the double difference location technique—improving hypocenter depth determination. *J Seismol* 17(1):83–94. doi:[10.1007/s10950-012-9322-7](https://doi.org/10.1007/s10950-012-9322-7)
- Sambridge M (1999) Geophysical inversion with a neighbourhood algorithm—I. Searching. *Geophys. J. Int.* 138:479–494. doi:[10.1046/j.1365-246X.1999.00876.x](https://doi.org/10.1046/j.1365-246X.1999.00876.x)
- Tarantola A (2005) Inverse Problem Theory and Methods for Model Parameter Estimation. SIAM, Philadelphia
- Teissseyre R (2011) Why rotation seismology: Confrontation between classic and asymmetric theories. *Bull Seismol Soc Am* 101(4):1683–1691. doi:[10.1785/0120100078](https://doi.org/10.1785/0120100078)
- Teissseyre R, Gorski M (2007) Physics of basic motions in assymetric continuum. *Acta Geophys* 55(2):119–132. doi:[10.2478/s11600-006-0008-4](https://doi.org/10.2478/s11600-006-0008-4)
- Teissseyre R, Gorski M (2009) Fundamental deformations in asymmetric continuum: motions and fracturing. *Bull Seismol Soc Am* 99(2B):1132–1136. doi:[10.1785/0120080091](https://doi.org/10.1785/0120080091)
- Telega J, Bielski W (2003) Flows in random porous media: effective models. *Comput Geotech* 30(4):271–288. doi:[10.1016/S0266-352X\(03\)00003-X](https://doi.org/10.1016/S0266-352X(03)00003-X)
- Telega J, Wojnar R (2007) Electrokinetics in random piezoelectric porous media. *Bull Pol Acad Sci Tech Sci* 55(1):125–128
- Torquato S (2002) Random heterogeneous materials: microstructure and macroscopic properties, Vol 16. Springer, New York
- Trifunac M (2009) Review: rotations in structural response. *Bull Seismol Soc Am* 99(2B):968–979. doi:[10.1785/0120080068](https://doi.org/10.1785/0120080068)
- Warren J, Root P (1963) The bahaviour of naturally fractured reservoirs. *Soc. Petroleum Engrs.* 3:245–255

- Yao ZS, Roberts RG, Tryggvason A (1999) Calculating resolution and covariance matrices for seismic tomography with the LSQR method. *Geophys J Int* 138:886–894. doi:[10.1046/j.1365-246x.1999.00925.x](https://doi.org/10.1046/j.1365-246x.1999.00925.x)
- Zembla Z (2009) Tutorial on surface rotations from wave passage effects: stochastic approach. *Bull Seismol Soc Am* 99(2B):1040–1049. doi:[10.1785/0120080102](https://doi.org/10.1785/0120080102)
- Zhdanov MS (2002) Geophysical Inverse Theory and Regularization Problems. Methods in Geochemistry and Geophysics, Vol 36. Elsevier, Amsterdam. doi: [10.1016/S0076-6895\(02\)80037-3](https://doi.org/10.1016/S0076-6895(02)80037-3)

Application of Passive Hydroacoustics in the Studies of Sea-Ice, Icebergs and Glaciers: Issues, Approaches and Future Needs

Oskar Glowacki and Mateusz Moskalik

Abstract Arctic and Southern Oceans are extremely noisy places. Various geophysical and biological processes generate underwater sounds at different frequencies. Using spectral, wavelet and statistical analysis, it becomes possible to distinguish almost all individual phenomena. This allows the assessment of, among other things, the rainfall intensity, various characteristics of wind-generated waves, abundance of marine organisms and shipping traffic. These issues are now relatively well-understood. What is more, for such studies hydroacoustic methods have been widely used for many years and provided satisfactory results. In the last decades, however, more and more attention is paid to sea-ice processes and properties, calving events and drifting icebergs. Melting ice and retreating tide-water glaciers are also sources of underwater ambient noise. This becomes more and more noticeable due to the observed climate shifts. Dynamic nature of these phenomena and harsh conditions encountered during field measurements still limit the progress in this area of research. In spite of all, recent preliminary studies show the possibility of using passive acoustic methods for both analyzing calving events in the Arctic fjords and investigating the behavior of icebergs. It became possible, for instance, to identify and describe various stages of calving processes: large rumbles, ice fractures, impacts on the water and iceberg oscillations. On the other hand, ambient noise related with freshwater outflows and sound propagation in the vicinity of glaciers are still unstudied. Moreover, underwater sounds associated with sea-ice processes occurring in small basins are also poorly understood, as well as their directivity and relationships with meteorological and oceanographic conditions. These topics require further investigation, which will enable the development of appropriate classification algorithms. For this purpose, new field experiments and methods of data analysis as well as state-of-the-art measuring devices are needed. A review of existing research articles concerning underwater cryogenic sounds is presented here, supplemented by a summary of the main gaps

O. Glowacki (✉) · M. Moskalik

Department of Polar Research, Institute of Geophysics, Polish Academy of Sciences,
Ksiegia Janusza 64, 01-452 Warsaw, Poland
e-mail: oglowacki@igf.edu.pl

and suggested future needs. All papers are sorted thematically and chronologically, showing the historical development of hydroacoustic methods and approaches in this area.

Keywords Underwater acoustics • Sea-ice • Icebergs • Glaciers • Calving events

1 Introduction

Recently observed global climate shifts result in increasing attention devoted to the Polar Regions and natural phenomena occurring in these areas. A large amount of fresh water provided by melting ice sheets, tidewater glaciers and icebergs (Meier et al. 2007), together with shrinking sea-ice cover in Arctic (e.g. Stroeve et al. 2007; Comiso 2012; Overland and Wang 2013), have become the major reasons for carrying out a number of research projects in high latitudes.

Remote sensing methods allow for continuous monitoring of the changing multiyear ice extent and sea level rise. Technological progress made it possible to acquire satellite images with high spatial and temporal resolution. Moreover, new numerical models and classification algorithms are still being developed as well. However, it is problematic to obtain information about the processes taking place in smaller scales, i.e. fjords, bays or straits. The complexity of mechanisms that are of interest forces the need to take them into account. Hence, basic knowledge of the sea-ice coverage in the Arctic, the rate of its transport, current area of glaciers or weather conditions is insufficient. Therefore, it is essential to use new tools in order to effectively investigate such phenomena as calving events, behavior of drifting icebergs and the development and evolution of various forms of sea-ice, characterized by a distinct resistance to mechanical deformations. Furthermore, difficulties resulting from the harsh polar conditions necessitate the use of automated measuring systems, which do not require constant human interventions.

New opportunities in this area are offered by passive and active underwater acoustics. Sound easily propagates in the water over long distances, allowing for non-invasive acquisition of information on various anthropogenic and natural events (e.g. Knudsen et al. 1948; Wenz 1962; Dahl et al. 2007; Hildebrand 2009). Importantly, the costs of research are relatively low compared with the use of satellite remote sensing methods. Depending on the needs and capabilities, analysis of underwater noise produced by individual objects or acoustic signals recorded after reflection or scattering of sound with specific amplitude-frequency characteristics is applied. In the last few decades, much attention has been paid to the use of hydroacoustic methods in the studies of sea-ice processes and properties. Furthermore, latest field experiments show their applicability for investigating the dynamics of tidewater glaciers and drifting icebergs. The usefulness of this approach for assessing information about strength of the relationship between various elements of the polar environment and meteorological and oceanographic

conditions was also demonstrated. Scientific projects were carried out in many aspects with consideration of different spatial and temporal scales.

This chapter presents an overview of hydroacoustic methods and tools already in use in the study of previously mentioned processes. What is more, future needs and gaps in knowledge are presented as well, together with the suggestions for further work.

2 Sea-Ice Dynamics, Properties and Sound Propagation Beneath the Sea-Ice Cover

Shrinking multiyear ice cover observed in the Northern Hemisphere is a visible effect of advancing climate shifts (e.g. Comiso 2012; Stroeve et al. 2012; Overland and Wang 2013). Sea-ice minimum extent in 2007 was the reason for speculations about the possible ice-free conditions in the summer of 2030 (Stroeve et al. 2007). Therefore, much attention is paid now to deepen our knowledge about the sea-ice processes and properties. For this purpose, satellite remote sensing is widely used and provides satisfactory results, especially for large-scale issues (e.g. Kwok 2011; Laxon et al. 2013). However, hydroacoustic methods have also been developed and applied since the 1960s. Hydroacoustics, in particular, gives the ability to perform continuous measurements in harsh polar environment without incurring large costs. Moreover, underwater acoustics can be used in small basins like fjords and bays, where satellite remote sensing does not provide sufficient spatial and temporal resolution. There are three main sea-ice related processes that generate underwater sounds: ice floe collisions, thermal cracking and interactions with waves (Fig. 1). Many authors have conducted hydroacoustic studies of sea-ice dynamics, properties and sound propagation beneath sea-ice.

Milne and Ganton (1964) made one of the first significant steps. They recorded ambient noise under the sea-ice cover in the Canadian Archipelago in three different environmental conditions: the late-summer, winter and spring. All measurements were performed using bottom-mounted or lowered hydrophones. Underwater sounds were recorded during short sessions lasting up to several minutes with various intervals. The authors demonstrated large variability of the characteristics of recorded ambient noises. They suggested the existence of two fundamental mechanisms of sound generation under the sea-ice cover: thermal stresses in winter and spring, and the movement of ice floes in late-summer. However, according to the authors, part of the signal well above instrument noise was produced probably by wind-driven granular snow moving along the surface of the ice cover. Milne and Ganton also showed that underwater sounds recorded under the sea-ice are mostly impulsive and sometimes highly non-Gaussian, which is different from the situation observed during ice-free conditions. What could be a little bit surprising, the noise levels in winter were often the same as for sea-state three.

Greene and Buck (1964) conducted hydroacoustic measurements in the Beaufort Sea during a two-week experiment in April 1963. They lowered a hydrophone 61 m

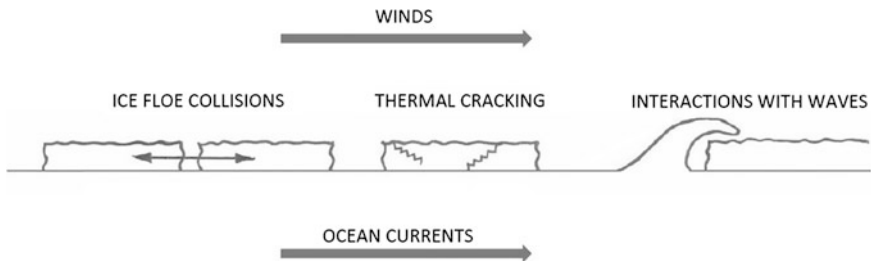


Fig. 1 Main sea-ice related processes that produce underwater ambient noise together with the most important external forces

below the surface from one of the ice floes. The primary objective of the study was to find spectral, directional and statistical properties of the underwater sound in the Arctic Ocean. The authors calculated daily-averaged spectrum levels for the frequency range 25–1000 Hz and, after further averaging over 3-day periods and finding the straight-line fit, compared their results with Knudsen's sea-state curves. The obtained curve was 6 dB above sea-state zero (extended) for 25 Hz. A correlation coefficient for the wind speed and spectrum levels at 50 Hz reached 0.47. A second hydrophone was lowered at a horizontal distance of 300 feet from the previous one to study the directionality of underwater sounds at two frequency ranges: 5–1,000 Hz and 20–60 Hz. Finally, probability-density analysis was performed for samples of the signal recorded during "noisy" conditions and "quiescent" periods to determine whether they are normally-distributed or not. Results showed that underwater sounds tend to be more Gaussian with increasing depth. Greene and Buck suggested that the recorded ambient noise may be more impulsive (and non-Gaussian) close to the ice cover due to the presence of ice cracking and popping events.

Other studies were carried out by Diachok (1976), who investigated the role of sea-ice ridges in influencing sound propagation patterns. For this purpose, he presented newly-developed heuristic under-ice reflection-model taking into account signal losses associated with the existence of these forms. Several parameters were chosen as the inputs for the model: numbers of ridges per km, grazing angle and average keel width and depth. Sea-ice ridges were considered as randomly distributed and infinitely long elliptical cylinders. Typical sound velocity profile, characteristic for the Arctic Ocean, was adopted for the calculations. Moreover, the complicated problem concerning high-frequency transmission losses occurring in the water column was taken into account. The results generated by the model showed reasonably good agreement with experimental data, which proved the validity of the assumptions. They demonstrated that their model can be also useful for frequencies below 50 Hz. However, in this case one must keep in mind uncertainties associated with the source levels, ray-theory computations and reflection-loss model. Finally, the authors pointed out the need for further experimental studies, including, e.g., sonar measurements of the sea-ice ridges.

Nielsen and Thomas (1987) focused on the analysis of a single recording lasting ~ 10 min in order to statistically describe the under-ice environment. The data was recorded in the Arctic Ocean from an ice floe in April 1980 using an omnidirectional hydrophone lowered to a depth of 91 m. Basing on five adjoining subsamples, each lasting about half a second, the authors generated empirical probability density function (pdf) plots of the signal's amplitude and showed that a member of the generalized Gaussian family can be used to model under-ice ambient noise. The performance levels of four detectors were compared to evaluate the effectiveness of the model: linear, amplitude limiter, time-varying linear and time-varying generalized Gaussian detector. However, none of the detection methods was significantly better than the others. The authors also computed power spectra for 0.5 s fragments of the signal using whole data set and found the unexpected relationship between its overall shape and the shape of the pdf. Moreover, they applied an adaptive notch filter to separate the sinusoidal signal (non-Gaussian) from the background noise (considered to be Gaussian). Their results demonstrated the potential of this method in removing narrowband components from the fragments containing a high-powered tonal, which in turn leads to the creation of nearly Gaussian signal. As emphasized, this is only possible when the distribution of original noise is not heavy-tailed.

Lewis and Denner (1988a) conducted a statistical study on the relationships between sea-ice kinematics and the properties of underwater ambient noise. The acoustic signal was recorded in the Beaufort Sea during the Arctic Ice Dynamics Joint Experiment (AIDJEX). Five components of the motion of ice parcel were obtained using satellite tracking system: shear deformation rate, normal deformation rate, vorticity, divergence, and translation rate. The authors calculated correlation coefficients between these kinematic parameters and their combinations and underwater ambient noise levels at 10, 32 and 1,000 Hz, taking into account parameterization of ice microfracturing generated by sensible heat flux. The analysis showed that summer sounds at all three frequencies are produced primarily by the sea-ice drift. During the fall, in turn, signals at 10 and 32 Hz are best correlated with the total change in shape in linear combination with the speed of ice parcel. This emphasized the role of colliding and reshaping ice floes in sound generation. Other kinematic parameters, such as ice convergence, were found to be responsible for lower frequency noises, but only during the winter season. In general, low correlation coefficients were reached for sounds at 1,000 Hz during fall and winter. The results of performed studies indicated a lack of knowledge about the origin of high-frequency sounds propagating in the Arctic Ocean.

This issue was further investigated by the same authors basing on previously described data set (Lewis and Denner 1988b). The authors selected recordings from nonsummer periods in order to find mechanisms responsible for the production of ambient noise at 1,000 Hz. They showed that thermal cracking is one of the main producers of higher frequency sounds, especially when amplitudes are larger than $10^3 \mu\text{Pa}$. Moreover, numerical simulations taking into account the daily heating cycle demonstrated that during periods without snow cover the maximum noise levels typically occurs in the evening, about 7 pm. Lewis and Denner made

the important point that sensible heat flux seems to have less impact on fracturing intensity than radiation heat balances. However, as emphasized by the authors, the ice fog and blowing snow may be important factors affecting the heat flux balance. Consequently, these phenomena can influence the generated ambient noise. According to the authors, it should also be kept in mind that ice drift explains up to 50 % of the variance of nonsummer underwater sound at 1,000 Hz. Finally, the obtained results indicated that sea-ice fracturing may produce ambient noise in wide bandwidth, i.e., down to 32 Hz.

Pritchard (1990) presented a new numerical model simulating underwater acoustic signal produced in compact sea-ice cover by various processes: mixed layer shearing, ridging and microcracking. Sound intensity was described in the proposed model as a sum of both these three different processes and the sum of intensities radiated from all source locations. An empirical propagation law, taken from the literature, was used in this work. Each process they considered, having its own spectral signature, is driven by a different environmental factor. Among these key variables, the author mentioned ice velocity (relative to the currents) and small-scale stresses and deformations (caused by both wind and currents). For the modeling purposes, these driving forces were converted to energy dissipation. Effects associated with changes in temperature were not taken into account. Pritchard showed that the model successfully simulated the characteristic of ambient noise measured under the Coordinated Eastern Arctic Experiment (CEAREX) in October 1988. Temporal variations in the ambient noise intensity at 31.5 Hz were well-reproduced by pressure and shear ridging and mixed layer shearing. Microcracking processes were not active during the analyzed period. One of the main conclusions of the study is that our knowledge about sea-ice processes and properties can be used in forecasting ambient noise levels in the Arctic Ocean.

Zakarauskas and Thorleifson (1991) lowered four hydrophones beneath the sea-ice cover over the Arctic continental shelf to measure the vertical directivity of ice cracking events. Instruments were spaced apart by 100 m along the vertical linear array. A bandpass filtration at the frequency range 40–1,250 Hz was applied. All acoustic pressure peaks extracted from 341 s sample of the signal were identified as potential indicators of sea-ice fracture events. The obtained results showed that most of the incoming sounds are arriving from directions 0–25° below the horizontal. In order to explain this situation, authors developed simple sound propagation model based on the ray theory and showed that the asymmetry in the angular distribution resulted from the source directivity. Acoustic rays refracted in the water column or reflected from the seabed usually arrived at negative angles. During these studies, the best fit to the measured data was produced by a dipole source. The results generated by the proposed model showed that angular distribution is generally insensitive to the type of bottom and to the features of source strength probability function. Finally, as was suggested, the angular distribution of the arriving ambient noise depends mostly on depths at which sensors are lowered.

Cousins (1991) conducted hydroacoustic measurements northeast of Svalbard under the previously mentioned CEAREX experiment. He recorded underwater

ambient noise beneath the ice using two omnidirectional hydrophones deployed at depths of 60 and 90 m. Samples lasting half a minute were averaged hourly in order to obtain 38-day time series at 10, 31.5 and 100 Hz. The mean noise levels in the investigated region were up to 30 dB higher than those usually recorded in the central part of the Arctic Ocean. Particularly active ridging processes occurring to the north of the Svalbard Archipelago were indicated as mechanisms responsible for this situation. However, the main objective of the study was to find relationships between the acoustic signal and various environmental components. Therefore, recorded ambient noise was correlated with the ice motion, air temperature and hourly-averaged wind speed. Cross-correlation coefficients about 0.4 were reached between underwater sound levels at all three analyzed frequencies and locally-measured averaged wind speed, with e-folding time reported to be 16 h. What is interesting, when the speed was rising above critical value of 12 m/s, the spectrum levels were no longer sensitive to the changing wind forcing. The coefficients for ice motion were similar for 10 and 31.5 Hz and slightly lower for 100 Hz. No relationship, in turn, was found for air temperature at 100 Hz, while for 10 and 31.5 Hz the correlations were significant. In general, the author showed that sea-ice movement is one of the major mechanisms controlling ambient noise levels. However, some exceptions were observed during periods with tidal/inertial oscillations contrary to the mean direction of the ice drift. Finally, Cousins pointed to the need of detailed measurements of ocean currents.

Xie (1991) investigated similar issues, but extended the study to mechanical properties of the sea-ice. He used data sets collected under two field experiments carried out in the Beaufort Sea and Central Canadian Arctic. The author paid particular attention to the cracking sounds generated by both multiyear ice and first-year ice. Images from synthetic aperture radar and other devices were analyzed to find relationships between the ambient noise recorded by a 3-D hydrophone array and different sea-ice types. According to Xie, when there is no snow cover, irregular multiyear ice produces most of the sounds associated with thermal cracking. What is interesting, in some cases the acoustic energy originating from smooth first-year ice radiated more horizontally than vertically. After obtaining these results, the author developed various analytical models, which made it possible to relate the characteristics of recorded ambient noise with thickness and Young's modulus of the sea-ice cover, as well as with the depths and lengths of the cracks. Moreover, the models showed that maximum acoustic energy originated from cracking events is usually radiated in direction of external forcing. Finally, a narrow band spectrum appeared during ice floe collisions. Further investigations with an application of the linear model demonstrated that frictional effects taking place at the ice floe edges are responsible for the peaks in frequency.

The same studies were continued and expanded by Xie and Farmer (1991). According to the authors, it was relatively easy to locate ice cracking events using 3-D array of hydrophones, located between first-year and multiyear ice cover. Moreover, thermal cracking processes occurring within the older sea-ice caused most of the recorded ambient noise. The authors applied a plate vibration theory and observed that angular distributions of the radiated sound were successfully

predicted. However, finite volume displacement theory seems to be more appropriate for larger cracks. Furthermore, Xie and Farmer observed that significantly shorter cracking noises were produced by the first-year ice. In order to investigate ambient noise produced by artificial sources and to partially evaluate elastic properties of sea-ice, they also performed an experiment with a hammer blow on the ice. In this case, the dominant frequency rose up to about 640 Hz with decreasing radiation angle, directly related to the increasing depth at which the hydrophone was deployed. The authors suggested that further description of sea-ice physics is needed to explain the reported phenomena.

Greening et al. (1992) presented observational and modeling study expanding earlier preliminary considerations about vertical directivity of ambient noise produced by ice-cracking events (Zakarauskas and Thorleifson 1991). Underwater sounds were recorded below the Arctic ice cover using twenty-two hydrophones creating a vertical array. The authors analyzed a total of 160 events with source angles between 1 and 80° and horizontal ranges of 40–2,000 m. They demonstrated that the directivity of the source pressure can be accurately fitted to a dipole when the range is greater than or equal to 40 wavelengths. A slightly different situation was reported for the shorter ranges due to the perturbations caused by several troughs and peaks occurring at varying angles. Moreover, for the angles from 60 to 65°, approximately 3-decibel rises in the pressure levels in relation to a dipole pattern were usually observed. The authors explained that this effect was induced by the coincidence between the acoustic mode at these source angles and the leaked longitudinal plate wave. In general, about 60 % of ice-cracking events fitted the proposed model with an average deviation remaining less than 0.75 dB.

Fricke and Unger (1995) conducted laboratory experiments and applied numerical and analytical methods to analyze scattering from elemental sea-ice features. The main objective of the study was to test the conjecture that old keels should be considered in models as elastic structures, while young keels are better represented by fluid structures. To simulate the natural conditions, different polypropylene materials were used as both types of keels. Laboratory tank with a pulse sound source characterized by the central frequency of 60 kHz was chosen as a location for the study. The results supported the previously mentioned conjecture concerning scattering characteristics of young and old keels. The authors suggested that a census of ridge types existing in the Arctic Ocean is needed in order to better reproduce natural conditions and more accurately estimate the propagation losses. However, Fricke and Unger emphasized that demonstrated outcomes may simplify the analytical modeling.

Ye (1995) investigated the process of underwater ambient noise generation by ice floe rubbing. The author developed a simple numerical model to characterize the horizontally polarized shear wave (SH) produced in the sea-ice during the occurrence of this phenomenon. Several limiting assumptions were made: displacement-independent rubbing stress, flat ice-water and ice-air boundaries, no sound attenuation and constant rubbing speed in one simulation. According to Ye, the lack of the first or last of these limitations would lead to nonlinearity and significant increase in complexity of the problem. The obtained results showed that

broadband sounds are possible when the rubbing speed is higher. For a smaller speed, the low-frequency modes seemed to dominate quite often. The author also demonstrated that the roughness of rubbing surfaces may be an important factor affecting the properties of generated SH waves and the resulting underwater sound. Moreover, Ye found an analogy between the discussed issues and the problems encountered in earthquake mechanics during the modeling of ruptures. Finally, he emphasized the need to conduct new experimental and theoretical studies as a requirement for further development of the proposed model and improving our knowledge about the relationships between sea-ice processes and underwater ambient noise.

Laible and Rajan (1996) studied temporal evolution of the sound reflection coefficient (R) at the ice-water boundary for the underwater noise. The research was based on the tomography experiment conducted between April 1992 and April 1993 in Sabine Bay of Melville Island. Both horizontal and vertical arrays of sixteen transmitters and fifteen receivers (in total) were used. Each of the transmitters, embedded in the ice or deployed in the water, was omnidirectional and set to generate sound at 12 kHz. Acoustic properties of the multiyear ice (including in particular the reflection coefficient) as a function of time were investigated together with the ice thickness and the roughness of its underside. Besides, the authors also calculated propagation times for different receiver-source pairs. Experiments were carried out every 3 days. Laible and Rajan found that for specular reflection grazing angles ranged from 20.2° in April 1993 to 26.9° in June 1992. A thermodynamic ice-growth model and an elastic model were developed to simulate sea-ice salinity, temperature and shear wave speeds. Finally, reflection coefficients were calculated for different input parameters and compared with those obtained from field measurements. Results showed that correlations between the modeled and measured R exist for the period from September to April. For the remaining months there was no correlation, which may be associated with changes in the properties of water column.

Gavrilov and Gudkovich (1996) presented results of their analysis of the relationships between mean square noise levels measured beneath the sea-ice and both wind speed and sea-ice deformation rates. The authors used experimental data collected in 1966–1967 on the drifting research station. Gavrilov and Gudkovich showed that the dynamic phenomena in the sea-ice cover results in the generation of specific underwater sounds. The main conclusion of this study is that knowing the relationships between ambient noise propagating under the sea-ice and various variables, such as wind velocity, air temperature and sea-ice divergence or convergence, it may be possible to obtain the equation of multicorrelation and estimate the stressed state of the ice cover.

Greening et al. (1997) applied the matched-field processing in order to investigate the possibility of localizing the broadband sources when the environmental conditions are poorly known. The author used simulated annealing inversion to search for the best match between the modeled and measured fields. This technique involves numerous perturbations of unknown parameters in a series of iterations. For more details, the reader is referred to the original paper. Presented

methods were illustrated on the process of creation of ice-ridges in the Arctic Ocean with nearly unknown bathymetry. Many aspects were taken into consideration, including the importance of simultaneous localization, the number of sources and the effect of errors in the bathymetry on the localization accuracy. The authors demonstrated that the proposed method provides a tool to localize multiple synthetic sources. They showed that such a situation occurs particularly when the spectral shape is known and the distance between the sources is relatively large. Finally, the data from ambient noise measurements conducted in the Lincoln Sea were also analyzed. A small number of the ridging sources were found sufficient to simulate measured fields.

Shaw (2000) investigated slightly different issues. A set of ambient noise data, recorded by two drifting buoys under the Surface Heat Budget of the Arctic Ocean (SHEBA) project in the period from 1997 to 1998, was used to characterize underwater sounds generated by the sea-ice activity in the Arctic Ocean. The information about sea-ice processes and properties were, in turn, obtained from the Polar Ice Prediction System (PIPS) and Radar Satellite Geophysical Processor System (RGPS) in order to identify the mechanisms responsible for the noise production. The conducted study demonstrated that during the winter the loudest sounds are radiated from pressure ridges, formed by eddy-like motions and the resulting strong convergence. However, the median winter noise levels were lower than those previously recorded in the same region. According to the authors, this situation was a result of the low number of storms. As a confirmation, a close relationship between the wind stress and recorded ambient noise was revealed in the cross-correlation analysis. Moreover, several observed and characterized events showed that distant processes can significantly affect the sound field. In general, one of the main conclusions is that the outputs from RGPSS (deformations rates) and PIPS (energy dissipation rate) systems may be potential inputs for the ambient noise models simulating the underwater sounds propagating beneath the ice cover.

Stamoulis and Dyer (2000) analyzed acoustic signals recorded during the Sea-Ice Mechanics Initiative (SIMI) experiment in 1994. The main objective of the study was to estimate the speed of sea-ice fracture events. The authors assumed in their work that each crack propagates unidirectionally. A total of 186 events were taken into consideration. In order to obtain the fracture velocity and orientation (strike angle), the motion-induced Doppler shifts were calculated and found to fall between 1 and 90 Hz. The fracture propagation speed was, in most cases, subsonic, i.e., in the range of 100–1100 m/s. In the previous studies, the Rayleigh wave speed (1,700 m/s) was usually posited for phenomena of this kind. Finally, the author concluded that a large variation in the obtained velocities can be caused by both the existence of different propagation stages in individual events, or of multiple fractures occurring simultaneously.

Gavrilov and Mikhalevsky (2006) conducted hydroacoustic research during the Arctic Climate Observations Using Underwater Sound (ACOUS) experiment. They investigated low-frequency propagation loss within the water column and its dependence on the seasonal changes of the sea-ice thickness. For this purpose, an

acoustic signal at a frequency of 20.5 Hz was generated every 4 days northwest from Franz Josef Land between October 1998 and December 1999. Receiving stations with vertical arrays of hydrophones were located at the ice camp APLIS in the Chukchi Sea north of Point Barrow, Alaska (2,720 km away) and in the Lincoln Sea (1,250 km from the source). The temporal variation in the sound velocity profiles, mode-coupling effects and the influence of sea-ice parameters were studied. The authors developed a numerical model of seasonal changes in sea-ice thickness to compare experimental data with performed simulations. They also used some upward-looking sonar observations to obtain comparative sea-ice draft on the analyzed path. Gavrilov and Mikhalevsky showed that modeling results are basically in agreement with fieldwork data. Thus, it was possible to correlate changing (temporally and spatially) sea-ice thickness with acoustic propagation loss. These results provide evidence that it may be possible to assess the thickness of Arctic ice using underwater remote sensing. However, according to the authors, transmitting the signal at a slightly higher frequency (e.g. 23 Hz) or locating the source and receivers into deeper waters would probably minimize interactions with seabed and improve the quality of the data.

In December 2009, Matsumoto et al. (2009) carried out hydroacoustic monitoring of the Scotia Sea near the South Georgia Island using five autonomous hydrophones (AUHs). The primary objective was to study ambient noise conditions across an area of 86,000 km². The authors expected that the results will help to differentiate naturally-generated sounds from anthropogenic noise produced by possible nuclear weapon tests. They presented a preliminary analysis of the 16-bit signal recorded during the 13 months of experiment, which illustrated typical bell-shaped ambient noise pattern. The formation of sea-ice cover and the activity of kinematic processes taking place during the fall were successfully captured. Moreover, the maximum ice extent observed in winter also had its own specific acoustic characteristics, which confirmed the significant seasonality of the ambient noise propagating in the Southern Ocean. What is extremely important, the AUHs recorded twice as many ice-related events than seismic stations located on land in different locations. This proved, among other things, the validity of the use of acoustic methods in the study of sea-ice processes and properties.

Nystuen (2011), in turn, presented various studies showing the possibilities offered by underwater acoustics in quantifying physical processes taking place in the marine environment. The author used data collected from the low-noise Passive Acoustic Listeners (PALs) with a low duty cycle around 1 % and high bandwidth (50 kHz). Among a variety of ambient noise sources, the importance of sea-ice was emphasized and some preliminary classification diagrams were also presented. As was proposed, distinctive spectral characteristics associated with different ice conditions, such as freezing ice, solid ice, melting ice or ice edge storm, may be useful in developing algorithms which will allow the remote identification of sea-ice types and extent. In this study, the ratio between sound levels at 8 kHz and spectral slopes from 8 to 20 kHz was chosen as a classification parameter. In general, Nystuen showed that underwater ambient noise recorded in Polar Regions potentially contains a lot of information about sea-ice processes,

coverage and its stage of development. Importantly, as is apparent from the first attempts of classification, the analysis of acoustic signals can help to obtain this information.

Roth et al. (2012) focused on the relationship between various sea-ice conditions and corresponding ambient noise. The analyzed acoustic signals were recorded on the continental slope by High-frequency Acoustic Recording Package (HARP) north of Barrow, Alaska, in the period from September 2006 to June 2009. Properties of the underwater sounds radiated during months with sea-ice coverage and both low wind and moderate wind speed were compared with the characteristics of ambient noise generated in open water conditions. Spectrum levels calculated for these three specific periods reached respectively the values of 65 dB re 1 $\mu\text{Pa}^2/\text{Hz}$ at 50 Hz, 70 dB at 50 Hz and 80–83 dB at 20–50 Hz. Moreover, fracture events observed in winter and in the first half of spring were found to be responsible for significant transient energy in the frequency range between 10 and 100 Hz. However, the authors reported much fewer transients in May, despite the fact that the ice cover was still present. This is probably the result of changing atmospheric forcing, which determines the formation of fractures. As a confirmation, it was demonstrated that ambient noise levels usually increased with wind speed by around 0.5 dB/m/s for almost complete sea-ice cover.

Alexander et al. (2012) studied the propagation of underwater sound beneath the sea-ice cover, thus continuing the research carried out by Gavrilov and Mikhalevsky (2006). At the beginning, they emphasized that correct modeling of the ambient noise in Polar Regions requires the solution of two problems: temporal and spatial variability of sea-ice properties and resulting changes in propagation losses. In order to simulate sound propagation paths, BELLHOP module of the Acoustic Toolbox from The Ocean Acoustic Library (<http://oalib.hlsresearch.com/>) was applied and tested with different input parameters. Furthermore, two ice canopy profiles measured by upward looking sonar mounted on a nuclear submarine were also implemented together with calculated statistics of the scattering parameters of sea-ice to model the impact of ice ridges. The coherent transmission loss and ray traces were derived using Gaussian beam tracing mode. Then, some advantages and limitations of the presented methods were discussed and few recommendations for future work were also proposed. Among them, the authors listed three main needs as the most crucial: implementation of better elastic properties, new statistical methods for describing environmental conditions, and the capability of determining the sea-ice properties at a given point and time.

Finally, the obtained results inspired the same research team to expand the study (Alexander et al. 2013). The authors carried out the research in order to provide a more detailed prediction of the sound field occurring beneath the sea-ice and, thereby, support deployments of Autonomous Underwater Vehicles (AUVs), which rely on acoustic communications. This time, they investigated the propagation losses of the acoustic signal generated at 20 m depth over a distance of 20 km. Ray and Beam propagation techniques were applied for typical sea-ice statistics to evaluate this situation. The authors performed their analysis for two different variants: firstly for completely flat ice canopy and then for rough ice

cover. The sea-ice roughness and deformations were taken into account using a Monte Carlo method. As was demonstrated basing on a real data, a strong defocussing in the direct path is created by certain polar sound speed profiles. Besides, the inclusion of surface roughness significantly reduced the impact of reflected paths. What is interesting, small areas of maximum defocussing with a boost to signal strength of up to 8 dB were also revealed. For perfectly flat ice cover, in turn, the transmission losses were decreased by 15–50 dB at a distance of 9–20 km. The presented work emphasized the importance of developing a suitable ice surface model that results from the complexity of the real sea-ice conditions.

Recently, first attempts of combining active and passive acoustic methods in order to investigate multifaceted ecosystem responses to changing ice conditions were also made. For instance, Miksis-Olds et al. (2013) deployed two subsurface oceanographic and hydroacoustic moorings in the Bering Sea to measure various environmental components during the period between September 25, 2008, and May 29, 2009. These moorings consisted of temperature, salinity, nitrate and chlorophyll fluorescence sensors and accompanying acoustic instruments: upward-looking ADCPs, one PAL and three-frequency echosounder system of Acoustic Water Column Profilers. All devices worked with specific time intervals. For example, echosounders were active for 5 min every half an hour. In March 2009, an unexpected seasonal sea-ice retreat was detected and carefully analyzed. By application of various previously-described measurement tools, it was possible to identify different biological and physical processes, including, e.g., changing sea-ice conditions, marine mammal vocalizations and migrations of fish and planktonic organisms. The authors emphasized that traditional ship-based observations do not allow collecting such a wide range of data sets. In general, the presented work demonstrated various benefits arising from the use of passive and active acoustic methods in interdisciplinary research conducted in ice-covered waters.

In spite of all the efforts described above, many questions remain unanswered. Firstly, there is still a large gap in our theoretical knowledge about sea-ice properties and physics, including seasonal changes in the properties of ice cover. This applies particularly when we consider small spatial scales, like those found in the Arctic fjords and straits, making it impossible to successfully forecast ambient noise field in such areas. Moreover, a lack of detailed measurements of ocean currents, local weather conditions, CTD profiles and sound fields limits the development of numerical models. Finally, just a little is known about the origin of high-frequency sounds propagating beneath the sea-ice.

3 Drifting, Disintegrating and Grounded Icebergs

In the last few years, much attention was also devoted to the behavior of drifting and grounded icebergs. Rising sea level, caused by melting of the glacial ice, is a primary motivation for conducting research. Detection and tracking of icebergs are carried out mainly by using high-resolution satellite images (e.g., Wesche and

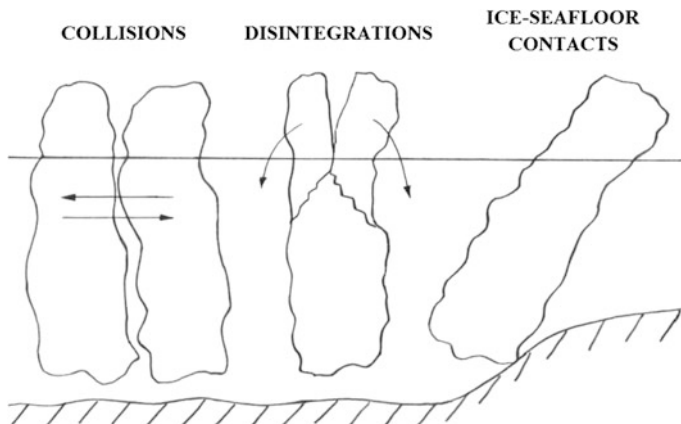


Fig. 2 Three key iceberg-related processes that generate underwater ambient noise

Dierking 2012; Tournadre et al. 2012). However, large pieces of glacial ice are also underwater sound sources, which is the result of their collisions, disintegrations and friction on the seabed (Fig. 2). Therefore, it is important to gain knowledge about iceberg-generated noise, including in particular its amplitude-frequency characteristics, generation mechanisms and contribution to the ambient sound budget. Few studies have been performed to find answers to these questions.

Urick (1971) deployed a number of sonobuoys at various distances from two selected icebergs, one of which was estimated to be 610 m long and 61 m high. Signals were analyzed in 1/3-oct frequency bands. The author showed that noise levels at low frequencies remain constant with changing distance from the berg. However, at frequencies higher than 1 kHz the levels increased when the buoys were getting closer to the analyzed block of glacier ice. It was stated that drifting icebergs were the sources of this high-frequency noise, which had a flat spectrum. According to the author, many factors determined the characteristics of generated sounds: pressure of the entrapped bubbles, air content, temperature of the surrounding water, and dimensions of icebergs.

Tolstoy et al. (2004) and Chapp et al. (2005) analyzed signals recorded at three hydroacoustic stations localized in the Indian Ocean: Diego Garcia North, Diego Garcia South and Cape Leeuwin. The main objective was to investigate the sound propagation through the Antarctic Convergence Zone with the lack of SOund Fixing And Ranging (SOFAR) channel in the high-latitudes of the Southern Ocean. The authors also studied the impact of shallow bathymetric features on the propagating sounds. Two major types of hydroacoustic signals were identified: variable harmonic tremor (HT) and cusped-pulsed tremor. The first of the above-mentioned signals, with fluctuating spectral peaks, was recognized as iceberg-related, previously reported by Talandier et al. (2002) on the basis of seismic data. A fundamental frequency was in the range of 4–10 Hz, but sometimes exceeded even 30 Hz. Durations of the HTs, in turn, varied between 1 and 30 min.

The authors successfully correlated the loudest episodes with the activity of large drifting iceberg B-15D, tracked by National Snow and Ice Data Centre. However, observations suggested that harmonic signals may also be linked with the drift of much smaller icebergs or calving activity on the coast of Antarctica. A second recorded type of signal was characterized by curved harmonic bands of energy in the range of 4–100 Hz, wherein its fundamental frequency ranged from 4 to 10 Hz. The duration of a single pulse varied from 26 to 60 s, whereas signal pulse trains sometimes persisted for 1 h. Basing on azimuthal and travel time calculations together with satellite imagery, the authors finally associated cusped-pulsed tremor with ice streams, responsible for significant part of ice flowing off Antarctica. The presented results indicated the resonance occurring in both an ice layer and fluid-filled cavity as a generator of two types of recorded signal. It was also shown that despite the lack of a well-developed SOFAR channel, ice-generated tremors can be recorded even in the equatorial zone.

Warren (2011), in turn, collected data from an array of hydrophones deployed between 01/01/2008 and 27/01/2009 in the Scotia Sea, principally to estimate the role of drifting icebergs in contributing to the overall ocean noise budget. Instruments were moored at a depth of about 500 m. Two types of hydroacoustic signals were recorded during the experiment: broadband signal with the spectral energy above 500 Hz and harmonic tremor, which accounted for less than 2 % of the catalog. The latter had fundamental harmonics in the frequency range from 3.5 to 36.7 Hz. The grouping of events around iceberg locations allowed the inference that both types of recorded signals were generated by drifting icebergs. According to the author's calculations, the annual energy produced by icebergs in the study area is 10.6 GJ/yr. Based on that, the total energy radiated from drifting Antarctic bergs was estimated to be 15.8 GJ/yr. Warren mentioned that a similar amount of energy would be generated by a supertanker during more than 19 years of operation. Thus, he showed that iceberg-related processes constitute an important source of sounds propagating in the Southern Ocean.

Dziak et al. (2013) recorded the full life-cycle of iceberg A53a. Hydrophones were deployed in the Bransfield Strait and Scotia Sea. The main objective of the research was to assess the amount of acoustic energy radiated to the ocean by icebergs. The investigated berg generated semicontinuous harmonic tremor for 6 days, when it had contact with the seafloor in the Weddel Sea. In the Bransfield Strait the duration of the tremors became shorter. Authors refer to the study of Martin et al. (2010) emphasizing the role of the iceberg speed and the duration and size of the ice-seafloor contact as the factors influencing tremors' signal lengths, overtone spacings and fundamental frequencies. In the deeper and warmer waters of the Scotia Sea, iceberg A53a began to melt and disintegrate. During this phase, short-duration signals in the frequency range between 1 and 440 Hz were recorded and assigned to the ice cracking and crack propagation. These sounds were easily distinguishable from HTs. Moreover, the authors also demonstrated that—similarly as in Warren's paper (2011)—the glacier ice can produce significantly greater noise than anthropogenic sources. Dziak et al. mentioned still unknown impact of iceberg-generated sounds on the marine life and the resulting need for further research.

It should be mentioned that harmonic tremors and other cryogenic signals are characterized by both acoustic and seismic phases and, thus, seismometers are also successfully used to study drifting, disintegrating and grounded icebergs. Hydroacoustic waves convert to local seismic waves (T phases) and are recorded, e.g., on the islands of the equatorial Pacific, while seismic phases are detectable in Antarctica.

For instance, several episodes of seismic tremors were recorded by Müller et al. (2005) at Neumayer Station in Antarctica. Using satellite images, it became possible to identify the source of signals—iceberg B-09A. The parts of the most spectacular event had spectrum consisted of narrow peaks and a fundamental frequency around 0.5 Hz. The authors suggested that water flowing through iceberg's crevasses and tunnels is responsible for elastic vibrations and, consequently, recorded tremor.

Talandier et al. (2006) collected data from different hydroacoustic and seismic stations to study signals generated by icebergs, either drifting in the Southern Pacific Ocean or grounded along the coast of Antarctica in the Indian Ocean. Signals were divided into two broad families, based on their spectral characteristics. The first group contained mainly monochromatic signals, but with frequency fluctuating in time during single sequence of emission. They were produced predominantly in the Indian Ocean, between latitudes 144 and 156°E (also called the ‘iceberg parking lot’) and interpreted as an effect of iceberg collisions. The other family had a much broader spectrum, with preferential frequencies constituting rather a background trend, and occurred both in the Southern Ocean and in the parking lot. In this case, exceptional episodes of the icebergs drift, e.g. when they passage over fronts like those determining the oceanographic southern convergence zone, were suggested as a source. The authors found different subgroups of signals in both families, distinguishable by variations in their spectra. As they showed, parked, drifting and colliding icebergs can generate hydroacoustic signals, detectable in the Southern Ocean.

MacAyeal et al. (2008) recorded harmonic tremors by placing seismometers on one of the icebergs in the Ross Sea. The objective was to identify mechanisms generating HT and explain their relevance to the iceberg life cycle. Long sequences of repeating episodes with stick-slip icequakes were identified as sources of detected harmonic tremors. Typically, thousands of individual subevents occurred during one hour when selected berg was subjected to collisions. As was established, iceberg fluid or elastic resonance modes were not associated with the observed signal. Finally, the authors suggested that wide knowledge about HTs may improve our understanding of various climate-driven processes, such us shelf disintegrations or iceberg dynamics.

A relatively small number of experiments concerning underwater sounds generated by drifting, disintegrating and grounded icebergs proved to be insufficient to answer all questions in this topic. Considering previous research, two fundamental gaps in our knowledge come to light. Firstly, virtually nothing is known on the impact of this noise on marine life. At the moment it is clear that these kinds of sounds make a significant contribution to the sound budget in the Southern Ocean,

in general. Secondly, there is a great need to improve our knowledge of harmonic tremors and their relationship with processes that are strongly associated with climate shifts.

4 Glacial Activity

The boundary between marine-terminating glaciers and ocean waters is the area with rapidly changing environmental conditions. Ice shelves and tidewater glaciers are subjected to the influence of tides, currents, wind-generated waves, swell and changeable water temperature (Benn et al. 2007). Calving events are responsible for the production of drifting icebergs and—as a result of melting—provide significant amounts of freshwater to the global ocean and contribute to sea level rise (Meier et al. 2007). Therefore, the intensity of these phenomena is one of the indicators of climate shifts. Together with submarine melt, they account for half of the mass loss from the Greenland ice sheet (van den Broeke et al. 2009) and almost the entire mass loss from the Antarctic ice sheet (Rignot et al. 2008, 2010). Tidewater glaciers and ice shelves are also the places where freshwater outflows took place. This modifies the local stratification in glacial bays and affects the diversity of marine organisms (Zajaczkowski and Legezynska 2001). Moreover, systems of eddies, upwellings and other structures are created.

Processes associated with the activity of marine-terminating glaciers are still poorly-understood. Remote sensing methods give the opportunity to observe disintegrations of large ice blocks, but without any information about smaller-scale events and freshwater outflows. In the last few years, these problems have been partially solved by the application of passive hydroacoustics. Several authors have studied “noisy processes” associated with the glacial activity (Fig. 3).

Tegowski et al. (2011) conducted hydroacoustic measurements in two Spitsbergen fjords. Hornsund fjord contains several glacial bays with tidewater glaciers, whereas Murchison fjord was filled with melting and colliding ice floes during field work. The authors used an omnidirectional hydrophone deployed from a drifting rubber boat at a depth of 18 m. Noise Spectrum Levels (NSLs) were computed from the 1-second segments of the analyzed signal. Results showed significant differences in spectral, wavelet and statistical characteristics of the ambient noise recorded in these areas. The most pronounced differences occurred for frequencies below 300 Hz. Moreover, one calving event was well-recognized with increase in NSL of up to 17 dB at 80 Hz in comparison with the quiescent period. The authors applied self-organized Kohonen’s neural network algorithm with various spectral and wavelet parameters, calculated over the range of 20 Hz–1 kHz, as input data to determine three classes reflecting different sources of ambient noise: ice cracking, glacier calving and general phenomena forming the noise field in the area. In this way, they initially showed the feasibility of acoustically detecting and classifying the calving events and other processes taking place in small Arctic fjords.

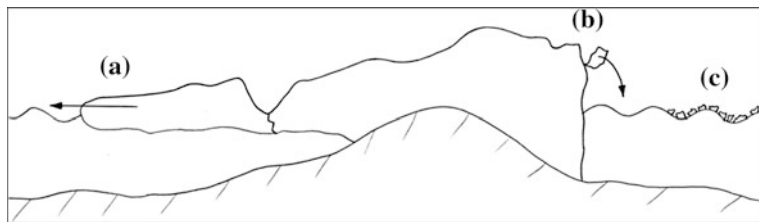


Fig. 3 Main “noisy processes” associated with glacial activity **a** large disintegration of the ice tongue **b** tidewater glacier calving **c** glacial ice melting (bubble creation) and collisions between chunks of ice

Additionally, the same team used data from the Hornsund Fjord to characterize underwater sounds associated with Stor Glacier activity (Tegowski et al. 2012). It was demonstrated that for low frequencies the pdf of the ambient noise significantly differs from the normal distribution, which probably gives information about the number and diversity of sound sources. The authors hypothesized that the long tail may represent calving and cracking events. They performed normality tests showing a central-limit type behavior for mid- and high-frequency range ($f > 2.5$ kHz). Subsequently, two averaged NSLs were compared: one complete and one without components of non-Gaussian origin. For the recorded big calving event the difference between these NSLs reached 7.5 dB. Further modeling of sound propagation in the study area and comparison with other acoustic measurements were suggested, as a possible way to classify individual processes.

Pettit et al. (2012), in turn, attempted to characterize three major processes associated with glacial activity: iceberg calving, ice melt and freshwater discharge. They recorded underwater noise in Icy Bay, Alaska, and suggested that the 1–3 kHz peak in sound pressure level is generated by air bubbles trapped inside the glacial ice and released during melting. The band is very narrow, which may be a result of the uniform distribution of pore sizes and pressures within the ice. The authors described different stages of bubble oscillations: initial high-frequency pulse connected with the first phase, strong fundamental mode oscillations just after bubble formation, damped oscillations while surfacing, and minimal oscillations at the end of the phenomenon. Furthermore, they also linked characteristic diurnal signal at 100 Hz, recorded during a three-day period, with freshwater outflows. It was expected that low-frequency sounds are generated when the water resonates in cracks and cavities, thereby causing creation of fractures in the glacial ice. The diurnal cycle was explained basing on the presumed similarity between tidewater glaciers and terrestrial glaciers.

Pettit (2012) carried out hydroacoustic research in the front of the Meares Glacier, recording signal 300 m from the ice cliff. Two omnidirectional hydrophones were used: one deployed at 30 m depth and the other at 16 m. As both hydrophones gave similar results, only data from the first one of the above-mentioned devices were chosen and processed using standard spectral analysis techniques. The author applied low-pass and bandpass Butterworth zero-phase filtering for the low-frequency time-

domain analysis. She selected one main subaerial calving event from about 2 h of observations to characterize different phases of this process. Finally, the author distinguished five stages: very low- (infrasound) and low-frequency onset, low-frequency pre-calving event activity, mid-frequency block impact, block oscillation and mini-tsunami and seiche action. In the first phase, which has a sudden onset, frequencies below 100 Hz dominate, in particular those between 6 and 8 Hz. Pettit hypothesized that during this stage the glacier loses its stability, as a result of the sudden movement, e.g., basal slip event. Subsequently, the author observed short-term (<1 s) increase in the intensity of low-frequency signal and reported that there was still not much noise at frequencies above 100 Hz. This part—as Pettit suggested—is probably related to detachment of the ice block, caused by rapidly propagating cracks. The third stage is characterized by sudden appearance of mid-frequency audible noise at a range of 100–600 Hz at the moment when the calved block falls into the water. Then, during the same phase, an increase in energy at high and ultrasonic frequencies occurs, as an effect of the water splash. Shortly after the impact, the piece of ice begins to oscillate. Spray and wave action, produced when it returns to the surface under the action of buoyancy forces, are responsible for the peak in high and ultrasonic frequencies. Soon after the first surfacing, oscillations dampen rapidly and it is difficult to distinguish subsequent oscillations from other wave action. Energy at low- and mid-frequencies remains relatively high for about five seconds from the impact and then begins to decrease, reaching almost the same level as that observed in the pre-calving phase. Infrasound noise at the range of 6–8 Hz does not dissipate and has a broad peak when the calved block is on the maximum depth. If the calving event is strong enough, mini-tsunamis are created in the last stage. Depending on the geometry of the glacial bay and the shape of the glacier front, the generated waves may reflect and return to the place of origin. Then, the wave interference leads to the formation of a pattern characteristic for seiche, with an accompanying increase in energy at high- and ultrasonic-frequency. For about 10 min sound pressure levels are still significantly higher than during quiescent period. Pettit pointed out that submarine calving event probably has a slightly different course with strong low-frequency content at the beginning. Moreover, no significant mid-frequency sound is expected due to the lack of impact on the water. The author suggested that the other phases should be the same as in the subaerial event.

Few studies were conducted to identify and describe underwater sounds associated with glacial events taking place along the Antarctic coast. However, in some of them the sources of recorded ambient noise were not clearly identified. According to the authors, these sounds can be generated by both the life cycle of drifting and grounded icebergs, or disintegration of ice shelves surrounding the continent.

Gavrilov and Vazquez (2005) collected data from one hydroacoustic station located 100 km of Cape Leeuwin, established as part of the International Monitoring System. The station consisted of one array of three hydrophones, spaced 2 km from each other. A majority of detected signals had a pulse-like waveform and frequency range between 5 and 30 Hz. Their spectrograms revealed typical characteristics for long-range propagation in the polar marine environment, with

strong waveguide dispersion. The intensity of hydroacoustic events was highly variable and mostly dependent on the season. In order to determine the location of sound sources, the authors modeled numerically the propagation of pulse-like signals from the Antarctic coast to the receiving station. Results showed that there were many locations in which particularly strong signals were produced. Finally, pointing out short duration at the origin, they suggested that recorded signals are most likely generated by calving events and ice rifting. Moreover, further development of the model of propagation was proposed as a way to gain a better understanding of the studied processes. Similar studies were conducted later by Li and Gavrilov (2006), but this time using data from two hydroacoustic stations. Thereby, it became possible to localize sound sources by applying back-azimuth bearing and compare results with those obtained with propagation model. Generally, the differences between computed localizations of the same events were smaller than 50 km, which verified numerical calculations. The authors also mentioned that the presence of islands and other topographic features between Antarctica and deployed hydrophones partially blocked the acoustic observations. Gavrilov and Li (2011), in turn, used data collected in 2002 and 2003 at two remote stations in the Indian Ocean to record signals associated with ice processes taking place in the Southern Ocean. Triangulation and bearing measurements were applied as tools for identifying the exact locations of sound sources. The obtained results showed that “noise generators” are concentrated mainly in the area of up to 200 km away from the coast of Antarctica. A large part of the signals were detected during austral summer, when there was no sea-ice. According to the authors, this situation showed that both calving events and drifting icebergs are major contributors to the ambient noise budget in the studied region.

The results of previous research clearly demonstrate the potential of hydroacoustic methods in the study of glacial activity. This applies particularly to the dynamics of tidewater glaciers and large ice shelves. However, there is a need for the development of new classification algorithms, which would allow the distinction of glaciological mechanisms responsible for different types of calving events. Moreover, the lack of effective methods for a quantitative assessment of the size of calved blocks makes it difficult to find relationships between the patterns of cryogenic sounds and climate-driven glacial processes. Finally, just a little is known about ambient noise generated by freshwater outflows.

5 Summary

As has been demonstrated, hydroacoustic methods have been successfully applied in the studies of sea-ice, glaciers and icebergs. However, the presented chapters have also shed light on hitherto unsolved problems, including lack of appropriate approaches in some areas, technological deficiencies, and the need for further field experiments. Some of these issues are considered to be particularly important and hence require special attention.

For instance, sound propagation beneath the sea-ice has been studied in various aspects and using a variety of research tools, such as numerical modeling, passive acoustics with the application of hydrophone arrays, and active acoustics with the deployment of specially designed emitters. However, several authors have emphasized the need for better understanding of the sea-ice physics and seasonal changes in the properties of the ice cover (e.g., Diachok 1976; Alexander et al. 2012, 2013). In contrast to this issue, actually a little is known about the propagation of underwater sounds generated in the vicinity of tidewater glaciers, including in particular the influence of extremely variable hydrological conditions. The necessity of conducting measurements close to the calving ice walls is one of the factors limiting the number of ongoing research. Hence, new measurement strategies are needed in combination with the use of state-of-the-art acoustic recorders, which would be able to continuously measure the ambient noise for a long period of time and with minimal risk of being damaged by drifting icebergs.

Another crucial issue is the ability to acoustically detect, identify and describe different types of calving events. Despite the fact that subaerial events were initially characterized in the fiords of Alaska (Pettit 2012; Pettit et al. 2012) and Svalbard (Tegowski et al. 2011, 2012), there are still many open questions. First of all, more experimental work should be carried out in order to confirm these preliminary results. Moreover, submarine calving events are poorly understood and there are only hypotheses about the ambient noise patterns produced by these phenomena. Finally, a quantitative assessment of the dimensions of detached blocks is extremely problematic due to the lack of appropriate methods. Therefore, there are no classification algorithms which use acoustic data as inputs and could be applied for automatic determination of the dynamics of tidewater glaciers and its relationships with environmental components. Besides, the radiation of acoustic energy from freshwater outflows, closely associated with the activity of the glaciers, is practically unstudied. In addition to the previously mentioned future needs, here the application of ADCPs and CTDs seems to be critical, because of the substantial need to localize and investigate changing hydrological structures.

In general, only a few hydroacoustic measurements were carried out in relatively small basins, like fjords or straits. These are places where satellite imagery is often insufficient to analyze sea-ice processes and properties, iceberg drifts, and glacial activity. However, first results have shown that application of underwater acoustics can be an effective method of determining sea-ice type and coverage in such areas (Nystuen 2011). What is more, the use of hydrophone arrays would allow the localization of different sound sources, such as individual sea-ice features, glaciers or icebergs, which has been done so far for both Arctic Ocean and Southern Ocean (e.g., Xie 1991; Xie and Farmer 1991; Li and Gavrilov 2006; Gavrilov and Li 2011). It should be remembered that directivity of underwater sound is one of the fundamental pieces of information, required for identification and categorization of various sound producers.

The possible impact of cryogenic underwater ambient noise on marine life is also an interesting but unsolved problem. Recently observed climate shifts lead to the enhanced melting and thereby increased production of these particular signals.

It is still unknown, however, whether this situation influences the migration, communication and the overall functioning of whales (Dziak et al. 2013). In this case, interdisciplinary studies combining marine biology with physical oceanography appear to be essential.

Summing up all issues discussed in this chapter, underwater acoustics is a relatively new research tool used in the Polar Regions, particularly in glacier bays. Despite the wide range of previously demonstrated capabilities, this area of research is still dynamically developing and, thus, constantly provides new scientific perspectives.

Acknowledgements We are grateful to Jaroslaw Tegowski and two anonymous reviewers for their valuable comments on the first version of our manuscript. This work was funded by the Polish National Science Centre, grant No. 2011/03/B/ST10/04275 and the statutory activity of the Institute of Geophysics Polish Academy of Sciences.

References

- Alexander PM, Duncan A, Bose N (2012) Modelling sound propagation under ice using the Ocean Acoustics Library's Acoustic Toolbox. In: McMinn T (ed) *Acoustics 2012 fremantle: acoustics, development and the environment, The 2012 conference of the Australian Acoustical Society, 21–23 Nov 2012. Fremantle, Western Australia, Australian Acoustical Society*
- Alexander PM, Duncan A, Bose N, Smith D (2013) Modelling acoustic transmission loss due to sea-ice cover. *Acoust Aus* 41:79–87
- Benn DI, Warren CW, Mottram RH (2007) Calving processes and the dynamics of calving glaciers. *Earth-Sci Rev* 82(3–4):143–179. doi:[10.1016/j.earscirev.2007.02.002](https://doi.org/10.1016/j.earscirev.2007.02.002)
- Chapp E, Bohnenstiehl DR, Tolstoy M (2005) Sound-channel observations of icegenerated tremor in the Indian Ocean. *Geochem Geophys Geosyst* 6, doi: [10.1029/2004GC000889](https://doi.org/10.1029/2004GC000889)
- Comiso JC (2012) Large decadal decline of the Arctic multilayer ice cover. *J Clim* 25:1176–1193. doi:[10.1175/JCLI-D-11-00113.1](https://doi.org/10.1175/JCLI-D-11-00113.1)
- Cousins JD (1991) Cearex ambient noise data measured northeast of Svalbard, Master's Thesis, Naval Postgraduate School, Monterey, California
- Dahl PH, Miller JH, Cato DH, Andrew RK (2007) Underwater ambient noise. *Acoust Today* 3(1):23–33. doi:[10.1121/1.2961145](https://doi.org/10.1121/1.2961145)
- Diachok OI (1976) Effects of sea-ice ridges on sound propagation in the Arctic Ocean. *J Acoust Soc Am* 59(5):1110–1120. doi:[10.1121/1.380965](https://doi.org/10.1121/1.380965)
- Dziak RP, Fowler MJ, Matsumoto H, Bohnenstiehl DR, Park M, Warren K, Lee WS (2013) Life and death sounds of Iceberg A53a. *Oceanography* 26(2), <http://dx.doi.org/10.5670/oceanog.2013.20>
- Fricke JR, Unger GL (1995) Acoustic scattering from elemental Arctic ice features: experimental results. *J Acoust Soc Am* 97(1):192–198. doi:[10.1121/1.412303](https://doi.org/10.1121/1.412303)
- Gavrilo VP, Gudkovich ZM (1996) Underwater ambient noise as indicator of the dynamic processes in the Arctic Sea-ice cover. *Int J Offshore Polar Eng* 6(2):152–158
- Gavrilov AN, Li B (2011) Location of ice noise sources in Antarctica, In: Proceedings of 4th UAM conference, 20–24 June, 2011, Kos, Greece
- Gavrilov AN, Mikhalevsky PN (2006) Low-frequency acoustic propagation loss in the Arctic Ocean: results of the Arctic climate observations using underwater sound experiment. *J Acoust Soc Am* 119(6):3694–3706. doi:[10.1121/1.2195255](https://doi.org/10.1121/1.2195255)

- Gavrillov AN, Vazques G (2005) Detection and localization of ice rifting and calving events in Antarctica using remote hydroacoustic stations, In: Proceedings of ACOUSTICS 2005, 9–11 Nov 2005, Busselton, Western Australia
- Greene CR, Buck BM (1964) Arctic Ocean ambient noise. *J Acoust Soc Am* 36(6):1218–1220. doi:[10.1121/1.1919192](https://doi.org/10.1121/1.1919192)
- Greening MV, Zakarauskas P, Dosso SE (1997) Matched-field localization for multiple sources in an uncertain environment, with application to Arctic ambient noise. *J Acoust Soc Am* 101(6):3525–3538. doi:[10.1121/1.418382](https://doi.org/10.1121/1.418382)
- Greening MV, Zakarauskas P, Verrall RI (1992) Vertical directivity of ice cracking. *J Acoust Soc Am* 92(2):1022–1030. doi:[10.1121/1.404031](https://doi.org/10.1121/1.404031)
- Hildebrand JA (2009) Anthropogenic and natural sources of ambient noise in the ocean. MEPS. doi:[10.3354/meps08353](https://doi.org/10.3354/meps08353)
- Knudsen VO, Alford RS, Emling JW (1948) Underwater ambient noise. *J Mar Res* 7:410–429
- Kwok R (2011) Satellite remote sensing of sea-ice thickness and kinematics: a review. *J Glacio* 56:200. doi:[10.3189/002214311796406167](https://doi.org/10.3189/002214311796406167)
- Laible HA, Rajan SD (1996) Temporal evolution of under ice reflectivity. *J Acoust Soc Am* 99(2):851–865. doi:[10.1121/1.414661](https://doi.org/10.1121/1.414661)
- Laxon SW, Giles KA, Ridout AL, Wingham DJ, Willatt R, Cullen R, Kwok R, Schweiger A, Zhang J, Haas C, Hendricks S, Krishfield R, Kurtz N, Farrell S, Davidson M (2013) CryoSat-2 estimates of Arctic sea-ice thickness and volume. *Geophys Res Lett* 40, doi: [10.1002/grl.50193](https://doi.org/10.1002/grl.50193)
- Lewis JK, Denner WW (1988a) Arctic ambient noise in the Beaufort Sea: seasonal relationships to sea-ice kinematics. *J Acoust Soc Am* 83(2):549–565. doi:[10.1121/1.396149](https://doi.org/10.1121/1.396149)
- Lewis JK, Denner WW (1988b) Higher frequency ambient noise in the Arctic Ocean. *J Acoust Soc Am* 84(4):1444–1455. doi:[10.1121/1.396591](https://doi.org/10.1121/1.396591)
- Li B, Gavrillov AN (2006) Hydroacoustic observation of Antarctic ice disintegration events in the Indian Ocean, in Proc. of ACOUSTICS 2006, Christchurch, New Zealand
- MacAyeal DR, Okal EA, Aster RC, Bassis JN (2008) Seismic and hydroacoustic tremor generated by colliding icebergs. *J Geophys Res* 113:F03011. doi:[10.1029/2008JF001005](https://doi.org/10.1029/2008JF001005)
- Martin S, Drucker R, Aster R, Davey F, Okal E, Scambos T, MacAyeal D (2010) Kinematic and seismic analysis of giant tabular iceberg breakup at Cape Adare. *Antarct J Geophy Res* 115:B06311. doi:[10.1029/2009JB006700](https://doi.org/10.1029/2009JB006700)
- Matsumoto H, Bohnenstiehl R, Dziak RP, Park M, Fowler MJ (2009) Hydroacoustic monitoring of the Scotia Sea: autonomous hydrophone experiment. In: Proceedings of the 2009 monitoring research review - ground-based nuclear explosion monitoring technologies, 21–23 Sep 2009, Tucson, Arizona
- Meier MF, Dyurgerov MB, Rick UK, O'Neil S, Pfeffer WT, Anderson RS, Anderson SP, Glazovsky AF (2007) Glaciers dominate eustatic sea-level rise in the 21st century. *Science* 317(5841):1064–1067. doi:[10.1126/science.1143906](https://doi.org/10.1126/science.1143906)
- Miksics-Olds JL, Stabeno PJ, Napp JM, Pinchuk AI, Nystuen JA, Warren JD, Denes SL (2013) Ecosystem response to a temporary sea-ice retreat in the Bering Sea: Winter 2009. *Prog Oceanogr* 111:38–51. doi:[10.1016/j.pocean.2012.10.010](https://doi.org/10.1016/j.pocean.2012.10.010)
- Milne AR, Ganton JH (1964) Ambient noise under Arctic-Sea-ice. *J Acoust Soc Am* 36(5):855–863. doi:[10.1121/1.1919103](https://doi.org/10.1121/1.1919103)
- Müller C, Schindwein V, Eckstaller A, Miller H (2005) Singing icebergs. *Science* 310(5752):1299–1299. doi:[10.1126/science.1117145](https://doi.org/10.1126/science.1117145)
- Nielsen PA, Thomas J (1987) Signal detection in Arctic under-ice noise. Proceedings of the twenty-fifth annual Allerton conference on communication, control, and computing, Urbana, IL, pp 172–177
- Nystuen JA (2011) Quantifying physical processes in the marine environment using underwater sound. In Proceedings of 4th UAM conference, 20–24 Jun 2011, Kos, Greece
- Overland JE, Wang M (2013) When will the summer Arctic be nearly sea-ice free? *Geophys Res Lett* 40:2097–2101. doi:[10.1002/grl.50316](https://doi.org/10.1002/grl.50316)

- Pettit EC (2012) Passive underwater acoustic evolution of a calving event. *Ann Glaciol* 53(60):113–122. doi:[10.3189/2012AoG60A137](https://doi.org/10.3189/2012AoG60A137)
- Pettit EC, Nystuen JA, O’Neil S (2012) Listening to glaciers: passive hydroacoustics near marine-terminating glaciers. *Oceanography* 25(3):104–105. doi:[10.5670/oceanog.2012.81](https://doi.org/10.5670/oceanog.2012.81)
- Pritchard RS (1990) Sea-ice noise-generating processes. *J Acoust Soc Am* 88(6):2830–2842. doi:[10.1121/1.399687](https://doi.org/10.1121/1.399687)
- Rignot E, Bamber JL, van den Broeke MR, Davis C, Li Y, van de Berg WJ, van Meijgaard E (2008) Recent Antarctic ice mass loss from radar interferometry and regional climate modelling. *Nat Geosci* 1(2):96–110. doi:[10.1038/ngeo102](https://doi.org/10.1038/ngeo102)
- Rignot E, Koppes M, Velicogna I (2010) Rapid submarine melting of the calving faces of West Greenland glaciers. *Nat Geosci* 3(3):141–145. doi:[10.1038/ngeo765](https://doi.org/10.1038/ngeo765)
- Roth EH, Hildebrand JA, Wiggins SM, Ross D (2012) Underwater ambient noise on the Chukchi Sea continental slope from 2006–2009. *J Acoust Soc Am* 131(1):104–110. doi:[10.1121/1.3664096](https://doi.org/10.1121/1.3664096)
- Shaw RR (2000) Ambient noise characteristics during the SHEBA experiment. Master’s thesis, Naval Postgraduate School, Monterey, CA
- Stamoulis C, Dyer I (2000) Acoustically derived ice-fracture velocity in central Arctic pack ice. *J Acoust Soc Am* 108(1):96–104. doi:[10.1121/1.429448](https://doi.org/10.1121/1.429448)
- Stroeve JC, Serreze MC, Holland M, Kay JE, Malanik J, Barrett AP (2012) The Arctic’s rapidly shrinking sea-ice cover: a research synthesis. *Clim Change* 110:1005–1027. doi:[10.1007/s10584-011-0101-1](https://doi.org/10.1007/s10584-011-0101-1)
- Stroeve JC, Holland MM, Meier W, Scambos T, Serreze M (2007) Arctic sea-ice decline: faster than forecast. *Geophys Res Lett* 34(9), doi: [10.1029/2007GL029703](https://doi.org/10.1029/2007GL029703)
- Talandier J, Hyvernaud O, Okal E, Piserchia P (2002) Long-range detection of hydroacoustic signals from large icebergs in the Ross Sea. *Antarct Earth Planetary Sci Lett* 203(1):519. doi:[10.1016/S0012-821X\(02\)00867-1](https://doi.org/10.1016/S0012-821X(02)00867-1)
- Talandier J, Hyvernaud O, Reymond D, Okal EA (2006) Hydroacoustic signals generated by parked and drifting icebergs in the Southern Indian and Pacific Oceans. *Geophys J Int* 165:817–834. doi:[10.1111/j.1365-246X.2006.02911.x](https://doi.org/10.1111/j.1365-246X.2006.02911.x)
- Tegowski J, Deane GB, Lisimenka A, Blondel P (2011) Detecting and analyzing underwater ambient noise of glaciers on Svalbard as indicator of dynamic processes in the Arctic. In: Proceedings of 4th UAM conference, 20–24 June, 2011, Kos, Greece
- Tegowski J, Deane G, Lisimenka A, Blondel P (2012) Spectral and statistical analyses of ambient noise in Spitsvergen Fjords and identification of glacier calving events. In: Proceedings of the 11th European conference on underwater acoustics, 2012-07-02 - 2012-07-06, Edinburgh
- Tolstoy M, Bohnenstiehl DR, Chapp E (2004) Long range acoustic propagation of high frequency energy in the Indian Ocean from icebergs and earthquakes. In: Proceedings of the 26th Seismic research review: trends in nuclear explosion monitoring, Orlando FL, pp 519–534
- Tournadre J, Girard-Ardhuin F, Legrésy B (2012) Antarctic icebergs distributions, 2002–2010. *J Geophys Res* 117:C05004. doi:[10.1029/2011JC007441](https://doi.org/10.1029/2011JC007441)
- Urick RJ (1971) Noise of melting icebergs. *J Acoust Soc Am* 50(1):337–341. doi:[10.1121/1.1912637](https://doi.org/10.1121/1.1912637)
- van den Broeke M, Bamber J, Ettema J, Rignot E, Schrama E, van de Berg WJ, van Meijgaard E, Velicogna I, Wouters B (2009) Partitioning recent greenland mass loss. *Science* 326(5955):984–986. doi:[10.1126/science.1178176](https://doi.org/10.1126/science.1178176)
- Warren K (2011) Underwater acoustic energy generated by icebergs in the Scotia Sea. M.S. Thesis, North Carolina State University, 100 pp, <http://repository.lib.ncsu.edu/ir/handle/1840.16/7365?mode=full>
- Wenz GM (1962) Acoustic ambient noise in the ocean: spectra and sources. *J Acoust Soc Am* 34(12):1936–1956. doi:[10.1121/1.1909155](https://doi.org/10.1121/1.1909155)
- Wesche C, Dierking W (2012) Iceberg signatures and detection in SAR images in two test regions of the Weddell Sea, Antarctica. *J Glaciol* 58(208), pp 325–339(15), doi: [10.3189/2012J0G11J020](https://doi.org/10.3189/2012J0G11J020)

- Xie Y (1991) An acoustical study of the properties and behavior of sea-ice. *J Acoust Soc Am* 90(4):2203–2203. doi:[10.1121/1.401650](https://doi.org/10.1121/1.401650)
- Xie Y, Farmer DM (1991) Acoustical radiation from thermally stressed sea-ice. *J Acoust Soc Am* 89(5):2215–2231. doi:[10.1121/1.400914](https://doi.org/10.1121/1.400914)
- Ye Z (1995) Sound generation by ice floe rubbing. *J Acoust Soc Am* 97(4):2191–2198. doi:[10.1121/1.411944](https://doi.org/10.1121/1.411944)
- Zajaczkowski MJ, Legezynska J (2001) Estimation of zooplankton mortality caused by an Arctic glacier outflow. *Oceanologia* 43(3):341–351
- Zakarauskas P, Thorleifson JM (1991) Directionality of ice cracking events. *J Acoust Soc Am* 89(2):722–734. doi:[10.1121/1.1894632](https://doi.org/10.1121/1.1894632)

Pigeon Navigation Model Based on a Vector Magnetometer

Jerzy Jankowski

Abstract A model of pigeon navigation is proposed. It is based on the assumption that a pigeon is in possession of a magnetometer to measure two geomagnetic field components. Another assumption is that in the linear approximation these components form a skew reference coordinate system. The model can explain not only how the birds find their way back home, but also a series of characteristic traits of their navigation, which, in spite of numerous experiments, still remain puzzling. An analysis of the model has also shown that the sensitivity of the magnetometer must be extremely high, in excess of the present-day technological achievements.

Keywords Pigeon navigation · Vector magnetometer · Magnetic maps

1 Introduction

One of the most interesting puzzles of nature is how animals, notably birds, navigate over unknown areas in order to reach a certain target. The principles of navigation, in particular as concerns pigeons, were searched for centuries. In the last 50 years, several facts were settled. The first is the finding that a pigeon has a few navigation systems and is able to use them skilfully. One of these is an astronomical system, based on the observation of the position of the Sun or stars.

This is a slightly updated version of the article prepared by the author in past years and published in Polish-language journal *Przegląd Geofizyczny* (see Jankowski 2010)

J. Jankowski (✉)

Polish Academy of Sciences, Institute of Geophysics, Księcia Janusza 64,
01-452 Warszawa, Poland
e-mail: jerzy@igf.edu.pl

Other hypotheses include orientation on the basis of smell or the effect of light polarization on the navigational systems. There are also evidences that pigeons sense infrasounds (Hagstrum 2013). Near home, the pigeon uses a topographic recognition of the area. All ornithologists agree that the pigeon possesses a magnetic sense, but what in fact it measures and how it makes use of this measurement is still a matter of discussion.

The problem of navigation of animals, in particular pigeons, has been widely discussed in the literature. The reader is referred to the review chapters by Matthews (1968), Keeton (1974), Schmidt-Koenig (1979), Schmidt-Koenig and Keeton (1978), Papi (1986), Elsner (1978), Wallraff (1990), Wiltschko and Wiltschko (1996, 2009) or to the monograph by Wiltschko and Wiltschko (1995).

The model presented in this chapter may explain the following experimental facts:

1. The finding of homeward azimuth from the release place, preceded by the reconnaissance flight consisting of several loops over an area of less than one square kilometer.
2. Small but systematic error in the direction of the homeward flight.
3. Characteristic dispersion of outflight direction and its dependence on magnetic activity.
4. Finding of return way home with an accuracy of a few kilometers.
5. Erroneous navigation when the pigeon is released in regions of magnetic anomalies.
6. Difficulty of finding the accurate home location on the basis of magnetic data alone.

In this chapter I propose a model of pigeon navigation based on features of the regional magnetic field. The model can explain the above-mentioned specific traits of pigeon navigation. I am aware that the pigeon can use other orientation systems as well, but I assume that it is guided by the magnetic field.

I want to emphasize that the assumption that the pigeon is guided by the magnetic field alone is the *a priori* assumption of this chapter. We will not argue whether it is correct or not, we just want to draw some conclusions about the parameters of the orientation system.

It is usually assumed that the pigeon measures the total magnetic field strength and is able to determine the magnetic north. This is not sufficient, though, for explaining the navigation system; some additional, independent information would be necessary. What this information may be is a matter of discussion for tens of years and evokes controversial opinions. For instance, Walker (1998) suggests that the other factor is the direction of maximum change of the field gradient, while Wallraff (1999) denies it and argues that the hypothesis of navigation according to the magnetic field has become outdated.

A possibility of using, along with the magnetic field strength, a second field component as well has also been considered for many years (Gould 1982; Walker et al. 2002). However, neither the navigation system nor the requirements as to the magnetometer's parameters resulting from it have been discussed in detail.

2 The Regular Features of the Magnetic Field

Let us begin with recalling the features of the magnetic field components. Its main constituent is the dipole component. The isolines of all the field components except of declination run along the magnetic parallels of latitude. The declination isolines run along the meridians for middle geomagnetic latitudes. The magnetic field contains also a non-dipole part, which modifies the above regular pattern. The non-dipole part modifies the magnetic field distribution in various regions of the Earth. To give an example of regional variations, we reproduce in Fig. 1 the magnetic charts of Suckdorff and Nevanlinna (1981) for Finland. The choice of Finland was arbitrary, but the variations in other regions seem to be similar.

In Fig. 2 we show the linear trends calculated from maps of Fig. 1 by the same authors. These linear trends represent the magnetic field distribution which will be used for an analysis of navigation system.

In the figures we show five components, but only three are independent. Let us consider what information contained in these charts can be used for navigation. Declination does not seem to be a possible candidate to be used for navigation, since the determination of astronomical meridian is difficult. The components F (total length of the vector) and Z (vertical component) are roughly parallel; the same is true about the inclination I (the angle calculated relative to the horizontal direction) and the horizontal component H . Isolines of F and Z have roughly speaking the direction of magnetic parallel of latitude, and H and I form an angle of about 30° with them. This skewness is of basic importance for the construction of the navigation model presented below. The regularities shown in the charts relate to a regional pattern, on which the local field anomalies, quite differing in amplitudes, are superimposed. Any combination of components of these two disjoint pairs can possibly be used for navigation. In the present chapter I decided to use H and Z , while Walker et al. (2002), considering a similar problem, made a choice of F and I . The model considerations made here can be equally well made for components F and I , and the conclusions would be the same. In order to be able to navigate according to the field components, the pigeon must be in possession of a vector magnetometer, i.e., an instrument which measures three independent field components. In terms of the geophysical nomenclature, it does not have to be a full vector magnetometer, which would be able to measure three components, usually perpendicular to each other. In our case it is enough to measure two components and to orient the magnetic meridian (equivalent of a magnetic compass). This may be, for instance, the measurement of vertical component and the maximum component in the horizontal plane.

Let us now derive simple mathematical formulae relating to the navigation system. Assume for simplicity that the Earth is locally flat and the origin of the x , y coordinate system is in the point of the field values H_0 and Z_0 . The x axis is directed towards E, and y towards N. Assuming that the field is characterized by linear trends, the expressions for H and Z at any point of the plane in the vicinity of point H_0 , Z_0 can be expressed as

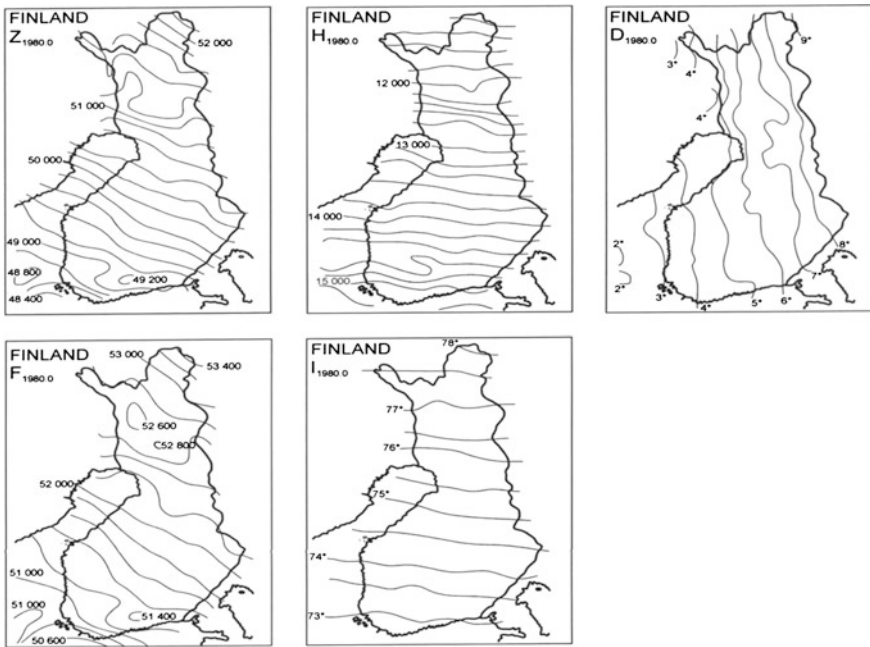


Fig. 1 Maps of geomagnetic components Z , H , D , F , and I for Finland, according to Suckdorff and Nevanlinna (1981)

$$H = H_0 + \frac{\partial H}{\partial x}x + \frac{\partial H}{\partial y}y,$$

$$Z = Z_0 + \frac{\partial Z}{\partial x}x + \frac{\partial Z}{\partial y}y.$$

Let us further denote the gradients $\frac{\partial H}{\partial x}$, $\frac{\partial H}{\partial y}$ and $\frac{\partial Z}{\partial x}$, $\frac{\partial Z}{\partial y}$ by symbols h_x , h_y , and z_x , z_y .
Then

$$Z = Z_0 + z_x x + z_y y$$

$$H = H_0 + h_x x + h_y y \quad (1)$$

This linear approximation is only valid for a limited area. In an arbitrary point of the plane in which the equations are satisfied, the knowledge of the components and gradient of the field enables us to easily find the coordinates x and y (under the assumption that the denominator differs from zero; its zeroing would mean that the isolines of both components are parallel)

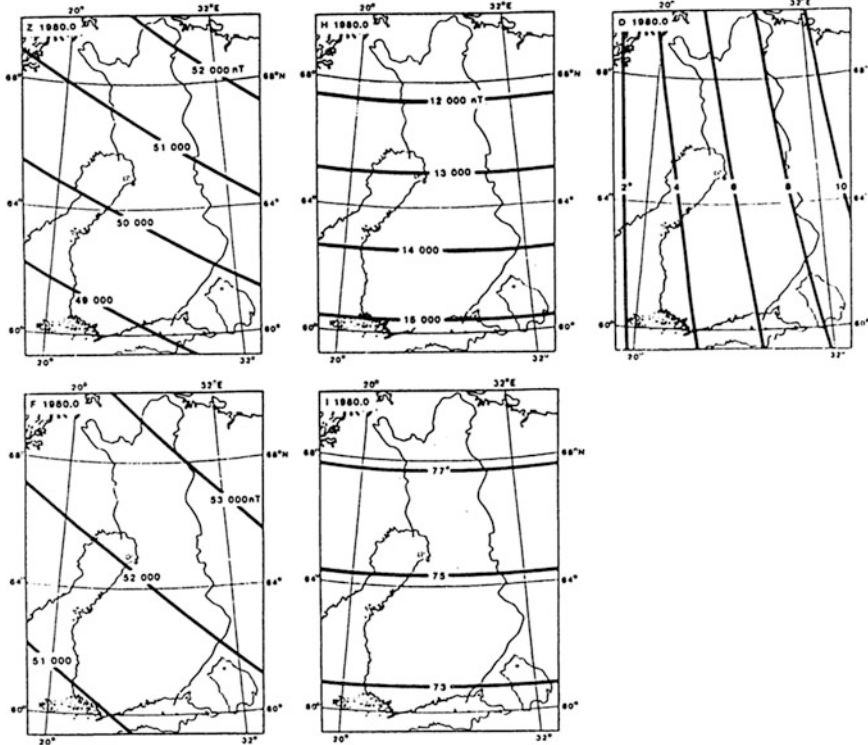


Fig. 2 Linear trends calculated from maps of Fig. 1 (Suckdorff and Nevanlinna 1981)

$$\begin{aligned} x &= (z_y(H - H_0) - h_y(Z - Z_0)) / (h_x z_y - h_y z_x), \\ y &= (h_x(Z - Z_0) - z_x(H - H_0)) / (h_x z_y - h_y z_x). \end{aligned} \quad (2)$$

The azimuth of the direction from home to the release site is described by the equation written below. The return direction differs by 180° .

$$\tan \alpha = (h_x(Z - Z_0) - z_x(H - H_0)) / (z_y(H - H_0) - h_y(Z - Z_0)) \quad (3)$$

If it were possible to describe the magnetic field by linear trends as those in Fig. 2, the navigation would be simple. In reality, the spatial distribution is more complicated. In what follows we will verify how the local discrepancies from the model may explain the real behavior of the pigeon in our considerations.

We assume that quantities H_0 and Z_0 are invariable. The model has 6 variable parameters: Z , H , h_x , h_y , z_x , z_y . The pigeon measures the sum of spatial and temporal changes. We will now briefly characterize the temporal changes in moderate geographical latitudes. In the Earth's magnetic field variations, the

following two components can be distinguished: quiet-sun variations and disturbed-period ones. The first of these have daily periodicity and are continuous. The amplitude of quiet changes in moderate geographical latitudes is some tens nT. Magnetic storms occur relatively rarely (few per year); the amplitude of changes during their occurrence may reach even a thousand nT. Of frequent occurrence, though, are irregular perturbations of variable amplitude; they are usually characterized by three-hour activity indices, named K indices.

The aim of this work is to numerically verify how the perturbation of input parameters of the model may affect the determination of azimuth. The model is used for numerical tests. Performing the test we only verify what information is needed in order to explain the features of pigeon navigation. We do not claim that the processing system is the same as that we use for data analysis. The pigeon may have quite different processing system, but information, e.g., about the magnetometer's resolution, remains valid. Later in this chapter we will present a much simpler method of how the data can be used.

An analysis of specific behaviors, as enumerated in points 1–6 (in the Introduction), will be discussed in the three subsections dealing with the regularities: (i) in the release place; (ii) on the path towards home; (iii) nearby home.

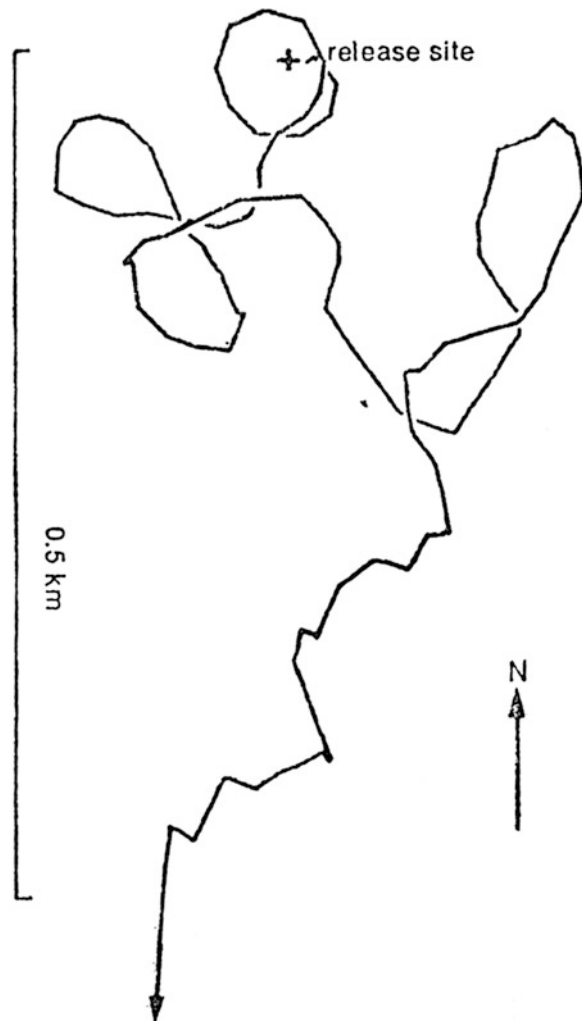
3 Pigeon Navigation Nearby the Release Site

All the examples presented have been taken from the literature and do not allow us to make a quantitative interpretation of the flight. The full numerical simulation is very difficult and would necessitate a series of experiments. Therefore, the analysis presented here will be to a large extent speculative; although I think it will yield interesting conclusions. A classical example how a pigeon behaves in the starting place is shown in Fig. 3.

It is seen that after making a few loops over an area of about 0.5 km diameter, the pigeon takes the flight direction (arrow in the figure). Interestingly, while making the reconnaissance loops the pigeon looks like it were searching for the missing information. Assume that it is collecting information that would enable it to calculate gradients. Finding gradients is a very difficult task. The gradient components amount to a few nT/km. At an area spanning half a kilometer, it is just few nT. To measure these tiny values, the magnetometer's sensitivity must be no less than 0.1 nT. The most difficult task is to stabilize the magnetometer in space. To achieve the 0.1 nT accuracy, the direction stability must be incredibly high, of the order of seconds of arc. Of course, it is not the pigeon's stability. It must only measure the component along the vertical direction and perpendicular to it; this means, the magnetometer must be in Cardan suspension, i.e., it must self-align along the gravity field.

Figure 3 presents the initial navigation of a single pigeon. The features of a group are shown in a circular diagram in Fig. 4.

Fig. 3 Pigeon navigation. The pigeon makes a few loops, and then chooses a homeward direction (after Gould 1982, reproduced with Nature Publishing Group permission)



The broken line depicts the real homeward direction. Dots are the individual departure directions. The arrow indicates the mean direction, and its length the direction variance. The diagram shows results for sunny and overcast days, relating to pigeons with a magnet attached or without it (according to Keeton et al. 1974).

The model should explain both the choice of direction and the systematic error relative to the true homeward direction, and also dispersions of these directions. The representation on a circular diagram is a standard in the literature and in all the cases the regular features are similar. I mean here the large dispersion of directions and the deviation of the mean direction from the true one. The examples of pigeon behavior have been taken from the literature. The authors of those chapters do not

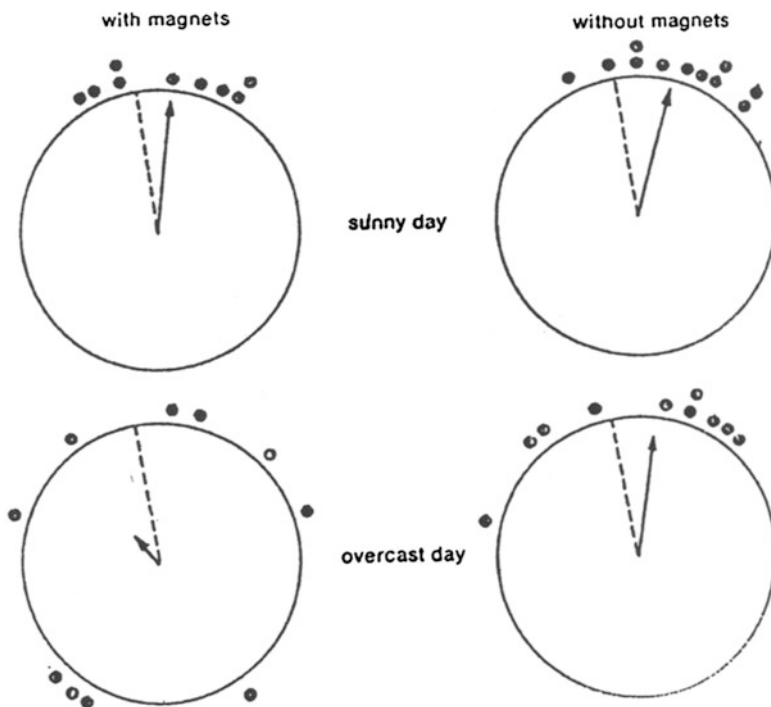
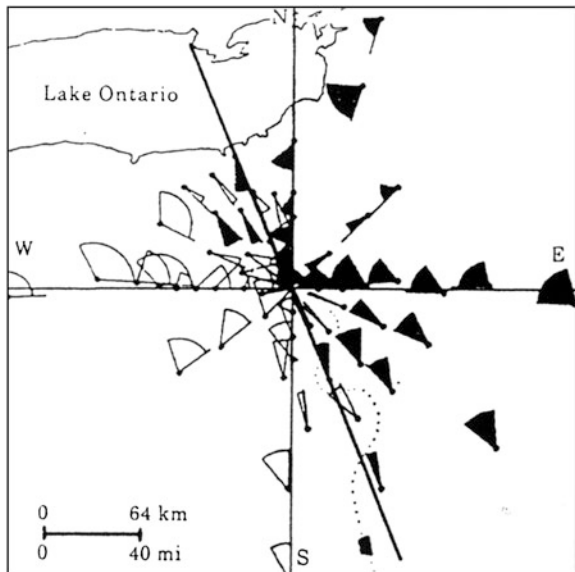


Fig. 4 Navigation of a group of pigeons. Dots indicate the directions of return flight of pigeons from a group. Dashed line indicates the true direction. The arrow represents the mean value of individual directions. The arrow length symbolizes the scattering. Diagram for pigeons with and without a magnet, in sunny and overcast days (Keeton et al. 1974)

provide the field values needed to make use of the equation for model azimuth. Hence, we do not intend to simulate the real flight of a pigeon. Yet we can make simple numerical calculations which will enable us to answer the question how the perturbation of initial conditions affects the flight azimuth (Fig. 5).

From Eqs. (1)–(3) we see that in this simplified case, the pigeon, having knowledge of the differences in the field values and its gradients in the N-S and E-W directions, may know in which place it is actually located and what is the azimuth of its return homeward path. Under the assumption that the pigeon is in possession of a vector magnetometer, the measurement of Z and H seems to be an easy task, but a question arises of how the bird can get knowledge about the gradients of changes. To estimate these gradients, the pigeon must measure both the direction and distance. Since it has a compass (the north is determined by the maximum value of H), the direction is no problem. The assessment of distance is a greater challenge, although this can be done basing on an optical evaluation of distance to some characteristic points on the area or by evaluation of the velocity and time of flight. As we already noted, it is enough to know the gradient with an accuracy to a common multiplier. From the former discussion on magnetometer's

Fig. 5 A map illustrating the distribution of systematic azimuth errors for pigeons starting from various places around home (Gould 1982, reproduced with Nature Publishing Group permission)



sensitivity it follows that the calculation of gradients, because of their small values, cannot be precise.

We will now use Eq. (3) for analyzing the azimuth changes in relation to the distribution of the field components. The task is not easy, since $\text{angl } \alpha$ is a function of 8 variables. We assume that the field values H_0 and Z_0 at home were remembered by the pigeon, and we will keep these values constant. The pigeon must measure the values of components H and Z in the release place, but this is not difficult provided that the pigeon has a vector magnetometer. An attempt at estimating gradients and their errors is much more difficult, though. If we assume that the pigeon calculates these gradients during the reconnaissance flight, we can only say that the estimate is not precise. Speaking about a pigeon I mean a virtual bird; as we will show later, for a real navigation, the pigeon does not have to know the gradients. However, the conclusions about the measurement system drawn from the model analysis remain valid. The model should explain both the systematic azimuth error as well as the scatter of its direction. The systematic error is affected by the discrepancies between the real field distribution and its linear approximation. Let us now make a series of calculations, the results of which are listed in Table 1. In this table we will vary the values of H and Z , as well as the gradient components.

In the table, the last column of the first line presents the azimuth calculated according to the linear model parameters. The last column of the next lines shows the azimuths calculated from Eq. (3) at various input values. The change of input parameters by some tens nT produces azimuth changes by a dozen or so degrees. The azimuth is also sensitive to changes in the values of gradient components. A 200 nT field change yields as much as 40° . A change on this order may be

Table 1 Return path azimuths for various input parameters [see Eq. (3)]

| H | Z | h_x | H_y | z_x | z_y | H_0 | Z_0 | α |
|--------|--------|-------|-------|-------|-------|--------|--------|----------|
| 13,000 | 50,600 | 0 | -3.3 | 1.1 | 2.6 | 13,400 | 50,200 | 57 |
| 2,950 | 50,640 | 0 | -3.3 | 1.1 | 2.6 | 13,400 | 50,200 | 60 |
| 13,000 | 50,550 | 0 | -3.3 | 1.1 | 2.6 | 13,400 | 50,200 | 75 |
| 13,200 | 50,550 | 0 | -3.3 | 1.1 | 2.6 | 13,400 | 50,200 | 19 |
| 12,900 | 50,650 | 0 | -3.3 | 1.1 | 2.6 | 13,400 | 50,200 | 72 |
| 13,200 | 50,550 | 0.1 | -0.1 | 1.2 | 2.8 | 13,400 | 50,200 | 27 |
| 12,950 | 50,640 | 0 | -2.9 | 1.1 | 2.6 | 13,400 | 50,200 | 78 |
| 12,950 | 50,640 | 0 | -2.9 | 1.3 | 2.8 | 13,400 | 50,200 | 88 |

needed for explaining the features presented in Fig. 6. The only conclusion that follows from the table is that real deviations of the azimuth may be qualitatively explained by the presented model.

The results of the experiment are presented in the form of fans, whose diameter characterizes the scattering of directions, and the homeward direction is a mean value. The blackened fans differ by the sense of the homeward direction deviation.

I find the results of the experiment to be very interesting. From the figure one can see not only direction deviations at particular locations and their dispersion, but also the regularities of spatial distribution.

It is clearly seen that the deviations in directions depend on the region, and also that the greater the systematic error the greater the dispersion of directions. These features can be explained by the magnetic anomalies in the study area, the systematic error by the normal field anomalies, and the dispersion by the less accurate determination of gradients in the anomalous field. Looking at Table 1 we see that the observed features can be qualitatively explained by the model.

Analyzing the pigeon behavior in the release point we will give another example. This is illustrated in Fig. 6 which shows the dependence of initial azimuth on variation. It is seen from Table 1 that this dependence can also be qualitatively explained by the analyzed model.

4 Homeward Navigation of Pigeons

Having determined the homeward direction, the pigeon begins its navigation back. The return paths are shown in Fig. 7 taken from Walcott (1978).

A characteristic trait is that the pigeon does not fly along the azimuth that has once been determined but its path is full of zigzags, so during this return journey the bird must collect additional information to enable it to correct the flight. I think, during the return flight it keeps determining the azimuths anew, making use of newly determined gradients and field component values. In my opinion, the bird evaluates the new azimuth not from an instantaneous value of the fields but takes an average over a certain segment. Such a procedure allows for a greater

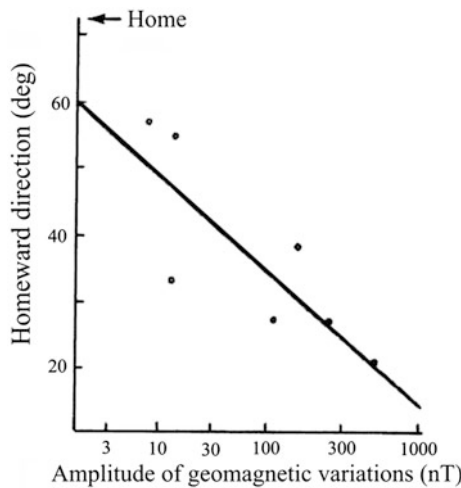


Fig. 6 Direction error as a function of magnetic activity (Gould 1982, reproduced with Nature Publishing Group permission)

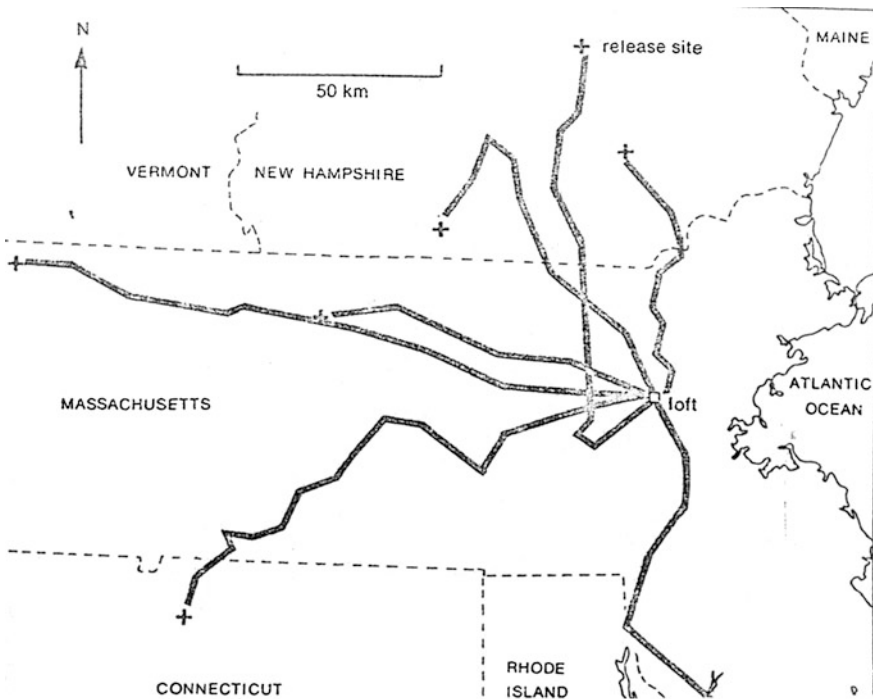


Fig. 7 Trajectories of pigeons released from 7 sites around home (Wallcott 1978)

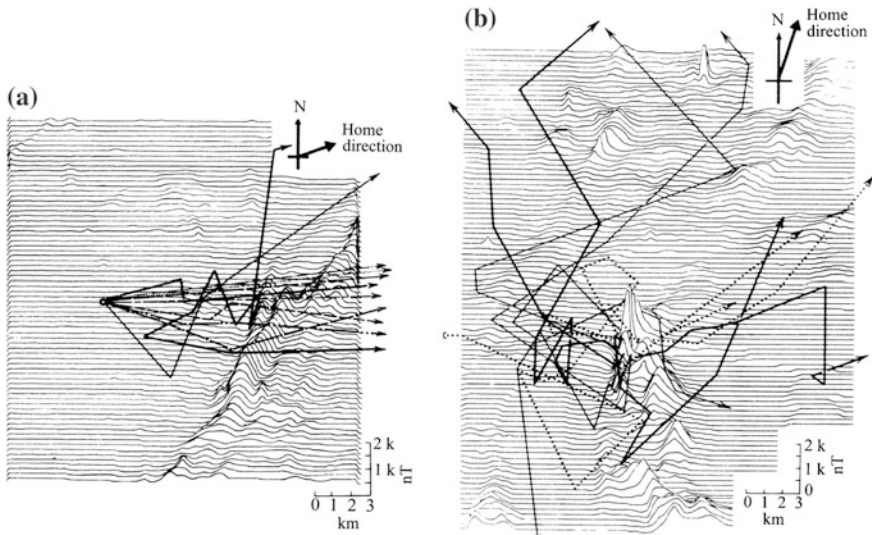


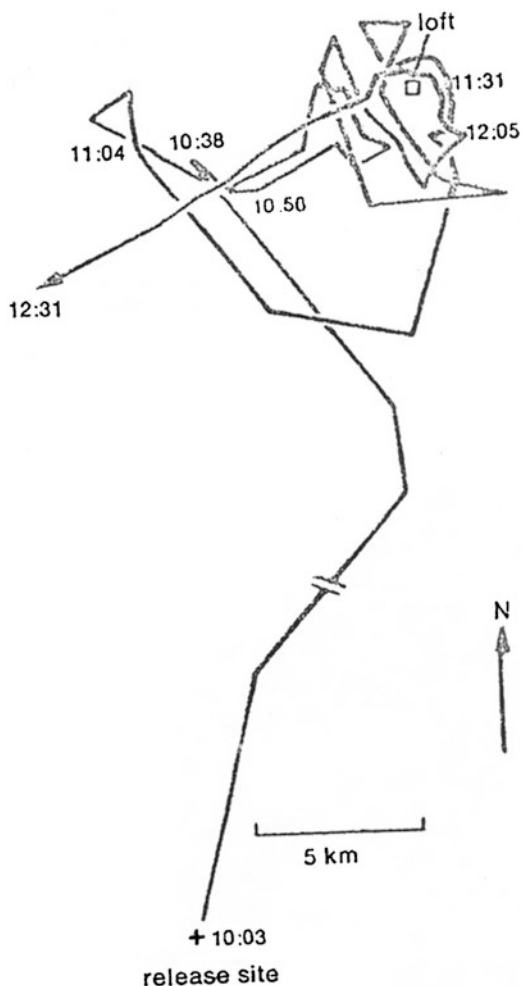
Fig. 8 Navigation of pigeons released at a site near Worcester, Massachusetts (a) and Iron Mine Hill, Rhode Island (b); more explanation in the text (Gould 1982, reproduced with Nature Publishing Group permission)

stability of the flight direction. This is essential for explaining the feature shown in Fig. 8a,b, presenting charts of the full field vector for the region near Worcester, Massachusetts (a), and Iron Mine Hill, Rhode Island (b) together with the pigeon flight paths. We see here an interesting phenomenon: when the pigeon is released at the area of quiet field distribution (Fig. 8a), and encounters magnetic anomalies later on its way, upon overpassing them it manages to find the proper direction and to keep it. The backward information is used in further navigation. The situation is different when the pigeon is released in the region of strong anomalies (Fig. 8b). In this case, the bird does not have enough data for stabilizing its direction and, as we see, it navigates falsely.

5 Pigeon Navigation Nearby its Home

Let us now consider how the pigeon can navigate in the vicinity of its home. We must keep in mind that the field undergoes changes in time, and the differences between the remembered and instantaneous fields may amount to tens nT, even in moderately-disturbed periods. This fact leads to the conclusion that, basing on magnetometric data, the pigeon cannot localize its home with an accuracy better than a few kilometers. Entering this region, it must switch into another navigation system; see Fig. 9 reproduced from Gould (1982), which shows how a blindfolded pigeon navigated around its home.

Fig. 9 Navigation around home of a blindfolded pigeon (Gould 1982; reproduced with Nature Publishing Group permission)



6 Parameters of Present-Day Magnetometric Systems

The magnetic field measurements are now performed making use of various physical phenomena. We have magnetometers based on superconductivity, nuclear resonance, optical pumping, or magnetic susceptibility nonlinearity (see, e.g., Jankowski and Suckdorff 1996). The resolution of 0.1 nT is relatively easily attainable, in particular in magnetometers that measure the field modulus (such magnetometers even attain an accuracy of 0.001 nT). It does not seem likely for a pigeon to make use of any of these phenomena. The high resolution of magnetometers does not mean that this is the accuracy with which they measure the components. The main difficulty is to properly align the measurement system's

axis. To attain the 0.1 nT accuracy, the vertical direction must be known with an accuracy of single seconds of arc. The direction can be stabilized either by means of gyroscope systems or by making digital recording of tilt and numerically correcting the readings. The stabilization of the vertical direction can also be obtained by applying Cardan's suspension of the sensor. The present technology, however, does not allow us to obtain, e.g., an aeromagnetic vector map with an accuracy of 0.1 nT. If a pigeon had such a system, it would have meant that it is superior to the contemporary technological achievements.

7 Plan of Future Experiments

In the last 50 years, ornithologists performed a lot of experiments to elucidate the pigeon navigation principles; some attempts were very intelligently designed and not easy to make. In the present chapter, we tried to use some of the results of these experiments. Still, the pigeon navigation conceals a mystery. The main way to approach the truth is to perform new experiments. First of all, they should confirm or deny the hypothesis that a pigeon is in possession of a vector magnetometer. To this end, we propose the following experiments:

1. We take a group of pigeons equipped with miniature position recorders (GPS) to a site that lies on an isoline of one field component, some 100 km from home. Then we wait for such conditions that all other navigation systems are most probably impossible to apply (I mean full overcast, homeward wind). The release of the pigeon on the isoline will automatically deprive it from the information coming from this component. If the released pigeons still select the proper direction, they must have additional information from, e.g., the measurement of the other component of the magnetic field. The experiment can be expanded by using isolines of different components. For a joint team of an ornithologist and geophysicist, the experiment is relatively easy to perform. Somewhat similar experiment was proposed by Źoltowski (1986)
2. The second experiment could be a modification of the one described by Gould (1982), the result of which has been shown in Fig. 5. The only difference is that we should select the area for which we are in possession of magnetic charts of all the field components. This region, some 100 km in diameter, must contain a few geomagnetic anomalies. This is difficult to perform since the pigeons must be released at many distant places.
3. The third proposition is sort of a wishful thinking, since its realization is difficult. I think that having a helicopter equipped with a proton magnetometer of 1 nT sensitivity one could make an attempt to find a home of known magnetic parameters, although the reconnaissance flight would involve greater loops.

Of course, much more experiments can be proposed.

8 Summary and Conclusions

An analysis of the proposed mathematical model gives grounds for drawing the following conclusions:

1. The assumption that the pigeon is in possession of a vector magnetometer makes it possible to explain the bird's navigation.
2. Navigation is possible when the linear trends of the two field components form a skew reference system.
3. The magnetometer's sensitivity must be very high, not worse than 0.1 nT.

I want to emphasize once again that I do not think the pigeon has the data processing system as proposed in the model. The model was used mainly in order to estimate how anomalies affect the flight direction. The information processing system may be different, but the conclusions presented above remain valid.

Below I describe a simpler navigation system. Its main assumption is that the pigeon chooses the direction at which the relative changes of both components are the same. Let ∂Z and ∂H denote the field differences between the release site and home, ∂Z and ∂H the local field changes, the latter being dependent on direction. If in the reconnaissance flights the pigeon finds the angle at which $\partial Z/\Delta Z$ is equal to $\partial h/\Delta H$, this will be the homeward direction. Please note that in this case it is not necessary to calculate the gradients. Nevertheless, the calculation of local increments reduces to the same. The pigeon will behave like "feeling" the home position. Of course, the direction the bird initially settled will be permanently verified and amended, basically in the same manner as in our model considerations.

The assumption that the pigeon has a vector magnetometer can be treated as a hypothesis. Whether it is true or not—it can only be verified by experiments. These can be planned easily enough since we know what questions should be answered. We have outlined the assumptions of a few experiments of this type, although one can imagine many other ones. The hypothesis has its strong and weak points. The strong points include a possibility of explaining practically all hitherto unexplained traits of navigation, while the weak ones—the extremely high requirements as to the magnetometer's sensitivity.

References

- Elsner B (1978) Accurate measurements of the initial tracks of homing pigeons. In: Schmidt-Koenig KK, Keeton WT (eds) Animal migration, navigation, and homing. Springer, Berlin, pp 194–198
- Gould JL (1982) The map sense of pigeons. Nature 296(5854):205–211
- Hagstrum JT (2013) Atmospheric propagation modeling indicates homing pigeons use loft-specific infrasonic map cues. J Exp Biol 216:687–699
- Jankowski J (2010) Model nawigacji gołębi oparty na wskazanich magetometru wektorowego (The pigeon navigation model based on vector magnetometer's indications) Przegląd Geofizyczny LV, 3–4:157–174

- Jankowski J, Suckdorff Ch (1996) Guide for magnetic measurements and observatory practice. IAGA, Warsaw 236 pp
- Keeton WT (1974) The orientational and navigational basis of homing in birds. In: DS Lehrman (ed) Advances in the study of behavior, vol 5. Academic Press, New York, pp 47–132
- Keeton WT, Larkin TS, Windsor DM (1974) Normal fluctuation in the earth's magnetic field influence pigeon orientation. *J Comp Physiol* 95:95–103
- Matthews GVT (1968) Bird navigation, 2nd edn. Cambridge University Press, Cambridge
- Papi F (1986) Pigeon navigation: solved problems and open questions. *Monit Zool Ital* 20:471–517
- Schmidt-Koenig KK, Keeton WT (eds) (1978) Animal migration navigation and homing. Springer, Berlin
- Schmidt-Koenig KK (1979) Avian orientation and navigation. Academic Press, London
- Sucksdorff CH, Nevanlinna H (1981) Magnetic charts for Finland (1980), Helsinki
- Walcott C (1978) Anomalies in the earth's magnetic field increase the scatter of pigeons' vanishing bearings. In: Schmidt-Koenig KK, Keeton WT (eds) Animal migration navigation and homing. Springer, Berlin, pp 143–151
- Walker MM (1998) On a wing and a vector: a model for magnetic navigation by homing pigeons. *J Theor Biol* 192:341–349
- Walker MM, Dennis TE, Kirschvink JL (2002) The magnetic sense and its use in long-distance navigation by animals. *Curr Opin Neurobiol* 12(6):735–744
- Wallraff HG (1990) Navigation by homing pigeons. *Ethol Ecol Evol* 2:81–115
- Wallraff HG (1999) The magnetic map of homing pigeons: an evergreen phantom. *J Theor Biol* 197(2):265–269. doi:[10.1006/jtbi.1998.0874](https://doi.org/10.1006/jtbi.1998.0874)
- Wiltschko R, Wiltschko W (1995) Magnetic orientation in animals. Springer, Berlin, p 297
- Wiltschko W, Wiltschko R (1996) Magnetic orientation in birds. *J Exp Biol* 199(1):29–38
- Wiltschko R, Wiltschko W (2009) Avian navigation the Auk—intern. *J Ornithol* 126(4):717–743. doi:[10.1525/auk.2009.11009](https://doi.org/10.1525/auk.2009.11009)
- Żółtowski AM (1986) On birds navigation in the Earth magnetic fields. *Proc Inst Geodesy Cartography* 1(76):87–111 (in Polish and English)

Analysis of Surface Ozone Variations Based on the Long-Term Measurement Series in Kraków (1854–1878), (2005–2013) and Belsk (1995–2012)

Izabela Pawlak and Janusz Jarosławski

Abstract One of the first long-term ozone measurement series in the world, as described in the chapter, was made in Poland (Kraków) during the period 1854–1878. The data obtained by the method of Schönbein papers reveal that annually averaged concentrations of ground level ozone in the second half of nineteenth century ranged between 11 and 24 ppb. For comparison, this chapter presents the results of contemporary measurements performed at rural background station in Belsk (1995–2012) and at urban background station in Kraków (2005–2013). Nowadays, annually averaged surface ozone values ranged between 22 and 31 ppb in Belsk and between 12 and 17 ppb in Kraków. Seasonal variation of nineteenth century Kraków series exhibited the highest surface ozone concentration during spring and early summer and the lowest in late autumn and winter. Current data present similar shape of distribution, although the sharp spring peak of high values has been replaced by a broad spring-summer maximum. Long-range averages of surface ozone concentration in rural areas are significantly higher than in urban areas (reaching 26 and 15 ppb, respectively).

Keywords Surface ozone · Schönbein paper · Linvill's chart

I. Pawlak (✉) · J. Jarosławski

Institute of Geophysics, Polish Academy of Sciences, 64 Księcia Janusza,
01-452 Warsaw, Poland
e-mail: izap@igf.edu.pl

J. Jarosławski
e-mail: januszj@igf.edu.pl

1 Discovery of Ozone, First Measurements and Speculations About its Origin

In 1839, German chemist Christian Friedrich Schönbein during his experiments on the electrolysis of water smelled a characteristic odor. Initially, due to oxidizing capacity of the newly discovered substance, he thought that it is chlorine or any of its variations, but soon changed his mind realizing that it is a variety of oxygen and proposed the new term “ozone”. Finally he stated that it is a natural component of air created as a result of chemical reactions or through the electrical activity in the atmosphere (Wierzbicki 1882). Andrews (1874) demonstrated that ozone is an allotropic variety of oxygen, most likely consisting of three atoms of oxygen. Furthermore, he confirmed Schönbein’s hypothesis that ozone is present in the air but it is also rapidly destroyed by smoke and other contaminations existing in the air of large towns. In his opinion, ozone is more abundant in rural than in urban regions, and in mountain areas than in the lowlands (Andrews 1874).

Those scientists, who believed in the existence of ozone tried to establish its potential sources. There existed numerous theories about the origin of ozone. The most widespread were associated with: (1) atmospheric electricity, (2) emission of ozone-rich-air by plants, (3) evaporation of water, and (4) action of sunlight on the leaves of green plants; in other theories it was supposed that ozone concentration is closely linked with species and height of the clouds (Wierzbicki 1882). Molecular formula of ozone was defined in 1865 by Soret and subsequently confirmed by him in 1867 (Rubin 2001).

The first measurements of ozone were made by its discoverer Christian Friedrich Schönbein. He exploited the fact that the compounds of iodide with potassium decompose under the influence of ozone. His method involved blotting paper dipped in starch glue with a leaven of potassium iodide. Dried “Schönbein paper” was exposed to ozone present in the air for several hours. Iodine, isolated due to decomposition of potassium iodide, acting on a starch changes its color to blue. More intense color meant more ozone in the air. Then the test-paper was compared with chromatic 10-grades scale and the result was used as a relative concentration of ozone in the atmospheric air. Number 0 means absence of ozone, while number 10 means very high amounts of ozone in the air. Schönbein’s method quickly turned out to be easily applicable and sensitive even if the concentration of ozone is very low (Wierzbicki 1882).

In the mid-1850s, about 300 measuring stations operated by medical doctors, pharmacists and university professors were located in Australia, Europe and North America, where only in the State of Michigan there were about 35 of such stations. Unfortunately, many series of measurements were not performed continuously and usually lasted for a short time (Bojkov 1986).

Despite the fact that Schönbein’s method was widespread around the world, it had also several disadvantages: (1) excretion of iodide in the first hours of exposure is more intense than later on, (2) subjective estimation of intensity of blue colour depending on the observer, and (3) strong dependency of this method on relative

humidity (Wierzbicki 1882). At low relative humidity, the colour has a little intensity even when ozone concentration was high and, vice versa, at high relative humidity the colour was intense even when ozone concentration was low. Also the presence of other gases influenced the colour of test-paper, and that is why measuring points were usually located away from potential sources, especially those of sulphurous acid (Linvill et al. 1980). The influence of relative humidity variations was a serious problem until 1980 when Linvill, Hooker and Olson proposed a conversion chart constructed to allow the conversion of Schönbein's data into units of ozone concentration used today (ppb). This chart was prepared based on measurements of ozone concentration within the chamber by a Dasibi ozone analyzer (Linvill et al. 1980).

Beside the qualitative method of ozone measurements discovered by Schönbein, also a quantitative method for the determination of ozone in the air was used. It is worth mentioning that the long-term measuring series performed by French chemist Albert Levy in the Meteorological Observatory of Montsouris, southern Paris, from 1876 to 1910. This method involved a process of arsenite oxidation. The basic element of the apparatus was a bottle filled with 20 cm^3 of 5×10^{-4} molar potassium arsenite (K_3AsO_3) and 2 cm^3 of a 3 % potassium iodide (KI) solution through which the atmospheric air was sucked. The ozone present in the air transformed arsenite into arsenate. The amounts of transformed arsenite were a basis for determining the ozone in the air (Volz and Kley 1988; Bojkov 1986). Volz and Kley decided to rebuild measuring apparatus to compare the obtained data with a modern UV-photometer. They proved that the uncertainty of Montsouris series is about 3 %. Their assessment is that the 30 year average of ozone concentration is about 11 ppb, in a range from 5 to 15 ppb (Kley 1994).

At the beginning of the twentieth century the interest in tropospheric ozone significantly decreased. According to Crutzen (1988) this was probably caused by poor quality of measurements, which made it difficult to determine reliable spatial and temporal patterns of ozone concentration. A big break-through came in the second decade of the twentieth century with the development optical techniques. Furthermore, by the end of the third decade the well-known chemical techniques based on conversion of potassium iodide (KI) to iodine (I_2) were improved. Measurements of this kind were commonly used in Europe in the half of twentieth century and their quality was regarded to be good. Because of the abundance of observations, in this chapter we mention only about two series of measurements performed on the territory of today's Poland. The first one was carried out by H. Cauer from June to October between 1934 and 1936 in the Tatra Mountains. Measurement points were located at different altitudes between 400 and 1000 m. a.s.l. According to these observations, the surface ozone concentration during day ranged from less than 10 to 25 ppbv. The second series of measurements using the same method was performed by H. Tichy between February and April in 1937 and 1938 in Schreiberhau (today: Szklarska Poręba, Poland) at 700 m altitude. The well-known diurnal cycle with maximum in the early afternoon hours was noticed. Tichy explained this fact by the correlation between surface ozone concentration and intensity of ultraviolet radiation. An average of early afternoon surface ozone concentration was generally in the range 10–15 ppbv (Crutzen 1988).

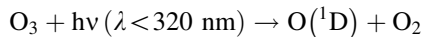
2 Theoretical Background

Ozone is a natural constituent of the atmosphere. About 90 % is located in the stratosphere where it is produced through the photolysis of molecular oxygen. The remaining 10 % is present in the troposphere where it is formed as a result different chemical processes.

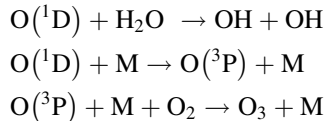
Until about 40 years ago, the dominant theory was that all ozone in the troposphere was previously created in the stratosphere. On the contrary to the common thinking, it is now proven that a significant part of ozone is formed and destroyed in the troposphere through numerous chemical reactions (Crutzen et al. 1998).

Surface ozone is a secondary air pollutant and its concentration is controlled by emission of the ozone precursors, the pollutants: nitrogen oxides (NOx), volatile organic compounds (VOCs) and carbon monoxide (CO) (Logan 1985). Interaction between O₃ and its precursors are often complex and nonlinear (Monks 2005).

The key chemical component that controls tropospheric chemistry (including the processes of ozone formation and destruction) is OH radicals, which are created from the photolysis of ozone itself:



Excited oxygen atom (O(¹D)) can either react with water vapour to produce OH radicals or form ozone following the collision with the other molecule "M" (predominantly O₂ or N₂).



where O(³P) is the oxygen atom in ground state, O(¹D) the oxygen atom in excited state.

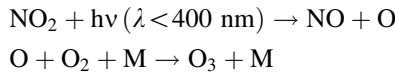
Hydroxyl radicals are responsible for processes of oxidation of different atmospheric pollutants, mainly CH₄ and CO, thereby initiating a series of reactions that produce or destroy ozone. Whether the above processes of oxidation lead to the ozone production is strongly dependent on the concentration of nitrogen oxides, NOx (NO + NO₂) (Crutzen et al. 1998). Non-linear relationship between O₃ and NOx is manifested by the fact that, depending on whether we are in the area of high or low NOx, an increase of NOx emission can promote or reduce the ozone formation. The area of high or low NOx is defined by a relative efficiency of radicals (S) production and NOx emission:

- When S > NOx emission = low NOx area, then the concentration of O₃ increases with decreasing amounts of NOx and almost does not depend on the amount of VOC.

- When $S < NO_x$ emission = high NO_x area, then the concentration of O_3 decreases with increasing amount of NO_x and increases with increasing amounts of VOC.

It can be concluded that an increase of concentration of VOCs generally promotes the ozone formation while an increase of NO_x emission can either promote or limit the ozone production.

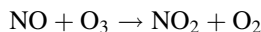
Meteorological conditions, beside the presence ozone precursors, are another factor that plays a crucial role in surface ozone formation. High ozone concentrations are usually associated with intense solar radiation, high temperature, low wind speed and low relative humidity (Pulikesi et al. 2006). Numerous observations have revealed that an increase of temperature and intensity of solar radiation on the cloudless days significantly affect the increase of ozone concentration (Pudasainee et al. 2006). Solar radiation is essential for the initiation of photochemical processes leading to ozone production. The only known method of ozone formation is the reaction of oxygen atom (O) with oxygen molecule (O_2). The main source of O near the Earth's surface is a process of photodissociation of NO_2 initiated by quantum of solar radiation at a wavelength below 400 nm:



Also the influence of temperature on the surface ozone content is not insignificant. High temperature enhances the rate of some chemical reactions (Science Policy Report 15/08 2008). Biogenic sources emit more VOCs at high temperature; especially the isoprene, due to its high reactivity plays a significant role in surface ozone production (Bell and Ellis 2004). Moreover, during daytime due to convective heating the processes of vertical mixing and simultaneously downward transport of ozone are most efficient (Lal et al. 2000).

The ozone concentration varies diurnally and seasonally, reaching its maximum during summer afternoon hours, when photochemical formation is most efficient. A secondary maximum during spring afternoons is additionally enhanced by the stratospheric-tropospheric exchange (Bloomer et al. 2010).

Analyzing the spatial variability of surface ozone concentration, the kind of study area turns out to be a very important factor. Distinction between rural and urban areas allows us to note that rural regions are often characterized by higher ozone concentration. The lower ozone amount in urban areas is generally connected with high concentration of NO_x and direct destruction of O_3 through the process:



During night, the lack of solar radiation hinders the process of photodissociation of NO_2 (to create O) and consequently makes ozone formation impossible.

Diurnal variations at high-altitude stations are quite different and do not show signs of daytime photochemical build-up characteristic of rural or urban areas. Relatively low values of daily ozone concentration are usually noticed at clear, elevated locations deprived of the influence of potential sources of pollutants (Oltmans and Levy 1994; Naja et al. 2003).

3 Objective of the Chapter

The main objective of this chapter is to present, known from the literature, ground-level ozone measurement series performed in the area of contemporary Poland. In this chapter we decided to use one of the first long-ranged ozone measurements series performed in Kraków in the second half of 19th century by Wierzbicki using Schönbein papers. Despite the poor uniformity of Schönbein method, already noted by Wierzbicki, we appreciate this extremely valuable series and used it to compare those data with current ozone observations. For this purpose we used Linvill's chart to convert Schönbein numbers into ppb units. Such an attempt has been already made by Degórska et al. (1996), who used data from Kraków to compare them with modern tropospheric ozone data from Belsk (Poland) and from Hohenpeissenberg (Germany).

In this work we present the results of the surface ozone measurements performed in Kraków (1854–1878) and Belsk (1995–2012). The analysis focuses on the daily (with the division into day and night) as well as the monthly, seasonal and annual variations of surface ozone concentration. The main objective of this work is to describe the surface ozone distribution observed in 19th century Kraków and contemporary Kraków and Belsk and determine the conditions governing the processes of surface ozone formation and destruction.

4 Experimental Details

One of the first long series of ground-level ozone measurements was performed by Wierzbicki in 1854–1878 in Kraków. Observations were carried out 2 times per day: at 6 am and 10 pm, thus the exposition time lasted 16 h during day and 8 h during night. The terms day and night used in the text refer to the above-mentioned time intervals. Daily average values were calculated as an average value over the day and night. Ozone papers were situated on the second floor of the Astronomical Observatory at a height of 11.7 m for the first 16 years (1854–1868) on the north-west, and then (1869–1878) on the south-west side of the building. For most of the time, until the beginning of 1875, measurements were carried out using papers prepared in trustful compliance with the original Schönbein's recipe using 10 point scale but later using papers produced in a factory of Lenz and Lender using 14 point scale. Shortly after the end of the measurements, the obtained results were

standardized and statistically compiled by Wierzbicki, and published by the Academy of Arts and Sciences in 1882.

Contemporary data were obtained from the Central Geophysical Observatory of the Institute of Geophysics, Polish Academy of Sciences at Belsk, which constitutes a background measuring station operating under the Regional Inspectorate of Environmental Protection in Warsaw. Daily average data as well as average day and night values were calculated based on hourly averaged data wherein the day and night values of ozone concentration are representative for the same time intervals as in Kraków (16 and 8 h, respectively). Measurements have been performed by Monitor Labs and Monitor Europe analyzers (model ML8810 and ML9810), operating on the basis of UV absorption by ozone at wavelength 253.7 nm, which is generated by a low pressure mercury lamp. The measurement consists of two parts:

- (1) Measurement of UV light passing through the sample of air without ozone to determine the reference light intensity (removal of ozone from the sample is done using ozone scrubber).
- (2) Measurement of UV light passing through the sample of air with ozone to determine intensity of light after absorption.

The degree of absorption is proportional to the amount of ozone, and, using Beer-Lambert absorption equation, it is possible to calculate the concentration of ozone in the air. The inlet for trace gas measurements is situated on the roof of the Laboratory building at a height of 7 m above the ground level.

5 Results and Discussion

5.1 Measurement Series in Kraków (1854–1878)

To describe temporal variability of surface ozone amount in the period 1854–1878 in Kraków, annually averaged concentrations are presented in Fig. 1.

In order to reveal the long-term changes, the annual data have been smoothed using the Locally weighted scatter plot smooth (LOWESS) technique. Analyzing this chart, the most conspicuous are small amounts of ozone in the second half of measurement series (1869–1878) in comparison to the first (1854–1868). The turning point, which occurred between 1868 and 1869, evidently divided 25 years of measurements into two parts. In the first one, the highest annual average was 51 ppb (1860), the lowest being 29 ppb (1856), while in the second one these values were 24 ppb (1874) and 11 ppb (1877), respectively. An average ozone concentration in the first part was more than 40 ppb, while in the second part only less than 17 ppb. Probably this was caused by changing the location of measuring point. Until 1869 the Schönbein papers were exposed from the north-west side of the building, near the street and the yard. It is well-known that such a location might have promoted accumulation of different components of the air, which could

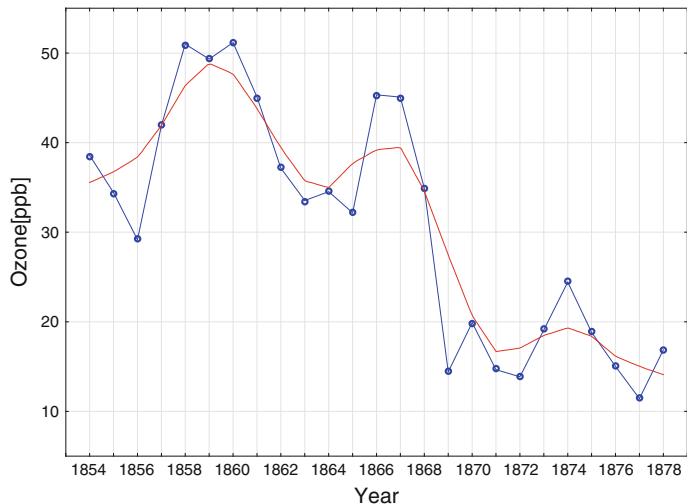


Fig. 1 Annually averaged concentration for 1854–1878 time series of surface ozone

influence on the color of paper. From 1869 to 1878 the test papers were exposed from the south-west side of the building, near the garden. To explain the influence of the location of measuring point during 22 April–31 May, Wierzbicki decided to perform the same kind of measurements in both places (Table 1).

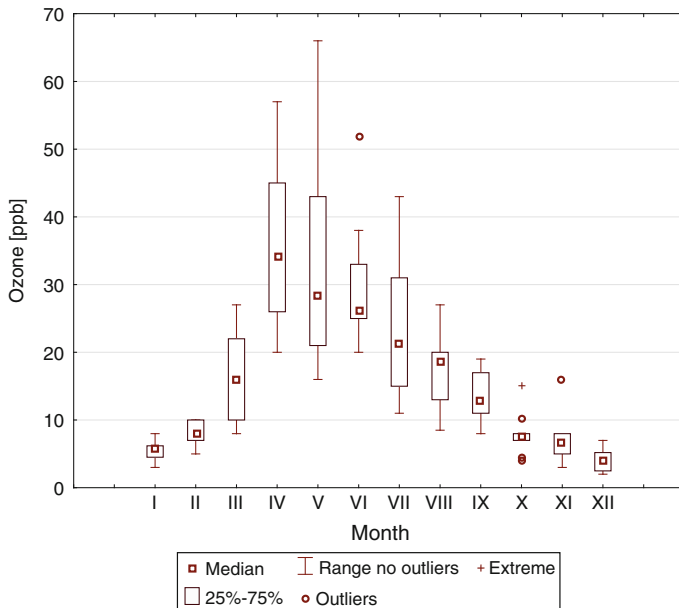
During forty days of observations performed on North location, the average daily ozone concentrations were significantly higher than those performed on the South. The differences ranged between 20 and 25 ppb. During nights, the situation was similar: average ozone concentrations performed on the North side were higher, although the differences were slightly lower than during day and oscillated between 2 and 23 ppb.

According to the recommendations of a researcher, who has performed these measurements, we decided to use in our chapter only data from 1869–1878 as the most reliable.

Analyzing seasonal variation of surface ozone in 1869–1878 (Fig. 2) it is possible to conclude what was the main mechanism that governed the distribution of ground-level ozone in the second part of 19th century. Very pronounced spring maximum indicates the dominant influence of the tropospheric-stratospheric exchange as the main source of ozone. Gradual decrease of surface ozone values throughout the summer and simultaneously significantly lower concentrations prove that photochemical production of ozone was of secondary importance in ozone budget. It was also found that surface ozone concentration varied in a broad range within a month, especially during spring and summer season. This can be explained by significantly higher potential of ozone production in summer. Based on statistics, the monthly median of surface ozone concentration ranged between 4 (December) and 34 (April) ppb, while the monthly average fluctuated in the range of 4.1 (December) and 35.1 (April) ppb.

Table 1 Average 10-days surface ozone values in Kraków

| Ten days | Average daily ozone concentration (ppb) | | | Average night ozone concentration (ppb) | | |
|----------|---|-------|------------|---|-------|------------|
| | North | South | Difference | North | South | Difference |
| I | 76 | 56 | 20 | 62 | 44 | 18 |
| II | 56 | 31 | 25 | 49 | 38 | 11 |
| III | 77 | 55 | 22 | 26 | 24 | 2 |
| IV | 98 | 78 | 20 | 94 | 71 | 23 |

**Fig. 2** Seasonal variations of surface ozone concentration for 1869–1878 time series

Analyzing the chart depicted in Fig. 3 we can further delve into the subject of seasonal variations of surface ozone concentration and notice again that the seasonal maximum of surface ozone concentration in each year occurred in spring. Slightly smaller values were noticed in summer, significantly lower values were observed during autumn, and the lowest during winter. The average values of seasonal surface ozone concentration for the period 1869–1878 were: 28 ppb in spring, 24 ppb in summer, 9 ppb in autumn, and—6 ppb in winter.

Looking at Table 2 we can state that in the years 1869–1873 the monthly maximum occurred in April (with the exception of 1869, when the maximum, amounting to 27 ppb, occurred in March).

The highest values varied from year to year and ranged between 26 and 57 ppb. In the subsequent years (1874–1878) the monthly maximum occurred alternately in May (1874—66 ppb, 1876—43 ppb) in June (1875—33 ppb, 1877—26 ppb) or

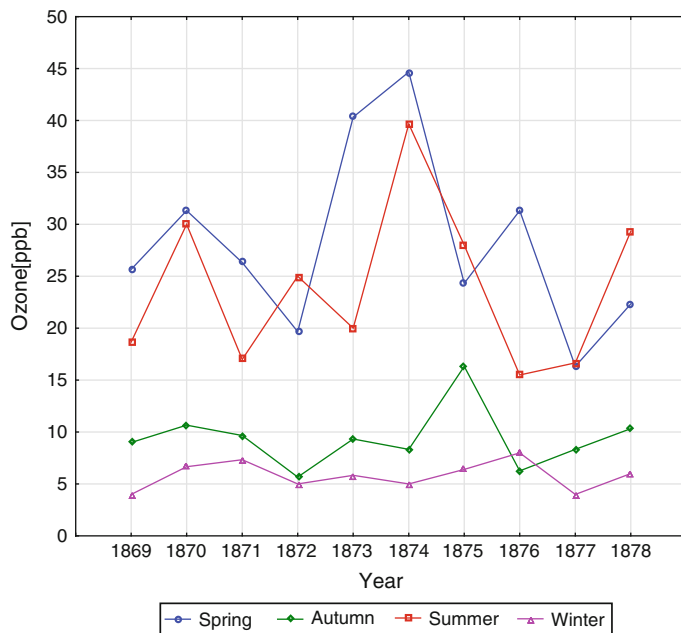


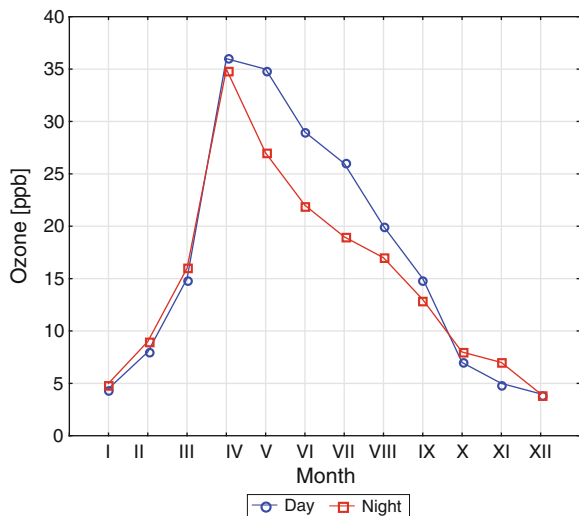
Fig. 3 Seasonal variations of surface ozone concentration for 1869–1878 time series divided into seasons

Table 2 Monthly averaged concentration of surface ozone (ppb) for 1869–1878 time series

| Year/Month | I | II | III | IV | V | VI | VII | VIII | IX | X | XI | XII |
|------------|-----|----|-----|----|----|----|-----|------|----|-----|-----|-----|
| 1869 | 4.5 | 5 | 27 | 26 | 24 | 20 | 18 | 18 | 11 | 8 | 8 | 4 |
| 1870 | 6 | 10 | 23 | 45 | 26 | 38 | 25 | 27 | 19 | 7 | 6.5 | 7 |
| 1871 | 7 | 8 | 10 | 35 | 34 | 25 | 15 | 11 | 11 | 10 | 8 | 2 |
| 1872 | 5 | 8 | 8 | 35 | 16 | 27 | 29 | 19 | 10 | 4 | 3 | 2.3 |
| 1873 | 5.2 | 10 | 15 | 57 | 49 | 26 | 17 | 17 | 14 | 7 | 7 | 5 |
| 1874 | 3 | 7 | 17 | 47 | 66 | 52 | 40 | 27 | 12 | 8 | 5 | 5.2 |
| 1875 | 6.2 | 8 | 14 | 28 | 31 | 33 | 31 | 20 | 18 | 15 | 16 | 6 |
| 1876 | 8 | 10 | 18 | 33 | 43 | 24 | 14 | 8.5 | 8 | 4.3 | 6.5 | 3 |
| 1877 | 4.2 | 5 | 8 | 20 | 21 | 26 | 11 | 13 | 14 | 7 | 4.2 | 4 |
| 1878 | 6 | 8 | 22 | 25 | 20 | 25 | 43 | 20 | 17 | 8 | 6 | 2.5 |

in July (43 ppb). Predominantly lowest monthly averaged values were in December (2–6 ppb) and in 2 years in January (1870—6 ppb, 1874—3 ppb). The highest values of surface ozone concentration may indicate a dominant role of stratospheric-tropospheric exchange as a main source of surface ozone (Volz and Kley 1988). Monthly averaged values of ground level ozone with division into day and night for the period 1869–1878 are presented in Fig. 4.

Fig. 4 Monthly averaged concentration of surface ozone with division into day and night for 1869–1878 time series



It is clearly seen that during months from April to September the ozone concentrations during day were higher than during night. The highest differences occurred in May, June and July and reached 8, 7 and 7 ppb, respectively. At this time, the potential of photochemical ozone production due to intensive solar radiation is the biggest. Opposite situation was noticed from October to March. In this case, differences were not so high and oscillated in a narrow range—up to 2 ppb. In the 19th century, the chemistry of atmosphere was dominated mainly by emission of SO_2 , CO and CO_2 as by-products of coal combustion. The absence of developed road transport was the reason why the NOx concentration level was significantly lower. In this case, it is especially important because during nighttime, NOx act as ozone destroyers ($\text{NO} + \text{O}_3 \rightarrow \text{NO}_2 + \text{O}_2$). In effect, locations distinguished by low concentration of NOx (even today) are characterized by relatively high surface ozone amounts during night. Furthermore, advection of frozen, fresh air from north and north-west directions during winter is generally responsible for the high ozone values. Most Arctic stations are characterized by the highest ozone concentrations in winter time (December–May) due to the weakness of ozone sinks during the dark period (Helmig et al. 2007). In winter months, photochemical production of ozone due to weak solar activity could be significantly smaller (as it is observed nowadays). We can suggest that air pollution associated for example with intensive domestic heating additionally limited the solar radiation. The poor efficiency of photochemical ozone formation under these conditions during day and reduced ozone titration processes at night resulted in similar values of surface ozone concentration during whole day (more details about the phenomenon of low ozone concentration during winter days in modern urban areas are contained in Sect. 5.3).

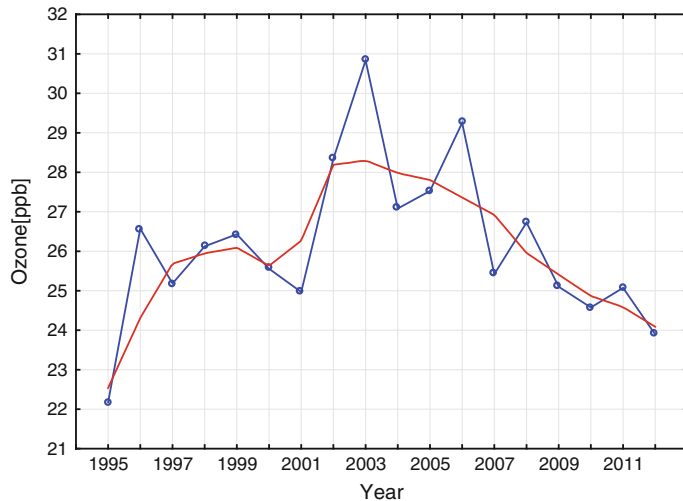


Fig. 5 Annually averaged concentration of surface ozone for 1995–2012 time series

5.2 Measurement Series in Belsk (1995–2012)

To describe temporal variability of surface ozone at station Belsk, annually averaged concentrations of surface ozone are presented in Fig. 5.

Data were smoothed using the LOWESS technique, which allows to track long-term changes of ozone. Analyzing this chart we can observe specific behavior of ozone concentration: from 1995 surface ozone concentration has been gradually increasing, revealing the maximum around 2003 and was steadily decreasing since that time. Probably such a situation was caused by decreasing emission to the atmosphere of contaminants of air being precursors of ozone. In the period 1990–2010 across the EEA-32 countries, significant decreases of NOx (−42 %), NMVOC (−53 %), CH₄ (−32 %) and CO (−61 %) were noticed. In Poland, the values were as follows: NOx (−30 %), NMVOC (−20 %), CH₄ (−25 %) and CO (−60 %). This improvement of air quality has been achieved by catalytic converters, which considerably reduced the amount of emission of NOx and CO from motor vehicles (EEA 2012).

Figure 6 depicts that minimum values of surface ozone occur in November and the increase in ozone concentration was then noticed, reaching the highest amount in April. Thereafter, through all the months until November, ozone concentrations decrease steadily. Based on statistics, the monthly median of surface ozone concentration ranged between 12.8 ppb (November) and 36.6 ppb (April) while the monthly average fluctuated in range from 13.3 (November) to 36.2 ppb (April).

Seasonally averaged surface ozone concentration presented in Fig. 7 allows to conclude that during the measurement period (1995–2012) the highest amounts of ozone occur in spring (35.11 ppb) and in summer (32.34 ppb). The lowest values

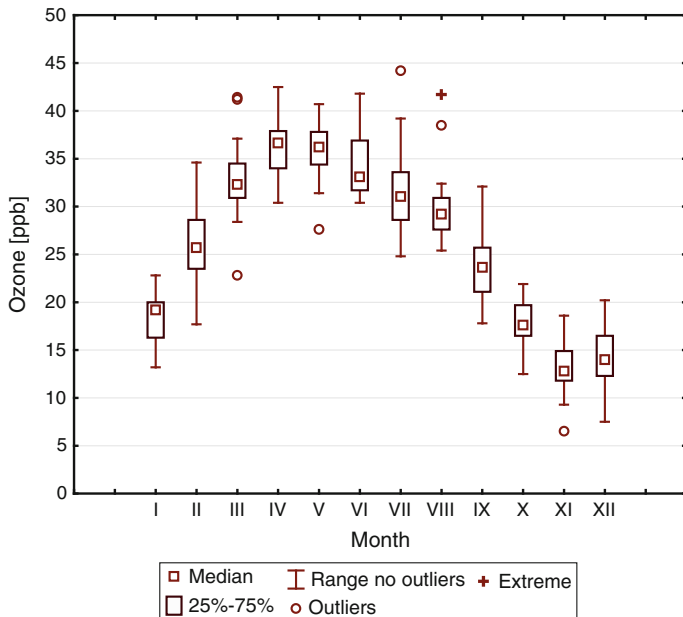
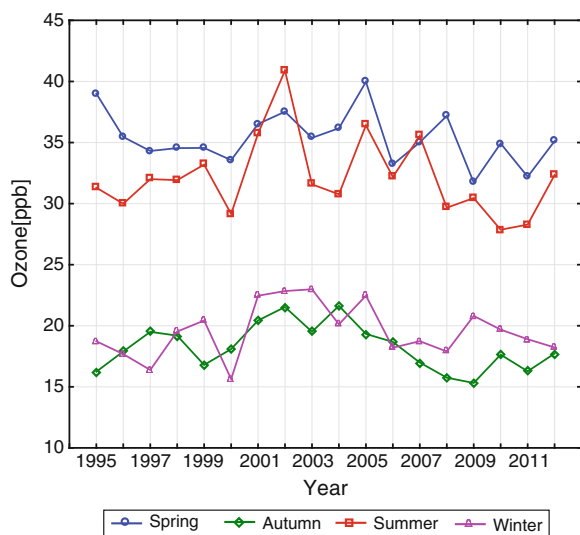


Fig. 6 Seasonal variations of surface ozone concentration for 1995–2012 time series

Fig. 7 Seasonal variations of surface ozone concentration for 1995–2012 time series divided into seasons



of surface ozone concentration occur in autumn (17.72 ppb) and in winter (18.22 ppb). As demonstrated by Volz and Kley (1988), the concentration of surface ozone in Europe in the last century almost doubled. Also the course of seasonal changes has been modified. The currently observed broad spring–summer

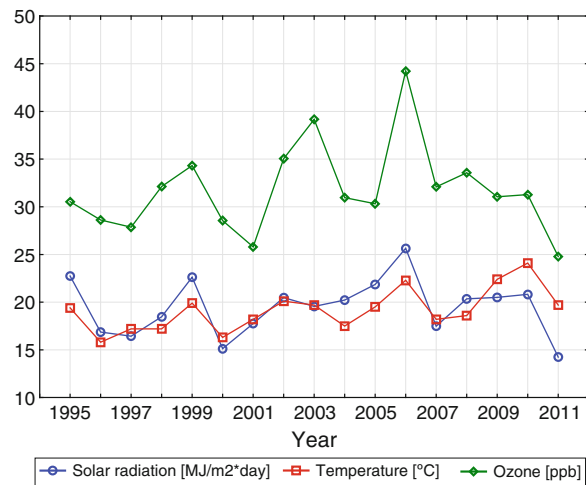
Table 3 Monthly averaged concentration of surface ozone (ppb) for 1995–2012 time series

| Year/Month | I | II | III | IV | V | VI | VII | VIII | IX | X | XI | XII |
|------------|------|------|------|------|------|------|------|------|------|------|------|------|
| 1995 | 17.5 | 17.7 | 22.8 | 30.4 | 31.4 | 31.7 | 30.5 | 29.4 | 24.1 | 16.5 | 6.5 | 7.5 |
| 1996 | 18.5 | 30.1 | 41.2 | 41.4 | 34.4 | 38 | 28.6 | 27.3 | 18.2 | 17.7 | 12.8 | 10.5 |
| 1997 | 14.6 | 27.9 | 31.7 | 37.9 | 36.8 | 32.4 | 27.9 | 29.7 | 23.5 | 18.1 | 12.1 | 9.7 |
| 1998 | 16 | 23.5 | 34.5 | 31.7 | 36.8 | 34.9 | 32.1 | 29 | 21.3 | 20.5 | 16.7 | 16.6 |
| 1999 | 14.7 | 27.3 | 31.9 | 34 | 37.8 | 30.5 | 34.3 | 30.9 | 26.3 | 18 | 13.3 | 18.2 |
| 2000 | 19.6 | 23.6 | 29.7 | 34 | 40 | 40.3 | 28.5 | 30.7 | 21.3 | 19.7 | 9.3 | 9.9 |
| 2001 | 13.2 | 23.8 | 30.9 | 32.7 | 37 | 32.8 | 25.8 | 28.9 | 19.1 | 16.7 | 18.6 | 20.2 |
| 2002 | 19.4 | 27.7 | 31.9 | 36.9 | 40.7 | 33.6 | 35 | 38.5 | 26.1 | 20.5 | 14.7 | 14.9 |
| 2003 | 19 | 34.6 | 37.1 | 37.9 | 37.5 | 41.8 | 39.2 | 41.7 | 30 | 21.9 | 12.7 | 16.5 |
| 2004 | 22.8 | 29.6 | 34.4 | 37.7 | 34 | 33.1 | 31 | 30.6 | 25.1 | 16.8 | 16.6 | 13.1 |
| 2005 | 21.7 | 25.6 | 36.7 | 37.3 | 34.5 | 34.5 | 30.3 | 27.5 | 32.1 | 20 | 12.8 | 17.4 |
| 2006 | 19.9 | 30.1 | 41.4 | 38.8 | 39.7 | 36.9 | 44.2 | 28.1 | 25.7 | 18.1 | 14.2 | 13.9 |
| 2007 | 21.3 | 19.4 | 28.4 | 35.9 | 35.2 | 33.1 | 32.1 | 31.4 | 23.3 | 15.3 | 17.3 | 12.3 |
| 2008 | 20.3 | 23.6 | 32.8 | 36.7 | 35.6 | 40.7 | 33.6 | 32.4 | 19.5 | 16.6 | 14.9 | 14.1 |
| 2009 | 16.3 | 23.3 | 30.8 | 42.5 | 38.2 | 30.4 | 31.1 | 27.6 | 23.8 | 12.5 | 11 | 13.9 |
| 2010 | 20 | 28.6 | 32.7 | 34.9 | 27.6 | 31.3 | 31.3 | 28.8 | 17.8 | 15.9 | 12.2 | 13.9 |
| 2011 | 19.4 | 25.8 | 32.7 | 36.6 | 35.5 | 32.9 | 24.8 | 25.9 | 23.8 | 17.5 | 11.6 | 14.4 |
| 2012 | 18.8 | 23.4 | 31 | 33.7 | 31.9 | 30.7 | 28.7 | 25.4 | 21.1 | 15.9 | 11.8 | 14.1 |

ozone maximum is probably a result of presence in the atmosphere of large amounts of ozone precursors, which are an important source of surface ozone during the summer maximum of solar radiation. Looking at Table 3 showing monthly averaged values of surface ozone concentrations for each year, we can notice that until 2004 the annual maximum generally occurred in May or in June.

Since 2004 we observe a shift in the early maximum, and the highest values are usually in April. This kind of annual ozone distribution is connected with two main sources of surface ozone: (1) photochemical reactions are more intense during spring and summer months, when values of temperature and solar radiation are significantly higher than in winter or autumn, (2) fluxes of stratospheric ozone are the most common during early spring months. The situation in recent years can be indicative of an important role of stratosphere-troposphere exchange as a source of surface ozone amount. A specific kind of distribution of ozone was noticed in 2006. This year was unusual in terms of meteorological situation in Europe. During the period 16 June–30 July, unusually high pressure systems settled over Europe, that alternately were connected with continental high from Russia. As a result, Poland was affected by tropical air masses from south-west, south and south-east directions. In this kind of circulation, solar radiation and temperature were very high and significantly exceeded long-term average values (Lorenc et al. 2006). As can be seen in Fig. 8, the surface ozone and solar radiation values in July were the highest during the measurement period (1995–2011) and were higher by 40 and 31 %, respectively, than long-term average values. It can be assumed that such meteorological conditions promoted the rate of reactions and in situ photochemical ozone production. Average temperature in July was also higher

Fig. 8 Variations of surface ozone concentration, solar radiation and temperature in July for 1995–2011



than the long-term value by 16 %. We can observe good compatibility between surface ozone and the above meteorological parameters. Correlation coefficients between surface ozone and solar radiation and temperature reach 0.72 and 0.43, respectively.

Monthly averaged surface ozone concentrations with division into day and night are presented in Fig. 9.

For each month, higher values during day than during night are observed. Processes of ozone formation during night do not take place. Furthermore, processes of ozone destruction, which are a result of ozone titration by NO ($\text{NO} + \text{O}_3 \rightarrow \text{NO}_2 + \text{O}_2$), lead to low values of surface ozone at night (Gerasopoulos et al. 2006).

5.3 Comparison of Seasonal Distribution of Measurement Series in Kraków (1869–1878) and Belsk (1995–2012)

Seasonal variations of surface ozone in Kraków (1869–1878) and Belsk (1995–2012) are presented in Fig. 10.

Comparing both curves, a significant difference in their shape is evident. Distribution in Kraków is characterized by a rapid growth of surface ozone concentration from January to April and then equally rapid decrease until December. Such a sharp peak in spring months indicates stratospheric fluxes of air rich in ozone as a main source of ground-level ozone. Distribution in Belsk is characterized by broad spring-summer surface ozone maximum. From March to August we can notice high ozone values and then gradual decrease of ozone values until winter months. This kind of distribution indicates troposphere-stratosphere exchange as a source of ozone near the ground but also (even more importantly) in situ photochemical ozone

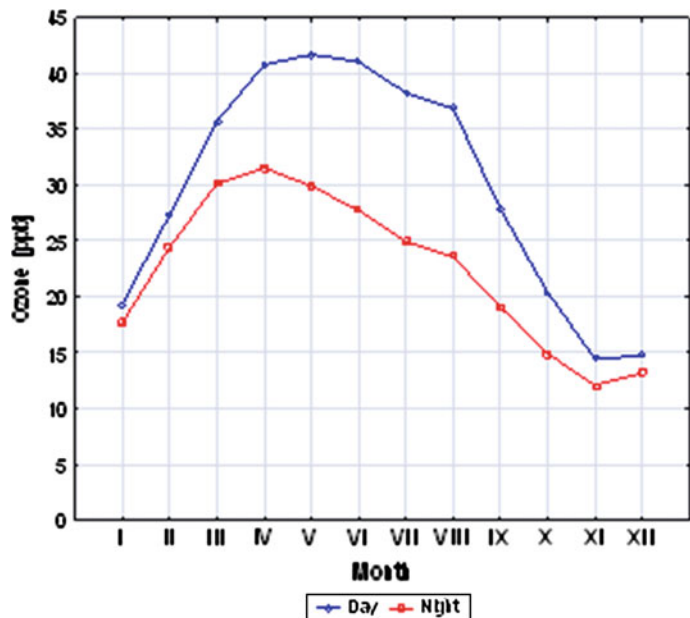
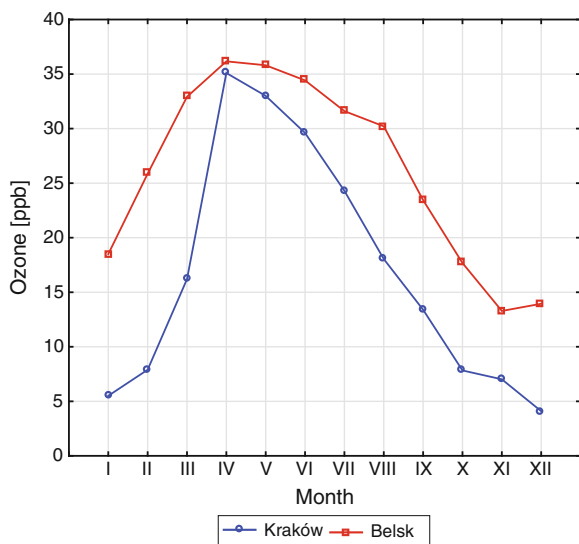


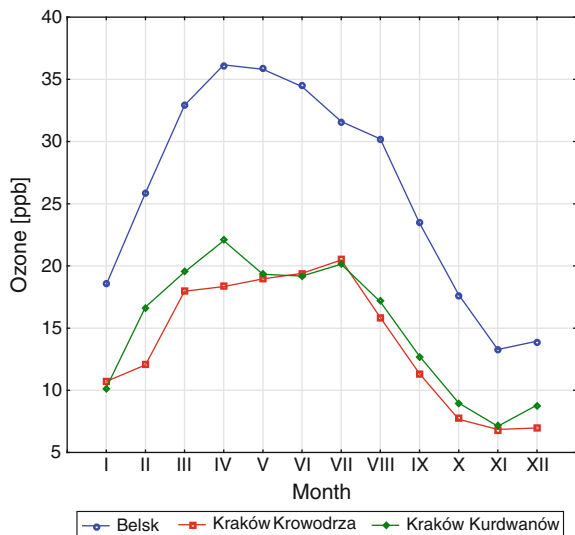
Fig. 9 Monthly averaged concentration of surface ozone with division into day and night for 1995–2012 time series

Fig. 10 Seasonal variations of surface ozone concentration in Kraków (1869–1878) and Belsk (1995–2012)



production. We suspect that an increase in photochemical ozone formation has been possible due to increased content of ozone precursors in the air. It is worth noting about the differences in average values of surface ozone concentration in these two

Fig. 11 Seasonal variations of surface ozone concentration in Kraków (2005–2013) and Belsk (2005–2013)



analyzed series. Average values in Belsk fluctuated between 13 and 36 ppb while in Kraków ranged from 4 to 35. The highest differences were during winter months (up to 18 ppb in February) and in March (17 ppb).

5.4 Comparison of Diurnal and Seasonal Distribution of Surface Ozone at Contemporary Rural (Belsk) and Urban (Kraków) Stations

The 9-year record (2005–2013) of the surface ozone data in Kraków and 18-year record (1995–2013) in Belsk were investigated to determine possible diurnal and seasonal distributions at 2 stations situated at different environments.

The surface ozone data set used in this study for Kraków were taken from the website of The Regional Inspectorate of Environmental Protection in Kraków. From January 1995 to February 2010 data were recorded in station Kraków-Krowodrza (north-west Kraków), from April 2010 to December 2013 in station Kraków-Kurdwanów (south Kraków). Both stations are urban background stations located at a distance of about 9 km.

Hourly averaged values were used to analyze variability during day and night. Monthly means were calculated based on daily values to study the seasonal cycle.

The seasonal variations of surface ozone in Kraków (urban stations) and Belsk (rural station), presented in Fig. 11, show a strong, characteristic variations with rural values of concentration being almost doubled compared to urban stations. The minimum values are observed in autumn (October, November) and winter (December, January) months. At the rural station, the values were reaching about

13–17 ppb and 13–18 ppb, respectively, whereas at the urban stations they were 7–9 ppb and 7–11 ppb, respectively. Broad spring-summer maximum at Belsk with the highest value in May and gradually decreasing during summer is replaced at urban stations by broad spring-summer maximum with 2 peaks during April and July. The first one is connected with stratospheric intrusions of air that was rich in ozone and the initiation of intensive photochemical ozone production, and the second one with photochemical ozone production with the participation of solar radiation and high temperature. The average ozone concentration is higher at rural site than at the urban, which can be associated with smaller number of sinks of ozone in the rural area and transport of precursors from mid or long distances (Saitanis 2003).

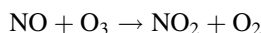
To better understand the big difference between surface ozone concentrations at rural and urban sites, diurnal variation of ozone in the form of day and night averages are presented in Fig. 12.

Diurnal variation of surface ozone is necessary to recognize and understand the different processes responsible for ozone production and destruction at a given area (Elampari and Chithambarathanu 2011). Diurnal ozone concentration is a result of both chemical processes (e.g., occurring with the participation of sunlight) and dynamic processes (e.g., advection of polluted air masses).

Higher concentration of surface ozone during day is evident at stations of both kinds. It is attributed to the photochemical reactions between ozone precursors and downward transport of air rich in ozone by the vertical mixing due to convective heating during the day (Lal et al. 2000). However, analyzing the ozone concentration at urban stations during November, December and January we can notice that values during nighttime are comparable with daytime. To explain this phenomenon we have to investigate surface ozone distribution during winter and summer months (Fig. 13).

The diurnal variation of surface ozone during July (Fig. 13a) is characterized by high concentration (up to 47 ppb for Belsk, up to 42 ppb for Kraków) during daytime and low concentration (down to 22 ppb for Belsk, down to—8 ppb for Kraków) during morning and evening.

The minimum ozone concentration is observed during the early morning hours. Since this moment, values start increasing rapidly and uniformly, coinciding with solar radiation reaching maximum during afternoon hours. From 17:00, together with less intense solar activity, ozone concentration gradually decreases, maintaining low values during evening and night hours. The nighttime minimum is more pronounced at the polluted urban area, associated with processes of ozone titration by NO expressed in the reaction:



Fresh NO emission in urban area contributes to removal of ozone and production of NO_2 and O_2 . Titration processes are remarkably visible during nighttime hours when the lack of solar radiation prevents the ozone formation (despite

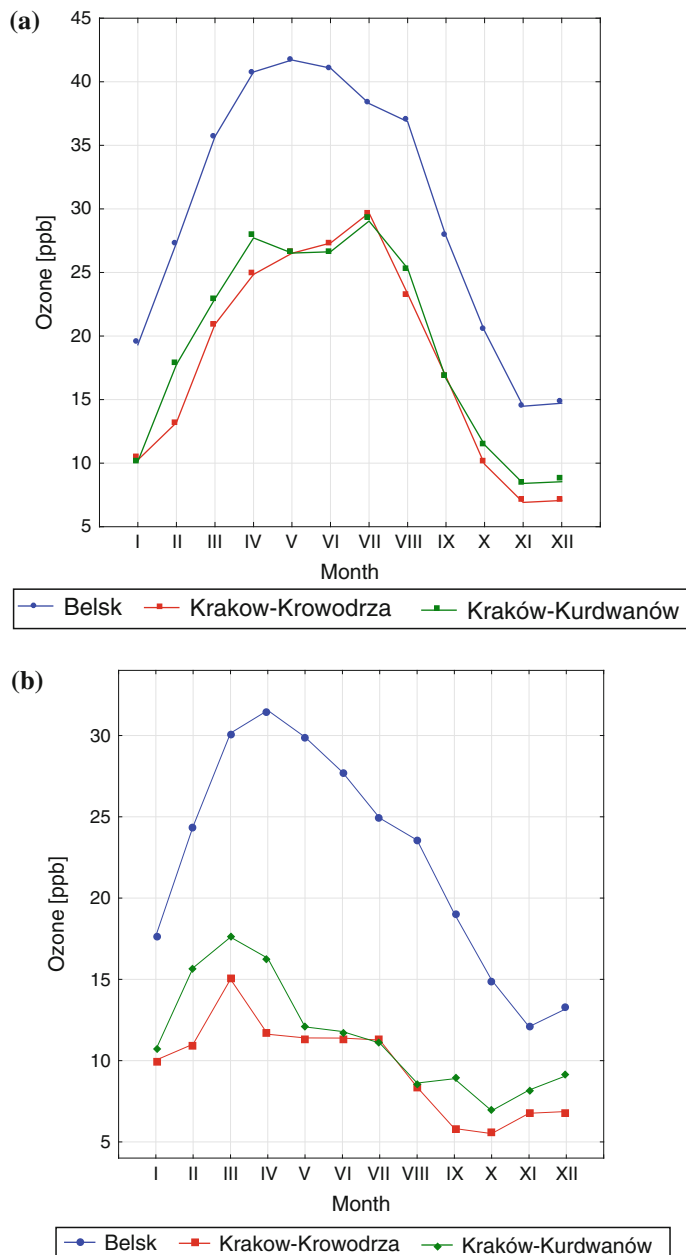
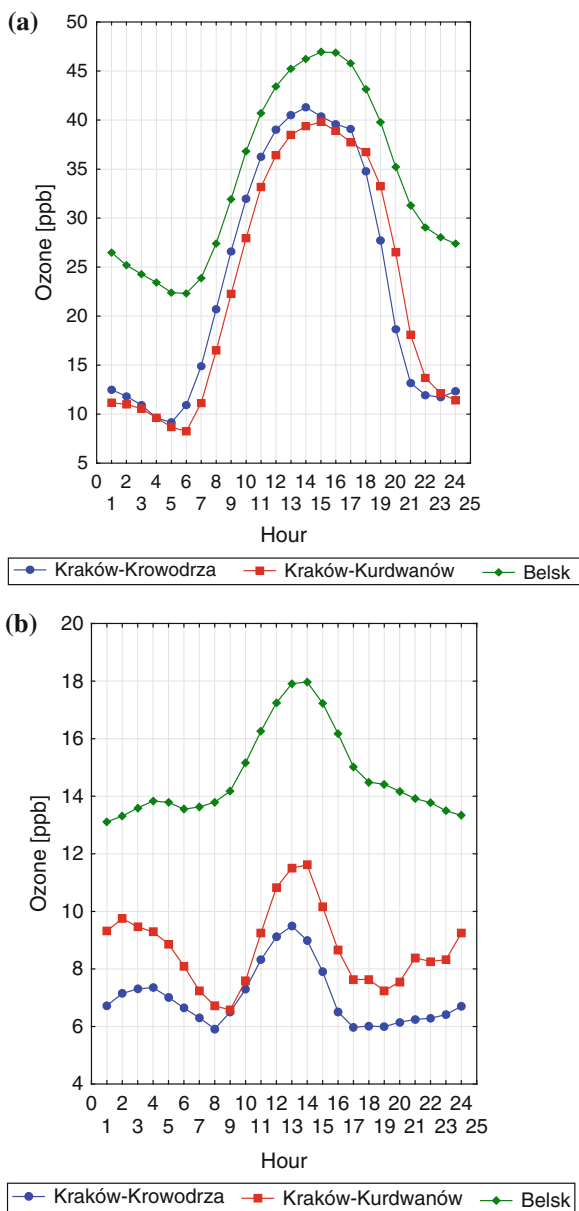


Fig. 12 Variations of surface ozone concentration in Kraków (2005–2013) and Belsk (2005–2013) in the form of average day (**a**) and night (**b**) values

Fig. 13 Diurnal variations of surface ozone concentration in July (a) and December (b) (2005–2013)



the production of NO_2). Indication of titration during daytime could be hidden by ozone production with the participation of solar radiation.

The variation of surface ozone during December (Fig. 13b) at urban stations is disrupted by deep ozone decreases during morning and evening hours, associated with rush hours and intensified emission of ozone precursors (e.g., NO_x). During

winter this effect together with limited photochemical ozone production are responsible for low surface ozone concentration. Less intense solar radiation during winter is not able to produce significant amounts of ozone during day to compensate for morning and evening declines and makes the net ozone concentration during day to be significantly higher than during night (like in spring and summer months).

6 Conclusions

Systematic measurements of surface ozone performed at Kraków Observatory from 1869 to 1878 have been compared with measurements of surface ozone carried out at Belsk Observatory from 1995 through 2012. Data were investigated in terms of annual, seasonal and diurnal cycles. Annually averaged surface ozone concentrations in the second half of the nineteenth century in Kraków ranged between 11 and 24 ppb. The highest values were noticed during spring and early summer months (April, May, June); in turn, the lowest were during late autumn and winter months (November, December, January). From April to September, concentrations of surface ozone during day were higher than during night by up to 8 ppb. From October to March, concentrations of surface ozone during night were higher than during day by up to 2 ppb. Annually averaged surface ozone concentration in recent years (1995–2012) at rural station ranged from 22 to 31 ppb. During whole measurement series we can distinguish the following stages: (1) gradual increase from 1995 to 2003, and (2) continuous decrease from 2004 to 2012. Annually averaged surface ozone concentrations in the last years (2005–2013) at urban station ranged between 12 and 17 ppb and were similar to those of nineteenth century Kraków. High number of sinks of ozone in the urban area is responsible for lower ozone concentration compared to rural places. An analysis of seasonal, contemporary concentrations of surface ozone revealed a distribution similar to that in the 19th century, with maximum in spring and summer and minimum in autumn and winter.

From the analysis performed in this chapter we may draw the following basic conclusions:

- (1) Urban places exposed to continuous emission of NO_x are characterized, on the average, by a low surface ozone concentration, comparable to that in the 19th century Kraków.
- (2) Rural sites, where emission of NO_x is significantly limited (due to low vehicle traffic) are characterized by significantly higher values of surface ozone concentration than those occurring in Kraków almost 150 years ago.
- (3) Since 2003, the background rural station in Belsk is characterized by gradual downward tendency of surface ozone concentration.

References

- Andrews T (1874) Address on ozone. *J Scott Meteorol Soc* 4:122–134
- Bell M, Ellis H (2004) Sensitivity analysis of tropospheric ozone to modified biogenic emissions for the Mid-Atlantic region. *Atmos Environ* 38:1879–1889
- Bloomer BJ, Vinnikov KY, Dickerson RR (2010) Changes in seasonal and diurnal cycles of ozone and temperature in the eastern U.S. *Atmos Environ* 30:1–9
- Bojkov RD (1986) Surface ozone during the second half of the nineteenth century. *J Clim Appl Meteorol* 25:343–352
- Crutzen PJ (1988) Tropospheric ozone: an overview. In: Isaksen ISA (ed) *Tropospheric ozone*. Reidel, Dordrecht, pp 3–32
- Crutzen PJ, Lawrence MG, Ulrich P (1998) On the background photochemistry of tropospheric ozone. *Tellus* 51A–B:123–146
- Degórska M, Rajewska-Więch B, Krzyścin J (1996) Seria obserwacji ozonu przyziemnego wykonana w Krakowie w latach 1854–1878 i próba oceny jej współczesnej wartości (Surface ozone observation series from Cracow in 1854–1878 and its nowadays importance). Publications of the Institute of Geophysics, Polish Academy of Sciences M-18 (273), pp 55–60
- EEA (2012) Emissions of ozone precursors (CSI 002/APE 008)
- Elampari K, Chithambarathanu T (2011) Diurnal and seasonal variations in surface ozone levels at tropical semi-urban site, Nagercoil, India and relationship with meteorological conditions. *Inter J Sci Tech* 1:80–88
- Gerasopoulos E, Kauvarakis G, Vrekoussis M, Donoussi C, Mihalopoulos N, Kanakidou M (2006) Photochemical ozone production in the Eastern Mediterranean. *Atmos Environ* 40: 3057–3069
- Helmig D, Oltmans SJ, Carlson D, Lamarque JF, Jones A, Labuschagne C, Anlauf K, Hayden K (2007) A review of surface ozone in the polar regions. *Atmos Environ* 41:5138–5161
- Kley D (1994) Tropospheric ozone in the global, regional and subregional context. In: Boutron CF (ed) *Topics in Atmospheric and Interstellar Physics and Chemistry*, ERCA, vol.1. EDP Les Ulis France, pp 161–184
- Lal S, Naja M, Subbaraya BH (2000) Seasonal variation in surface ozone and its precursors over an urban site in India. *Atmos Environ* 34:2713–2724
- Linville DE, Hooker WJ, Olson B (1980) Ozone in Michigan's environment 1876–1880. *Mon Weather Rev* 108:1883–1891
- Logan JA (1985) Tropospheric ozone: seasonal behavior. Trends and anthropogenic influence. *J Geophys Res* 90(D6):10463–10482
- Lorenc H, Laskowska A, Ceran M, Mirkiewicz M, Sasim M (2006) Susza w Polsce – 2006 rok. (Drought in Poland – 2006), Raport Instytutu Meteorologii i Gospodarki wodnej, Warszawa
- Monks PS (2005) Gas phase radical chemistry in the troposphere. *Chem Soc Rev* 34:376–395
- Naja M, Lal S, Chand D (2003) Diurnal and seasonal variabilities in surface ozone at a high-altitude site Mt. Abu (24.6°N. 72.7°E. 1680 m asl) in India. *Atmos Environ* 37:4205–4215
- Oltmans SJ, Levy H II (1994) Surface ozone measurements from a global network. *Atmos Environ* 28:9–24
- Pudasainee D, Sapkota B, Lal Shrestha M, Kaga A, Kondo A, Inoue Y (2006) Ground level ozone concentrations and its association with NO_x and meteorological parameters in Kathmandu valley, Nepal. *Atmos Environ* 40:8081–8087
- Pulikesi M, Baskaralingam P, Rayudu VN, Elango D, Ramamurthi V, Sivanesan S (2006) Surface Ozone measurements at urban coastal site Chennai. in India. *J Hazard Mater* 137(3): 1554–1559
- Rubin M (2001) The history of Ozone. The Schönbein period. 1839–1868. *Bull Hist Chem* 26(1):40–56
- Saitanis CJ (2003) Background ozone monitoring and phytodetection in the greater rural area of Corinth-Greece. *Chemosphere* 51(9):913–923

- Science Policy Report 15/08 (2008) Ground-level ozone in the 21st century: future trends. im-pacts and policy implications. The Royal Society 2008
- Volz A, Kley D (1988) Evaluation of the Montsouris series of ozone measurements made in the nineteenth century. *Nature* 332:240–242
- Wierzbicki D (1882) Ozon atmosferyczny i roczny ruch jego według dwudziesto-pięcioletnich spostrzeżeń obliczony (Atmospheric ozone and its annual variation calculated from 25-year observations). *Rozprawy i Sprawozdania z Posiedzeń Wydziału Matematyczno-Przyrodniczego Akademii Umiejętności*. Tom IX. Kraków

Dissolved Oxygen in Rivers: Concepts and Measuring Techniques

Agnieszka Rajwa, Robert J. Bialik, Mikołaj Karpiński
and Bartłomiej Luks

Abstract This chapter presents the basic concepts of methods and techniques used in the measurement of dissolved oxygen in flowing water. Based on field tests carried out on the Narew, Świdra and Vistula Rivers, sensor performance was analysed. The results show that the comparability of sensors depends not only on their accuracy, but also on the hydrological conditions under measurement, as well as the duration of measurement and sensor location. For diel measurement, the time delay between the maximum temperature and minimum oxygen concentration is acknowledged and briefly discussed. Moreover, in contrast to other studies, the main attention has been focused on abiotic factors that affect oxygen conditions in rivers. Finally, the key research challenges are highlighted.

Keywords Dissolved oxygen · Optical sensors · Winkler titration · Electrochemical methods · Accuracy · Oversaturation

1 Introduction

Dissolved oxygen (DO) in water ecosystems has attracted growing attention over the last century in different disciplines of science and can be considered from many aspects; either from a solely ecological perspective, or in terms of its nature and driving mechanisms. The topic covers three major aspects, which have usually been considered separately in the past and contemporary investigations, such as gas transfer at the air-water interface, the advective transport of dissolved substances in rivers and the impact of vegetation on oxygen conditions in aquatic ecosystems. In nature, these aspects overlap and some of the methods developed

A. Rajwa (✉) · R. J. Bialik · M. Karpiński · B. Luks
Institute of Geophysics, Polish Academy of Sciences, Księcia Janusza 64,
01-452 Warsaw, Poland
e-mail: arajwa@igf.edu.pl

within these study categories should be modified or used simultaneously. Recent investigations have highlighted the importance of DO, not only from the stand-point of water quality management, as it is used in estimation of primary production in flowing waters (e.g., Odum 1956; Reichert et al. 2009; Demars et al. 2011a), but also for understanding processes and factors that regulate its dynamics in rivers (e.g., O'Connor 1967; Demars et al. 2011b; Helton et al. 2012; Hondzo et al. 2013; O'Connor et al. 2012) and developing models able to deal with such complex interactions (e.g., Manson et al. 2011; Birkel et al. 2013; Li et al. 2013).

In view of current studies, we have attempted to analyse whether the available devices allow us to solve particular problems or how far we can generalise results. Therefore, the goal of this chapter is to summarise selected sensing techniques used for the measurement of dissolved oxygen in natural waters and to demonstrate their suitability for certain study cases. In particular, the study aims to identify potential problems in field applications arising from the use of various sensing methods (optical and galvanic) and abiotic factors that affect oxygen concentration in rivers. In this context, the performance of the sensors is discussed and their potential application in future challenges is highlighted. In the following sections, the main focus is placed on the sensing techniques, current devices used in field measurements, and examples of results obtained from field investigations, together with a critical discussion.

2 Sensing Techniques

Over the last century, a variety of approaches have been developed and employed in oxygen measurements. These methods vary widely in precision and differ in their utility. For many years, dissolved oxygen could only be determined by iodometric titration of the water sample, which is widely known as the Winkler method (Dojlido 1980). The traditional Winkler method (Winkler 1888) defined as a standard method (Skoog et al. 1988; APHA 1995) with its later modifications is still used in laboratory practice, whereas in the field it has been superseded by electrochemical sensors. For decades, it has been widely used for the calibration of electrochemical sensors with solutions of a known oxygen concentration (Helman et al. 2012). However, its accuracy strongly depends on the experience of the worker. Moreover, the Winkler method is demanding and subject to many interfaces, such as contamination of the water sample by atmospheric oxygen (Jalukse et al. 2008). The other drawback is related to a short time between sampling and analyte detection in the laboratory, due to the risk of changes in the oxygen content of the analysed sample. Furthermore, the method does not allow the collection of a large number of samples, which is necessary to understand the drivers of spatial heterogeneity and temporal dynamics of dissolved oxygen. Each extracted sample represents only a small part of the river and is isolated from the hydrodynamic setting. Thus, scaling the results of that sampling might generate errors.

Electrochemical methods have solved the limitations of Winkler's titration, especially in real-time fieldwork applications. The protagonist of polarographic sensors was an American biochemist, Leland Clark, who was working on a bubble oxygenator for use in cardiac surgery. Although his results were subjected to some criticism initially, further studies led to the development of Clark's cell (1956), which was used for measuring oxygen in blood and also in water and other liquids. From a technical point of view, the Clark's sensor is a cell that consists of two electrodes immersed in an electrolyte. The cell is separated from the measured medium by a gas-permeable membrane. The principle underlying the measurement is based on the diffusion of oxygen through the membrane to the measuring cell, where it is immediately reduced at the cathode, forming a steady-state current that is proportional to the amount of oxygen in the medium (Cygański 1995; Harvey 1999). Because oxygen is consumed during measurements, the sensor is flow-dependent, meaning that it requires a continuous flow of oxygen through the measurement cell. In contrast, newer types of sensors introduced in 1964 by Macreth (UMCES 2004) do not require an external power source to provide polarisation. This stems from the fact that electrodes are made of other materials to ensure a sufficient difference in potential between anode and cathode; thus, a voltage is generated by the electrodes themselves, similar to a battery. As a consequence, the cell is always ready for deployment and there is no warm-up time (YSI handbook 2009). This type of sensor is usually referred as a galvanic or internally polarised sensor.

More recently, advances in optical detectors and data processing have led to a breakthrough in the measurement of dissolved oxygen. Optical sensors of oxygen rely on luminescence quenching by molecular oxygen. Although this phenomenon has already been observed in 1931 by Kautsky and Hirsh (1931) (Kautsky 1939), one of the earliest descriptions of the complete optical sensor system was provided by Bergman in the late 1960s (Narayanaswamy and Wolfbeis 2004). In this technique, sensing is based on intensity or lifetime changes (Mills 1997; Demas et al. 1999; Grist et al. 2010). Luminescence is inversely proportional to the oxygen concentration in regions of high linearity of the Stern–Volmer plot (Stern and Volmer 1919; Amao 2003; Mitchell 2006; Lakowicz 2006). However, the signal is especially sensitive to high oxygen concentrations, which gives a downwards-sloping curve of the Stern–Volmer plot (YSI handbook 2009; Gewehr and Delpy 1994). Therefore, to overcome this non-linearity, the equation is modified depending on the particular manufacturer of the sensor. In contrast to electrochemical methods, optical sensors do not involve chemical reactions and thus, oxygen is not consumed during measurements (Rommel 2004; Chu et al. 2011). Finally, optical sensors are less prone to drift in long-term monitoring and require less-frequent calibration (Johnston and Williams 2005).

Electrochemical and optical methods have revolutionised measurements and have provided a technological grounding for future research, due to their simplicity and efficiency. The differences between these sensors result in their application for particular purposes. In fact, the development of electrochemical and optical techniques have improved measurements and enabled long-term monitoring of DO, temperature and other parameters at specified time intervals.

3 Study Sites and Field Equipment

To test the sensors, field surveys were carried out on three rivers, characterised by different hydrological settings; namely, the Vistula and its tributaries, the Świder and the Narew (Fig. 1).

The Vistula is the largest river in Poland, having a catchment area of 194,700 km² (Dojlido 1997). Measurements on the Vistula were carried out on its meander, which is located 20 km south of Warsaw and is part of the Świderskie Islands Reserve. In cross-section, the river has a discharge $Q = 300 \text{ m}^3/\text{s}$, a mean width $B = 500 \text{ m}$, with a varying depth of 0.3–1.8 m.

The Świder joins the Vistula at Świder Village, which is located 20 km south of Warsaw. The river has a natural shape with numerous meanders, and the channel consists of sand material, which forms fluvial bedforms such as dunes and ripples. The measurements have been taken in the Świder River Reserve. In measured cross-section, the river has a discharge $Q = 3 \text{ m}^3/\text{s}$, a mean width $B = 25 \text{ m}$ and a depth $H = 0.5 \text{ m}$.

The Narew represents an anastomosing river characterised by multiple channels separated by islands covered with dense channels and bank vegetation. The width of channels varies from a few to 30 m. The main channels are about 4–5 m deep, whereas the smaller ones are 1.5–3.0 m deep (Gradziński et al. 2003). For the present study, measurements were carried out on a weir in Rzędziany Village, located in the Narew National Park. In cross-section (20 m above the weir), the river has discharge $Q = 10 \text{ m}^3/\text{s}$, a mean width $B = 20 \text{ m}$, and a depth $H = 2 \text{ m}$.

Dissolved oxygen in mg/L and percentage saturation, water temperature and barometric pressure were measured with an optical technique using a ProODO meter and the galvanic technique using a ProPlus meter (1.25 mil PE), both manufactured by YSI Inc., Yellow Springs, Ohio, USA (Fig. 2).

Several procedures are commonly used to calibrate oxygen sensors, such as water-saturated air, air-saturated water, and a two-point calibration with a zero oxygen solution using sodium sulphite and noted earlier in the Winkler titration. Since the last three procedures are either time-consuming or require some preparation time, the first procedure is generally recommended. Therefore, the calibration was performed before deployment of the sensors using 100 % saturated air for both devices.

4 Results

This section is structured as follows: Section 4.1 verifies the accuracy of measuring devices with a special emphasis on differences in the measurements. Section 4.2 discusses the oxygen oversaturation in flowing water, using the Vistula and the Świder rivers as examples. Section 4.3 provides an insight into differences between short- and long-term measurements. Section 4.4 discusses the importance of the sensor location, with a special focus on the influence of hydraulic structures.

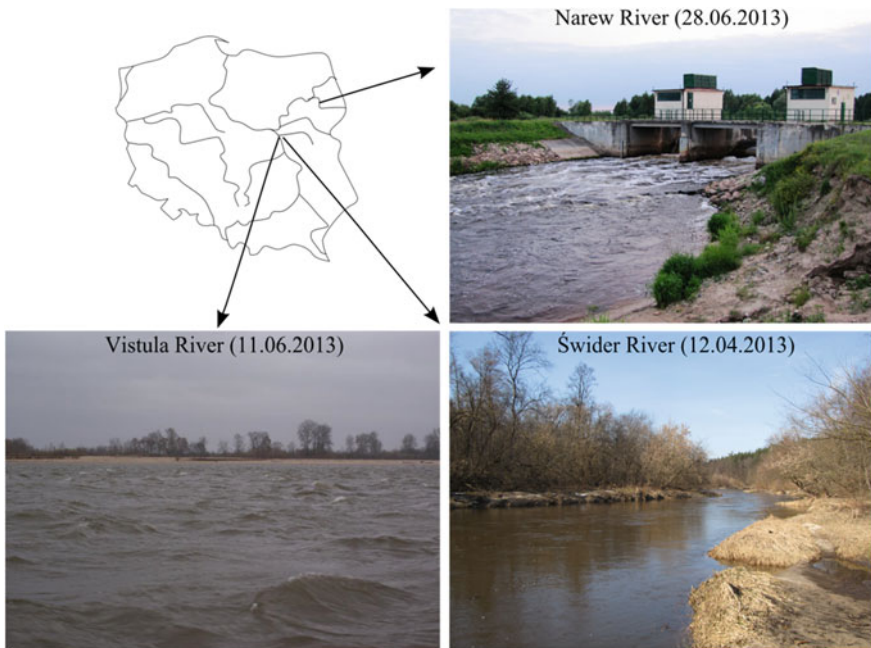


Fig. 1 Location of study sites

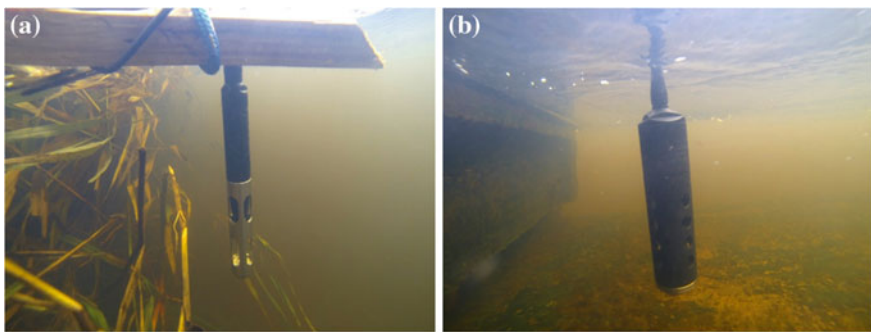
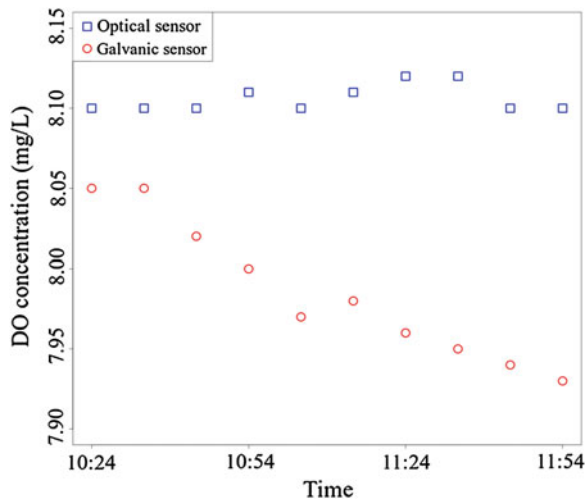


Fig. 2 **a** ProODO with the optical sensor; **b** ProPlus with the galvanic sensor (1.25 mil PE)

4.1 Accuracy and Resolution of Sensors

One of the main considerations in performing oxygen balance or metabolism calculations for a certain river reach, irrespective of whether a galvanic or optical technique is used, is the accuracy of measurements. In fact, considerably more attention has been paid to finite resolution (or precision) than to the accuracy of measuring devices (e.g., McCutchan et al. 1998). A potential problem arises when

Fig. 3 Recordings at 10-min. intervals obtained using galvanic and optical sensors in the Świder River (June, 2013)



two different sensors are employed simultaneously. Although both sensors have the same range and resolution, they might differ in accuracy. Bearing this in mind, a difference in readings at the 2 % level in the case of saturation and 0.2 mg/L concentration should not be taken into account because the recordings are equally valid. The performance of galvanic and optical sensors installed side-by-side in the Świder River is shown in Fig. 3; note the concentration range. Apart from the discrepancy between these sensors, the differences are within the margins of error.

4.2 Oversaturation of Dissolved Oxygen

As has been reported in the literature, for super-saturation states, optical sensors are favoured over electrochemical sensors (YSI handbook 2009; Mitchell 2006). In fact, oversaturation is a common phenomenon in natural waters. During our measurements, oversaturation was reported twice; at the beginning of April and in July 2013; however, the origins of this state were different. In spring, water of the Świder maintained near-equilibrium saturation concentration due to surface recharge from melting snow, which resulted in a decrease in water temperature and enhanced oxygen solubility in water. Additionally, during this time, the discharge ($Q = 19.3 \text{ m}^3/\text{s}$), mean velocity and water depth ($H = 1.93 \text{ m}$) in the cross-section were relatively high, which might have resulted in higher re-aeration.

The state of super-saturation observed in July on the Vistula was apparently driven by meteorological conditions. The measurements of DO concentrations were taken from a boat along the river at a distance of 3 km, in horizontal cross-sections (above the inflow of the Świder) at a distance of 700 m (Fig. 4) and in one vertical profile (approximately 2 m depth). Both optical and galvanic sensors showed that the water was highly oxygenated, with a saturation of about 150 % and a DO

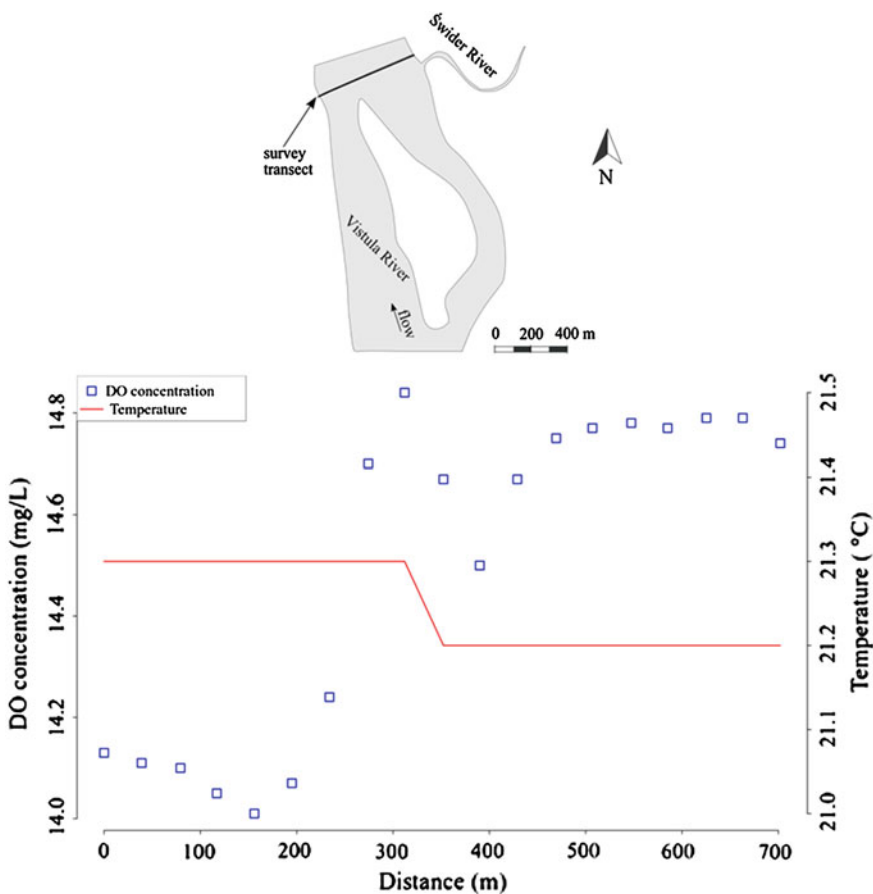


Fig. 4 Distribution of dissolved oxygen in the horizontal cross-section along the *black line* depicted on the map. Measurements were taken from a moving boat every 30 s from the *left* to the *right* bank of the Vistula, above the Świder inflow (July, 2013)

concentration of 14 mg/L, whereas water temperature was 21.3 °C. In fact, these values are very far from equilibrium, implying that additional factors might affect the concentration level. Therefore, if we take a sample of water but maintain the same temperature and air pressure, the concentration of oxygen, after a certain period, will be lowered to the equilibrium state (about 9 mg/L). For comparison, measurements taken on the same day in the Świder at about 1.5 km from the river mouth have shown that the oxygen concentration and saturation, and water temperature, were lower than the values recorded on the Vistula; however, amounting to 9.7 mg/L, 18.9 °C and 103 %, respectively, they were still above the saturation level. On the other hand, the relatively small oversaturation in the Świder may just as well be within our measurement errors. Because the water surface of the Vistula was covered with breaking waves accompanied with a strong wind (about 11.0 m/s), we

can hypothesise that wind was the driving factor. Furthermore, according to the measurements taken 1 week earlier, which did not show oversaturation, we can also reject intensified photosynthesis as a factor. Unfortunately, due to limited data the contribution of wind reaeration has not been estimated. Although there was no difference in the vertical profile, meaning that the water was fully mixed, small differences were observed in the horizontal cross-section, as presented in Fig. 4. Although waters of the Świder are less oxygenated, we observed a higher oxygen concentration on the right bank of the Vistula. This can partly be explained by the temperature decrease and mixing effect, which enhances oxygen absorption. Although the difference was recorded by two sensors, this evidence is not strong, because it is at the limit of the error level and requires further verification.

Ample evidence exists that DO should be measured in the field and that results obtained in the laboratory are deprived of a hydrodynamic setting. This is essential, for example, in re-aeration research, during the planning of experiments and the self-purification of rivers.

Although the oxygen oversaturation has been reported in the literature many times, there is still a lack of knowledge concerning the acceptance of these data and the uncertainty of the results. Apart from calibration errors, oversaturation is usually attributed to photosynthesis of green plants or to sharp changes in water temperature or air pressure during storm events, especially in slow flowing waters (YSI 2003, 2005, Tech Note). However, changes in dissolved oxygen can be attributed to photosynthesis and respiration only when biotic changes in oxygen concentration exceed the rate of change due to diffusion. This explains why oversaturation also occurs in the turbulent waters of mountain streams and large rivers exposed to wind activity. This implies that the commonly used saturation levels and concentrations do not appear to be an accurate measure (Truesdale and Downing 1954; Allen 1955).

4.3 Short- and Long-Term Measurements

One of the main aspects involved in high frequency data collection is the response time of a sensor. Among YSI products, this is defined as T-95 and reflects the length of time that the sensor requires to reach 95 % of the final reading during its transferral from fully saturated water to oxygen-deprived water (YSI handbook 2009). From a practical point of view, this value determines how long dissolved oxygen should be measured at a certain point to obtain a correct result and defines the shortest time interval between recordings.

The time interval between measurements and their duration is important in terms of short-term measurements (less than 1 day). The recordings of oxygen concentrations in the Narew River measured continuously at one point for 3.5 h at a 5-min intervals are shown in Fig. 5; note the concentration range. The distribution of points suggests a rising trend, whereas the changes in concentration are within the error level and the temperature remained constant.

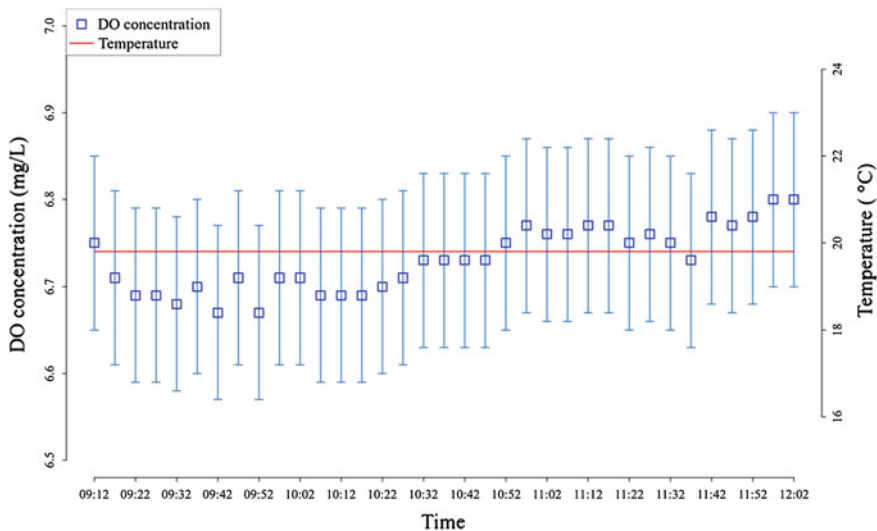


Fig. 5 DO concentration during a 3-hour recording at 5-min. intervals measured below the weir on the Narew (June, 2013)

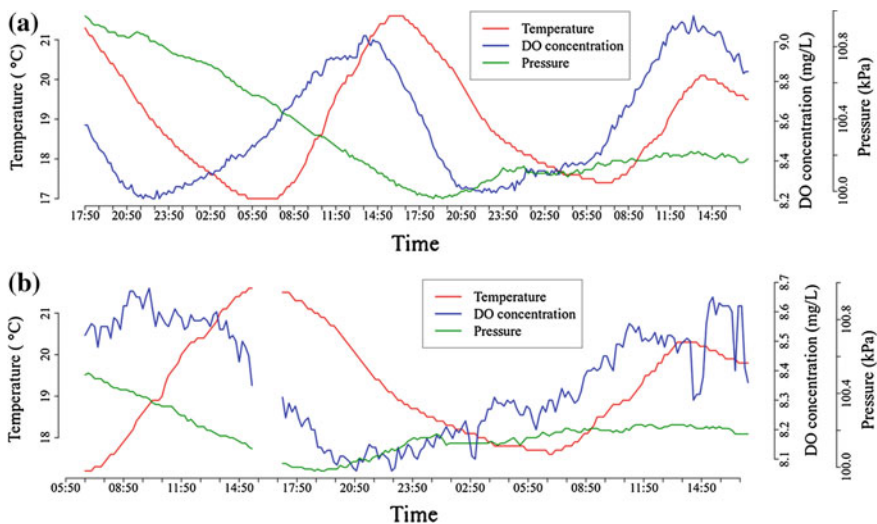


Fig. 6 Daily curves of dissolved oxygen in the Świdra at 10-min. intervals; **a** recordings taken with the optical sensor; **b** recordings taken with the galvanic sensor

Changes in oxygen concentration in the Świdra were readily observed over periods covering whole days, as presented in Fig. 6a, b. The lowest concentrations of dissolved oxygen occurred at night, despite the favourable low temperatures. In spite of the absence of channel vegetation, oxygen deficit (calculated according to the

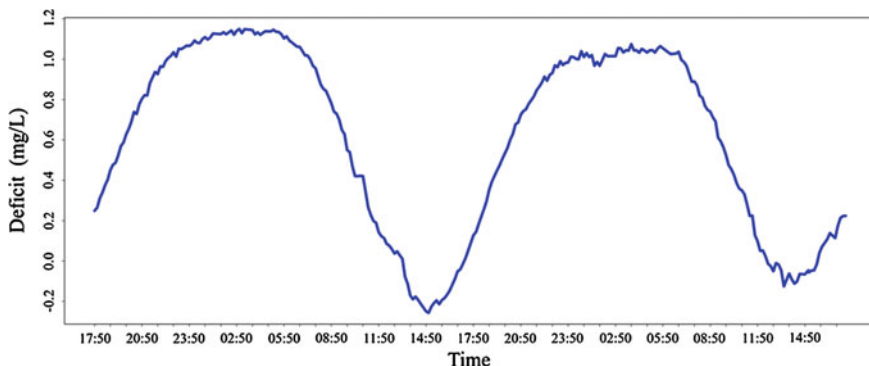


Fig. 7 Daily curves of oxygen deficit in the Świdra calculated from Fig. 6a

APHA 1995) at night was relatively high (Fig. 7), which can be attributed to a high sediment oxygen demand during the decomposition of organic matter as observed in the Vistula by Opaliński and Puczko (2009). They explain that the consumption of oxygen is the result of energetic processes of interstitial organisms, which form a film on the surface of sand grains or/and inhabit the pore spaces.

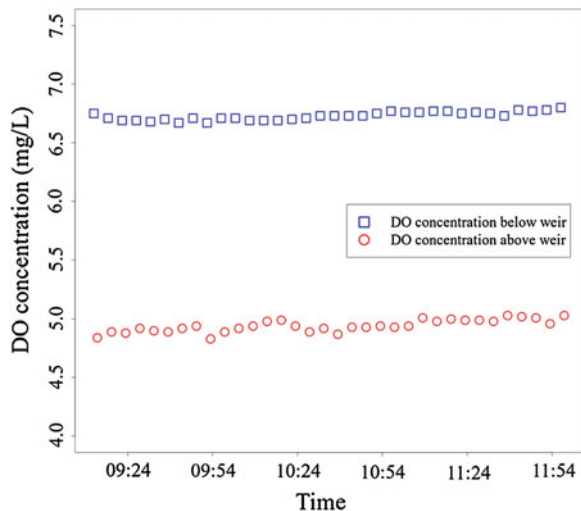
One observation is that the rising limb of DO concentration is longer than the falling limb (Fig. 6b), indicating that the absorption of oxygen takes more time than its release. However, this is an uncommon pattern, and to the best of our knowledge, has not been reported in the literature. Another observation worth noting here is the phase shift in time between oxygen concentration and water temperature, which ranges from 6 (Fig. 6a) to 8 h (Fig. 6b), depending on whether it is for minimum or maximum values of both concentration and temperature. This discrepancy is probably related to the flow ratio and river depth. However, further research is required to estimate the impact of the river geomorphology and flow properties on oxygen dynamics.

From a technical point of view, visual differences occur when comparing Fig. 6a, b. The distribution of points in Fig. 6b appears to be more random. This can apparently be attributed to the higher noise of the galvanic sensor as it is flow-dependent. As was reported elsewhere, the galvanic sensor is more sensitive to the velocity of the current, as oxygen passes through the membrane and becomes depleted in the water surrounding the tip of the sensor.

4.4 Sensor Location

In complex river channels, the location of sensors plays a significant role. Due to the heterogeneity of rivers associated with the presence of areas of stagnant water such as dead zones and oxbows, oxygen sensors should be placed stationary at two or more (if possible) sites to give the best representation of the river. The measurements should be carried out in a period of steady flow at relatively short time intervals,

Fig. 8 Differences in oxygen content above and below the weir on the Narew in Rzedziany



which for stream metabolism studies is approximately 5–15 min. In shallow rivers, it is also crucial to observe the mean depth of the river, to properly estimate the depth of sensor deployment during measurements. This ensures that the sensors are constantly below the water surface. Furthermore, sensor selection is crucial; the galvanic sensor is flow-dependent, meaning that water should flow through the membrane with a speed of approximately 7.62–30.48 cm/s, depending on the membrane material (YSI handbook 2009). Therefore, galvanic sensors should be installed at locations of sufficient flow to avoid artificially low readings. Although the performance of the sensor improves with stirring, it is not feasible to perform this in long-term field measurements.

The differences in the spatial distribution of oxygen along the river are readily apparent in the Narew. The Narew is characterised by a network of channels, dead zones and oxbows of varying depths, shaded by dense riparian and channel vegetation. The water warms at different rates and thus, differences in DO occur. In consequence, water in oxbows is characterised by a less stable oxygen regime than in rivers (Kalinowski et al. 2011). In the Narew, anoxic conditions have been observed often, depending on the location along the river because, in contrast to the Świdra, which is dominated by submerged bed forms, the Narew is dominated by dense vegetation. Thus, as reported by Caraco and Cole (2002), vegetated rivers have lower DO concentrations on average. Moreover, in densely vegetated channels, oxygen consumption during respiration is higher, even though the concentration during the afternoon reaches an adequate level (Kaenel et al. 2000). Consequently, water flowing through the Narew National Park loses oxygen, and below the Park it tends to have very low oxygen content, apart from where weirs are present.

Although the presence of weirs oxygenates the water to some extent, this might be a temporal effect only below the weir (Fig. 8). Therefore, in some cases, the concentration at a particular distance below the weir would resemble that above the weir.

Despite the considerable number of studies devoted to re-aeration on hydraulic structures (e.g., Butts and Evans 1983; Gulliver and Rindels 1993; Gulliver et al. 1998), their impact on oxygen content is debatable. Apparently, these discrepancies arise from the initial conditions; thus, less saturated water has a greater oxygen capacity than fully saturated water. Therefore, less saturated water would tend to absorb more oxygen at hydraulic structures, whereas fully saturated water would tend to desorb it. Undoubtedly, hydraulic structures are places of high mass transfer, which is a function of the geometry of hydraulic structures and the inflow conditions (Tebbutt 1972; Toombes and Chanson 2005).

5 Conclusions

To conclude, oxygen studies constitute an important part of water quality management and environmental engineering. Future studies should focus on relationships between hydrodynamics and biophysical processes occurring in rivers. The development of methods and technology has improved measurements and has identified four broad research objectives:

1. Re-aeration mechanisms in rivers. Does the time length of desorption and absorption of oxygen (oxygen fluxes) relate to river hydrodynamics, e.g., velocity fluctuations?
2. Does the geomorphology of the river, channel geometry (size of dead zones) and stream-flow affect spatial differences in the distribution of oxygen content and the dynamics of DO concentrations?
3. Does the mixing of water from tributaries affect diel oxygen curves? Does it show a periodic cycle corresponding to changes in water temperature and light conditions or depend on flow rate and mixing?
4. How can these measurements be applied to the modelling of oxygen transport in rivers and to water quality predictions?

Acknowledgments Funding for this research was provided in part by the Institute of Geophysics of the Polish Academy of Sciences through the project for Young Scientists No. 500-10-15 and by the Ministry of Sciences and Higher Education within statutory activities No 3841/E-41/S/2014 and within the “IUVENTUS PLUS II” project No. 0028/IP2/2011/71. The authors are grateful to P.M. Rowiński for stimulating discussions on this topic. The authors would also like to thank three reviewers for their constructive comments, which helped to improve the manuscript.

References

- AHPA (1995) Standard methods for the examination of water and wastewater. 19th edition. American public health association, American waterworks association, and water environment federation, Washington, DC
- Allen JA (1955) Solubility of oxygen in water. Nature 175:83

- Amao Y (2003) Probes and polymers for optical sensing of oxygen. *Microchim Acta* 2143:1–12
- Birkel C, Soulsby C, Malcolm I, Tetzlaff D (2013) Modeling the dynamics of metabolism in montane streams using continuous dissolved oxygen measurements. *Water Resour Res* 49:5260–5275
- Butts T, Evans R (1983) Small stream channel dam aeration characteristics. *J Environ Eng* 109(3):555–573
- Caraco NF, Cole JJ (2002) Contrasting impacts of native and alien macrophytes on dissolved oxygen in a large river. *Ecol Appl* 12:1496–1509
- Chu ChS, Lo YL, Sung TW (2011) Review on recent developments of fluorescent oxygen and carbon optical fiber sensors. *Photonic Sensors* 1(3):234–250
- Clark LC Jr (1956) Monitor and control of blood and tissue O₂ tensions. *Trans Am Soc Artif Intern Organs* 2:41–48
- Cygański A (1995) Metody elektroanalizyczne (Electroanalytical methods). WNT, Warszawa. ISBN 83-204-1876-3 (in Polish)
- Demars BOL, Manson JR, Olafsson JS, Gislason GM, Gudmundsdottir R, Woodward G, Reiss J, Pichler D, Rasmussen JJ, Friberg N (2011a) Temperature and metabolic balance of streams. *Freshwater Biol* 56:1106–1121
- Demars BOL, Manson JR, Olafsson JS, Gislason GM, Friberg N (2011b) Stream hydraulics and temperature determine the metabolism of geothermal Icelandic streams. *Knowl Manag Aquat Ecosyst* 402(5):1–17
- Demas JN, De Graff BA, Coleman P (1999) Oxygen sensors based on luminescence quenching. *Anal Chem* 71:793A–800A
- Dojlido J (1980) Instrumentalne metody badania wody i ścieków (Instrumental methods for the examination of water and wastewater). Arkady, Warszawa
- Dojlido J (1997) Water quality in the Vistula basin. In: Best GA, Bogacka T, Niemirycz E (eds) International river water quality. Pollution and Restoration. Taylor and Francis, London, p 21–32
- Gewehr PM, Delpy DT (1994) Analysis of non-linearity of optical oxygen sensors based upon phosphorescence lifetime quenching. *Med Biol Eng Comput* 32:659–664
- Gradziński R, Baryła J, Dotor M, Gmür D, Gradziński M, Kędzior A, Paszkowski M, Soja R, Zieliński T, Żurek S (2003) Vegetation-controlled modern anastomosing system of the upper Narew River (NE Poland) and its sediments. *Sed Geol* 157:253–276
- Grist S, Chrostowski L, Cheung KC (2010) Optical oxygen sensors for applications in microfluidic cell culture. *Sensors* 10:9286–9316
- Gulliver JS, Rindels A (1993) Measurement of air-water oxygen transfer at hydraulic structures. *J Hydraul Eng* 119(3):327–349
- Gulliver JS, Wilhelms SC, Parkhill KL (1998) Predictive capabilities in oxygen transfer at hydraulic structures. *J Hydraul Eng* 124(7):664–671
- Harvey D (1999) Modern analytical chemistry. McGraw-Hill, Boston
- Helman I, Jalukse L, Leito I (2012) A highly accurate method for determination of dissolved oxygen: Gravimetric Winkler method. *Anal Chim Acta* 741:21–31
- Helton AM, Poole GC, Payn RA, Izurieta C, Stanford JA (2012) Scaling flow path processes to fluvial landscapes: an integrated field and model assessment of temperature and dissolved oxygen dynamics in a river-floodplain-aquifer system. *J Geophys Res* 117:G00N14
- Hondzo M, Voller VR, Morris M, Foufoula-Georgiou E, Finlay J, Ganti V, Power ME (2013) Estimating and scaling stream ecosystem metabolism along channels with heterogeneous substrate. *Ecohydrology* 6:679–688
- Jalukse L, Helm I, Saks O (2008) On the accuracy of micro Winkler titration procedures: a case study. *Accred Qual Assur* 13:575–589
- Johnston MW, Williams JS (2005) Filed comparison of optical and Clark cell dissolved oxygen sensors in the Tualatin River, Oregon, 2005. USGS Open-File Report 2006–1047
- Kaenel BR, Buehrer H, Uehlinger U (2000) Effects of aquatic plant management on stream metabolism and oxygen balance in streams. *Freshwater Biol* 45(1):85–95

- Kalinowski A, Burandt P, Glińska-Lewczuk K (2011) Wpływ czynników hydrologicznych na warunki termiczno-tlenowe starorzeczy na przykładzie Doliny Drwęcy (Effect of hydrological factors on temperature and oxygen distribution in floodplain lakes. A case study of the Drwęca floodplain). *Proc of ECOpole* 5(1):245–250
- Kautsky H, Hirsch A (1931) Neue Versuche zur Kohlensaureassimilation. *Naturwissenschaften* 19:964
- Kautsky H (1939) Quenching of luminescence by oxygen. *Trans Faraday Soc* 35:216–219
- Lakowicz JR (2006) Principle of fluorescence spectroscopy. Springer, Baltimore
- Li J, Liu H, Li Y, Mei K, Dahlgren R, Zhang M (2013) Monitoring and modeling dissolved oxygen dynamics through continuous longitudinal sampling: a case study in Wen-Rui Tang River, Wenzhou, China. *Hydrol Process* 27:3502–3510
- Manson JR, Demars BOL, Wallis SG (2011) Integrated experimental and computational hydraulic science in a unique natural laboratory. In: Rowinski P (ed) Experimental methods in hydraulic research. Springer Book Series, Geoplanet: Earth and Planetary Sciences 1:123–131
- McCutchan JH Jr, Lewis WM Jr, Saunders JF III (1998) Uncertainty in the estimation of stream metabolism from open-channel oxygen concentrations. *J North Am Benthol Soc* 17:155–164
- Mills A (1997) Optical oxygen sensors. *Platinum Met Rev* 41:115–127
- Mitchell TO (2006) Luminescence based measurement of dissolved oxygen in natural waters. Hach Company, p 1–8
- Narayanaswamy R, Wolfbeis OS (2004) Optical sensors: industrial, environmental and diagnostic applications. Springer series on chemical sensors and biosensors 01. Springer, Berlin
- Odum HT (1956) Primary production in flowing waters. *Limnol Oceanogr* 1(2):102–117
- O'Connor BL, Harvey JW, McPhillips LE (2012) Thresholds of flow-induced bed disturbances and their effects on stream metabolism in an agricultural river. *Water Resour Res* 48:W08504
- O'Connor DJ (1967) The temporal and spatial distribution of dissolved oxygen in streams. *Water Resour Res* 3(1):65–79
- Opaliński KW, Puczko M (2009) Oxygen consumption in Vistula River sandy beach. In: J Dojlido, K Dęguś (ed) Problems of water protection in the Bug and Narew river catchments. Monograph—Oficyna WSEiZ, Warsaw, p 33–64
- Reichert P, Uehlinger U, Acuña V (2009) Estimating stream metabolism from oxygen concentrations: effect of spatial heterogeneity. *J Geophys Res* 114:G03016
- Rommel K (2004) Oxygen measurement: optically or electrochemically?—comparison of theory and practical experience in online measurements. *Asian Environ Technol* 8(4):1–2
- Skoog DA, West DM, Holler FJ (1988) Fundamentals of analytical chemistry, 5th edn. Saunders, Philadelphia
- Stern O, Volmer M (1919) The fading time of fluorescence. *Phys Z* 20:183–188
- Tebbutt THY (1972) Some studies on reaeration in cascades. *Water Res* 6(3):297–304
- Toombes L, Chanson K (2005) Air–water mass transfer on a stepped waterway. *J Environ Eng* 131(10):1377–1386
- Truesdale GA, Downing AL (1954) Solubility of oxygen in water. *Nature* 173:1236
- UMCES, (2004) Workshop Proceedings, State of Technology in the Development and Application of Dissolved Oxygen Sensors, Alliance for coastal technologies, UMCES Technical report Series: TS-444-04-CBL/Ref No [UMCES] CBL 04-089
- Winkler LW (1888) Die Bestimmung des im Wasser gelösten Sauerstoffes. *Ber Dtsch Chem Ges* 21:2843–2854
- YSI (2009), The Dissolved Oxygen Handbook
- YSI (2003, 2005) Environmental Dissolved Oxygen Values Above 100 % Air Saturation. Pure Data for a Healthy Planet. Technical Note

Gradient-Based Similarity in the Stable Atmospheric Boundary Layer

Zbigniew Sorbjan

Abstract A structure of the stably-stratified atmospheric boundary layer is examined in terms of a novel gradient-based similarity theory. The presented approach introduces similarity scales based on the vertical gradient of the potential temperature, contrary to the traditional method, which is based on momentum and temperature fluxes. The length scale, defined using the semi-empirical form of the mixing length, is demonstrated to be effective in the entire stable boundary layer. In more complex cases, an alternative formulation of the mixing length, based on vertical velocity or temperature variances, can be employed. The empirical similarity functions of the Richardson number are expressed in analytical form, valid in the entire stable boundary layer. The introduced similarity approach allows for evaluating the minimum values of the dimensionless turbulent heat flux and the temperature standard deviation as functions of the Richardson number. It can also be used as a closure scheme for a single column model.

Keywords Atmospheric boundary layer • Gradient-based similarity • Stable boundary layer • Turbulence

1 Introduction

Small-scale processes in the atmosphere are fundamental to both weather and climate. Consequently, weather and climate forecasting models must include realistic representations of such processes through physical parameterizations.

Z. Sorbjan (✉)

Institute of Geophysics, Polish Academy of Sciences, Warsaw, Poland
e-mail: sorbjan@igf.edu.pl; zbigniew.sorbjan@mu.edu

Z. Sorbjan

Department of Physics, Marquette University, Milwaukee, USA

This chapter aims to review recent progress in the development of parameterizations for the stable (nocturnal) boundary layer in the atmosphere.

Parameterization of nocturnal turbulence is not a trivial problem. Data collected in the atmospheric boundary layer during recent years indicate that the structure of the stable regime is more complex than previously anticipated. High-resolution soundings of temperature, wind speed, direction, and other parameters exhibit small-scale zigzag-like fluctuations with height (e.g., Sorbjan and Balsley 2008). Large-eddy simulations show that such fluctuations are associated with front-like coherent vortical structures, which emanate from the surface, tilt forward, and fill the boundary layer (Sullivan 2014). Stable turbulence is often found to survive at Richardson numbers exceeding the critical value $Ri_{cr} = 1/4$ (e.g., Galperin et al. 2007). It can have either a continuous or intermittent character (e.g., Coulter and Doran 2002; Van de Wiel et al. 2003), within weakly stable or very stable regimes (e.g., Oyha et al. 1997; Mahrt 1998). The weakly stable case is associated with significant wind shear, clouds, continuous turbulence near the surface, and sub-critical values of the Richardson number. In contrast, the very stable regime is defined by a lesser wind shear, clear skies, supercritical values of the Richardson number, and weak turbulence. It may assume an “upside-down” character (Mahrt 1999), with the strongest turbulence in the upper part of the boundary layer (Newsom and Banta 2003; Banta 2008; Cuxart 2008). Weak turbulence in very stable conditions limits the validity of the Monin-Obukhov similarity, regarded as the major tool for understanding near-surface turbulence (e.g., Sorbjan 2006a, b). The similarity functions are formally valid only in the lower portion of the stable boundary layer, and in sub-critical cases. They cannot be accurately estimated due to the uncertainty introduced by small values of fluxes, and also due to self-correlation errors (Klipp and Mahrt 2004; Baas et al. 2006).

The chapter focuses on the gradient-based similarity theory in the stable boundary layer and its applications. It has the following structure. The similarity scaling systems are discussed in Sect. 2. The empirical verification of gradient-based similarity functions is presented in Sect. 3. Applications of the introduced approach are discussed in Sect. 4. Final remarks are provided in Sect. 5.

2 Scaling Systems

2.1 Governing Parameters

Let us consider the most basic dependence between fluxes and gradients in the stable boundary layer of the atmosphere. According to the classic K-theory, the turbulent kinematic fluxes of momentum τ and temperature H in the horizontally homogeneous flow can be expressed in terms of the mean wind shear $S = \sqrt{(dU/dz)^2 + (dV/dz)^2}$ and the vertical gradient of the virtual potential temperature gradient $\Gamma = d\Theta/dz$ (Sorbjan 2010; Sorbjan and Grachev 2010):

$$\tau = K_m S \quad (1a)$$

$$H = -K_h \Gamma \quad (1b)$$

where U and V are components of the wind vector, and the coefficients K_m and K_h can be written in the form:

$$K_m = l^2 S f_m(Ri) \quad (2a)$$

$$K_h = l^2 S f_h(Ri) \quad (2b)$$

where l is the mixing length in neutrally stratified layer, f_m , and f_h are empirical stability functions of the Richardson number $Ri = N^2/S^2$, $N = \sqrt{\beta\Gamma}$ is the Brunt-Väisälä frequency, $\beta = g/T_o$ is the buoyancy parameter, g is the gravity acceleration, and T_o is the reference temperature. The functions f_m and f_h are equal to unity in neutral conditions (when $Ri = 0$), and are expected to decrease with increasing Ri . The eddy diffusivity K_h is defined analogously to K_m .

Equation (2a) follows from an expressions for the eddy viscosity $K_m = l^2 S$ of Prandtl (1932), derived under assumption that thermal stratification is neutral. The mixing length l characterizes dominant eddies, and is formally defined as $l = \tau^{1/2}/S$. In the close proximity of the underlying surface, observations show that $S = u_*/(\kappa z)$, where $u_* = \tau^{1/2}$ is the friction velocity, $\kappa = 0.4$ is the von Karman constant, and z is height. This implies that the mixing length in the neutral surface layer is a linear function of height:

$$l = \kappa z \quad (3a)$$

Farther from the surface, the growth of the mixing length with height is expected to be gentler. This fact can be taken into consideration by adopting the inverse linear approximation of Delage (1974), between the limits of the mixing length near the underlying surface ($= \kappa z$) and above the surface ($= \lambda_o$): $1/l = 1/(\kappa z) + 1/\lambda_o$, which is equivalent to:

$$l = \frac{\kappa z}{1 + \frac{\kappa z}{\lambda_o}} \quad (3b)$$

Sorbian (2012a) found that $\lambda_o = 12$ for the CASES-99 data set in stable conditions. Blackadar (1962) suggested that $\lambda_o = 0.009 u_* f$, where f is the Coriolis parameter.

Huang et al. (2013) and Sorbian (2013) employed additional modification of the mixing length of the form: $1/l = 1/(\kappa z) + 1/\lambda_m$, where $1/\lambda_m = 1/\lambda_o + 1/\lambda_B$, and λ_B is a stability parameter. This yields:

$$l = \frac{\kappa z}{1 + \frac{\kappa z}{\lambda_o} (1 + \lambda_o/\lambda_B)} \quad (3c)$$

Huang et al. (2013) concluded, based on a series of large-eddy simulations, that $\lambda_B = \lambda_s/Ri$. The parameter λ_s was assumed equal to 1 m by Sorbjan (2013). Note that when $Ri \rightarrow 0$, $\lambda_o/\lambda_B \rightarrow 0$, and $l \rightarrow \kappa z/(1 + \kappa z/\lambda_o)$, which coincides with (3b).

When the empirical functions f_m , f_h and l are specified, the system (1a, 1b)–(2a, 2b) is closed. It describes the relationship between the fluxes τ , H and parameters S , Γ , β , z . Based on this fact, some general conclusions can be derived by employing the approach of the dimensional analysis (e.g., Barenblatt 1996).

Note that the choice of the similarity scales for the set of six variables: $\{\tau, H, S, \Gamma, l, \beta\}$, with three independent units, (m), (s), (K), is not unique and can be performed in a number of ways. Generally, any three dimensionally independent parameters in the above list can be selected to build a system of three scales for length, temperature, and velocity. In the next sections, we will consider scaling systems, based on the following choice of the parameters:

$$\{\tau, H, \beta\} \quad (4a)$$

and

$$\{l, \Gamma, \beta\} \quad (4b)$$

The system defined by the first set of parameters will be referred to as “flux-based scaling”, while the remaining system will be called “gradient-based scaling”. It should be mentioned that other gradient-based scaling systems can also be proposed in the stable regime, e.g. by using shear S instead of Γ in (4b), as shown in Sect. 4.1 of this chapter, or augmenting the list of similarity parameters by additional characteristics of turbulence, e.g. standard deviations σ_w , σ_θ of the vertical velocity and temperature, as in Sect. 3.3, or by the dissipation rate ε (Sorbjan and Balsley 2008).

2.2 The Flux-Based Scaling

Historically, the first similarity scaling system was proposed by Monin and Obukhov (1954) for the surface layer, where the turbulent fluxes can be assumed to be nearly constant with height. The surface values of fluxes τ_o , H_o from the list (4a) were employed to construct 3 scales: for length $L_* = -\tau_o^{3/2}/(\kappa\beta H_o)$, for temperature $T_* = -H_o/u_*$, and for velocity $u_* = \sqrt{\tau_o}$. Based on a dimensional analysis, Monin and Obukhov concluded that the non-dimensional products of statistical moments in the surface layer (e.g. σ_w , σ_θ , S , Γ), and the flux-based scales, are universal functions φ of a single dimensionless height z/L_* (Sorbjan 1989):

$$\frac{X}{u_*^a T_*^b L_*^c} = \varphi_x(z/L_*) \quad (5)$$

where X is a statistical moment, and the exponents a, b, c are chosen in such a way that φ_x is dimensionless.

The above expression conveys the so-called “self-similarity”, a property, which manifests itself in the reduction of the number of independent dimensionless variables in comparison to the number of dimensional ones (e.g., Barenblatt 1996). Self-similarity substantially simplifies the description of phenomena and their experimental, analytical and computational analysis. It can be noted, however, that the presence of fluxes τ_o, H_o in definitions of scales u_*, T_*, L_* , and in the dimensionless parameter z/L_* , introduces “self-correlation” errors of universal functions φ_x (e.g. Baas et al. 2006).

By using second-order closure model, Nieuwstadt (1984) demonstrated that the assumption of the constancy of fluxes with height is not necessary in the lower part of the boundary layer, so that the scales in the stable boundary layer can be height-dependent (local):

$$U_*(z) = \sqrt{\tau}, \quad \vartheta_*(z) = -\frac{H}{U_*}, \quad \Lambda_*(z) = -\frac{\tau^{3/2}}{\kappa\beta H} \quad (6)$$

where capital letters are used to mark the local (z -dependent) scales. Sorbjan (e.g., 1986a, b, c, 1988) argued that the functional form of similarity functions φ_x of the argument z/Λ_* and of z/Λ_* is identical in stable conditions. As a result, one might write for shear S and temperature gradient Γ :

$$\frac{\kappa z}{U_*} S = \varphi_m(z/\Lambda_*) \quad (7a)$$

$$\frac{\kappa z}{\vartheta_*} \Gamma = \varphi_h(z/\Lambda_*) \quad (7b)$$

where φ_m, φ_h are functions evaluated based on observations in the surface layer. Applying the definition of the Richardson number yields:

$$Ri = \frac{z}{\Lambda_*} \frac{\varphi_h(z/\Lambda_*)}{\varphi_m^2(z/\Lambda_*)} \quad (8)$$

Equation (8) shows that Ri is a function of z/Λ_* . This fact allows rewriting (7a, 7b) in the equivalent form:

$$\frac{\kappa z}{U_*} S = \psi_m(Ri) \quad (9a)$$

$$\frac{\kappa z}{\vartheta_*} \Gamma = \psi_h(Ri) \quad (9b)$$

where ψ_m, ψ_h are the similarity functions of the Richardson number. The same result can be formally obtained based on (1a, 1b)–(2a, 2b), with $\psi_m \sim 1/f_m^{1/2}$, $\psi_h \sim f_m^{1/2}/f_h$, and $l = \kappa z$.

2.3 The Gradient-Based Scaling

An alternative similarity scaling was introduced by Sorbjan (2010), who used parameters listed in (4b), namely, the temperature gradient Γ , the buoyancy parameter β , and the mixing length l , to formulate gradient-based scales:

$$U_N(z) = lN, \quad T_N(z) = l\Gamma, \quad L_N(z) = l \quad (10)$$

where l is a generic mixing length. The scales (10) are valid when the Brunt-Väisälä frequency N is positive and sufficiently large.

Employing (10), one can obtain from (1a, 1b)–(2a, 2b) that:

$$\frac{\tau}{U_N^2} = G_t(Ri) \quad (11a)$$

$$-\frac{H}{U_N T_N} = G_h(Ri) \quad (11b)$$

where $G_t \sim f_m/Ri$, $G_h = f_h/Ri^{1/2}$. Note also that $G_t = 1/(Ri \psi_m^2)$, and $G_h = 1/(Ri^{1/2} \psi_m \psi_h)$. The above result can be generalized by stating that the non-dimensional products of statistical moments X in the surface layer and the above scales must be universal functions of a single dimensionless parameter Ri :

$$\frac{X}{U_N^a T_N^b L_N^c} = G_x(Ri) \quad (12)$$

which is an analog of (5).

Applying (12) to the standard deviations of the vertical velocity and temperature, yields

$$\frac{\sigma_w}{U_N} = G_w(Ri) \quad (13a)$$

$$\frac{\sigma_\theta}{T_N} = G_\theta(Ri) \quad (13b)$$

Note that the temperature gradient Γ appears on both sides of (13a, 13b), i.e. within the similarity scales and in the definition of the Richardson number. This fact implies self-correlation, due to the relative errors in the evaluation of the temperature gradient Γ . One can expect, however, that such errors are relatively small when the gradient observations are accurately evaluated, and temperature gradient is sufficiently large.

We will show in Sect. 3 that the generic mixing length l can be described by (3a) in the surface layer. In the lower part of the stable boundary layer, l can be

expressed by (3b). In the entire stable boundary layer, l can be described by (3c). For any of these cases, the dependence of the similarity functions G_t , G_h , G_w , G_θ on the Richardson number Ri remains unchanged.

3 Empirical Verification

In this section we will evaluate and examine the gradient-based similarity functions, using three data sets collected during SHEBA, CASES-99 experiments, and on the BAO tower in Colorado. The SHEBA observations, which were performed in a relatively close proximity from the underlying surface, will be used to test gradient-based similarity in the surface layer. The CASES-99 data will allow us to examine similarity predictions in the lower half of the stable boundary layer, and also to generalize results for the entire stable boundary layer. The BAO data include observations in more complex situations.

3.1 Verification in the Stable Surface Layer (The Length Scale $L_N = \kappa z$)

3.1.1 The SHEBA Experiment

The gradient-based approach was first examined in the surface layer, based on data collected during the SHEBA experiment (Sorbian 2010; Sorbian and Grachev 2010). The experiment took place over the Arctic pack ice, drifting in the Beaufort Gyre to the north of Alaska (latitude from 74°N–81°N) from October 1997 through September 1998 (Andreas et al. 1999, 2003, 2006; Persson et al. 2002; Grachev et al. 2005, 2007a, b, 2008). The sub-polar localization offered a number of advantages, especially due to the stationarity of weather conditions, and the lack of contamination by drainage or strong advective flows. Except for rare periods, instruments ran almost continuously for 11 months and produced well over 6,000 h of useful data, covering a wide range of stability conditions.

Measurements during SHEBA were performed on the 20 m main tower and collected at five levels, located at 2.2 m (level 1), 3.2 m (level 2), 5.1 m (level 3), 8.9 m (level 4), and 18.2 or 14 m above the surface (level 5) (Grachev et al. 2007a). The variances and covariances at each level were evaluated based on 1 h averaging, and derived through frequency integration of spectra and cospectra. Vertical gradients of the mean wind velocity and the potential temperature were obtained by fitting a second-order polynomial through the 1 h profiles, followed by an evaluation of the derivative with respect to z for levels 1–5. The data points were based on a bin-averaging of the individual 1 h data at levels 2, 3, 4, and 5. For this purpose, data were first sorted into bins for the Richardson number Ri as

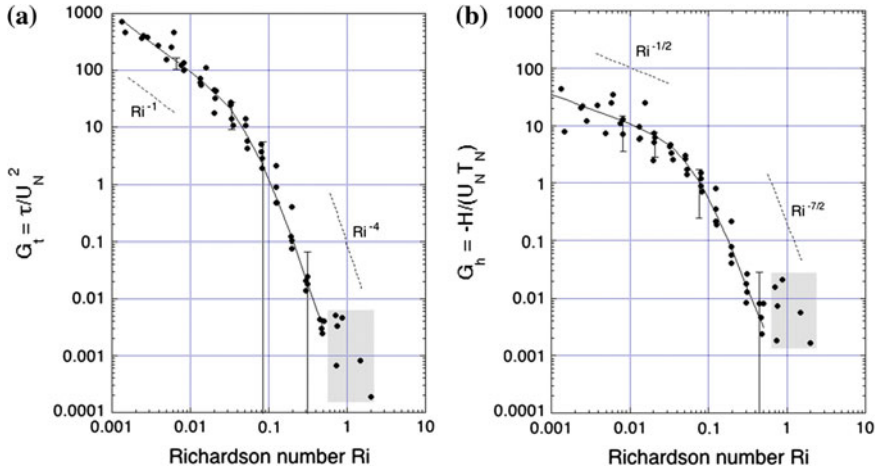


Fig. 1 Dependence of the bin-averaged values of the dimensionless: **a** momentum flux $G_t = \tau/U_N^2$, **b** heat flux $G_h = -H/(U_N T_N)$, on the Richardson number Ri , obtained based on SHEBA data. The solid lines are plotted based on Eqs. 16a and 16b. The vertical lines represent the confidence intervals evaluated at level 5 of the mast. Data points within the “extremely-stable” domain are marked by the shaded box (based on Sorbian 2010)

the sorting parameter. Then the mean values of relevant parameters were computed for each bin (e.g., Grachev et al. 2008). A special prerequisite was applied on the data to limit the influence of outliers on the bin-averaging. It had the following form: $0.5Ri_e < Ri < 2Ri_e$, where the value of the Richardson number Ri_e is estimated based on an equation analogous to (8), and the analytical form of the Monin-Obukhov similarity functions φ_h and φ_m of z/L_* , obtained by Grachev et al. (2007a, 2008). If the actual value of a Richardson number Ri was not in the range defined by Ri_e , the data point was rejected.

3.1.2 Empirical Similarity Functions

The dependence of the dimensionless fluxes, $G_t = \tau/U_N^2$ and $G_h = -H/(U_N T_N)$, on the Richardson number Ri is shown in Fig. 1. The similarity scales in the considered case of SHEBA data were assumed in the form: $L_N = \kappa z$, $U_N = \kappa z N$, $T_N = \kappa z T$. The vertical lines with horizontal bars represent the confidence intervals, obtained by adding or subtracting the standard deviation to, or from the mean values, evaluated at level 3 of the mast. Because the ordinate is logarithmic, the confidence intervals are asymmetric. The dimensionless moments $G_w = \sigma_w/U_N$ and $G_\theta = \sigma_\theta/T_N$ are depicted in Fig. 2. A clustering of data points in Figs. 1 and 2 is caused by the fact that the Richardson number Ri is a sorting parameter for the displayed levels 2–5.

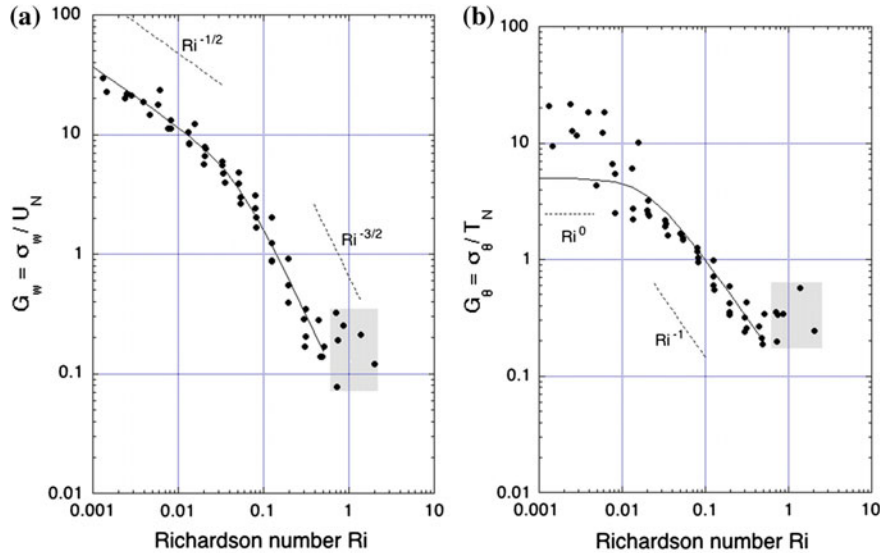


Fig. 2 Dependence of the bin-averaged values of the dimensionless standard deviations for: **a** vertical velocity $G_w = \sigma_w/U_N$, **b** temperature $G_\theta = \sigma_\theta/T_N$, on the Richardson number Ri , obtained based on SHEBA data. The *solid lines* are plotted based on Eqs. 16c and 16d. Data points within the “extremely-stable” domain are marked by the *shaded box* (based on Sorbjan 2010)

It can be noticed that the scatter of data points in Fig. 2b (especially for small values of Ri) is larger than in Fig. 2a. This effect can be associated with thermal inhomogeneity around the observational site (e.g., Kukharets and Tsvang 1998; Tsvang et al. 1998). The ice floe around the main tower was multi-year pack ice, with varying degrees of thickness, with a surface composed of ice of a different type and salinity, snow of a different depth and age, melt-ponds, and even leads (e.g., Sorbjan and Grachev 2010). These surface patches were characterized by different albedo, thermal capacity and conductivity and, therefore, by different temperatures. Andreas et al. (1998) reported analogous behavior for humidity statistics over a surface with vegetation that was patchy at meter scales.

In order to further evaluate the presented results, let us first notice that in nearly-neutral conditions, $\tau \sim (\kappa z S)^2$, $\sigma_w \sim \kappa z S$, and also that $H \sim (\kappa z)^2 S N^2 / \beta$, $\sigma_\theta \sim \kappa z N^2 / \beta$. Thus, we can conclude that in such conditions

$$G_t \sim Ri^{-1}, \quad G_h \sim Ri^{-1/2}, \quad G_w \sim Ri^{-1/2}, \quad G_\theta \sim Ri^0. \quad (14)$$

Figures 1a, b and 2a confirm the above predictions for $Ri < 0.01$. The observational values of the dimensionless temperature variance G_θ , in Fig. 2b, are larger than expected in the nearly-neutral range, most likely due to effects associated with thermal inhomogeneity around the observational site.

In the range $Ri < 0.7$, the values of the similarity functions fall off in a coherent fashion for the increasing values of Ri . This indicates the presence of a self-similar regime in very stable conditions. The dimensional analysis, however, does not allow the formulation of any constructive similarity prediction. Therefore, we will assume, based on the presented empirical evidence, that the similarity functions obey the following power laws:

$$G_t \sim Ri^{-4}, \quad G_h \sim Ri^{-7/2}, \quad G_w \sim Ri^{-3/2}, \quad G_\theta \sim Ri^{-1} \quad (15)$$

valid approximately in the range $0.1 < Ri < 0.7$, as indicated by the dotted lines in the figures. Above this range, the values of similarity functions are incoherent and scattered. Such behaviour indicates a lack of any general similarity laws for larger values of Ri . Consequently, we will limit our analysis to the range of $Ri < 0.7$, and disregard the domain marked by the shaded boxes in Figs. 1–2, and also in the remaining figures.

Taking (14) and (15) into consideration, we will adopt the following approximations of the similarity functions:

$$G_t \equiv \frac{\tau}{U_N^2} = \frac{f_m}{Ri} = \frac{1}{Ri(1 + 300Ri^2)^{3/2}} \quad (16a)$$

$$G_h \equiv -\frac{H}{U_N T_N} = \frac{f_h}{Ri^{1/2}} = \frac{1}{0.9 Ri^{1/2} (1 + 250 Ri^2)^{3/2}} \quad (16b)$$

$$G_w \equiv \frac{\sigma_w}{U_N} = \frac{1}{0.85 Ri^{1/2} (1 + 450 Ri^2)^{1/2}} \quad (16c)$$

$$G_\theta \equiv \frac{\sigma_\theta}{T_N} = \frac{5}{(1 + 2500 Ri^2)^{1/2}} \quad (16d)$$

The above equations are represented in Figs. 1 and 2 by solid curves. From (2a, 2b) it also follows that

$$\frac{K_m}{l^2 S} = Ri G_t = f_m = \frac{1}{(1 + 300 Ri^2)^{3/2}} \quad (17a)$$

$$\frac{K_h}{l^2 S} = Ri^{1/2} G_h = f_h = \frac{1}{0.9(1 + 250 Ri^2)^{3/2}} \quad (17b)$$

Using (6) and (10), we will also obtain for the flux-based similarity functions (9a, 9b):

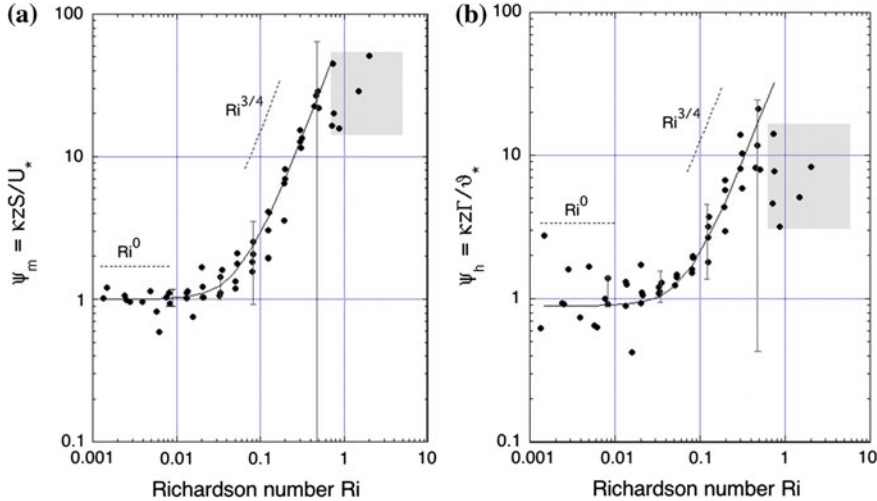


Fig. 3 Dependence of the bin-averaged values of the flux-based similarity functions, **a** ψ_m , and **b** ψ_h , on the Richardson number Ri , obtained based on SHEBA data. The *solid curves* are described by Eqs. 18a and 18b. The *vertical lines* represent the confidence intervals evaluated at level 5 of the mast. The “extremely-stable” domain is marked by the *shaded box* (based on Sorbjan and Grachev 2010)

$$\psi_m \equiv \frac{lS}{U_*} = \frac{1}{Ri^{1/2} G_t^{1/2}} = \frac{1}{f_m^{1/2}} = (1 + 300Ri^2)^{3/4} \quad (18a)$$

$$\psi_h \equiv \frac{l\Gamma}{v_*} = \frac{G_t^{1/2}}{G_h} = \frac{f_m^{1/2}}{f_h} = 0.9 \frac{(1 + 250Ri^2)^{3/2}}{(1 + 300Ri^2)^{3/4}} \quad (18b)$$

in the range $Ri < 0.7$.

The values of the similarity functions ψ_m , ψ_h are plotted in Fig. 3. Data points in the figure agree with curves, defined by expressions (18a, 18b), except for the outliers in the shaded box, which are highly scattered. The scatter of data points for ψ_h is larger than for ψ_m , which could be associated with the effects of thermal inhomogeneity around the observational site.

3.1.3 Structure of Stable Turbulence

Let us now consider the flux Richardson number, defined as $Rf = -\beta H/(\tau S)$. Employing (16a, 16b), we obtain:

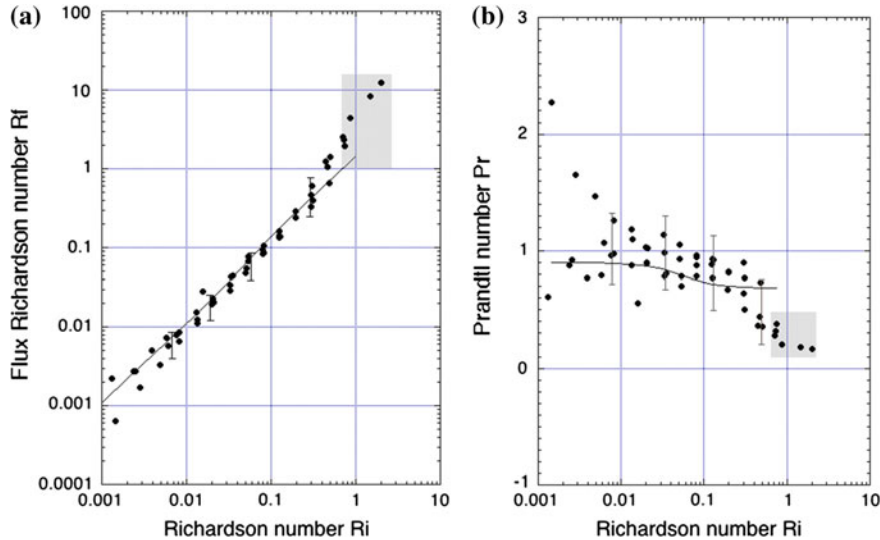


Fig. 4 Dependence of the bin-averaged values of: **a** the flux Richardson number Rf (the *solid line* is plotted based on Eq. 19), and **b** the Prandtl number Pr , on the gradient Richardson number Ri (the *solid line* is plotted based on Eq. 20). Points represent the SHEBA data. The *vertical lines* represent the confidence intervals for evaluated at level 5 of the mast (based on Sorbjan 2010)

$$Rf = \frac{G_h}{G_t} Ri^{1/2} = \frac{f_h}{f_m} Ri = \frac{Ri (1 + 300Ri^2)^{3/2}}{0.9(1 + 250Ri^2)^{3/2}} \quad (19)$$

in the range $Ri < 0.7$. The above expression is depicted in Fig. 4a as a solid curve. In accordance with (19), $Rf = 1.11 Ri$ in nearly-neutral conditions, and $Rf = 1.46 Ri$ for large values of Ri . Consequently, the curve in the figure differs only slightly from a straight line.

Taking into consideration that the Prandtl number $Pr = K_m/K_h = Ri/Rf$, we can also receive from (17a, 17b) or (19) that:

$$Pr = \frac{f_m}{f_h} = 0.9 \frac{(1 + 250Ri^2)^{3/2}}{(1 + 300Ri^2)^{3/2}} \quad (20)$$

in the range $Ri < 0.7$. The above expression is shown in Fig. 4b as a solid curve.

Equation (20) indicates that the value of the Prandtl number is equal to $Pr_o = 0.9$ in nearly-neutral conditions, and to 0.7 for larger values of Ri . When all displayed data points are considered, the resulting mean value of the Prandtl number is 0.83, the median is equal to 0.85, and the standard deviation is 0.36.

The resulting neutral value 0.9 is larger than the value $Pr_o = 0.74$ of Businger (1973), than the neutral limit of 0.8 proposed by Churchill (2002), and than the value 0.85, obtained by Kader and Yaglom (1990). According to Ohya (2001),

Grachev et al. (2007b), Esau and Grachev (2007), Zilitinkevich et al. (2008), Anderson (2009), the Prandtl number increases with Ri in supercritical conditions. A detailed analysis of Grachev et al. (2007b) implies, however, that such a result is spurious. When the special prerequisite limiting the influence of outliers on the bin-averaging, discussed in Sect. 3.1, is not imposed, the resulting SHEBA points indeed show that Pr increases with the increasing values of Ri . With the prerequisite applied, however, the Prandtl number decreases slightly, as shown in Fig. 4b (Sorjan and Grachev 2010).

Note that the steady-state, turbulent energy budget can also be expressed in the following form (e.g., Sorjan 1989):

$$K_m S^2 (1 - Rf) = \varepsilon \quad (21)$$

Since the dissipation rate ε is positive-definite, the above equation allows us to conclude that the steady state, which results from a balance of shear production and buoyant-dissipative destruction, takes place only for $Rf < 1$.

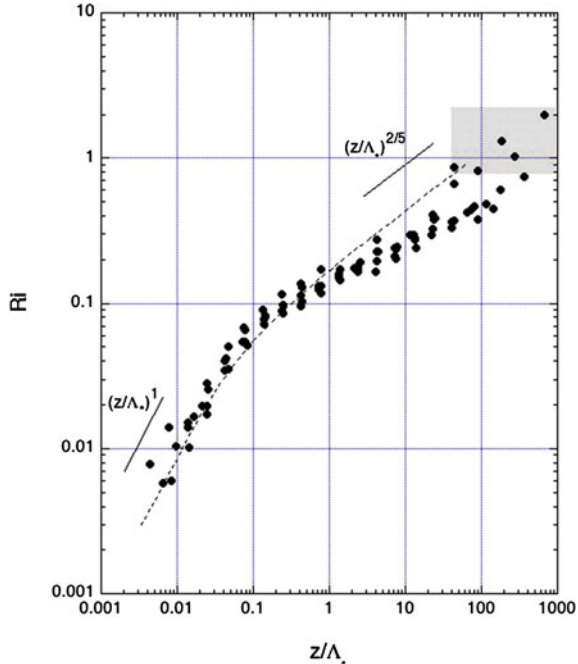
Figure 4b indicates that $Rf = 1$ at $Ri = 0.7$. Thus, at the Richardson number Ri exceeding the value $Ri_s = 0.7$ (which is larger than the critical value $Ri_{cr} = 0.25$ indicated by the linear stability evaluation), the steady-state turbulence would not be present. In other words, at $Ri > R_s$, turbulence is non-stationary and decaying or sporadic. The inequality $Ri < R_{cr} = 0.25$ is a sufficient condition for the presence of steady-state turbulence, i.e., if satisfied, it guarantees that steady-state turbulence exists. The inequality $Ri < R_s = 0.7$ is a necessary condition for the presence of steady-state turbulence, i.e., it must be satisfied for steady-state turbulence to take place. This conclusion generally coincides with Abarbanel et al. (1984), who found, based on non-linear stability analysis, that the transition from turbulence to laminar flow takes place at $Ri = 1$. A similar conclusion was reached by Cheng et al. (2002), and Fernando (2003). Nonetheless, Grachev et al. (2013) argued that at $Ri > 0.25$, turbulence dies in the inertial range, associated with the Richardson-Kolmogorov cascade, and vertical turbulent fluxes become small.

Figure 5 shows the dependence between the Richardson number Ri and the stability parameter $l/(\kappa A_*)$ equal to z/A_* in the surface layer. The plot was obtained by employing z/A_* as a sorting parameter for SHEBA data. As a result, the number of SHEBA data points differs from those in previous figures. The values in the figure generally agree with the results of Yagüe et al. (2006). The figure shows, for example, that at $z/A_* \approx 4$, Ri is about 0.25, which coincides with the results of Businger et al. (1967), and Dyer (1974), and disagrees with Holtslag and De Bruin (1988) and Beljaars and Holtslag (1991), who obtained that the corresponding value of Ri is much higher, and in the range of 0.7–0.9.

The solid curve in Fig. 5 is derived from the following equation:

$$\frac{l}{\kappa A_*} = Ri \frac{\psi_m^2}{\psi_h} = Ri \frac{f_h}{f_m^{3/2}} = \frac{Ri (1 + 300Ri^2)^{9/4}}{0.9 (1 + 250Ri^2)^{3/2}} \quad (22)$$

Fig. 5 Dependence of the bin-averaged values of the gradient Richardson number Ri and the dimensionless parameter $l/(\kappa\Lambda^*) = z/\Lambda_*$ in the surface layer, obtained based on SHEBA data. The solid line is based on Eq. 22. The vertical lines represent the confidence intervals evaluated at level 5 of the mast. The “extremely-stable” domain is marked by the shaded box (based on Sorbjan and Grachev 2010)



which was obtained by using (18a, 18b), and $l = \kappa z$. The above equation is also displayed in Fig. 5. It indicates that the critical value $Ri_s = 0.7$ corresponds to the value $z/\Lambda_* \approx 50$. The figure shows an agreement between the solid curve and the data points for $z/\Lambda_* < 1$, and a disagreement for very stable conditions, when $z/\Lambda_* > 1$. Such a discrepancy can be interpreted as a result of using the stable parameter z/Λ_* as a sorting parameter, and also of relatively large errors in evaluation of this parameter (which is defined as a ratio of fluxes) at $Ri > 0.2$.

Referring to Fig. 5 and Eq. (22), one can identify four stable regimes within the stable surface layer. They can be named: “nearly-neutral”, “weakly-stable”, “very-stable”, and “extremely-stable”. In the “nearly-neutral” regime ($0 < Ri < 0.02$) the dimensionless gradients ψ_m and ψ_h are nearly constant (see Fig. 3), and the dependence of $l/(\kappa\Lambda_*)$ on Ri is linear. The “weakly-stable” regime ($0.02 < Ri < 0.12$) is the transition between “nearly-neutral” and “very-stable” conditions. In the “very-stable” regime ($0.12 < Ri < 0.7$), the dimensionless gradients ψ_m and ψ_h are exponential, as is the dependence of $l/(\kappa\Lambda_*)$ and Ri . The presence of any scaling laws in “extremely-stable” conditions, when $Ri > 0.7$, is doubtful (e.g., Cheng et al. 2002), since turbulence in this case can be impacted by local influences, such as surface non-heterogeneity, or propagating gravity waves. The specified regimes are controlled by local stability parameters and can generally occur at any height within the stably stratified boundary layer.

3.2 Verification Above the Surface Layer

$$[L_N = \kappa z / (1 + \kappa z / \lambda_o)]$$

3.2.1 The CASES-99 Experiment

The experimental was carried out from October 1 to 31, 1999, near Leon, Kansas (50 km) east of Wichita, Kansas with a 3 day intercomparison and instrument testing period from September 27 to 30. This area was chosen due to its relative lack of obstacles and flat terrain (average slopes of 0.5°), and reasonable access to power and phone lines. Instrumentation included a heavily instrumented 60 m tower, numerous 10 m towers (many with flux measurements), multiple radars, lidars, scintillometers, tethersondes, rawinsondes and research aircraft.

The resulting data set contains the momentum and heat fluxes, vertical velocity and temperature variances, wind shear S and temperature gradient Γ , available at nine levels: 0.5, 1.5, 5, 10, 20, 30, 40, 50, and 55 m above the underlying surface, during the period between 1,800 LST and 0600 LST, collected over 18 days of the experiment. The processed fluxes do not contain mesoscale fluctuations, which were removed based on the method of Vickers and Mahrt (2003, 2006). Data, which could be affected by booms of anemometers at certain wind directions, were also eliminated. The block averaging interval for obtaining mean variables was 10 min. The gradients of wind velocity components are based on log-linear functions of height, fitted to data points at three levels: the level where the wind shear is calculated, the level above it and the one below it. Because of the fine vertical resolution of the temperature observation, central differences were used to calculate the vertical temperature gradients, for points above and below each calculation level.

3.2.2 Empirical Similarity Functions

The plots of the resulting dimensionless fluxes and variances are presented in Figs. 6 and 7. They were obtained for the gradient-based similarity scales (10), with the mixing length l defined by both, (3a) or (3b). The value $\lambda_o = 12$ m in (3b) was found to be optimal in the latter case. Two levels, at 10 and 50 m above the underlying surface, were selected as representative for the surface layer and for the layer above it.

The dimensionless heat flux $-H/(U_N T_N)$ is shown in Fig. 6a. The values of the dimensionless flux, obtained for $U_N = \kappa z N$ and $T_N = \kappa z \Gamma$, are marked by red circles, while the values obtained for $U_N = \kappa z N / (1 + \kappa z / \lambda_o)$ and $T_N = \kappa z \Gamma / (1 + \kappa z / \lambda_o)$ are indicated by black diamonds. The stability function (16b) is represented by a blue curve. The impact of the mixing length correction (proportional to λ_o) in Fig. 6a (level of 10 m) is small. At the level of 50 m, the impact of the mixing length correction is significant. Most of the red circles at $Ri > 0.1$ in Fig. 6b are located below the blue curve, while the black diamonds are shifted closer to the blue curve. This proves that using the mixing length (3b) above the surface layer is more appropriate.

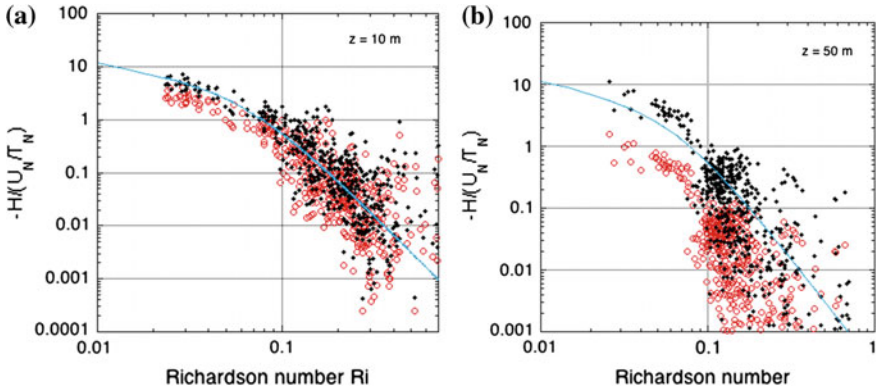


Fig. 6 A comparison of the dimensionless heat flux flux $-H/(U_N T_N)$ during CASES-99 at: **a** $z = 10 \text{ m}$, and **b** $z = 50 \text{ m}$, obtained for $U_N = \kappa z N$, $T_N = \kappa z \Gamma$ (red circles), and for $U_N = \kappa z N / (1 + \kappa z / \lambda_o)$, $T_N = \kappa z \Gamma / (1 + \kappa z / \lambda_o)$, with $\lambda_o = 12 \text{ m}$ (black diamonds). The stability function of the Richardson number Ri (blue line) is described by Eq. 16b (based on Sorbjan 2012b)

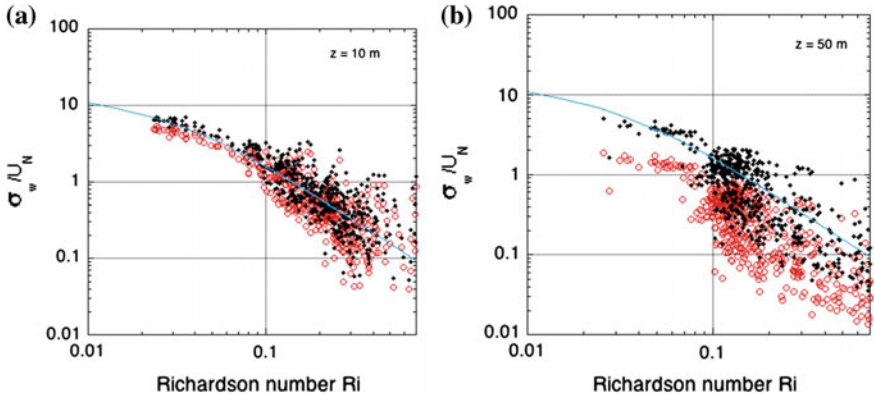


Fig. 7 A comparison of the dimensionless standard deviation of the vertical velocity σ_w / U_N during CASES-99 at: **a** $z = 10 \text{ m}$, and **b** $z = 50 \text{ m}$, obtained for $U_N = \kappa z N$ (red circles), and for $U_N = \kappa z N / (1 + \kappa z / \lambda_o)$, with $\lambda_o = 12$ (black diamonds). The stability function of the Richardson number Ri (blue line) is described by Eq. 16c (based on Sorbjan 2012a)

Figure 7 shows a comparison of the dimensionless standard deviation of the vertical velocity σ_w / U_N , obtained for $U_N = \kappa z N$ (red circles) and for $U_N = \kappa z N / (1 + \kappa z / \lambda_o)$. The stability function (16c) is represented by the blue curve. As in Fig. 6, the effect of the mixing length correction is relatively small on the level of 10 m in Fig. 7a, and significant at the level of 50 m (Fig. 7b). Most of the red circles at $z = 50 \text{ m}$, obtained by assuming the linear mixing length, are located below the blue curve. The black diamonds are situated closer to the blue curve.

The modification of the similarity scales by using the mixing length defined by (3b), instead of (3a), does not alter the dependence of similarity functions on the Richardson number Ri in the surface layer. However, it causes a noticeable improvement above the surface layer. Based on this observation, the validity of the gradient-based similarity functions of the Richardson number can be extended for the entire boundary layer, by using (3c) in the definition of the similarity scales (10).

3.3 Verification in the Boundary Layer Affected by Gravity Waves [$L_N = \sigma_w N$, or $L_N = \beta \sigma_\theta N^2$]

In order to investigate effects of interactions between turbulence and gravity waves in the stable boundary layer on similarity relationships, Sorbjan and Czerwinski (2013) examined a dataset collected by Hunt et al. (1985) during three April nights in 1978 and in 1980 on the 300 m tower of the Boulder Atmospheric Observatory (BAO). The BAO site, located in Erie, Colorado, USA, 30 km east of the foothills of the Rocky Mountains, has been known for the frequent detection of wave activities. Results showed that the scaling (10), based on the semi-empirical expressions for the mixing length (3b), is inefficient for the considered data set.

Alternatively, the considered data were normalized by two other local, gradient-based scaling systems. The first scaling system was based on (10), with the mixing length dependent on local values of the vertical-velocity variance σ_w and the Brunt-Väisälä frequency N (the σ_w scaling):

$$L_w = \frac{\sigma_w}{N}, \quad U_w = L_w N \equiv \sigma_w, \quad T_w = L_w \Gamma \equiv \frac{N \sigma_w}{\beta} \quad (23)$$

and the second one was defined using the temperature variance σ_θ and N (the σ_θ scaling):

$$L_\theta = \frac{\beta \sigma_\theta}{N^2} \quad U_\theta = L_\theta N \equiv \frac{\beta \sigma_\theta}{N} \quad T_\theta = L_\theta \Gamma \equiv \sigma_\theta \quad (24)$$

The similarity functions for the σ_w scaling can be found by employing (16a, 16b) and (23):

$$\frac{\tau}{U_w^2} = G_t/G_w^2 = 0.72 \frac{(1 + 450Ri^2)}{(1 + 300Ri^2)^{3/2}} \quad (25a)$$

$$-\frac{H}{U_w T_w} = G_h/G_w^2 = 0.80 Ri^{1/2} \frac{(1 + 450Ri^2)}{(1 + 250Ri^2)^{3/2}} \quad (25b)$$

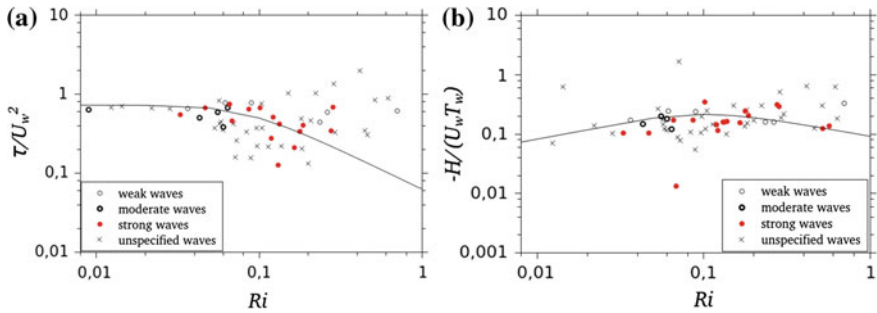


Fig. 8 A dependence of the dimensionless moments on the Richardson number Ri : **a** the momentum flux τ/U_w^2 , **b** the temperature flux $H/(U_w T_w)$, obtained from the BAO data (based on Sorbjan and Czerwinska 2013)

$$\frac{\sigma_\theta}{T_w} = G_\theta/G_w = 4.25Ri^{1/2} \frac{(1 + 450Ri^2)^{1/2}}{(1 + 2500Ri^2)^{1/2}} \quad (25c)$$

An analogous functions can be obtained for the σ_θ scaling (24) (Sorbjan 2010). The above expressions are valid throughout the entire stable boundary layer, and in the range $Ri < 0.7$.

A comparison of analytical (Eqs. 25a, 25b, 25c) and empirical values of the dimensionless momentum flux τ/U_w^2 and the temperature flux $H/(U_w T_w)$, as functions of the Richardson number Ri , is shown in Fig. 8. The figure shows some departures from the analytical similarity functions (25a, 25b, 25c)—derived during the SHEBA experiment; nonetheless, the overall dependency of dimensionless moments on the Richardson number is maintained.

4 Applications

In this section we will discuss two applications of the introduced approach. The first one deals with the realizability condition for the temperature flux in the stable boundary layer. The second one describes a single-column model, constructed based on the diagnostic closure scheme introduced in Sect. 2.1.

4.1 The Temperature-Flux Realizability Condition

It can be noted that the temperature flux H drops to zero in neutral condition, when $Ri \rightarrow 0$, and vanishes in very stable condition, when $Ri \rightarrow Ri_s$. This allows us to conclude that H , as a function of the Richardson number Ri , has an extremum at

some point in the range $(0, Ri_s)$. To investigate this notion, let us consider an alternative gradient-based scaling system of the following form (Sorbian 2013):

$$U_S = lS, \quad T_S = lS^2/\beta, \quad (26)$$

The above scales involve shear S , and therefore can be referred to as the “gradient-based S -scales”. It can be easily verified that

$$U_S = U_N Ri^{-1/2}, \quad T_S = T_N Ri^{-1} \quad (27)$$

Using (27), the expression (16b) can be rewritten as

$$-\frac{H}{U_S T_S} = Ri^{3/2} G_h = \frac{Ri}{0.9(1 + 250Ri^2)^{3/2}} \quad (28)$$

The above dimensionless function is plotted in Fig. 9a. The function has a minimum, where its first derivative with respect to Ri is zero. It can easily be verified that the minimum, equal to -0.027 , is reached at $Ri_{\min} = 0.0447$. Taking this result into consideration, we can obtain:

$$\frac{H_{\min}}{U_S T_S} = -0.027 \quad (29a)$$

$$H_{\min}(z) = -0.27 U_S T_S = -0.027 \frac{l^2(z) S^3(z)}{\beta} \quad (29b)$$

which constitutes the realizability condition for the temperature flux $H(z)$ at a specific level z . The inequality $0 > H(z) \geq H_{\min}(z)$ must be satisfied at any height z in the stable boundary layer.

An expression analogous to (29b) was derived by Van de Wiel et al. (2011), based on Monin-Obukhov similarity formulation in the surface layer. The authors obtained that the minimum of the temperature flux occurs at a larger value of $Ri_{\min} = 0.07$. According to Grachev (2012), the bin-averaged temperature flux, measured at five levels during SHEBA experiment show a similar minimum at the stability parameter z/L_* in the range 10^{-2} – 10^{-1} .

It could also be mentioned that by using (16d, 18b), and the definition of T_N in (10), the following expression for the standard deviation of temperature can be obtained:

$$\frac{\sigma_\theta}{\vartheta_*} = \frac{4.5}{(1 + 2500Ri^2)^{1/2}} \frac{(1 + 250Ri^2)^{3/2}}{(1 + 300Ri^2)^{3/4}}. \quad (30)$$

The above dimensionless function is plotted in Fig. 9b. The figure indicates that $\sigma_\theta/\vartheta_*$ is equal to 4.5 in nearly neutral conditions. At $Ri = 0.09$, it reaches a

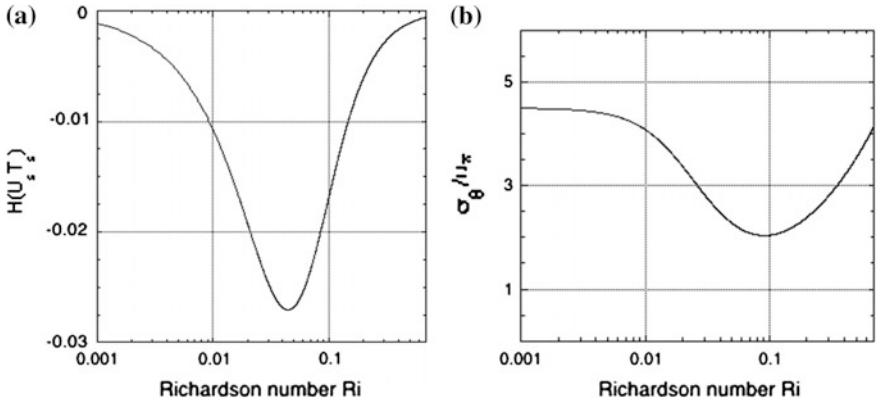


Fig. 9 The dimensionless: **a** the temperature flux $H/(U_s T_s)$, and **b** the temperature standard deviation $\sigma_\theta/\vartheta_*$ as functions of the Richardson number Ri in the stable boundary layer. Plots are based on Eqs. 28 and 30

minimum equal to 2, and increases to about 4 at $Ri = 0.7$. This result agrees with SHEBA data of Grachev et al. (2013, private communication), which show the minimum value reached in the range $0.1 < z/L_* < 1$, which is equivalent to $0.05 < Ri < 0.15$.

4.2 Single-Column Modeling

Let us consider a single-column model (SCM), defined by the following equations (Sorbjan 2013):

$$\frac{d\hat{X}}{dt} = \hat{F} + \frac{d}{dz} K_x \frac{d\hat{X}}{dz} \quad (31)$$

where $\hat{X} = \{U, V, \Theta\}^T$ is the vector of unknown variables (i.e. two components of the wind velocity and the potential temperature), $\hat{F} = \{fV, -f(U-G), 0\}^T$ is the applied dynamic forcing (due to the Coriolis force and the pressure gradient force), G is the geostrophic wind, f is the Coriolis parameter, and $K_x = K_m$ or K_h , and the letter T indicates the transpose of a vector.

The turbulence closure of the model is diagnostic, based on the K-theory approach (1a, 1b), (17a, 17b), with a semi-empirical form of the mixing length (3c). As a result, the model results, expressed in terms of local similarity scales, exactly satisfy the similarity expressions (16a)–(16b), (18a)–(18b) in the entire SBL, at any level and any moment of time. The model employs one internal, governing stability parameter—the Richardson number Ri , which dynamically adjusts to the boundary conditions and to the external forcing.

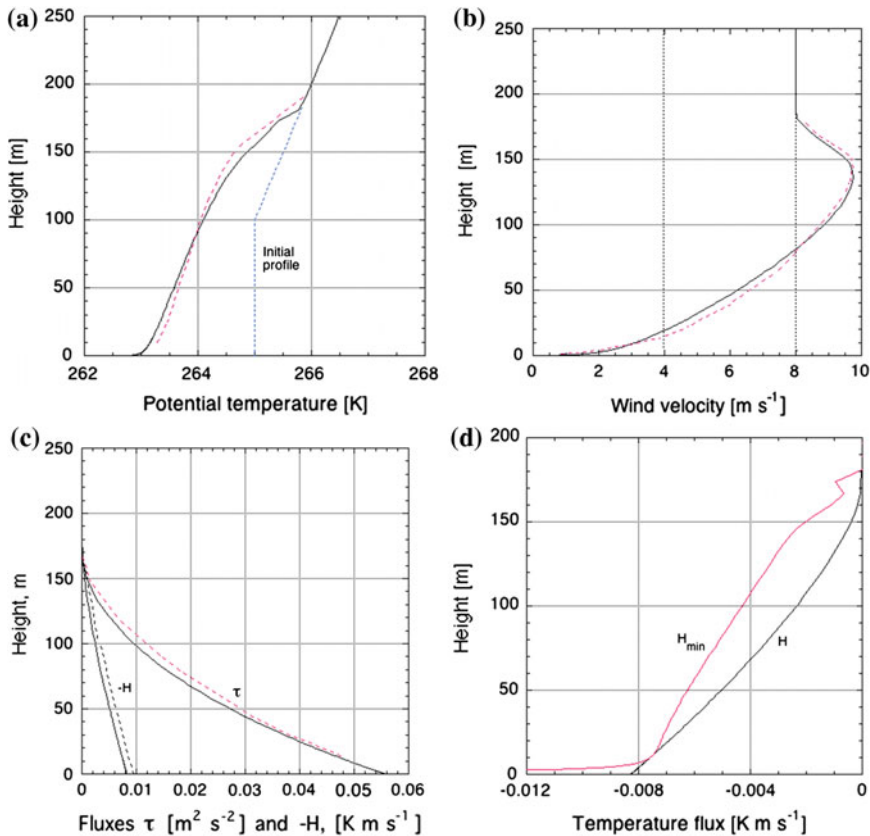


Fig. 10 Results of the single-column model, obtained in the 9 h basic run: **a** the potential temperature, **b** the wind velocity modulus, **c** the (negative) heat flux $-H$, and the modulus of the momentum flux τ , **d** the actual temperature flux H and the minimum allowable flux H_{\min} (red line, see Eqs. 29a, 29b) as a function of height. Note that $H = H_{\min}$ at $z = 11$ m, and at $z = 180$ m. Profiles obtained in the University of Hannover large-eddy simulations (Raasch and Etling 1991; Raasch and Schröter 2001) are indicated by red dashed lines (based on Sorbjan 2013)

The resulting vertical profiles of the potential temperature, wind velocity, and turbulent fluxes, obtained from the basic 9 h run of such a model, are shown in Fig. 10a–c. They were evaluated for the initial condition defined as a neutrally stratified layer with a potential temperature $\Theta_0 = 265$ K, extending up to 100 m. Above the 100 m layer, the potential temperature increased at the gradient $\gamma = 0.01 \text{ Km}^{-1}$. The x -axis of the coordinate system was aligned with the geostrophic wind vector, G was set to 8 ms^{-1} , the Coriolis parameter was $f = 1.39 \times 10^{-4} \text{ s}^{-1}$, which corresponds to latitude 73°N , and the roughness parameter is $z_o = 0.1$ m. A prescribed surface cooling rate of $C_R = 0.25 \text{ Kh}^{-1}$ was applied for 9 h.

The resulting potential temperature after 9 h basic SCM run is depicted in Fig. 10a together with the initial condition. The local wind maximum (low level jet) in Fig. 1b is about 9.5 ms^{-1} , and takes place at the altitude of about 140 m. Both turbulent fluxes, $-H$ and τ , decrease with height (in Fig. 10c), and reach relatively small values at levels above 150 m.

Results from high-resolution large-eddy simulations, performed at the University of Hannover (Raasch and Etling 1991; Raasch and Schröter 2001), are also presented in Fig. 10a–c. The LES and the SCM runs were performed for analogous initial conditions and forcing. The SCM results are presented as solid lines in the figure. They closely agree with the LES results, which are represented by dashed red lines. This fact can be treated as indirect prove that the gradient-based similarity scales based on (3c), and that the introduced similarity functions of the Richardson number, are valid in the entire stable boundary layer.

In Fig. 10d, the actual heat flux H and the minimum permissible heat flux H_{\min} are plotted as functions of height. Values of both functions, H and H_{\min} , are equal at $z = 11 \text{ m}$. Below and above this level, the actual heat flux is larger than the permissible one. At the top of the stable boundary layer, both values are equal to zero.

5 Final Remarks

Properties of the stably stratified boundary layer were examined by using the gradient-based similarity theory. The approach introduces similarity scales based on gradients of the potential temperature (or wind velocity components). The empirical similarity functions of the Richardson number Ri , for fluxes and variances as well as other characteristics of turbulence, were evaluated in the surface layer, based on tower data collected during the SHEBA field program. Subsequently, they were examined in the lower part of the stable boundary layer using data collected during the CASES-99 experiment.

The gradient-based similarity scales, built on the explicit, semi-empirical form of the mixing length, were found to be effective in the entire stable boundary layer. In more complex cases, however, alternative formulation of the mixing length, based on vertical velocity or temperature variances, is recommended.

The introduced similarity approach allows evaluating the minimum values of the dimensionless turbulent temperature flux and the standard deviation of temperature in the stable conditions, as functions of the Richardson number. It can also be used as a closure scheme for a single-column model. A comparison of such a single-column model with a large-eddy simulation modelled showed a very close agreement.

Acknowledgments The work has been supported by the US National Science Foundation grant ATM-0938293, and by the Polish National Science Centre grant 0572/B/P01/2011/40.

References

- Abarbanel HD, Holm DD, Madsen JE, Ratiu T (1984) Richardson number criterion for the nonlinear stability of three-dimensional stratified flow. *Phys Rev Lett* 52:2352–2355
- Anderson PS (2009) Measurement of Prandtl number as function of Richardson number avoiding self-correlation. *Boundary-Layer Meteorol* 131:345–362
- Andreas EL, Hill RJ, Gosz JR, Moore DI, Otto WD, Sarma AD (1998) Statistics of surface-layer turbulence over terrain with metre-scale heterogeneity. *Boundary-Layer Meteorol* 86:379–408
- Andreas EL, Fairall CW, Guest PS, Persson POG (1999) An overview of the SHEBA atmospheric surface flux program. In: 13th symposium on boundary layers and turbulence. American Meteorological Society, Proceedings, Dallas, TX, pp 550–555
- Andreas EL, Fairall CW, Grachev AA, Guest PS, Horst TW, Jordan RE, and Persson POG (2003) Turbulent transfer coefficients and roughness lengths over sea ice: the SHEBA results. In: Seventh conference on polar meteorology and oceanography and joint symposium on high-latitude climate variations, American Meteorological Society. 12–16 May 2003, Hyannis, Massachusetts, AMS Preprint CD-ROM
- Andreas EL, Claffey KJ, Jordan RE, Fairall CW, Guest PS, Persson POG, Grachev AA (2006) Evaluations of the von Kármán Constant in the Atmospheric Surface Layer. *J Fluid Mech* 559:117–149
- Baas P, Steeneveld GJ, van de Wiel BJH, Holtslag AAM (2006) Exploring self-correlation in flux-gradient relationships for stably stratified conditions. *J Atmos Sci* 63:3045–3054
- Banta RM (2008) Stable-boundary-layer regimes from the perspective of the low-level jet. *Acta Geophys* 56:58–87
- Barenblatt GI (1996) Scaling, self-similarity laws, and intermediate asymptotes. In: Cambridge Texts in Applied Mathematics, vol 14. Cambridge University Press, Cambridge, p 380
- Beljaars ACM, Holtslag AAM (1991) Flux parameterization over land surfaces for atmospheric models. *J Appl Meteor* 30:327–341
- Blackadar AK (1962) The vertical distribution of wind and turbulent exchange in neutral atmosphere. *J Geoph Res* 67:3095–3103
- Businger JA (1973) Turbulent transfer in the atmospheric surface layer, Chapter 2. In: Haugen DA (ed) Workshop on Micrometeorology. American Meteorological Society, Boston, pp 67–100
- Businger JA, Miyake M, Dyer AJ, Bradley F (1967) On the direct determination of the turbulent heat flux near the ground. *J Appl Meteor* 6:1025–1032
- Cheng Y, Canuto VM, Howard AM (2002) An improved model for the turbulent PBL. *J Atmos Sci* 59:1550–1565
- Churchill SW (2002) A reinterpretation of the turbulent Prandtl number. *Ind Eng Chem Res* 41:6393–6401
- Coulter RL, Doran JC (2002) Spatial and temporal occurrences of intermittent turbulence during CASES-99. *Boundary-Layer Meteorol* 105:329–349
- Cuxart J (2008) Nocturnal basin low-level jets: an integrated study. *Acta Geophys* 56:100–113
- Delage Y (1974) A numerical study of the nocturnal atmospheric boundary layer. *Quart J Roy Meteorol Soc* 100:351–364
- Esau I, Grachev A (2007) Turbulent Prandtl number in stably stratified atmospheric boundary layer: intercomparison between LES and SHEBA data. *e-WindEng*, 006: 01–17
- Fernando HJS (2003) Turbulent patches in stratified shear flow. *Phys Fluids* 15:3164–3169
- Galperin B, Sukoriansky S, Anderson PS (2007) On the critical Richardson number in stably stratified turbulence, *Atmos Sci Letters ASL.153*
- Grachev AA, Fairall CW, Persson POG, Andreas EL, Guest PS (2005) Stable boundary-layer scaling regimes: the SHEBA data. *Boundary-Layer Meteorol* 116:201–235
- Grachev AA, Andreas EL, Fairall CW, Guest PS, Persson POG (2007a) SHEBA Flux profile relationships in the stable atmospheric boundary layer'. *Boundary-Layer Meteorol* 124:315–333

- Grachev AA, Andreas EL, Fairall CW, Guest PS, Persson POG (2007b) On the turbulent Prandtl Number in the Stable Atmospheric Boundary Layer. *Boundary-Layer Meteorol* 125:329–341
- Grachev AA, Andreas EL, Fairall CW, Guest PS, Persson POG (2008) Turbulent measurements in the stable atmospheric boundary layer during SHEBA: ten years after. *Acta Geophys* 56:142–166
- Grachev AA (2012) Private communication
- Grachev AA, Andreas EL, Fairall CW, Guest PS, Persson OG (2013) The critical richardson number and limits of applicability of local similarity theory in the stable boundary layer. *Boundary-Layer Meteorol* 147(1):51–82
- Holtslag AAM and De Bruin FTM (1988) Applied modeling of night-time surface energy balance over land. *J Appl Meteor* 27:689–704
- Huang J, Bou-Zeid E, Golaz JC (2013) Turbulence and vertical fluxes in the stable boundary layer. Part II: a novel mixing-length model. *J Atmos Sci* 111:793–815
- Hunt JCR, Kaimal JC, Gaynor JE (1985) Some observations of turbulence structure in stable layers. *Quart J Roy Meteorol Soc* 130:2087–2103
- Kader BA, Yaglom AM (1990) Mean fields and fluctuation moments in unstably stratified turbulent boundary layers. *J Fluid Mech* 212:637–662
- Klipp CL, Mahrt L (2004) Flux-gradient relationship, self-correlation and intermittency in the stable boundary layer. *Quart J Roy Meteorol Soc* 130:2087–2103
- Kukharets VP, Tsvang LR (1998) Atmospheric turbulence characteristics over a temperature-inhomogeneous land surface. Part I: statistical characteristics of small-scale spatial inhomogeneities of land surface temperature. *Boundary-Layer Meteorol* 86:89–101
- Mahrt L (1998) Stratified atmospheric boundary layers. *Boundary-Layer Meteorol* 90:375–396
- Mahrt L (1999) Stratified atmospheric boundary layers. *Boundary-Layer Meteorol* 90:375–396
- Monin AS, Obukhov AM (1954) Basic laws of turbulence mixing in the surface layer of the atmosphere. *Trudy Geof Inst AN SSSR* 24:163–187
- Newsom KR, Banta RM (2003) Shear-flow instability in the stable nocturnal boundary layer as observed by Doppler lidar during CASES-99. *J Atmos Sci* 60:16–33
- Nieuwstadt FTM (1984) The turbulent structure of the stable, nocturnal boundary layer. *J Atmos Sci* 41:2202–2216
- Oyha YD, Neff E, Meroney EN (1997) Turbulence structure in a stratified boundary layer under stable conditions. *Boundary-Layer Meteorol* 83:139–161
- Oyha YD (2001) Wind tunnel study of atmospheric stable boundary layers over a rough surface. *Boundary-Layer Meteorol* 98:57–82
- Persson POG, Fairall CW, Andreas EL, Guest PS, Perovich DK (2002) Measurements near the atmospheric surface flux group tower at SHEBA: near-surface conditions and surface energy budget. *J Geophys Res* 107: 8045, doi: [10.1029/2000JC000705](https://doi.org/10.1029/2000JC000705)
- Prandtl L (1932) Meteorologische anwendungen der stromungslehre. *Beitr Phys Atmosph* 19:188–202
- Raasch S, Etling D (1991) Numerical simulations of rotating turbulent thermal convection. *Beitr Phys Atmos* 64:185–199
- Raasch S, Schröter M (2001) PALM: a large-eddy simulation model performing on massively parallel computers. *Meteor Z* 10:363–372
- Sorbjan Z (1986a) On similarity in the atmospheric boundary layer. *Boundary-Layer Meteorol* 34:377–397
- Sorbjan Z (1986b) On the vertical distribution of passive species in the atmospheric boundary layer. *Boundary-Layer Meteorol* 35:73–81
- Sorbjan Z (1986c) Local similarity of spectral and cospectral characteristics in the stable-continuous boundary layer. *Boundary-Layer Meteorol* 35:257–275
- Sorbjan Z (1988) Structure of the stably-stratified boundary layer during the Sesame-1979 experiment. *Boundary-Layer Meteorol* 44:255–260
- Sorbjan Z (1989) Structure of the atmospheric boundary layer. Prentice-Hall, New Jersey, p 316
- Sorbjan Z (2006a) Local structure of turbulence in stably-stratified boundary layers. *J Atmos Sci* 63:526–537

- Sorbian Z (2006b) Comments on “Flux-gradient relationship, self-correlation and intermittency in the stable boundary layer”. *Q J Roy Meteorol Soc B* 617(132):1371–1373
- Sorbian Z, Balsley BB (2008) Microstructure of turbulence in the nocturnal boundary layer. *Boundary-Layer Meteorol* 129:191–210
- Sorbian Z (2010) Gradient-based scales and similarity laws in the stable boundary layer. *Quart J Roy Meteorol Soc* 136:1243–1254
- Sorbian Z, Grachev AA (2010) An evaluation of the flux-gradient relationship in the stable boundary layer. *Boundary-Layer Meteorol* 135:385–405
- Sorbian Z (2012a) The height correction of similarity functions in the stable boundary layer. *Boundary-Layer Meteorol* 142:21–31
- Sorbian Z (2012b) A study of the stable boundary layer based on a single-column K-theory model. *Boundary-Layer Meteorol* 142:33–53
- Sorbian Z, Czerwinska A (2013) Statistics of turbulence in the stable boundary layer affected by gravity waves. *Boundary-Layer Meteorol* 148(1):73–91
- Sorbian Z (2013) Modelling of the evolving stable boundary layer. *Boundary-Layer Meteorol* DOI [10.1007/s10546-013-9893-z](https://doi.org/10.1007/s10546-013-9893-z)
- Sullivan PP (2014) Structures, temperature fronts, and intermittent behavior in stable boundary layers. In: 21st Symposium on boundary layers and turbulence, 9–13 Jun 2014, Leeds, United Kingdom
- Tsvang LR, Kukharets VP, Perepelkin VG (1998) Atmospheric turbulence characteristics over a temperature-inhomogeneous Land Surface Part II: the effect of small-scale inhomogeneities of surface temperature on some characteristics of the atmospheric surface layer. *Boundary-Layer Meteorol* 86:103–124
- Van de Wiel BJH, Moene A, Hartogenesis G, De Bruin HA, Holtslag AAM (2003) Intermittent turbulence in the stable boundary layer over land. Part III. A classification for observations during CASES-99. *J Atmos Sci* 60:2509–2522
- Van de Wiel BJH, Basu S, Moene AF, Jonker HJJ, Steenveld GJ, Baas P, Holtslag AAM (2011) Comments on “An extremum solution of the Monin-Obukhov similarity equations”. *J. Atmos Sci* 68:1405–1408
- Vickers D, Mahrt L (2003) The cospectral gap and turbulent flux calculations. *J Atmos Ocean Technol* 20:660–672
- Vickers D, Mahrt L (2006) A solution for flux contamination by mesoscale motions with very weak turbulence. *Boundary-Layer Meteorol* 111:431–447
- Yagüe C, Viana S, Maqueda G, Redondo JM (2006) Influence of stability on the flux-profile relationships for wind speed, φ_m , and temperature, φ_h , for the stable atmospheric boundary layer. *Nonlin Processes Geophys* 13:185–203
- Zilitinkevich S, Elperin T, Kleorin N, Rogachevkii I, Esau I, Mauritzen T, Miles M (2008) Turbulence energetics in stably stratified geophysical flows: strong and weak mixing regimes. *Quart J Roy Meteorol Soc* 134:793–799

Asymmetric Continuum Theory: Fracture Processes in Seismology and Extreme Fluid Dynamics

Roman Teisseyre

Abstract A new joint approach to deformations and motions in solids and fluids is presented. For the theory of solids, in addition to the shear and rotation strains, we define the molecular transport, while for fluids we consider the transport motions and the shear and rotation molecular strains. In this way we arrive at a common asymmetric theory for solids and fluids. Thus, for solids we present the release-rebound relations and related wave equations for strains, while for fluids we present the Navier-Stokes transport relations; moreover, for solids the included molecular transport and for fluids the molecular rotation and shear strains are considered additionally. The molecular transport in solids helps us to understand the fracture preparation processes. Of course, to each of these continua we include an influence of pressure; thus, in fluids we have both the pressure and its time derivative, that is, the molecular pressure related to sound phenomena.

Keywords Shear and rotation strains · Molecular rotation and shear strains · Transport motion · Molecular transport

1 Introduction

We make an attempt to present a common basis for describing motions in solids and fluids. For fluids, we are dealing with the Navier-Stokes relations for transport motions and include an influence of the molecular strains, while for solids we use here relations for the antisymmetric strains (we add rotation strains as explained further on) and the molecular transport motions. This approach makes it possible to explain, among other things, the strain propagation, as shown in Fig. 1, and the

R. Teisseyre (✉)

Institute of Geophysics, Polish Academy of Sciences, ul. Ksiegia Janusza 64,
01-452 Warsaw, Poland
e-mail: rt@igf.edu.pl

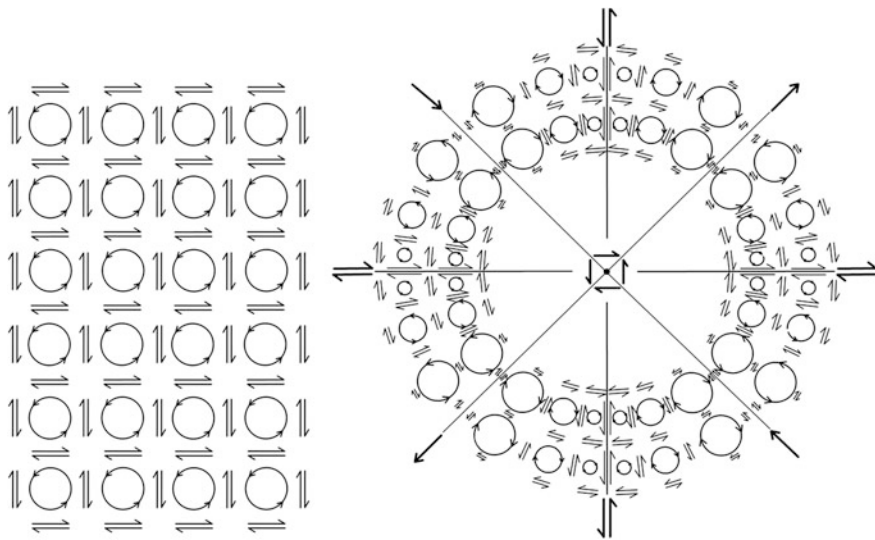


Fig. 1 Sketch of linear parallel and radial wave propagation as combined due to the mutual interaction of shear and rotation strains

formation of a fracture process in solids; for fluids, the molecular strains help to introduce, among other things, the asymmetric fluid viscous stress tensor. Without such a mutually combined system it is difficult to understand the related propagation motions.

The recording of seismic waves, even very long, means that in fact we record the deformation, $D_{ik} = \partial u_k / \partial x_i$, which becomes integrated during the adequate time by a seismometer to reveal the displacement motion ($u_k = \int \sum (\partial u_k / \partial x_i) \Delta x_i dt$;

where Δx means a rigid element of seismometer's platform); this displacement means an abstract element, a potential function, while a real displacement reveals itself only in a fracture process (its description might be done only outside of the continuum theory).

Our global seismological network is solely based on recordings of displacements by a system of seismometers; to trace and watch any strain changes in a global scale we would need a global network of shear and rotation strains. However, we should admit that in some separate seismically active regions a local system of strain-meters, even somewhere including rotation strain deformations, does already exist.

However, our new theoretical approach helps us also to describe some preparation processes leading to the fracturing; such a concise theory allows to describe the independent and correlated fracture release-rebound processes in an expected source region and to analyze the correlations between some recorded seismic waves.

We should underline that in fracture release processes the strain deformations, axial, shear and rotational (rotation strains), may appear independently; thus, instead of analyzing the displacement motions on the basis of the world-wide seismic network only, it is necessary to record the strain and rotation strain waves as well. We should keep in mind that only a new global system based directly on the strain-meters and rotation devices might reveal these independent strain motions; a local recording system of this kind already exists only in very few seismic regions. Therefore, it is necessary to express an urgent need for such a new complex world-wide seismic system, especially the one that would record the strain waves and also the very long global molecular displacements.

We may note that in the frame of Asymmetric Continuum Theory it may be possible to describe all release-rebound motions and deformations appearing in an expected earthquake source, and properly interpret these deformations and motions from the data obtained from the proper recording devices which should be included in a desired world-network. Especially important for earthquake risk studies is a possibility to trace the slow changes appearing in the global strain system.

The Asymmetric Theory includes the rotation strain motions. Many attempts have been made in the past to improve the classic elasticity. Since the end of the nineteenth century, there were many trials to construct a more adequate and powerful theory of continua. The first attempt to include rotations into the theory is due to Voigt in 1887. A complete theory, with the displacement vector and rotation vector, was proposed by the Cosserat brothers in 1896 (see Cosserat and Cosserat 1909). A powerful approach has been provided by the elastic micropolar and micromorphic theories developed by Eringen and his co-workers (see, e.g., Eringen and Suhubi 1964; Mindlin 1965, as well as two important monographs: Eringen 1999, 2001).

Another approach to generalize the classic theory is due to Kröner's papers, in which an elastic field is given as a difference between the total fields and the self-fields representing a continuous distribution of internal nuclei (e.g., Kröner 1981).

The main problems related with the classical theories are as follows:

- In the classical elastic theory, the balance of angular momentum holds only for the symmetric stresses, while the angular motions can be only introduced in an artificial way with the help of a characteristic length element and the reference points.
- Fracture pattern reveals usually an asymmetric pattern with the main slip plane with the granulation and fragmentation processes which include the rotation motions.
- Searching for the fault-slip solutions we should use the friction constitutive laws introduced additionally as the elastodynamic solutions for slip propagation and friction effects.
- Geometry of earthquake fracture and premonitory processes usually reveals an asymmetric pattern.

- Any solution for an edge dislocation presents asymmetry in the strain components in the plane perpendicular to the dislocation line (wedge line).
- Any continuous distribution of dislocations leads to confrontation between the symmetry of shear strains and asymmetry of stresses.

The Asymmetric Continuum Theory for solids (Teisseyre 2008a, b, 2009, 2011) has been constructed to avoid these numerous insufficiencies of the classic symmetric theory and to explain some phenomena found by seismological observations. Similar considerations can be presented for fluids; the molecular strains produce symmetric and anti-symmetric molecular deformations (Teisseyre 2009).

Let us recall again some attempts for improving the classical elasticity, namely

- The Cosserat brothers' theory of elasticity (Cosserat and Cosserat 1909), which included the displacements and rotations;
- The micropolar and micromorphic elastic theories (cf., Eringen and Suhubi 1964; Mindlin 1965; Nowacki 1986; for an advanced review, see Eringen 1999, 2001).

The micropolar and micromorphic theories present a very powerful tool for describing the complicated problems (see, e.g., Teisseyre 1973, 1974). However, these theories are very complicated and their use in common seismological studies requires that we know many additional material constants.

A similar approach can be made for fluids; the molecular strains may present the symmetric and anti-symmetric molecular deformations (Teisseyre 2009). We will meet there additional complications when considering the non-laminar and turbulent motions; moreover, the density variation in gases will be of great importance. The first trials in these directions have already been undertaken in the frame of micropolar and micromorphic theories (Eringen 2001; see also Teisseyre 1973, 1974).

Finally we should remember that the records of rotation motions have been obtained by means of the Sagnac measurement system at the end of last century (cf., Lee et al. 2009). We may also mention the discovered wave groups correlated with rotational oscillations (Teisseyre 2007).

Another very important feature of rotation strain deformations, $E_{\varphi\varphi}$ (angular squeeze in the horizontal plane) has been discovered in strain measurement related to earthquake events by Gomberg and Agnew (1996). In these authors' original opinion, related to the classic elastic theory, this squeeze angular strain, $E_{\varphi\varphi}$, should be estimated from the solution for the displacement potentials. These authors, using the scalar and vector potentials, Φ and Ψ , considered the asymptotic solution for the cylindrical waves excited by an earthquake source (m and k are constants):

$$(\Phi, \Psi) \rightarrow f(r, \varphi, t) = AJ_m(k, r) \exp[i(m\varphi - \varpi t)]$$

$$\text{for } m = 0 \quad (\Phi, \Psi) \approx A \sqrt{\frac{2}{\pi kr}} \exp\left[i(kr - \varpi t - \frac{\pi}{4})\right] \quad (1)$$

We can assume that the induced shears and fragmentation depend on the applied load and defect content. Such induced angular squeeze, $E_{\varphi\varphi}$, can be related to the applied axial stresses due to the defect co-action:

$$\sum S_{ss} = \varepsilon E_{\varphi\varphi} \quad (2)$$

where we insert a new constant, ε , which may relate to the unknown angular squeeze material properties and to a specific angular squeeze structure.

Note a difference between the component $E_{\varphi\varphi}$ and the E_{rr} , E_{zz} ones; the latter components represent typical compression strains, while $E_{\varphi\varphi}$ represents a circular squeeze which seems to fit to the local fragmentation in circular-shape processes under a high confining load. For processes in which a constant load is applied, $E_{rr} + E_{zz}$, we arrive at (cf., Udiás 2002):

$$\mu \left(\frac{\partial}{r \partial r} \left(\frac{r \partial}{\partial r} \right) + \frac{\partial^2}{r^2 \partial \psi^2} + \frac{\partial^2}{\partial z^2} \right) E_{\varphi\varphi} - \rho \frac{\partial^2}{\partial t^2} E_{\varphi\varphi} = \left(\frac{\mu}{\lambda + 2\mu} \right)^{1/2} \frac{\partial F_\varphi}{r \partial \psi} \quad (3a)$$

where $\psi = \varphi \left(\frac{\mu}{\lambda + 2\mu} \right)^{1/2}$ and F is the force.

An asymptotic expression for the angular squeeze strain (Gomberg and Agnew 1996) decays rapidly with distance:

$$E_{\varphi\varphi} \approx \frac{u_r}{r} + i \frac{u_\varphi}{r} \quad (3b)$$

These authors wanted to explain the experimentally discovered angular squeeze strains discovered by the systematic squeeze measurements; however, the obtained theoretical result forced them to assume that these experimentally discovered angular squeeze strains appear only as some local distortions of the strain fields; they formulated this statement in spite of the fact that for all analysed events the obtained $E_{\varphi\varphi}$ values have been estimated as significant.

The presented strange and controversial results may be explained when using the relations valid in the Asymmetric Continuum Theory. In this case, instead of the solution (3b) we arrive at the Bessel wave solution for this angular term:

$$E_{\varphi\varphi} = AJ_m(kr) \exp[i(k_z z + m\psi - \varpi t)]; \quad \psi = \varphi \left(\frac{\mu}{\lambda + 2\mu} \right)^{1/2} \quad (4a)$$

The asymptotic expression can be given by an expansion of the Bessel functions:

$$\begin{aligned} E_{\varphi\varphi} \alpha \sqrt{\frac{2}{\pi k_r r}} \exp[i(k_r r + k_z z + m\psi - \varpi t - \pi/4)] \\ \approx \sqrt{\frac{2}{\pi k_r r}} \exp\left[i\left(k_r r + k_z z + \frac{m\varphi}{\sqrt{3}} - \varpi t - \pi/4\right)\right] \end{aligned} \quad (4b)$$

In this solution, the angular squeeze decays with r quite differently than for the former solution (3b) related to the classic theory and we arrive at much greater effects which do not decay rapidly. The observed significant deformations, $E_{\varphi\varphi}$, present an agreement between observations and Asymmetric Theory. We repeat that the angular squeeze strains considered by Gomberg and Agnew (1996) were recorded as significant for all the events they analyzed; their experimental discovery is extremely important. Finally, we may quote some other direct observations of the rotation strain propagation, see, e.g., Teisseyre KP (2007), Schreiber et al. (2009), Lee et al. (2009) and Zembaty (2009).

2 Solids: Basic Relations

The motion equation for deformation, $D_{ni} = \frac{\partial u_i}{\partial x_n}$, follows from the derivatives of the classic Newton formula:

$$\begin{aligned} \mu \sum_s \frac{\partial^2 u_i}{\partial x_s \partial x_s} - \rho \frac{\partial^2 u_i}{\partial t^2} + (\lambda + \mu) \frac{\partial}{\partial x_i} \sum_s \frac{\partial u_s}{\partial x_s} = 0; \\ D_{ni} = \frac{\partial u_i}{\partial x_n}, \quad E_{(ni)} = \frac{1}{2} \left(\frac{\partial u_i}{\partial x_n} + \frac{\partial u_n}{\partial x_i} \right), \quad E_{[ni]} = \frac{1}{2} \left(\frac{\partial u_i}{\partial x_n} - \frac{\partial u_n}{\partial x_i} \right) \end{aligned} \quad (5a)$$

where the displacements may be considered only as the potential reference fields, \bar{u}_s , \hat{u}_s , \check{u}_s , as follows:

$$\begin{aligned} \bar{E} = \frac{1}{3} \sum_s E_{ss} = \frac{1}{3} \sum_s \frac{\partial \bar{u}_s}{\partial x_s} &- \text{ total axial strain} \\ E_{(ik)}^D = E_{(ik)} - \delta_{ik} \frac{1}{3} \sum_{s=1}^3 E_{(ss)} &= \frac{1}{2} \left(\frac{\partial \hat{u}_k}{\partial x_i} + \frac{\partial \hat{u}_i}{\partial x_k} \right) - \delta_{ik} \frac{1}{3} \sum_{s=1}^3 \frac{\partial \hat{u}_s}{\partial x_s} &- \text{ deviatoric shears} \\ E_{[ik]} &= \frac{1}{2} \left(\frac{\partial \check{u}_k}{\partial x_i} - \frac{\partial \check{u}_i}{\partial x_k} \right) - \text{ rotation strain} \end{aligned} \quad (5b)$$

where some inter-relations between the reference displacements written above may be related to the joint processes in a source; in general, the relation to common, phase shifted or independent displacements may be expressed as:

$$\bar{u}_s = \xi^0 u_s, \hat{u}_s = e^0 u_s, \check{u}_s = \chi^0 u'_s; \quad \{\xi^0, e^0, \chi^0\} = \{0, \pm 1, \pm i\} \quad (5c)$$

Accordingly, for symmetric and anti-symmetric strains we obtain:

$$\begin{aligned} \mu \sum_s \frac{\partial^2}{\partial x_s \partial x_s} E_{(nl)} - \rho \frac{\partial^2}{\partial t^2} E_{(nl)} &= -(\lambda + \mu) \frac{\partial^2}{\partial x_n \partial x_l} \sum_s E_{(ss)}; \\ E_{(nl)} &= \frac{1}{2} \left(\frac{\partial u_l}{\partial x_n} + \frac{\partial u_n}{\partial x_l} \right) \end{aligned} \quad (6a)$$

$$\mu \sum_s \frac{\partial^2}{\partial x_s \partial x_s} E_{[nl]} - \rho \frac{\partial^2}{\partial t^2} E_{[nl]} = 0; \quad E_{[nl]} = \frac{1}{2} \left(\frac{\partial \bar{u}_l}{\partial x_n} - \frac{\partial \bar{u}_n}{\partial x_l} \right) \quad (6b)$$

where in all these formulae we may use the different reference displacement motions as explained above (see Eqs. 5a–5c); we have also omitted the external forces.

For the constitutive relations joining stresses and strains we choose the simplest relations for the axial, deviatoric and rotation stresses:

$$\begin{aligned} S_{kl} &= S_{(kl)} + S_{[kl]} = \delta_{kl} \bar{S} + S_{(kl)}^D + S_{[kl]}; \\ \bar{S} &= \frac{1}{3} \sum_{s=1}^3 S_{(ss)}, \quad S_{(ik)}^D = S_{(ik)} - \delta_{ik} \frac{1}{3} \sum_{s=1}^3 S_{(ss)} \end{aligned} \quad (7a)$$

and we get:

$$S_{(ik)} = 2\mu E_{(ik)} + \lambda \delta_{ik} E_{(ss)}; \quad S_{[ik]} = 2\mu E_{[ik]} \quad (7b)$$

$$\bar{S} = (2\mu + 3\lambda \delta_{ik}) \bar{E}; \quad S_{(ik)}^D = 2\mu E_{(ik)}^D; \quad S_{[ik]} = 2\mu E_{[ik]} \quad (7c)$$

Note that the fracture source processes could run according to the release-rebound processes, similarly to the propagation pattern (cf., Teisseyre 1980, 1985, 2009, 2011).

For constant total axial stresses, the release-rebound system may be described by the linear relations between the time and space derivatives; these unique relations are similar to the Maxwell-like ones. In the special coordinate system, the deviatoric strains can be represented by the off-diagonal tensor,

$$E_{(ik)} - \delta_{ik} \frac{1}{3} \sum_{s=1}^3 E_{(ss)} \rightarrow E_{(k)} = \begin{bmatrix} 0 & E_{(12)} & E_{(13)} \\ E_{(12)} & 0 & E_{(23)} \\ E_{(13)} & E_{(23)} & 0 \end{bmatrix} \quad (8)$$

In this system, the shear vector can be defined as follows:

$$E_{(k)} = \{E_{(23)}, E_{(31)}, E_{(12)}\} \quad (9a)$$

and we can always define the rotation vector:

$$E_{[k]} = \{E_{[23]}, E_{[31]}, E_{[12]}\} \quad (9b)$$

The strain rotation vector is invariant, but the shear vector is not; however, we may mention that using the 4D approach the shear vector \hat{E}_i could be also defined invariantly with the help of invariant Dirac tensors (cf., Teisseyre 2009).

The release-rebound process may mean a break of some bonds on a molecular level—a release of rotation field, $\partial E_{[]} / \partial t$, and then, in a rebound motion, there will appear the rotation of shears, $\text{rot } E_{()}$. Reversely, a release of shear field, $\partial E_{()} / \partial t$, causes the rebound change of the rotation strains, $\text{rot } E_{[]}$. Such a process may be also valid for source processes; a shear strain may cause a slip motion at the source, then a rotation strain appears and these source processes lead to a wave propagation process. These release-rebound processes are adequately described by the Maxwell-like relations (Teisseyre 2009, 2011):

$$\text{rot } E_{[]} - \frac{\kappa \partial E_{()}}{c \partial t} = 0, \quad \text{rot } E_{()} + \frac{\kappa \partial E_{[]}}{c \partial t} = 0; \quad \frac{c}{\kappa} = V = V^S = \sqrt{\frac{\mu}{\rho}} \quad (10)$$

where κ is an adequate material parameter depending, first of all, on pressure, and c is the light velocity; here $E_{()}$ means shear strain and $E_{[]}$, the rotation strain.

From these relations we may obtain the wave equations which coincide with the previously derived formulae (6a) and (6b).

When the pressure remains constant ($S = (2\mu + 3\lambda\delta_{ik})\bar{E} = \text{const}$) we obtain the pure wave relations for rotation and shear fields, which, de facto, are mutually correlated, as shown in the previous equation:

$$\Delta E_{()} - \frac{\partial^2 E_{()}}{V^2 \partial t^2} = 0 \quad \text{and} \quad \Delta E_{[]} - \frac{\partial^2 E_{[]}}{V^2 \partial t^2} = 0 \quad (11)$$

The related wave mosaic (Teisseyre and Gorski 2011) explains the interrelated propagation pattern of the shear and rotation motions, as presented in Fig. 1 and described equivalently by Eq. (10) or (11).

The release-rebound relation has a universal character; it could describe both the propagation system (e.g., shear and rotation strains waves), but also some local events (e.g., fracture processes). Such a universal character of the release-rebound mechanism permits us to use it also for the sub-molecular processes with an adequate parameter related to the local material responses to shear-rotation time changes.

We will return to the problems of fracture preparation processes at a seismic or any other source in the final considerations.

3 Solids: Induced Strains

Further on, we may consider relations between the asymmetric stresses and dislocation fields and the formation of defect arrays. Local stresses formed due to the dislocation arrays might significantly reorganize the applied loads. The presented theory of induced stresses is formulated basing on the Peach-Koehler definition of forces acting on dislocations (Peach and Koehler 1950). We should underline that the action of induced stresses is particularly significant for a confining stress load; the extreme confining load usually leads to the shear and fragmentation (rotational) fractures, being caused de facto by the induced strains.

At a very high concentration of defects, e.g., in a seismic zone, there are formed arrays of linear defects leading to concentration of an applied external stress field (Eshelby et al. 1951); at the top of such an array we will have concentration of the applied field, S^{Top} , which might lead to a crack (Teisseyre 1980, 1985):

$$S^{Top} = nS \quad (12)$$

On such dislocations (defect lines), there are exerted the Peach-Koehler forces (Peach and Koehler 1950)

$$F_n = \varepsilon_{nsq} \sum_k S_{sk} b_k v_q \quad (13)$$

where S_{sk} means the applied stress field, b_k is a dislocation slip vector, v_q is a dislocation line versor and ε_{nsq} the fully asymmetric tensor $(1, -1, 0)$.

Such defect concentration might lead to the formation of a crack; two cracks could join each other to form a bigger crack; the opposite edges of these cracks (or arrays) become mutually annihilated and the energies concentrated released (simple fracture model, see Droste and Teisseyre 1959).

For defect density fields we may transform the Peach-Koehler expression (13), introducing a defect density using a dislocation slip vector and dislocation line versor:

$$\alpha_{qk} = v_q b_k \quad (14a)$$

Then using relations (12) and (13) we can define the induced stresses as a product of the Peach-Koehler force and normal to the defect plane, $F_n n_p$:

$$S_{np}^{Ind} = F_n n_p = \varepsilon_{nsq} \sum_k \alpha_{qk} S_{sk} n_p, \quad S_{[np]}^{Ind} = S_{(np)}^{Ind} + S_{[np]}^{Ind} \quad (14b)$$

and

$$\begin{aligned} S_{(np)}^{Ind} &= \frac{1}{2} \varepsilon_{nsq} \sum_k \alpha_{qk} S_{sk} n_p + \frac{1}{2} \varepsilon_{psq} \sum_k \alpha_{qk} S_{sk} n_n \\ S_{[np]}^{Ind} &= \frac{1}{2} \varepsilon_{nsq} \sum_k \alpha_{qk} S_{sk} n_p - \frac{1}{2} \varepsilon_{psq} \sum_k \alpha_{qk} S_{sk} n_n \end{aligned} \quad (14c)$$

The total stresses mean reorganized stresses due to the defect field:

$$S_{np}^T = S_{np} + S_{[np]}^{Ind} = S_{(np)} + S_{[np]} + S_{(np)}^{Ind} + S_{[np]}^{Ind} \quad (15)$$

Our considerations on the seismic energy releases might bring several important results for seismology and, more generally, for continuum and fracture mechanics and thermodynamics. Dynamic fracture processes, e.g., earthquakes, could be well described by the release-rebound equation system with special adequate parameters.

Considering the applied stress field as given by the constant total axial stresses only (constant pressure)

$$S_{np}^T = -p \delta_{np} + S_{np}^{Ind} \quad (16a)$$

we obtain from Eqs. 14a–14c and 15 that the non-diagonal component of asymmetric total stresses will be related to the defect content (here, n_p means a normal to the defect plane):

$$S_{12}^T = p(\alpha_{23} - \alpha_{32})n_2, \quad S_{23}^T = p(\alpha_{31} - \alpha_{13})n_3, \quad S_{31}^T = p(\alpha_{12} - \alpha_{21})n_1 \quad (16b)$$

while for the axial fields we obtain:

$$S_{11}^T = p(\alpha_{23} - \alpha_{32} - 1)n_1, \quad S_{22}^T = p(\alpha_{31} - \alpha_{13} - 1)n_2, \quad S_{33}^T = p(\alpha_{12} - \alpha_{21} - 1)n_3 \quad (16c)$$

This is an important expression: a fracture under pressure may partly run as a shear and partly as a strain rotation, both mutually related. This result confirms the known experimental fact that under applied pressure the fragmentation has both a shear and a rotational character.

Two cracks can join each other to form a bigger crack; in such a process the stresses concentrated at the opposite edges of these cracks (or arrays) become mutually annihilated; that means their energies become released. This simple fracture model (cf., Droste and Teisseyre 1959) could be applied to a continuum with high defect content.

We will return to the problem of fracture preparation processes at the end of this chapter.

4 Fluids: Basic Theory

In the frame of Continuum Theory we will also present a new approach to the fluid dynamics. The transport processes based on the Navier-Stokes equations should be enriched also by the rotational transport term leading to vortex processes. Besides the molecular shear strains, the non-vanishing time rates of shears, we should include the molecular rotation strains and stresses, the time rate of rotation strains (Teisseyre 2010).

The main problems encountered in the classic elasticity have been discussed earlier in this chapter. Let us now recall the transport motion, the Navier-Stokes relations:

$$\rho \frac{dv_i}{dt} = \rho \frac{\partial v_i}{\partial t} + \rho v_s \frac{\partial v_i}{\partial x_s} = \eta \frac{\partial^2 v_i}{\partial x_k \partial x_k} - \tilde{F}_i \quad (17a)$$

where \tilde{F} are the body forces, including pressure, v is the displacement velocity, η is the dynamic viscosity.

We may present this relation in a different form, with the molecular strains (strain time derivatives), $\tilde{E}_{(ki)}(v)$ and $\tilde{E}_{[ki]}(v)$:

$$\begin{aligned} \rho \frac{dv_i}{dt} &\rightarrow \rho \frac{\partial v_i}{\partial t} + \rho v_s \frac{\partial v_i}{\partial x_s} = \eta \frac{\partial}{\partial x_k} \tilde{E}_{ki} - \tilde{F}_i \\ \tilde{E}_{ki} &= \tilde{E}_{(ki)} + \tilde{E}_{[ki]} = \frac{\partial v_i}{\partial x_k} \end{aligned} \quad (17b)$$

For complex transport motions we may consider several float transport relations and we assume that these different float transports may remain mutually independent. Thus, we may write:

$$\begin{aligned} \rho \frac{dv_i^A}{dt} &= \rho \frac{\partial v_i^A}{\partial t} + \rho \left(\sum_s v_s^A \frac{\partial v_i^A}{\partial x_s} + \sum_s v_s^B \frac{\partial v_i^A}{\partial x_s} + \sum_s v_s^C \frac{\partial v_i^A}{\partial x_s} \right) = \eta \sum_s \frac{\partial^2 v_i^A}{\partial x_s^2} + F_i^A \\ \rho \frac{dv_i^B}{dt} &= \rho \frac{\partial v_i^B}{\partial t} + \rho \left(\sum_s v_s^A \frac{\partial v_i^B}{\partial x_s} + \sum_s v_s^B \frac{\partial v_i^B}{\partial x_s} + \sum_s v_s^C \frac{\partial v_i^B}{\partial x_s} \right) = \eta \sum_s \frac{\partial^2 v_i^B}{\partial x_s^2} + F_i^B \\ \rho \frac{dv_i^C}{dt} &= \rho \frac{\partial v_i^C}{\partial t} + \rho \left(\sum_s v_s^A \frac{\partial v_i^C}{\partial x_s} + \sum_s v_s^B \frac{\partial v_i^C}{\partial x_s} + \sum_s v_s^C \frac{\partial v_i^C}{\partial x_s} \right) = \eta \sum_s \frac{\partial^2 v_i^C}{\partial x_s^2} + F_i^C \end{aligned} \quad (18a)$$

and for a total float, $v_i^T = v_i^A + v_i^B + v_i^C$, we have:

$$\rho \frac{dv_i^T}{dt} = \rho \frac{\partial v_i^T}{\partial t} + \rho \sum_s v_s^T \frac{\partial v_i^T}{\partial x_s} = \eta \sum_s \frac{\partial^2 v_i^T}{\partial x_s^2} + F_i^T \quad (18b)$$

We should consider also the molecular vortex motions, instead of the classic approach for the vorticity ζ in fluids:

$$\zeta_k = \varepsilon_{kpi} \frac{\partial v_i}{\partial x_p} \Leftrightarrow \zeta = \text{rot } v \quad (19)$$

However, we are convinced that we should define the vortex motion as the helical transport terms included in the Navier-Stokes equations in the cylindrical system (r, φ, z) :

$$\begin{aligned} \rho \frac{\partial v_r}{\partial t} + \rho \left(v_r \frac{\partial v_r}{\partial r} + v_\varphi \frac{\partial v_r}{r \partial \varphi} + v_z \frac{\partial v_r}{\partial z} \right) - \eta \left(\frac{\partial}{r \partial r} \left(r \frac{\partial v_r}{\partial r} \right) + \frac{\partial^2 v_r}{r^2 \partial \varphi^2} + \frac{\partial^2 v_r}{\partial z^2} \right) &= F_r \\ \rho \frac{\partial v_\varphi}{\partial t} + \rho \left(v_r \frac{\partial v_\varphi}{\partial r} + v_\varphi \frac{\partial v_\varphi}{r \partial \varphi} + v_z \frac{\partial v_\varphi}{\partial z} \right) - \eta \left(\frac{\partial}{r \partial r} \left(r \frac{\partial v_\varphi}{\partial r} \right) + \frac{\partial^2 v_\varphi}{r^2 \partial \varphi^2} + \frac{\partial^2 v_\varphi}{\partial z^2} \right) &= F_\varphi \\ \rho \frac{\partial v_z}{\partial t} + \rho \left(v_r \frac{\partial v_z}{\partial r} + v_\varphi \frac{\partial v_z}{r \partial \varphi} + v_z \frac{\partial v_z}{\partial z} \right) - \eta \left(\frac{\partial}{r \partial r} \left(r \frac{\partial v_z}{\partial r} \right) + \frac{\partial^2 v_z}{r^2 \partial \varphi^2} + \frac{\partial^2 v_z}{\partial z^2} \right) &= F_z \end{aligned} \quad (20)$$

The difference between the classic vortex definition and this approach (Fig. 2) indicates that the classical approach presents only three degrees of freedom, instead of six. Thus, the points in a fluid may have the six degrees of freedom: displacement velocity and rotation rate—spin.

Here, we might also consider the molecular rotation motion which may remind us the vortex processes (see Fig. 3). Note that these vortex motions might have different forms.

Similarly to Eqs. (18a), (18b) and (20), for the simultaneous linear and vortex transports, v_s and $\vec{v} = (\vec{v}_r, \vec{v}_\varphi, \vec{v}_z)$, we may write

$$\begin{aligned} \rho \frac{\partial v_x}{\partial t} + \rho \left(\sum_s v_s \frac{\partial v_x}{\partial x_s} + \vec{v}_r \frac{\partial v_x}{\partial r} + \vec{v}_\varphi \frac{\partial v_x}{r \partial \varphi} + \vec{v}_z \frac{\partial v_x}{\partial z} \right) &= \eta \Delta v_x + F_x \\ \rho \frac{\partial v_y}{\partial t} + \rho \left(\sum_s v_s \frac{\partial v_y}{\partial x_s} + \vec{v}_r \frac{\partial v_y}{\partial r} + \vec{v}_\varphi \frac{\partial v_y}{r \partial \varphi} + \vec{v}_z \frac{\partial v_y}{\partial z} \right) &= \eta \Delta v_y + F_y \\ \rho \frac{\partial v_z}{\partial t} + \rho \left(\sum_s v_s \frac{\partial v_z}{\partial x_s} + \vec{v}_r \frac{\partial v_z}{\partial r} + \vec{v}_\varphi \frac{\partial v_z}{r \partial \varphi} + \vec{v}_z \frac{\partial v_z}{\partial z} \right) &= \eta \Delta v_z + F_z \end{aligned} \quad (21)$$

Fig. 2 Sketch of vortex transport with points having three degrees of freedom in space (classic vorticity) (*left part*) and six degrees of freedom for the vortex defined in the Asymmetric Continuum Theory (*right*); on a plane, we observe only one degree of freedom (*left*) and two degrees (*right*)

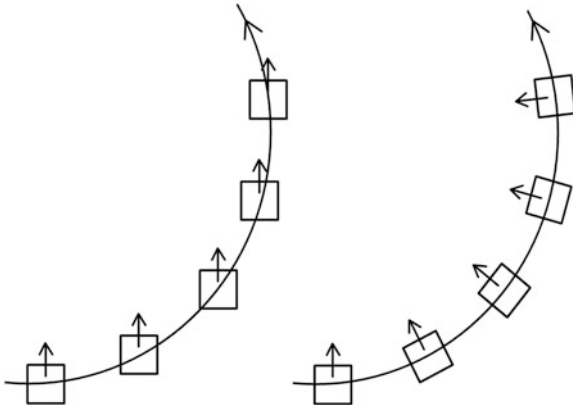
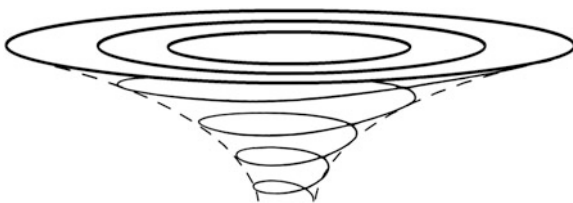


Fig. 3 An example of molecular rotation related to a vortex motion



and

$$\begin{aligned} \rho \frac{\partial \vec{v}_r}{\partial t} + \rho \left(\sum_s v_s \frac{\partial \vec{v}_r}{\partial x_s} + \vec{v}_\varphi v_x \frac{\sin \varphi}{r} - \vec{v}_\varphi v_y \frac{\cos \varphi}{r} + \vec{v}_r \frac{\partial \vec{v}_r}{\partial r} + \vec{v}_\varphi \frac{\partial \vec{v}_r}{\partial \varphi} + \vec{v}_z \frac{\partial \vec{v}_r}{\partial z} - \frac{\vec{v}_\varphi^2}{r} \right) &= \eta \Delta \vec{v}_r + \vec{F}_r \\ \rho \frac{\partial \vec{v}_\varphi}{\partial t} + \rho \left(\sum_s v_s \frac{\partial \vec{v}_\varphi}{\partial x_s} - \vec{v}_r v_x \frac{\sin \varphi}{r} + \vec{v}_r v_y \frac{\cos \varphi}{r} + \vec{v}_r \frac{\partial \vec{v}_\varphi}{\partial r} + \vec{v}_\varphi \frac{\partial \vec{v}_\varphi}{\partial \varphi} + \vec{v}_z \frac{\partial \vec{v}_\varphi}{\partial z} + \frac{\vec{v}_r \vec{v}_\varphi}{r} \right) &= \eta \Delta \vec{v}_\varphi + \vec{F}_\varphi \\ \rho \frac{\partial \vec{v}_z}{\partial t} + \rho \left(\sum_s v_s \frac{\partial \vec{v}_z}{\partial x_s} + \vec{v}_r \frac{\partial \vec{v}_z}{\partial r} + \vec{v}_\varphi \frac{\partial \vec{v}_z}{\partial \varphi} + \vec{v}_z \frac{\partial \vec{v}_z}{\partial z} \right) &= \eta \Delta \vec{v}_z + \vec{F}_z \end{aligned} \quad (22)$$

where $\Delta \Rightarrow \frac{\partial}{\partial r} \left(r \frac{\partial}{\partial r} \right) + \frac{\partial^2}{r^2 \partial \varphi^2} + \frac{\partial^2}{\partial z^2}$

Such processes may be important to explain some phenomena in fluids, e.g., turbulence and the Coriolis effect. Turbulence with stochastic properties and unsteady vortices appears probably due to the high rates of momentum and to breaks related to a viscous laminar flow.

Of course, we follow the Asymmetric Continuum Theory developed in our former papers (Teissseyre 2008a, b, 2009, 2011); we assume that beside the symmetric molecular strains (strain rates) there appear also the antisymmetric molecular strain rates (spins); for the related molecular stresses we write:

$$\begin{aligned}\tilde{S}_{kl} &= \tilde{S}_{(kl)} + \tilde{S}_{[kl]}, \quad \tilde{E}_{kl} = \tilde{E}_{(kl)} + \tilde{E}_{[kl]}; \\ \tilde{S}_{(kl)}^D &= \tilde{S}_{(kl)} - \frac{1}{3} \delta_{kl} \sum_s \tilde{S}_{ss}, \quad \tilde{E}_{(kl)}^D = \tilde{E}_{(kl)} - \frac{1}{3} \delta_{kl} \sum_s \tilde{E}_{ss}\end{aligned}\quad (23a)$$

and for the constitutive relations we may put:

$$\frac{1}{3} \sum_s \tilde{S}_{ss} = -\frac{\partial p}{\partial t} = \frac{1}{3} k \sum_s \tilde{E}_{ss}, \quad \tilde{S}_{(kl)}^D = \eta \tilde{E}_{(kl)}^D, \quad \tilde{S}_{[kl]} = \eta \tilde{E}_{[kl]} \quad (23b)$$

where $\tilde{S}_{(kl)}^D$ and $\tilde{E}_{(kl)}^D$ mean the deviatoric parts of tensors and η is the viscosity; we have assumed the same constant, η , for symmetric and antisymmetric parts as these fields should propagate at the same velocity.

The molecular strain rates could be related to the derivatives of some transport displacement velocities:

$$\tilde{E}_{(kl)} = \frac{1}{2} \left(\frac{\partial v_l}{\partial x_k} + \frac{\partial v_k}{\partial x_l} \right), \quad \tilde{E}_{[kl]} = \frac{1}{2} \left[\frac{\partial v_i}{\partial x_k} - \frac{\partial v_k}{\partial x_i} \right] \quad (24a)$$

and we obtain:

$$\tilde{S}_{(kl)}^D + \tilde{S}_{[kl]} = \eta \frac{\partial v_l}{\partial x_k} = \eta (\tilde{E}_{(kl)}^D + \tilde{E}_{[kl]}) \quad (24b)$$

Thus, in motions with advanced vorticity dynamics we assume that a transport can be related both to transport velocity and the vortex motions; we follow the approach applied to fragmentation and slip in the fracture processes (Teisseyre 2009). For a large Reynolds number, the laminar motions become unstable and the double transport process with displacement velocities and spin motions may generate the micro-vortices; a kind of dynamic vortex structure can be formed, simultaneously undergoing a displacement transport process. However, under some special conditions, an isolated vortex center can be formed; inside it, the displacement velocity transport might be negligible.

We should also take into account that on any liquid/gas surface (gas viscosity is about 1,000 times smaller than the liquid viscosity), including surfaces of drops and bubbles, we expect a co-action of the shear and rotation tensions in this 2D space; the molecular strains—rotational and shear—existing in fluids, become there, on these surfaces, the real strains. Therefore, this process explains also the formation of a meniscus in a fluid at an existing solid element; a liquid-gas surface should approach that solid element parallelly in order to meet the same strain system in this liquid-gas surface and in the corresponding solid element with its boundary strain system.

It seems important to find some mathematical expression to define a difference between a liquid and a gas. We should remember that a difference between solids and fluids is that in fluids we deal with the molecular strains; thus we may suppose

that a difference between liquids and gas might be that in liquids we have the molecular strains (time derivative of strains), but in a gas we have the sub-molecular strains (second order of the time derivative of strains).

5 Conclusions: Joint Continuum Theory for Solids and Fluids

Keeping in mind that the main elements of the classic thermodynamics remain valid when considering the Asymmetric Strain Theory solids and Newtonian fluids, we will focus here only on some necessary corrections related to the rotational components appearing due to the presented new approach related to the motions and deformations.

In our considerations, important influences on the thermodynamic parameters in solids have been exerted by defects; therefore, we follow the $cB\Omega$ thermodynamical model (Varotsos and Alexopoulos 1984a, b, 1986), confirmed by a number of empirical relations and leading, among other things, to an important search of earthquake precursors.

We can define also the super-lattice related to the distribution of the linear defects. The formation of a defect line leads to the negative contribution to the Gibbs free energy; therefore, we cannot reach a minimum for any number of dislocations; however, we can omit this problem when introducing the dislocation super-lattice and adding to the Gibbs free energy a related difference between the dislocation super-lattice and a number of dislocations.

Moreover, we adopt the standard approach to the expression for released energies which contains, besides the symmetric stresses, also their antisymmetric parts; thus, the energy drops may include the rotational stress fields as well.

The main relations for solids, release-rebound strains and related wave equations, and for fluids, the Navier-Stokes transport relations, relate to the strains in solids and transport motions in fluids. However, in fluids we additionally have the molecular strains as a complementary field which may influence a transport motion. Reversely, in solids we propose to introduce the molecular transport in order to understand the fracture preparation processes. Of course, to any continuum we include an influence of pressure; thus, in fluids we have both the pressure and its time derivative, the molecular pressure related to sound.

A molecular transport in solids is necessary to understand some nucleation processes which can lead to fracture. The real displacements, even very weak, do not exist in a solid continuum, but can appear there due to the integration processes of these introduced molecular transport motions. Such a combined system may permit to understand the fracture nucleation processes and propagation of the shear and rotation strains due to the related common interactions.

Thus, we present the Asymmetric Continuum Theory with the axial, shear and rotation strains and with the transport processes which are a common theoretical

basis for solids and fluids; the related differences between solids and fluids are as follows:

- **in solids** we consider the asymmetric strains and we include, moreover, the molecular transport processes,
- **in fluids** we consider, reversely, the transport motions and molecular strains.

For fluids, as already presented in the new approach to the vortex processes, instead of the classic definition of vorticity, we consider the vortex motion system based on the transport with a variable arm and rotation flow as presented in the cylindrical coordinates. This new definition provides an explanation for the degrees of freedom desired in a vortex motion.

For solids, in a similar manner, we will have asymmetric strains and, moreover, the molecular transport processes. Here, we should underline that some important relations, e.g., the release-rebound processes achievable only in a special coordinate system in the 3D space (see Eqs. 8 and 9a, 9b), may become invariant when presented in the 4D space-time system. At an earthquake process, or other fracture processes, a break of molecular bonds, e.g., related to a release of shear strains, $\partial E_{()} / \partial t$, should cause a rebound process (rotation of strain rotation), $\text{rot}E_{[]}$, and, vice versa, a release of rotation $\partial E_{[]} / \partial t$ should cause a rebound, rotation of shears: $\text{rot}E_{()}$. A wave propagation follows these release-rebound mechanisms (compare to Eq. 10; cf., Teisseyre 1985, 2011).

Into the molecular transport we can include also a number of independent motions, e.g., the linear transport fields and the vortex transports in a cylindrical system:

$$w_s = \frac{\partial v_s}{\partial x_s} \rightarrow \left(\frac{\partial v_r}{\partial x_r}, \frac{\partial v_\varphi}{r \partial \varphi}, \frac{\partial v_z}{\partial z} \right) \text{ and } \check{w} = \left(\frac{\partial \check{w}_r}{\partial r}, \frac{\partial \check{w}_\varphi}{r \partial \varphi}, \frac{\partial \check{w}_z}{\partial z} \right) \quad (25)$$

For these two simultaneous molecular transports, $w^T = w + \check{w}$, we use the relations similar to the Navier-Stokes equations:

$$\rho \frac{dv^T}{dt} = \rho \frac{\partial w^T}{\partial t} + \rho (w^T \cdot \text{grad}) w^T = \vec{\eta} \Delta w^T - \vec{\kappa} F \quad (26)$$

where we introduce the new adequate parameters, $\vec{\eta}$ and $\vec{\kappa}$. According to Eq. 24a we may write for the sub-molecular strains, \vec{E}_{kl} :

$$\frac{\partial w_l}{\partial x_k} = \vec{\eta} (\vec{E}_{(kl)}^D + \vec{E}_{[kl]}) \quad (27)$$

Note that when the surface tension is included, the relations for the surface waves must be modified.

Let us also note that these sub-molecular strains, \vec{E}_{kl} , could be related to the local internal relations similar to Eq. (10):

$$\text{rot } \vec{E} - \frac{\vec{\kappa}}{c} \frac{\partial \vec{E}}{\partial t} = 0, \quad \text{rot } \hat{\vec{E}} + \frac{\vec{\kappa}}{c} \frac{\partial \vec{E}}{\partial t} = 0; \quad \frac{c}{\vec{\kappa}} = \vec{V} \quad (28)$$

where \vec{V} would mean a fracture velocity.

It is to be added that this apparent propagation of molecular transport in solids should be realized, in fact, through an influence of the real wave motions (propagation of strains) acting on the molecular behavior.

It is also worth to repeat that pressure can induce defects forming the centers with opposite-sense shears and rotations assuring a mutual compensation of those induced fields. Such material micro-destructions relate to very complicated non-linear processes. Due to existing differences related to the various defect densities, we may explain some different effects produced by a given load; these different effects are related to the unknown distribution of the internal defects or to some influence of different human activities. The theory of dislocation and dislocation arrays (Eshelby et al. 1951; cf., Rybicki 1986) permits us to understand the role of defect densities and applied stresses (cf., Kossecka and DeWitt 1977 and Teisseyre and Górska 2012).

Of course, we cannot directly describe a fracture process in terms of the Continuum Theory; we may only state that such a fracture is caused by an interaction of the real shear and rotation strains and related molecular displacements. Any molecular propagation is only apparent; these changes are related only to the real propagation of strains in a solid, or real transport in fluids. However, the molecular transport motions may exist in a whole space; the related mechanism may help us to understand an influence of the appearance of another fracture even at a large distance.

In the final remark let us repeat that the Asymmetric Continuum Theory includes the strain waves, with shears and rotations, and the transport motions; for solids, these are the strains and molecular transport, and for fluids the transport and molecular strains. Moreover, an important difference between the Classic and Asymmetric theories follows from the assumption that in the Asymmetric Theory we may admit a simultaneous use of a number of fields independently released in some source, e.g., an earthquake source. A release and propagation of some physical fields, e.g., shear and rotation strains and the different transport motions (including the vortex transport in fluids, and the molecular transports in solids), makes it possible to better understand the related complex processes.

More information and more detail analyses can be found in a comprehensive monograph by Teisseyre and Teisseyre-Jeleńska (2014).

References

- Cosserat E, Cosserat F (1909) Théorie des Corps Déformables. A. Hermann et Fils, Paris
- Droste Z, Teisseyre R (1959) The mechanism of earthquakes according to dislocation theory. *Sci Rep Tohoku Univ Ser 5, Geophys* 11(1):55–71
- Eringen AC (1999) Microcontinuum field theories I, foundations and solids. Springer, Berlin, p 325
- Eringen AC (2001) Microcontinuum field theories II, fluent media. Springer, Berlin, p 340
- Eringen AC, Suhubi ES (1964) Non-linear theory of simple microelastic solids-1. *Int J Eng Sci* 2:189–203
- Eshelby JD, Frank FC, Nabarro FRN (1951) The equilibrium of linear arrays of dislocations. *Philos Mag* 42:351–364
- Gomberg J, Agnew DC (1996) The accuracy of seismic estimates of dynamic strains from pinyon flat observatory, California, strainmeter and seismograph data. *Bull Seismol Soc Am* 86:212–220
- Kossecka E, DeWitt R (1977) Disclination kinematic. *Arch Mech* 29:633–651
- Kröner E (1981) Continuum theory of defect. In: Balian R, Kleman M, Poirier JP (eds) *Les Houches, session XXXV, 1980, physics of defects*. North Holland, Amsterdam
- Lee WHK, Celebi M, Todorovska MI, Igel H (2009) Introduction to special issue on rotational seismology and engineering applications. *Bull Seismol Soc Am* 62(2B):945–957
- Mindlin RD (1965) On the equations of elastic materials with microstructure. *Int J Solid Struct* 1(1):73
- Nowacki W (1986) Theory of asymmetric elasticity. Pergamon Press, PWN, Warszawa
- Peach M, Koehler JS (1950) The forces exerted on dislocations and the stress fields produced by them. *Phys Rev* 80:436–439
- Rybicki K (1986) Dislocations and their geophysical applications. In: Teisseyre R (ed) *Continuum theories in solid earth physics*. Elsevier-PWN, Warsaw, pp 18–186
- Schreiber KU, Hautman JN, Velikoseltsev A, Wassermann J, Igel H, Otero J, Vernon F, Wells J-PR (2009) Ring laser measurements of ground rotations for seismology. *Bull Seismol Soc Am* 99(2B):1190–1198
- Teisseyre KP (2007) Analysis of a group of seismic events using rotational components. *Acta Geophys* 55:535–553
- Teisseyre R (1973) Earthquake processes in a micromorphic continuum. *Pure Appl Geophys* 102:15–28
- Teisseyre R (1974) Symmetric micromorphic continuum: wave propagation, point source solutions and some applications to earthquake processes. In: Thoft-Christensen P (ed) *Continuum mechanics aspects of geodynamics and rock fracture mechanics*, pp 201–244
- Teisseyre R (1980) Earthquake premonitory sequence—dislocation processes and fracturing. *Boll Geofis Teor Appl* 22:245–254
- Teisseyre R (1985a) Creep-flow and earthquake rebound: system of the internal stress evolution. *Acta Geophys Pol* XXXIII(1):11–23
- Teisseyre R (1985b) New earthquake rebound theory. *Phys Earth Planet Inter* 39(1):1–4
- Teisseyre R (2008a) Introduction to asymmetric continuum: dislocations in solids and extreme phenomena in fluids. *Acta Geophys* 56:259–269
- Teisseyre R (2008b) Asymmetric continuum: standard theory. In: Teisseyre R, Nagahama H, Majewski E (eds) *Physics of asymmetric continua: extreme and fracture processes*. Springer, Berlin, pp 95–109
- Teisseyre R (2009) Tutorial on new development in physics of rotation motions. *Bull Seismol Soc Am* 99(2B):1028–1039
- Teisseyre R (2010) Fluid theory with asymmetric molecular stresses: difference between vorticity and spin equations. *Acta Geophys* 58(6):1056–1071T
- Teisseyre R (2011) Why rotation seismology: confrontation between classic and asymmetric theories. *Bull Seismol Soc Am* 101(4):1683–1691

- Teisseyre R, Górski M (2009) Fundamental deformations in asymmetric continuum: motions and fracturing. *Bull Seismol Soc Am* 99(2B):1028–1039
- Teisseyre R, Górski M (2011) Earthquake fragmentation and slip processes: spin and shear-twist wave mosaic. *Acta Geophys* 59(3):453–469
- Teisseyre R, Górski M (2012) Induced strains and defect continuum theory: internal reorganization of load. *Acta Geophys* 60(1):24–42
- Teisseyre R, Teisseyre-Jeleńska M (2014) Asymmetric continuum: extreme processes in solids and fluids. *GeoPlanet Series*, Springer, Berlin
- Udias A (2002) Theoretical seismology: an introduction. In: Lee WHK, Kanamori H, Jennings PC, Kisslinger C (eds) International handbook of earthquake & engineering seismology, part a. Academic Press, New York, pp 81–102
- Varotsos P, Alexopoulos K (1984a) Physical properties of the variations of the electric field of the earth preceding earthquakes, I. *Tectonophysics* 110:73–98
- Varotsos P, Alexopoulos K (1984b) Physical properties of the variations of the electric field of the earth preceding earthquakes, II. Determination of epicenter and magnitude. *Tectonophysics* 110:99–125
- Varotsos P, Alexopoulos K (1986) Thermodynamics of point defects and their relation with the bulk properties. Elsevier Science Ltd, North Holland
- Zemba Z (2009) Tutorial on surface rotations from wave passage effects: stochastic approach. *Bull Seismol Soc Am* 99(2B):1040–1049

Time Scales: Towards Extending the Finite Difference Technique for Non-homogeneous Grids

Kamil Waśkiewicz and Wojciech Dębski

Abstract Tremendous progress in seismology over last years is greatly due to availability of high quality seismic waveforms. Their availability prompts the new mathematical and numerical algorithms for their more detailed analysis. This analysis usually takes a form of the inverse problems—an estimation of physical parameters from seismic waveforms called the full waveform inversion (FWI). No matter which inversion algorithm is used, the FWI technique requires precise modeling of synthetic seismograms for a given lithological model. This is by no means a trivial task from the algorithmic point of view, as it requires solving (usually numerically) the wave equation describing propagation of seismic waves in complex 3D media, taking into account such effects as spatial heterogeneities of media properties, anisotropy, and energy attenuation, to name a few. Although many numerical algorithms have been developed to handle this task, there is still a need for further development as there is no single universal approach equally good for all tasks in hand. In this chapter, the possibility of using the Time Scale Calculus formalism to advance the synthetic seismograms calculation is discussed. This modern approach developed the late 1990s with the aim of unifying analytical and numerical calculations provides the very promising basement for developing new computational methods for seismological, or more general geophysical applications. In this chapter we review the basic elements of the Time Scale Calculus keeping in mind its application in seismology but also we extend the initial concept of Hilger's derivative towards the backward-type and central-type derivatives using the unified approach and compare their properties for various time scales. Using these results we define the second order differential operators (laplacians) and provide explicit formulas for different time scales. Finally, the formalism of time scales is used for solving 1D linear, acoustic wave equation for a velocity model with large velocity discontinuities. Based on this simple example

K. Waśkiewicz · W. Dębski (✉)

Institute of Geophysics, Polish Academy of Sciences, ul. Ks. Janusza 64,
01-452 Warsaw, Poland
e-mail: debski@igf.edu.pl

we demonstrate that even in such a simple case using an extension of the classical finite difference schemata towards irregular grid leads to a significant improvement of computational efficiency.

Keywords Synthetic seismograms · Time scale calculus · Finite difference

1 Introduction

Precise answer to many seismological questions requires a very accurate modeling of seismic waveforms since it is a significant part of most of seismological analyses (Virieux et al. 2009; Debski 2008, 2010). Unfortunately, for most of realistic media this can be achieved only approximating the original continuous seismic wave equation by some discrete version suitable for numerical computations. The most popular approach, called the finite difference (FD) method (see, e.g., Moczo et al. 2007), relays on a simple discretization of the partial differential equation by replacing continuous differential operators by its discrete counterparts. This leads to a very simple set of discrete equations easy for numerical treatment. As a consequence, the method is very fast and requires relatively small amount of computer memory. However, the method can hardly incorporate complicated boundary conditions and its stability (explicit schemata) requires careful choice of parameters. To avoid these problems, using nonuniform grids like in the case of finite element method is advisable (de Rivas 1972; Pitarka 1999). However, such a generalization is a real challenge at least for the elastic wave equation used to generate synthetic seismograms and there is still no general consensus of how to achieve it (Moczo et al. 2007, 2011). From this point of view a very promising approach has recently been developed and is connected with an attempt of unifying the continuous and discrete mathematics. It is called the Time Scale Calculus (TSC).

The concept of Time Scales has been formulated by Hilger (1990, 1997) in order to unify continuous and discrete mathematical analysis. Its particular application is in the field of partial differential and difference equations (Agarwal et al. 2002; Agarwal and Bohner 1999) which have a broad range of applications in many scientific and engineering problems. In geophysics, for example, many analyses relay on solving such equations like wave equation, Poisson equation, Maxwell equations, or various differential equations originating from fluid dynamics, including Navier-Stokes equation. The TSC approach, besides its mathematical aspects (see, e.g., Cieslinski 2007, 2012), due to its universality seems to have a large potential when practical applications are considered (Agarwal and Bohner 1999; Atici et al. 2006; Dryl et al. 2013). This is because it is a method for extending the classical finite difference schemata including both uniform and nonuniform grids towards non-homogeneous grids consisting of a combination of continuous sets and discrete grids together (Atici et al. 2006).

Besides this, TSC provides an elegant mathematical framework for considering the general finite difference methods. Thus, we have decided to bring the Time Scale calculus concept closer to geophysical, or more precisely to seismological applications.

From the numerical, i.e. applicational point of view, the TSC can be regarded as an extension of the finite difference schemata for the complex non-homogeneous domains. It includes both ordinary and partial differential equation solvers (Bohner and Peterson 2001; Agarwal et al. 2002) as well as integration and variational methods (Ferreira and Torres 2008; Dryl et al. 2013). In this chapter we explore a possibility of using the TSC in geophysics in the context of numerical solution of the linear wave equation (Aki and Richards 1985). From this point of view, the TSC approach introduces first of all the new possibilities of solving the wave equation using complex spatial domains consisting of continuous sets and discrete grids. Using this possibility is potentially interesting, for example, for marine seismic explorations. This prospecting technique is based on simulation of the seismic wave propagation in the sea bedrock generated by sources located in water. Since the uppermost part of model used in such simulations—the water layer—has a relatively simple velocity structure, the propagation of waves in this medium can be described analytically while the propagation of seismic waves in the “bedrock part” of the model has to be implemented numerically. Thus, the TSC approach can address this issue.

Secondly, if the domain of interest is discretized by means of any regular or irregular grid, the TSC approach provides a uniform mathematical methods of describing such problems. Although such analyses are already well known (see, e.g. Pitarka 1999; de Rivas 1972; Vesnauer 1996), the TSC brings a unified, mathematically elegant approach to this task.

This chapter is a basic introduction to the time scales calculus in the seismological context and presents beginning of our attempt of extending classical FD technique towards the non-homogeneous, multi-dimensional time scales. We firstly wish to reformulate the classical finite difference methods based on both uniform and nonuniform grids in the language of TSC (this chapter), next extend it towards the fully non-homogeneous time scales, and finally addresses the problems in two and three dimensions.

The chapter is organized as follow. Firstly, after giving the formal definitions, we introduce a general time scale classification introducing the notion of homogeneous and non-homogeneous time scales depending on type of points of time scales. Next, the basic elements of TSC are presented. In the next part, the acoustic wave equation in the Hamiltonian formulation is presented and the explicit formula for numerical iterative schemata on an arbitrary homogeneous spatial time scale is given. Then we illustrate its use with a simple 1D model showing the well known advantages of using the nonuniform grids (Pitarka 1999), especially avoiding spatial oversampling by adopting the grid to the velocity model in hand. The chapter ends with general comments on further perspectives of using TSC for building new numerical schemata of simulation of seismic wave propagation.

2 Time Scales: Basic Concepts

The concept of time scales analysis is a fairly new idea as it was introduced by Hilger (1990). At the mathematical level, it combines the traditional areas of continuous and discrete analysis into one theory which unifies methods for analysis of the differential and difference equations. The most visible differences between these two groups of equations are essentially different domains of equations. In case of the difference equation (continuous case) the domain can be identified with the space of the real numbers (\mathbb{R} or in multidimensional cases \mathbb{R}^N) or some of its subsets, while the natural domain for difference equations (discrete case) is a set of integers or natural numbers. The discussed time scale calculus concept relays on the basic generalization of the considered domains into the so-called time scales denoted here as \mathbb{T} . By definition, the time scale (in 1D) is any (non-empty) closed subset of real numbers. Thus, \mathbb{R} , \mathbb{Z} , i.e., the real numbers and the integers are examples of time scales. Time scales can also have a more complex structure as, for example, the sum of closed subsets like $[0; 1] \cup [2; 3]$ or combinations like $[0; 1] \cup \mathbb{N}$.

To illustrate the basic properties of time scales and different operators defined later on, we shall consider the following time scales:

They are shown graphically in Fig. 1.

Given a time scale \mathbb{T} , we define the following two operators which we shall use to generalize the concept of the classical notion of derivative. These are the forward jump operator:

$$\sigma : \mathbb{T} \rightarrow \mathbb{T} \quad \sigma(t) := \inf\{s \in \mathbb{T} : s > t\} \quad (1)$$

and the backward jump operator

$$\rho : \mathbb{T} \rightarrow \mathbb{T} \quad \rho(t) := \sup\{s \in \mathbb{T} : s < t\}. \quad (2)$$

With respect to the defined above operators σ and ρ defined above, one can classify all points on the time scale as follows:

- if $\sigma(t) > t$ then t is called the right-scattered point,
- if $\sigma(t) = t$ then t is called the right-dense point,
- if $\rho(t) < t$ then t is called the left-scattered point,
- if $\rho(t) = t$ then t is called the left-dense point,
- if $\rho(t) < t < \sigma(t)$ we say that t is the scattered (isolated) point.

The meaning of the notions introduced above is obvious and their geometric interpretation is shown in Fig. 2.

The time scales composed of only dense or scattered points shall be called *homogeneous*. The homogeneous time scales consisting of scattered points can be *regular* if distances between points are changing in a regular manner over the whole time scale (for example, the distance between points is constant, or their ratio is constant), or *irregular* if no such “global” feature exists. An example of

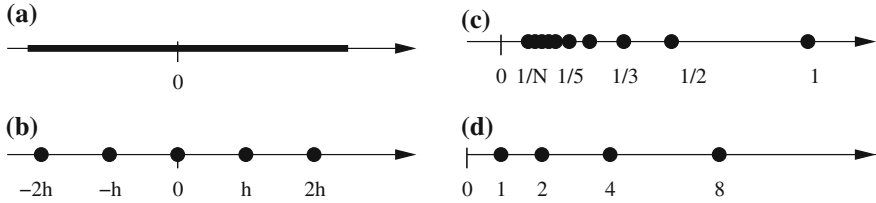


Fig. 1 Geometric illustration of considered time scales. **a** $\mathbb{T}_R = \mathbb{R}$ —the set of all real numbers. Actually, in this case the time scale calculus reduces to the classical continuum mathematics, **b** $\mathbb{T}_Z = h\mathbb{Z}$ —the set of real numbers $h\mathbb{Z} := \{\dots, -h, 0, h, 2h, \dots\}$ with h being the “distance” between subsequent points, **c** $\mathbb{T}_N = \{\frac{c}{n} : n \in [1, N]\} = \{c, c/2, c/3, \dots, c/N\}$ —the simple time scale with non-uniformly distributed separate points, **d** $\mathbb{T}_Q = \{1\} \cup \{q^N : q > 1\} = \{1, q, q^2, \dots\}$ —another grainy time scale with non-uniformly distributed points being the set of real numbers of the constant ratio q between subsequent points. A similar time scale but with $q < 1$ is considered, for example, by Atici and Eloe (2007)



Fig. 2 Geometric illustration of different types of points at general time scales

the regular time scale is thus the classical uniform grid (Moczo et al. 2007) while various nonuniform grids (see, e.g. Pitarka 1999) will be mostly classified as the irregular ones. All “discrete” time scales considered in this chapter ($\mathbb{T}_Z - \mathbb{T}_Q$) are homogeneous and regular.

Let us now define another two functions, $\mu(t)$ and $v(t)$ called the graininess functions

$$\begin{aligned}\mu(t) &:= \sigma(t) - t \\ v(t) &:= \rho(t) - t\end{aligned}\tag{3}$$

which will be used to measure a forward and backward “continuity” or “graininess” of time scales.

The explicit form of $\sigma(t)$, $\rho(t)$, $\mu(t)$ and $v(t)$ for the considered time scales can be easily obtained from the above definitions:

A. $\mathbb{T} = \mathbb{T}_R$. In this case

$$\sigma(t) = \inf\{s \in \mathbb{R} : s > t\} = \inf(t; \infty) = t\tag{4}$$

and by analogy

$$\rho(t) = t\tag{5}$$

One can easily verify that each point t is both left-, and right-dense points. Latter on we shall refer to such points as density points. The graininess functions for this case read:

$$\begin{aligned}\mu(t) &= \sigma(t) - t = 0 \\ v(t) &= \rho(t) - t = 0\end{aligned}\tag{6}$$

which simply means that the time scale is a “continuous” set.

B. $\mathbb{T} = \mathbb{T}_{\mathbb{Z}}$. One can easily verify that in this case for each $t \in \mathbb{T}$ the following relation holds:

$$\sigma(t) = \inf\{s \in h\mathbb{Z} : s > t\} = \inf(t + h; t + 2h; \dots) = t + h\tag{7}$$

and $\rho(t) = t - h$. All points $t \in \mathbb{T}$ are now scattered points and the graininess functions read

$$\begin{aligned}\mu(t) &= \sigma(t) - t = h \\ v(t) &= \rho(t) - t = -h\end{aligned}\tag{8}$$

C. $\mathbb{T} = \mathbb{T}_{\mathbb{N}}$. Following the definition of the jump operators one can easily find that for this time scale

$$\sigma(t = c/n) = \inf\{c, c/2, \dots, c/(n-1)\} = \frac{ct}{c-t}\tag{9}$$

$$\rho(t) = \sup\{c/(n+1), c/(n+2), \dots\} = \frac{ct}{c+t}\tag{10}$$

and the graininess functions read:

$$\begin{aligned}\mu(t) &= \frac{t^2}{c-t} \\ v(t) &= \frac{t^2}{c+t}\end{aligned}\tag{11}$$

D. $\mathbb{T} = \mathbb{T}_{\mathbb{Q}}$. For this geometric-type time scale the jump operators read:

$$\begin{aligned}\sigma(t) &= q \cdot t \\ \rho(t) &= q^{-1} \cdot t\end{aligned}\tag{12}$$

All points $t \in \mathbb{T}_{\mathbb{Q}}$ are now scattered points and the graininess functions read

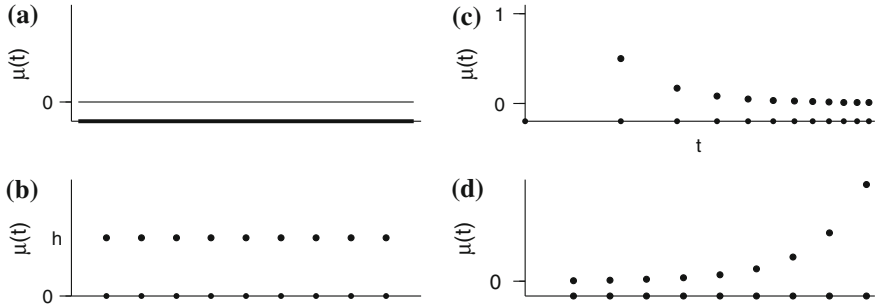


Fig. 3 Illustration of the graininess function for the considered time scales. Dots and thick lines represents actual time scales

$$\begin{aligned}\mu(t) &= (q - 1) \cdot t \\ v(t) &= (1 - q)/q \cdot t\end{aligned}\quad (13)$$

Figure 3 represents graphically the graininess function $\mu(t)$ for the considered time scales.

2.1 Differential Operators

Equipped with the definitions of jump operators let us define the Hilger Derivative operation.

For any scalar function $f : \mathbb{T} \rightarrow \mathbb{R}$ and $t \in \mathbb{T}^k$, where \mathbb{T}^k are time scales with the rightmost point removed, let us define Hilger's derivative denoted by $f^\triangleright(t)$ in such a way that for any $\varepsilon > 0$, there exists a neighborhood U of t , constructed as $U = (t - \delta; t + \delta) \cap \mathbb{T}$ for $\delta > 0$ such that:

$$|f(\sigma(t)) - f(s) - f^\triangleright(t)[\sigma(t) - s]| \leq \varepsilon |\sigma(t) - s| \quad (14)$$

We shall call $f^\triangleright(t)$ the delta derivative of f on \mathbb{T}^k . One can prove (Agarwal and Bohner 1999; Agarwal et al. 2002) the following properties of the $f^\triangleright(t)$ operator:

- If f is continuous at t and t is the right-scattered point, then f is differentiable at t with:

$$f^\triangleright(t) = \frac{f(\sigma(t)) - f(t)}{\mu(t)} \quad (15)$$

- If t is the right-dense point, then f is differentiable at t if the limit: $\lim_{s \rightarrow t} \frac{f(t) - f(s)}{t - s}$ exists and is finite. In this case

$$f^\triangleright(t) = \lim_{s \rightarrow t, s > t} \frac{f(t) - f(s)}{t - s} \quad (16)$$

- If f is differentiable at t , then:

$$f(\sigma(t)) = f(t) + \mu(t)f^\triangleright(t). \quad (17)$$

The above derivative operator acting on general time scales has the properties very similar to the ones well known from the continuous case. For example, assuming that $f, g : \mathbb{T} \rightarrow \mathbb{R}$ are two differentiable functions on the time scale \mathbb{T}^k the following relations hold:

1.

$$(f + g)^\triangleright(t) = f^\triangleright(t) + g^\triangleright(t)$$

2.

$$(\alpha f)^\triangleright(t) = \alpha \cdot f^\triangleright(t)$$

3.

$$(f \cdot g)^\triangleright(t) = f^\triangleright(t)g(t) + f(\sigma(t))g^\triangleright(t) = f(t)g^\triangleright(t) + f^\triangleright(t)g(\sigma(t))$$

4.

$$\left(\frac{1}{f}\right)^\triangleright(t) = -\frac{f^\triangleright(t)}{f(t)f(\sigma(t))}$$

5.

$$\left(\frac{f}{g}\right)^\triangleright(t) = \frac{f^\triangleright(t)g(t) - f(t)g^\triangleright(t)}{g(t)g(\sigma(t))}$$

Let us finish this basic introduction by commenting that in a similar way as above one can define the delta derivative which for grainy time scales will reproduce the backward-type finite difference operator. This requires the redefinition of the delta derivative function, replacing the $\sigma(t)$ function by $\rho(t)$ in its definition (Eq. 3) and corresponding changes in the definition of the graininess function (Eq. 14) as follows:

$$f^\triangleleft(t) = \frac{f(\rho(t)) - f(t)}{\nu(t)} \quad (18)$$

Table 1 Hilger's derivatives for considered time scales

| Time scale | Hilger's derivative |
|------------------|--|
| $T_{\mathbb{R}}$ | $f^{\triangleright}(t) = \frac{df}{dt}$ |
| $T_{\mathbb{Z}}$ | $f^{\triangleright}(t) = \frac{f(t+h)-f(t)}{h}$ |
| $T_{\mathbb{N}}$ | $f^{\triangleright}(t) = \frac{c-t}{t^2} [f(\frac{ct}{c-t}) - f(t)]$ |
| $T_{\mathbb{Q}}$ | $f^{\triangleright}(t) = \frac{f(qt)-f(t)}{t(q-1)}$ |

Table 2 Hilger's derivatives of the test function

$$f(t) = \sin(t)$$

| Time scale | Hilger's derivative |
|------------------|--|
| $T_{\mathbb{R}}$ | $\cos(t)$ |
| $T_{\mathbb{Z}}$ | $\frac{2}{h} \sin\left(\frac{h}{2}\right) \cos\left(\frac{2t+h}{2}\right)$ |
| $T_{\mathbb{N}}$ | $\frac{2(c-t)}{t^2} \sin\left[\frac{t^2}{2(c-t)}\right] \cos\left[\frac{(2c-t)t}{2(c-t)}\right]$ |
| $T_{\mathbb{Q}}$ | $\frac{2}{t(q-1)} \sin\left[\frac{t(q-1)}{2}\right] \cos\left[\frac{t(q+1)}{2}\right]$ |

The backward derivative operators $f^{\triangleleft}(t)$ holds all the same properties as the forward one $f^{\triangleright}(t)$.

Following Eqs. 15 and 16 it is easy to write down the explicit formulas for the Hilger's derivative on the considered time scales. They are collected in Table 1 and the explicit formulas for the test function $f(t) = \sin(t)$ are listed in Table 2 and plotted in Fig. 4. In addition the differences between the analytical and Hilger's derivatives for the $\sin(t)$ function are shown in Fig. 5.

Let us note Hilger's derivatives of the $\sin(t)$ function can be put down in the generic form

$$(\sin)^{\triangleright}(t) = \frac{\sin(\mu(t)/2)}{\mu(t)/2} \cos(t + \mu(t)/2) \quad (19)$$

This example illustrates that for discrete time scales with nonzero graininess the Hilger's derivative introduces some phase shift and amplitude correction with respect to the analytical one which depends on the local graininess of the time scale. The influence of the finite graininess of the time scale ($\mu(t) \neq 0$) on the approximation errors of the continuous derivative for the $f(t) = \sin(t)$ function is clearly visible in Fig. 5. Two effects are noticeable. The first one is the observation that the approximation errors are nonuniformly distributed even for the uniform $T_{\mathbb{Z}}$ time scale (case B in Fig. 5). Secondly, the non-uniformity of time scales enhances this effect.

The approximation errors depend, of course, on the definition of time scales. Changing the parameters controlling the graininess of the time scales we can control the overall accuracy of approximating the continuous derivative by

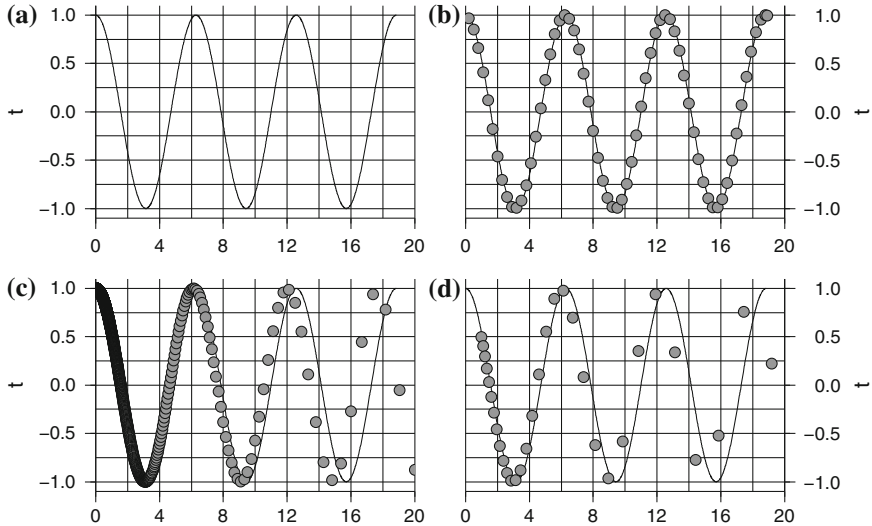


Fig. 4 Plot of Hilger's derivatives of $f(t) = \sin(t)$ function for the considered time scales (a, $\mathbb{T}_{\mathbb{R}}$, b, $\mathbb{T}_{\mathbb{Z}}$, c, $\mathbb{T}_{\mathbb{N}}$, d, $\mathbb{T}_{\mathbb{Q}}$). The $\cos(t)$ function being the exact, continuous derivative of $\sin(t)$ is plotted for reference. The following settings defining the time scales is used **b** $h = 0.1$, **c** $C = 8\pi$, $N = 500$, **d** $q = 1.1$

Hilger's one. For example, using the explicit form of the Hilger's derivatives (Eq. 19) for the $\sin(t)$ function in the limit $\mu(t) < 1$ we obtain

$$Err(t) = [f'(t) - f^{\triangleright}(t)]^2 = (\mu(t)/2)^2 \sin^2(t) + O(\mu^2(t)) \quad (20)$$

It is thus evident that in case of “simplest”, uniform time scale $\mathbb{T}_{\mathbb{Z}}$ for which $\mu(t) = h$, decreasing the h parameter improves the approximation to continuous derivative, since $Err(t) \approx h^2/4 \sin^2(t)$. In case of non-uniform time scales the situation is more complicated because of additional (possibly strong) variability of $\mu(t)$. Particularly, the asymptotic form given by Eq. 20 may not hold over the entire time scale. A good example is the $\mathbb{T}_{\mathbb{N}}$ time scale for which the graininess for the k -th point ($t_k = c/k$) reads

$$\mu(t_k) = -\frac{c}{k(k-1)} \quad (21)$$

and, depending on setting of the C parameter, $\mu(t)$ can be much larger than 1 for first points while simultaneously the condition $\mu(t) < 1$ can be satisfied for respectively “distant” ($k > \sqrt{c}$) points of $\mathbb{T}_{\mathbb{N}}$. In this case, the approximating errors calculated for “distant points” according to Eq. 20 will be much smaller than the overall upper limit for the entire time scale which, according to Eq. 19, is equal to 1. A similar situation occurs for the $\mathbb{T}_{\mathbb{Q}}$ time scale but in this case, because $q > 1$, the errors increase with subsequent points, as can be observed in Fig. 5.

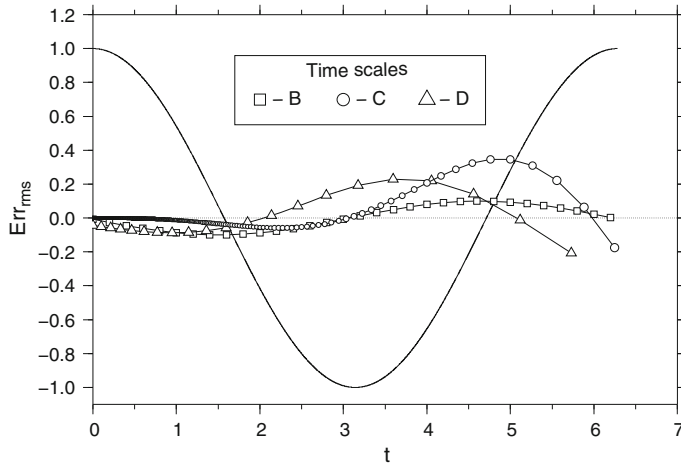


Fig. 5 Difference between the analytical and the Hilger's derivatives of $f(t) = \sin(t)$ function for the considered time scales. The analytical solution $f'(t) = \cos(t)$ is also shown for the reference (*bare line*). The following settings defining the time scales is used B: $h = 0.1$, C: $C = 100$, $N = 1000$, D: $q = 1.1$

3 Second Order Derivatives: Laplace Operators

In a similar way one can define higher order derivatives, among which the second order derivatives are very important since they appear in many physical equations, like wave equation, diffusion equation, etc. In this section we consider formulation of such derivatives on time scales. Actually, considering second (and higher orders) derivatives we explicitly touch the problem of dimensionality of space because in multidimensional spaces already second order derivatives can contain mixed first-order derivatives with respect to different space dimensions. However, in this chapter we do not address this point and consider the 1D time scales only, for which the second order derivative is unique (for continuous case). Bearing in mind future analysis, we shall refer to such second order derivatives as the Laplacian.

Defining the higher order differential operators we have to keep in mind that one can use both forward and/or backward Hilger's differential operators and, in general, they do not commute. This gives us four different possibilities of defining the Laplace operator on time scales as follow:

$$\begin{aligned}\Delta_{ff}(f) &= (f^{\triangleright})^{\triangleright} \\ \Delta_{bb}(f) &= (f^{\triangleleft})^{\triangleleft} \\ \Delta_{fb}(f) &= (f^{\triangleright})^{\triangleleft} \\ \Delta_{bf}(f) &= (f^{\triangleleft})^{\triangleright}\end{aligned}\tag{22}$$

Let us observe that the above formulas are obviously not equivalent if the distance to the nearest point on the left-hand side is not equal to the distance to the nearest point on the right-hand side.

Applying twice the derivative operators according to Eq. 25 and using the formulas for derivatives of the product and ratio of two functions, one can find out, after simple calculations, the explicit formulas of the Laplace operators defined above

$$\begin{aligned} f^{\triangleright\triangleright} &= \frac{1}{\mu\mu_\sigma} f_{2\sigma} - \frac{1}{\mu} \left(\frac{1}{\mu} + \frac{1}{\mu_\sigma} \right) f_\sigma + \frac{1}{\mu^2} f \\ f^{\triangleleft\triangleleft} &= \frac{1}{vv_\rho} f_{2\rho} - \frac{1}{v} \left(\frac{1}{v} + \frac{1}{v_\rho} \right) f_\rho + \frac{1}{v^2} f \\ f^{\triangleright\triangleleft} &= \frac{1}{\mu v_\sigma} f_{\rho\sigma} + \frac{1}{\mu v} f - \frac{1}{\mu v_\sigma} f_\sigma - \frac{1}{\mu v} f_\rho \\ f^{\triangleleft\triangleright} &= \frac{1}{v\mu_\rho} f_{\sigma\rho} + \frac{1}{\mu v} f - \frac{1}{v\mu_\rho} f_\rho - \frac{1}{\mu v} f_\sigma \end{aligned} \quad (23)$$

where the following shorthand notation is used: $f_\sigma = f(\sigma(t))$, $f_\rho = f(\rho(t))$, $f_{2\sigma} = f(\sigma(\sigma(t)))$, $f_{\rho\sigma} = f(\rho(\sigma(t)))$, etc.

The formulas in Eq. 23 can be further simplified since the following relations hold:

$$\begin{aligned} v_\sigma &= -\mu \\ \mu_\rho &= -v \\ \rho(\sigma(t)) &= \sigma(\rho(t)) = t \end{aligned} \quad (24)$$

In such a case, the Laplace operators read

$$\begin{aligned} f^{\triangleright\triangleright} &= \frac{1}{\mu\mu_\sigma} f_{2\sigma} - \frac{1}{\mu} \left(\frac{1}{\mu} + \frac{1}{\mu_\sigma} \right) f_\sigma + \frac{1}{\mu^2} f \\ f^{\triangleleft\triangleleft} &= \frac{1}{vv_\rho} f_{2\rho} - \frac{1}{v} \left(\frac{1}{v} + \frac{1}{v_\rho} \right) f_\rho + \frac{1}{v^2} f \\ f^{\triangleright\triangleleft} &= \frac{1}{\mu} \left(\frac{1}{v} - \frac{1}{\mu} \right) f + \frac{1}{\mu^2} f_\sigma - \frac{1}{\mu v} f_\rho \\ f^{\triangleleft\triangleright} &= \frac{1}{v} \left(\frac{1}{\mu} - \frac{1}{v} \right) f + \frac{1}{v^2} f_\rho - \frac{1}{\mu v} f_\sigma \end{aligned} \quad (25)$$

Let us note that Laplacians $f^{\triangleright\triangleright}$ and $f^{\triangleright\triangleleft}$ at a given point t are determined by values of f at the point t and its left and right neighborhoods: $t + \rho$ and $t + \sigma$. In case of $f^{\triangleright\triangleright}$ and $f^{\triangleleft\triangleleft}$ the additional points used to determine $f^{\triangleright\triangleright}$ and $f^{\triangleleft\triangleleft}$ are always larger or smaller than t , respectively. In Table 3 the explicit formulas of the Laplace operators for the time scales $\mathbb{T}_{\mathbb{Z}}$, $\mathbb{T}_{\mathbb{N}}$, and $\mathbb{T}_{\mathbb{Q}}$ are gathered.

Table 3 Laplace operators for the considered time scales

| Time scale | Laplace operator |
|---------------------------|---|
| $\mathbb{T}_{\mathbb{R}}$ | $f^{\gg}(t) = f^{\triangleleft}(t) = f^{\triangleleft\triangle}(t) = f^{\triangleleft\triangle\triangle}(t) = \frac{d^2f}{dt^2}$ |
| $\mathbb{T}_{\mathbb{Z}}$ | $f^{\gg}(t) = \frac{f(t+2h) - 2f(t+h) + f(t)}{h^2}$ $f^{\triangleleft}(t) = \frac{f(t-2h) - 2f(t-h) + f(t)}{h^2}$ $f^{\triangleleft\triangle}(t) = \frac{f(t+h) - 2f(t) + f(t-h)}{h^2}$ |
| $\mathbb{T}_{\mathbb{N}}$ | $f^{\gg}(t) = \left(\frac{c-t}{t^2}\right)^2 \left[\frac{c-2t}{c} f\left(\frac{ct}{c-2t}\right) - 2 \frac{c-t}{c} f\left(\frac{ct}{c-t}\right) + f(t) \right]$ $f^{\triangleleft}(t) = \left(\frac{c+t}{t^2}\right)^2 \left[\frac{c+2t}{c} f\left(\frac{ct}{c+2t}\right) - 2 \frac{c+t}{c} f\left(\frac{ct}{c+t}\right) + f(t) \right]$ $f^{\triangleleft\triangle}(t) = \frac{c-t}{t^4} [(c-t)f\left(\frac{ct}{c-t}\right) - 2cf(t) + (c+t)f\left(\frac{ct}{c+t}\right)]$ $f^{\triangleleft\triangle\triangle}(t) = \frac{c+t}{t^4} [(c-t)f\left(\frac{ct}{c-t}\right) - 2cf(t) + (c+t)f\left(\frac{ct}{c+t}\right)]$ |
| $\mathbb{T}_{\mathbb{Q}}$ | $f^{\gg}(t) = \frac{1}{t^2(q-1)^2} \left[\frac{1}{q} f(q^2 t) - f(qt) \frac{1+q}{q} + f(t) \right]$ $f^{\triangleleft}(t) = \frac{q^2}{t^2(1-q)^2} \left[qf\left(\frac{t}{q^2}\right) - f\left(\frac{t}{q}\right)(q-1) + f(t) \right]$ $f^{\triangleleft\triangle}(t) = \frac{1}{t^2(q-1)^2} \left[-qf\left(\frac{t}{q}\right) + f(t)(q-1) + f(qt) \right]$ $f^{\triangleleft\triangle\triangle}(t) = \frac{q}{t^2(q-1)^2} \left[-f(qt) + f(t)(q-1) - f\left(\frac{t}{q}\right)q \right]$ |

4 Acoustic Wave Equation in 1D

The seismic waves are examples of elastic (mechanical) waves propagating in elastic solid medium. Their description (see, e.g. Aki and Richards 1985) includes the three components of particles motion and its temporal and spatial variability through the vectorial hyperbolic-type second order partial differential equation (Aki and Richards 1985). However, in some seismological applications it is reasonable to use simplified approach and consider pressure disturbances instead of the full vector of displacement. In such a case, the elastic wave equation reduces to much simpler scalar-type acoustic equations which for non-attenuating, isotropic medium can be casted into the Hamiltonian type equations:

$$\begin{cases} \dot{\rho}(r, t) &= \frac{\partial H}{\partial p} \\ \dot{p}(r, t) &= -\frac{\partial H}{\partial \rho} \end{cases} \quad (26)$$

where p and ρ stand for the pressure and density disturbances, $\dot{\rho}, \dot{p}$ denote the time derivatives of ρ and p , respectively. The Hamiltonian density for perfectly elastic medium reads

$$H(\rho, p) = \frac{\rho^2}{2\rho_o} + \kappa(\nabla p)^2 \quad (27)$$

where ρ_o is the undisturbed medium density and κ is the bulk modulus. Independence of H of time implies the energy conservation: $H(p, q) = \text{const.}$ during the wave propagation.

The set of Eq. 26 (called sometimes velocity-stress formulation) is very convenient for numerical treatment. However, in seismological applications they are usually transformed into the second order differential equation:

$$\frac{1}{c^2} \frac{\partial^2 p}{\partial t^2} - \Delta p = S(r, t) \quad (28)$$

where c denotes waves velocity and the external source term $S(r, t)$ has been added. Analysis of general solution of Eq. 28 in two and three dimensions on time scales will be discussed elsewhere and here we consider only 1D case. Let us begin the discussion of numerical solutions by recalling the analytical solution for the homogeneous medium ($c = \text{const.}$)

The solution of the homogeneous wave equation, i.e., Eq. 28 but without the S term on the right hand side, with initial conditions $p(x, t) = f(x), \partial p / \partial t = g(x)$ is given by the well known formula due to d'Alambert (see, e.g. Courant and Hilbert 1962) and reads

$$p_h(x, t) = \frac{1}{2}(f(x + ct) - f(x - ct)) + \frac{1}{2c} \int_{x-ct}^{x+ct} g(s) ds \quad (29)$$

The solution of the inhomogeneous equation can be obtained using the fact that if $\psi(x, t; s)$, where s is an auxiliary real parameter is the solution of the wave equation with the Dirichlet's boundary condition

$$\begin{aligned} 1/c^2 \partial^2 \psi / \partial t^2 - \partial^2 \psi / \partial x^2 &= 0 \\ \psi(x, 0; s) &= 0 \\ \partial \psi / \partial t &= S(x, t; s) \end{aligned} \quad (30)$$

then

$$p(x, t) = \int_{-\infty}^t \psi(x, t - s; s) ds \quad (31)$$

is a solution to the inhomogeneous wave equation with zero initial condition

$$\begin{aligned} 1/c^2 \partial^2 p / \partial t^2 - \partial^2 p / \partial x^2 &= S(x, t) \\ p(x, 0) &= 0 \\ \partial p / \partial t &= 0 \end{aligned} \quad (32)$$

Using this result, the solution to Eq. 28 with vanishing initial condition after simple manipulation can be written down as

$$p(x, t) = \frac{c}{2} \int_{-\infty}^t \int_{-c(t-s)}^{c(t-s)} S(x + r, s) dr ds \quad (33)$$

This is the solution to the inhomogeneous problem which vanishes at $t < 0$. Actually, this solution is the most interesting from the seismological point of view since it describes the transient waves due to an abrupt rock movement in seismic source foci.

The above solution concerns the homogeneous velocity distribution and its extension to the general velocity model is problematic and the numerical methods of solving Eq. 28 are necessary.

Using the time scale concept presented in the previous sections, the discretization of Eq. 28 necessary for the numerical treatment can be achieved by a simple changing of the domain at which the solution is sought: $\mathbb{R} \times \mathbb{R} \Rightarrow \mathbb{T} \times \mathbb{Z}$ where the first and second subspaces refer to the spatial and time coordinates, respectively. Following the classical finite difference technique we shall assume the regular $dt\mathbb{Z}$ scale for time and thus the wave equation (Eq. 28) can be written down in the following form

$$p^{n+1}(x_i) = 2p^n(x_i) - p^{n-1}(x_i) + (c(x_i)dt)^2 \left[(\Delta p)_{x_i}^n + S^n(x_i) \right] \quad (34)$$

where the temporal derivative was approximated by Δ_{fb} , the subscripts n refers to n_{th} point of temporal time scale ($t_n = nh_t$), x_i is the i th point of the used spatial time scale, and dt is the time step. Choosing $\mathbb{T} = h\mathbb{Z}$ leads to the classical finite difference formula (Moczo et al. 2007) which is an obvious choice in situation when velocity c is constant or varying slowly in space.

The main power of the time scale based approach revealed in a situation when velocity significantly changes in space. The reasons are following.

The explicit, time marching numerical schemata for partial differential equations are well known (Moczo et al. 2007) to be potentially unstable: the numerical errors blow up in time leading to false solutions. In order to get the stable solution being a reasonable approximation to the analytical solution, the Courant-Friedrichs-Lowy stability condition has to be fulfilled (Courant et al. 1928). It reads

$$\frac{(dt)c(x_i)}{\mu(x_i)} \leq 1. \quad (35)$$

This condition imposes the restriction on the time length step dt or, equivalently on $\mu(t)$ if dt is kept fixed. The classical finite difference approach based on regular grid ($\mathbb{T} = h\mathbb{Z}$) address the problem by taking the grid node distance h small enough to fulfill the above condition. However, such a choice is not optimal from computational efficiency point of view since small h is required only if $c(x_i)$ is small. Thus using the irregular grid, or, in other words, more complex than $h\mathbb{Z}$ time scales for spatial coordinate would improve the performance of the algorithm.

Let us illustrate this point simulating the wave propagation using the numerical schemata of Eq. 34 with different grids (time scales) for the velocity model:

$$c(x) = \begin{cases} 8 \text{ km/s} & 0 < x \leq 500 \text{ m} \\ 5 \text{ km/s} & 500 < x \leq 1500 \text{ m} \\ 2 \text{ km/s} & 1500 < x \leq 2000 \text{ m} \end{cases} \quad (36)$$

assuming the point source located at $x = 1000$ and having the Gaussian-type time dependence: $s(x, t) = \delta(x - 1000) \exp((t - 0.012)/0.04)^2$. For the purpose of the simulation we assumed the time step $dt = 0.1$ ms and the simulation was continuing up to $T = 200$ ms. Three time scales were used:

- classical uniform grid: $\mathbb{T} = h\mathbb{Z}$ with $h = 2$ m,
- blocked type grid typically used in multi-domain methods,
- irregular grid with graininess function nonlineary interpolated between 5 and 2 m

among which the first two are used in the classical- and domain-type finite difference analysis (Kopriva 1989; Kaser and Igel 2001) while the last one is explicite based on the time scales formalism.

In the first simulation (case A) we have assumed $\mathbb{T} = h\mathbb{Z}$ with $h = 2$ m so the method coincided with the classical finite difference approach. The snapshot of waveforms at $t = 0.13$ s is shown in Fig. 6. This is our reference solution which is a very good approximation of the semi-analytical solution (Bouchon 2003).

In the next case, B, the solution was calculated using the time scale being a combination of three $h\mathbb{Z}$ -type time scales defined by the graininess function

$$\mu(x) = \begin{cases} 10 \text{ m} & 0 < x \leq 500 \text{ m} \\ 5 \text{ m} & 500 < x \leq 1500 \text{ m} \\ 2 \text{ m} & 1500 < x \leq 2000 \text{ m} \end{cases} \quad (37)$$

Such a discretization is typically used in domain-decomposition methods (see, e.g. Bamberger et al. 1997; Carcione 1991). The snapshot for $t = 0.13$ s is shown in Fig. 7. Evident numerical artifacts are visible in the solution. Finally (case C), we have defined the “smooth” irregular time scale shown in Fig. 8. The solution

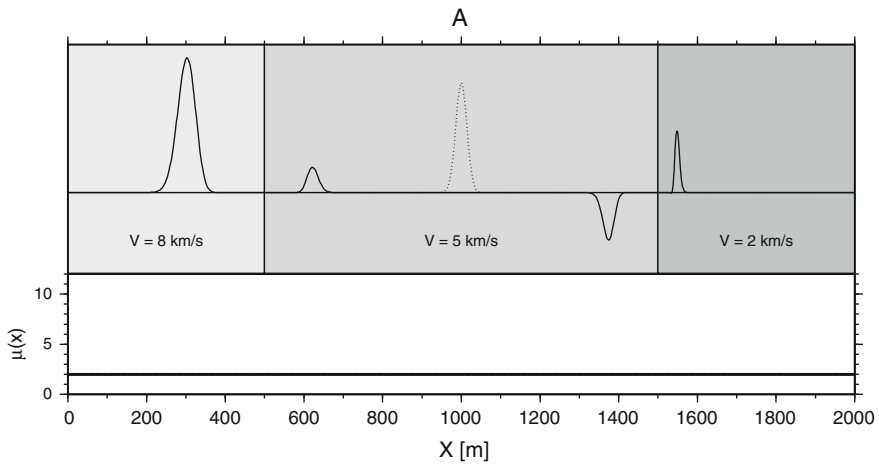


Fig. 6 Snapshot at $t = 0.13$ s of the propagating waves (*upper part*) in 1D velocity model consisting of three homogeneous blocks. The original source is depicted by the *dotted line*. The graininess function $\mu(x)$ defining the used time scale is shown in the *lower part*. This is the reference solution equivalent to the classical finite difference method. Calculation time for this simulation was 35 s

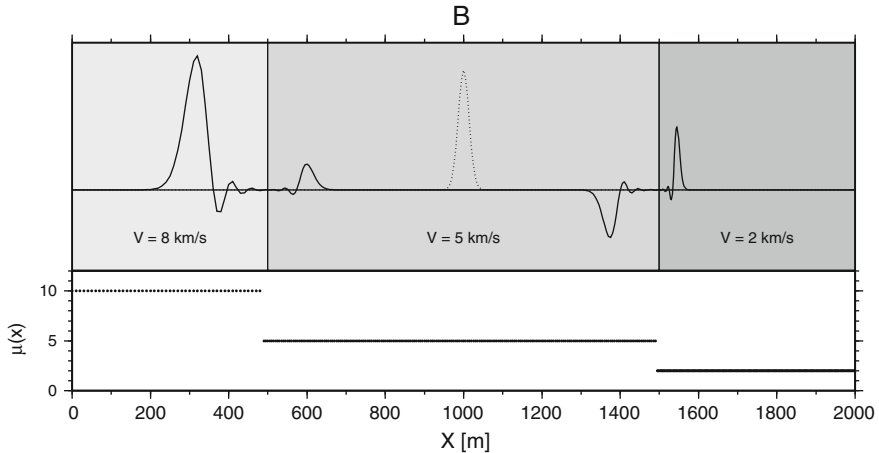


Fig. 7 Snapshot at $t = 0.13$ s of the propagating waves (*upper part*) in 1D velocity model consisting of three homogeneous blocks. The original source is depicted by the *dotted line*. The graininess function $\mu(x)$ defining the used time scale is shown in the *lower part*. This is the roughest, but fastest (calculation time 16 s) solution

obtained for this time scale is very similar to the reference one and in most situations will be quite satisfactory. The complexity and efficiency of calculations for all three setups is summarized in Table 4.

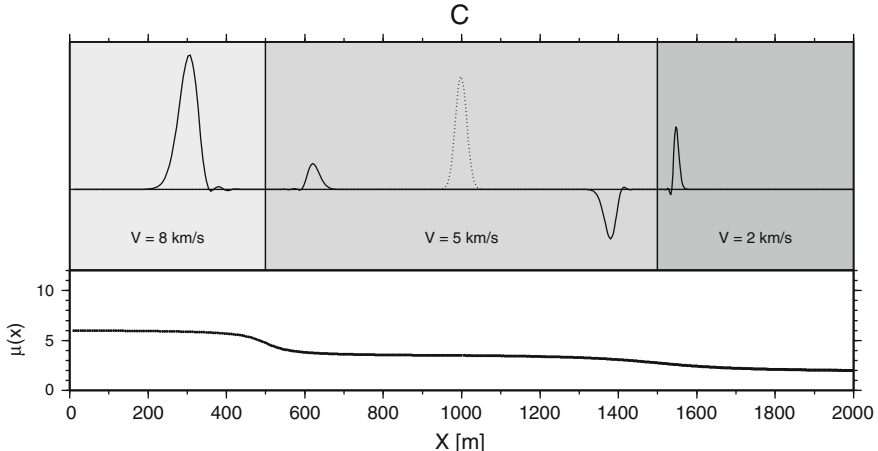


Fig. 8 Snapshot at $t = 0.13$ s of the propagating waves (*upper part*) in 1D velocity model consisting of three homogeneous blocks. The original source is depicted by the *dotted line*. The graininess function $\mu(x)$ defining the used time scale is shown in the *lower part*. Using a “smooth” time scale allowed to obtain solution very similar to the reference one (case A) but calculation time was reduced by about 35 %

Table 4 Comparison of number of grid nodes and computational times for three different time scales

| Case | No of nodes | Time [s] |
|------|-------------|----------|
| A | 1000 | 35 |
| B | 503 | 16 |
| C | 600 | 22 |

It is clear that using the irregular spatial time scale (case C) has led to the method which is as accurate as the refined finite difference approach but simultaneously it is significantly faster. In this case, the very high accuracy is achieved with the smaller number of grid nodes, which automatically means shorter computation time.

5 Conclusions

The concept of time scales has been developed for mathematical purpose—unification and thus simplification of continuous and discrete mathematical considerations like, for example, avoiding double proofing of some mathematical theorems. However, from practical point of view we think that the time scale approach opens new possibilities in developing new forward modeling algorithms providing the necessary tools for extending the classical finite difference approach

towards non-homogeneous grids. Presently, we see two different seismological applications of this particular feature of TSC to calculations of synthetic seismograms. The first one concerns the marine seismic prospecting. In this type of survey, the uppermost part of the velocity models used for calculation of synthetic seismograms is a water layer which is assumed to be homogeneous or, in some special cases (Yamada et al. 2002; Obana et al. 2000; Debski and Ando 2002) layered. In both cases, seismic waves propagation in this part of the model can be described analytically or semi-analytically (Bouchon 2003), while the more demanding numerical computations are left for the “hard-rock” part of the model. The second situation in which the non-homogeneous time scale is potentially important is simulation of seismic wave propagation in deep mines. No matter what mining technology is used, the mining area consists of hard rock-masses cut out by a large number of tunnels and/or chambers. Detailed calculation of synthetic seismograms, especially their high frequency spectrum, requires taking into account an existence of these technological “empty areas”. It can be done efficiently using appropriate, mixed-type TSC.

The different possibility of TSC approach potentially important in seismology is an ability of defining numerical schemata for differential equations using the irregular grids. This can be used to improve the performance of the seismic waveform tomographic inversion when the thought velocity perturbations are relatively small with respect to the background velocity model. In such a situation, one can try to use the complex, irregular or even non-homogeneous time scales for spatial differential operator discretization which will accommodate for the velocity background model, thus making the numerical schemata less dispersive for a given number of grid nodes with respect to the classical FD approaches (Pitarka 1999; de Rivas 1972).

Another possible application of time scales is a more accurate treatment of the boundary conditions, especially at sharp interfaces across the media. Such discontinuities in velocity models are known to be sources of large numerical errors, especially when the interface does not align with the used grid (see, e.g., Gottlieb et al. 1982; Moczo et al. 2007). Local densification of the grid points with the neighborhood of such interface can significantly improve the FD performance without the significant lost of the numerical efficiency. In case of the fully non-linear waveform inversion, when velocity models used during subsequent inversion steps can be quite different, the time scales formulation can be used in iterative grid refinements to keep forward modelling errors as small as possible (see, e.g., Gottlieb et al. 1982; Zhang et al. 2013).

Our expectations mentioned above as well as many other similar “technical” points still remain open questions and require extensive studies. With this chapter we have only begun such research. Putting forward some ideas of using the concepts of time scale calculus in the geophysical numerical analysis we wish to initialize further discussion and research on this subject which we believe will be significant part of future research work carried out at the Institute of Geophysics PAS.

Acknowledgements This chapter was partially support by the grants No. 2011/01/B/ST10/07305 from the National Science Centre, Poland. K.W. acknowledges the financial support within the grant for young scientists no. 500-10-13 from IGF PAS. K. Nowozynski and anonymous reviewers are acknowledged for their help in improving the manuscript.

References

- Agarwal R, Bohner M (1999) Basic calculus on time scales and some of its applications. *Results Math* 35:3–22. doi:[10.1007/BF03322019](https://doi.org/10.1007/BF03322019)
- Agarwal R, Bohner M, O'Regan D (2002) Dynamic Equations on time scales: a survey. *J Comp Appl Math* 141(1-2):1–26. doi:[10.1016/S0377-0427\(01\)00432-0](https://doi.org/10.1016/S0377-0427(01)00432-0)
- Aki K, Richards PG (1985) Quantitative seismology. Freeman and Co, San Francisco
- Atici F, Biles D, Lebedinsky A (2006) An application of time scales to economics. *Math Comput Model* 43:718–726. doi:[10.1016/j.mcm.2005.08.014](https://doi.org/10.1016/j.mcm.2005.08.014)
- Atici F, Eloe P (2007) Fractional q-Calculus on a time scale. *J Nonlinear Math Phys* 14(3):341–352. doi:[10.2991/jnmp.2007.14.3.4](https://doi.org/10.2991/jnmp.2007.14.3.4)
- Bamberger A, Glowinski R, Tran QH (1997) Domain decomposition method for the acoustic wave equation with discontinuous coefficients and grid changes. *J Numer Anal* 34:603–639
- Bohner M, Peterson A (2001) First and second order linear dynamics equations on time scales. *J Differ Equ Appl* 7:767–792
- Bouchon M (2003) Review of the discrete wavenumber method. *Pure Appl Geophys* 160(3-4):445–465. doi:[10.1007/PL00012545](https://doi.org/10.1007/PL00012545)
- Carcione JM (1991) Domain decomposition for wave propagation problems. *J Sci Comput* 6:453–472
- Cieslinski J (2007) Pseudospherical surfaces on time scales: a geometric definition and the spectral approach. *J Phys A Math Theor* 40:12525–12538. doi:[10.1088/1751-8113/40/42/S02](https://doi.org/10.1088/1751-8113/40/42/S02)
- Cieslinski J (2012) New definitions of exponential, hyperbolic and trigonometric functions on time scales. *J Math Anal Appl* 388:8–22. doi:[10.1016/j.jmaa.2011.11.023](https://doi.org/10.1016/j.jmaa.2011.11.023)
- Courant R, Friedrichs K, Lewy H (1928) Über die partiellen Differenzengleichungen der mathematischen Physik. *Math Ann* 100(1):32–74. doi:[10.1007/BF01448839](https://doi.org/10.1007/BF01448839)
- Courant R, Hilbert D (1962) Methods of mathematical physics. vol 2, Wiley, New York. doi:[10.1002/9783527617234](https://doi.org/10.1002/9783527617234)
- de Rivas E (1972) On the use of nonuniform grids in finite-difference equations. *J Comput Phys* 10(2):202–210. doi:[10.1016/0021-9991\(72\)90060-5](https://doi.org/10.1016/0021-9991(72)90060-5)
- Debski W (2008) Estimating the source time function by Markov Chain Monte Carlo sampling. *Pure Appl Geophys* 165:1263–1287. doi:[10.1007/s0024-008-0357-1](https://doi.org/10.1007/s0024-008-0357-1)
- Debski W (2010) Probabilistic inverse theory. *Adv Geophys* 52:1–102. doi:[10.1016/S0065-2687\(10\)52001-6](https://doi.org/10.1016/S0065-2687(10)52001-6)
- Debski W, Ando M (2002) Robust and accurate seismic/acoustic ray tracer. In The 2002 Japan-Taiwan joint seminar on earthquake mechanisms and hazard. Nagoya Japan, pp 317–327
- Dryl M, Malinowska A, Torres D (2013) A time-scale variational approach to inflation, Unemployment and social loss. *arXiv:1304.5269v1*, pp 718–726
- Ferreira R, Torres D (2008) Higher-order calculus of variations on time scales. Springer, Berlin
- Gottlieb D, Gunzberger MD, Turkel E (1982) On numerical boundary treatment for hyperbolic systems for finite difference and finite element methods. *SIAM-JNA* 19:671–682. doi:[10.1137/0719047](https://doi.org/10.1137/0719047)
- Hilger S (1990) Analysis on measure chains—a unified approach to continuous and discrete calculus. *Res Math* 18(1-2):18–56. doi:[10.1007/BF03323153](https://doi.org/10.1007/BF03323153)
- Hilger S (1997) Differential and difference calculus—unified! *Nonlinear Anal Theor Meth Appl* 30:2683–2694. doi:[10.1016/50362-546X\(96\)00204-0](https://doi.org/10.1016/50362-546X(96)00204-0)

- Kaser M, Igel H (2001) Numerical simulation of 2D wave propagation on unstructured grids using explicit differential operators. *Geophys Prosp* 49:607–619
- Kopriva DA (1989) Domain decomposition with both spectral and finite difference methods for the accurate computation of flows with shocks. *Appl Numer Math* 6:141–151
- Moczo P, Kristek J, Galis M, Chaljub E, Etienne V (2011) 3-D finite-difference, finite-element, discontinuous-Galerkin and spectral-element schemes analysed for their accuracy with respect to P-wave to S-wave speed ratio. *Geophys J Int* 187(3):1645–1667. doi:[10.1111/j.1365-246X.2011.05221.x](https://doi.org/10.1111/j.1365-246X.2011.05221.x)
- Moczo P, Robertsson J, Eisner L (2007) The Finite-difference time-domain method for modelling of seismic wave propagation, *Advances in geophysics*, vol 48. Elsevier u2013 Academic Press, New York: doi:[10.1016/S0065-2687\(06\)48008-0](https://doi.org/10.1016/S0065-2687(06)48008-0)
- Obana K, Katao H, Ando M (2000) Seafloor positioning system with GPS-acoustic link for crustal dynamics observation- preliminary result from experiments in the sea. *Earth Planets Space* 52:415–423
- Pitarka A (1999) 3D Elastic finite-difference modeling of seismic motion using staggered grids with nonuniform spacing. *Bull Seismol Soc Am* 89(1):54–68
- Vesnauer A (1996) Ray tracing based on Fermat's principle in irregular grids. *Geophys Prosp* 44(5):741–760
- Virieux J, Operto S, Ben-Hadj-Ali H, Brossier R, Etienne V, Sourbier F (2009) Seismic wave modeling for seismic imaging. *Lead Edge* 28(5):538–544. doi:[10.1190/1.3124928](https://doi.org/10.1190/1.3124928)
- Yamada, T., M. Ando, K. Tadokoro, K. Sato, and T. O. and (2002). Error evaluation in acoustic positioning of a single transponder. *Earth Planets Space.* 54, 871–881
- Zhang Z, Wei Z, Hong L, Xiaofei C (2013) Stable discontinuous grid implementation for collocated-grid finite-difference seismic wave modelling. *Geophys J Int* 192(3):1179–1188. doi:[10.1093/gji/ggs069](https://doi.org/10.1093/gji/ggs069)